

ACTA RADIOLOGICA

FOUNDED IN 1921 BY GOSTA FORSELL

OFFICIAL ORGAN OF THE RADIOLOGICAL SOCIETIES OF DENMARK, FINLAND NORWAY AND SWEDEN

EDITOR ERIK LINDGRÉN

ASSOCIATE EDITORS

Radiodiagnosis OLLE OLSSON

Radiotherapy

Radiophysics KURT LIDÉN

Radiobiology ARNE FORSBERG

EDITORIAL BOARD

Denmark S. KAAE G. THOMSEN

Finland S. MUSTAKALLIO P. VIRTAMA

Norway E. POPPE J. FRIMANN DASIL

Sweden F. KNUTSON

DIAGNOSIS

SEVENTH SYMPOSIUM

COLLECT

NEURORADIOLOGICUM

NEW YORK

21—25 September 1964

PART II

Pneumography — Ventriculography

Radioisotopes — Ultrasound — Thermography

Spine examinations — Myelography

ACTA RADIOLOGICA

OFFICIAL ORGAN OF THE RADIOLOGICAL SOCIETIES OF
DENMARK FINLAND NORWAY AND SWEDEN

Vol 5

DIAGNOSIS

1966

SEVENTH SYMPOSIUM NEURORADIOLOGICUM NEW YORK

21—25 September 1964

PART II

Table of Contents

PNEUMOGRAPHY VENTRICULOGRAPHY

PERNE A S and LOURIE H	Hemorrhage into cistern of velum interpositum in infants	635
DIECKMANN G SCHMIDT K and PRAGER J	Positional changes of intracranial structures after encephalography and during stereotaxic operations	644
DE BOLLAY G	Pulsatile movements in the CSF pathways (not reviewed)	—
ISSERWOOD I MAWDSLEY C and FERGUSON F R	Pneumoencephalographic changes in boxers	654
JIMENEZ A P LYONNET J and SILVA F E	A new diagnostic method by trans-oval cisternography	662
LEMAI M and ABRAVOWICZ A	Encephalography in the diagnosis of cerebellar atrophy	667
LEWIS A A and JEFFERSON A A	The carotid cistern — A source of diagnostic difficulties with suprasellar extensions of pituitary adenomata	675
LOOP J W	A device for encephalography in infants	691
PORTER A	Pan ventriculography — A new technique utilizing emulsified Pantopaque	693
RIGLIERO G	Encephalography today — Refinements in technique and progress in diagnosis	703
THIEBAULT F WACK ENHET A VOLSOS C CUCIBRANA M	Atrophies du vermis cérébelleux	716

RADIOISOTOPES ULTRASOUND THERMOGRAPHY

ABE Y IANAKI K WA I I and ITO K	Diagnosis of intracranial hemorrhage using ultrasound	721
ALAN B D CHASE N F KRICHFF I I and BAPTISTA A F	B scan encephalography	730

NOTICE TO AUTHORS

ACTA RADIOLOGICA publishes selected original papers on medical radiology and nuclear medicine. The articles are printed in English, French, or German according to the wishes of the author, and are subject to editorial revision; the right is reserved to introduce such changes as may be necessary to make the contributions conform to editorial standards. Acta Radiologica does not hold itself responsible for opinions expressed by the authors.

Papers should not exceed 24 pages, including space for figures and tables. Only in exceptional cases will contributions requiring more space be accepted for publication in the journal. More extensive articles may be published as Supplements for which special conditions apply.

All contributions should ordinarily be addressed to the *Editorial Secretary Acta Radiologica Box 2052 Stockholm 2 Sweden*. Papers from Denmark, Finland, and Norway may for convenience be submitted to the Editors of the respective countries for preliminary revision. The name and address of the department or hospital at which the work was carried out should be given at the top of the paper; the author should add an address to which correspondence can be directed and retain a copy of the typescript for reference.

Contributions should be as clear and concise as possible and typewritten with adequate margins and double spacing (with at least 1 cm between each line). It is important to avoid unessential matter; the typescript should therefore be carefully revised before submission. Alterations at the proof stage are expensive and with the exception of small corrections will be charged to the author. Footnotes should be avoided.

Illustrations and tabular material should be unmounted and attached to the typescript in an individual cover; they must be provided with suitable short legends comprehensible without reference to the text and typewritten on a separate page. Numbering or any arrowing or lettering

should not be drawn on the front of the prints submitted but should be marked lightly in pencil on the reverse side together with author's name. To ensure good reproduction, lines as well as numerals and lettering in diagrams and schematic illustrations should be sharp and well defined and drawn in black Indian ink (never in blue). The thickness of such lines and lettering should allow for adequate reduction. The Editor reserves the right to reduce the size of illustrations as considered appropriate. If the prints supplied are not of a sufficiently high standard for reproduction purposes, the author will be required to submit the original films. Colour drawings or colour photographs are not ordinarily acceptable.

A short summary not exceeding 75 words must be included. The references should be arranged in alphabetical order of the author's name followed by initial full title of the paper, and name of the periodical — abbreviated preferably according to the latest edition of *World Medical Periodicals* published by WHO and UNESCO, otherwise according to FISHBEIN *Medical Writing* or to the *Quarterly Cumulative Index Medicus*. The volume number, year within brackets, and number of the first page of the article should follow. Reference to books and monographs should indicate the author, title and edition of the book, the name of the publishers and the city and year of publication.

Examples

BOJSEN E and DAIN I. Selective angiography of bronchial and intercostal arteries. *Acta radiol. Diagnosis* 3 (1965), 513.

KERRIT A. Human embryology and morphology. 6th edition. p. 523. Arnold & Co. London 1948.

Fifty reprints of each paper are supplied free; additional reprints may be purchased at cost provided the necessary order is given when the proof is returned.

SUBSCRIPTIONS

	in Scandinavia	outside Scandinavia
Acta Radiologica new series for diagnostics (red) for therapeutics (blue) (including physics and biology)	} both vols Sw Kr 90	Sw Kr 100
Acta Radiologica new series for diagnostics (red)	one vol Sw Kr 60	Sw Kr 67
Acta Radiologica new series for therapeutics (blue)	one vol Sw Kr 60	Sw Kr 67

All rates include regular mailing costs

*All communications in regard to advertising, subscription, change of address, etc. should be sent to
Acta Radiologica Box 2052, Stockholm 2 Sweden*

ACTA RADIOLOGICA

OFFICIAL ORGAN OF THE RADIOLOGICAL SOCIETIES OF
DENMARK FINLAND NORWAY AND SWEDEN

Vol 5

DIAGNOSIS

1966

SEVENTH SYMPOSIUM NEURORADIOLOGICUM NEW YORK

21—25 September 1964

PART II

Table of Contents

PNEUMOGRAPHY VENTRICULOGRAPHY

BERNE A D and LOURIE H	Hemorrhage into cistern of velum interpositum in infants	635
DIEGAMANN G SCHINDT K and PRAGER J	Positional changes of intracranial structures after encephalography and during stereotaxic operations	644
DU BOULAY G	Pulsatile movements in the CSF pathways (not reviewed)	—
INVERNODI I MAWDSLEY C and FERGUSON F R	Pneumoencephalographic changes in boxers	654
JIMENEZ A L LONNET J and SILVA F R	A new diagnostic method by trans-oval cisternography	662
LE MAY M and ABRAMOWICZ A	Encephalography in the diagnosis of cerebellar atrophy	667
LEWIS A A and JEFFERSON A A	The carotid cistern — A source of diagnostic difficulties with suprasellar extensions of pituitary adenomata	675
LOOP J W	A device for encephalography in infants	691
LORTERA A	Pan ventriculography — A new technique utilizing emulsified Pantopaque	693
R HRO G	Encephalography today — Refinements in technique and progress in diagnosis	705
THIEBAULT F WACK ENHEIM A VROUSOS C and SUBIRANA M	Atrophies du vermis cérébelleux	716

RADIOISOTOPES ULTRASOUND THERMOGRAPHY

ANDY TANAKA K	Diagnosis of intracranial hemorrhage using ultrasound	721
WANG T and ITO K	B scan encephalography	730
MAJON B D CHASE A F KRICHFF I I and BATTISTA A F		

NOTICE TO AUTHORS

ACTA RADIOLOGICA publishes selected original papers on medical radiology and nuclear medicine. The articles are printed in English, French or German according to the wishes of the author, and are subject to editorial revision: the right is reserved to introduce such changes as may be necessary to make the contributions conform to editorial standards. Acta Radiologica does not hold itself responsible for opinions expressed by the authors.

Papers should not exceed 24 pages including space for figures and tables. Only in exceptional cases will contributions requiring more space be accepted for publication in the journal. More extensive articles may be published as Supplements for which special conditions apply.

All contributions should ordinarily be addressed, to the *Editorial Secretary, Acta Radiologica, Box 2052, Stockholm 2, Sweden*. Papers from Denmark, Finland and Norway may for convenience be submitted to the Editors of the respective countries for preliminary revision. The name and address of the department or hospital at which the work was carried out should be given at the top of the paper; the author should add an address to which correspondence can be directed and retain a copy of the typescript for reference.

Contributions should be as clear and concise as possible and typewritten with adequate margins and double spacing (with at least 1 cm between each line). It is important to avoid unessential matter; the typescript should therefore be carefully revised before submission. Alterations at the proof stage are expensive and with the exception of small corrections will be charged to the author. Footnotes should be avoided.

Illustrations and tabular material should be unmounted and attached to the typescript in an individual cover; they must be provided with suitable short legends comprehensible without reference to the text and typewritten on a separate page. Numbering or any arrowing or let-

tering should not be drawn on the front of the print submitted but should be marked lightly in pencil on the reverse side together with author's name. To ensure good reproduction, lines as well as numerals and lettering in diagrams and schematic illustrations should be sharp and well defined and drawn in black Indian ink (never in blue). The thickness of such lines and lettering should allow for adequate reduction. The Editor reserves the right to reduce the size of illustrations as considered appropriate. If the prints supplied are not of a sufficiently high standard for reproduction purposes the author will be required to submit the original films. Colour drawings or colour photographs are not ordinarily acceptable.

A short summary not exceeding 75 words must be included. The references should be arranged in alphabetical order of the author's name followed by initials, full title of the paper, and name of the periodical — abbreviated preferably according to the latest edition of *World Medical Periodicals* published by WHO and UNESCO otherwise according to *FISHBEIN Medical Writing* or to the *Quarterly Cumulative Index Medicus*. The volume number, year within brackets and number of the first page of the article should follow. Reference to books and monographs should indicate the author, title and edition of the book, the name of the publishers and the city and year of publication.

Examples

BOJSEN E. and DAHV I. Selective angiography of bronchial and intercostal arteries. *Acta radiol. Diagnosis* 3 (1965), 513.

KERRI A. Human embryology and morphology. 6th edition. p. 523. Arnold & Co. London 1948.

Fifty reprints of each paper are supplied free; additional reprints may be purchased at cost provided the necessary order is given when the proof is returned.

SUBSCRIPTIONS

		in Scandinavia	outside Scandinavia
Acta Radiologica new series (for diagnostics (red) for therapeutics (blue) (including physics and biology)	} both vols	Sw Kr 90	Sw Kr 100
Acta Radiologica new series (for diagnostics (red)	one vol	Sw Kr 60	Sw Kr 67
Acta Radiologica new series for therapeutics (blue)	one vol	Sw Kr 60	Sw Kr 67

All rates include regular mailing costs.

All communications in regard to advertising, subscription change of address etc. should be sent to Acta Radiologica, Box 2052, Stockholm 2, Sweden.

ROLLER C J and PRIEBRAH H F W	Lumbosacral intradural lipoma and sacral agenesis (not reced)	—
TANAKA K and ITO K	Diagnosis of brain tumor using ultrasound	915
WENDE S	Verlaufsuntersuchungen bei Hirntumoren mit radioaktiven Isotopen	928
WHITE D A and BLANCHARD J B	Studies in ultrasonic echoencephalography II — An objective technique for the A scan presentation of the cerebral midline structures	936
WILCKE O	Hirndurchblutungsmessung mit Isotopen und ihr kli- nischer Wert	953
WOOD E H and HILL R P	Thermography in the diagnosis of cerebrovascular occlu- sive disease	961
ZINGESER L MANDELL S and SCHECHTER M	Gamma encephalograms in extracerebral hematomas	972

SPINE AND MYELOGRAPHY

BACIOCCO A GALLIZZO A and SASSAROLI S	Experiences with SH-617 L myelography	981
CALABRO A and SMALINO F	Urea in positive contrast myelography	984
DI GIRO G	Observations on the circulation of the cerebrospinal fluid	988
DORFMAN J	Radiological aspects of spinal cysticercosis	1003
EPSTEIN B S and EPSTEIN J A	Syphonage technique for removal of Pantopaque	1007
GARDNER W J	Embryologic origin of spinal malformations	1013
HEINE E R BRINKER R A and TAVERAS J M	Advantages of a less dense Pantopaque contrast material for myelography	1024
HOWLAND W J and CURRY J L	Pantopaque arachnoiditis — Experimental study of blood as a potentiating agent and corticosteroids as an ameliorating agent	1032
JIROUT J	Mobility of the spinal cord under abnormal conditions	1042
LOMBARDI G and PASERINI A	Congenital tumours of the spinal cord	1047
LUYENDIJK W and VAN VOORTHUSEN A F	Contrast examination of the spinal epidural space	1051
MELOT C J BRILLIAT J JEANMART L et GOMPEL C	Les hémangiomes du rachis cervical	1067
METZGER J ENGEL PH DILENCE D et ABOLIKER J	La myélobulbographie gazeuse dans les myélopathies chroniques	1079
PENNINC L and VAN DER ZWAAG I	Biomechanical aspects of spondylotic myelopathy	1090
REZENDE T	Double contrast myelography	1104
SAMON G LOUIS R et CERINFL C	Le fourreau dural lombo-sacré — Étude radio-anatom- ique	1107
SCHECHTER M M and ZINGESER L H	The spinal arteries	1124

BELL R L	Cerebral blood flow measured with radioactive isotopes	740
BRINKER R A and TAVERAS J M	Ultrasound cross sectional pictures of the head	745
BULL J W D	Topographical criteria for pathological diagnosis of intra cranial masses by means of gamma encephalography	754
CRONQVIST S INGVAR D H and LASSEN N A	Quantitative measurements of regional cerebral blood flow related to neuroradiological findings	760
DRESE M J HAYES G J and KEMPE L G	Evaluating intracranial hematoma by echo EG	767
FERIA L G and RÄDBERG C	Complete gas myelography via lumbar injection under pressure (not received)	—
FRIEDMANN G und WILCKE O	Gegenüberstellung der serienangiographischen und szintigraphischen Ergebnisse bei 242 Hirntumoren	774
GELETNIKOV C L	Echoencephalographie bei cerebralen Erkrankungen im Sauglings und Kindersalter	779
GOLDBERG H I HEINZ E R and TAVERAS J M	Thermography in neurological patients — Preliminary experiences	786
GORDON D	Ultrasonic surgery of the central nervous system	796
GROSCH M WACK FRIEDEMANN A VROUSOS C et SUBIRANA M	Scintigraphie cisternale	804
DE GUTIERREZ MAHONEY C G and CLEVAS VERDU C	Palencephalography	813
HARPER P V FINK R A CHARLSTON D B BLACK R N LATHROP K A and EVANS J P	Rapid brain scanning with Technetium 99m	819
KAZNER E und SCHIEFER W	Echoencephalographische Untersuchungsergebnisse bei Schädel Hirnverletzungen	832
KUHL D E PITTS F W and TUCKER S H	Brain scanning of children using body section techniques and pertechnetate ^{99m} Tc	843
MAKOW D M WISLOUZIL W WHITE D N and BLANCHARD J	Novel immersion scanner and display system for ultra sonic brain tomography	855
MCKINNEY W M TOOLE J F SHARP W T MACMILLAN E A GIBSON J W and SOUTH B D	Evaluation of five hundred psychiatric in patients by midline echoencephalography	865
MEALEY JR J and CAMPELL J A	Scintillography of infantile subdural effusions and its clinical application	871
MORELLO F GIORDANO G P ALVISE C and SCIASCIA R	Scintiscanning of cerebral neoplasms by radioactive mercury (Neohydrin ²⁰³ Hg)	884
MURPHY K	Isotope encephalometry — A simplified and rapid scan ning procedure	890
MULLER D	Die Cisterna terminalis des Duraalsackes bei Spina bifida occulta mit peridurale Lipomatose oder occulte Me ningocele (not received)	—
OJEMANN R G ARONOW S and SWEET W H	Scanning with positron emitting isotopes in cerebrovascu lar disease	894
PLANIOL TH METZGER J DAVID M et FISCHCOLD H	Explorations techniques ambulatoires dans le diagnostic des tumeurs cérébrales hémisphériques	906

ROLLER C J and PRIEBRAM H F W	Lumbosacral intradural lipoma and sacral agenesis (not received)	—
TANAKA K and ITO K	Diagnosis of brain tumor using ultrasound	915
WENDE S	Verlaufsuntersuchungen bei Hirntumoren mit radioaktiven Isotopen	928
WHITE D N and BLANCHARD J B	Studies in ultrasonic echoencephalography II — An objective technique for the A scan presentation of the cerebral midline structures	936
WILCKE O	Hirndurchblutungsmessung mit Isotopen und ihr klinischer Wert	953
WOOD E H and HILL R P	Thermography in the diagnosis of cerebrovascular occlusive disease	961
ZINGESSER L, MANDELL S and SCHECHTER M	Gamma encephalograms in extracerebral hematomas	972

SPINE AND MYELOGRAPHY

BACIOCIO A, GALLUZZO A and BASSAROLI S	Experiences with SH 617 L myelography	981
CALABRO A and SMALTINO F	Urea in positive contrast myelography	984
DI CIPRO G	Observations on the circulation of the cerebrospinal fluid	988
DORFSMAN J	Radiological aspects of spinal cysticercosis	1003
EPSTEIN B S and EPSTEIN J A	Syphonage technique for removal of Pantopaque	1007
CARDNER W J	Embryologic origin of spinal malformations	1013
HEINZ E R, BRINKER R A and TAVERAS J M	Advantages of a less dense Pantopaque contrast material for myelography	1024
HOWLAND W J and CURRY J L	Pantopaque arachnoiditis — Experimental study of blood as a potentiating agent and corticosteroids as an ameliorating agent	1032
JIROUT J	Mobility of the spinal cord under abnormal conditions	1042
LOMBARDI G and PASSERINI A	Congenital tumours of the spinal cord	1047
LUYENDIJK W and VAN VOORTHUSEN A E	Contrast examination of the spinal epidural space	1051
MELOT C J, BRIHAYE J, JEANMART L et COMPEL C	Les hémangiomes du rachis cervical	1067
MITZGER J, ENGEL P et DILENG D et ABOLKER J	La myélobulbographie gazeuse dans les myélopathies chroniques	1079
PENNINC L and VAN DER ZWAAG P	Biomechanical aspects of spondylotic myelopathy	1090
REZENDE T	Double contrast myelography	1104
SALAMON G, LOUIS R et CUTRINEL G	Le fourreau dural lombo-sacré — Étude radio-anatomique	1107
SCHUCHTER M M and ZINGESSER L H	The spinal arteries	1124

SOLF LLENAS J, ROTÉS QUEROL J and DALMAU GRIÀ M	Radiologic aspects of spinal brucellosis	1132
THOMSON J L C	Myelography in dorsal disc protrusion	1140
TUCKER H J, SIBLER W A and LAPHAM I W	Cauda equina damage after thorium dioxide myelography	1147
Réflexions après le VIIème Symposium		1155

List of Authors

- | | | |
|-----------------------|-----------------------------|--------------------------|
| Abe Y 721 | Coldberg H I 786 | Ojemann R C 894 |
| Aboulker J 1079 | Compel C 1067 | |
| Abramowicz A 667 | Cordon D 796 | Passerini A 1047 |
| Adipou B D 730 | Cro C M 804 | Penning L 1090 |
| Ali C 884 | Cuermel C 1107 | Pitts F W 813 |
| Aronow S 894 | de Cudrérez Mahoney C C 813 | Planiol Th 906 |
| | | Portera A 693 |
| | | Rager J 444 |
| Baclocco A 981 | Harper I A 819 | |
| Battista A I 730 | Hayes C J 767 | Rezende T 1104 |
| Beck K N 819 | Heinz L R 786 1024 | Rotés Querol J 1132 |
| Bell R I 740 | Hill R P 961 | Ruggiero C 705 |
| Berne A S 635 | Howland W J 1034 | |
| Blanchard J B 855 936 | | |
| Brihaye J 1067 | Ingram D H 760 | Salmon G 1107 |
| Brunker R A 745 1024 | Isherwood I 654 | Saravali S 981 |
| Bull J W D 754 | Ito K 721 915 | Schechter M M 977 1124 |
| | | Schielke W 837 |
| Calabro A 984 | Jeanmart I 1067 | Schmidt K 644 |
| Campbell J A 871 | Jefferson A A 675 | Serseri R 884 |
| Charleston D B 819 | Jimenez A P 612 | Sharp W T 865 |
| Chase N F 730 | Jirout J 1042 | Sibley W A 1147 |
| Cronqvist S 760 | | Silva I 662 |
| Cuevas Verdu C 813 | Kazner F 832 | Smallino F 984 |
| Curry J I 1032 | Kenpe L C 767 | Solf Llenas J 1132 |
| | Krichoff I I 730 | South B D 865 |
| | Kuhl D E 843 | Subirana M 716 804 |
| Dalmau Grià M 1132 | | Sweet W H 894 |
| David M 906 | Lapham L W 1147 | |
| Di Chiro C 989 | Lassen N A 760 | Tanaka K 721 915 |
| Dieckmann C 644 | Lithrop K A 819 | Taveras J M 747 786 1024 |
| Dilenge D 1079 | Elmazy M 617 | Thiébaud I 716 |
| Dorfman J 1003 | Lewtas N A 675 | Thomson J L C 1140 |
| Dreese M J 767 | Lombardi C 1047 | Toole J I 865 |
| | Loop J W 691 | Tucker H J 1147 |
| Engel H 1079 | Louis R 1107 | Tucker S H 843 |
| Epstein B S 1007 | Lourie H 635 | |
| Epstein J A 1007 | Luyendyk W 1051 | van Voorthuysen A F 1051 |
| Farras J I 819 | Lyonnet J 662 | Vrousos C 716 804 |
| | | |
| Ferguson F P 654 | McMuney W M 865 | Wackenheim A 716 804 |
| Fink R A 819 | MacMillan E A 867 | Wagui T 721 |
| Fischgold H 906 1155 | Makow D M 855 | Wende S 978 |
| Friedmann C 774 | Mandell S 972 | White D N 855 936 |
| | Mawdsley C 654 | Wilcke O 774 953 |
| Giluzzo A 991 | Mealey Jr J 871 | Wood E M 961 |
| Gardner W J 1013 | Meltz C J 1067 | Wyslounski W 855 |
| Celetnky C L 779 | Meizger J 904 1079 | |
| Gibson J W 865 | Morello I 884 | Zingesser I H 977 1124 |
| Giordano C P 884 | Myhre K 890 | van der Zwag P 1090 |

HEMORRHAGE INTO CISTERN OF VELUM INTERPOSITUM IN INFANTS

by

ALFRED S. BERNE and HERBERT LOURIE

There are many reports concerning intracranial hemorrhage in the immediate perinatal period (4-5) and in young children (6-7-8). However, a review of the literature failed to disclose a report of the type of intracranial hemorrhage in young infants as will be recorded here. Furthermore, we have found no description of the pneumographic findings in subarachnoid hemorrhage in infancy similar to those to be described. The clinical and radiologic features of these three cases of subarachnoid hemorrhage into the cistern of the velum interpositum in infants constitute a specific entity. Analysis of these features adds information which appears to confirm the hypothetical etiologic relationship between perinatal intracranial hemorrhage and congenital communicating hydrocephalus (1) and incriminates fetal hypoxia as the precipitating factor.

Case reports

Case 1 This 4-month-old girl was delivered as a vertex presentation after 16 hours of induced labor. She appeared well until the day of admission to the hospital, when she suddenly screamed several times, became decerebrate, and lapsed into coma. Lumbar and ventricular

SOLE LLENAS J, ROTÉS QUEROL J and DALMAU CRIÀ M	Radiologic aspects of spinal brucellosis	1132
THOMSON J L G	Myelography in dorsal disc protrusion	1140
TUCKER H J SIBLEY W A and LAPHAM I W	Cauda equina damage after thorium dioxide myelography	1147
Réflexions apres le VIIème Symposium		1155

List of Authors

- Abe Y 721
 Aboulker J 1079
 Abramowicz A 667
 Adapon B D 730
 Aharin C 884
 Aronow S 894
 Baciocco A 981
 Battista A J 730
 Beck R N 819
 Bell R I 740
 Berne A S 635
 Blanchard J B 855 936
 Brinaye J 1067
 Brinker R A 745 1024
 Bull J W D 754
 Calabro A 984
 Campbell J A 871
 Charleston D B 819
 Chase N F 730
 Cronqvist S 760
 Cuevas Verdu C 813
 Curry J I 1032
 Dalmau Crià M 1132
 David M 906
 Di Chiro C 988
 Diekmann C 644
 Dilenge D 1079
 Dorfman J 1003
 Dreese M J 767
 Engel Ph 1079
 Epstein B S 1007
 Epstein J A 1007
 Evans J P 819
 Ferguson F P 654
 Fink R A 819
 Fischgold H 906 1155
 Friedmann G 774
 Galuzzo A 981
 Gardner W J 1013
 Geletneky C I 779
 Gibson J W 865
 Giordano C P 884
 Goldberg H I 786
 Gompel C 1067
 Gordon D 796
 Gro C M 804
 Guerinel G 1107
 de Gutiérrez Mahoney C C 813
 Harper P A 819
 Hayes C J 767
 Heinz L R 786 1024
 Hill R P 961
 Howard W J 1034
 Ingvar D H 760
 Isherwood I 654
 Ito K 721 915
 Jeannart I 1067
 Jefferson A A 675
 Jimenez A P 667
 Jirout J 1042
 Kärner F 832
 Kempe L G 767
 Kricheff I I 730
 Kuhl D E 843
 Lapham L W 1147
 Lassen N A 760
 Lathrop K A 819
 LeMay M 667
 Lewtas N A 675
 Lombardi G 1047
 Loop J W 691
 Louis R 1107
 Lourie H 635
 Luyendyk W 1051
 Lyonnet J 662
 McKinney W M 865
 MacMillan F A 865
 Makow D M 825
 Mandell S 972
 Mawdsley C 654
 Mexley Jr J 871
 Melor C J 1067
 Metzger J 906 1079
 Morello I 884
 Myhre K 890
 Ojemann R C 894
 Passeri A 1047
 Penning I 1090
 Pitts F W 843
 Planiol Th 906
 Portera A 693
 Prager J 644
 Rezende T 1104
 Rotés Querol J 1132
 Ruggiero C 705
 Salamon C 1107
 Sassaroli S 981
 Schlechter M M 972 1124
 Schiefer W 832
 Schmidt K 644
 Scarsa R 884
 Sharp W T 865
 Sibley W A 1147
 Silva F 662
 Smalino F 984
 Sole Ikenas J 1132
 South B D 865
 Subirana M 716 804
 Sweet W H 894
 Tanaka K 721 915
 Taveras J M 745 786 1024
 Thiebaut J 716
 Thomson J L C 1140
 Toole J I 865
 Tucker H J 1147
 Tucker S H 843
 van Voorthuisen A E 1051
 Vrousos C 716 804
 Wackenheim A 716 804
 Wagon T 721
 Wende S 928
 White D N 855 936
 Wilcke O 774 953
 Wood E M 961
 Wydoszil W 855
 Zingesser I H 972 1124
 van der Zwaag P 1090



Fig 2 Case 2 supine position (a, b) and prone position (c). Two lateral smooth masses extending from region of foramen of Monro to atria and projecting into lateral ventricles; the right mass is the larger. Compression of right superior portion of lateral ventricle by the mass (arrow). Dilated cisterna magna, moderate hydrocephalus. Needle track seen in right frontal region (n).

Case 2 This 7 week-old boy was delivered as a vertex presentation. Borderline cephalopelvic disproportion was present and the child was obviously hypoxic at birth (graded 5 on the Apgar scale). He made an apparent complete recovery and was doing well until one week before hospital admission when he vomited suddenly and became decerebrate. Lumbar puncture at that time produced bloody spinal fluid and the infant improved considerably over the next 6 days. He was then transferred to this hospital for evaluation of an enlarged head.



a



b



c

Fig 1 Case 1 Half axial and lateral projections supine position (a, b) and prone position (c). Bilateral smoothly outlined masses projecting from floor into lateral ventricles; the masses (→) extend from the foramina of Monro to the atria; depression of roof of third ventricle (↔) minimal hydrocephalus

traps yielded slowly bloody fluid. Serial cerebral angiography was performed and was normal. Ventriculography was then done (Fig 1). The patient expired before therapy could be instituted.

Autopsy revealed a solid clot which originated in the transverse cerebral fissure and had ruptured into the left lateral ventricle. Extensive softening and hemorrhagic infarction of the left thalamus were present.

This acute case with an overwhelming hemorrhage into the cavum velum interpositum and fatal intraventricular rupture is the prototype of the less severe subacute and chronic stages of this syndrome.

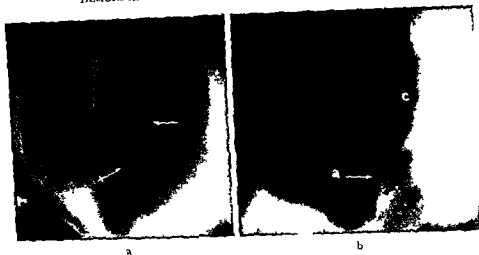


Fig 4 Case 3 Ventriculography supine position Smooth mass projecting into lateral ventricles much larger on the left (a→) compression of left side of roof of third ventricle (←→) cyst of cavum Verga (x c) moderate to marked hydrocephalus (g) greater on left

The hydrocephalus was arrested for 6 weeks. Then megacephaly was again obvious and encephalography and ventriculography were performed (Fig 5). The marked communicating hydrocephalus has been successfully treated with a ventriculogugular shunt.

Discussion

The many similarities in these three cases constitute a distinct and well defined clinical and radiologic syndrome. Each child was full term and the first born, two were definitely hypoxic at birth and the third infant was born after 16 hours of induced labor. Each patient was apparently healthy at the time of occurrence of a sudden intracranial hemorrhage. The initial air study in each individual showed a mass in the cistern of the velum interpositum. Later in the patients who survived, as the mass disappeared, a communicating hydrocephalus of increasing severity developed (Figs 1 to 5). Finally, in none of these patients was an obvious cause for hemorrhage found (i.e. vascular anomaly, tumor, blood dyscrasia, etc.).

The exhaustive study and review by HALLER, NESBITT & ANDERSON (5) of perinatal intracranial hemorrhage is particularly informative. These authors and others (2, 3, 4) stress that perinatal anoxia frequently causes overwhelming fatal hemorrhages into the area of the brain under discussion in this paper — the velum interpositum and the neighboring spaces of the transverse cerebral fissure (Fig 6). These hemorrhages are in contradistinction to the

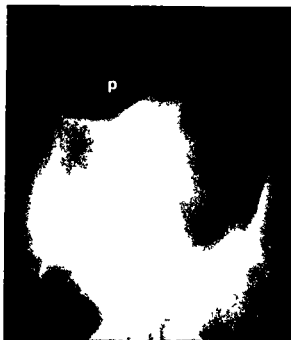


Fig. 3 Case 2 Ventriculography supine position 2 months after examination in fig. 2. No masses projecting into lateral ventricles; the hydrocephalus is more marked; a porencephalic cyst has developed at the site of the needle track (p).

Pink, deeply xanthochromic fluid was obtained at ventricular tap performed for ventriculography 7 days after the acute episode (Fig. 2). The head size stabilized and the baby again improved after ventricular tap.

Six weeks later, at the age of 14 weeks, the baby was readmitted because of increasing head size. Otherwise the infant's general state of health had been good. Repeat ventriculograms were made (Fig. 3). The mass in the cistern of the velum interpositum had disappeared; the hydrocephalus was greater, and a porencephalic cyst had developed at the site of the needle track made at the original ventriculography. Intraventricular exploration through this cyst revealed only blood-stained ependyma in the floor of the lateral ventricle; no mass or vascular anomaly was found. The baby expired postoperatively. Permission for autopsy was refused.

Case 3. This female infant was delivered as a breech presentation. The delivery was complicated by a terminal abruptio placentae. One loop of umbilical cord encircled the child's neck. She was lethargic and nursed poorly for the first 3 days of life. At age 5 days she appeared very well and was discharged from the hospital. Thirty-six hours later she became restless, suddenly cried out in a strange manner, became decerebrate, and lapsed into coma. Lumbar puncture produced bloody fluid. Progressive improvement followed the tap and the baby was discharged from the hospital.

At age 5 weeks an enlarged head was noted at a well-baby check-up, and she was readmitted to the hospital. Carotid angiography was unsuccessful on two occasions. Ventriculograms were made (Fig. 4). Cytologic study of the ventricular fluid, which was deeply xanthochromic, was reported as class V (malignant glioma). Because of this report the mass seen on ventriculography was explored surgically (HL). A cystic dilatation of the cavum velum interpositum and hemosiderin-stained ependyma were found. The abnormal cells originally reported were re-examined and reclassified as primitive ependymal cells.

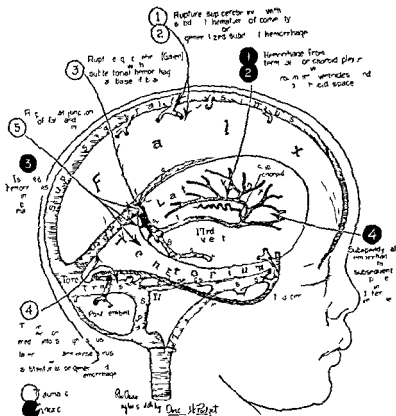


Fig 6 Schematic drawing to show frequent sites of injury and hemorrhage at birth. The sites of noxious lesions are indicated by numbers encircled in black and traumatic lesions by numbers encircled in white. (From HALLER, NEBITT & ANDERSON: Obstetrical and Gynecological Survey Vol 11 1956)

disease a severe communicating hydrocephalus develops as a result of the obliterative arachnoiditis which occurs secondary to the blood in the cistern of the velum interpositum and the adjoining ambient cisterns (1)

The radiologic diagnosis can be clearly established by its pneumographic features. In the subacute or intermediate stage a mass conforming to the boundaries of the velum interpositum is demonstrated. The mass extends anteriorly to the foramen of Monro and posteriorly to the atrial region and is smooth in outline. It projects bilaterally into the bodies of the lateral ventricles and causes impression upon and depression of the roof of the third ventricle (Figs 1, 2 and 4). The chronic or late stage is characterized by the usual radiographic features of a communicating non absorptive hydrocephalus



Fig. 3. Case 3. Pneumography 4 months after the ventriculographic examination in fig. 4. a) Erect lateral encephalogram. Dilated interpeduncular cistern and gas rising into crural portion of ambient cistern (arrow) but not rising above level of tentorial notch. b) Ventriculogram, supine position. The hydrocephalus has increased in severity. A porencephalic cyst has developed at site of surgical exploration (x); the mass has disappeared.

traumatic perinatal intracranial hemorrhages which occur in relation to the large dural sinuses.

The similarity of the anatomical sites of hemorrhage in the cases reported here to those of the fatal anoxic hemorrhages reported in neonates, and the hypoxic circumstances surrounding our patients' births appears to be more than coincidental. If this hypothesis is accepted the evolution and pathogenesis of the syndrome described here become clear. A newborn infant suffers a moderately severe but non-fatal hypoxic episode at birth. This results in hemorrhagic softening in the deep structures surrounding the cisterna velum interpositum and probable damage (9) to the walls of the many veins and venules in this region (10).

Subsequently, these weakened blood vessels, with the loss of their usual glial support, rupture into the cistern of the velum interpositum. If the hemorrhage does not rupture into the ventricles the infant survives. Pneumograms made at this stage of the disease will demonstrate a mass in the cistern of the velum interpositum as seen in Cases 2 and 3 (Figs 2 and 4). After the mass will disappear as was demonstrated by the second pneumography performed in Cases 2 and 3 (Figs 3 and 5). At this time the late and final stage of the

REFERENCES

- 1 GRANHOLM L and RADBERG C Congenital communicating hydrocephalus *J Neurosurg* 20 (1963) 338
- 2 GRONTOFT O Intracerebral and meningeal haemorrhages in perinatally deceased infants I Intracerebral haemorrhages *Acta Obstet gynec scand* 32 (1953) 308
- 3 — Intracerebral and meningeal haemorrhages in perinatally deceased infants II Meningeal haemorrhages *Acta Obstet gynec scand* 32 (1953) 485
- 4 GLENWALD P Subependymal cerebral hemorrhage in premature infants and its relation to various injurious influences at birth *Amer J Obstet Gynec* 6 (1951) 1285
- 5 HALLER E S NESBITT R E L JR and ANDERSON G W Clinical and pathological concepts of gross intracranial hemorrhage in perinatal mortality *Obstet gynec Surv* 11 (1956) 179
- 6 KING R B Spontaneous subarachnoid hemorrhage in children *Postgraduate Medicine* 28 (1960) 130
- 7 MILLER H G Spontaneous subarachnoid hemorrhage in children *Arch Dis Childhood* 13 (1938) 258
- 8 SEDZIMIR C B Intracranial hemorrhage in children (Abstract) *J Neurol Neurosurg Psychiat* 22 (1959) 78
- 9 THORNER M W and LEWIS F H The effects of repeated anoxia on the brain A histopathologic study *J Amer med Ass* 115 (1940) 1595
- 10 WOLF B S and HUANG Y P The subependymal veins of the lateral ventricles *Amer J Roentgenol* 91 (1964) 406

1 c, dilated ventricles, dilated basal cisterns, and failure of gas to ascend above the tentorial notch to fill the supratentorial cisterns and cerebral sulci (1) (Figs 3 and 5)

Our experience would suggest that therapy during the acute and subacute stages of this syndrome be directed towards relieving intracranial pressure by ventricular and lumbar taps. The clot in the transverse fissure will resolve and need not be attacked directly in these young infants. Later, if necessary, a shunt can be inserted to control the hydrocephalus.

The evolution of this syndrome, from delayed hemorrhage into the midline cistern of the velum interpositum to that of classical "congenital" communicating hydrocephalus as it occurred in our cases, gives strong support to the theory that communicating hydrocephalus developing in other young infants is in fact related to perinatal hypoxic subarachnoid hemorrhage.

Acknowledgements

The authors express their appreciation to Dr. Arthur Ecker for permission to use Case 1. Case 2 was brought to our attention by Dr. William Stewart and Case 3 by Dr. Willet Bowen.

SUMMARY

Three instances of hemorrhage into the cistern of the velum interpositum in young infants are described. This delayed hemorrhage is related to perinatal hypoxia. The acute stage may terminate fatally by intraventricular rupture of the hemorrhage. The subacute stage is characterized by the presence of a mass occupying the cistern of the velum interpositum as shown by pneumography. In the chronic stage pneumography will demonstrate an increasingly severe communicating hydrocephalus and disappearance of the mass from the cistern of the velum interpositum.

ZUSAMMENFASSUNG

Es werden drei Beispiele von Blutungen in die Cisterna veli interpositi bei Kleinkindern beschrieben. Diese verzögerte Blutung wird zu perinataler Hypoxie in Beziehung gesetzt. Das akute Stadium kann infolge Ruptur der Blutung in die Ventrikel tödlich enden. Das subakute Stadium ist durch eine Masse, die die Cisterna veli interpositi ausfüllt, wie mittels Pneumoencephalographie gezeigt werden konnte — gekennzeichnet. Im chronischen Stadium zeigt die Pneumographie einen zunehmenden kommunizierenden Hydrozephalus und ein Verschwinden der Veränderung in der Cisterna veli interpositi.

RÉSUMÉ

Présentation de trois cas d'hémorragie dans la citerne de velum interpositum chez des nourrissons. Cette hémorragie retardée est en rapport avec l'hypoxie périnatale. La phase aiguë peut se terminer par la mort du fait de la rupture intraventriculaire de l'hémorragie. La phase subaiguë est caractérisée par la présence d'une masse occupant la citerne du velum interpositum et mise en évidence par pneumographie. À la phase chronique, la pneumographie montre une hydrocéphalie communicante qui va en s'aggravant et la disparition de la masse qui occupait la citerne du velum interpositum.

calcifications are also found it was of interest to find out whether these calcifications may shift in relation to the bony reference points of the skull base. These reference points are used for the transfer of the target point from the pneumogram in the sitting position to the supine horizontal roentgenogram during operation by the methods mentioned above.

2 The second question concerns the significance of possible shifts of intracranial structures due to the collection of extracerebral air during stereotaxic brain operations. It was of interest to ascertain to what extent the identification of shifts resulting from gravitational influence is possible by observing the clinical effects of coagulations in the pallidum.

Methods

Positional changes in sharply delineated pineal or habenular calcifications were chosen as indicators of relative shift in brain structures. Localization of calcifications was determined in the brow up pneumogram by means of two landmarks appearing as bony irregularities in the regions of the dorsum sellae and planum sphenoidale. From these two points (the endpoints of line C in Fig. 1) lines were erected to form a triangle with the point of calcification (represented by F in Fig. 1). The same triangle was then constructed in the subsequent conventional film taken in the supine horizontal position and revealing a large amount of extracerebral air. (For comparison films were used in which the endpoints of line C coincided with an error of 0.10 mm or less.) By measuring lines D and E (see Fig. 1) localization of the calcified points could be compared and the distances between them measured. The direction and the extent of shifts are indicated by arrows the real extent of which was multiplied by 30 to produce better clarity. The several calcified points which actually differ in their localization in different skulls were indicated as the single point F. The thickness of the amount of extracerebral air was measured as the maximal distance from the inner wall of the skull to the cortex.

From the total material of 1800 operated patients 14 cases were selected for analysis. The small sample resulted from the fact that comparable films showing both calcifications and a significant amount of extracerebral air were infrequently found. For control purposes 4 cases without extracerebral air were selected and the localization of calcifications in different head positions was determined in the manner described above.

It was expected that positional changes of brain structures in patients with a large amount of extracerebral air might be reflected in the clinical effects of coagulations in the pallidum. Since a somatotopic representation

POSITIONAL CHANGES OF INTRACRANIAL STRUCTURES AFTER ENCEPHALOGRAPHY AND DURING STEREOTAXIC OPERATIONS

by

G DIECKMANN, K SCHMIDT and J PRAGER

In stereotaxic brain operations at the Freiburger Neurochirurgische Universitätsklinik it is customary to perform the encephalography required for target point determination prior to the operation itself. In 1 800 operations performed between 1952 and 1962, it was found that in 13 % of the cases some extracerebral air had collected before the skull was opened. This air, resulting from encephalography prior to the stereotaxic procedure, later gathered in the rostral subarachnoid space. Pneumograms to determine target points were obtained while the patient was in a sitting position. During the stereotaxic operation the target point was transposed to the conventional skull films taken while the patient was in a supine position according to the localization method of HASSLER & REICHERT (1954) and after the technique of REICHERT & MUNDINGER (1955). Two major questions arose.

1. The first concerned the possibility of positional changes of intracranial structures due to gravitational influence, when an extracerebral intracranial amount of air exists. In cases where sharply delineated pineal or habenular

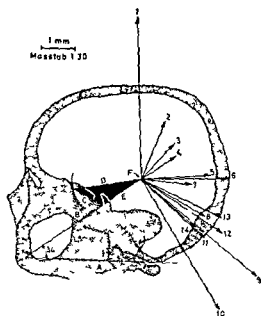


Fig 1 Direction and extent of positional change of pineal or habenular calcifications (F) associated with extracerebral air after encephalography. Arrows indicate the direction of shift according to the localization of the extracerebral air: 2—4 fronto-basal; 6—7 frontal; and 8—14 high frontal air. Cases 1 and 5 did not shift according to expectation. Triangle CDE was required to determine different positions of F in the compared films.

8, 9, 10, 11, 12, 13 and 14 in two anomalous cases shifts did not occur in the expected manner but rather in the direction indicated by arrows 1 and 5.

It is evident that the direction of shift in these examples generally corresponds with the localization of extracerebral air, signifying that the calcifications and thus the brain is shifted primarily in the direction of gravity.

Four control cases without extracerebral air gave no indication of shift in calcifications.

In the total number of pallidotomies for Parkinsonism 19 cases were noted in which no extracerebral air was seen during encephalography. However, skull films obtained 3 or 4 days later prior to the operation or after the opening of the dura revealed the presence of a significant amount of extracerebral air. It was expected that especially in the transitional zone between arm and leg representation which is always entirely penetrated during operation, shifts of the target area would be expressed in combined coagulation effects for arm and leg. The clinical effects which indicate the pallidum coagulation are evidenced by an improvement of rigidity and to a lesser degree in tremor.

Fig 2 shows a gross outline of the pallidum. Above is the foramen of Monro with the base line. The line labeled V indicates the direction of positional changes of intracranial calcifications. The distance from the origin of line V to the upper angle of the black triangle is the average extent of shifts. The line

of the areas for face and upper and lower extremities exists in the pallidum which follow the order of penetration by the coagulating electrode (HASSLER & RIECHERT 1958, MUNDINGER & POTTHOFF 1960). In the total operative material we observed 627 cases of pallidotomies. Of these cases, 19 had a significant accumulation of extracerebral air, and 50 pallidotomies without air furnished comparative controls. For determination of the pallidum internum we constructed a transparent model for superimposition on the film as a lateral projection view, as described by MUNDINGER & POTTHOFF (1960).

In cases with extracerebral air the direction of gravity and thus the direction of expected shifting was determined by a perpendicular line to the base of the air pockets, the mean direction of which was indicated by line V in Fig. 2 and shows the mean direction of shift. The base line was transposed from pneumograms to conventional skull films with the coagulating electrode in situ, by means of the bony reference points. By constructing a perpendicular line from the tip of the electrode to the base line, and noting the distance from the intersection of the perpendicular with the base line to the interventricular foramen, the position of the tip of the electrode could be determined in each case. The angle between the base line and the coagulating electrode was used for the construction of line W, which indicates the direction of electrode penetration. According to the operation protocols the position of performed coagulations was marked on line W. The clinically observed coagulation effect was then compared with the actual site of the coagulating electrode, and the clinical effect was marked in the schematic pallidum by means of symbols. Because the coagulating electrode was introduced into the brain at an angle to the midsagittal plane, thereby causing the zone of penetration to appear foreshortened in the lateral sagittal view, it was necessary to correct for foreshortening by determining the cosine of the incident angle.

Results

Fig. 1 indicates the direction and extent of shifts in the position of pineal or habenular calcifications in 14 cases with an extracerebral amount of air, calculated from films taken both in the sitting and the supine positions. Each arrow shows the relative extent and direction of shift in mm per case. The average shift of calcifications for all 14 cases was 2.48 ± 1.08 mm. The average maximum diameter of air pockets was 7.1 ± 2.15 mm.

Relative to the direction of shift, the following is shown in Fig. 1. Shifts resulting from air collection in the frontobasal extracerebral area are indicated by arrows 2, 3 and 4, frontal extracerebral air caused shifts in the direction of arrows 6 and 7, high frontal air accumulation corresponds to arrows

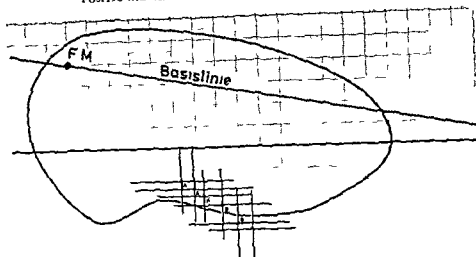


Fig 3 Shift of target area indicated in segregated arm (A) leg (B) and combined (K) coagulation effects in pallidotomy. Rostral crosses of each letter denote target area in control cases caudal crosses of each letter target area in cases with extracerebral air

than in control cases. This follows from the necessity in all operations to begin coagulations at the calculated target area and proceed normally, though in reality (and unknown to the operator) the shifted target region is at a distance of a few millimeters beyond the normally predetermined target point. Nevertheless, the range of penetration in the control cases was 7.3 mm, and in the others only 8.3 mm. Such a small difference is explainable by the fact that in cases where the target area had shifted the entire arm and leg region was not actually penetrated in its total range, in order to avoid possible extension beyond the pallidum.

Fig 3 contains drawn means and standard deviations of the above mentioned combined coagulation effects (arm and leg) labeled K, and separate arm and leg effects labeled A and B respectively. The mean coagulation effects for cases with air are always lying more caudally according to gravitational influence. Crosses A rostral and caudal are situated relatively close together. The distance between crosses B rostral and caudal representing leg effects is greater than for crosses A representing arm effects, but is still not as large as for combined effects K. This is not surprising because the total range of arm and leg representation was not penetrated. However, the distance between leg effects B rostral and caudal could be expected to be even greater, if the range of electrode penetration were not restricted in practice by the possibility of extending beyond the pallidum in cases with air. While the interval between

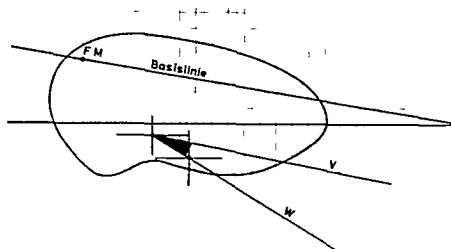


Fig. 2. Shifting of target point in pallidotomies with frontal extracerebral air according to the maximal coagulation effect. Rostral cross indicates mean and standard deviation of coagulation effect in control cases without extra-cerebral air. Caudal cross the same in cases with frontal air. Line V notes the direction of gravitational influence, line W the direction of penetrating coagulating electrode. The black triangle is used to indicate the extent of expected shifting.

labeled W is an empirical representation of the direction of electrode penetration during operation. The perpendicular line from line V to line W defines the theoretical expectation of shift of the target point based on the measured average shifts of the calcifications mentioned before. The intersection of caudal crossed lines on line W shows the area of maximal obtained coagulation effect, an average calculated from the point of maximal effect in each of the 19 cases with air. The length of the crossed lines from the intersection depicts the standard deviation around the mean in this illustration for only the vertical and horizontal sagittal dimensions. The intersection of the rostral crossed lines depicts the average point of maximal coagulation effect in 50 control cases without air. Length of vertical and horizontal lines denotes the standard deviation of measurements as above.

The difference of 2.7 mm between point of maximal effect for control cases shown rostrally, and the analogous point for cases with air shown caudally, is statistically significant at the 0.01 level, both for the ordinates and abscissas of the crossed lines (ordinates $p < 0.0005$, abscissas $p \approx 0.0025$). This suggests that the shift of the target area in patients with air is a real one. The recorded shift in target area for cases with air is close to the theoretically expected target shift, estimated on the basis of positional changes of the calcifications.

According to the positional change of the target for cases with air it would be expected that the range of electrode penetration would be greater

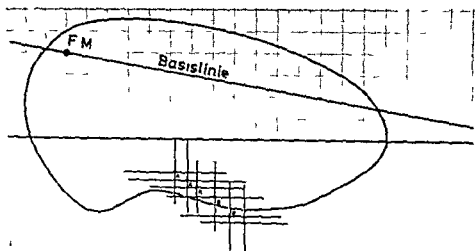


Fig. 3 Shifting of target area indicated in segregated arm (A) leg (B) and combined (K) coagulation effects in palidotomies. Rostral crosses of each letter denote target area in control cases caudal crosses of each letter target area in cases with extracerebral air

than in control cases. This follows from the necessity in all operations to begin coagulations at the calculated target area and proceed normally, though in reality (and unknown to the operator) the shifted target region is at a distance of a few millimeters beyond the normally predetermined target point. Nevertheless, the range of penetration in the control cases was 7.3 mm, and in the others only 8.3 mm. Such a small difference is explainable by the fact that in cases where the target area had shifted the entire arm and leg region was not actually penetrated in its total range in order to avoid possible extension beyond the pallidum.

Fig. 3 contains drawn means and standard deviations of the above mentioned combined coagulation effects (arm and leg) labeled K, and separate arm and leg effects labeled A and B respectively. The mean coagulation effects for cases with air are always lying more caudally according to gravitational influence. Crosses A rostral and caudal are situated relatively close together. The distance between crosses B rostral and caudal representing leg effects is greater than for crosses A representing arm effects but is still not as large as for combined effects K. This is not surprising because the total range of arm and leg representation was not penetrated. However, the distance between leg effects B rostral and caudal could be expected to be even greater if the range of electrode penetration were not restricted in practice by the possibility of extending beyond the pallidum in cases with air. While the interval between

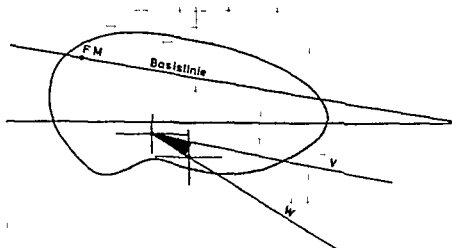


Fig. 2. Shifting of target point in pallidotomies with frontal extracerebral air according to the maximal coagulation effect. Rostral cross indicates mean and standard deviation of coagulation effect in control cases without extracerebral air. Caudal cross the same in cases with frontal air. Line V notes the direction of gravitational influence, line W the direction of penetrating coagulating electrode. The black triangle is used to indicate the extent of expected shifting.

labeled W is an empirical representation of the direction of electrode penetration during operation. The perpendicular line from line V to line W defines the theoretical expectation of shift of the target point based on the measured average shifts of the calcifications mentioned before. The intersection of caudal crossed lines on line W shows the area of maximal obtained coagulation effect, an average calculated from the point of maximal effect in each of the 19 cases with air. The length of the crossed lines from the intersection depicts the standard deviation around the mean in this illustration for only the vertical and horizontal sagittal dimensions. The intersection of the rostral crossed lines depicts the average point of maximal coagulation effect in 50 control cases without air. Length of vertical and horizontal lines denotes the standard deviation of measurements as above.

The difference of 2.7 mm between point of maximal effect for control cases shown rostrally, and the analogous point for cases with air shown caudally, is statistically significant at the 0.01 level, both for the ordinates and abscissas of the crossed lines (ordinates $p \approx 0.0005$, abscissas $p \approx 0.0025$). This suggests that the shift of the target area in patients with air is a real one. The recorded shift in target area for cases with air is close to the theoretically expected target shift, estimated on the basis of positional changes of the calcifications.

According to the positional change of the target for cases with air it would be expected that the range of electrode penetration would be greater



Fig. 5 Positional change of target point in a case of thalamotomy. The target area was anticipated at the exit of the string electrode (\rightarrow) but was actually situated in the region of the tip of the string electrode (\rightarrow).

The decrease of the coagulating effect according to the penetration of the electrode in ventro-caudal direction in the control cases and the increase of the combined coagulating effects in the 19 patients with air according to the shift of the target point in direction of gravity is quite clear. The action of gravity and the resulting shift of the target point is also evident though not so regular for leg effects. We can notice a decrease according to the penetration of the electrode in control cases without air and an increase in cases with air. Such correlations are not so obvious in cases of coagulation in the area of arm representation. Since the zone of arm and leg representation were not penetrated in their entire length it is understandable that in these circumstances the effects would be more ambivalent.

The practical consequences of these investigations are demonstrated in Fig. 5 which depicts a case of thalamotomy with a large amount of frontal air. The calculated target point was anticipated at the exit of the string electrode. Due to the shift of the target point in the direction of gravity it was in fact localized significantly more caudally. Only by penetrating with the string electrode in the direction of gravity was it possible to obtain a good coagulation effect.

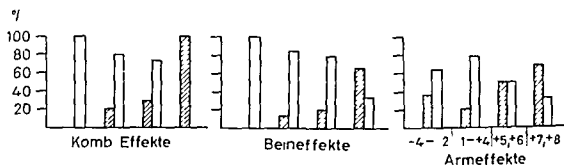


Fig. 4. Histogram showing the decrease of coagulation effect in control cases without air (white columns) and the increase of coagulation effect in cases with air (hatched columns) according to the position of coagulating electrode. Numbers on the abscissa indicate the position of the coagulating electrode with regard to the calculated target point. Negative numbers mean positions rostral from the target point, positive numbers mean ventro caudal positions from the target point.

specific effects for control cases and cases with air is not so impressive as for combined effects, the general trend of target point shift in the direction of gravity is clear, and congruent with theoretical expectation. It would also appear that the leg effects as well as combined effects are situated outside of the schematic pallidum. Moreover, the distribution of effects in this figure based on the most impressive clinical observations during operations seems to correspond to the localization and extent of the ansa lenticularis, from which maximal coagulating effects can be obtained as is well known.

Isolated and combined effects are further elaborated in the histograms of Fig. 4. On the abscissa is shown the distance in mm from the tip of the coagulating electrode to the calculated target point in the zone of penetration. Numbers with negative signs signify withdrawal of the electrode from the target point in a dorso rostral direction. Numbers with positive signs signify extension of the electrode beyond the target point in a ventro caudal direction. The distances are divided into four groups. White columns represent the control cases, and the hatched columns patients with extracerebral air. The total number of operated patients in which coagulations were performed according to the area marked on the abscissa is taken as 100%. The ordinates represent the percentage of cases per group with air or without air in which effects were observed in arm, leg, or combined categories.

Regarding the category of combined effects, in the range of -4 to -2 we observe only cases without extracerebral air. From the range of -1 to $+4$ we begin to see an occurrence of patients with air, but control cases are still more prevalent. More patients with air cases appear in the third group $+5$ to $+6$, while for the extremely ventro caudally situated coagulations only cases with extracerebral air are observed.

ZUSAMMENFASSUNG

Intracranielle extracerebrale Luftansammlungen von mehr als 4 mm Dicke bedingen eine Verschiebung einer verkalkten Glandula pinealis oder Commissura habenularum wie Verschiebungen zwischen im Sitzen angefertigten Encephalogrammen und später im Liegen aufgenommenen Leerbildern zeigen. Die Verschiebung beträgt bei einer Luftschichtstärke von 4 ± 2.15 mm im Mittel 2.48 ± 1.08 mm. Pallidotomie Effekte bei Patienten mit und ohne frontalen Luftkappen sprechen für eine Verschiebung stereotaktischer Zielgebiete um etwa 7 mm in Richtung der Schwerkraft bei Fällen mit extracerebraler Luftansammlung.

RESUMÉ

La présence d'air dans le crâne en dehors du cerveau en une couche de plus de 4 mm d'épaisseur cause un déplacement des calcifications pinéale ou habénulaires dans le sens de la pesanteur apprécié par comparaison de radiographies simples prises en décubitus et de pneumographies en position assise. Les calcifications se déplacent de 2.48 ± 1.08 mm quand l'air extracérébral est épais de 7.4 ± 2.15 mm. Les auteurs ont comparé les effets des coagulations chez des malades avec et sans air extracérébral. Les régions-cibles donnant les effets chimiques associés du membre supérieur et du membre inférieur ont été déplacées dans le sens de la pesanteur d'environ 2.7 mm dans les cas avec air.

REFERENCES

- FRORIEP A. Zur Kenntnis der Lagebeziehungen zwischen Grosshirn und Schädeldach bei Menschen verschiedener Kopfform. Zugleich ein Beitrag zur Vergleichung des Schädels mit der Todtenmaske. Veit & Co. Leipzig 1897.
- HÄSSLER R. und RIECHERT T. Indikationen und Lokalisationsmethode der gezielten Hirnoperationen. Nervenarzt 25 (1954) 441.
- — Über die Symptomatik und operative Behandlung der extrapyramidalen Bewegungsstörungen. Med. Klin. 53 (1958) 817.
- MUNDINGER R. und POTTIOFF P. Encephalographische und klinische Untersuchungen zur funktionellen Somatopik des Pallidum internum bei stereotaktischen Pallidotomien. Arch. Psychiat. Nervenkr. 201 (1960) 151.
- RIECHERT T. und MUNDINGER F. Beschreibung und Anwendung eines Zielgerätes für stereotaktische Hirnoperationen (II. Modell). Acta neurochir. (Wien) Suppl. III (1955) 308.
- VAN BUREN J. M. and MACCUBBIN D. A. An outline atlas of the human basal ganglia with estimation of anatomical variants. J. Neurosurg. 19 (1962) 811.

Discussion

FRORIER (1897) has demonstrated the possibility of brain shifting in the post mortem state due to loss of cerebrospinal fluid. Similar shifts were expected with evacuation of the subarachnoid fluid in stereotaxic operations after opening the dura mater, especially in cases with cortical atrophy of marked degree. In these circumstances we observed a change in the relation of intracerebral points to bony reference points. The significance for stereotaxic operations with previous pneumography seems to be evident. Nevertheless, during encephalography with replacement of the subarachnoid fluid by air, VAN BUREN & MACCUBBIN (1962) did not find a significant positional change of intracerebral landmarks as in the 14 cases described above. They noted an average shift of 0.7 mm with gravity and of 0.5 mm against gravity unrelated to the thickness of extracerebral air. An explanation of this discrepancy in results appears difficult. The possibility of errors in measurements and technique as described by VAN BUREN & MACCUBBIN we believe were avoided by us. The important question of the influence of head rotation along the vertical axis investigated by these authors in a model experiment perhaps is not of significance here, because our intracerebral landmarks lie so near the region of the vertical rotation axis of the head. On the other hand, the bony reference points used in our study are nearer this vertical axis than the glabella used by VAN BUREN & MACCUBBIN in their pneumographic studies. Perhaps it is a question of different filling techniques in encephalography, although our cases did not show a subdural filling. However, we can note a correspondence between the results of pneumographic studies as shown in Fig. 1 and the findings during stereotaxic operations in cases with subdural air.

The problems mentioned above should be considered only in a descriptive and statistical manner. Anatomical points of view concerning the numerous possibilities of variation with which the stereotaxic operator is often confronted remain deliberately unmentioned. The question of the somatotopic differentiation of the pallidum not yet acknowledged by all authors, is not discussed here, but it would seem that such a differentiation is confirmed by the above investigation.

SUMMARY

Intracranial extracerebral air more than 4 mm wide is associated with shifts of the pineal or habenular calcifications in the direction of gravity when supine conventional roentgenograms are compared to upright pneumograms. Calcifications shifted 2.48 ± 1.08 mm with a thickness of extracerebral air of 7.4 ± 2.15 mm. Coagulation effects in patients with and without extracerebral air were compared. Target areas for clinically observed combined arm and leg effects shifted approximately 2.7 mm in the direction of gravity for cases with air.

Table

Analysis of the radiological changes observed during encephalography

Case No	Cavum septi pellucidum	Brain atrophy			
		Ventricular enlargement	Cortical atrophy	Cerebellar atrophy	Dilatation of cistern of lamina terminalis
1	x	x		x	
2		x	x		
3	x	x			
4					
5	x	x		x	
6	x		x		
7	x	x			
8					
9		x			
10					
11					
12		x			
13				x	
14	x	x			
15	x	x			x
16					

Cavum septi pellucidum Changes in the septum pellucidum are of particular interest (Fig. 1). The septum is a thin triangular shaped membranous partition separating the lateral ventricles and consisting of two laminae. It is attached above to the corpus callosum below to the anterior part of the fornix posteriorly and the reflected portion of the corpus callosum anteriorly.

Various abnormalities of the septum have been described in anatomical and autopsy studies. Perforation of the septum is well recognised and DAWDY (1931) considered many such perforations to be acquired. Three types of cavum septi pellucidum have been recorded (VAN WEGENEN & AIRD 1943) the non communicating type the communicating type with openings into the lateral or third ventricles and the type associated with internal hydrocephalus.

In this series of cases in order to demonstrate the integrity of the septum pellucidum or the walls of a cavum septi pellucidum an antero posterior film using a horizontal beam with the patient lying on his side was taken. Antero posterior tomography was also carried out in some of the patients. The antero posterior horizontal view will in normal circumstances demonstrate some air trapped in the lowermost ventricle whereas in a perforated septum air will

PNEUMOENCEPHALOGRAPHIC CHANGES IN BOXERS

by

IAN ISHERWOOD, C MAWDSLEY and F R FERGUSON

In recent years interest has been directed towards neurological disease in boxers. Associated encephalographic changes were first observed by SPILLANE (1962) in a study of five boxers, four of whom had abnormal encephalograms. We have had the opportunity to carry out encephalographic studies in a further sixteen ex boxers, all of whom had evidence of neurological disease. The clinical features of some of these patients have been the subject of discussion in a previous communication by MAWDSLEY & FERGUSON (1963).

The main purpose of this paper is to classify the radiological changes which have been observed in association with this type of traumatic encephalopathy and to assess their significance and diagnostic value.

Results

Of the sixteen patients in the present study, three had normal encephalograms whilst the remaining thirteen had a variety of abnormalities (see Table). The abnormal findings were (1) crura septi pellucidi in 9 cases (2) evidence of brain atrophy (generalised ventricular enlargement in 11 cases, cerebral cortical atrophy in 3 cases, cerebellar atrophy in 1 case) (3) enlargement of the cistern of the lamina terminalis in 4 cases.

Table

Analysis of the radiological changes observed during encephalography

Case No	Cavum septi pellucidi	Brain atrophy			
		Ventricular enlargement	Cortical atrophy	Cerebellar atrophy	Dilatation of cistern of lamina terminalis
1	x	x		^	
2		x	x		
3	x				
4					
5		x		x	
6	x		x		
7		x			
8					
9		/			
10		x			
11					
12				/	
13				x	x
14		x			
15		x			
16		x			

Cavum septi pellucidi Changes in the septum pellucidum are of particular interest (Fig. 1). The septum is a thin triangular shaped membranous partition separating the lateral ventricles and consisting of two laminae. It is attached above to the corpus callosum below to the anterior part of the fornix posteriorly and the reflected portion of the corpus callosum anteriorly.

Various abnormalities of the septum have been described in anatomical and autopsy studies. Perforation of the septum is well recognised and DANDY (1931) considered many such perforations to be acquired. Three types of cavum septi pellucidi have been recorded (VAN WEGENEN & AIRD 1943) the non communicating type the communicating type with openings into the lateral or third ventricles and the type associated with internal hydrocephalus.

In this series of cases in order to demonstrate the integrity of the septum pellucidum or the walls of a cavum septi pellucidi an antero posterior film using a horizontal beam with the patient lying on his side was taken. Antero posterior tomography was also carried out in some of the patients. The antero posterior horizontal view will in normal circumstances demonstrate some air trapped in the lowermost ventricle whereas in a perforated septum air will

PNEUMOENCEPHALOGRAPHIC CHANGES IN BOXERS

by

IAN ISHERWOOD, C MAWDSLEY and F R FERGUSON

In recent years interest has been directed towards neurological disease in boxers. Associated encephalographic changes were first observed by SPILLANI (1962) in a study of five boxers, four of whom had abnormal encephalograms. We have had the opportunity to carry out encephalographic studies in a further sixteen ex boxers, all of whom had evidence of neurological disease. The clinical features of some of these patients have been the subject of discussion in a previous communication by MAWDSLEY & FERGUSON (1963).

The main purpose of this paper is to classify the radiological changes which have been observed in association with this type of traumatic encephalopathy and to assess their significance and diagnostic value.

Results

Of the sixteen patients in the present study, three had normal encephalograms, whilst the remaining thirteen had a variety of abnormalities (see Table). The abnormal findings were (1) *cavum septi pellucidum* in 9 cases, (2) evidence of brain atrophy (generalised ventricular enlargement in 11 cases, cerebral cortical atrophy in 3 cases, cerebellar atrophy in 1 case) (3) enlargement of the cistern of the *lamina terminalis* in 4 cases.



Fig 4 Oblique view of autopsy specimen demonstrating multiple perforations in walls of cavum septi pellucidum

In the present series of sixteen cases nine patients had evidence of a communicating cavum septi pellucidum; an incidence of 56%. If the cases described by SPILLANE (1962) are considered the recorded incidence of abnormal communication between the lateral ventricles with or without a cavum in boxers is 13 out of 21 patients i.e., 62%.

The natural incidence of a communicating cavum septi pellucidum has never previously been determined accurately, though THIEFFREY *et coll* (1958) suggested 1%. In the last 300 unselected encephalographies carried out in the Manchester Royal Infirmary three cases have been recorded, giving a similar incidence.

Tomography demonstrated the walls of the cavum to be intact anteriorly but to have multiple perforations behind the foramina of Monro increasing in number posteriorly (Fig 3). These observations have been confirmed by an autopsy study of the brain of an ex boxer where it was noted that the fenestrations increased posteriorly to a point where only a few residual strands of the lamellae remained (Fig 4). A free communication between the posterior ends of the lateral ventricles was thus allowed.

It is of interest that in the three cases of cavum septi pellucidum observed incidentally none of whom were ex boxers two showed evidence of communication with one lateral ventricle only and in the third patient the cavum septi pellucidum communicated with a well developed cavum vergae. These variations have not been recorded in any of the boxers in the series.



Fig 1 A p film The cavum septi pellucidi is visible ventricular enlargement



Fig 2 A p film right lateral decubitus position All air has risen to upper ventricle due to septal perforation

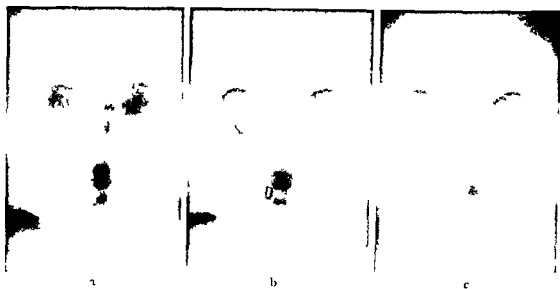


Fig 3 Tomography a) Walls of cavum septi pellucidi intact anteriorly b) and c) Multiple perforations in walls of cavum septi pellucidi from foramina of Monro posteriorly

rise to the upper ventricle (Fig 2). Some air may of course spill through the foramina of Monro but in a series of over 300 unselected encephalograms where this procedure was employed, this only occurred in 4 cases all of whom had large ventricles. Where linear tomography during encephalography was carried out it was found essential to employ transverse movement of the tube in relation to the patient's head in order to avoid linear blur of the septal structures under investigation.



Fig 8 Tomography in mid sagittal plane. Dilatation of cistern of lamina terminalis, cistern of septum pellucidum visible

recorded from 20 % by SCHWIDDE (1952) to 60 % by SCHUKA (1963) where the average separation of the leaves has been 3 mm

It is suggested that dilatation of the cistern and perforation of its walls precedes the occasional disappearance of the septum as observed in one patient described by SPILLANE (1962) and that this disappearance occurs first posteriorly (Fig 5). None of the boxers without a communicating cistern, however, showed any radiological evidence of widening of the septum.

Evidence of brain atrophy. Generalised ventricular enlargement. In ten of the patients ventricular enlargement was observed. This was recorded initially as a subjective impression. A further review employing a variety of generally accepted methods of measurement (ENGESER 1964) to assess ventricular size has confirmed these findings.

Cerebral cortical atrophy. In three patients the cerebral sulci were widened.

Cerebellar atrophy. In four patients the subarachnoid space around the cerebellum was markedly increased in size (Fig 6).

The radiological changes indicating brain atrophy, i.e. ventricular enlargement, cortical and cerebellar atrophy, have been observed after head injury (FRIEDMAN 1932; JACKSON & FLEMINGER 1946; TROLAND et al. 1946).

Direct brain damage due to mechanical acceleration and rotation strains together with localised petechial haemorrhages gives rise to glial replacement



Fig 5 P a film Complete disappearance of septum posteriorly



Fig 6 Dilatation of subarachnoid space around cerebellum in an ex boxer



a



b

Fig 7 Dilatation of cistern of lamina terminalis a) Patient erect Fluid level evident b) Brow up

There seems no doubt therefore, that the changes observed in the septum pellucidum in boxers are a significant feature and the role of trauma in their production must be considered proven. The changes may be produced by a sudden elevation in ventricular pressure with rupture of the floor or walls of the potential *cavum septi pellucidum*. Later pressure rises might cause dilatation of the *cavum* and perforation of its walls.

A potential space between the leaves of the septum pellucidum is normally present and the incidence of a non communicating *cavum* has been variously

REFERENCES

- DANDY W. Congenital cerebral cysts of cavum septi pellucidi (fifth ventricle) & cavum vergae (sixth ventricle) Diagnosis and treatment Arch Neurol Psychiat (Chicago) 25 (1931) 44
- ENGSEST A and SKRAASTAD E. Methods of measurement in encephalography Neurology 14 (1964) 381
- FRIEDMAN E D. Head injuries effects and their appraisal encephalographic observations Arch Neurol Psychiat (Chicago) 27 (1932) 791
- JACKSON H and FLEMINGER J J. Discussion on cortical atrophy Proc roy Soc Med 39 (1946) 423
- MAWDSLEY C and FERGUSON F R. Neurological disease in boxers Lancet (1963) 795
- SCHLACK H. Congenital dilatations of the septum pellucidum Radiology 81 (1963) 610
- SCHWIDDE J T. Incidence of cavum septum pellucidum & cavum vergae in 1032 human brains Arch Neurol Psychiat (Chicago) 67 (1952) 625
- SPILLANE J D. 5 boxers Brit med J ii (1962) 1705
- THIEFFREY S, LEFEBRE J, LEPINTRE J, FAURE C et MASSELIN S. Contribution à l'étude radiologique des malformations du plan sagittal interhémisphérique à propos de 45 observations Acta radiol Stockholm 50 (1958) 242
- TROLAND C E, BAXTER D H and SCHATZKI R. Observations on encephalographic findings in cerebral trauma J Neurosurg 3 (1946) 390
- VAN WEGENEN W P and AIRD R B. Dilatation of cavity of septum pellucidum & cavum vergae report of cases Amer J Cancer 70 (1934) 539

Such changes may result in local atrophy. It is suggested that there is a correlation between the degree and distribution of atrophy demonstrated radiologically and the severity and type of neurological affection evinced clinically.

Enlargement of the cistern of the lamina terminalis. In four of the patients an unusual dilatation of the cistern of the lamina terminalis was observed (Fig. 7), a phenomenon not previously recorded. Three of the patients exhibiting this dilatation also had a cavum septi pellucidi. Tomography in the mid sagittal plane demonstrated the dilated cistern clearly, together with its relationship to the cavum septi pellucidi (Fig. 8). The mechanism of production of this dilatation is uncertain, but the repetitive transient elevation of intracranial pressure brought about by traumatic deformation of the skull may be responsible. It is possible that this mechanism may also result in a rupture of the floor or walls of the cavum septi pellucidi.

Conclusions

In the investigation of neurological disorder in boxers, the demonstration of a communicating cavum septi pellucidi, particularly in association with ventricular enlargement, cortical or cerebellar atrophy, or enlargement of the cistern of the lamina terminalis, is very strong evidence in favour of a traumatic origin of the disease.

SUMMARY

The radiologic changes observed in 16 ex boxers have been described with particular reference to tomography and encephalography and their significance and diagnostic value as compared with a normal control group. A possible mechanism for the production of some of these changes is suggested.

ZUSAMMENFASSUNG

Die an 16 Exboxern beobachteten röntgenologischen Veränderungen werden mit besonderer Berücksichtigung von Tomographie und Encephalographie beschrieben. Ihre Bedeutung und ihr diagnostischer Wert wird mit den Befunden einer normalen Kontrollgruppe verglichen. Ein Mechanismus, der für die Entstehung einiger dieser Schäden in Betracht kommt, wird vermutet.

RESUMÉ

Les auteurs décrivent les signes radiologiques observés chez 16 anciens boxeurs en particulier les signes tomographiques et encéphalographiques et examinent leur importance et leur valeur diagnostique en les comparant à un groupe témoin normal. Les auteurs proposent un mécanisme possible de la production de certains de ces signes.

REFERENCES

- DANDY W Congenital cerebral cysts of cavum septi pellucidi (fifth ventricle) & cavum vergae (sixth ventricle) Diagnosis and treatment Arch Neurol Psychiat (Chicago) 25 (1931) 44
- ENGSET A and SKRAASTAD E Methods of measurement in encephalography Neurology 14 (1964) 381
- FRIEDMAN E D Head injuries effects and their appraisal encephalographic observations Arch Neurol Psychiat (Chicago) 27 (1932) 791
- JACKSON H and FLEWINGER J J Discussion on cortical atrophy Proc roy Soc Med 39 (1946) 423
- MAYDSLEY C and FERGLSON F R Neurological disease in boxers Lancet (1963) 793
- SCHLAK H Congenital dilatations of the septum pellucidum Radiology 81 (1963) 610
- SCHLITDE J T Incidence of cavum septum pellucidi & cavum vergae in 1032 human brains Arch Neurol Psychiat (Chicago) 67 (1952) 625
- SPILLANE J D 5 boxers Brit med J ii (1962) 1203
- THIEFFREY S LEFEBRE J LEPINTRE J FAURE C et MASSELIN S Contribution a l'étude radiologique des malformations du plan sagittal interhémisphérique à propos de 45 observations Acta radiol Stockholm 50 (1958) 242
- TROLAND C E BAXTER D H and SCHATZKI R Observations on encephalographic findings in cerebral trauma J Neurosurg 3 (1946) 390
- VAN WEGENEN W P and AIRD R B Dilatation of cavity of septum pellucidum & cavum vergae report of cases Amer J Cancer 20 (1934) 539

A NEW DIAGNOSTIC METHOD BY TRANS-OVAL CISTERNOGRAPHY

by

ABEL P. JIMENEZ, JULIO LYONNET and FERNANDO SILVA

The radiological diagnosis of cerebello pontine angle tumours is usually established by the classic methods: conventional films of the skull, angiography, and encephalography. Sometimes, however, there are problems which make the diagnosis difficult. For these cases we are using a new method with very good results.

Basically, it consists in putting a positive contrast material into the trigeminal cistern, which lies within the *cavum mecklii* and freely communicates posteriorly with the basal cisterns (Fig. 1).

The approach used is the same as that employed by LYONNET & SILVA (1963) for percutaneous trigeminal neurolysis. The patient is placed in the supine position with the head hyperextended, as in Hirtz's position. We draw a line on the skin between the most lateral part of the bony margin of the orbit and the mandibular angle, then we mark the inferior orbital foramen, and the zygomatic tubercle, both easily palpable (Fig. 2). The inferior orbital foramen, the zygomatic tubercle, and the foramen ovale lie in one plane and form a right angled triangle in which the right angle is the foramen ovale. Bearing in mind these landmarks, it is easy to find blindly the foramen ovale.



Fig 1 The posterior fossa viewed from above after incision and separation of the tentorium. Meckel's cavity at arrow.



Fig 2 Anatomical specimen showing the needle track and its landmarks.



Fig 3 Normal cisternogram.



Fig 4 Subarachnoid cyst. Absence of filling of the circumferential cistern in the posterior part.

A NEW DIAGNOSTIC METHOD BY TRANS OVAL CISTERNOGRAPHY

by

ABEL P. JIMENEZ, JULIO LYONNET and FERNANDO SILVA

The radiological diagnosis of cerebello pontine angle tumours is usually established by the classic methods: conventional films of the skull, angiography, and encephalography. Sometimes, however, there are problems which make the diagnosis difficult. For these cases we are using a new method with very good results.

Basically, it consists in putting a positive contrast material into the trigeminal cistern, which lies within the cranium mecklii and freely communicates posteriorly with the basal cisterns (Fig. 1).

The approach used is the same as that employed by LYONNET & SILVA (1963) for percutaneous trigeminal neurolysis. The patient is placed in the supine position with the head hyperextended, as in Hirtz's position. We draw a line on the skin between the most lateral part of the bony margin of the orbit and the mandibular angle, then we mark the infraorbital foramen, and the zygomatic tubercle, both easily palpable (Fig. 2). The infraorbital foramen, the zygomatic tubercle, and the foramen ovale lie in one plane and form a right angled triangle, in which the right angle is the foramen ovale. Bearing in mind these landmarks, it is easy to find blindly the foramen ovale.



Fig 1 The posterior fossa viewed from above after incision and separation of the tentorium. Meckel's cavity at arrow



Fig 2 Anatomical specimen showing the needle track and its landmarks



Fig 3 Normal cisternography



Fig 4 Subarachnoid cyst. Absence of filling of the cisterna magna posteriorly (arrow)



Fig. 5 Glioma of the pons in a child. As in fig. 4 stop in the circumponuncular cistern: the contrast medium does not go down to the cistern of the vein of Galen.

With an approximately 15 cm long spinal puncture needle, we pierce the skin of the cheek, immediately below the malar bone and immediately inside the mandibular ramus. The needle is placed perpendicular to the drawn line. Viewed laterally, the needle points toward the zygomatic tubercle, and looking frontally it points toward the infraorbital foramen. The end of the needle thus reaches the foramen ovale. When passing through it we feel the same sensation as when we pierce the dura mater in a lumbar puncture. At this stage, we advance the needle one centimeter and we then pass into the trigeminal cistern. We can prove this in two ways: first, when withdrawing the stylet a few drops of cerebrospinal fluid will emerge, second, by taking an antero-posterior roentgenogram of the skull with the beam parallel to the orbito-malar line the tip of the needle will be at the level of the petrous ridge. Having these proofs (and with possible errors corrected), we inject 1.5 or 2 ml of an iodized oil. The medium being heavier than the CSF, it will go through the only possible way, on account of the position of the patient's head, and the substance will fall into the adjoining basal cisterns. Before the needle is removed we inject corticosteroids through it, as in myelography when we use the same contrast medium. Then we obtain the roentgenograms. The first, submento-vertex, is the main one (Fig. 3). It shows a complete image of the cisterns, as seen in Fig. 1. We also take a lateral and a half-vertex view. Any possible space-occupying lesion within the cisterns or their vicinity, of sufficient size, will alter the anatomical sketch and thus alteration is clearly shown at the cisternography.



Fig 6 N u noma of the trigeminal Tumor completely surrounded by the positive contrast

The early roentgen sign of abnormality is absence of filling of the circumponuncular cistern (Figs 4 and 5). The contrast medium does not pass down to the vein of Galen cistern as it normally does. When the tumor lies on the wider part of the cisterns, it is sharply outlined showing a lacunar image completely surrounded by the positive contrast. In this case the tumor is well delineated and localized (Fig 6).

The technique is much easier than it seems from the description. We have experienced no significant complications. There is the possibility of arachnoid irritation as a reaction to the iodized oil. Future improvement of the contrast media will lessen this risk. Trans-oval cisternography does not alter the tensional equilibrium between the endocranial and spinal fluid and can be used without hazard with high intracranial pressure. We have tried to change the positive contrast for air but we have not been able to obtain satisfactory results.

We see other possibilities for this new method such as implantation of radioactive substances for diagnostic and therapeutic purposes.

SUMMARY

We present a new diagnostic method especially useful for cerebello-pontine angle tumours. The technical aspects of the procedure are described and normal and pathological cases are shown.

ZUSAMMENFASSUNG

Eine neue diagnostische Methode wird beschrieben, die besonders für die Diagnose von Brückenwinkeltumoren von Nutzen ist. Normale und pathologische Fälle werden gezeigt.

RÉSUMÉ

Présentation d'une nouvelle méthode diagnostique particulièrement utile pour les tumeurs de l'angle ponto-cérébelleux. Description de la technique et présentation de cas normaux et pathologiques.

REFERENCES

- LYONNET J. e SILVA F. Neuralgia del trigémino. Editorial Braga. Buenos Aires 1963.
PENMAN J. A simple radiological aid to gasserian injection. *Lancet* 245 (1949) 268.
— Some developments in the technique of trigeminal injection. *Lancet* 264 (1953) 760.
PUTNAM T. J. and HAMPTON A. O. A technique of injection into the gasserian ganglion under roentgenographic control. *Arch. Neurol. Psychiat.* 35 (1936) 92.

ENCEPHALOGRAPHY IN THE DIAGNOSIS OF CEREBELLAR ATROPHY

by

MARJORIE LEMAY and ARTUR ABRAMOWICZ

Most of the published articles describing the encephalographic findings in atrophic lesions of the cerebellum have been case reports of patients with the diagnosis established clinically or pathologically (EPSTEIN & DAVIDOFF 1946 ELLERMAN 1943 MURPHY & ARANA 1947 UZMAN 1948). The cerebellar folia are usually not well demonstrated in routine air studies and the radiologic diagnosis of atrophy often has been made upon indirect evidence derived from demonstration of a large cisterna magna or fourth ventricle. This is analogous to the indirect evidence frequently used in the radiologic diagnosis of cerebral atrophy yet it is being recognized that enlargement of the lateral ventricles does not necessarily denote cerebral cortical atrophy and that there is often little correlation between the volume of the ventricular system and clinical symptomatology (HAMMERBERG & FOG 1959 STALLWORTHY & SAVAGE 1955).

The present work was carried out on a series of patients whose cerebellar sulci were well demonstrated at encephalography in order to study the relationship between the radiologic and neurologic diagnosis of atrophy. The size of the fourth ventricle and cisterna magna were measured and contrasted



Fig. 1. Normal cerebellar sulci.

with the width of the cerebellar sulci and the data thus obtained correlated with the clinical symptomatology presented by the patients.

Material and Method. A total of 700 consecutive encephalographic examinations were reviewed. In 72 of these cases the cerebellar sulci were well outlined. Some of the patients were studied by the technique described by TIMBAUT, WACKENHEIM & VROUSOS (1959) in which it is usually possible to demonstrate the cerebellar sulci without using large amounts of air. In none of the cases was an attempt made to drain the spinal fluid completely and replace it with air. In most of the patients 40 to 60 ml of air were injected and slightly less fluid removed.

The 72 cases were divided into three groups: a normal group in which the cerebellar folia were separated from each other by not more, and usually less, than 2 mm wide air spaces (Fig. 1), a group in whom a mild to moderate degree of cerebellar atrophy was judged to be present on the basis of 2 to 4 mm wide air spaces separating the folia (Fig. 2) and a group classified as marked atrophy, with separation of the cerebellar folia by air spaces wider than 4 mm (Fig. 3).

The clinical records of the 72 cases were reviewed independently without reference to the encephalographic findings and a note was made of pertinent clinical history and neurologic symptoms that might be indicative of a cerebellar deficit. Among these patients 35 were found to have such symptoms, 37 did not.



Fig 2 Slightly enlarged sulci. Primary fissure not over 4 mm in width



Fig 3 Cerebellum is small and the sulci measure over 4 mm in width

Results

The relationship found between the size of the cerebellar sulci and clinical findings referable to cerebellar disease is seen in Table 1

Normal cerebellar sulci A total of 33 patients were classified as having normal cerebellar sulci. The average of the group was 40.5 years with a spread of the ages between 22 and 67 years. Eight had symptoms referable to the cerebellum.

Slight to moderate cerebellar cortical atrophy A total of 28 patients, 42.5 years old on the average, with an age spread from 31 to 63 years, were classified as having a mild to moderate degree of cerebellar atrophy. 17 of these patients had definite cerebellar symptoms and signs.

Table 1

Relationship between size of cerebellar sulci and clinical findings in 72 cases

Cerebellar sulci	No. of cases	Av. age	No. of patients with cerebellar symptom
Normal	33	40.55	8 (24%)
Slight to moderately enlarged	28	42.5	17 (61%)
Grossly enlarged	11	54.0	10 (91%)
	72		35 (49%)

Table 2

Relationship of the clinical symptoms with the size of the fourth ventricle cisterna magna and enlarged cerebellar sulci

	No of patients	No of patients with a large cisterna magna	No of patients with a large fourth ventricle	No of patients with large sulci
Cerebellar symptoms	35	9 (25 %)	4 (11 %)	27 (77 %)
No cerebellar symptoms	37	3 (9 %)	1	12 (33 %)

Marked cerebellar cortical atrophy Eleven patients were classified as having severe cerebellar atrophy. The average age of the group was 54.2 years with a spread of ages from 41 to 71 years. Of these cases, 10 showed moderate or severe symptoms indicative of cerebellar dysfunction.

Large fourth ventricle and/or large cisterna magna The correlation between the clinical findings and the variations in size of the cerebellar sulci in patients with enlargement of the fourth ventricle or cisterna magna is evident from Table 2. Of the 35 patients with clinical suspicion of cerebellar dysfunction only 9 had enlargement of the cisterna magna. Of the 37 patients without evidence of cerebellar dysfunction, 3 had enlargement of this structure. Of 35 patients with symptoms of cerebellar disorder only 4 had an enlarged fourth ventricle according to the criterion of SUTTON (1950). Of these 4 patients, 3 also had large cisternae magnae. The one patient with an enlarged fourth ventricle but without cerebellar dysfunction had a small cisterna magna.

Discussion

The close correlation between the clinical and the direct radiologic findings in the group of patients with marked cerebellar atrophy shows the value of attempting to demonstrate the cerebellar sulci. Only three of the patients with grossly enlarged sulci had indirect radiologic evidence suggesting a possible cerebellar defect, i.e. a large fourth ventricle and/or large cisterna magna. If the sulci had not been demonstrated, therefore, a radiologic diagnosis of cerebellar atrophy could not have been made. The one patient in this group without clinical evidence of a cerebellar deficit was a chronic alcoholic with mild dementia and clinical evidence of liver disease.

Among the 72 cases studied, 39 had radiologic evidence of mild, moderate or severe cerebellar atrophy and among these cases with abnormal cerebellar encephalographic findings, 27 (69 %) had clinical evidence of a cerebellar

Table 3

Clinical findings in eight patients with normal sulci and symptoms suggestive of a cerebellar deficit

Ag	Height of IV ventricle	Cisterna magna	Cerebellar findings	Clinical diagnosis
Ac 34	15 mm	small	Ataxic gait Head titubation	
Cr 49	10	small	Unilateral tandem walk or stand on one foot Ataxia	Chronic alcoholism with several episodes of DTs
Do 67	21	large	Tremor Ataxia lower extremities	Ependymoma of L2 with block on myelogram Past history of cerebral hemorrhage requiring burr holes
Ed 33	16	large	Ataxic gait	Chronic alcoholism with cirrhosis Seizures Skull fracture one year ago
Lo 41	18	small	Unsteadiness of gait and posture	Epilepsy At least one episode of barbiturate intoxication
Re 42	16	small	Poor coordination and falling to either side Finger-to-nose and heel-to-knee tests — poor	Temporal lobe epilepsy with several episodes of delirium toxication
Wa 57	16	small	Progressive gait difficulty	Generalized arteriosclerosis and secondary myelopathy
Wr 51	21	small	Nystagmus Mild ataxia	Chronic alcoholism Lentescence of cirrhosis Autopsy — no gross cerebellar atrophy

deficit (Table 1). By contrast among the 33 patients with normal encephalograms only 24% had signs of possible cerebellar dysfunction. Among 37 patients without clinical evidence or suspicion of cerebellar disease, 12 had encephalographic abnormalities. Of these, however, 6 were severe alcoholics and may well have had occult cerebellar atrophy. LICHTENSTEIN & LEVINSKY (1946) have shown that gross cerebellar atrophy may be present in the absence of specific cerebellar clinical symptoms.



Fig. 4. From a patient with hereditary olivopontocerebellar degeneration. The cerebellar sulci are slightly enlarged and the fourth ventricle and cisterna pontis are large.

Of the 33 patients whose sulci appeared normal 8 had symptoms referable to the cerebellum. Table 3 gives the clinical diagnosis in these patients, 6 of them were patients with chronic alcoholism or were epileptics who had received dilantin for many years. One patient, a 67 year old man with hypertensive vascular disease, had a very large cisterna magna and a fourth ventricle measuring 21 mm in height, and it would seem probable that the patient had atrophy which was more marked in the hemispheres than along the midline structures where the sulci are outlined best.

Two of the patients classified as having only slight cortical atrophy were patients with hereditary olivopontocerebellar degeneration. The fourth ventricle was enlarged in both of these patients and the pontine cisterns were enlarged, measuring 12 mm in both. Fig. 4 shows the findings in one of these cases. At necropsy these two patients had gross atrophy of the pons and some generalized cerebellar atrophy, but the atrophy was maximal in the hemispheres and the vermis was grossly only slightly abnormal. Since it often is not possible to differentiate clinically between olivopontocerebellar and chronic cortical degeneration, encephalography may be determinative.

The difference in the average ages of the group with normal cerebellar sulci, 40.5 years, and the group manifesting severe atrophy, 51.5 years, is significant. Only 3 of the 33 patients with normal sulci were over 60 years of age while 5 of the 11 patients with marked cerebellar atrophy were over 60 years of age. All but one of the patients with severe atrophy had enlargement of the lateral and third ventricles. An increase in ventricular size commonly

occurs with aging but it seems unlikely that severe peripheral cortical atrophy can be explained by an age factor alone. This concept is supported by the observation that in the patients with normal studies as opposed to those with slight moderate atrophy there was no significant age differential.

The demonstration of the cerebellar sulci depends more on the position of the head during the introduction of the air at encephalography than on the amount of gas used. UZMAN (1948) attempted total replacement of fluid in five patients with cerebellar symptoms and only in one of them was there adequate filling of the sulci to demonstrate the folia. Recent superb studies by THIÉBAUT, WACKENHEIM & VROUSOS (1959) have outlined the most reliable maneuvers to be followed for filling the sulci. The same authors, as well as EPSTEIN & DAVIDOFF (1946), DI CHIRO (1964) and BASSANI & AMICI (1960) have stressed the value of tomography during encephalography. The cerebellar sulci demonstrated most readily at encephalography are those of the vermis, fortunately the majority of cases of cerebellar atrophy are represented by the nutritional alcoholic group and in these it is predominantly the cerebellar vermis which undergoes degeneration (VICTOR et coll. 1959).

SUMMARY

The results indicate that encephalography has a definite value in disclosing and diagnosing the presence of cerebellar atrophy and is probably more useful than the indirect criteria based upon enlargement of the cisterna magna and/or fourth ventricle.

ZUSAMMENFASSUNG

Die Ergebnisse weisen darauf hin, dass der Encephalographie beim Nachweis und für Diagnosestellung von cerebellärer Atrophie ein eindeutiger Wert zukommt. Diese Untersuchung ist wahrscheinlich wichtiger als die indirekten Kriterien, die bei Vergrößerung der Cisterna magna und/oder des vierten Ventrikels in Erscheinung treten.

RÉSUMÉ

Les résultats des auteurs montrent que l'encéphalographie a une grande valeur pour le diagnostic de l'atrophie cérébelleuse et est probablement plus utile que les critères indirects basés sur l'agrandissement de la grande citerne et/ou du quatrième ventricule.

REFERENCES

- BASSANI G. and AMICI F. On the radiological diagnosis of cerebellar atrophy. *Ann. Radiol. diagn.* (Bologna) 33 (1960) 26.
 DI CHIRO G. Axial transverse encephalography. *Amer. J. Roentgenol.* 92 (1964) 441.
 UZMAN M. A case of cerebellar atrophy. *J. nerv. ment. Dis.* 97 (1943) 389.

- ERSTEIN B S and DAVIDOFF L M The use of laminography with encephalography in the diagnosis of middle and subtotal brain tumors *Amer J Roentgenol* 55 (1946) 675
- HABERLAND C Cerebellar degeneration with clinical manifestation in chronic epileptic patients *Psychiat et Neurol (Basel)* 143 (1962)
- HÄMMERBERG P E and FOG T The clinical value of the x ray diagnosis *atrophia cerebri* *Acta Psychiat scand Suppl* 137 (1959)
- LICHTENSTEIN B W and LEVINSON S A Cortical cerebellar atrophy without ataxia II primary circumscribed variety *J Neuropath exp Neurol* 5 (1946) 29
- MURPHY J P and ARANA R The pneumoencephalogram of cerebellar atrophy *Amer J Roentgenol* 57 (1947) 545
- STALLWORTHY K R and SAVAGE P P E Clinical aspects of cerebral atrophy revealed by encephalography *N Z med J* 54 1955
- SUTTON D The radiological assessment of the normal aqueduct and fourth ventricle *Brit J Radiol* 23 (1950) 208
- THIEBAUT F WACKENHEIM A and VROLSOS C Atrophies cerebelleuses la pneumostératographie sagittale médiane du crâne *Presse méd (Atlas Radiol clin)* (1959) 120
- UZMAN L Pneumoencephalography in the diagnosis of cerebellar atrophy report of five cases *Amer J Roentgenol* 60 (1948) 293
- VICTOR M ADAMS R D and MANCILL E A restricted form of cerebellar cortical degeneration occurring in alcoholic patients *A M A Arch Neurol & Psychiat* Vol 1 (1959) 579

THE CAROTID CISTERN A SOURCE OF DIAGNOSTIC DIFFICULTIES WITH SUPRASellar EXTENSIONS OF PITUITARY ADENOMATA

by

N A LEWTAS and A A JEFFERSON

When studying patients with chromophobe pituitary adenomata we have frequently observed discrepancies between the dimensions of the suprasellar portion of the lesion as they appear at encephalography and as found at operation. Air which projects over the suprasellar region in lateral films but which lies lateral to the midline is the source of this disparity. We have come to realise that one of the most important regions in which this air collects is around the carotid artery. Because this periarterial subarachnoid space is large we shall refer to it as the carotid cistern.

It is the purpose of this communication to describe and to illustrate the radiographic appearances of the carotid cistern and to describe the techniques available for overcoming the difficulties which its presence creates.

One of the reasons why the precise suprasellar extent of a pituitary adenoma cannot easily be recognised is because its anterior wall is rarely seen. In a consecutive series of 33 encephalographies for chromophobe pituitary adenomata we have outlined the anterior border of the suprasellar portion of the tumour on only three occasions.

- FRSTEIN B S and DAVIDOFF L M The use of laminography with encephalography in the diagnosis of middle and subtotal brain tumors *Amer J Roentgenol* 55 (1946) 675
- HABERLAND C Cerebellar degeneration with clinical manifestation in chronic epileptic patients *Psychiat et Neurol (Basel)* 143 (1962)
- HAMMERBERG P E and FOG T The clinical value of the x ray diagnosis atrofia cerebri *Acta Psychiat scand Suppl* 137 (1959)
- LICHTENSTEIN B W and LEVINSON S A Cortical cerebellar atrophy without ataxia II primary circumscribed variety *J Neuropath exp Neurol* 5 (1946) 29
- MURPHY J P and ARANA R The pneumoencephalogram of cerebellar atrophy *Amer J Roentgenol* 57 (1947) 545
- STALLWORTH K R and SAVAGE P P E Clinical aspects of cerebral atrophy revealed by encephalography *N Z med J* 54 1955
- SUTTON D The radiological assessment of the normal aqueduct and fourth ventricle *Brit J Radiol* 23 (1950) 208
- THIEBAUT F WACKENHEIM A and VROULOS C Atrophies cerebelleuses la pneumostratigraphie sagittale mediane du cervelet *Presse méd (Atlas Radiol clin)* (1959) 120
- UZMAN L Pneumoencephalography in the diagnosis of cerebellar atrophy report of five cases *Amer J Roentgenol* 60 (1948) 293
- VICTOR M ADAMS R D and MANCALL E A restricted form of cerebellar cortical degeneration occurring in alcoholic patients *A M A Arch Neurol & Psychiat* Vol 1 (1959) 579

THE CAROTID CISTERN A SOURCE OF DIAGNOSTIC DIFFICULTIES WITH SUPRASellar EXTENSIONS OF PITUITARY ADENOMATA

by

N A LEWTAS and A A JEFFERSON

When studying patients with chromophobe pituitary adenomata we have frequently observed discrepancies between the dimensions of the suprasellar portion of the lesion as they appear at encephalography and as found at operation. Air which projects over the suprasellar region in lateral films but which lies lateral to the midline is the source of this disparity. We have come to realise that one of the most important regions in which this air collects is around the carotid artery. Because this periarterial subarachnoid space is large we shall refer to it as the carotid cistern.

It is the purpose of this communication to describe and to illustrate the radiographic appearances of the carotid cistern and to describe the techniques available for overcoming the difficulties which its presence creates.

One of the reasons why the precise suprasellar extent of a pituitary adenoma cannot easily be recognised is because its anterior wall is rarely seen. In a consecutive series of 33 encephalographies for chromophobe pituitary adenomata we have outlined the anterior border of the suprasellar portion of the tumour on only three occasions.

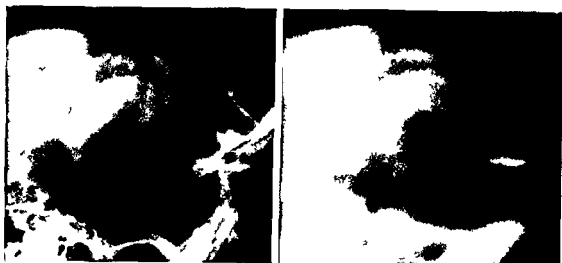
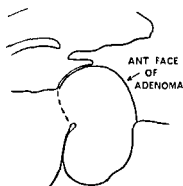


Fig. 1 *Left* Lateral encephalogram. A large suprasellar extension of a chromophobe adenoma deforms the front of the third ventricle. Only the apex of the lesion is outlined. Subarachnoid air overlies the suprasellar region. *Right* A midline sagittal tomogram outlines the anterior border of the tumour. Despite tomographic blurring parasellar subarachnoid air is still apparent.



Results

An enlarged sella and also a clear indentation of the antero-inferior aspect of the third ventricle are seen in Fig. 1. Because the suprasellar region is obscured by irregular collections of air it would be hard to define the true outlines of the tumour. The approximate position of the posterior wall of the adenoma may be derived from a line joining the posterior clinoid processes to the lowest part of the indentation in the third ventricle. However, the anterior face of the lesion would be drawn in by guess work alone were it not for the information provided by the tomogram where the convex anterior face of the suprasellar portion of the adenoma is well seen.

A similar appearance is shown in Fig. 2 in which the anterior wall of a (partially calcified) adenoma was well outlined during routine encephalography. In our third case the findings were almost identical. We feel it necessary to stress this appearance because numerous authorities have given credence to

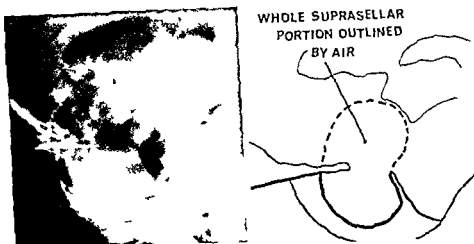


Fig 2 Lateral encephalogram. Fortuitous delineation of the whole suprasellar mass

the view that the suprasellar portion of the adenoma may consist only of a triangular portion involving the posterior part of the suprasellar region.

An example of this artefact from our own series is illustrated in Fig 3 (top). A film obtained later in the examination showed the third ventricle to be indented by a tumour which was far larger than the triangular portion previously indicated. We feel strongly that the interpretation suggested in the schematic diagram must always be incorrect for the surgical findings with such lesions are consistently those shown in Fig 4 where the lesion bulges forwards between the optic nerves and is contiguous with the tuberculum sellae.

Sometimes the artefact present in the suprasellar region takes the form of an M (Fig 5). At other times and perhaps only in the atrophic brain there may be a large sheet of air which completely obscures the whole suprasellar region (Fig 6).

In order to understand the origin of these appearances one must consider the normal anatomy. It has long been recognised that the carotid artery may be seen in the lateral projection during encephalography. We suggest that the presence of air adjacent to the carotid artery helps to create the artefacts illustrated in Figs 3 and 5. The subarachnoid space which surrounds the carotid artery is in most anatomical descriptions (e.g. LUNQUEST 1959) merely listed as part of the cisterna chiasmatis. However when one explores the carotid artery surgically one invariably finds a capacious space around it. We propose to refer to the large subarachnoid space which surrounds the

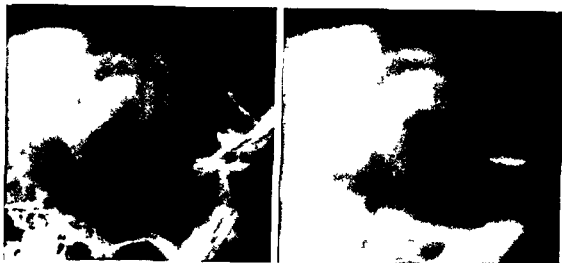
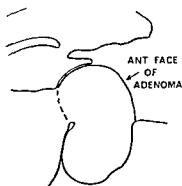


Fig. 1 *Left* Lateral encephalogram. A large suprasellar extension of a chromophobe adenoma deforms the front of the third ventricle. Only the apex of the lesion is outlined. Subarachnoid air overlies the suprasellar region. *Right* A midline sagittal tomogram outlines the anterior border of the tumour. Despite tomographic blurring parasellar subarachnoid air is still apparent.



Results

An enlarged sella and also a clear indentation of the antero-inferior aspect of the third ventricle are seen in Fig. 1. Because the suprasellar region is obscured by irregular collections of air it would be hard to define the true outlines of the tumour. The approximate position of the posterior wall of the adenoma may be derived from a line joining the posterior clinoid processes to the lowest part of the indentation in the third ventricle. However, the anterior face of the lesion would be drawn in by guess work alone were it not for the information provided by the tomogram where the convex anterior face of the suprasellar portion of the adenoma is well seen.

A similar appearance is shown in Fig. 2 in which the anterior wall of a (partially calcified) adenoma was well outlined during routine encephalography. In our third case the findings were almost identical. We feel it necessary to stress this appearance because numerous authorities have given credence to

Floor of Ant Fossa

Free edge of Falx

Tuberculum
sellae

Adenoma

Chiasmatic
cistern

Retractor

R Optic n



Fig 4 Operation photograph. Suprasellar mass bulges forwards medial to right optic nerve and contiguous with tuberculum sellae.

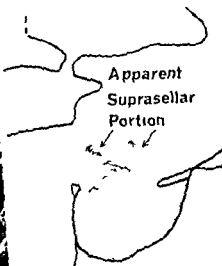


Fig 5 Lateral cephalogram. Sella and the false V-shaped outline of adenoma. True sella shown by third ventricle.

internal carotid artery as the carotid cistern. The extent of the carotid cistern can be recognised on tomography and in some cuts the carotid artery may be seen within it. In Fig 8 comparison between the straight film and a tomographic cut in the midline clearly discriminates between air lying in the

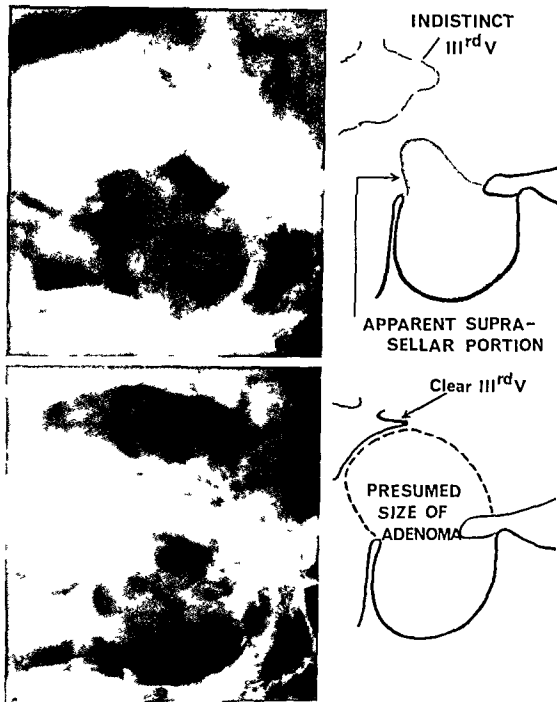


Fig 3 Lateral encephalograms. *Top* Third ventricle indistinct. Subarachnoid suprasellar air creates false outline of tumour. *Bottom* Later film. True size of tumour shown by indented third ventricle.

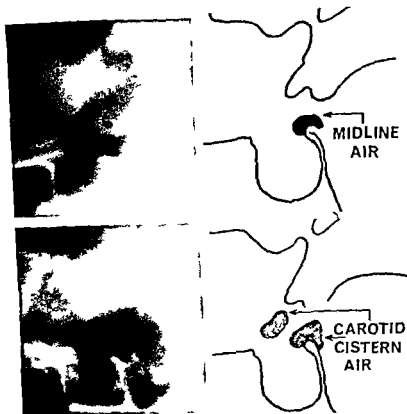
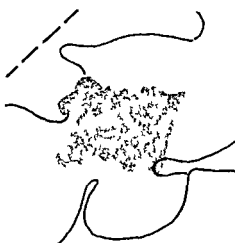


Fig 8 Intrasellar chromophobe adenoma. *Top* Sagittal tomogram shows only a small amount of air in the midline. *Bottom* Conventional film shows much larger quantity of air in carotid cistern.

reproduces the films of a patient with a massive suprasellar tumour in whom the third ventricle was not clearly seen on any of the films. There was no significant enlargement of the lateral ventricles and the fact that the foramen of Monro was almost occluded was not recognised. In consequence of this error this patient underwent operation and died some 36 hours later. This occurred 10 years ago and if we had then realised the true proportions of this lesion operation would have been strictly avoided.

Because in our opinion it is vitally important clearly to see the antero-inferior limits of the third ventricle we have considered how this may be achieved with certainty. We have reviewed the encephalograms of a series of operable cases (i.e. those without massive suprasellar extensions). Among twenty-nine patients the antero-inferior limits of the third ventricle were



SUBARACHNOID AIR OBSCURING CRITICAL AREAS

Fig 6 Lateral encephalogram in patient with relatively small suprasellar mass and cerebral atrophy. Large sheet of air obscures suprasellar region



CAROTID SIPHON



Fig 7 Normal lateral air encephalogram in which the internal carotid artery is clearly outlined by air

midline and air lying more laterally surrounding the carotid siphon. It will be noted that the air in the carotid cistern is by far the larger collection. In coronal tomograms the carotid cistern may also be demonstrated. In Fig 9, there is relatively little air in the sylvian fissure, but if there is extensive cerebral atrophy a large amount of air may become trapped along its length (Fig 10). This air, when viewed in the lateral projection, may densely obscure the suprasellar region (see Fig 6).

Clear demonstration of the third ventricle, or failure to identify it, can literally make the difference between life and death. For example Fig 11

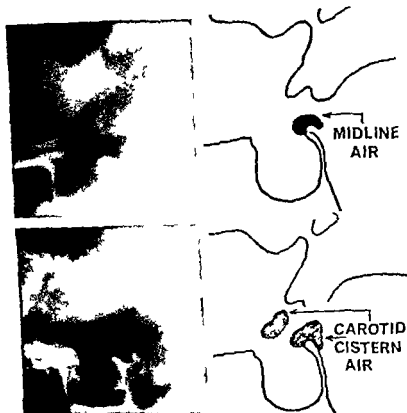


Fig 8 Intrasellar chromophobe adenoma. *T p S* gital tomogram shows only a small amount of air in the midline. *Conventional* film shows much larger quantity of air in carotid cistern.

reproduces the films of a patient with a massive suprasellar tumour in whom the third ventricle was not clearly seen on any of the films. There was no significant enlargement of the lateral ventricles and the fact that the foramen of Monro was almost occluded was not recognised. In consequence of this error this patient underwent operation and died some 36 hours later. This occurred 10 years ago and if we had then realised the true proportions of this lesion operation would have been strictly avoided.

Because in our opinion it is vitally important clearly to see the antero-inferior limits of the third ventricle we have considered how this may be achieved with certainty. We have reviewed the encephalograms of a series of operable cases (i.e. those without massive suprasellar extensions). Among twenty-nine patients the antero-inferior limits of the third ventricle were

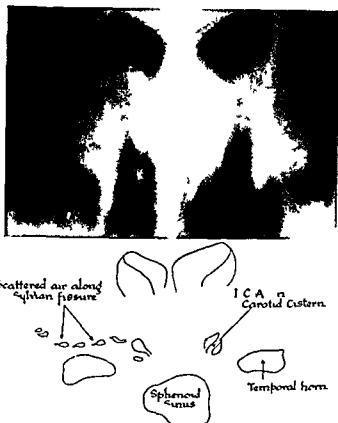


Fig 9 Pituitary adenoma (see also Figs 4 and 13) Coronal tomogram shows left internal carotid artery within the carotid cistern

not recognisable in eight, they were difficult to define in six, and were well seen in fifteen. Thus, using old methods of encephalography we were failing precisely to outline the area critical to the investigation in half our patients. Originally, this deficiency did not greatly trouble us, because our main aim during encephalography with these patients had been to certify the case as suitable for surgery by excluding the presence of a massive suprasellar lesion. However, because there will always be a small proportion of patients in whom the clinical diagnosis is in doubt we feel that precision in the routine techniques is essential. Tomography provides the chief means by which the antero-inferior portion of the third ventricle may be clearly seen. We have employed sagittal 'cuts' in the brow-up position using a vertical arc of tube swing. This invariably gives a clear outline of the anterior portion of the third ventricle, and eliminates to a considerable extent overlying subarachnoid air. An example of this technique is shown in Fig. 12 where the straight lateral projection shows only a small suprasellar mass whose size cannot be

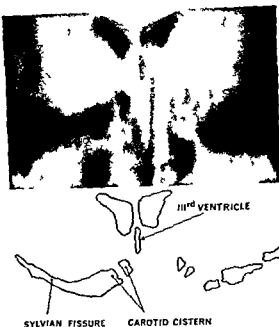


Fig 10 Same patient as in fig 6
Coronal tomogram shows large collection of air in Sylvian fissure and carotid cistern

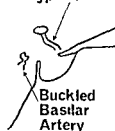
properly estimated because the third ventricle remains indistinct. The tomogram shows the true size of the tumour.

An additional virtue of tomography is that by revealing obliteration of the midline portion of the cisterna chiasmatis it will help to reveal the presence of relatively small adenomata which are large enough to compress the visual pathways but too small to distort the third ventricle to any great extent. Fig 13 reproduces a film from a patient with suspicious visual changes and with an almost normal supraoptic recess. However in this case the air which lay in the pontine cistern outlined the posterior face of the suprasellar mass. In cases in which the suprasellar mass is relatively small and the third ventricle lies anatomically either high or posterior or both relative to the pituitary fossa midline sagittal tomography would obviously assist correct diagnosis.

Because the necessary specialized apparatus for the brow up sagittal tomographic cuts may not always be available, we have also studied two alternative techniques. The first and more elegant of these is to employ auto tomography. With care one may achieve results which match those so beautifully illustrated by SCHLICHTER & GUTIÉRREZ MAHONEY (1962). The second alternative makes



Stretched and
elevated Carotid
Syphon



Buckled
Basilar
Artery

Fig 11 Lateral encephalogram with massive supra-sellar adenoma. (The third ventricle was not seen in any of the films.) Deformation of carotid and basilar arteries.

use of the old observation that, following encephalography, the subarachnoid air disappears before the intraventricular air. Fig 14 illustrates a patient in whom, on the initial roentgenograms, the third ventricle was not clearly defined, and the air in the basal cisterns thoroughly obscured the suprasellar region. Twelve hours later the subarachnoid air had almost all been absorbed and a lateral film, taken with the head over extended, allowed a considerable indentation in the front wall of the third ventricle to be clearly recognised. It should be noted that the small collection of apparently suprasellar air in Fig 14 (top sketch) must actually lie laterally in the carotid cistern. It is possible to make this statement categorically for these films relate to the same patient whose operation findings have been illustrated in Fig 4.

Discussion

Every surgeon who operates in the postero-medial subfrontal region will be familiar with the amount of cerebrospinal fluid which escapes from around the internal carotid artery whenever the cistern which contains it is first opened. It was when we realised the capaciousness of this subarachnoid space that we sought to discover whether air contained within it could obscure the suprasellar region when viewed in the lateral projection. It is the size of this subarachnoid

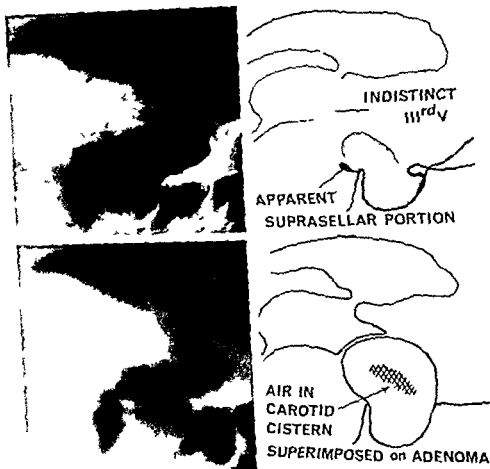


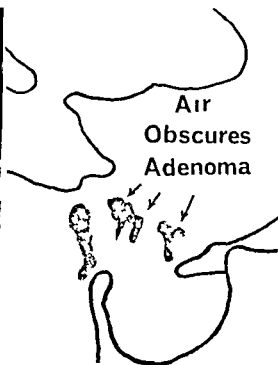
Fig. 17. Top: Lateral cephalogram, straight lateral projection. Small suprasellar mass, third ventricle indistinct. Bottom: Sagittal tomogram. Dilated third ventricle shows true size of tumour. Pituitary stalk still visible in midline cut.

space as seen at operation and as demonstrated by tomography (see Figs 8, 9 and 10) that has made us wish to identify it as the carotid cistern. Since the capacity of the carotid cistern is far larger than the central portion of the cisterna chiasmatis it seems logical to differentiate between them. We feel that there is every reason to suppose that confusing artefacts of the types displayed in Figs 3 and 5 are caused by air which is pooled in the carotid cisterns.

HAAS in 1925 made the suggestion that encephalography would allow one to define the upper border of the pituitary gland. However it was HEIDRICH (1928 and 1929) who first reported using encephalography in an attempt to



FIG. 13 Lateral encephalogram
Third ventricle lies high and posterior
to tumour and is little deformed
Only posterior face of tumour is out-
lined



determine the suprasellar extent of pituitary adenomata. He studied the changes in the basal cisterns and was anxious to avoid intracranial operations with massive lesions. HEIDRICH was also concerned to distinguish between tumours which were mainly suprasellar and those which were mainly intrasellar. He wished to use this information to decide whether operation should be undertaken via the nasopharynx or intracranially.

The next serious attempt to add precision to encephalography was that of DYKE & DAVIDOFF (1934) who studied particularly the changes in the basal cisterns in a wide range of pathological lesions. With pituitary adenomata, they reported changes similar to those described by HEIDRICH, but like him they did not refer specifically to the diagnostic deformities of the third ventricle.

In 1940 BALADO & ORIBE described a technique in which they used encephalography associated with stereoscopic radiography in the extended head position. They described a series of four cases investigated by this means and claimed that it gave great diagnostic precision. They found that the increased information provided by stereoscopy helped them to recognise obliteration of the chiasmatic cistern by a suprasellar mass, together with elevation of the adjacent portion of the third ventricle. They observed that, without stereoscopy, these features were often obscured by superimposed air. In the years that

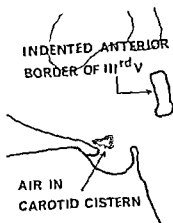
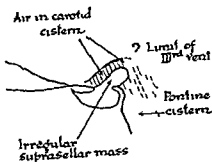


Fig. 14 Lateral cephalograms (see also figs 4 and 8). *Top*: Large amount of subarachnoid space; all relevant details of third ventricle not clearly seen. *Bottom*: Two hours later, loss of subarachnoid space; now absorbed and deformity of third ventricle is plainly seen.

Following this contribution, encephalography came to be more and more accepted as a routine measure in the investigation of pituitary tumours. The writings of BAKAY & WHITE (1953) and of DAVIDOFF & EPSTEIN (1955) bear witness to this process. However, in our hands at least until the last few years we tended, when performing encephalography, to be more interested in detecting the presence of tumours too large for surgery among a series of patients in whom, on other grounds, we had no reasonable doubt concerning the pathology. Apart from the dangers inherent in inexact radiography, we have for the past four years recognised the need for the greatest precision following an experience in which one of us (A. J.) was led to operate unnecessarily. The patient had optic atrophy, a clear bitemporal hemianopia, an

enlarged pituitary fossa and a very short history. At operation, it was found that the adenoma had spontaneously infarcted and was confined within the pituitary fossa. In retrospect, the short history related to recent suprarenal insufficiency and the patient had ignored (preceding) bi-temporal hemianopia until hospital investigations made her aware of it. This error arose from failure clearly to demonstrate the antero-inferior portion of the third ventricle.

For many years it has been recognised that during encephalography overlying collections of air obscure the suprasellar region. TWINE in 1937 predicted that tomography would play an important part in resolving this kind of difficulty. He felt that it would 'come more and more into routine use' and added that 'if we ask it (tomography) the right questions, we shall get the right answers'. TWINE's forecast was confirmed by the appearance of studies such as those of EPSTEIN & DAVIDOFF (1946) which was concerned with midline tumours, and of LOMBARDI (1949) which so beautifully illustrated the normal basal cisterns.

Tomography provides an invaluable means of displaying the midline portion of the cisternal chiasmatis, of occasionally showing the anterior border of the lesion, and it is a method which should invariably be employed when there is real diagnostic difficulty. We cannot emphasise too strongly that, in the presence of suprasellar masses, most of the air which appears suprasellar in position (in the lateral film) is in reality lateral to the midline. The importance of identifying the plane in which this air is lying has been recognised by others. BONNANT (1953) who had failed to solve the problem by tomography, attempted to do so with stereoscopic radiography. Stereoscopic techniques were also used, as mentioned above, by BALADO & ORIBE (1940) and by DAVIDOFF & EPSTEIN (1955) for the study of the basal cisterns. These last workers had previously been successful in displaying clearly the third ventricle by means of tomography (EPSTEIN & DAVIDOFF 1946).

PALEIRAC, LABAUGE & BASSEDE (1953) described the use of tomography with the head over extended to show the dispersal of air in the basal cisterns. They obtained 'cuts' in the midline and 1 cm to each side of it, and remarked that this technique eliminated vascular structures which were superimposed on pathologic processes. (No further details on this point were given, however.)

Although autotomography with encephalography was originally described in 1950 by ZIEDSIS DES PLANTES, for some curious reason its merits were generally ignored for many years. Its value was however recognized by SCHWARCZ (1959), who also modified the technique. SCHECHTER & GUTIÉRRIEZ-MAHONEY in 1962 published a comprehensive report brilliantly displaying the possibilities of the method. Certainly autotomography when

carefully performed brow up with the neck fully extended will provide excellent detail of the front of the third ventricle (cf SCHVARCZ 1959). The less satisfactory technique of repeating the lateral views after the overlying subarachnoid air has been largely absorbed has very real limitations for one is automatically bound to remain ignorant of the contours in the space above the sella and below the brain. In this we agree with SCHVARCZ.

Only by a full understanding both of the ways in which difficulties of interpretation arise and of the means by which such difficulties may be surmounted can we hope to arrive at consistently correct diagnosis and thus to offer appropriate treatment to our patients.

Acknowledgements

Figures 1, 8, 9, 10 and 12 are a tribute to the skill of Mr A. Robson, F.S.R., and we are grateful to him for his help. The remaining figures have been obtained by Miss J. M. Osborne and her staff at the Royal Infirmary, to all of whom we continue to be greatly indebted. It is a pleasure to record our thanks to Mr G. Swann, of the Photographic Department, for his careful work in preparing the illustrations, and to Miss A. Mason, whose typing never needs correction.

SUMMARY

Because the third ventricle may not be completely outlined by conventional techniques during air encephalography, it is often difficult to define the precise suprasellar extent of chromophobe adenomata. The commonest cause is air surrounding the carotid artery and obscuring the suprasellar region in the lateral projection. The difficulties may be circumvented by employing tomography.

ZUSAMMENFASSUNG

Da bei konventioneller Luftencephalographie der dritte Ventrikel unvollständig gefüllt sein kann, ist es oft schwierig, die suprasellare Ausbreitung von chromophoben Adenomen zu bestimmen. Die häufigste Ursache hierfür ist, dass die Luft die Art. carotis umgibt und in der Seitenprojektion die suprasellare Region überlagert. Diese Schwierigkeiten können mittels Tomographie vermieden werden.

RÉSUMÉ

Il arrive qu'il ne soit pas possible d'étudier complètement le troisième ventricule par les techniques classiques d'encéphalographie gazeuse, ce qui rend souvent difficile la délimitation précise de l'extension suprasellaire des adénomes chromophobes. La cause la plus commune est l'air qui entoure l'artère carotide et se superpose à la région suprasellaire sur la radiographie de profil. Ces difficultés peuvent être évitées par l'emploi de la tomographie.

REFERENCES

- BARAK L and WHITE J C Pneumoencephalography in chromophobe adenomas of the hypophysis *J Neurosurg* 10 (1953) 284
- BALADO M e ORIBE F La encephalografia en el diagnostico de las lesiones quiasmáticas e hipofisarias *Sem Med* 1 (1940) 1173
- BONNANT M Cisternographie stéréoscopique et adénomes pituitaires *Rev méd Suisse rom* 73 (1953) 108
- DAVIDOFF L M and EPSTEIN B S The abnormal pneumoencephalogram 2nd edition p 187 Lea & Febiger Philadelphia 1955
- DYKE C G and DAVIDOFF L M Significance of abnormally shaped subarachnoid cisterns as seen in the encephalogram *Amer J Roentgenol* 32 (1934) 743
- EPSTEIN B S and DAVIDOFF L M The use of laminography with encephalography in the diagnosis of midline and subtentorial brain tumours *Amer J Roentgenol* 55 (1946) 675
- HAAS L Erfahrungen auf dem Gebiete der radiologischen selladiagnostik *Fortschr Röntgenstr* 33 (1925) 419 and 469
- HEIDRICH L Zur chirurgie der hypophyse insbesondere die darstellung von hypophysen tumoren im encephalogram *Bruns Beitr klin Chir* 142 (1928) 837
- Weiterer beitrage zur frage der darstellung suprasellarer hypophysentumoren im encephalogram *Bruns Beitr klin Chir* 145 (1929) 628
- LILIEQUIST B The subarachnoid cisterns *Acta radiol Suppl* 185 (1959) p 64
- LOMBARDI G Studio radiologico delle cisterne cerebrali in condizioni normali *Radiol med* 5 (1919) 395
- PALEIRAC R LABAUCE R et BASSÈDE J Premiers resultats de la tomo isternographie *J Radiol Electrol* 34 (1953) 98
- SCHRECHTER M M and CURRIERREZ MATHONFAY C G Autotomography *Brit J Radiol* 35 (1962) 438
- SCHWARZ J Autotomography of the fourth ventricle and the floor of the third ventricle *Acta radiol* 52 (1959) 465
- TWING E W Discussion on the clinical value of the tomograph *Proc roy Soc Med* 31 (1937) 386
- ZIEDSDES DES LANTIS B C Examen du troisième et du quatrième ventricule *Acta radiol* 34 (1950) 399

A DEVICE FOR ENCEPHALOGRAPHY IN INFANTS

by

JOHN W. LOOP

Encephalography in infants and small children presents a variety of technical problems. Moving the very young into proper position for exposing the films may be rather difficult because of the relatively large and heavy head compared to the tiny trunk. Apparatuses which are scaled to adult dimensions are often not easily adaptable to children. Normally the smooth routine is frequently disrupted because the examiner needs to improvise. These problems are to some extent aggravated by the predictable non cooperation of wakeful infants and the encumbrances of those who have been anesthetized. For these reasons it was thought useful to develop a special device for handling infants during encephalography.

The figure shows a free standing metal frame with closed transparent upper sections and adjustable shoulder and hip yokes and foot plate. The patient is enclosed within this frame and strapped to the shoulder and foot sections. These with the hip section can be raised until the head is inside the closed upper part. Here it is centered and fixed by inflating a pair of transparent bag. Head tilting and rotation are thus eliminated and the head and trunk thereafter move together as a unit. The unit can be quickly moved from position to position and either forward or backward somersaults (controlled encephalography) can be accomplished with ease. The design permits exposing of films in inverted positions and allows identical frontal projections in right and left lateral recumbency, as well as standard encephalographic views.

REFERENCES

- BAKAY L and WHITE J C Pneumoencephalography in chromophobe adenomas of the hypophysis *J Neurosurg* 10 (1953) 284
- BALADO M e ORRIF F La encephalografia en el diagnóstico de las lesiones quiasmáticas e hipofisarias *Sem Med* 1 (1940) 1173
- BONNANT M Cisternographie stéréoscopique et adénomes pituitaires *Rev méd Suisse rom* 73 (1953) 108
- DAVIDOFF L M and EPSTEIN B S The abnormal pneumoencephalogram 2nd edition p 187 Lea & Febiger Philadelphia 1955
- DYKE C G and DAVIDOFF L M Significance of abnormally shaped subarachnoid cisterns as seen in the encephalogram *Amer J Roentgenol* 32 (1934) 743
- EPSTEIN B S and DAVIDOFF L M The use of laminography with encephalography in the diagnosis of midline and subtentorial brain tumours *Amer J Roentgenol* 55 (1946) 675
- HAAS L Erfahrungen auf dem Gebiete der radiologischen selladiagnostik *Fortschr Röntgenstr* 33 (1925), 419 and 469
- HEIDRICH L Zur chirurgie der hypophyse insbesondere die darstellung von hypophysen tumoren im encephalogram *Bruns Beitr klin Chir* 142 (1928) 837
- Weiterer beitrage zur frage der darstellung suprasellarer hypophysentumoren im encephalogram *Bruns Beitr klin Chir* 145 (1929) 628
- LILIEQUIST B The subarachnoid cisterns *Acta radiol Suppl* 185 (1959) p 64
- LOMBARDI G Studio radiologico delle cisterne cerebrali in condizioni normali *Radiol med* 5 (1949) 395
- PALEIRAC R LABAUGE R et BASSÈDE J Premiers resultats de la tomo isternographie *J Radiol Électrol* 34 (1953) 98
- SCHIECHTER M M and GUTIERREZ MAHONEY C G Autotomography *Brit J Radiol* 35 (1962) 438
- SCHWARCZ J Autotomography of the fourth ventricle and the floor of the third ventricle *Acta radiol* 52 (1959) 465
- TWINING E W Discussion on the clinical value of the tomograph *Proc roy Soc Med* 31 (1937) 386
- ZIEDESS DES PLANTES B C Examen du troisième et du quatrième ventricule *Acta radiol* 34 (1950) 393

A DEVICE FOR ENCEPHALOGRAPHY IN INFANTS

by

JOHN W. LOOP

Encephalography in infants and small children presents a variety of technical problems. Moving the very young into proper position for exposing the films may be rather difficult because of the relatively large and heavy head compared to the tiny trunk. Apparatuses which are scaled to adult dimensions are often not easily adaptable to children. Normally the smooth routine is frequently disrupted because the examiner needs to improvise. These problems are to some extent aggravated by the predictable non-cooperation of wakeful infants and the encumbrances of those who have been anesthetized. For these reasons it was thought useful to develop a special device for handling infants during encephalography.

The figure shows a free standing metal frame with closed transparent upper sections and adjustable shoulder and hip yokes and foot plate. The patient is enclosed within this frame and strapped to the shoulder and foot sections. These with the hip section can be raised until the head is inside the closed upper part. Here it is centered and fixed by inflating a pair of transparent bags. Head tilting and rotation are thus eliminated and the head and trunk thereafter move together as a unit. The unit can be quickly moved from position to position and either forward or backward somersaults (controlled encephalography) can be accomplished with ease. The design permits exposing of films in inverted positions and allows identical frontal projections in right and left lateral recumbency as well as standard encephalographic views.



Figure Device for holding infants for encephalography. The two inflatable plastic bags used to center and secure the patient's head may be removed.

Fluoroscopic and cinematographic examination is also convenienceed by this system of immobilization.

SUMMARY

A device for positioning infants and small children for encephalography is described.

ZUSAMMENFASSUNG

Eine Vorrichtung zur Lagerung und Fixierung für die Encephalographie bei Säuglingen und Kleinkindern wird angegeben.

RÉSUMÉ

Description d'un dispositif pour maintenir les nourrissons et les petits enfants pendant l'encephalographie.

PAN VENTRICULOGRAPHY

A new technique utilizing emulsified Pantopaque

by

ALBERTO PORTERA

LUCKETT (1913) accidentally discovered air outlining the ventricular system in a routine roentgenogram of the skull in a man with a skull fracture. Since then much effort has been directed towards finding an ideal contrast medium for delineation of the ventricular system and subarachnoid space. Since the development of air ventriculography and encephalography by DANDY (1918—1919) air has been used as an excellent contrast medium despite the frequently disagreeable side effects. Through wide use this technique has been perfected to such a degree that it is now possible to outline practically all of the cerebrospinal fluid containing cavities and hence to assess abnormalities within them. However these techniques in general commonly require the use of such special equipment as tilting chairs and tomographs as well as multiple injections of air with numerous roentgen exposures and consequent discomfort to the patient.

In addition to interpret this series of positional films correctly a high degree of skill and experience is needed and the proper use of air as a contrast medium has therefore become limited to well trained neuro radiologists and those departments where the above mentioned special equipment is available.

These considerations have led to further studies to find other contrast media and more simplified techniques

BALADO (1928) introduced Lipiodol into the ventricular system through a burr hole, and by using multiple exposures of the head in various positions he was able to obtain a complete survey of the ventricular system. Since then, this method has been in wide use but Pantopaque has replaced Lipiodol because of its less irritating qualities. MATSUBARA (1960) used isobaric Lipiodol emulsified with a neutral isotonic solution prepared with sodium lauryl sulphate. He was able to obtain complete demonstration of the ventricular system without apparent complication. The use of these oily contrast media has some advantage over air since they are painless and the patient's only discomfort is the trouble some head positions. However, their non absorbability is a disadvantage because frequently, several ml must be injected in order to obtain complete demonstration of the ventricular system. This particular disadvantage has led to the use of the presently available absorbable contrast media for injection into the ventricles. Unfortunately, recent communications (CAMPBELL 1964) have indicated that frequent and severe complications limit their utilisation in man. More recently DI CHIRO (1964) has introduced RISA into the ventricular system to supplement information found by examinations using air as the contrast medium. His paper cites some of the disadvantages of air. He found RISA ventriculography especially useful for detecting intraventricular tumors and internal hydrocephalus, and concluded that RISA ventriculography has a definite place among neuroradiologic diagnostic methods.

The work of BLEISEL (1961) using emulsified Pantopaque for lumbar myelography prompted us to use this technique for our own myelographies. As the complications were no greater than with ordinary Pantopaque and as emulsified Pantopaque is less dense, we introduced the use of this emulsion in those cases in which ventriculography was indicated.

Method

The surgical technique is the same as in classical ventriculography with air but only one burr hole is needed. Only local anesthesia is required. A right frontal burr hole is made and the patient is placed on the radiographic couch in the supine position with the head flexed by using a radio transparent prop. The roentgen tube is positioned to take a lateral roentgenogram with the usual settings for a standard skull film, with an exposure time of less than half a second, if possible.

A ventricular cannula is introduced through the burr hole (or through the fontanel in the case of an infant) into the frontal horn of the right lateral



Fig 1 Case 1 a) Film taken about 2 sec after injection of the emulsion (2 ml Pantopaque and 6 ml cerebrospinal fluid). The ventricular system is outlined in detail. Abnormal angulation in upper part of aqueduct b) Anteroposterior projection obtained without moving the patient. Asymmetry of 4th ventricle with flattening of right lateral recess

ventricle. An amount of 8 to 15 ml of ventricular fluid is collected in a sterile 20 ml syringe depending on the expected size of the ventricle. Pantopaque in an amount approximately one fourth of the volume of the spinal fluid collected is introduced into the syringe. In addition 5 ml of air is also introduced into the same syringe to facilitate emulsification. A sterile cap is applied to the syringe and it is then shaken vigorously for 20 seconds. The exact proportion of Pantopaque to ventricular fluid is not critical for we have used a range of ratios from 1/6th to 1/3rd of the spinal fluid with equally satisfactory results. Higher concentrations are recommended in children with obstructive hydrocephalus with extremely large ventricles.

The air in the syringe is then ejected and the milky emulsion is injected into the ventricle through the cannula. The injection must be done rapidly and smoothly at the rate of an ordinary intramuscular injection.

The intraventricular cannula should be left in place for 24 hours in cases in which a complete block is found. This will allow removal of excessive ventricular fluid should it accumulate prior to a definitive surgical procedure.

A lateral film is taken one second after the end of the injection. Without moving the patient the position of the tube is changed and an a.p. film is taken (Fig 1 a and b). We have studied a series of lateral views taken with a film changer at half-second intervals starting at the beginning of the injection. The Pantopaque in fine emulsified droplets enters the

These considerations have led to further studies to find other contrast media and more simplified techniques

BALADO (1928) introduced Lipiodol into the ventricular system through a burr hole, and by using multiple exposures of the head in various positions he was able to obtain a complete survey of the ventricular system. Since then, this method has been in wide use but Pantopaque has replaced Lipiodol because of its less irritating qualities. MATSUBARA (1960) used isobaric Lipiodol emulsified with a neutral isotonic solution prepared with sodium lauryl sulphate. He was able to obtain complete demonstration of the ventricular system without apparent complication. The use of these oily contrast media has some advantage over air since they are painless and the patient's only discomfort is the trouble some head positions. However, their non absorbability is a disadvantage because frequently, several ml must be injected in order to obtain complete demonstration of the ventricular system. This particular disadvantage has led to the use of the presently available absorbable contrast media for injection into the ventricles. Unfortunately, recent communications (CAMPBELL 1964) have indicated that frequent and severe complications limit their utilisation in man. More recently DI CUIRO (1964) has introduced RISA into the ventricular system to supplement information found by examinations using air as the contrast medium. His paper cites some of the disadvantages of air. He found RISA ventriculography especially useful for detecting intraventricular tumors and internal hydrocephalus, and concluded that RISA ventriculography has a definite place among neuroradiologic diagnostic methods.

The work of BLEASEL (1961) using emulsified Pantopaque for lumbar myelography prompted us to use this technique for our own myelographies. As the complications were no greater than with ordinary Pantopaque and as emulsified Pantopaque is less dense, we introduced the use of this emulsion in those cases in which ventriculography was indicated.

Method

The surgical technique is the same as in classical ventriculography with air but only one burr hole is needed. Only local anesthesia is required. A right frontal burr hole is made and the patient is placed on the radiographic couch in the supine position with the head flexed by using a radio transparent prop. The roentgen tube is positioned to take a lateral roentgenogram with the usual settings for a standard skull film with an exposure time of less than half a second, if possible.

A ventricular cannula is introduced through the burr hole (or through the fontanel in the case of an infant) into the frontal horn of the right lateral



Figs 4-6 (cf. figs 2-3) At the 3rd sec (upper left) the whole ventricular system is filled with contrast material. At the end of the 4th sec (upper right) some contrast can be seen in the upper cervical subarachnoid space. 5 min later (lower left) the emulsion has broken down and the Pantopaque has pooled in dependent areas including the cisterna magna.

present Ventriculography. Dilatation of the aqueduct and a block at the level of the fourth ventricle with marked displacement of the aqueduct and the fourth ventricle to the left demonstrated (Fig. 7a). At operation a large right-sided acoustic neuroma was found.

Case 3. This 7-year-old child had a history of intermittent headache and difficulty with gait of five months duration. Diplopia developed two months and nausea and vomiting two weeks prior to admission. Examination revealed bilateral pyramidal tract disease and a bilateral internuclear ophthalmoplegia. Fig. 8 shows upward and backward displacement of the aqueduct. Surgical exploration revealed a pineal tumor.

Case 4. An 11-year-old boy with a six-month history of constant diplopia and with difficulty in moving his left eye outward. Intermittent headache and vomiting appeared one month



Figs 2—3 Films obtained with a rapid film changer. At the end of the 1st second (left) the emulsion has partially filled the lateral and 3rd ventricles and in the second film (right) at the end of 2 sec the emulsion has filled the occipital horns of the lateral ventricles and entered the 4th ventricle.

ventricle with a turbulence which results in extremely rapid and complete dispersal throughout the entire ventricular system. Fig. 2 shows the state of turbulence at the end of the first second and Figs 3 to 6 the distribution and rapid dispersal of the contrast medium during the first five minutes.

In general, we have chosen the lateral position for the first film as it gives the most information for a survey of the entire ventricular system. This is followed by obtaining an a.p. view without moving the patient, thus allowing a clear view of displacement of the midline portions of the ventricular system. This sequence could be reversed in a particular case, or biplane serial films obtained if the equipment is available.

To illustrate clinical examples where the value of this technique is evident, five cases will be briefly presented.

Case reports

Case 1 A 23 year old girl with a history of severe headaches of six months duration and progressive loss of vision for one month. On examination she showed marked bilateral papille-dema and slight incoordination of the right hand. In Fig. 1 a and b slight dislocation of the upper third of the aqueduct and a flattening of the lateral recess of the fourth ventricle are clearly demonstrated. At operation a tuberculoma of the right inferior pole of the cerebellum was found.

Case 2 A 32 year old man presented with typical symptoms of a right acoustic neurinoma of three years duration. On examination right sided deafness, right facial hypalgesia and a mild right facial palsy of peripheral type were noted. Bilateral severe papilledema was also



Fig 8 Case 3 Pontine tumor in a child
Film taken a few seconds after the turbulence
ceased Elevation and posterior displacement
of the aqueduct

and 19 males. The same indications for air ventriculography or ordinary Pantopaque ventriculography were used in the selection of cases—that is, the presence of clinical evidence of increased intracranial pressure. In these cases the performance of encephalography is usually considered dangerous. This method was also used in 3 patients for localization of landmarks prior to stereotactic thalamotomy for Parkinson's syndrome (Fig 10). During stereotactic surgery the commissures can be seen throughout the operation. This method has proved very valuable for this type of operation where critical and permanent landmarks are indispensable.

We have found this method specially useful in detecting displacements, distortions or blocks of the midline portions of the ventricular system. It is also valuable in outlining both temporal and occipital horns simultaneously. In most cases the frontal horns and bodies of the ventricles can be seen if the film is taken during the state of turbulence immediately following the injection. The use of a rapid film changer facilitates critical timing. We have also found that the small amount of air which forms part of the emulsion is helpful in outlining the frontal horns of the injected side. This air is liberated during the first minutes following injection as the emulsion breaks down.

Diagnostically the technique has proved to be accurate and reliable. In the 27 cases of suspected brain tumors studied, 18 showed abnormalities of

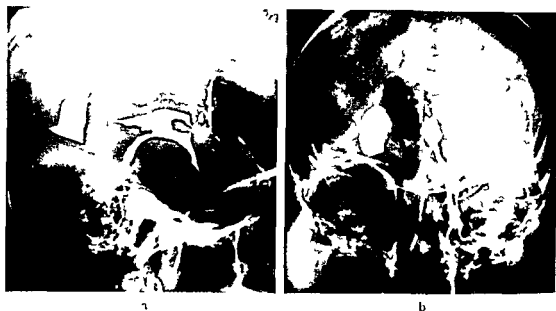


Fig 7 Case 2 a) Lateral film in acoustic neuroma. Elevation and dilatation of the aqueduct together with distortion of the 4th ventricle. Film taken more than four sec after injection. Turbulence is no longer present. b) A p view. Displacement of 3rd ventricle and aqueduct and narrowing of 4th ventricle.

prior to admission. He also complained of paresthesias and pain in the left periorbital region. Examination revealed bilateral papilledema and a complete left sixth nerve palsy. He also had a diminished left corneal reflex and hypalgesia in the area of distribution of the first and second divisions of the left trigeminal nerve. Ventriculography. Hydrocephalus due to a block at the rostral end of the aqueduct was found as well as displacement of the floor and the posterior part of the third ventricle upward and laterally (Fig 9 a and b). To obtain good contrast filling of the temporal horns the head of the patient was brought from the brow up position to the brow down position. In Fig 9 c a p a film shows marked elevation of the left temporal horn which appears collapsed. The space occupying lesion has also displaced the anterior part of the third ventricle to the right. At operation a large tumor was found occupying a great part of the left middle fossa and displacing the temporal lobe upward. The tumor was found to extend in dumb bell fashion below the tentorium into the anterior portion of the left cerebello pontine angle cistern. Microscopic studies of the tumor revealed it to be a neurinoma which presumably originated in the left 6th nerve.

Case 5 A 45 year old patient with a five year history of rightsided parkinsonism was selected for stereotactic thalamotomy. Fig 10 shows a lateral film taken while the patient was on the operating table with the craniostat in place. The emulsion clearly outlines the commissures of the third ventricle which are the most commonly used landmarks for this type of surgery.

Discussion

We have now used this method in 38 patients: 13 children from 6 months to 13 years of age and 25 adults from 20 to 70 years of age. There were 19 females

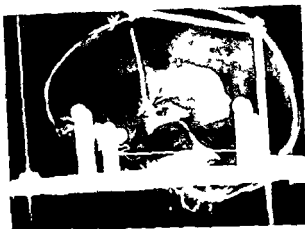


Fig 10 Case 5 Emulsified Pantopaque was used for delineation of the commissures of the 3rd ventricle in stereotactic surgery

than 24 hours. Occasionally mild headaches were reported 4 to 8 hours after the procedure but these responded promptly to analgesics. Two 13 year old children manifested a more severe febrile reaction accompanied by an aseptic meningitis syndrome. Temperatures ranged to over 39 C but symptomatic treatment resulted in remission of symptoms and complete recovery in 48 hours. Three infants under one year of age who had been subjected to the procedure by needle-puncture of the anterior fontanel developed the mild febrile reaction seen in the adults. We have now followed our patients for periods up to 18 months. No symptoms attributable to Pantopaque have been found. In some patients we were able to obtain roentgen films of the skull and lumbosacral region at random intervals of approximately 3 and 6 months. They showed that most of the Pantopaque injected in the ventricles dispersed throughout the sacral roots much in the same manner as found after lumbar myelography. A negligible amount of Pantopaque remained inside the ventricles.

The mild toxic reactions seen in our groups of cases are in sharp contrast to the experience of JAEGER (1950) in his work with dogs. He prepared Pantopaque in a colloid mill emulsifying it with artificial dispersing agents such as aracia. The particle size achieved in the mill was in the order of 10 microns. The emulsion was very stable and persisted through autoclave sterilization. Following the injection of this emulsion into the ventricles of five dogs death occurred within the first 10 minutes in all animals. He assumes in his paper that the tiny dispersed particles of the Pantopaque were responsible for the ill effects found in his dogs.

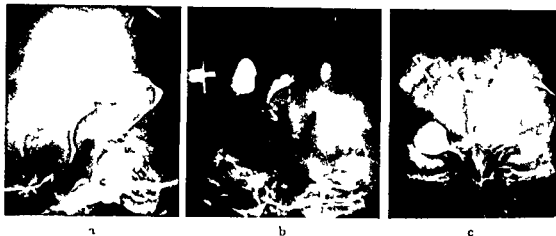


Fig 9 Case 4 a) Lateral film Complete block at origin of aqueduct The turbulence has disappeared Elevation of posterior part of floor of 3rd ventricle and dilatation of the ventricles b) A p view Film taken five minutes after the injection without moving the head The floor of the 3rd ventricle appears amputated and displaced upwards and to the right c) P a view By tilting the head forward both temporal horns and anterior part of 3rd ventricle are demonstrated The Pantopaque occupies the lowest portions of the ventricular system The neoplasm has elevated and collapsed the left temporal horn and displaced the anterior part of the 3rd ventricle to the right

the ventricular system suggesting the presence of a space occupying lesion. In all abnormal cases a brain tumor was confirmed at surgery. There have been no false positive studies. This high degree of reliability is probably a result of the excellent detail with which the midline portions of the ventricular system are demonstrated. In most cases two single films, a lateral and an a p projection, are necessary for correct localization of the lesion, in rare instances a third or fourth film may be required. This may be obtained after making simple maneuvers of the head of the patient.

This method can only be used for study of the ventricular system and through a burr hole. Where demonstration of the cisterns is desired encephalography can be performed during the same diagnostic session. The injection of air can be safely done via a lumbar tap because the danger of brain stem herniation is minimized following ventricular tap.

It should be emphasized that this procedure is done under local anesthesia and is painless. Thus, the patient may cooperate and this further simplifies the examination. Since most of the information is obtained with two films, the need for multiple positional changes of the patient is eliminated. Obviously the large number of films necessary with air or standard Pantopaque techniques are greatly reduced.

Mild complications have been encountered. In 28 cases low grade febrile reactions occurred, the temperatures were less than 39° C and persisted less

patient. The anatomical detail achieved is impressive. Because of the demonstration of the entire ventricular system in one film the interpretation is greatly simplified as compared to the complexity of analysing multiple films such as are required in air studies. The technique does not limit the possibility of examining the subarachnoid cisterns with air at the same session.

Only transitory side effects have been encountered and these have been generally less severe than those common to air ventriculography. A specialized application of this method is the accurate localization of landmarks for stereotactic surgery. We consider this method of special value in the study of posterior fossa or midline middle fossa lesions. Also blocks of the cerebrospinal fluid pathways are readily demonstrated.

In our experience to date, emulsified Pantopaque ventriculography has been the method of choice for studying the midline portions of the ventricular system in patients with increased intracranial pressure.

SUMMARY

Pantopaque emulsified with cerebrospinal fluid from the patient under study has been used in cerebral ventriculography in 38 patients. The entire ventricular system can be demonstrated in two films in the a p and lateral projections. Side effects have been minimal and of short duration. The examination is performed under local anesthesia and causes little or no discomfort. Only 2 ml or less of Pantopaque are used for the emulsion.

ZUSAMMENFASSUNG

Pantopaque emulgiert im Liquor des jeweiligen Patienten wurde bei 38 Patienten zur cerebralen Ventrikulographie verwendet. Das gesamte Ventrikelsystem kann auf zwei Filmen in bzw. a p und laterale Projektionen dargestellt werden. Nebenwirkungen waren minimal und nur von kurzer Dauer. Die Untersuchung wird unter Lokalanästhesie ausgeführt und ist mit wenig oder gar keinem Unbehagen verbunden. Die Menge Pantopaque die für die Emulsion benötigt wird beträgt nur 2 ml oder weniger.

RÉSUMÉ

L'auteur a utilisé dans 38 cas en ventriculographie cérébrale une émulsion de Pantopaque dans le liquide céphalo-rachidien du malade. On peut mettre en évidence la totalité du système ventriculaire sur deux films en incidence de face et de profil. Les effets secondaires ont été minimes et de courte durée. L'examen est fait sous anesthésie locale et n'est que peu ou pas pénible. Il ne faut que 2 ml ou moins de Pantopaque pour l'émulsion.

With our technique the emulsification is achieved by manually shaking Pantopaque with the cerebrospinal fluid of the patient. No artificial dispersing agents are used. The size of the droplets is extremely variable and has been measured as being from 20 to 400 microns. The resulting emulsion is very unstable. In Fig. 6 the film was taken 5 minutes after the injection of the emulsion. It is readily seen that it has broken down and that the Pantopaque has pooled in the dependent portions of the ventricular system.

In view of the differences between our study and JAEGER's work with dogs, it is possible to speculate that the size of the droplets or the nature of the dispersing agent may be responsible for the production of complications. Perhaps the small size of the particles increases ependymal and arachnoid irritation because of longer lasting contact with the membrane surfaces.

We have recently obtained findings from a postmortem examination of a child who was subjected to our method of ventriculography about one year ago. At that time the diagnosis of obstructive hydrocephalus was made and was subsequently surgically alleviated by a shunt procedure. The patient did well for more than a year but died of injuries sustained in an automobile accident. Careful microscopic study of the ventricular ependyma and the arachnoid membranes of the posterior fossa revealed no abnormalities. Roentgen examination of the removed brain failed to show any Pantopaque within the ventricles or in the subarachnoid space.

Our experience with this type of emulsification of Pantopaque has been without severe complications. Because of the short duration of the emulsion due to large particle size this procedure is tolerated in the same manner as standard Pantopaque ventriculography. This contrast medium has been widely used for over 20 years as the best available compound for myelography. There have been occasional clinical reports of unfavorable reactions of the use of Pantopaque but repeated experiments with laboratory animals have failed to demonstrate anything but minimal transitory reactions when injected in the subarachnoid space (MEAGHAM 1963). Another factor which should contribute to minimizing the possible toxic effects of Pantopaque with our method is the small volume used. Normally this is less than 2 ml in contrast to the 6 to 9 ml generally used in myelography.

Conclusions

A simple technique utilizing emulsified Pantopaque for study of the ventricular system is offered. No special neuroradiographic equipment is required. The time needed to perform the examination is much less than with air or Pantopaque ventriculography. Little or no discomfort is experienced by the

patient. The anatomical detail achieved is impressive. Because of the demonstration of the entire ventricular system in one film the interpretation is greatly simplified as compared to the complexity of analysing multiple films such as are required in air studies. The technique does not limit the possibility of examining the subarachnoid cisterns with air at the same session.

Only transitory side effects have been encountered and these have been generally less severe than those common to air ventriculography. A specialized application of this method is the accurate localization of landmarks for stereotactic surgery. We consider this method of special value in the study of posterior fossa or midline middle fossa lesions. Also blocks of the cerebrospinal fluid pathways are readily demonstrated.

In our experience to date emulsified Pantopaque ventriculography has been the method of choice for studying the midline portions of the ventricular system in patients with increased intracranial pressure.

SUMMARY

Pantopaque emulsified with cerebrospinal fluid from the patient under study has been used in cerebral ventriculography in 38 patients. The entire ventricular system can be demonstrated in two films in the *a p* and lateral projections. Side effects have been minimal and of short duration. The examination is performed under local anesthesia and causes little or no discomfort. Only 2 ml or less of Pantopaque are used for the emulsion.

ZUSAMMENFASSUNG

Pantopaque emulgiert im Liquor des jeweiligen Patienten wurde bei 38 Patienten zur cerebralen Ventrikulographie verwendet. Das gesamte Ventrikelsystem kann auf zwei Filmen in *bzw.* *a p* und laterale Projektionen dargestellt werden. Nebenwirkungen waren minimal und nur von kurzer Dauer. Die Untersuchung wird unter Lokalanästhesie ausgeführt und ist mit wenig oder gar keinem Unbehagen verbunden. Die Menge Pantopaque, die für die Emulsion benötigt wird, beträgt nur 2 ml oder weniger.

RÉSUMÉ

L'auteur a utilisé dans 38 cas en ventriculographie cérébrale une émulsion de Pantopaque dans le liquide céphalorachidien du malade. On peut mettre en évidence la totalité du système ventriculaire sur deux films en incidence de face et de profil. Les effets secondaires ont été minimes et de courte durée. L'examen est fait sous anesthésie locale et n'est que peu ou pas pénible. Il ne faut que 2 ml ou moins de Pantopaque pour l'émulsion.

With our technique the emulsification is achieved by manually shaking Pantopaque with the cerebrospinal fluid of the patient. No artificial dispersing agents are used. The size of the droplets is extremely variable and has been measured as being from 20 to 400 microns. The resulting emulsion is very unstable. In Fig. 6 the film was taken 5 minutes after the injection of the emulsion. It is readily seen that it has broken down and that the Pantopaque has pooled in the dependent portions of the ventricular system.

In view of the differences between our study and JAEGER's work with dogs, it is possible to speculate that the size of the droplets or the nature of the dispersing agent may be responsible for the production of complications. Perhaps the small size of the particles increases ependymal and arachnoid irritation because of longer-lasting contact with the membrane surfaces.

We have recently obtained findings from a postmortem examination of a child who was subjected to our method of ventriculography about one year ago. At that time the diagnosis of obstructive hydrocephalus was made and was subsequently surgically alleviated by a shunt procedure. The patient did well for more than a year but died of injuries sustained in an automobile accident. Careful microscopic study of the ventricular ependyma and the arachnoid membranes of the posterior fossa revealed no abnormalities. Roentgen examination of the removed brain failed to show any Pantopaque within the ventricles or in the subarachnoid space.

Our experience with this type of emulsification of Pantopaque has been without severe complications. Because of the short duration of the emulsion due to large particle size this procedure is tolerated in the same manner as standard Pantopaque ventriculography. This contrast medium has been widely used for over 20 years as the best available compound for myelography. There have been occasional clinical reports of unfavorable reactions of the use of Pantopaque but repeated experiments with laboratory animals have failed to demonstrate anything but minimal transitory reactions when injected in the subarachnoid space (MEACHAM 1963). Another factor which should contribute to minimizing the possible toxic effects of Pantopaque with our method is the small volume used. Normally this is less than 2 ml in contrast to the 6 to 9 ml generally used in myelography.

Conclusions

A simple technique utilizing emulsified Pantopaque for study of the ventricular system is offered. No special neuroradiographic equipment is required. The time needed to perform the examination is much less than with air or Pantopaque ventriculography. Little or no discomfort is experienced by the

ENCEPHALOGRAPHY TODAY

Refinements in technique and progress in diagnosis

by

GIOVANNI RUGGIERO

The present paper received the privilege of opening the scientific session of the VII Symposium Neuroradiologicum. I take this as a sign that its subject is still of great interest to neuroradiologists. Neuroradiologic techniques have recently become quite popular and consequently there is at present a certain tendency to make use of examinations which are technically relatively easier than encephalography which is a complicated procedure requiring skill in performance. After fifteen years of experience I am however more convinced than ever that encephalography is still and by far the most accurate means of investigation for a proper radiologic diagnosis of cerebral lesions. This is emphasized by Fig. 1 which shows the incidence of encephalography in our department where it is the second most frequent examination after carotid angiography.

In 1951 I published a monograph (7) summarizing our past experiences with encephalography. The main purpose of the present paper is to point out the progress that has been achieved since then. This progress has been twofold: better technique and more accurate diagnosis. These two factors are interdependent and cannot be discussed separately.

REFERENCES

- BALADO M La radiografía del tercer ventrículo mediante la inyección intraventricular de Lipiodol Arch argent Neurol 2 (1928) 69
- BLEASEL K Nerve root radiography Brit J Radiol 34 (1961) 596
- CAMPBELL R L, CAMPBELL J A, HIENBURGER R F, KALSBECK J F and MFALY J Ventriculography and myelography with absorbable radiopaque medium Radiology 82 (1964) 286
- DANDY W F Ventriculography following the injection of air into the cerebral ventricles Ann Surg 68 (1918) 5
- Roentgenography of the brain after the injection of air into the spinal canal Ann Surg 70 (1919) 397
- DI GIUO G, REAMES P M and MATTHEWS W B JR RIS A ventriculography and RIS A cisternography Neurology 14 (1964) 185
- JAEGER R Irritating effect of iodized vegetable oils on the brain and spinal cord when divided into small particles Arch Neurol Psychiat 64 (1950) 715
- LUCKETT W H Air in the ventricles of the brain following a fracture of the skull Surg Gynec Obstet 17 (1913) 237
- MATSUBARA T and NOMURA T Emulsified iodized oil ventriculography Amer J Roentgenol 84 (1960) 52
- MURCHAM W F The ependymal response to long term intraventricular Pantopaque J Neurol Neurosurg Psychiat 26 (1963) 559
- PORTERA A, BRAVO G and PARERA C Emulsified Pantopaque ventriculography J Neurosurg 21 (1964) 422

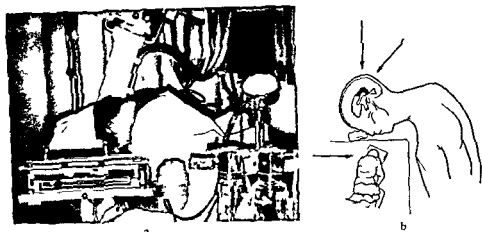


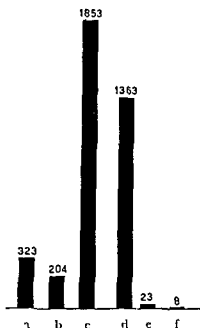
Fig. 2. Examination of occipital horns in sitting position. a) Position of patient. The manometer for measuring the arterial pressure is incorporated in the set up for the general anesthesia and remains attached to the patient during the entire examination. b) Centering for lateral, postero-anterior and lateral-postero-anterior projections. The head is slightly extended but this does not influence the quality of the roentgenograms; only the fluid level appears slightly oblique.

amplifier television system with those obtained from the use of the Mimer. With the present system it is however difficult to use the image intensifier in the frontal projection in the sitting position and impossible when the patient is lying down. (We have not had an opportunity to use Mimer II which is especially constructed for encephalographic examinations using image amplifier TV and was presented at the XI International Congress of Radiology in Rome 1966.)

Examination of occipital horns in sitting position. This is carried out shortly after investigating the posterior fossa structures and before examining the frontal horns (9). With our present technique (Fig. 2) the temporal horns can be rapidly investigated by performing a simple manoeuvre which does not necessitate the patient being previously in the prone position during the examination. It is surprising how greatly this simplifies the whole technique, especially when dealing with fat or deformed subjects for whom the centering can be difficult also in the prone position. In the sitting position the fluid level in the ventricular carrefour or the posterior portion of the temporal horn may appear oblique in patients in whom it is not possible to obtain a complete flexion of the neck, but this does not interfere with the diagnostic value of the radiographic images.

A simpler manoeuvre for filling the temporal horn. LINDGREN (4) has demonstrated the necessity of studying the temporal horn in the supine position taking

Fig. 1 Cerebral contrast examinations at the Neuroradiologic Department of Ospedale Maggiore between November 1st 1961 and June 7th 1964 a — Percutaneous vertebral angiography b — Percutaneous external carotid angiography c — Percutaneous common and internal carotid angiography d — Frictional encephalography e — Cisternography f — Positive contrast ventriculography



Our radiographic technique

At the symposium, a movie showing the present technique in detail was presented

Utilisation of an image intensifier under television control An image intensifier is now used routinely in our department. This allows a shorter examination time than earlier, especially that part which is carried out with the patient in the sitting position, and makes the examination much better tolerated.

Using the image amplifier, it is possible to check quickly whether the contrast medium has passed into the desired portion of the ventricular system or subarachnoid space, whether it is equally distributed within the two lateral ventricles, and whether the amount of air injected is sufficient. It is also possible to evaluate rapidly the success of some special manoeuvres as for instance, those for filling the temporal horn or the antero-inferior portion of the third ventricle. One important point needs to be emphasized however: the images observed on the television screen can never be regarded as a substitute for the films, and have no diagnostic value unless they are recorded radiocinematically. It is also essential that the intensifier TV unit be fixed in such a way that none of the basic principles of the encephalographic technique as first established by LINDGREN (5) have to be set aside. We use a set up designed for our department with the aim of combining the advantages of the image

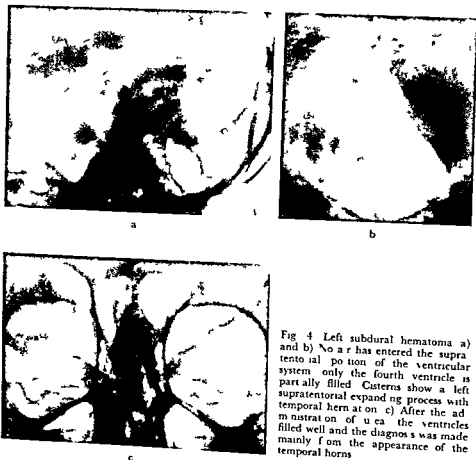


Fig 4 Left subdural hematoma a) and b) No air has entered the supratentorial portion of the ventricular system only the fourth ventricle is partially filled c) Cisterns show a left supratentorial expanding process with temporal herniation c) After the administration of uca the ventricles filled well and the diagnosis was made mainly from the appearance of the temporal horns

to let any CSF escape whereas in cases of atrophy of the brain or communicating hydrocephalus in which large amounts of air necessarily have to be injected it may be necessary to withdraw a certain amount of CSF in order to avoid too much discomfort to the patient

Late radiographic control In 1959 we (14) proposed the performance of a radiographic control 24 hours after encephalography. Since the air in the subarachnoid space is usually absorbed before the air in the ventricles one can so to speak perform a ventriculography without ventricular puncture. It is thus possible to obtain better demonstration of some ventricular details which might have been hidden by superimposed air in the subarachnoid spaces or not filled at all at the first examination. Continued experience has demonstrated

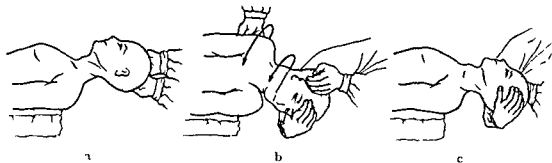


FIG. 3 Technique for filling the temporal horn in supine position. After (c) the head is placed in the same position as in (a).

lateral views with a horizontal beam in order to demonstrate the anterior portion in its entirety. Our technique for filling the temporal horn is as follows: after the occipital horns have been studied in the sitting position the shoulder homolateral to the temporal horn which is to be filled is lifted up and the head is slowly turned towards the opposite side and then lowered by accentuating the rotation, in order that the midpoint of the forehead will lie at a lower level than the midpoint of the occiput. The head is then rotated back to a forward facing position while still hyperextended, and finally is quickly raised and placed in the correct position for radiography (Fig. 3). Experience with our technique has convinced us that it can also provide good demonstration of one temporal horn alone.

Modality of gas injection. It has recently (3, 15, 16, 17) been suggested, especially by AZAMBUJA's (1) experiments, that a fractionated air study can be tolerated much better if no cerebrospinal fluid (CSF) is removed, or if its removal is minimal. The principle of such a technique is based on the observation that the increase of CSF pressure following the injection of air is only of short duration, much shorter in any case than the time necessary for a decreased CSF pressure due to a withdrawal of fluid to return to normal values. A transient hypertension in the subarachnoid space is supposed to be less dangerous than a prolonged hypotension. We have been using this technique for a fairly long time. We have not found differences as striking as those reported by other authors, but this technique seems to be useful mainly to prevent late complications. Even the original technique of LINDGREN (5, 7) has always been a benign procedure in our hands. Injection of more air than the amount of CSF withdrawn has always been a basic rule in fractional encephalography (9). In a case of posterior fossa tumour with increased intracranial pressure in which only a small amount of air is necessary it will be strictly contraindicated.

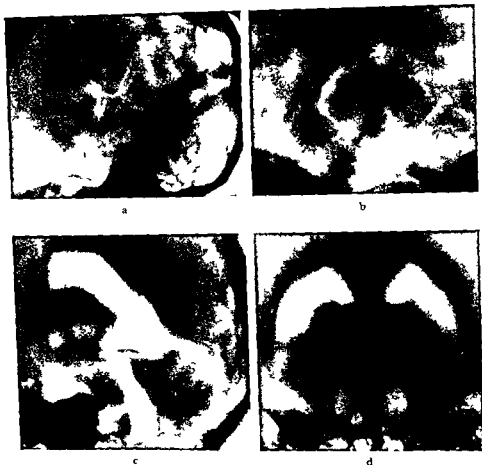


Fig 6 Unverified brain stem tumour. A contrast medium does not enter the ventricular system (only the posterior part of the third ventricle is very poorly filled) despite administration of urea (a) and (b). However, the diagnosis of pontine tumour was easily made on the basis of the displacement of the cisterns of the brain stem. It was anatomically verified by a ventriculography (c) and (d) made at the surgeon's request.

might be caused by several factors and aggravated by the sitting position. The blood pressure is measured in the sitting position just before the lumbar puncture and compared with the patient's usual pressure. It is important that the blood pressure at the time of the examination should not be significantly lower than the usual pressure. If it is lower it must be increased before the examination is begun. The blood pressure is also controlled at the end of the examination in the sitting position, at the end of the whole examination, and every time it is considered necessary. In the presence of any untoward reaction

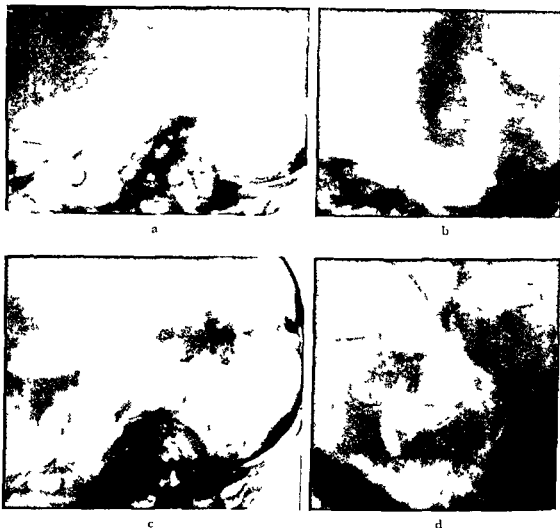


Fig. 5. Left sided medulloblastoma invading the fourth ventricle. No gas enters the ventricular system. Pontine cistern irregularly filled and left cerebello pontine angle cistern not filled (a) and (b). After urea administration the ventricular system filled perfectly. The aqueduct is dilated (c) and there is a filling defect in the fourth ventricle which is not dilated (d).

that 24 hours is too long an interval and we now routinely take control films of our patients about 6 hours after the examination, except in patients in very poor general condition with a clear diagnosis or in patients to be operated upon immediately after the encephalography.

Measuring of the blood pressure The examination should never be started before the blood pressure has been measured. We are firmly convinced that the great majority of accidents reported as episodes of acute cerebral herniation are instead the results of cerebral ischemia due to arterial hypotension, which



Fig 8 Verified post traumatic left frontal intraventricular hematoma. Bilateral angiography was negative. The encephalography is diagnostic.

is usually performed by the senior members of the team. In any case we try to avoid general anesthesia as much as possible and tend to consider it contraindicated in tumours of the posterior fossa and brain stem. The only three serious accidents (two of which were fatalities) observed after encephalography were in patients under general anesthesia. (These patients however were in poor general condition before the examination.) It should be remembered that general anesthesia both depresses the bulbar centers especially the respiratory ones, and increases the CSF pressure.

Urea technique. At the time of my monograph one main problem remained to be solved: the diagnosis of those supratentorial tumours in which because of the cerebral edema no air entered the supratentorial portion of the ventricular system. The use of a perfusion of urea solution in encephalography was suggested by ENGSET & HALGE (2). Independently of their publication we had also started to use urea employing another technique which in our opinion is more suitable to the principles of encephalography (12-13). We consider the use of urea to be a giant step forward towards a more accurate encephalographic diagnosis (Fig 4). When the present paper was being prepared the urea technique had been used in 22 cases of supratentorial space occupying lesions: only in 4 of them was there failure of ventricular filling after the urea administration (a deep central tumour, a suspected metastatic tumour which could not be verified either at surgery or at autopsy, a case of radiologically verified multiple metastases with suspected cerebellar metastases, and a parietal glioma which at surgery did not seem to invade the deep midline structures or the upper brain stem: the latter case was the only one in which we could not clearly explain the lack of success).

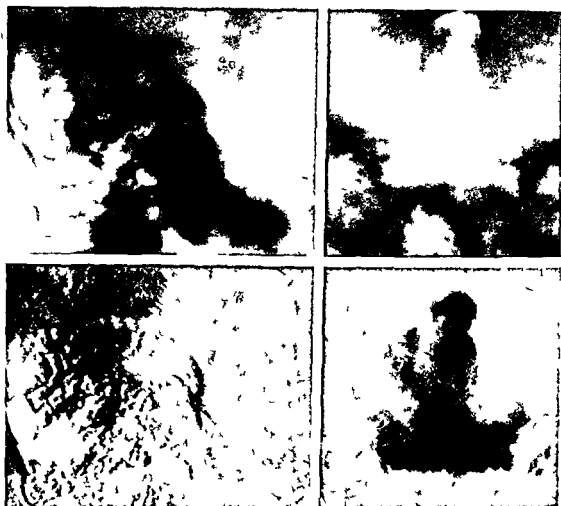


Fig. 7. Subtraction in a case of negative encephalography. The fluid level in the great cistern is much better outlined.

we have often observed a sudden decrease in the arterial pressure which might explain other vegetative troubles such as profuse sweating and coldness of the skin. Usually these disorders disappear with the return of the blood pressure to the 'normal' limits.

General anesthesia. A point of paramount importance is whether or not encephalography should be carried out under general anesthesia. Our investigations on the variations of CSF pressure during encephalography seem to demonstrate that such variations, especially those between the initial and final pressure, are more 'regular' in those examinations carried out without anesthesia. This seems to be even more marked in cases of brain tumour, but I think that it should be borne in mind that in cases of tumour the examination

RESUME

L'auteur analyse les principaux aspects de la technique de l'encephalographie fractionnée telle qu'elle est pratiquée actuellement dans son service

REFERENCES

- 1 AZAMBUJA N. Experimental variations of CSF pressure following injection and removal of CSF. Personal communication
- 2 ENGESET A and HALGE T. Urea as an aid in encephalography. *Acta radiol. Diagnosis* 1 (1963) 565
- 3 HULTSCH E G und SEEBERG A. Die Pneumoencephalographie unter Überdruck und die medikamentöse Behandlung des vegetativen Symptomenkomplexes. *Nervenarzt* 28 (1957) 49
- 4 LINDGREN E. A pneumographic study of the temporal horn. *Acta radiol.* (1948) Suppl No 69
- 5 — Some aspects of the technique of encephalography. *Acta radiol.* 31 (1949) 161
- 6 NELSON D A, YEFFREYS W H, LEANING R H and McDOWELL F. Encephalography by the displacement technique. *Arch. Neurol. Psychiat.* 79 (1958) 498
- 7 RLOGIERO G. L'encephalographie fractionnée. Vol 1 p 509. Masson et Cie Paris 1957
- 8 — Encefalografia e ventricolografia nei tumori della fossa posteriore. *Bull. Sci. med.* 1 (1963) 103
- 9 — Technique neuroradiologique. Vol 1 p 358. In *Traité de technique chirurgicale*. Tome II. Masson et Cie Paris 1959
- 10 — e DETTORI P. Una nuova tecnica di encefalografia. Nota preliminare. *Bull. Sci. med.* 3 (1964) 223
- 11 — — Ulteriori esperienze con la sottrazione di immagini in neuroradiologia. *Bull. Sci. med.* 2 (1964) 132
- 12 — et PACIFICO L. Quelques aspects techniques nouveaux de l'encephalographie fractionnée. *Neuro-chirurgie* 9 (1963) 92
- 13 — — LEIGHTON R S et PACIFICO L. Encefalografia con urea. *Bull. Sci. med.* 4 (1963) 493
- 14 — and SMALTING F. Appearance of the ventricular system 24 hours after encephalography. A preliminary report. *Acta radiol.* 53 (1960) 279
- 15 SHEALY N C and NEW P F J. Cerebrospinal fluid pressure changes in fractional pneumoencephalography without removal of cerebrospinal fluid. *Radiology* 81 (1963) 493
- 16 SLOSBERG P and BORNSTEIN M. Pneumoencephalography with minimal fluid. *Arch. Neurol. Psychiat.* 74 (1955) 334
- 17 — — and LICHTENSTEIN T. Pneumoencephalography with minimal withdrawal of cerebrospinal fluid. *J. Mt. Sinai Hosp.* 21 (1955) 299
- 18 ZIEDELDES ILANTES B G. Eine röntgenographische Methode zur separaten Abbildung bestimmter Teile des Objektes. *Fortschr. Röntgenstr.* 52 (1935) 69

In cerebellar and fourth ventricle tumours, the study of the cisterns alone can always indicate the site of the lesion in the posterior portion of the posterior fossa but not always its exact localization, i.e. in a cerebellar hemisphere, or in the midline. There is no doubt that greater experience in encephalography with a more profound knowledge of the encephalographic anatomy has greatly improved the diagnosis, but it might still be rather elaborate. The urea perfusion technique is useful also in these cases (Fig. 5), but sometimes only indirectly. If the administration of urea does not influence the filling of the fourth ventricle and aqueduct one might believe that this lack of filling is not due to a compression of these structures from an edematous cerebellar lobe but to their direct involvement by the tumour, which invades and obstructs the normal pathways between the subarachnoid space and the ventricular system.

Subtraction. The subtraction technique was first suggested by ZIFDZES DES PLANTIS (18). We have had only limited experience with it, but it seems as if this technique can be very useful in studying the cisterns around the occipital foramen.

Encephalography in vascular accidents. Encephalography has proved useful in cases of brain hemorrhage either traumatic or spontaneous, by demonstrating the presence of an intraventricular clot when a bilateral angiography is negative. In all patients in whom the angiographic study is negative, one should not hesitate to perform an encephalography even if they are in poor general condition, one is dealing, usually, with subjects under the control of the anesthesiologists and the examination can be carried out quickly, especially since a complete study is often unnecessary.

SUMMARY

The main aspects of the author's technique of fractional encephalography are described. With this technique the examination time is shortened and consequently the procedure is safer and better tolerated.

ZUSAMMENFASSUNG

Der Verfasser gibt einen Bericht über seine Technik bei fraktionierter Encephalographie mit welcher die Zeit der Untersuchung verkürzt werden kann und damit besser toleriert wird.

ATROPHIES DU VERMIS CÉRÉBELLEUX



Fig 1 Dilatation de la cistérne périvermienne sans insufflation des sillons vermiens (négative)
Fig 2 Image de lobulation impaire vermis cérébelleux postéro inférieure. Les vermes antérieurs sont sufflés et ne



Fig 3 Atrophies vermiennes corticales 1 Local et au culmen 2 Culmen et déclivité 3 Diffuse

que ces cas correspondent à une atrophie vermienne sous corticale. On ne peut pas partir de la nosographie des atrophies vermiennes proprement dites.

En dehors de ces cas nous disposons de 22 observations radio-recrutées parmi 3 035 pneumostratigraphies sagittales médianes de la base postérieure qui se divisent en trois groupes.

A. Les images d'atrophie vermienne corticale. Nos 17 observations de ce type se caractérisent par une dilatation des sillons vermiens et des cisternes vermiennes. On reconnaît parfaitement l'atrophie localisée à l'un ou à plusieurs ou à l'ensemble des lobules vermiens. Les corrélations radio-cliniques permettent de distinguer 3 formes (Fig 3).

ATROPHIES DU VERMIS CÉRÉBELLEUX

par

J THIEBAUT, A WACKENHEIM, C VROUSOS et M SUBIRANA

La nosographie des atrophies cérébelleuses est très complexe et peu précise. Les neuro pathologistes distinguent de nombreuses formes dont certaines n'ont que des caractères microscopiques.

La pratique de l'encéphalographie gazeuse a conduit à des conclusions souvent erronées basées uniquement sur l'accumulation de grande quantité d'air dans la fosse postérieure. La pneumostratigraphie sagittale médiane de la fosse postérieure, telle que nous la pratiquons depuis 1958 permet de préciser ces images et de distinguer celles qui correspondent réellement à une réduction volumétrique du parenchyme vermien, avec dilatation pathologique des sillons. On connaît par contre beaucoup d'observations d'états malformatifs que nous avons décrits ailleurs, à savoir l'image de mégaciterne (Fig 1) caractérisée par une dilatation de la grande citerne sans représentation des sillons vermiens, l'image de lobulation vermienne imparfaite (Fig 2) caractérisée par la présence de sillons vermiens antérieurs normaux avec absence de sillons vermiens postérieurs et l'image de cervelet infantile caractérisé par son petit volume et sa morphologie harmonieuse.

Dans ce travail nous n'avons pas tenu compte des dilatations du IV^e ventricule qui s'inscrivent dans le cadre d'une dilatation ventriculaire diffuse. Bien

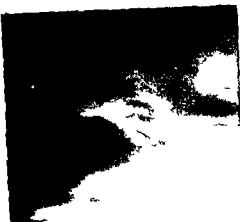


Fig. 7 Atrophie vermiennne cortico-sous corticale de l'enfant

B. *Les images d'atrophie vermiennne cortico sous corticale de l'adulte* Dans nos 2 cas de ce groupe il existe d'une part une dilatation des sillons vermiens et d'autre part une nette dilatation du IV^e ventricule (Fig. 7) Un syndrome cérébelleux n'existe que dans l'un de ces deux cas

C. *Les images d'atrophie cortico sous corticale de l'enfant* (Fig. 8) Dans nos trois observations nous relevons une formule pneumostratigraphique tout a fait superposable Les anomalies sont tres caractéristiques et se distinguent nettement de celles de l'adulte Il existe en effet

- 1 Une forte dilatation du IV^e ventricule dont le toit est arrondi
- 2 Une dilatation des sillons vermiens cette dilatation quoique nette est toutefois moins accusée que la dilatation du IV^e ventricule
- 3 La réduction du parenchyme vermien predomine sur le vermis postero inferieur contrairement aux formes de l'adulte qui predominent sur le vermis antero-supérieur Chez l'enfant la region flocculo nodulo uvulaire est reduite a une mince languette opaque

Cliniquement il existe un syndrome cerebelleux statique cinétique et progressif dans les trois cas

RÉSUMÉ

Les auteurs étudient 22 observations radio-cliniques d'atrophie localisée au vermis cérébelleux. Grâce à leur technique de pneumostratigraphie sagittale médiane de la fosse postérieure ils distinguent 3 grands groupes d'images d'atrophie vermiennne à savoir l'atrophie vermiennne corticale localisée ou diffuse l'atrophie vermiennne cortico-sous-corticale de l'adulte et l'atrophie vermiennne cortico-sous-corticale de l'enfant. Les auteurs étudient ensuite les corrélations radio-cliniques dans ces trois groupes de cas.



Fig 4 Atrophie vermiennne corticale localisée au culmen



Fig 5 Atrophie vermiennne corticale localisée au culmen et declive



Fig 6 Atrophie vermiennne corticale diffuse (a) et cortico sous corticale de l'adulte (b)



1 *Atrophie localisée à un lobule* (7 cas) Cette anomalie relativement fréquente est cliniquement asymptomatique (Fig 4)

2 *Atrophie vermiennne supérieure* (culmen et declive 5 cas) Elle s'accompagne d'une nette dilatation du sillon transverse antérieur. Ces atrophies (Fig 5) relativement étendues s'accompagnent ou non d'une symptomatologie clinique de type cérébelleux. Sur nos 5 malades de ce groupe, 3 présentent un syndrome cérébelleux à prédominance statique

3 *Atrophie vermiennne diffuse* (Fig 6) caractérisée par une nette dilatation de tous les sillons vermiens (5 cas). Ces malades présentent tous un syndrome cérébelleux statique et cinétique

FROM THE SURGICAL DEPARTMENT II JUTENDO UNIVERSITY SCHOOL OF MEDICINE,
HONGO, TOKYO JAPAN

DIAGNOSIS OF INTRACRANIAL HEMORRHAGE USING ULTRASOUND

by

YUICHI ABE KENJI TANAKA TOSHIO WAGAI and KAZUFUMI ITO

Ultrasound has recently been remarkably developed and advanced in various fields especially in industry and at the same time medical application of ultrasound has been acquiring status as a diagnostic and surgical tool

Since 1931 we have been applying the echo method for the diagnosis of various intracranial diseases especially brain tumor and the present authors have since 1953 been successful in achieving early diagnosis of intracranial hemorrhage

It is difficult but very important accurately to differentiate hypertensive intracerebral hemorrhage from other forms of stroke in order to decide between conservative management or surgical treatment This is especially important since angiography is usually inevitable for the differential diagnosis of hypertensive intracerebral hemorrhage brain softening and subarachnoid hemorrhage We have found the ultrasonic echo method to be more advantageous for this purpose than the ordinary neurologic examination This is especially true as the technique is quick and easily performed without harm to the patient

SUMMARY

Twenty two radioclinically established cases of atrophy of the vermis cerebelli have been studied by a special technique of sagittal median stratigraphy of the posterior fossa. It was possible to distinguish three main groups: cortical atrophy either localised or diffuse; cortico-subcortical atrophy in adults; and cortico-subcortical atrophy in children. Radioclinical correlations between these three groups were also studied.

ZUSAMMENFASSUNG

Es wurden 22 röntgenologisch und klinisch gesicherte Fälle von Atrophie des vermis cerebelli mittels einer Spezialtechnik von sagittaler medianer Stratigraphie der Hinteren Schädelsgrube studiert. Es war möglich drei Hauptgruppen zu unterscheiden: Cortikale Atrophie lokal oder diffus; corticosubcorticale Atrophie bei Erwachsenen und cortico-subcorticale Atrophie bei Kindern. Es wurden ebenfalls die Korrelationen zwischen diesen drei Gruppen studiert.

BIBLIOGRAPHIE

- LEMAIRE J. Contribution à l'étude des atrophies cérébelleuses par la pneumostratigraphie sagittale médiane de la fosse postérieure. Thèse de Médecine, Strasbourg 1964.
- SUBIRANA M. et VROUSOS C. Pneumostratigraphie frontale des hémisphères cérébelleux. J. Radiol. Électrol. 45 (1964) 225.
- THIÉBAUT F., WACKENHEIM A. et VROUSOS C. Le diagnostic radiologique des différentes variétés de hernie amygdalienne dans le trou occipital par la pneumostratigraphie médiane. Rev. neurol. 104 (1961) 548.
- — — Radioanatomie de l'insula en pneumostratigraphie horizontale. J. Radiol. Électrol. 44 (1963) 463.
- — — Pneumostratigraphie sagittale médiane de la fosse postérieure. Acta radiol. Vol. 1 (1963) 638 (On trouvera toute la bibliographie complète jusqu'à 1961).
- — — Radioanatomie normale et pathologique des cisternes du tronc cérébral supérieur en pneumostratigraphie. Ann. Radiol. 7 (1964) 211.
- WACKENHEIM A. et VROUSOS C. La cisterna prébulbaire. Radioanatomie pneumographique normale et modifications dans les processus expansifs extra-cérébraux prébulbaires. Ann. Radiol. 6 (1963) 95.
- — et SUBIRANA M. Le diagnostic radiologique des cavités kystiques cervico-bulbaires non communicantes. J. de Neuro-radiologie de Strasbourg (1963).

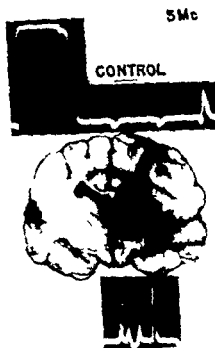


Fig. 2 Intracerebral hematoma in a cat. Continuous sharp echo.

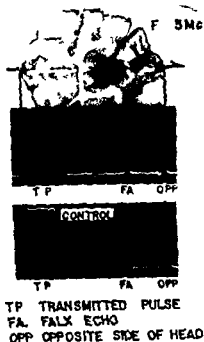


Fig. 3 Brain softening in a cat. No echo.

Extracerebral hematomas were made by injecting blood coagulum into the epi- and subdural space of a cat. The echo from the hematoma can be detected by using ultrasound at 5 megacycles per second. On the other hand, in the case of an intracerebral hematoma made by injecting 0.1 or 5 ml of blood coagulum into the hemisphere of a cat's brain, the echo from the hematoma shows a characteristic pattern which consists of continuous sharp echo similar to hypertensive intracerebral hemorrhage (Fig. 2). On the contrary, in the case of brain softening made by injecting 5% agar into the internal carotid artery of the cat, these echoes were not observed (Fig. 3).

In addition to the analysis of the echoes, the measurements of ultrasonic attenuation in brain tissue are very important. For example, it is found clinically that patients who are in the stage of brain edema have the highest level of ultrasonic attenuation. For detection of ultrasonic attenuation in brain tissue and blood, the heat production in these samples due to irradiation of ultrasound was measured. It was found that the ultrasonic attenuation in blood was smaller than in meningioma. The transmission and reflection method

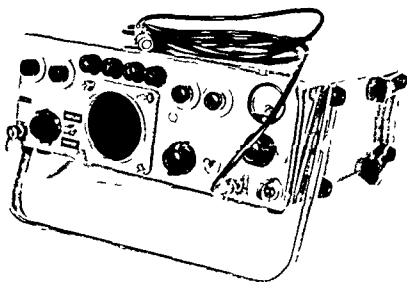


Fig. 1 Ultrasonic apparatus from Japan Radio Co. Aloka model SSD 2

Apparatus The standard ultrasonic apparatus (Aloka model SSD 2, Japan Radio Co) was used with an adapted camera (Fig. 1). The echoes were displayed on the Braun tube by A scope indication. Being portable, the instrument may be carried to the bedside and plugged into the main electrical supply.

The transducers used were barium titanate (1 and 2.25 megacycle) and piezoelectric quartz crystal (5 and 10 megacycle). The following types of probes were used: 1 and 2.5 megacycle 10 mm in diameter, for the examination through the intact skull; 5 and 10 megacycle 10 mm in diameter for direct application on the brain.

Experimental studies

The acoustic velocity for brain tissue was found to be 1460 m/sec, and for blood 1560 m/sec. Fresh human blood and brain tissue show an acoustic impedance of 1660 g/cm²/sec and 1510 g/cm²/sec respectively. The velocity in glioma tissue is 1600–1660 m/sec. Thus it is theoretically possible that the border between brain tissue and blood will cause an acoustic reflection. This possibility could also be demonstrated in animal experiments.

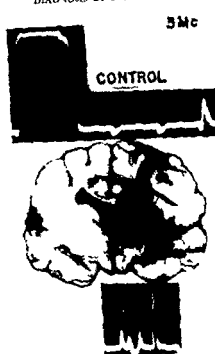


Fig 2 Intracerebral hematoma in a cat. Control shows sharp echo.

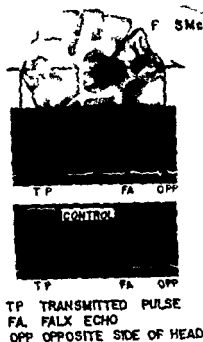


Fig 3 Brain softening in a cat. No echo.

Extracerebral hematomas were made by injecting blood coagulum into the *epi* and subdural space of a cat. The echo from the hematoma can be detected by using ultrasound at 5 megacycles per second. On the other hand, in the case of an intracerebral hematoma made by injecting 0.1 or 5 ml of blood coagulum into the hemisphere of a cat's brain, the echo from the hematoma shows a characteristic pattern which consists of continuous sharp echo similar to hypertensive intracerebral hemorrhage (Fig 2). On the contrary, in the case of brain softening made by injecting 5% agar into the internal carotid artery of the cat, these echoes were not observed (Fig 3).

In addition to the analysis of the echoes, the measurements of ultrasonic attenuation in brain tissue are very important. For example, it is found clinically that patients who are in the stage of brain edema have the highest level of ultrasonic attenuation. For detection of ultrasonic attenuation in brain tissue and blood, the heat production in these samples due to irradiation of ultrasound was measured. It was found that the ultrasonic attenuation in blood was smaller than in meningioma. The transmission and reflection method

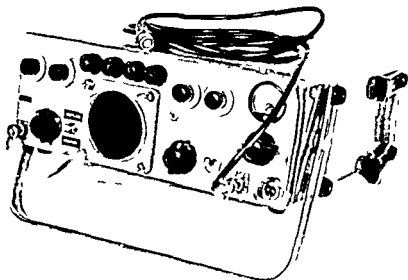


Fig. 1 Ultrasonic apparatus from Japan Radio Co. Aloka model SSD 2

Apparatus The standard ultrasonic apparatus (Aloka model SSD 2, Japan Radio Co) was used with an adapted camera (Fig. 1). The echoes were displayed on the Braun tube by A scope indication. Being portable, the instrument may be carried to the bedside and plugged into the main electrical supply.

The transducers used were barium titanate (1 and 2.25 megacycle) and piezoelectric quartz crystal (5 and 10 megacycle). The following types of probes were used: 1 and 2.5 megacycle 10 mm in diameter, for the examination through the intact skull; 5 and 10 megacycle 10 mm in diameter for direct application on the brain.

Experimental studies

The acoustic velocity for brain tissue was found to be 1460 m/sec, and for blood 1560 m/sec. Fresh human blood and brain tissue show an acoustic impedance of 1660 g/cm²/sec and 1510 g/cm²/sec respectively. The velocity in glioma tissue is 1600–1660 m/sec. Thus it is theoretically possible that the border between brain tissue and blood will cause an acoustic reflection. This possibility could also be demonstrated in animal experiments.

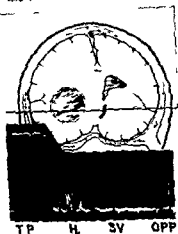


Fig 6 Case 2 1 transcranial hemorrhage Irregularly grouped echors H = H matoma echoes



Fig 7 [Case 3 Brain softening & abnormal echoes

of a shift of the third ventricle is useful for screening while the detection of the hematoma echo is necessary for the diagnosis of intracranial hematoma. The sharp bottom echo of the hematoma is detected either by the examination from the same side as the lesion, or from the opposite side of the lesion (Fig 4). The ultrasonic attenuation increases on the hematoma side as compared with the normal side of the head.

Case 1 A 58-year-old male who had had a head injury four months prior to admission was admitted in a state of coma with right hemiplegia. At the neurologic examination the deep reflexes on the right were exaggerated and Babinski's sign was positive on the right side. Right hemiplegia and bilateral choked optic discs were noted.

At the ultrasonic examination through the right temporal region the third ventricle echo was shifted to the right and the sharp echo from the hematoma was observed just before the opposite side of the head (Fig 5). Left carotid angiography showed displacement of the pericallosal artery to the right side and an avascular area in the left parieto-temporal region. A subdural hematoma was evacuated from the left parieto-temporal region.

Ultrasonic examination was performed on 369 cases with head injuries, and out of 38 cases of extracerebral hematoma 35 cases were correctly diagnosed (26 out of 27 subdural hematomas, both cases of subdural hygroma and 7 out of 9 epidural hematomas).

In the postoperative follow-up observation of these cases the return of the displaced third ventricle echo to the normal position can be observed. It

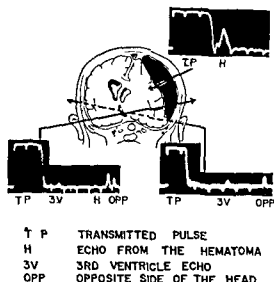


Fig 4 Intracerebral hematoma. The sharp bottom echo of the hematoma was detected by examination from both sides

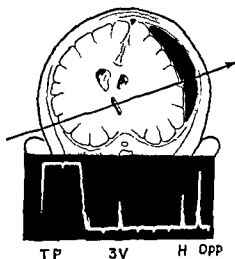


Fig 5 Case 1 Extracerebral hematoma

of ultrasonic pulse was used for the detection of ultrasound attenuation in the clinical studies

The experimental studies of the characteristics of hematoma echoes were performed as follows

The samples given below were put into a beaker 4 cm in diameter: 1) Degassed water, 2) blood with heparin, 3) blood with brain fragments, 4) blood containing heparin and brain fragments, 5) blood containing coagula and brain fragments. The samples were then examined with a transducer of 5 megacycles, 10 mm in diameter.

Except for the degassed water, continuous sharp echoes from the samples, especially in the case of blood including brain fragments, were observed. On the other hand, no special echoes were observed in the case of degassed water. It was clear, experimentally, that the echoes from the hematoma were influenced by brain fragments included in the hematoma.

Clinical studies

Diagnosis of extracerebral hematoma

A shift of the third ventricle echo does not always prove the presence of a hematoma because the shift of this echo can also be caused by unilateral edema, hygroma and tumor. Furthermore, in the case of bilateral hematoma, a shift of the third ventricle echo could not be observed. Thus, the observation

Examination of brain softening

Case 3 A 66-year-old male was admitted with delirium and mental change. Neurologic examination revealed a hypnotic male with disorientation, emotional instability, and nuchal rigidity. The deep reflexes were exaggerated, and Hoffman's sign was positive on the left side. Lumbar puncture revealed an initial pressure of 150 mm of water with xanthochromia.

At the ultrasonic examination, abnormal echoes were not disclosed in either of the frontal regions and the third ventricle echo was not displaced. The attenuation of ultrasonic energy in brain tissue was normal (Fig. 7). Multiple softening in the frontal lobe was disclosed at autopsy.

In the case of brain softening and subarachnoid hemorrhage, neither an abnormal echo nor a shift of the third ventricle echo were observed; these conditions show a normal level of ultrasonic attenuation in most cases.

Ultrasonic examination was performed in 108 cases with so-called apoplexy, including hypertensive intracerebral hemorrhage, brain softening, and subarachnoid hemorrhage. The ultrasonic diagnosis was intracranial hemorrhage in 41 patients, brain softening in 60, and subarachnoid hemorrhage in 7 (see tabulation below). In the patients with intracerebral hemorrhage, the ultrasonic echogram showed clear evidence of the lesion.

	Ultrasonic diagnosis	Clinical diagnosis
Subarachnoid hemorrhage	7	8
Brain softening	60	57
Cerebral hemorrhage	41	31
So-called apoplexy		12

The ultrasonic characteristics of hematoma echoes were examined with a transducer of 5 megacycles/sec on the dura mater. The hematoma echo reveals a characteristic continuous sharp echo, while a tumor echo is observed as a continuous irregular echo.

The writers confirmed clinically that the hematoma echo is basically different from the tumor echo (Fig. 8).

Conclusions

In patients with extracerebral hematoma, a shift of the third ventricle echo to the opposite side of the lesion is observed together with a hematoma echo. Usually the sharp bottom echo of the hematoma is detected by the examination from the opposite side of the lesion.

In intracerebral hemorrhage, an abnormal echo from the hemorrhage is observed as a characteristic continuous sharp echo and can be differentiated from tumor echoes which are characterized by continuous irregular echoes.

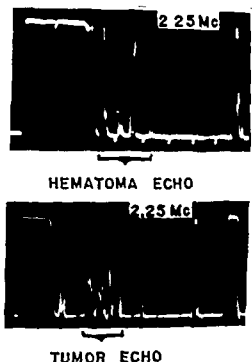


Fig. 8. Difference between hematoma and tumor echo.

took 1 to 4 weeks after the evacuation of the extracerebral hematoma for the echo to return to normal. Thus, a continuous observation of the third ventricle echo is very useful for the postoperative management of intracranial hematoma.

Diagnosis of intracerebral haemorrhage

Case 2. A 52-year-old male was admitted in a state of semi-coma with right hemiplegia. He had had sudden attacks of unconsciousness thereafter vomiting had begun. At the same time he noted weakness in the right arm and leg which was slowly progressing. At the neurologic examination right hemiplegia and exaggeration of the deep tendon reflexes on the right was noted and Babinski's sign was positive bilaterally. Lumbar puncture revealed an initial pressure of 200 mm of water and the cerebrospinal fluid was xanthochromic.

At the ultrasonic examination the third ventricle echo was shifted to the right about 10 mm and the ultrasonic attenuation was increased on the left side. The abnormal echoes were detected 3 to 6 cm inside the left fronto-temporal region. There were irregularly grouped echoes (Fig. 6). Under local anesthesia the blood coagulum was evacuated in the fronto-temporal region.

The present writers thus confirmed that the ultrasonic findings of intracerebral hemorrhage were as follows: 1) detection of an intracerebral abnormal echo, 2) shift of the third ventricle echo, (3) increase of ultrasonic attenuation.

- JEFFSON S Echo-encephalography III *Acta chir scand* 119 (1960) 455
- KIKUCHI Y UCHIDA R TANAKA K and WAGAI T Early cancer diagnosis through ultrasonics *J acoust Soc Amer* 29 (1959) 824
- LEKSELL L Echo-encephalography I *Acta chir scand* 110 (1955/56) 301
- Echo-encephalography II *Acta med scand* 115 (1958) 255
- LITHLANDER B The clinical use of echo-encephalography *Acta psychiat scand* 35 (1960) 241
- TANAKA K Ultrasonic diagnosis of brain tumor *Nolt* January 1967
- and ITO K Ultrasonic diagnosis of intracranial diseases *Recent Advances in Research on the Nervous System* 7 (1963) 335
- KIKUCHI Y and UCHIDA R Ultrasonic diagnosis of brain tumor *Proc Third International Congress Acoustics* p 1191 Stuttgart 1959
- — Ultrasonic diagnosis of intracranial diseases *Proc Surg Soc Japan* 53 (1953) 242
- ITO K and ISHIKAWA S Ultrasonic diagnosis of brain tumor (Japanese) *Medicine* 18 (1961) 297
- — and UEMATSU S Ultrasonoechography in children (Japanese) *J pediat Practice* 25 (1962) 976
- et coll Diagnosis of brain tumors using ultrasound (Japanese) *Japan J clin Med* 21 (1963) 2195
- TAYLOR J C NEWELL J A and HARVOLDIS P Ultrasonics in the diagnosis of intracranial space-occupying lesions *Lancet* 3 (1961) 1197

In brain softening and subarachnoid hemorrhage on the other hand, an abnormal echo and a shift of the third ventricle is not observed.

In addition to the analysis of the echoes, observation of the degree of ultrasonic attenuation in the brain, especially on the hematoma side, is very important. From this standpoint, extra and intracerebral hematomas are characterized by an increase in the ultrasonic attenuation. Brain softening and subarachnoid hemorrhage, on the other hand, have a normal level of ultrasonic attenuation in most cases.

The ultrasonic examination is useful for quick diagnosis of extracerebral hematoma in patients with head injury and for the differential diagnosis of apoplexy.

SUMMARY

The clinical value of ultrasonic diagnosis in intracranial hemorrhage is discussed. The ultrasound equipment used was the Aloka model SSD 2 manufactured by the Japan Radio Co. Ultrasonic examination is useful for a rapid diagnosis of extracerebral hematoma in patients with head injury and in the differential diagnosis from apoplexy.

ZUSAMMENFASSUNG

Es wird über den klinischen Wert der Ultraschalldiagnose bei intrakraniellen Blutungen berichtet. Es kam das Aloka Modell SSD 2 hergestellt von der Japan Radio Co. zur Verwendung. Ultraschalluntersuchung ist wertvoll für die rasche Diagnosestellung von extracerebralen Hämatomen nach Schädelverletzungen und in der Differentialdiagnose gegenüber Apoplexie.

RÉSUMÉ

Ies auteurs montrent l'intérêt clinique de l'examen par les ultrasons dans les hémorragies intracranienues. L'appareil utilisé est le modèle Aloka SSD 2 fabriqué par la Japan Radio Co. L'examen par les ultrasons est utile pour le diagnostic rapide des hématomes extracérébraux chez les traumatisés crâniens et pour le diagnostic différentiel avec l'apoplexie.

REFERENCES

- BRAAK J. W. G. ter, GRANDIA W. A. M. and VLIJECER M. de. Echo encephalography as an aid in the diagnosis of subdural and extradural hematomas. Recent neurological research. Elsevier Amsterdam 1959 p. 37.
- FORD R. and AMBROSE J. Echoencephalography. The measurement of the position of midline structures in the skull with high frequency pulsed ultrasound. Brain 86 (1963) 189.
- CORDON D. Echo encephalography — ultrasonic rays in diagnostic radiology. Rev. neurof. 99 (1958) 652.
- Echoencephalography. Brit. med. J. 1 (1959) 1500.

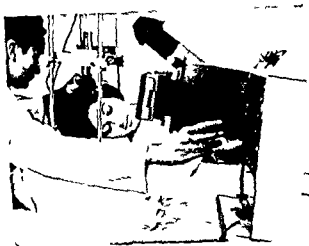


Fig. 1 Method of examination showing mechanical scanning bridge which holds and moves the transducer on the patient's head. The technician guides the direction of the transducer to permit good acoustic contact during the entire scanning period.

The purpose of this paper is to illustrate our techniques and early experience with a simple 'B' scanning in patients with intracranial masses.

Description of the system The technical details are not within the scope of this paper. The system involves the production of an ultrasonic pulse (1 to 2 mc/sec frequency) from a piezoelectric crystal which is transmitted through the skull by a transducer. A water or glycerine coupling medium between the transducer probe and the skull provides acoustic contact. The reflected echoes are received by the same transducer and are then amplified electronically and displayed on the cathode ray tube as many bright spots.

The A scan presents a one dimensional evaluation of echoes which can be used to determine the position of the interfaces of tissue structures such as the midline of the brain.

For B scanning the transducer is coupled to a mechanical scanning bridge which moves it over the surface of the skull (Fig. 1). The scanning bridge also moves the point of the cathode ray tube trace over a path which is linked to the movement of the transducer. The echo signals received by the transducer and displayed on the cathode ray tube are intensity modulated so that the echoes appear on the oscilloscope face as spots whose brightness is proportional to echo strength rather than height of pulse. The echoes are recorded in their proper geometrical relationship by making a photographic record of the cathode ray tube during the entire scanning.

'B' SCAN ENCEPHALOGRAPHY

by

B D ADAPON, N E CHASE, I I KRICHIEFF and A F BATTISTA

The use of ultrasonic acoustic waves to demonstrate the structure of biological tissues is well known (21). The principles are roughly similar to those of marine sonar equipment used for detection of submarines.

WILD delineated the structure of bowel segments by means of ultrasound in 1950 (20). Since then, various modifications of the pulse echo have been used to delineate normal and abnormal body structures including the localization of gall stones, soft tissue tumors, ocular foreign bodies, renal, hepatic, uterine, breast and pelvic tumors (2, 4, 8, 9, 10, 11, 17, 22). These examinations required the immersion of the parts being studied in a fluid containing chamber or the use of a water containing plastic bag for the adequate functioning of the system. HOLMES & HOWRY (9) using elaborate equipment have constructed a compound circular 'B' scanning system that gives differential echo images of the neck, extremities and abdominal structures.

In the brain, the application of the ultrasound pulse for diagnosis has been limited to the localization of the midline structures (1, 5, 7, 13, 15). This 'A' scanning has also been extended by other investigators to the study of abnormal pulses by intracranial masses such as subdural hematomas and ventricular size (3, 16, 18, 19). TANAKA, KIKUCHI and others (6, 14), obtained differential echo images in brain masses during operation and in pathological specimens.

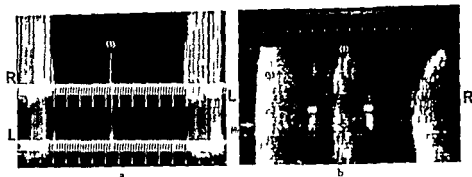


Fig 3 Normal scans a) Sample A scan for detection of midline structures obtained by conventional method with stationary transducer (1) Midline (3) skull tables b) Normal B scan obtained with moving transducer (see fig 2) demonstrates cross section or tomogram of brain at level of scanning (1) Midline echo (2) lateral ventricles (choroid plexus) (3) skull tables (4) level of external auditory meatus

60 were proven to have intracranial expansive lesions and the remainder (67) were diagnostically negative after all investigations

The classification and location of the intracranial expansive lesions (60 cases) are given below

	Not demonstrated	Demonstrated	
		Indirect	Direct
Subdural hematomas	5	5	1
Intracerebral hematomas	1	4	
Pituitary tumors	1		1
Hypophyseal tumors	1	1	2
Multiple masses	2	3	2
Supratentorial tumors			
Anterior frontal		4	1
Sphenoidal	4	3	2
Infratentorial		3	3
Retrolental	1		1
Thalamic and deep frontal		1	3
Hydrocephalus	1		4
Totals	16 (26.6%)	24 (40%)	20 (33.4%)

There were 11 subdural hematomas 5 intracerebral hematomas 5 meningiomas 21 gliomas 7 multiple masses, 4 hypophyseal tumors and 2 infratentorial lesions

The intracranial lesions were demonstrated by B scan tomography either directly or indirectly in 44 patients (73.4%). The B scan failed to demonstrate a mass in 16 (26.6%) although all of these cases had displaced midline

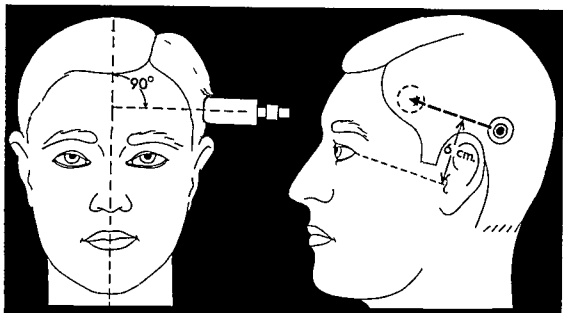


Fig 2 Diagrammatic sketch of transducer pathway on patient's head. Reference mark at level of external auditory meatus.

Method of examination The patient is placed in the decubitus position and the transducer probe is applied along a line drawn on the occipitotemporal frontal region 6 cm above the canthomeatal line (Fig 2). The transducer is moved from posterior to anterior and the tracing is marked at the level of the external auditory meatus. The speed of the probe is usually 2.5 cm/sec, which is regulated by the motorized transducer holder. The direction in which the transducer is aimed may be adjusted up to 30° from the vertical. This aids in obtaining a proper beam entrance and good acoustical contact along irregular contours.

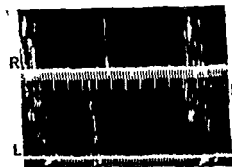
Paired tracings are obtained on both sides of the skull and the tracings are photographed with the Polaroid Land Camera (Fig 3).

In some cases the transducer path is 5 or 7 cm from the canthomeatal line depending on the presumed level of tumor clinically.

Clinical material and results

A total of 127 patients were studied. There were 41 females and 86 males with ages from 1 month to 80 years with a mean age of 40.5 years. All patients had conventional neuroradiologic diagnostic procedures (encephalography or cerebral angiography) and/or surgical exploration or autopsy examination,

Fig 7 a) Acute subdural hematoma in right temporo-parietal frontal convexity in a 38 year-old male b) A scan Midline shift right to left 7 mm c) B scan Absence of echoes in the right frontotemporal convexity and displacement of lepton meninges by subdural collection



echoes in the A scan. There were five false positives. 2 had the appearance of subdural hematomas and 3 had displaced lateral echoes on one side only. These cases proved to be normal except for one with diffuse cerebral atrophy.

Echographic findings The space occupying lesions may be detected by direct sonic demonstration of the mass (23) or by indirect signs. The former may occur in two ways:

1. The lesion may reflect more sound than the normal tissue echo background (Fig 4). In addition, abnormally directed echoes may be observed. We believe that the abnormal cluster of echoes is produced by the multiple tissue interfaces of the mass with polarity that varies from the surrounding normal brain tissue.

2. Other lesions reflect less sound than the normal tissue background and may appear as a 'hole' or less dense area of echoes (Fig 5).

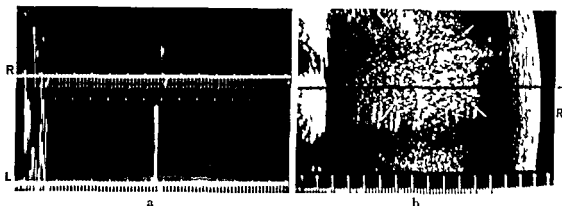


Fig 4 Direct positive demonstration on a 49 year old male with large posterior frontal parietal glioblastoma a) A scan Midline shift right to left 3 mm b) B scan Abnormal cluster of echoes with different echo polarity in region of tumor

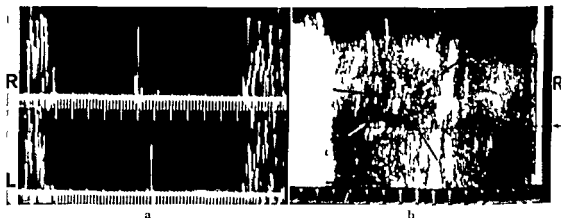


Fig 5 Direct negative demonstration of left deep fronto thalamic glioblastomas in a 37 year old female a) A scan Midline shift left to right 5 mm b) B scan Spherical area of tumor with displaced strong midline echo

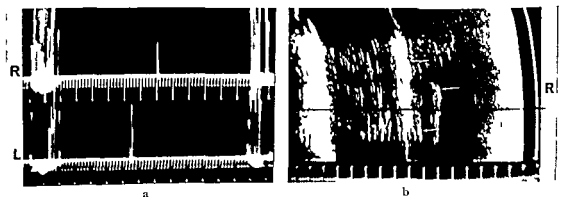


Fig 6 Indirect demonstration of deep temporo thalamic intracerebral clot in a 40 year old male a) A scan Midline shift right to left 7.5 mm b) B scan Lateral and midline echoes markedly displaced towards left



Fig 9 B scan tomogram superimposed on horizontal cross-section of the brain specimen scanned demonstrating the various midline structures that may give rise to the midline echo. Strong midline echoes from anterior and posterior portions of interhemispheric fissure, the third ventricle and fornix septum pellucidum, strong echoes from the insula.

Discussion

The oscillographic display of reflected echoes from tissue interfaces depends upon the acoustic impedance of the reflecting substance and the angle of incidence of the sound beam (12). Tissue interfaces with large changes in acoustic impedance may reflect enough of a differential echo to permit these interfaces to be identified.

Also following the law of reflection, the greatest amount of ultrasonic echoes will be picked up when the sound strikes tissue interfaces at right angles. A differential echo pattern will thus be shown when the abnormal masses are disposed perpendicular to the ultrasound beam. Unfortunately, the axes of the different tumor masses studied were not always perpendicular to the main axis of the transducer beam because at the present time the transducer pathway is limited to 1 or 2 levels of cross section. This is due to the difficulty in obtaining good acoustic linkage at higher or lower levels on the skull.

For example, among the gliomas, the frontal and low supratentorial masses were picked up readily. The main axis of the tumor bulk in these locations is



Fig 8 From infant with hydrocephalus secondary to aqueductal stenosis a) A scan Midline shift left to right 4 mm b) B scan Huge lateral ventricles seen left greater than right

Indirectly, the tumor may be demonstrated by the displacement or obliteration of normal tissue structures (Fig 6). Echoes may be either the strong midline echo shifted to one side or the more laterally placed echoes from the insula being absent or shifted medially or laterally.

In cases with subdural hematoma (see Fig 7) the displacements of the leptomeninges by an accumulation of clot may be demonstrated. Unfortunately, the immediate 8 to 10 mm beneath the inner table of the ipsilateral side of the skull is masked by the main bang of echoes arising from the cranial vault. For this reason only subdural hematomas over 1 cm in thickness could be demonstrated.

Enlarged lateral ventricles were noted directly in 5 patients with hydrocephalus. The echo failed to demonstrate enlarged ventricles in one case. The reason for this is not clear. The enlarged ventricles are seen as areas of echo lack in an otherwise normal tissue background (Fig 8). The lateral echoes are also correspondingly displaced.

Source of normal echoes Normal formalized brain specimens were scanned with techniques as nearly similar to those used in living subjects as possible. In Fig 9, the resulting B scan is superimposed on the horizontal cross section of the brain at the level of scanning. Strong echoes are seen reflected from the midline structures as well as the insula and portions of the lateral ventricles. It can be seen that the strong and constant midline echo originates from different structures in the midline, normally the anterior and posterior portions of the interhemispheric fissure, the third ventricle and the septum pellucidum. Thus, the echo source can vary according to the placement of the transducer probe and the shape of the skull.

- 4 DONALD I MACVICAR J and BROU N T Investigation of abdominal masses by pulsed ultrasound *Lancet* 1 (1958) 1188
- 5 FORD R and AMBROSE J Echoencephalography measurement of position of midline structures in the skull with high frequency pulsed ultrasound *Brain* 86 (1963) 189
- 6 FRENCH L WILD J and NEAL D Experimental application of ultrasound for localization of brain tumors *J Neurosurg* 8 (1951) 198
- 7 GORDON D Echoencephalography Ultrasonic rays in diagnostic radiology *Brit med J* 1 (1959) 1500
- 8 HAYASHI S WAGAI T and MAYAZOWA R Ultrasound diagnosis of breast tumors and cholelithiasis *West. J Surg* 70 (1962) 34
- 9 HOLMES J and HOWRY D Ultrasonic diagnosis of abdominal diseases *Amer J dig Dis* 8 (1963) 12
- 10 HOWRY D H and BLISS W R Ultrasonic visualization of soft tissue structures of the body *J Lab clin Med* 40 (1953) 579
- 11 — STOTT D A and BLISS W R Ultrasonic visualization of carcinoma of the breast and other soft tissue structures *Cancer* 7 (1954) 354
- 12 HUETER T and BOLT R *Sonics* (N.Y.) 38 (1955) 65
- 13 JEPSON S The midline echo An evaluation of its usefulness for diagnosis of intracranial masses and its source *Acta chir scand Suppl* 272 (1961)
- 14 KIKUCHI Y and TANAKA K Intracranial masses by pulsed ultrasound *J acoust Soc Amer* 29 (1957) 824
- 15 LEKSELL L Echoencephalography Detection of intracranial complications following head injury *Acta chir scand* 110 (1955) 301
- 16 LITHANDER B Origin of echoes in the echoencephalogram *J Neurol Neurosurg Psychiat* 24 (1961) 22
- 17 OKSALA A and LEHTINEN A The use of the echogram in the localization and diagnosis of intraocular foreign bodies *Brit J Ophthal* 43 (1959) 744
- 18 TANAKA K, KIKUCHI Y and UCHIDA R Detection of intracranial diseases by ultrasound *J Jap surg Soc* 54 (1953) 242
- 19 VILIEGER M and RIDDER H Use of echoencephalography *Neurology* 9 (1959) 216
- 20 WILD J J The use of ultrasonic pulses for the measurement of biologic tissues and the detection of density changes *Surgery* 27 (1950) 161
- 21 — and RETZ J The application of echo ranging techniques in the determination of biologic tissues *Science* 115 (1952) 226
- 22 — — Further pilot echographic studies on the histological structures of tumors of the living human breast *Amer J Path* 28 (1952) 839
- 23 — — Progress in techniques of soft tissue examination *Ultrasound in Biology and Medicine* (Ed by E Kelley) p 30 Waverly Press Baltimore Md 1957

approximately perpendicular to the transducer pathway. The parasagittal and high convexity tumors as well as the low lying temporal masses were not demonstrated because they were centered above or below the line of scan. These masses are only seen indirectly i.e. in the degree they displace normal tissues.

Acknowledgements

This work was supported in part by the New York City Health Research Council Contract No. U 1175 and in part by the National Institutes of Health (National Institute for Neurological Diseases and Blindness) Contract No. 5433 01. It would not have been possible without the hard work and cooperation of Mr. Ralph Majoral and Mr. Ramon Santana.

SUMMARY

Sixty patients with various types of intracranial masses were subjected to A and B scanning. Forty-four of them showed abnormal echographic findings on the B scan either directly or indirectly and in 16 the lesion could not be observed by B scanning although the midline displacement was noted in the A scan.

ZUSAMMENFASSUNG

Sechzig Patienten mit verschiedenen Typen von intrakraniellen Tumoren wurden mittels A und B Scintillographie untersucht. Vierzig davon zeigten im B Scintillogramm einen normalen echographischen Befund, entweder direkt oder indirekt. Bei 16 Patienten konnte keine Veränderung im B Scintillogramm gefunden werden, obwohl eine Seitenverschiebung im A Scintillogramm vorhanden war.

RÉSUMÉ

Soixante malades atteints de diverses tumeurs intracrâniennes ont été examinés par les explorations A et B. Quarante quatre d'entre eux ont présenté des signes échographiques anormaux sur l'examen B, directement ou indirectement et seize n'ont pas présenté de signe de leur lésion sur l'examen B, bien que l'examen A montrait un déplacement de la ligne médiane.

REFERENCES

1. AMBROSE J. Pulsed ultrasound. Illustrations of clinical significance. *Brit. J. Radiol.* 37 (1964) 165.
2. BAUM G. and GREENWOOD I. Orbital lesion localization by 3 dimensional ultrasonography. *N.Y. St. J. Med.* 61 (1961) 414.
3. BRAAK J. W. ter CREZEE P. GRANDIA W. and VLIJCKER M. Significance of some reflections in echo encephalography. *Acta neurochir.* 9 (1961) 382.



Fig 1 Position of patient and probes for recording at start of injection

of the material as it passes through the torcula. In the more recent observations the two probes have been positioned for a series of three injections (Fig 2b). The standard positions are: 1) The timing of the event which is obtained in the standard carotid innom position; 2) The second recording is made with one probe centered over the midline at a fixed distance anterior to the innom; 3) The final measurement is made over the carotid on a 3 cm center so that it is possible to obtain a carotid input velocity and a jugular output velocity. It is necessary to use more than one injection because of the inability to obtain more probes at present. We are able to obtain through this group of curves an appreciation of average velocities and to relate these to specific times in the entire event.

Results

If velocity measurements are made in a normotensive individual having only minimal neurological deficit, no gross cerebral vascular disease, and no space-occupying mass, we are able to obtain a series of points which are velocities which can be plotted versus time. A straight line relationship exists which indicates that there is a velocity gradient from artery, to sinus, to vein in decreasing order (Fig 3a). This order holds as long as a process does not favor the development of shunts. If a patient has arterial hypertension, the input velocity is greater and the gradient is much steeper (Fig 3b). This has been true during several observations in hypertensive patients.

In the presence of increased intracranial pressure, the relationships lose their linearity, and there is an arrival of bolus at the innom ahead of the anterior

CEREBRAL BLOOD FLOW MEASURED WITH RADIOACTIVE ISOTOPES

by

ROBERT L. BELL

For several years, we have been interested in observing changes in the shape of a radioactive bolus as it has passed from the carotid arterial circulation through the brain, and its alteration in configuration at the venous output. These observations have been considered a dynamic indicator of the status of the cerebral circulation.

Instrumentation Basically, the cerebral circulation has two carotid inputs and two vertebral inputs, whereas the venous outputs are numerous. In our first efforts to observe the bolus, we recorded only at the arterial input over the carotid artery and the venous output at the union. The patient (Fig 1) is positioned so that 0.2 ml of RISA can be injected through the carotid artery after the completion of angiography. The scintillation probes are positioned so that the observations are made at the desired anatomical sites. The recording instruments process the data and from these we are able to obtain records for evaluation of the events per unit of time. In Fig 2a, the top line of the recording shows an input spike, the second rise is the output slug as it passes in the jugular vein adjacent to the carotid artery. The lower tracing indicates the distribution

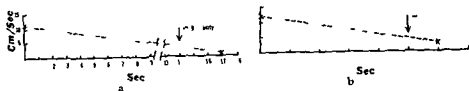


Fig. 4 Velocity gradient in a patient with increased intracranial pressure (a) and in a patient with a glioma (b)

In the presence of a tumor (Fig. 4b) the shunts via a deep glioma permit blood to enter the deeper venous circulation and the torcula in advance of the sagittal sinus. It might be said that an asynchronism develops where a negative velocity is assigned and because of incomplete shunting there is a prolonged discharge pattern through the jugular vein. In some patients we have observed pulsatile discharge over the jugular output.

Discussion

Like all physiological measurements no two observations are the same. It was hoped at the start that the simpler records could be analyzed in the same fashion as a cardiac output curve. This would lead to the application of an analogous technique which would give answers to problems of cerebral blood flow. Because of complex curves and variability between cases calculations would be prohibitive and would necessitate computer techniques. However from these studies we have gained knowledge in conjunction with angiography which indicates that there are considerable alterations in the circulation time and variations contributed by vascular shunts. If large numbers of patients are studied with these techniques certain similarities may be observed in the tracings.

Most radiologists know the major anastomotic pathways of the circulation but few realize how critical these shunts become when there is abnormal intracranial pressure caused by space occupying lesions. By the application of more probes at strategic locations and the use of shorter half life isotopes more measurements can be obtained from each patient. We would advocate evaluation of both hemispheres simultaneously in order to detect leaks through the opposite jugular vein.

Of theoretical consideration would be how to improve the relationships. Conceivably by altering the cardiac output the gradients could be readjusted. However this would not induce blood to flow in the regular gradient in presence of increased intracranial pressure. If however a decompression were

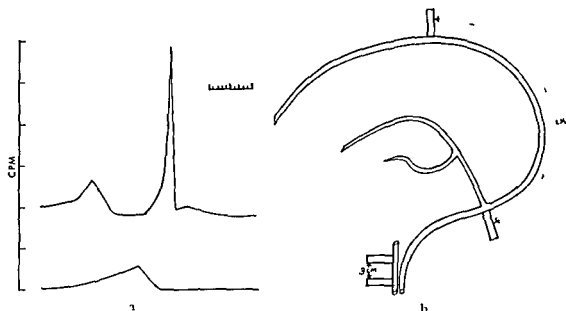


Fig 2 a) Tracing of a recording, showing on top line the input arterial spike. Later there is an attenuation and a reappearance of material in the jugular vein. Bottom line reveals material as it flows through union. Time markers 1 sec. Vertical scale count/minute. b) Diagram of position of probes for velocity measurements.

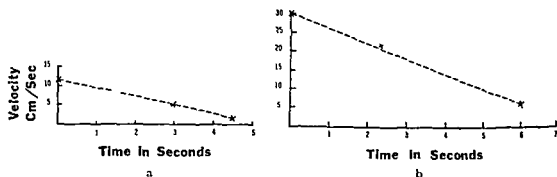


Fig 3 Velocity gradient in a normotensive patient (a) and in a hypertensive patient (b)

sinus measurement (Fig 1a). This means that we must either consider the velocity as negative or negative in relation to time. Both of these concepts are hard to resolve unless one remembers that shunts may channel material to the union before the material can travel by way of the sagittal sinus, i.e., there is absence of the configuration of a normal velocity gradient. This particular patient had generalized cerebral swelling with impairment of the circulation of the veins emptying into the sagittal sinus and apparently faster emptying through the deep venous midline circulation. All of these factors were evaluated and correlated with the concomitant angiography.

ULTRASOUND CROSS SECTIONAL PICTURES OF THE HEAD

by

RAY A BRINKER and JUAN M TAVERAS

Ultrasound has played an increasingly important role in neurological diagnosis since its first application by LENSELL in 1956. Originally the equipment used was borrowed from the engineering field of nondestructive testing and was relatively crude in its application for biological work. Gradually over the intervening years more sophisticated equipment both from the mechanical and electronic standpoints has been developed and this has led to improved methodology for its use.

Midline echoencephalography has now become a well established method for diagnosis. In working with classical midline echoencephalography equipment many workers (CARLIN 1960, GORDON 1964, JEPPESON 1961, RICHARDSON 1962) have been intrigued by the number of echoes occurring from ultrasonic interfaces other than the midline. If a method could be found to record these interfaces, cross sectional anatomical pictures of the brain could be made. To this end the procedures and equipment described in this paper were developed.

History

The first attempt to define intracranial anatomy in pictorial form was described by DLUSSIK et coll (1947) and later by BALLENTINE (1950). Unfortu-

afforded, it might be possible to show the establishment of the normal gradient. Indeed this may be the case in a decompressive procedure, such as removal of the mass or the performance of a lobectomy.

Conclusions

It is possible to demonstrate a linear velocity time relationship between arterial input, sagittal sinus and venous output in the patient who does not have increased intracranial pressure. In those having increased intracranial pressure, there is an alteration of the velocity occurring in the region of the superior sagittal sinus and its tributaries. In this instance, either sinusoids in the tumor bed, or well known venous shunts, alter the velocities observed at the sagittal sinus/junction outflow and favor an inversion of the normal relationships.

SUMMARY

By proper placement of scintillation probes vascular velocity gradients can be measured in the central nervous system. Full exploration of techniques could permit evaluation of blood flow including shunts.

ZUSAMMENFASSUNG

Mittels geeigneter Anbringung von Scintillationssonden kann der Gradient der Blutstromgeschwindigkeit im ZNS gemessen werden. Bei voller Ausnutzung der Technik kann das Ausmass der Blutzirkulation inklusive shunts bestimmt werden.

RÉSUMÉ

La mise en place convenable de sondes à scintillations permet de mesurer dans le système nerveux central des gradients de vitesse circulatoire. L'étude complète de ces techniques pourrait permettre la mesure de débit sanguin y compris dans les shunts.

REFERENCES

- BELL R. L. Observations of cerebral arterio venous transit times using radio iodinated human serum albumin. J. nucl. Med. 5 (1964) 9.

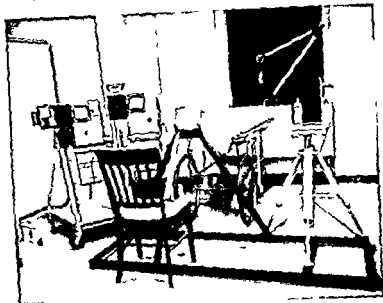


Fig. 1 Apparatus used for scanning. The patient lies supine on the stretcher with his head in the holder and the examiner sits facing the top of the patient's head. Scanning frame supported on its tripod to the right. Oscilloscope screen opens to the left.

side of the head in a normal subject, and if displaced indicates the presence of a mass lesion on the side indicated. A transmission trace is then utilized as a check as originally introduced by LITHANDER (1960). The accuracy of this method has been determined by many workers (JEFFERSON 1961).

In our equipment (Porta scan — Physionics Engineering Inc. Longmont Colorado) the transducer is fixed to three rigid arms (Fig. 1), which in turn are connected to a movable frame. Each arm is connected to this reference frame by fine steel wires. Movement of any of these three arms will be accurately recorded on the oscilloscope both in position and direction. The mechanical and electronic apparatus is to be discussed in a separate paper.

There is a great difference in the relative amplitude of ultrasonic signals returning from the head which is dependent upon the angle of reflection, the size of the interface and the difference in the specific acoustic impedance of the interface. At present there is no satisfactory method of utilizing the information concerning the amplitude or width of the interface. The authors therefore decided to use only the information that an interface is or is not present at some particular point in space. For this purpose a video activated pulser has been designed and built. This unit will cause a minute dot on the

nately, the transmission method used did not result in meaningful pictures of the intracranial contents, due to varying thickness of the skullbone over the scanned region. This line of investigation was abandoned.

FIRESTONE, in 1945, introduced the pulse echo technique into ultrasound. In this manner ultrasound is sent into the structure under study and echoes are received back from it. This so called echo ranging technique has been developed extensively in industry and is the method applied for present day neurological application as echoencephalography.

DE VIEGLER, in 1963, recorded attempts to make intracranial pictures utilizing water path and contact scanning. His pioneering work in the field has resulted in some pictorial representations which have not, as yet, been well correlated with the actual position of intracranial structures. TANAKA et coll. (1962) have also done work in the neurological area in attempting to make intracranial pictures.

The technique of compound ultrasound tomography was extensively developed and used by HOWRY et coll. (1956) in parts of the body other than the head. More recent work by HOLMES & HOWRY (1963) and others has further extended this, so that examinations of the kidney and liver are now fairly routine. BAUM & GREENWOOD (1961) have used compound scanning at high frequency ranges to make outstanding cross sectional pictures of the eye.

Equipment

In a classical A scan echoencephalography the transducer is placed in contact with the side of the head at a point approximately above the external auditory canal. The ultrasound energy passes into the head and returns from the region of the posterior third ventricle to the transducer face, after a delay indicated by the speed of sound in the head. This minute returning echo is fed into a preamplifier, amplifier, and is then detected in a wide band video system.

The time base sweep from left to right of the oscilloscope face is adjusted either to the speed of sound in the head or to some known multiple for ease of recording the results. In our equipment the horizontal type base is adjusted to exactly half the speed of ultrasound in the head so that the resultant pictures are minified by half. The time base is amplitude modulated by the reflected energy from the ultrasonic interfaces and causes a deflection on the base of the oscilloscope trace. In this manner, by knowing the speed of the time base sweep, the actual distance from the transducer face to the interface under study, in this case the posterior third ventricle, can be ascertained. Obviously, the distance to the posterior third ventricle should be the same from either

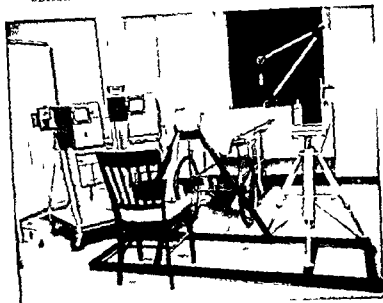
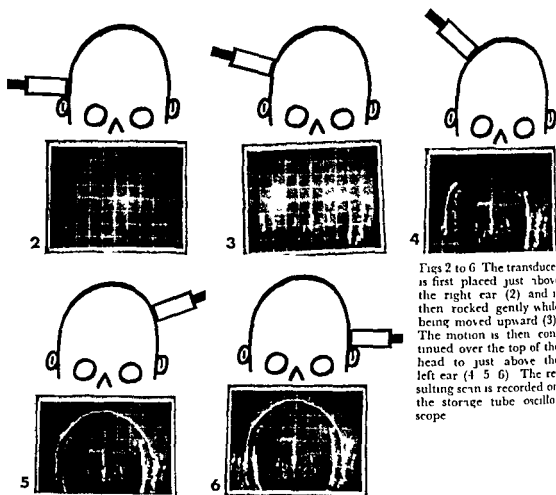


Fig 1 Apparatus used for scanning. The patient lies supine on the stretcher with his head in the holder and the examiner is facing the top of the patient's head. Scanning frame supported on its tripod to the right. Oscilloscope to the left.

side of the head in a normal subject, and if displaced indicates the presence of a mass lesion on the side indicated. A transmission trace is then utilized as a check as originally introduced by LITHANDER (1960). The accuracy of this method has been determined by many workers (JEPPSON 1961).

In our equipment (Porta scan — Physionics Engineering Inc. Longmont, Colorado) the transducer is fixed to three rigid arms (Fig 1) which in turn are connected to a movable frame. Each arm is connected to this reference frame by fine steel wires. Movement of any of these three arms will be accurately recorded on the oscilloscope both in position and direction. The mechanical and electronic apparatus is to be discussed in a separate paper.

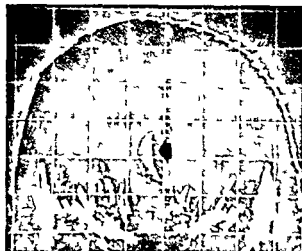
There is a great difference in the relative amplitude of ultrasonic signals returning from the head which is dependent upon the angle of reflection, the size of the interface and the difference in the specific acoustic impedance of the interface. At present there is no satisfactory method of utilizing the information concerning the amplitude or width of the interface. The authors therefore decided to use only the information that an interface is or is not present at some particular point in space. For this purpose a video activated pulser has been designed and built. This unit will cause a minute dot on the



Figs 2 to 6 The transducer is first placed just above the right ear (2) and is then rocked gently while being moved upward (3). The motion is then continued over the top of the head to just above the left ear (4 5 6). The resulting scan is recorded on the storage tube oscilloscope.

face of the read out oscilloscope whenever an ultrasonic interface is seen. The specific operation of this unit will be the subject of a separate paper.

Patient immobilization. The inability to hold the patient's head in a fixed position was a great problem in obtaining ultrasonic pictures. Several attempts at head immobilization led to less than satisfactory results, and an ultrasonic headholder was therefore designed and built. This unit consists of a rigid angle iron frame holding both the headholder and scanner frame. The headholder has adjustable posts which come in from either side and press on the patient's head just below the zygoma in front of the ear. Another arm comes from beneath and presses on the patient's head just inferior to the external occipital protuberance. A U shaped chinholder is then used, and this can be pressed up against the patient's chin (Fig. 1). An auxiliary unit has been designed which will press gently on the roof of the mouth when an anesthetized

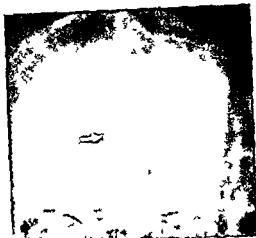
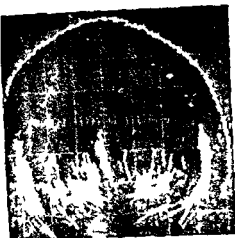


Figs 9 to 11 Ultrasound scan (top left) lateral arterial phase (lower right) and lateral venous phase of angiography (top right) of first patient. The arrow shows the displacement of the posterior 3rd ventricle on both the ultrasound scan and the lateral angiogram (Case of proven metastasis to the left cerebral hemisphere from a carcinoma of the lung)

Results

The present work has concentrated on doing coronal scans. The scanning plane we have most frequently used is from a point halfway between the trasion and the external occipital protuberance to a plane connecting the two external auditory canals. Anatomically, this will pass through a plane of the head as shown in Fig. 7.

As shown in Fig. 8 which is a representative example of the scans obtained, there is close correlation between the anatomical structure shown in the cross section and the structures shown on the ultrasonic coronal scan. By actually superimposing Figs. 7 and 8 we can show the following structures with some assurance: 1) pons, 2) ambient cisterns, 3) medial tips of the temporal lobes, 4) possibly the upper portion of the aqueduct, 5) posterior third ventricle and the petrous bone.



Figs 12 to 14 Ultrasound scan (top left) lateral arterial phase (lower right) and a p venous phase (top right) of second patient. The arrow shows identical placement of the posterior 3rd ventricle (Case of proven glioblastoma of the left temporal lobe)

The midline structure extends slightly higher than we would expect by superimposing it on the anatomical picture. This may in part be due to the anatomical picture being slightly anterior to the plane of the cut and the higher extent of the midline structure being the interhemispheric fissure and/or the falx cerebri.

There are other structures noted in the region of the lateral ventricles. These have not been shown with sufficient clarity in our studies to be positively identified. In part they may represent portions of the lateral wall of the lateral ventricles, choroid plexus, and/or the internal capsule. Also, some lateral structures have been identified in the region of the sylvian fissure.

The coronal scan from a patient with a primary carcinoma of the lung and clinical symptoms suggesting metastasis to the left cerebral hemisphere is shown in Fig 9. The midline echo, presumably the posterior third ventricle, is shown to be displaced 5 mm to the right of the midline. The companion

structures laterally are fairly symmetrical and there is no evidence of distortion of the pons. The lateral arteriogram, as well as the a p venous phase of the angiography, are reproduced in Figs 10 and 11. By superimposition, the position of the posterior third ventricle, as shown in the a p venous phase of the angiography, is identical with the structure shown in the echoencephalogram.

In Fig 12 is shown the coronal scan of a patient whose clinical symptoms suggested a space occupying mass in the left cerebral hemisphere. The scan shows a 1 cm displacement of the upper portion of the third ventricle to the right, and structures lateral to it, as well as the appearance of the pons, give the impression of midbrain rotation. The lateral arterial phase and the a p venous phase are reproduced in Figs 13 and 14 and, again, the echo picture can be superimposed on the venous phase of the angiography.

We are currently investigating the coronal sections behind or in front of the plane illustrated here as well as use of the transverse scans.

Acknowledgement

Supported in part by Grant NB 04884-01 from the National Institute of Neurological Diseases and Blindness.

SUMMARY

Cross sectional pictures of the head which are of definite clinical usefulness have been made. By outlining the midbrain structures as well as the posterior third ventricular structures definite information can be gained as to the presence of a mass lesion.

ZUSAMMENFASSUNG

Es wurden Transversalschnittbilder des Schädels deren klinischer Wert bewiesen war angefertigt. Durch Darstellung der Mittelhirnstrukturen wie auch des hinteren Teiles des III Ventrikels kann man sichere Information über die Anwesenheit eines Tumors erhalten.

RÉSUMÉ

Les auteurs ont obtenu au moyen des ultra sons des images de coupes de la tête qui présentent un réel intérêt clinique. La mise en évidence des structures mésencéphaliques et de la partie postérieure du troisième ventricule renseigne sur la présence d'une tumeur.

REFERENCES

- BALLENTINE H T JR, LUDWIG G D, BOLT R H and HUETER T F. Ultrasonic localization of the cerebral ventricles. *Trans Amer Neurol Ass* 75 (1950) 38.
 BAUM G and GREENWOOD I. Orbital lesion localization by three-dimensional ultrasonography. *NY St J Med* 61 (1961) 414.

- CARLIN B. *Ultrasonics* 2nd edition McGraw Hill New York 1960
- DE VIEGLER N, DE STERKE A, MOLIN C E and VAN DER VEN C. *Ultrasound for two-dimensional echoencephalography* *Ultrasonics* 1 (1963) 1948
- DONALD I and BROWN T G. Demonstration of tissue interfaces within the body by ultrasonic echo-sounding *Brit J Radiol* 34 (1961) 539
- DUSIK K T, DUSIK F and WYT L. Auf dem Wege Zur Hyperphonographie des Gehirnes *Wien med Wschr* 97 (1947) 425
- FIRESTONE F A. Supersonic reflectoscope for interior inspection *Metal Progress* 48 (1945) 505
- GORDON D. *Ultrasound as a diagnostic and surgical tool* E & S Livingstone Ltd Teviot Place Edinburgh Scotland 1964
- HOLMES J and HOWRY D. Ultrasonic diagnosis of abdominal disease *Amer J dig Dis* 8 (1963) 12
- HOWRY D H, POSAKONY G J, CUSHMAN C R and HOLMES J H. Three dimensional and stereoscopic observations of body structures by ultrasound *J appl Physiol* 9 (1956) 304
- JEPPSON S. *Echoencephalography* IV. The midline echo: an evaluation of its usefulness for diagnosing intracranial expansivities and an investigation into its source *Acta chir scand Suppl* 272 (1961)
- KOSSOFF G, ROBINSON D E, LIU C N and GARRETT W J. Design criteria for ultrasonic visualization systems *Ultrasonics* 2 (1964) 29
- LEKSELL L. *Echoencephalography* Detection of intracranial complications following head injury *Acta chir scand* 110 (1956) 301
- LITTHANDER B. A control method for echoencephalography *Acta psychiat scand* 35 (1960) 741
- RICHARDSON E G. *Ultrasonic Physics* 2nd edition American Elsevier New York 1962
- TANAKA K, ITO K, ISHIKAWA S and UEMATSU S. Ultrasonic diagnosis of brain tumor in children (in Japanese) *Japan Pediat Pract* 25 (1962) 130

TOPOGRAPHICAL CRITERIA FOR PATHOLOGICAL DIAGNOSIS OF INTRACRANIAL MASSES BY MEANS OF GAMMA ENCEPHALOGRAPHY

by

JAMES W. D. BULL

The purpose of this paper is to indicate to what extent the pathology of a given mass can be determined by photoscanning. It is well known that the size, shape and position can be clearly defined. Greater anatomical accuracy has recently been achieved by the method devised by MARRIAT & BULL (1964). It consists in taking an under exposed roentgenogram of the skull and leaving the image latent until after the scan. When the film is processed, both the image of the scan and the skull outline are obtained. This is illustrated in Figs 3, 4 and 5. It has been found that by reference to certain anatomical landmarks and their relation to the mass, the pathology can often be predicted. Anatomical structures to which these masses have been related are (1) the dura, (2) the falx cerebri, (3) the tentorium cerebelli and (4) the corpus callosum. Fig. 1 shows the normal anatomy of the falx, tentorium and corpus callosum. A fifth factor which has been taken into account is the presence of multiple masses. By studying these various features it has been possible very often to predict the pathology of three common tumour types: (1) meningiomas, (2) astrocytomas and (3) metastases.

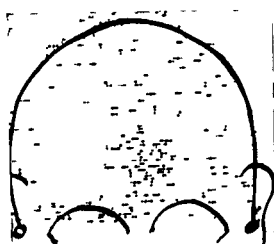


Fig 2

Fig 2 Bifrontal meningioma confirmed by surgical removal

Fig 3 Convexity meningioma confirmed by surgical removal

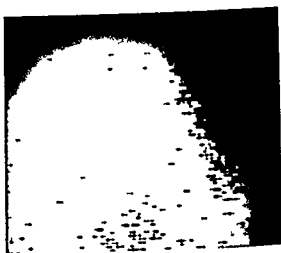


Fig 3

— can add further confirmation to the site of the mass. Such a projection was used in the case illustrated (Fig 4, c and d).

It is likely that the vertical projection will play an increasing part in the future examinations, it has not yet been fully exploited.

4 *Recurrences* The diagnosis was simple in three recurrent cases in that the previous site of the tumour and the pathology were both known. One involved the tentorium (Fig 5).

Astrocytomas

Of the 31 astrocytomas, 6 were diagnosed on the scans as involving the corpus callosum unequivocally, and in three others it was strongly suspected.

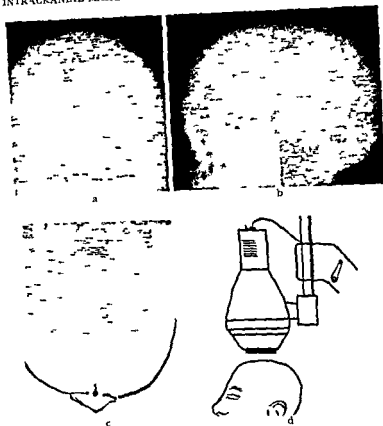


Fig 4 Falx meningioma confirmed by surgical removal

The diagnosis was made in most cases by biopsy occasionally by operation and three were confirmed at autopsy. Fig 6 illustrates the scan of one of the cases confirmed at autopsy.

Involvement of the corpus callosum is often very difficult to demonstrate by pneumography and angiography although it is sometimes possible. It is submitted that the scanning method is the most reliable available and it serves two purposes (1) to demonstrate the site of the neoplasm and (2) to allow a very confident pathological diagnosis to be made on the basis of the scan.

In 1957 BULL & ROY studied 100 cases of supratentorial astrocytomas confirmed at autopsy with the object of assessing the accuracy of pneumography and angiography in delineating the extent of the tumours. The corpus callosum was involved in one third of the cases.



Fig 2

Fig 2 Bifrontal meningioma confirmed by surgical removal

Fig 3 Convexity meningioma confirmed by surgical removal

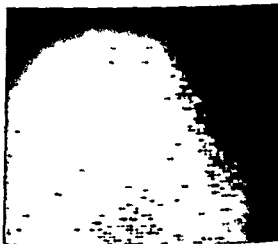


Fig 3

— can add further confirmation to the site of the mass. Such a projection was used in the case illustrated (Fig 4, c and d).

It is likely that the vertical projection will play an increasing part in the future examinations, it has not yet been fully exploited.

† *Recurrences* The diagnosis was simple in three recurrent cases in that the previous site of the tumour and the pathology were both known. One involved the tentorium (Fig 5).

Astrocytomas

Of the 31 astrocytomas 6 were diagnosed on the scan as involving the corpus callosum unequivocally, and in three others it was strongly suspected

Acknowledgement

This work was made possible with the aid of a grant from the British Empire Cancer Campaign

SUMMARY

By studying the topography of tumours demonstrated by photoscanning it is frequently possible to predict the pathology particularly in the case of meningiomas astrocytomas and metastases. Meningiomas can often be diagnosed by noting their relation to the dura falx or tentorium. Astrocytomas can be confidently diagnosed when the corpus callosum is seen to be involved. When metastases are present multiple lesions were often shown thus enabling a diagnosis to be made.

ZUSAMMENFASSUNG

Beim Studium der Topographie von Tumoren die mittels Photo-Scintillographie dargestellt werden, ist es oft möglich die Pathologie vorauszusagen besonders bei Fällen von Meningiomen Astrocytomen und Metastasen. Meningiome können oft diagnostiziert werden wenn man ihre Beziehung zur Dura Falx oder Tentorium beachtet. Astrocytome können mit Sicherheit festgestellt werden wenn das Corpus callosum befallen ist. Bei Vorliegen von Metastasen zeigen sich oft multiple Veränderungen wodurch die Diagnose gestellt werden kann.

RÉSUMÉ

L'étude de la topographie des tumeurs montrées par la scintigraphie permet souvent de prévoir leur nature anatomopathologique en particulier dans le cas de méningiomes d'astrocytomes et de métastases. Leurs rapports avec la dure mère la faux ou la tente permettent souvent de diagnostiquer les méningiomes. L'atteinte du corps calleux permet le diagnostic d'astrocytome. Dans le cas de métastases la multiplicité fréquente des lésions permet le diagnostic.

REFERENCES

- BELL J. W. D. and ROY R. L. The radiographic localisation of intracerebral gliomata. *J. Fac. Radiol.* 8 (1957) 147.
MARRYAT J. and BELL J. W. D. An apparatus providing a combined radiograph and gamma scan. *Brit. J. Radiol.* 37 (1964) 711.



Fig. 5. Tentorial meningioma (recurrence)

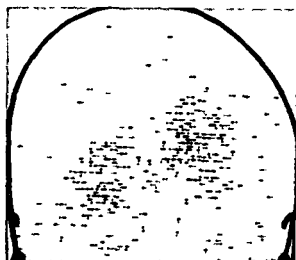


Fig. 6. Astrocytoma splenium of corpus callosum and both parieto-occipital lobes (Confirmed at autopsy)

Metastases

There were 17 cases of metastases, 10 had single masses and the remaining 7 multiple. Without clinical or radiological aid, a correct pathological diagnosis clearly could not be made in the ten cases where a single mass was shown. However, in the remaining seven cases the pathology could be accurately predicted. Two metastases were shown in five, three in one and four in the seventh case.

It is thought that multiple metastases are more readily demonstrated by scanning than by either pneumography or angiography.

Acknowledgement

This work was made possible with the aid of a grant from the British Empire Cancer Campaign

SUMMARY

By studying the topography of tumours demonstrated by photoscanning it is frequently possible to predict the pathology particularly in the case of meningiomas astrocytomas and metastases. Meningiomas can often be diagnosed by noting their relation to the dura falx or tentorium. Astrocytomas can be confidently diagnosed when the corpus callosum is seen to be involved. When metastases are present multiple lesions were often shown thus enabling a diagnosis to be made.

ZUSAMMENFASSUNG

Beim Studium der Topographie von Tumoren die mittels Photo-Scintullographie dargestellt werden ist es oft möglich die Pathologie vorauszusagen besonders bei Fällen von Meningeomen Astrocytomen und Metastasen. Meningeome können oft diagnostiziert werden wenn man ihre Beziehung zur Dura Falx oder Tentorium beachtet. Astrocytome können mit Sicherheit festgestellt werden wenn das Corpus callosum befallen ist. Bei Vorliegen von Metastasen zeigen sich oft multiple Veränderungen wodurch die Diagnose gestellt werden kann.

RÉSUMÉ

L'étude de la topographie des tumeurs montrées par la scintigraphie permet souvent de prévoir leur nature anatomopathologique en particulier dans le cas de méningiomes d'astrocytomes et de métastases. Leurs rapports avec la dure mère la faux ou la tente permettent souvent de diagnostiquer les méningiomes. L'atteinte du corps calleux permet le diagnostic d'astrocytome. Dans le cas de métastases la multiplicité fréquente des lésions permet le diagnostic.

REFERENCES

- BULL J W D and ROYCE R L. The radiographic localisation of intracerebral gliomata
J Fac Radiol 8 (1957) 147
MARRYAT J and BULL J W D. An apparatus providing a combined radiograph and gamma scan
Brit J Radiol 37 (1964) 711

QUANTITATIVE MEASUREMENTS OF REGIONAL CEREBRAL BLOOD FLOW RELATED TO NEURORADIOLOGICAL FINDINGS

by

STEN CRONQVIST, DAVID H. INGVAR and NIELS A. LASSEN

The majority of the disorders of the central nervous system are regional in character. It is a well known fact, however, that conventional neuroradiological procedures will give a definite diagnosis in only a part of such cases. It is therefore desirable to supplement our present techniques with others which yield information on regional disturbances within the brain.

One such method is the isotope clearance method, recently worked out by LASSEN *et coll.* (1963). This method permits measurements of the regional cerebral blood flow. In the following, a brief description of the method will be given, as well as some results obtained and their relation to the neuroradiological findings in a few typical cases. A detailed review is being prepared at present (INGVAR, CRONQVIST, EKBORG *et coll.*).

Two isotopes were used, ^{133}Xe and ^{85}Kr . Both are freely diffusible gamma emitting inert gases, which can be easily dissolved in small amounts of saline. For the clinical studies we have usually used about 0.5 mCi ^{133}Xe in 2 to 5 ml saline which was injected rapidly into the internal carotid artery. The uptake

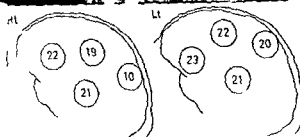


Fig 1 Male 77 years old. Intracranial hemorrhage in right parietal region. B lateral decrease of blood flow values in all region is measured. Area of normal flow (10 ml/100 g/min) on the right side corresponds with expansivity as evident in angiogram.

of the isotope and the subsequent clearance was recorded by means of four collimated detectors over different regions of the hemisphere.

It can be shown that the clearance curve is a function of the blood flow in the regions covered by each detector. This curve is an almost pure wash out curve since there is practically no recirculation due to the rapid elimination of the radioactive gas by the lungs. Since the partition coefficient for the gases between the blood and the tissue is known, it is possible to calculate the regional cerebral blood flow from the curves in terms of millilitres per 100 gram per minute (INGVAR & LASSEN 1962; HOEDT RASMUSSEN, SVEINSDOTTIR & LASSEN 1966).

Analysis of the clearance curves has shown that they consist of two components which represent a slow and a fast type of flow. There are reasons to believe that they are related to the blood flow within the grey and the white matter respectively (HOEDT RASMUSSEN, SVEINSDOTTIR & LASSEN 1966).

Normal values for the method were obtained in seven young healthy male volunteers (INGVAR, CROQVIST, EKBERG, RISBERG & HOEDT RASMUSSEN).

QUANTITATIVE MEASUREMENTS OF REGIONAL CEREBRAL BLOOD FLOW RELATED TO NEURORADIOLOGICAL FINDINGS

by

STEN CRONQVIST, DAVID H. INGVAR and NIELS A. LASSEN

The majority of the disorders of the central nervous system are regional in character. It is a well known fact, however, that conventional neuroradiological procedures will give a definite diagnosis in only a part of such cases. It is therefore desirable to supplement our present techniques with others which yield information on regional disturbances within the brain.

One such method is the isotope clearance method, recently worked out by LASSEN et coll (1963). This method permits measurements of the regional cerebral blood flow. In the following a brief description of the method will be given, as well as some results obtained and their relation to the neuroradiological findings in a few typical cases. A detailed review is being prepared at present (INGVAR, CRONQVIST, EKBERG et coll.).

Two isotopes were used, ^{133}Xe and ^{86}Kr . Both are freely diffusible gamma emitting inert gases, which can be easily dissolved in small amounts of saline. For the clinical studies we have usually used about 0.5 mCi ^{133}Xe in 2 to 5 ml saline which was injected rapidly into the internal carotid artery. The uptake

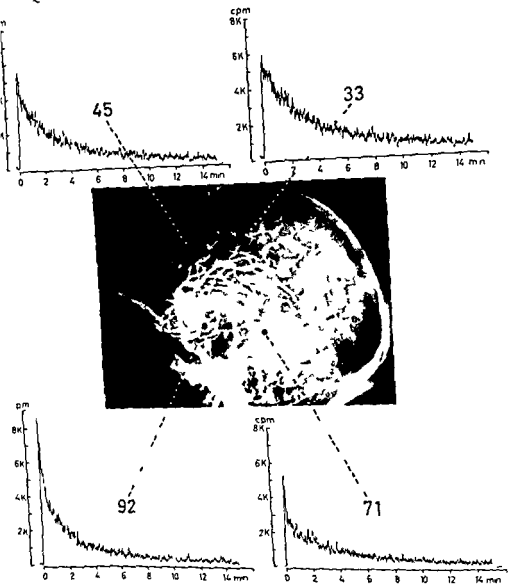


Fig 3 Woman 68 years old. Malignant glioma with abundant arterio-venous shunts in left temporal region. Flow values within and close to the tumour region are highly increased. In surrounding areas values are significantly lower than normal. In the first peak in clearance curves from tumour area characteristic of arterio-venous shunts.

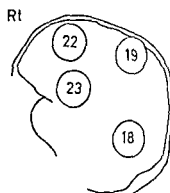


Fig 2 Male 60 years old. Occlusion of right middle cerebral artery. The regional blood flow within occluded area is lower than in the rest of the hemisphere

1965) The average regional cerebral blood flow value measured in four standard regions was found to be $54.5 \text{ ml}/100 \text{ g}/\text{min}$ ($\pm \text{SD } 5.1$), a figure corresponding well with values obtained with the nitrous oxide technique of KETY & SCHMIDT (1918). The relation between the fast type of flow and the slow type was about 4 to 1.

The cases to be related here illustrate the value of regional measurements of the cerebral blood flow in different brain disorders.

The first case pertains to the *cerebrovascular group* (Fig 1). This patient had suffered from a left-sided hemiplegia with slow onset. A carotid angiography showed a large expansive lesion in the left parietal region. In the corresponding area the regional blood flow was found to be only about one fifth of the normal. Two days later the patient died and the autopsy confirmed the presence of a massive intracerebral hemorrhage in the region where the changes of the angiogram were seen and where the minimal cerebral blood flow was measured.

In this case, as well as in similar ones, it was also noted that the flow in other regions surrounding the lesion and on the contralateral side, was very much reduced. Similar findings with the same method have been reported by HOEDT, RASMUSSEN & SKINHOJ (1961).

Fig 2 shows a case with an occlusion of the right middle cerebral artery. The regional blood flow within the occluded area is lower than in the rest of the hemisphere. All flow values show a significant decrease, however, as in the first case presented.

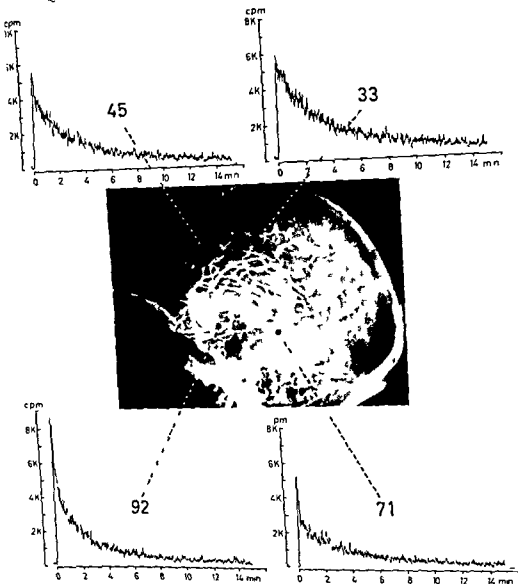


Fig 3 Woman 68 years old. Malignant glioma with abundant arteriovenous shunts in left temporal region. Flow values within and close to the tumour region are highly increased. In surrounding areas values are significantly lower than normal. Initial peak in clearance curves from tumour area has a characteristic of arteriovenous shunts.

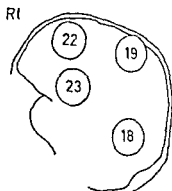
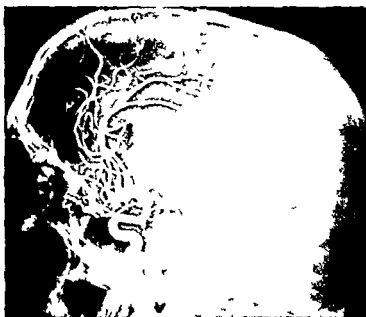


Fig 2 Male 60 years old Occlusion of right middle cerebral artery. The regional blood flow within occluded area is lower than in the rest of the hemisphere

1965) The average regional cerebral blood flow value measured in four standard regions was found to be $54.5 \text{ ml/100 g/min}$ ($\pm \text{S.D. } 5.1$), a figure corresponding well with values obtained with the nitrous oxide technique of KETY & SCHMIDT (1948). The relation between the fast type of flow and the slow type was about 4 to 1.

The cases to be related here illustrate the value of regional measurements of the cerebral blood flow in different brain disorders.

The first case pertains to the *cerebrovascular group* (Fig. 1). This patient had suffered from a left-sided hemiplegia with slow onset. A carotid angiography showed a large expansive lesion in the left parietal region. In the corresponding area the regional blood flow was found to be only about one fifth of the normal. Two days later the patient died and the autopsy confirmed the presence of a massive intracerebral hemorrhage in the region where the changes of the angiogram were seen and where the minimal cerebral blood flow was measured.

In this case, as well as in similar ones, it was also noted that the flow in other regions surrounding the lesion and on the contralateral side, was very much reduced. Similar findings with the same method have been reported by HOEDT RASMUSSEN & SKINHOJ (1964).

Fig. 2 shows a case with an occlusion of the right middle cerebral artery. The regional blood flow within the occluded area is lower than in the rest of the hemisphere. All flow values show a significant decrease, however, as in the first case presented.

pared to that at low pressure. It was furthermore noted that the diameter of the cerebral arteries was larger at the high pressure, indicating that a general vasodilatation at least of the largest cerebral vessels had taken place. A group of similar cases are at present being studied systematically and the results will be published later (CRONQVIST, INGVAR & LUNDBERG).

Conclusions

The present new method permits a simultaneous quantitative measurement of the blood flow in different regions of the brain.

In cases with regional abnormalities as shown by neuroradiological examinations it has been possible to confirm and to quantitate these abnormalities in terms of regional blood flow per 100 gram tissue and minute.

In several cases with normal radiological findings the measurements of the cerebral blood flow have nevertheless revealed abnormal conditions in most cases a decrease of the flow.

A combined study of the cerebral circulation both from a morphological standpoint in neuroradiological procedures and physiologically by means of the isotope technique presented has enabled a study of new aspects of cerebral hemodynamic conditions.

Acknowledgements

The present investigation was supported by grants from the Swedish Medical Research Council, the Wallenberg Foundation and the Fylgia Insurance Company.

SUMMARY

The uptake and clearance within the brain tissue of ^{133}Xe dissolved in saline and injected into the internal carotid artery have been recorded. Multiple regions have been measured simultaneously through the intact skull. Blood flow was calculated in terms of ml per gram per minute. The results in normal subjects and in patients with different lesions of the brain are briefly reported.

ZUSAMMENFASSUNG

Aufnahme und Clearance von ^{133}Xe das in einer Salzlosung in die Art. carotis int. injiziert wurden war wurde registriert. Es wurden viele Stellen gleichzeitig durch den intakten Schadel hindurch gemessen. Die Blutzirkulation wurde in Milliliter per Gramm per Minute errechnet. Es wird über die Resultate bei Normalen und Patienten mit verschiedenen Hirnschaden berichtet.

These two cases with regional cerebral circulatory disturbances showed a fair correlation between the angiographic findings and the regional blood flow measurements. Within the cerebrovascular group so far investigated there are, however, other cases, usually with less severe symptoms or with symptoms of the transient type, which do not show any abnormality angiographically and which have a normal circulation time angiographically determined. Such cases usually have shown an overall decrease of the cerebral blood flow, determined with isotope methods, but so far we have not been able to detect significant regional circulatory difference with the present collimator equipment. We are exploring the possibility of increasing the resolution of the method by other forms of collimators.

Cases with *general cerebral atrophy* have in most instances shown an overall reduction of the flow with no apparent regional differences. One such case was a woman of 74 with severe dementia and cerebral atrophy. A carotid angiography was normal. The regional cerebral blood flow in three regions measured (the premotor, the central and the parietal region) was found to be about equally reduced (36, 31 and 33 ml per 100 gram per minute, respectively). In another similar case, a woman of 74, also with severe dementia and cerebral atrophy, an overall reduction of the flow was found in four areas measured to be about 30 % below the normal without any apparent regional differences.

Fig. 3 shows a case from the *brain tumour* series with a malignant glioma in the left temporal region with abundant arterio venous shunts. The figure demonstrates the clearance curves obtained from different parts of the hemisphere on the tumour side. It is seen that the flow values within, and close to, the tumour region are highly increased, in comparison to those in the regions surrounding the tumour, which were significantly lower than normal. The high values are explained by the shunts which give a marked initial peak in the clearance curves, due to the very rapid elimination of part of the isotope by the pathological vessels (HAGGENDAL et coll. 1965).

In this patient another most interesting finding was made. She suffered from increased intracranial pressure with so called plateau waves (LUNDBERG 1960), that is, recurrent spontaneous periods of markedly elevated intraventricular pressure. Measurements of the blood flow were made when the pressure was low, and when it was high during a plateau wave. A significant difference was found with a flow value of 40 ml/100 g/min at an average pressure of 25 mm Hg and 28 ml/100 g/min at the high pressure (about 80 mm Hg).

The corresponding angiograms showed that during the high pressure, when the flow was decreased, the circulation time was markedly elongated as com-

EVALUATING INTRACRANIAL HEMATOMA BY ECHO EG

by

M J DRESE G J HAYES and L G KEMPE

Unlike intracranial neoplasm that often determines prognosis by position and inherent degree of malignancy intracranial hematoma may be less a determinant than our response to it. The rapid diagnosis of acute epidural hematoma frequently results in early craniotomy and recovery from a potentially fatal lesion. Acute and chronic subdural hematoma although usually not of such immediate threat if unrecognized can also cause death (9).

Need for craniotomy is usually based on clinical and arteriographic findings. The history and physical examination frequently allow ischemic and hemorrhagic disease to be distinguished but evaluation of a comatose patient for whom an adequate history is unobtainable may be most difficult. There are occasions too when arteriography is not used for a definitive diagnosis. If extra cerebral hematoma is suspected in elderly patients trephination may be preferred to angiography because of the higher incidence of arteriographic complications in this age group. Arteriography is widely used but trephination is still available in localities lacking facilities for contrast studies. Early trephination may be life saving on occasion and cannot be delayed. There are occasions

RÉSUMÉ

Les auteurs ont enregistré la fixation et la clearance dans le tissu cérébral du ^{133}Xe dissous dans une solution salée physiologique injectée dans l'artère carotide interne. Ils ont mesuré simultanément à travers le crâne intact l'activité de plusieurs régions cérébrales. Ils ont calculé le débit sanguin en ml par gramme par minute. Ils rapportent brièvement les résultats obtenus chez des sujets normaux et chez des malades atteints de diverses lésions cérébrales.

REFERENCES

- CRONQVIST S, INGVAR D H and LUNDBERG N To be published
- HACCEFDAL F, INGVAR D H, LASSEN N A, NILSSON N J, NORLIN G, WICKBOM I and ZWETNOW N Intra and postoperative measurements of regional cerebral blood flow in three cases of intracranial arterio-venous aneurysm *J Neurosurg* 22 (1965) 1
- HOFDT RASMUSSEN K and SKINHOJ E Transneural depression of the cerebral hemispheric metabolism in man *Acta neurol scand* 10 (1964) 41
- SÄFVINSDDTTIR F and LASSEN N A The inert gas intra arterial injection method for determining regional cerebral blood flow in man through the intact skull *J clin Invest* (1966), In press
- INGVAR D H, CRONQVIST S, EKBFRG R, RISEFRG J and HOFDT RASMUSSEN K Normal values of regional cerebral blood flow in man including flow and weight estimates of gray and white matter *Acta neurol scand* (1965) Suppl 14 Regional cerebral blood flow. An Intern Symposium University of Lund March 5 1965
- and LASSEN N A Regional blood flow of the cerebral cortex determined by Krypton⁸⁵ *Acta physiol scand* 34 (1962) 325
- KETY S S and SCHMIDT C I The nitrous oxide method for determination of cerebral blood flow in man: theory, procedure and normal values *J clin Invest* 27 (1948) 476
- LASSEN N A, HOFDT RASMUSSEN K, SORENSEN S C, SKINHOJ L, CRONQVIST S, BODFORS B and INGVAR D H Regional cerebral blood flow in man determined by Krypton⁸⁵ *Neurology* 13 (1963) 719
- LUNDBERG N Continuous recording and control of ventricular fluid pressure in neurosurgical practice *Acta psychiat scand* (1960) Suppl 149

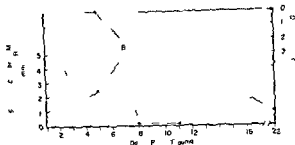
TEMPORAL CORRELATION OF MIDLINE SHIFT
AND STATE OF CONSCIOUSNESS

Fig 1 Correlation of cerebral midline shift and state of consciousness. Carotid arteriography showed cerebral edema (A). Repeat arteriography demonstrated a subdural hematoma (B). Lessening of both confusion (upper graph) and midline shift (lower graph) followed removal of the hematoma.

seen two days after sustaining cranial trauma. The echogram showed a cerebral midline shift of 5 mm later confirmed by angiography although no hematoma was seen. His recovery from cerebral concussion was evidenced both by lessening of confusion and midline shift. After initial improvement, he again became disoriented and was found to have a progressive recurrence of a 5 mm midline shift. Repeat angiography revealed a subdural hematoma. After craniotomy, midline shift disappeared and the patient became and remained mentally alert. Although it was not possible on the basis of a single reading of midline shift correctly to differentiate edema from hematoma, discovery of recurrence of shift several days after initial improvement was most suggestive of hematoma formation. As with EEG, the information gained from serial studies may be of greater value than from multiple readings considered individually.

Although serial Echo EG findings are useful in evaluating cranial trauma, it would be of great value to have a means of detecting intracranial hematoma at the time of initial examination.

Acute cranial trauma if severe usually results in both hemorrhage and cerebral swelling. Nevertheless, even when swelling is prominent, removal of a complicating hematoma might be life saving (1), especially where *uncal herniation* impending. Decompression by removal of calvarium is not without risks in the presence of cerebral edema severe enough to shift the midline. Drugs used to decrease cerebral swelling should not be used if intracranial bleeding is suspected. Despite the possibility of complications, angiography has been needed to verify the presence of acute intracranial hemorrhage (4, 1, 10, 2, 7, 8). Reliable Echo EG detection of acute hematoma would thus be most valuable when serial examinations are not possible. For this difference in the Echo EG pattern between intracranial hemorrhage and swelling must be found.

Our experience to date suggests that although no single difference is diagnostic, several echographic variations when combined may be quite helpful.

when arteriography, although valuable and indicated, cannot be performed. Permission may be refused and rarely, sensitivity to contrast media may exist.

Clearly, despite its high diagnostic reliability, arteriography may be a less than satisfactory means of diagnosing extracerebral hemorrhage in a specific case. It may be refused, unavailable, relatively contraindicated, or rejected because of clinical need of immediate craniotomy.

On these occasions, Echo EG, a useful adjunct to arteriography (5), becomes especially valuable. Although less information is gained from Echo EG than from arteriography, it is valuable more quickly and often gives adequate data to indicate the need for trephination. Under such circumstances, the ready availability of Echo EG compensates for less detailed data.

However, Echo EG is not the definitive study of choice in cases of suspected extracerebral hemorrhage because of the occurrence of false positive and negative findings. Until Echo EG refinements can prevent false negative studies from bilateral hematoma and false positive studies from cerebral edema, it cannot approach the diagnostic reliability of arteriography. A single midline determination may be of aid to clinical judgement, but although it may indicate a need for definitive arteriography, it cannot itself establish or disprove the presence of hematoma with certainty. In practice the delay and added risk of certain diagnosis is often balanced against the benefits of direct trephination. Improved Echo EG reliability would aid in making this decision.

There appear to be at least two means of increasing the value of Echo EG in these cases. Accumulating knowledge of the predicted pattern of midline shift from various lesions may be applied, to interpret serial Echo EG readings more correctly, and the technique of Echo EG can be modified by use of lateral echoes, to increase the yield of data. Examples are given from three years' experience where both methods proved of clinical value. The illustrative cases are chosen from over 150 patients seen because of suspected intracranial hematoma.

Consideration of the time interval between cranial trauma and the initial Echogram may suggest the cause of the shift. For example, presence of cerebral midline shift days after cranial trauma is suggestive of hemorrhage. It is not known however, just how many days shift may remain from posttraumatic swelling alone. Incomplete evidence suggests lessening of traumatic cerebral edema in three to five days but more data are needed before patterns of shift occurrence and resolution are well established (11). Nevertheless, whereas interpretation of a single reading is difficult, serial Echo EG readings are often clinically useful. Midline shifts secondary to acute trauma may result from either swelling or cerebral hemorrhage. Serial readings may suggest which is responsible, as shown in the following case (Fig. 1). A 20 year old soldier was

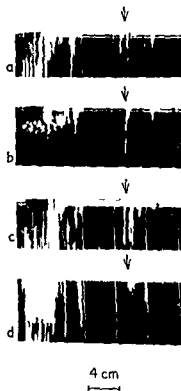


Fig. 4. Comparison of echo EG recordings before and after removal of extracerebral hematomas in two cases: a) Subdural hematoma: the ultrasound passed through the brain and reflected from the opposite skull table seen to the right of the arrow. An echo is also seen to the left of the arrow prior to removal of the clot; b) Postoperative echogram. The unusual echo is no longer present; c) and d) Epidural hematoma: the echo to the left of the arrow seen preoperatively; c) is absent after removal of the epidural hematoma (d).

ment toward the inner table of the skull would be expected. This is in fact seen (Fig. 2 a). These data suggest that the extent of insular as well as midline shift may be useful in evaluating cranial trauma. To compare bilateral structures measurements must be made from points consistently related to fixed external symmetrical anatomic structures such as the external auditory meatus. Subsequent measurements should be made from the points originally chosen. Insular determinations are usually taken about 4 cm above and 2 cm anterior to the external auditory meatus.

The usefulness of the insular echoes was not fully realized when the echograms shown by the first figure were taken. In retrospect the echogram taken when the midline shift resulted from swelling was compared to the echograms with shift from hematoma. Fig. 3 thus compares two echograms from the same 20-year-old patient. Normal insular position was seen (Fig. 3 a) when arteriography showed only diffuse hemispherical swelling, whereas medial insular shift is seen (Fig. 3 b) when an extracerebral hematoma had developed.

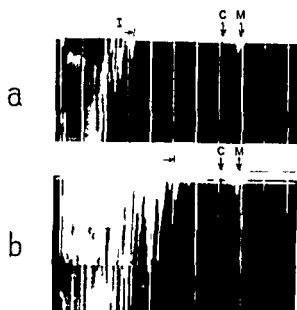


Fig 2 Comparison of lateral echoes from 2 patients with equal extent of midline shift. a) Cerebral edema: solid arrows indicate positions of both cranial and cerebral midline. Echo from cerebral midline (M) is displaced to right of midline control position (C). Insular echoes (I) extend only 3 cm deep to probe position on far left. b) Subdural hematoma: the extent of cerebral midline shift equals that seen in a) whereas lateral echoes extend 5 cm toward the shifted midline suggesting shift of both insula and cerebral midline structures.

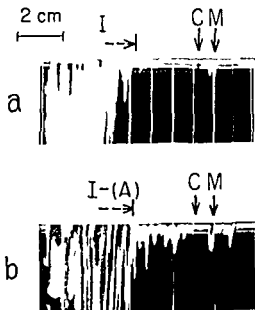


Fig 3 Comparison of echograms of the same patient studied on two occasions. a) Cerebral edema: the cerebral midline structures (M) are displaced to the right of the cranial midline (C). b) Subdural hematoma: the cerebral midline echo is displaced equally as in a) but prominent echoes appear further from the probe because the insula as well as midline structures are now shifted by subdural hematoma. The broken arrow indicates the initial depth of insular echoes.

The first example is shown by cases 2 and 3 (Fig 2). Fig 2, a and b are enlarged echograms of two patients evaluated for cranial trauma. The cranial midline control distance of both patients was fortuitously equal, and the cerebral midlines were shifted 9 mm. Both echograms showed identical cranial midlines and equal extent of cerebral shift.

The lesions responsible for the shift were found to be quite different, however. The first patient (Fig 2 a) died, and was found at necropsy to have a diffusely swollen brain without extracerebral hemorrhage. The second patient (Fig 2 b) recovered after evacuation of a subdural hematoma. The two echograms differ in the extent of lateral echoes. These echoes located several centimeters deep to the inner table arise from the operculum of the temporal lobe and extend to the insula (6). Extra-cerebral hematoma superficial to the insula causes considerable insular, as well as midline shift (Fig 2 b). Diffuse hemispherical swelling would not be expected to cause significant insular displacement. Indeed, if swelling medial to the insula were relatively more severe, displace-

ung war bei der Differenzialdiagnose zwischen Ödem und Hamatom wertvoll. Echos die direkt von epiduralen — und subduralen Hamatomen ausgehen werden mit chirurgischen und radiologischen Kontrolluntersuchungen verglichen.

RÉSUMÉ

Il faut utiliser pour le diagnostic tous les renseignements que peut donner l'écho encéphalographique. Cette technique se compare plutôt à la radioscopie qu'à la radiographie. L'enregistrement en série du déplacement de la ligne médiane et celle des échos latéraux donne des renseignements que ne fournit pas le seul enregistrement de la ligne médiane. La comparaison du déplacement insulaire et du déplacement de la ligne médiane est utile pour distinguer l'œdème de l'hématome. Les échos provenant directement d'hématomes extra-duraux et sous-duraux ont été comparés aux examens radiologiques et per opératoires.

REFERENCES

- 1 ABBOTT K. H. GAY J. R. and GOODALL R. J. Clinical complications of cerebral angiography. *J. Neurosurg.* 9 (1952) 258.
- 2 BAUER R. B. SHEPHAN S. WECHSLER N. and MEYER J. S. Arteriographic study of sites incidence and treatment of arteriosclerotic cerebrovascular lesions. *Neurology* 12 (1962) 698.
- 3 TER BRAAK J. W. G. GRANDIA W. A. M. and DE V. LIEGER M. Echo-encephalography as an aid in the diagnosis of subdural and extradural haematomas. (Recent Neurological Research.) A. Biemond Editor 37.
- 4 BROMAN T. FORSSMAN B. and OLSSON O. Further experimental investigations of injuries from contrast media in cerebral angiography. *Acta radiol.* 34 (1950) 135.
- 5 DRESE M. J. and NETSKY M. G. The clinical use of echo-encephalography. *Va. Med. Monthly* 90 (1963) 539.
- 6 — — Studies of lateral reflections in the echo-encephalogram. *Neurology* 14 (1964) 521.
- 7 JOHNSON J. H. and KINSLEY M. H. Intravascular agglutination of the flowing blood following the injection of radiopaque contrast media. *Neurology* 12 (1962) 560.
- 8 KUTT H. MILHORAT T. H. and McDOWELL F. The effect of ioditized contrast media upon blood proteins, electrolytes and red cells. *Neurology* 13 (1963) 492.
- 9 McLAURIN R. L. and TUTOR F. T. Acute subdural hematoma. Review of ninety cases. *J. Neurosurg.* 18 (1961) 61.
- 10 PATTERSON R. H. GOODALL H. and DUNNING H. S. Complications of carotid arteriography. *Arch. Neurol.* 10 (1964) 513.
- 11 WHITE J. C. BROOKS J. R. GOLDTHWAIT J. C. and ADAMS R. D. Changes in brain volume and blood content after experimental concussion. *Ann. Surg.* 118 (1943) 619.

The time sequence of shift recurrence was most helpful in this case, although in retrospect even more data were present but unrecognized.

Another aid in detecting extracerebral hemorrhage is to note presence or absence of extra echoes inside the far skull table when recording from the side opposite a suspected hematoma. This technique is not original, and we found, as have others (3), both false positive and negative readings. Two illustrative cases follow, however, where echoes did originate from hematoma. The echograms of two patients before and after surgery were compared (Fig 4). The inner table echo is to the right of the arrow, but in both cases an unusual echo appeared inside to the left of the arrow before surgery. The lesion responsible for midline shift (Fig 4 a) and occupying the region of the unusual echo source was found to be a subdural hematoma enclosed by membranes. A repeat echogram after craniotomy showed the echo inside the inner table to be absent (Fig 4 b). There was no midline displacement. The second patient (Fig 4 c) was shown by angiography to have an epidural hematoma. An echogram following craniotomy showed disappearance of the unusual echo (Fig 4 d) previously seen to arise from the position of the dural hematoma interface.

Because both false positive and negative findings occur, little reliability can presently be given to hematoma echoes alone. When evaluated together with the extent of midline shift, position of insular echoes and neurological history and findings, they become much more meaningful.

Acknowledgements

The authors express appreciation to Col Levens, Chief of Neurology, for permission to study patients on his Service and to Maurice Swinnen and Bartley Gordon for technical electronic assistance.

SUMMARY

All possible clues obtainable by Echo EG must be used if the diagnostic potential is to be achieved. The study is best likened to fluoroscopy not radiography. Serial recordings of midline shift and use of lateral echoes gave valuable information not available from a single midline recording. Comparison of insular to midline shift was useful in distinguishing edema from hematoma. Echoes arising directly from epidural and subdural hematomas are compared to surgical and radiographic controls.

ZUSAMMENFASSUNG

Alle möglichen Spuren die man mittels Echo EG erhalten kann, müssen für die Diagnose ausgenutzt werden. Die Untersuchung ähnelt eher der Durchleuchtung als der Radiographie. Wiederholte Untersuchungen geben Informationen, die man mit einer einzigen Mittellinien Untersuchung nicht erhalten kann. Vergleich der Insel- und Mittellinien-Verschieb

Im Angiogramm ergibt sich die Lokalisation des Tumors aus der Gefäßverlagerung und die Artdiagnose aus der Tumoranfärbung in einer bestimmten für die Tumorart typischen Phase der Zirkulation des Kontrastmittels sowie aus charakteristischen arterio-venösen Kurzschlußverbindungen und der dadurch erfolgenden vorzeitigen Venenfüllung. Bei der Positronenszintigraphie (PCG) sind aus dem Ort und dem Grad der Anreicherung lokalisatorische und artdiagnostische Schlüsse zu ziehen, wobei sich auch aus einer Zone verminderter Aktivitätsaufnahme (WILCKE 1961) in Verbindung mit dem angiographischen Befund Hinweise für die Artdiagnose ergeben können.

Meningiome (71) sind von allen raumfordernden intracraniellen Prozessen im PCG durch ihre besonders starke und zumeist umschriebene Anreicherung der Aktivität am sichersten zu erfassen. In 96 % der Fälle war eine entsprechende Lokalisation und in 72 % der Fälle zudem die Artdiagnose mit großer Wahrscheinlichkeit zu stellen. Das Angiogramm erbrachte bei 69 der 71 Patienten den Nachweis eines raumfordernden Prozesses und erlaubte auf Grund der typischen homogenen Anfärbung in der venösen Phase in 70 % der Fälle die Artdiagnose festzulegen. Bei dem Vergleich der Untersuchungsbefunde zeigte es sich, daß die Anwendung der PCG besonders dann indiziert ist, wenn infolge der atypischen oder fehlenden Anfärbung die Entscheidung Meningiom/Gliom offen bleiben muß. Dies trifft besonders für die parietal und occipital neben der Medianen liegenden Meningiome zu, die im Gefäßbild häufiger nur eine Abdrängung und Verlagerung einzelner Gefäßabschnitte bedingen. Im Szintigramm hingegen zu einer kräftigen Anreicherung führen und dadurch ihrer Art nach bestimmt werden können. Andererseits sind die mittelständigen para- oder suprasellar gelegenen Meningiome im Szintigramm ganz allgemein und besonders hinsichtlich ihrer Artdiagnose schlechter nachzuweisen als im Angiogramm, da die Aktivität in Temporalmuskel die Tumoranreicherung überdeckt. Durch die Kombination von Angiographie und Szintigraphie war in 93 % der Fälle eine Artdiagnose möglich. Bei den verbleibenden 7 % handelte es sich fast ausschließlich um die Gruppe der suprasellaren Meningiome.

Astrozytome (43) sind im PCG von allen Tumoren am schlechtesten nachzuweisen, manche Typen nehmen keinerlei Aktivität auf, so daß dann sogar die Aktivität der gesunden Seite überwiegt. So war nur in knapp 60 % der Fälle mit dem ICG mit der Angiographie jedoch bei 88 % die Tumorlokalisation möglich. Beide Methoden zusammen erbrachten bei 91 % eine zutreffende Lagebestimmung. Für die artdiagnostische Zuordnung läßt sich außer der Anamnese und Klinik die durchweg geringe Anreicherung der

GEGENÜBERSTELLUNG DER SERIENANGIO- GRAPHISCHEN UND SZINTIGRAPHISCHEN ERGEBNISSE BEI 242 HIRNTUMOREN

von

G. FRIEDMANN und O. WILCKE

Der klinische Wert der Cerebralen Serienangiographie zum Nachweis und zur Artbestimmung von Hirntumoren ist unbestritten. Um jedoch die Bedeutung der erst seit wenigen Jahren gebräuchlichen Isotopen-Methoden endgültig zu klären, bedarf es hinsichtlich der diagnostischen Möglichkeiten noch weiterer Erfahrung und vergleichender Untersuchungen. Aus diesem Grund soll über die angiographischen und szintigraphischen Befunde und die dabei gewonnenen Erkenntnisse bei 242 auch operativ bzw. histologisch gesicherten Hirntumoren berichtet werden.

Die Serienangiographie erfolgte nach der Methode von TONNIS & SCHIEFER (1959), die Szintigraphie wurde mit den Positronenstrahlern Arsen (^{74}As) und Kupfer (^{64}Cu) nach den Angaben von BROWNELL & SWEET (1956) vorgenommen.

Im Einzelnen handelte es sich um 71 Meningiome, 43 Astrozytome, 37 Glioblastome, 28 Oligodendrogliome, 27 Metastasen, 16 Hypophysentumoren, 8 Epidermoide, 6 Ependymome und 6 Sarkome.

Im Angiogramm ergibt sich die Lokalisation des Tumors aus der Gefäßverlagerung und die Artdiagnose aus der Tumoranfärbung in einer bestimmten für die Tumorart typischen Phase der Zirkulation des Kontrastmittels sowie aus charakteristischen arterio-venösen Kurzschlußverbindungen und der dadurch erfolgenden vorzeitigen Venenfüllung. Bei der Positronenszintigraphie (PCG) sind aus dem Ort und dem Grad der Anreicherung lokalisatorische und artdiagnostische Schlüsse zu ziehen wobei sich auch aus einer Zone verminderter Aktivitätsaufnahme (WILCKE 1961) in Verbindung mit dem angiographischen Befund Hinweise für die Artdiagnose ergeben können.

Meningiome (71) sind von allen raumfordernden intracraniellen Prozessen im PCG durch ihre besonders starke und zumeist umschriebene Anreicherung der Aktivität am sichersten zu erfassen. In 96 % der Fälle war eine entsprechende Lokalisation und in 72 % der Fälle zudem die Artdiagnose mit großer Wahrscheinlichkeit zu stellen. Das Angiogramm erbrachte bei 69 der 71 Patienten den Nachweis eines raumfordernden Prozesses und erlaubte auf Grund der typischen homogenen Anfärbung in der venösen Phase in 70 % der Fälle die Artdiagnose festzulegen. Bei dem Vergleich der Untersuchungsbefunde zeigte es sich, daß die Anwendung der PCG besonders dann indiziert ist wenn infolge der atypischen oder fehlenden Anfärbung die Entscheidung Meningiom, Gliom offen bleiben muß. Dies trifft besonders für die parietal und occipital neben der Medianen liegenden Meningiome zu, die im Gefäßbild häufiger nur eine Abdrängung und Verlagerung einzelner Gefäßabschnitte bedingen. Im Szintigramm hingegen zu einer kräftigen Anreicherung führen und dadurch ihrer Art nach bestimmt werden können. Andererseits sind die mittelständigen para- oder suprasellar gelegenen Meningiome im Szintigramm ganz allgemein und besonders hinsichtlich ihrer Artdiagnose schlechter nachzuweisen als im Angiogramm, da die Aktivität in Temporalmuskel die Tumoranreicherung überdeckt. Durch die Kombination von Angiographie und Szintigraphie war in 93 % der Fälle eine Artdiagnose möglich. Bei den verbleibenden 7 % handelte es sich fast ausschließlich um die Gruppe der suprasellaren Meningiome.

Astrozytome (43) sind im PCG von allen Tumoren am schlechtesten nachzuweisen, manche Typen nehmen keinerlei Aktivität auf so daß dann sogar die Aktivität der gesunden Seite überwiegt. So war nur in knapp 60 % der Fälle mit dem PCG mit der Angiographie jedoch bei 88 % die Tumork Lokalisation möglich. Beide Methoden zusammen erbrachten bei 91 % eine zutreffende Lagebestimmung. Für die artdiagnostische Zuordnung läßt sich außer der Anamnese und Klinik die durchweg geringe Anreicherung der

Aktivität in der gesamten Hemisphäre und insbesondere im Tumorgebiet in Verbindung mit der fehlenden Anfärbung im Angiogramm verwerten

Glioblastome (37) führen im PCG in der Mehrzahl zu einer in ihrer Intensität den Meningiomen ähnlichen Anreicherung. Eine Unterscheidung ergibt sich vielfach aber durch die im Vergleich zu den Meningiomen mehr diffuse und weniger gut gegen die Umgebung abgesetzte Anreicherungszone. 82,5 % der Glioblastome konnten szintigraphisch, 97 % anhand des Angiogramms lokalisiert werden. Da es sich bei dieser Gruppe von Patienten zumeist um atypisch verlaufende Glioblastome handelt, finden sich nur bei gut der Hälfte der Fälle typische angiographische Kriterien. Im Szintigramm konnte bei 16 Patienten aus der Art der erwähnten Anreicherung auf das Vorliegen eines Glioblastoms geschlossen werden. Die Kombination beider Methoden ergab bei 68 % eine richtige Artldiagnose.

Oligodendrogliome (28) zeigen ebenfalls eine nur geringe Aktivitätsaufnahme, die unseren Erfahrungen nach aber doch durchweg etwas ausgeprägter ist als bei den Astrozytomen. Wenn daher auch aus dem PCG allein keine Artldiagnose zu stellen ist, so eignet sich die Methode doch sehr gut zum Ausschluß eines Meningioms oder Glioblastoms. Insgesamt wurden von den 28 Oligodendrogliomen 21 (75 %) im PCG und 25 (89 %) im Angiogramm erfaßt. Durch die Kombination beider Methoden erhöhte sich der Prozentsatz sogar auf 96 % = 27 Patienten.

Metastasen (27) reichern die Aktivität in sehr unterschiedlichem Maße an, in der Regel nehmen Metastasen eines Mamma-Carcinoms mehr Aktivität auf als die cerebralen Absiedlungen der Bronchial-Carcinome und Melanome, so daß bei ersteren am häufigsten der szintigraphische Nachweis gelingt. Insgesamt war bei 4/5 aller Fälle im PCG ein pathologischer Befund vorhanden. Verschiedentlich konnte die Diagnose auf Grund mehrerer Anreicherungs-zonen im Szintigramm exakt gestellt werden. Im Angiogramm kam es bei 24 Fällen (89 %) zur Darstellung eines krankhaften Befundes. Durch die Kombination von Angiographie und PCG gelingt es ohne Ausnahme einen raumfordernden Prozess nachzuweisen.

Hypophysentumoren (16) nehmen in diesem Rahmen insofern eine Sonderstellung ein, als zu ihrem Nachweis meist eine Nativaufnahme des Schädels und insbesondere des Sellagebietes genügt, so daß die Angiographie nur bei besonderen Fragestellungen zur Klärung der supra- oder parasellären Ausdehnung des Tumors benötigt wird. Aus diesem Grund ist ein nur unvoll-

ständiger Vergleich mit den szintigraphischen Untersuchungen möglich bei denen es 12 mal zu einer stärkeren Anreicherung der Aktivität kam. Diese gute Nachweisbarkeit im PCG ist offenbar dadurch bedingt, daß die Anreicherung im Adenom nicht wie z. B. bei den gliomatösen Tumoren über eine Störung der Blut-Hirnschranken-Funktion erfolgt, sondern diese Tumoren ähnlich den parenchymatösen Organen anderer Körperregionen mehr Radioaktivität aufnehmen als normales Hirngewebe.

Epidermoide (8) reichern keine Aktivität an. Die Lokalisation und sogar die Artdiagnose gelingen jedoch recht häufig, wenn das Angiogramm nur eine Gefäßverlagerung, aber keine Anfärbung zeigt. Im Szintigramm aber auf der gesunden kontralateralen Seite mehr Aktivität aufgenommen wurde als in der Tumorregion. Dies war bei unseren Beobachtungen mit einer Ausnahme der Fall. Hier bestanden bereits erhebliche allgemeine Hirndruckzeichen.

Ependymome (6) werden auf Grund ihrer Lokalisation in der Regel durch die Hirnkammerluftfüllung diagnostiziert. Von den 6 angiographisch untersuchten Fällen zeigten 5 einen pathologischen Befund im Sinne einer Gefäßverlagerung oder geringen Anfärbung. Im Szintigramm war 4 mal eine deutliche Anreicherung der Aktivität zu beobachten. Kriterien, die zur Artdiagnose herangezogen werden konnten, fanden sich allerdings nicht.

Sarkome (6) bewirken besonders wenn es sich um ein sarkomatos entartetes Meningiom handelt, eine ähnlich starke Anreicherung wie die Meningiome und sind daher artdiagnostisch allein im PCG nicht von ihnen zu differenzieren. 5 der 6 Sarkome wiesen im Szintigramm eine erhebliche Aktivitätsaufnahme auf, während einmal keine Anreicherung zustande kam. Angiographisch war bei allen Fällen die Tumorlokalisation infolge einer Gefäßverlagerung möglich. 4 mal kam es außerdem zu einer Anfärbung, die in einem Fall die Charakteristika eines Meningioms aufwies.

ZUSAMMENFASSUNG

Sinn der Ausführungen war die Möglichkeiten und Grenzen der angiographischen und szintigraphischen Diagnostik der Großhirnhemisphärentumoren aufzuzeigen. Die Angiographie ist sowohl hinsichtlich der Tumorlokalisation als auch der Artdiagnose für den Nachweis gliomatöser Tumoren zuverlässiger als die Szintigraphie, während bei den Meningiomen beide Verfahren nahezu Gleichwertiges leisten. Die Kombination der Methoden führt mit Sicherheit zu einer eindeutigen Verbesserung der Resultate.

Aktivität in der gesamten Hemisphäre und insbesondere im Tumorgebiet in Verbindung mit der fehlenden Anfärbung im Angiogramm verwerten

Glioblastome (37) führen im PCG in der Mehrzahl zu einer in ihrer Intensität den Meningiomen ähnlichen Anreicherung. Eine Unterscheidung ergibt sich vielfach aber durch die im Vergleich zu den Meningiomen mehr diffuse und weniger gut gegen die Umgebung abgesetzte Anreicherungszone. 82,5 % der Glioblastome konnten szintigraphisch, 97 % anhand des Angiogramms lokalisiert werden. Da es sich bei dieser Gruppe von Patienten zumeist um atypisch verlaufende Glioblastome handelt, finden sich nur bei gut der Hälfte der Fälle typische angiographische Kriterien. Im Szintigramm konnte bei 16 Patienten aus der Art der erwähnten Anreicherung auf das Vorliegen eines Glioblastoms geschlossen werden. Die Kombination beider Methoden ergab bei 68 % eine richtige Art diagnosis.

Oligodendrogliome (28) zeigen ebenfalls eine nur geringe Aktivitätsaufnahme, die unseren Erfahrungen nach aber doch durchweg etwas ausgeprägter ist als bei den Astrozytomen. Wenn daher auch aus dem PCG allein keine Art diagnosis zu stellen ist, so eignet sich die Methode doch sehr gut zum Ausschluß eines Meningioms oder Glioblastoms. Insgesamt wurden von den 28 Oligodendrogliomen 21 (75 %) im PCG und 25 (89 %) im Angiogramm erfaßt. Durch die Kombination beider Methoden erhöhte sich der Prozentsatz sogar auf 96 % = 27 Patienten.

Metastasen (27) reichern die Aktivität in sehr unterschiedlichem Maße an, in der Regel nehmen Metastasen eines Mammacarcinoms mehr Aktivität auf als die cerebralen Absiedlungen der Bronchialcarcinome und Melanome, so daß bei ersteren am häufigsten der szintigraphische Nachweis gelingt. Insgesamt war bei 4/5 aller Fälle im PCG ein pathologischer Befund vorhanden. Verschiedentlich konnte die Diagnose auf Grund mehrerer Anreicherungs zonen im Szintigramm exakt gestellt werden. Im Angiogramm kam es bei 24 Fällen (89 %) zur Darstellung eines krankhaften Befundes. Durch die Kombination von Angiographie und PCG gelang es ohne Ausnahme einen raumfordernden Prozess nachzuweisen.

Hypophysentumoren (16) nehmen in diesem Rahmen insofern eine Sonderstellung ein, als zu ihrem Nachweis meist eine Nativaufnahme des Schädels und insbesondere des Sellagebietes genügt, so daß die Angiographie nur bei besonderen Fragestellungen zur Klärung der supra oder parasellären Ausdehnung des Tumors benötigt wird. Aus diesem Grund ist ein nur unvoll

ECHOENCEPHALOGRAPHIE BEI CEREBRALEN ERKRANKUNGEN IM SAUGLINGS UND KINDESALTER

VON

CARL LUDWIG GELETNYKY

Die Echoencephalographie im Kindesalter beruht grundsätzlich auf den gleichen bisher erarbeiteten physikalischen Grundlagen wie im Erwachsenenalter. Besondere Erwähnung über das normale Echoencephalogramm und die Mittellinienstrukturen bei Kindern finden sich in den Arbeiten von JEPSSON und LITHANDER. In der zusammenfassenden Arbeit von SHIEFER, KAZNER & BRUCKER wird besonders auf den kindlichen Hydrocephalus eingegangen.

Wir untersuchten echoencephalogisch 120 Kinder mit cerebralen Erkrankungen. Besonders günstige Voraussetzungen für die Anwendung der Echoencephalographie in diesem Alter waren:

1. Atrophische und zystische Veränderungen als Folge der spezifischen Reaktionsweise des unreifen Gehirns, die Häufigkeit subduraler Hämatome und Hydrome verschiedenartiger Hydrocephalusformen und damit die Fixierung von Medien und Grenzflächen verschiedener Schallgeschwindigkeit.

2. Die anatomischen Verhältnisse des kindlichen Schädels mit dünnem Lamellenknochen (0,5–4 mm) und tiefstehende Schädelbasis, somit hohe Echoamplituden infolge geringer Schallabsorption und Fortfall von störenden Reflexen durch basale Strukturen.

SUMMARY

An attempt is made to demonstrate the possibilities and the limits of the angiographic and scintigraphic diagnosis of tumours of the cerebral hemispheres. Angiography appears more successful in demonstrating the site and character of the lesion in the case of gliomas but both methods seem to have equal merits in angiomas. The combination of the two methods leads undoubtedly to more reliable results.

RÉSUMÉ

Le but de ce travail était de déterminer les possibilités et les limites du diagnostic angiographique et scintigraphique des tumeurs des hémisphères cérébraux. L'angiographie est plus fidèle que la scintigraphie pour la localisation et le diagnostic de nature des tumeurs gliomateuses alors que pour les méningiomes les résultats des deux méthodes sont à peu près équivalents. L'association des deux méthodes apporte incontestablement une notable amélioration des résultats.

LITERATUR

- BROWNELL G. L. and SWIFT W. H. Scanning of positron emitting isotopes in diagnosis of intracranial and other lesions. *Acta radiol.* 45 (1956) 425.
- FRIEDMANN G. und WILCKE O. Vergleichende Untersuchungen der Kontrastmittel und Isotopendiagnostik bei Hirntumoren. *Deutsch. med. Wschr.* 87 (1962) 2311.
- — Vergleichende Untersuchungen zum Nachweis der Meningiome anhand des Nativbildes des Isotopentestes und der Carotisserienangiographie. *Zbl. Neurochir.* 25 (1963) 198.
- MAURER W. und WILCKE O. Diagnose von Hirntumoren mit radioaktiven Isotopen. *Handbuch der Neurochirurgie*. Herausgegeben von OLIVIERO TONNIS. Bd. IV/3. Springer Verlag, Berlin Göttingen Heidelberg (1962).
- SWIFT W. H. External localization of intracranial lesions with radioactive isotopes. *Schweiz. med. Wschr.* 92 (1962) 1545.
- TONNIS W. und SCHIEFFER W. Zirkulationsstörung des Gehirns im Serienangiogramm. Springer Verlag, Berlin Göttingen Heidelberg (1959).
- WILCKE O. Die differentialdiagnostischen Möglichkeiten der Positronencephalographie (Cu 64 und As 74). *Fédération Mondiale de Neurologie*, Strasbourg, 23—24 IX 1963.
- Möglichkeiten und Grenzen der Hirntumordiagnostik mit Positronenstrahlern (Cu 64 und As 74). *Neurochirurgia* 7 (1964) 33.
- Results of positron scanning in 1200 cases for diagnosis of intracranial lesions. *Intern. Atomic Energy Agency Sympos. on Med. Radioisotopes*, Scanning, Athens 20—24 IV 1964.

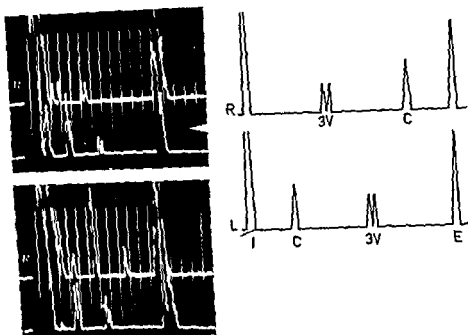


Abb 3 Ly tisches Flexuspapillom im Bereich des linken Parietallappens

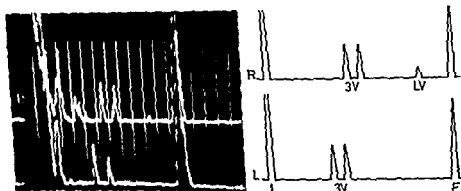
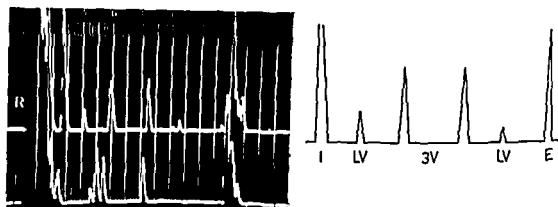
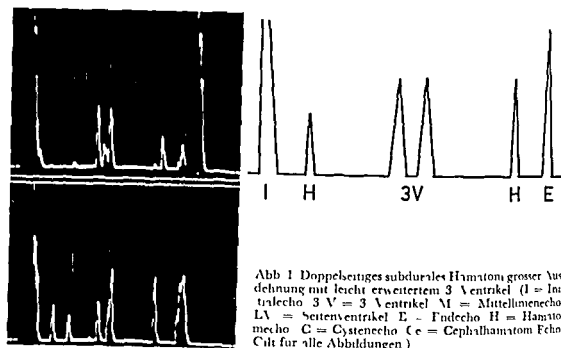


Abb 4 Linksseitige Hemiatrophie

Hydrocephalus Die Diagnose des Hydrocephalus aller Formen ist durch die Weite des 3 Ventrikels, der Seitenventrikel und die Messung der Hirnmanteldicke möglich. Kennzeichnend bei der Untersuchung sind sehr hohe Echoimplutuden. Schädelasymmetrien können die Beurteilung erschweren. Da die Größe des Hydrocephalus exakt bestimmt werden kann, stellen Verlaufsbeobachtungen während der Entstehung eines Hydrocephalus bzw. seiner Rück-



Diese idealen Vorbedingungen erlauben eine breite Indikation der Echoencephalographie im Kindesalter

Subdurale Hämatome und Hygrome sind im Kindesalter meist doppelseitig und liegen parasagittal. Durch Ausbildung von Membranen sind sie im Echoencephalogramm erfassbar, nicht immer im bitemporalen Strahlengang, sondern oft erst bei Beschallung in biparietaler Richtung. Das ist besonders wichtig zur Erfassung kleinerer Hämatome. Ein begleitender Hydrocephalus ist nachweisbar. Verlaufsuntersuchungen erlauben eine Kontrolle der Rückbildung und Vergrößerung der Hämatome (Abb 1)

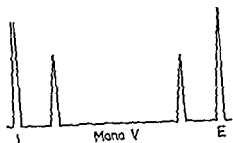


Abb 6 Monoventrikulie

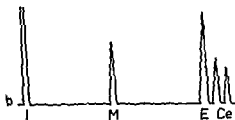
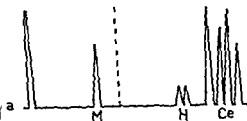
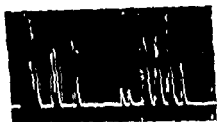


Abb 7 Epiduralhämatom und Kephalthämatom b) Kephalthämatom

ablenierten Gefäßen durchzogen sein können. Die Erweiterung des Seitenventrikels auf der atrophischen Seite ist meist zu erfassen. Zu beachten sind die stets begleitenden Schädelsymmetrien mit unterschiedlichen Echoamplituden bei Beschallung mit gleicher Impulsstärke von beiden Seiten offensichtlich als Ausdruck der unterschiedlichen Kalottendicke.

Postoperative Verlaufsuntersuchungen nach Hemisphärektomien können zur Aufdeckung von Komplikationen beitragen wie etwa ein Monroe Verschuß mit Erweiterung der Seitenventrikel der verbliebenen Hemisphäre oder Zunahme der Verlagerung des 3. Ventrikels.

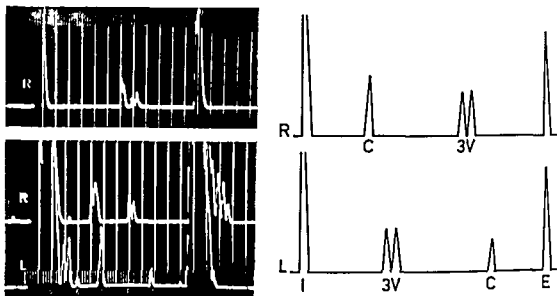


Abb. 2 Subarachnoidalzyste im Bereich der rechten Hemisphäre (Die obere linke Echokurve zeigt bei parietalem Strahlengang die Tiefe der Zyste)

bildung nach operativen Maßnahmen eine wirksame diagnostische Bereicherung dar. Das gilt besonders für Verlaufsbeobachtungen nach atrioventrikulärer Anastomose wegen der in diesen Fällen nicht möglichen Encephalographie (SCHIEFFR, KAZNER & BRUCKNER) (Abb. 2).

Verstündlicherweise ist die Differentialdiagnose eines Hydrocephalus occlusus bzw. communicans nicht möglich. Eine Ausnahme scheinen Tumoren des 3. Ventrikels und seiner Nachbarschaft zu machen. In einem solchen Fall ließen sich die erweiterten Seitenventrikel darstellen, während eine Reflektion des 3. Ventrikels fehlte.

Für Großhirntumoren gelten die gleichen Verhältnisse wie beim Erwachsenen. Auf solide Tumoren ist lediglich aus der Massenverschiebung mit Verlagerung des 3. Ventrikels zu schließen. Bei zystischen Tumoren ist der Nachweis der Zyste und entsprechend die Lokalisation möglich. Große Zysten können bei günstiger Durchschallungsrichtung in ihrer Tiefe bestimmt werden (Abb. 3). Häufiger sind jedoch Zysten in einem gekammerten oder kleineren Tumor durch multiple hohe Amplituden im Echoencephalogramm charakterisiert.

Große Bedeutung hat die Echoencephalographie bei den infantilen Encephalopathien verschiedener Ätiologie. Bei Hemiratiohien ist das wichtigste Kriterium die Mittellinienverlagerung zur homolateralen atrophischen Seite (Abb. 4). Zystische Erweichungen etwa nach Mediaverschluß mit Hemiatrophien, sind nicht immer im Echoencephalogramm darzustellen, da sie von

la largeur du troisième ventricule et des ventricules latéraux ainsi que par la mesure de l'épaisseur du parenchyme cérébral. Les tumeurs des hémisphères cérébraux se traduisent par le déplacement de l'écho médian. Les kystes assez volumineux sont décelables par l'écho-encéphalographie. Les hémorragies se traduisent par un déplacement homolatéral de l'écho médian. Dans les traumatismes crânio-cérébraux récents l'écho-encéphalographie est peu satisfaisante en raison de l'apparition le plus souvent rapide de l'œdème cérébral. Les gros hémistomes extra durs sont décelables.

LITERATUR

- JEPSSON S. Echoencephalography. Acta chir. scand. Suppl. 272 (1961).
LITHIANDER B. Origin of echoes in the echo-encephalogram. J. Neurol. Psychiatr. 24 (1961) 21.
SCHIFFER W., KAZNER E. und BRUCKNER H. Die Echoencephalographie: ihre Anwendungswiese und klinische Ergebnisse. Fortschr. Neurol. Psychiatr. 31 (1963) 457.

Glatt begrenzte Zysten, wie etwa eine Arachnoidzyste oder eine Zyste des Septum pellucidum, sind leicht nachweisbar (Abb 5) Die Leistungsfähigkeit der Echoencephalographie ist gerade in diesen Fällen besonders groß So ließ sich etwa ein Fall mit Monoventrikulie nachweisen (Abb 6)

In allen akuten Fällen, etwa bei frischem *Schädelhirntrauma*, ist die Echoencephalographie weniger leistungsfähig, da im Gegensatz zum Erwachsenen älter Verlagerungen des 3. Ventrikels trotz zum Teil ausgedehnter Hämatom meist fehlen Dafür scheint das meist schnell auftretende und intensive Hirnodem verantwortlich zu sein Das epidurale Hämatom verhält sich wie im Erwachsenenalter Das für das Kindesalter typische Kephallhämatom macht kennzeichnende Impulse nach dem Endecho (Abb 7)

Nach den bisherigen Untersuchungen kann gesagt werden, daß gerade in diesem Lebensabschnitt wegen der besonderen anatomischen und pathologischen Verhältnisse die Echoencephalographie einen wichtigen Beitrag zur Diagnose und Differenzialdiagnose leisten kann

ZUSAMMENFASSUNG

Es wurden 125 Kinder mit verschiedenen cerebralen Erkrankungen echoencephalographisch untersucht Besonders günstige Voraussetzungen waren dabei atrophische und zystische Veränderungen und die anatomischen Verhältnisse des kindlichen Schädels Die subduralen Hämatome sind durch die Ausbildung von Membranen im Echoencephalogramm erfassbar Der Hydrocephalus kann durch die Weite des 3. Ventrikels und der Seitenventrikel sowie die Messung der Hirnrindendicke erfaßt werden Großhirntumoren sind durch Mittellinienverlagerungen gekennzeichnet Größere Zysten lassen sich im Echoencephalogramm darstellen Hemiatrophien sind durch die homolateralen Mittellinienverlagerungen erkennbar Bei frischen Schädelhirntraumen ist die Echoencephalographie wenig leistungsfähig bedingt durch das meist schnell auftretende Hirnodem Große epidurale Blutungen sind nachweisbar

SUMMARY

Echoencephalography was used in 125 children with cerebral anomalies Atrophy and cystic conditions as well as the anatomic peculiarities of the juvenile skull were favourable factors Due to the formation of a capsule the subdural haematomas are recognisable by this method Hydrocephalus is identifiable by enlargement of the third ventricle and the lateral ventricles and by the measurement of the cerebral cortex Cerebral tumours are recognised by displacement of the midline echo major cysts are readily diagnosable Characteristic of atrophy is displacement of the midline echo towards the affected side Due to rapidly developing cerebral oedema the method is of little value in recent cerebral injuries Major epidural haematomas are well demonstrated

RÉSUMÉ

L'auteur a examiné par échoencéphalographie 125 enfants atteints de diverses affections cérébrales Les lésions atrophiques et kystiques ainsi que les caractéristiques du crâne de l'enfant favorisent cet examen Les hématomes sous durux se reconnaissent sur l'écho encéphalogramme grâce à la formation de membranes L'hydrocéphalie est reconnaissable par

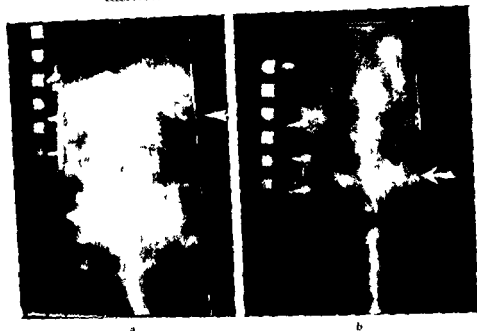


Fig. 1. Thermograms of normal low back. a) Level of posterior iliac crest (L4-L5 interspace). In anterioral white stripe at bottom represents inguital cleft and diffuse patchy heat pattern with small nodular accentuations most marked at level of L4-L5 slightly to left of midline. b) Arrangement of level of posterior iliac crest nodular midline heat pattern superimposed on a diffuse midline grayness with slight accentuation of level of L5.

surface by either evaporation or perspiration convection by air currents or emission of infrared radiation and 3) the amount of heat being absorbed by the skin from the surrounding environment. In order to ensure that the thermogram reflects only the condition of the underlying body temperature it is necessary to let the skin come to an equilibrium temperature with the surrounding atmosphere. This can usually be satisfactorily accomplished by exposing the part to be examined in a non drafty cool environment of about 10 to 21°C for at least 30 minutes before the thermographic scan is obtained.

Skin temperature is not uniform over the entire body even under ideal ambient conditions. This is probably in part a reflection of varying degrees of metabolic activity of underlying tissues and also in part a reflection of differences in the vascular architecture of the skin and subcutaneous region (De Souza & Soveral Rodrigues 1962). The surface of the body overlying large collections of adipose tissue such as the buttocks appears relatively cold due to the excellent insulating property of fat (Hardy 1954). The hair also is a

THERMOGRAPHY IN NEUROLOGICAL PATIENTS

Preliminary experiences

by

H I GOLDBERG E R HEINZ and J M TAKEAS

The local change in temperature of the skin is utilized by most clinicians in the detection of underlying vascular inflammatory and neoplastic disease.

Extremely sensitive heat recording instruments have recently been developed which permit rapid photographic temperature mapping of the body surface. These thermographic cameras contain thermal sensitive resistors of nickel cobalt and magnesium oxides which respond to the infrared radiations being emitted from the surface of the body (BARNES 1963). The Barnes infrared camera used in the present evaluation employs a rapid linear scanning system which records up to 60 000 individual temperature measurements in the maximum 10×20 angular degree field of view covered. Since the human skin is an almost perfect emitter of infrared radiation (with an emissivity of 0.99), in the wavelengths utilized from 3 to 15 microns the level of radiation recorded is therefore a direct function of the temperature at the surface of the body (BARNES 1963, BARNES & GLASSMAN COHEN 1963, LAWSON 1957).

The normal skin temperature at any one moment is a result of many factors and may vary greatly. It depends on: 1) the amount of heat conducted to the surface from the underlying tissue, 2) the amount of heat being lost from the

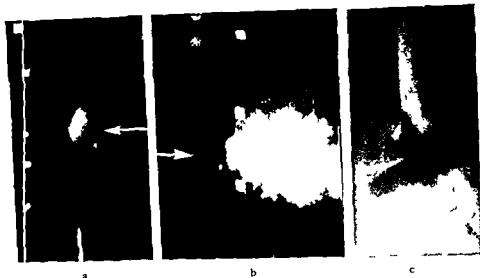


Fig 3 Back thermograms in patients with symptomatic malalignment of lumbar spine. a) Dominant heat pattern (arrow) 5 cm above level of iliac crest in a patient with malalignment between L3 and L4. b) Dramatic heat pattern spreading diffusely over low back most accentuated at level of L5 (arrow). Patient had a spondylolisthesis between L4 and L5. c) A severe compression of the spinal canal present from dorsally thickened ligaments and bone at level of malignment at L4-L5. Nodular filling defects in the opaque column below the level of compression represent dilated veins secondary to the partial obstruction.

gram surrounded by the large cold (dark) area represents the midline intergluteal cleft with the adjacent buttocks which is always relatively cold due to its thick covering of adipose tissue. This stripe is a useful midline orienting landmark. Heated wires were placed above the skin at known distances from the iliac crest. From the lowest up these were situated 5 cm below the crest, at the crest, 5 cm above the crest and 15 cm above the crest. These markers are seen at the side of the thermograms. The multiple different geometric forms also seen on the side of the scans represent a known temperature scale.

A second normal heat pattern for the low back is seen in Fig 1b. Here there is basically a midline increase of skin temperature which again consists of multiple nodular hot spots superimposed on a more homogeneous background. The warmest and frequently the broadest accentuation of heat is usually located at the L4 and L5 level.

In general therefore we found the normal low back thermogram to consist of patchy areas of increased heat with superimposed small nodular hot spots located in the midline and paraspinal region and most marked at the L4 and L5

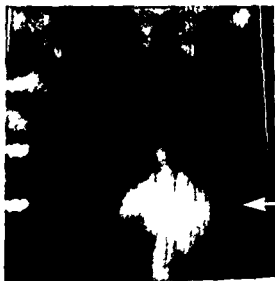


Fig 2 Thermogram of low back in patient with acute intervertebral disc herniation at L5—S1 level dominant area of increased heat at L5—S1 level (arrow)

good insulator and does not permit the transmission of skin temperature if the covering is heavy. In the thermographic scans the whiter the area the warmer its relative temperature. The number at the lower portion of some of the pictures indicates the sensitivity setting of the camera and defines the temperature range recorded between the pure white and the pure black regions of the film. The sensitivity scale extends from 0 to 100 and indicates a temperature range on the film of 10.4°C for a setting of 0 down to 1.2°C for a setting of 100. At number 20 the gray scale range amounts to 4.1°C .

Thermographic evaluation of the back and the head was carried out on a series of 75 patients at the Neurological Institute of New York and this study is being continued at the Albert Einstein Medical Center in Philadelphia. Some observations will be presented on our preliminary experience with thermography in each of these two categories.

Back

The heat picture of the normal back varies greatly from person to person. Several general patterns and characteristics of normal heat distribution can, however, be recognized in the low back. One of the common normal patterns seen was a diffuse increased heat in the midline and paraspinal area of the lumbosacral region consisting of ill defined patchy areas within which there were seen small nodular like accentuations of the heat (Fig 1a). The warmest areas were usually seen at about the level of L4 and L5 and frequently were slightly eccentrically situated. The vertical white stripe at the lower end of the thermo-

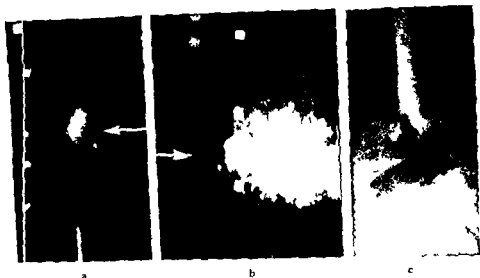


Fig 3 Ba x thermograms in patients with symptomatic mal alignment of lumbar spine a) Dominant heat pattern (arrow) 5 cm above level of iliac crest in a patient with malalignment between L3 and L4 b) Dominant heat pattern spreading diffusely over low back most accentuated at level of L5 (arrow) Patient had a spondylolisthesis between L4 and L5 c) A severe compression of the spinal canal is present from dorsally thickened ligaments and bone at level of malalignment at L4—L5 Nodular filling defects in the opaque column below the level of compression represent dilated veins secondary to the partial obstruction

gram surrounded by the large cold (dark) area represents the midline intergluteal cleft with the adjacent buttocks which is always relatively cold due to its thick covering of adipose tissue. This stripe is a useful midline orienting landmark. Heated wires were placed above the skin at known distances from the iliac crest. From the lowest up these were situated 5 cm below the crest, at the crest, 5 cm above the crest and 15 cm above the crest. These markers are seen at the side of the thermograms. The multiple different geometric forms also seen on the side of the scans represent a known temperature scale.

A second normal heat pattern for the low back is seen in Fig 1b. Here there is basically a midline increase of skin temperature which again consists of multiple nodular hot spots superimposed on a more homogeneous background. The warmest and frequently the broadest accentuation of heat is usually located at the L4 and L5 level.

In general therefore we found the normal low back thermogram to consist of patchy areas of increased heat with superimposed small nodular hot spots located in the midline and paraspinal region and most marked at the L4 and L5



Fig 2 Thermogram of low back in patient with acute intervertebral disc herniation at L5—S1 level dominant area of increased heat at L5—S1 level (arrow)

good insulator and does not permit the transmission of skin temperature if the covering is heavy. In the thermographic scans the whiter the area the warmer its relative temperature. The number at the lower portion of some of the pictures indicates the sensitivity setting of the camera and defines the temperature range recorded between the pure white and the pure black regions of the film. The sensitivity scale extends from 0 to 100 and indicates a temperature range on the film of 10.4°C for a setting of 0 down to 1.2°C for a setting of 100. At number 20 the gray scale range amounts to 4.1°C .

Thermographic evaluation of the back and the head was carried out on a series of 75 patients at the Neurological Institute of New York and this study is being continued at the Albert Einstein Medical Center in Philadelphia. Some observations will be presented on our preliminary experience with thermography in each of these two categories.

Back

The heat picture of the normal back varies greatly from person to person. Several general patterns and characteristics of normal heat distribution can, however, be recognized in the low back. One of the common normal patterns seen was a diffuse increased heat in the midline and paraspinal area of the lumbosacral region consisting of ill defined patchy areas within which there were seen small nodular like accentuations of the heat (Fig 1a). The warmest areas were usually seen at about the level of L4 and L5 and frequently were slightly eccentrically situated. The vertical white stripe at the lower end of the thermo-

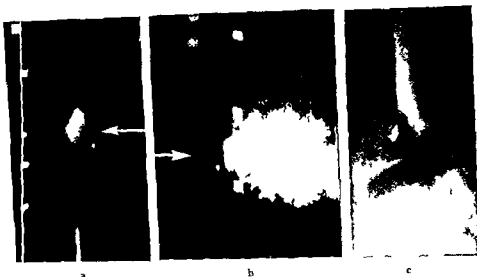


Fig 3 Back thermograms in patients with symptomatic lumbar spondylosis. a) Dominant heat pattern (arrow) 5 cm above level of iliac crest in a patient with malalignment between L3 and L4. b) Dominant heat pattern spreading diffusely over low back most accentuated at level of L5 (arrow). Patient had a spondylolisthesis between L4 and L5. c) A severe compression of the spinal canal is present from dorsally thickened ligaments and bone at level of malalignment at L4-L5. Nodular filling defects in opaque column below the level of compression represent dilated veins secondary to the partial obstruction.

gram surrounded by the large cold (dark) area represents the midline intergluteal cleft with the adjacent buttocks which is always relatively cold due to its thick covering of adipose tissue. This stripe is a useful midline orienting landmark. Heated wires were placed above the skin at known distances from the iliac crest. From the lowest up these were situated 5 cm below the crest, at the crest, 5 cm above the crest, and 15 cm above the crest. These markers are seen at the side of the thermograms. The multiple different geometric forms also seen on the side of the scans represent a known temperature scale.

A second normal heat pattern for the low back is seen in Fig 1b. Here there is basically a midline increase of skin temperature which again consists of multiple nodular hot spots superimposed on a more homogeneous background. The warmest and frequently the broadest accentuation of heat is usually located at the L4 and L5 level.

In general, therefore, we found the normal low back thermogram to consist of patchy areas of increased heat with superimposed small nodular hot spots located in the midline and paraspinal region and most marked at the L4 and L5



Fig. 4

Fig. 4. Low back thermogram in a patient with an intraspinal vascular malformation at level of L2—L3. A marked accentuation over the normal heat pattern is present in the upper lumbar region in the midline (arrow).



Fig. 5

Fig. 5. Normal face thermogram. Symmetrical heat pattern of forehead below hair line (arrow).

levels. For a heat pattern to be considered abnormal, the thermogram had to reveal a dominant well defined hot spot which was definitely larger than the normal small nodular hot spots.

Twenty six cases with proven herniated intervertebral discs were thermographed. Only 4 of 21 lumbar herniations had what we considered to be abnormal heat patterns (Fig. 2). No cases with abnormal patterns were seen in the five herniated thoracic or cervical discs.

In a small group of patients with back pain and malalignment of the lumbar spine, pathologic thermograms were consistently present (Fig. 3). The malalignment in all four cases was secondary to degenerative intervertebral disc and posterior joint disease. On myelography in these cases various degrees of block were present due to the abnormal alignment and thickening of ligaments dorsally (Fig. 3c).

Of six cases with intraspinal and paraspinal tumors three revealed abnormal heat patterns. Two of the three positive thermograms were in patients



Fig 6 Face thermogram in 26 year-old patient with an old left supraclinoid internal carotid artery occlusion with collateral filling of a hypoplastic middle cerebral artery. There is marked related coolness of left side of forehead (arrow)

with intradural neurofibromas that produced significant blocks on myelography. The hot spots on the thermograms corresponded to the level of the myelographic block.

An intraspinal vascular malformation produced a well localized dramatic hot spot in the low back (Fig 4). Two cases of osteomyelitis of the spine, one being chronic and two cases of metastatic spinal and paraspinal malignant disease had abnormal thermograms.

Three positive thermograms were encountered in symptomatic patients in whom no definite pathology could be discovered on routine radiological examination: myelography or surgery.

Head

Sixteen patients with diseases of the brain and skull were evaluated. The results of thermography in this group are given below. For satisfactory thermo-

	Patients	Tests
Meningioma	3	3
Intercerebral tumor	3	3
Pituitary adenomas	1	2
Multifocal sclerosis	1	1
Carotid occlusion	1	1
Cerebellar tumor	0	1
Sinus mucocoeles	0	2



Fig 4

Fig 4 Low back thermogram in a patient with an intraspinal vascular malformation at level of T2-L3. A marked accentuation over the normal heat pattern is present in the upper lumbar region in the midline (arrow)



Fig 5

Fig 5 Normal face thermogram. Symmetrical heat pattern of forehead below hair line (arrow)

levels. For a heat pattern to be considered abnormal, the thermogram had to reveal a dominant well defined hot spot which was definitely larger than the normal small nodular hot spots.

Twenty six cases with proven herniated intervertebral discs were thermographed. Only 4 of 21 lumbar herniations had what we considered to be abnormal heat patterns (Fig 2). No cases with abnormal patterns were seen in the five herniated thoracic or cervical discs.

In a small group of patients with back pain and malalignment of the lumbar spine, pathologic thermograms were consistently present (Fig 3). The malalignment in all four cases was secondary to degenerative intervertebral disc and posterior joint disease. On myelography in these cases various degrees of block were present due to the abnormal alignment and thickening of ligaments dorsally (Fig 3c).

Of six cases with intraspinal and paraspinal tumors, three revealed abnormal heat patterns. Two of the three positive thermograms were in patients

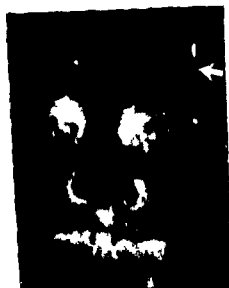


Fig 6 Face thermogram in 26-year-old patient with an old left supraclinoid internal carotid artery occlusion with collateral filling of a hypoplastic middle cerebral artery. There is marked related coolness of left side of forehead (arrow).

with intradural neurofibromas that produced significant blocks on myelography. The hot spots on the thermograms corresponded to the level of the myelographic block.

An intraspinal vascular malformation produced a well localized dramatic hot spot in the low back (Fig 4). Two cases of osteomyelitis of the spine, one being chronic and two cases of metastatic spinal and paraspinal malignant disease had abnormal thermograms.

Three positive thermograms were encountered in symptomatic patients in whom no definite pathology could be discovered on routine radiological examination: myelography or surgery.

Head

Sixteen patients with diseases of the brain and skull were evaluated. The results of thermography in this group are given below. For satisfactory thermo-

	Patient	Total
Meningiomas	3	3
Frontal lobe tumor	3	3
Pituitary adenoma	1	2
Multiple sclerosis	1	1
Carotid occlusion	1	1
Cerebellar tumor	0	1
Sinus mucocoeles	0	2



Fig 4

Fig 4 Low back thermogram in a patient with an intraspinal vascular malformation at level of T2—L3. A marked accentuation over the normal heat pattern is present in the upper lumbar region in the midline (arrow).



Fig 5

Fig 5 Normal face thermogram. Symmetrical heat pattern of forehead below hair line (arrow).

levels. For a heat pattern to be considered abnormal, the thermogram had to reveal a dominant well defined hot spot which was definitely larger than the normal small nodular hot spots.

Twenty six cases with proven herniated intervertebral discs were thermographed. Only 4 of 21 lumbar herniations had what we considered to be abnormal heat patterns (Fig 2). No cases with abnormal patterns were seen in the five herniated thoracic or cervical discs.

In a small group of patients with back pain and malalignment of the lumbar spine, pathologic thermograms were consistently present (Fig 3). The malalignment in all four cases was secondary to degenerative intervertebral disc and posterior joint disease. On myelography in these cases various degrees of block were present due to the abnormal alignment and thickening of ligaments dorsally (Fig 3c).

Of six cases with intraspinal and paraspinal tumors, three revealed abnormal heat patterns. Two of the three positive thermograms were in patients



Fig 6 Face thermogram in 26-year-old patient with an old left sup ached internal carotid artery occlusion with collateral filling of a hypoplastic middle cerebral artery. There is marked related coolness of left side of forehead (arrow)

with intradural neurofibromas that produced significant blocks on myelography. The hot spots on the thermograms corresponded to the level of the myelographic block.

An intraspinal vascular malformation produced a well localized dramatic hot spot in the low back (Fig 4). Two cases of osteomyelitis of the spine, one being chronic and two cases of metastatic spinal and paraspinal malignant disease had abnormal thermograms.

Three positive thermograms were encountered in symptomatic patients in whom no definite pathology could be discovered on routine radiological examination, myelography or surgery.

Head

Sixteen patients with diseases of the brain and skull were evaluated. The results of thermography in this group are given below. For satisfactory thermo-

	Positive	Total
Meningiomas	3	3
Intercerebral tumor	3	5
Pituitary adenoma	1	2
Multiple sclerosis	1	1
Carotid occlusion	1	1
Cerebellar tumor	0	1
Sinus mucocoeles	0	2



Fig. 4

Fig. 4 Low back thermogram in a patient with an intraspinal vascular malformation at level of L2—L3. A marked accentuation over the normal heat pattern is present in the upper lumbar region in the midline (arrow)



Fig. 5

Fig. 5 Normal face thermogram. Symmetrical heat pattern of forehead below hair line (arrow)

levels. For a heat pattern to be considered abnormal, the thermogram had to reveal a dominant well defined hot spot which was definitely larger than the normal small nodular hot spots.

Twenty six cases with proven herniated intervertebral discs were thermographed. Only 4 of 21 lumbar herniations had what we considered to be abnormal heat patterns (Fig. 2). No cases with abnormal patterns were seen in the five herniated thoracic or cervical discs.

In a small group of patients with back pain and malalignment of the lumbar spine, pathologic thermograms were consistently present (Fig. 3). The malalignment in all four cases was secondary to degenerative intervertebral disc and posterior joint disease. On myelography in these cases various degrees of block were present due to the abnormal alignment and thickening of ligaments dorsally (Fig. 3c).

Of six cases with intraspinal and paraspinal tumors three revealed abnormal heat patterns. Two of the three positive thermograms were in patients



Fig 8 Patient with a proven left mid supratentorial malignant glioma. a) Bilateral head thermograms showing pathologically warm region on left (arrow) above ear. Compare with symmetrical area on opposite side. b) Left carotid angiogram, arterial phase. The typical displacement of the superficial arteries (arrow) can be seen localizing the tumor to same region as the thermographic abnormality.

Discussion

Increased skin temperature overlying malignant tumors of the breast as well as in other soft tissues and bone has been amply documented (BARNES & GERSHON COHEN 1963, 1963, LAWSON 1957). It was somewhat surprising to find localized areas of increased back temperature when only benign underlying spinal conditions existed such as malalignment, intraspinal neurofibromata and occasionally herniated intervertebral discs. In most of these abnormal back thermograms some degree of chronic block existed in the subarachnoid pathway as seen myelographically. This block may in some way be related to the increased skin warmth either from alteration in the route of venous drainage or possibly from vasodilation secondary to nerve injury.

The warm area of the scalp overlying some intracranial neoplasms is possibly due to the direct conduction of tumor heat secondary to increased metabolism to the surface through the calvarium. In meningioma the increased surface vascularity probably contributes to the local temperature rise. The decreased heat of the forehead found in the patient with the old internal carotid artery occlusion and hypoplastic middle cerebral artery appears to be related to the lower metabolic activity of the underlying poorly vascularized portion of the brain. If further work shows this difference in cranial thermographic patterns between tumor and occlusive vascular disease to be consistent and valid it will be of great help in the evaluation of certain selective cases.



Fig. 7 Bilateral head thermogram in a patient with a large right pterional meningioma. Thermogram positioned so that each side of head is facing towards middle of film. Asymmetrical increased brightness on right in front of ear.

grams of the head to be obtained, it was necessary to have the hair closely clipped due to the barrier the hair imposed on recording infrared radiation coming from the scalp. On occasion a thermogram of the forehead provided some useful information. The normal face thermogram (Fig. 5) reveals a symmetrical heat pattern in the forehead region. At the hair line there is a sharp cutoff to the transmission of scalp warmth.

An abnormal face thermogram was encountered in a 26 year old patient with a moderate right sided weakness dating back to childhood (Fig. 6). An asymmetrical coolness of the left side of the forehead was present with sparing of the parmidline region. On angiography an occlusion of the supraclinoid segment of the left internal carotid artery was found with filling of a hypoplastic left middle cerebral artery through collateral circulation via the lenticulo striate arteries. The external carotid circulation was normal.

Three patients with meningiomas were thermographed. All had abnormal heat patterns. An asymmetrical hot region is seen in front of the right ear in a patient with a pterional meningioma (Fig. 7).

Five patients with intracerebral tumors were evaluated. Three of them showed asymmetrical heat patterns with increased warmth being recorded in the overlying scalp. An asymmetrical warm area can be identified in Fig. 8a on the left above and slightly in front of the ear. The lateral left carotid angiogram demonstrated the vascular displacement indicating the localization of the underlying cerebral tumor which at craniotomy was found to be a glioma with malignant change (Fig. 8b).

RÉSUMÉ

Les auteurs ont fait une expérimentation préliminaire avec un appareil spécial pour la mesure de la température cutanée chez des malades neurologiques atteints d'affections intracrâniennes et intrarachidiennes. Certaines lésions peuvent être détectées par cette méthode. Les propriétés isolantes de la chevelure gênent considérablement la détection au niveau de la tête. Les disques intervertébraux herniés n'ont pas donné des résultats constants. Certaines tumeurs intrarachidiennes ont été détectées ainsi que des lésions inflammatoires, néoplasiques et spondyliques.

REFERENCES

- BARNES R. B. *Thermography of the human body*, Science 140 (1963) 870
BARNES R. B. and GERSHON COHEN J. *Clinical thermography*, J. Amer. med. Ass. 185 (1963) 949
— — *Thermomastography*, J. A. Einstein med. Cent. 11 (1963) 107
DE SOL A. A. and SOVERAL RODRIGUES F. *Angioarchitecture of the skin*, Amer. J. Roentgenol. 88 (1967) 112
HARDY J. D. *Summary review of the influence of thermal radiation on human skin*, U.S. Naval Air Development Center, Johnsville, Pa. Report No. NADC-NA 5415, 1954
LAWSON R. N. *Thermography—a new tool in the investigation of breast lesions*, Canad. Serv. med. J. 13 (1957) 517

Conclusions

Thermography of the spine and head was performed in the evaluation of many of the common conditions encountered in a neuroradiological clinic. The number of cases in each entity studied was too small to permit any definite conclusions. The results to date, however, have shown that thermography of the back was negative in most cases of herniated intervertebral discs. All four patients with symptomatic malalignment of the lumbar spine had abnormal hot spots on the scans. Three of six patients with intraspinal and paraspinal tumors revealed localized warm areas along with one case of an intracranial spinal vascular malformation, two cases of spinal bacterial inflammatory disease and two cases of metastatic malignancy to the back. The great variability of the normal back thermographic pattern makes interpretation of possible minor abnormalities difficult.

In the head the need for completely clipping the hair restricts to a great extent its routine use in the evaluation of intracranial disease. Sixteen cases with intracranial and cranial disease were thermographed. All three surface meningiomas presented asymmetric warm areas over the tumors. Three of five intracerebral tumors were localized on the thermograms as pathologic areas with increased temperature. A case with an old internal carotid artery occlusion and secondary hypoplasia of the middle cerebral artery revealed a relative cool region of the forehead on the side of the occlusion.

Acknowledgement

Supported in part by the National Institute of Neurological Diseases and Blindness Fellowship Numbers 2F11NB976 02 and 2F11NB973 C2.

SUMMARY

Preliminary experiences with the use of a special apparatus for the measurement of the skin temperature in neurological patients with intracranial and intraspinal diseases is presented. It appears that certain lesions can be detected by this method. In the head the technique is severely handicapped by the insulating properties of hair. In the spine herniated intervertebral discs have not produced consistent results. Certain tumours have been detected and inflammatory, neoplastic and spondylitic processes have also been shown.

ZUSAMMENFASSUNG

Preliminäre Erfahrungen in der Anwendung einer Specialapparatur zur Messung der Hauttemperatur von neurologischen Patienten mit intrakraniellen und intraspinalen Erkrankungen werden mitgeteilt. Es scheint, dass bestimmte Erkrankungen mit dieser Methode entdeckt werden können. Am Schädel ist diese Technik durch die isolierenden Eigenschaften des Haares sehr beeinträchtigt. An der Wirbelsäule hat man bei Diskushernien keine einstim- migen Resultate erhalten. Man konnte inflammatorische, neoplastische und spondylitische Prozesse zeigen.



Fig 1 Focal ultrasonic lesion in cat brain
(Courtesy of R. WARWICK)

even more important, the relative immunity of the blood vessels over capillary size

In the ARSLAN technique the bone over the lateral semicircular canal is reduced to less than 0.5 mm thickness. With the true focusing technique used in neurosurgery the craniotomy is temporarily removed over a wide area.

The complete removal of bone alters the whole picture. Instead of the absorption, refraction and reflection produced by the skull vault, the rays travel virtually without deviation from the transducer through a coupling bath, through the membranes and brain tissue to reach a focus at a predictable site.

The technical features of this procedure will be omitted here, as they will be given in a paper at the IEEE Symposium in October and most have already been published in chapter 20 of *Ultrasound as a diagnostic and surgical tool*. The transducers used by the American workers employed a flat quartz crystal and a plastic lens. The modern ceramic crystals ground to form a focusing bowl suffer from frequency instability with temperature and have not been accepted in America. This disadvantage has been overcome by improved methods of monitoring and self-tuning and their inherent advantages of constancy of focus position and low operating voltage can now be used without hesitation.

Owing to the large solid angle of radiation employed, the intensity rises very rapidly to a high level and as rapidly falls once the focus has been passed. In this way it is possible to produce localized areas of cell necrosis in the brain with no overlying damage (Fig 1).

Both FRY and BALLANTINE employed a very fine thermocouple probe to identify the position of the focus. This requires elaborate special equipment

ULTRASONIC SURGERY OF THE CENTRAL NERVOUS SYSTEM

by

DOUGLAS GORDON

The President of the Symposium in his opening address referred to the first paper on ultrasonic diagnosis read at the 1955 Symposium in London and to the way in which the new departure had become accepted as part of neuroradiology. As the author of the 1955 paper I now venture to suggest a subject that will become accepted by the Symposium of 1973.

Ever since the original paper one has been tempted to look forward to the day when ultrasonic tomograms through the skull would replace the cephalogram. Nearly eleven years of experience has convinced me that the physical limitations imposed by the cranial vault make such an end result very unlikely. The future of ultrasonic tomography is in the soft tissues that are not protected by dense bone, e.g. the liver, the eye, the uterus, etc.

For the past five years I have been engaged in work on the ultrasonic destruction of the vestibular apparatus of the inner ear by the technique first invented by ARSLAN (1964). His position as the Father of Ultrasonic Surgery is as unique as that of DUSSEK in ultrasonic diagnosis.

The use of highly focused ultrasound has been developed in the U.S.A. by FRY and his colleagues by MYERS and by LELL & BASARI. These investigators established the remarkable sensitivity of nerve tissue to ultrasound and,

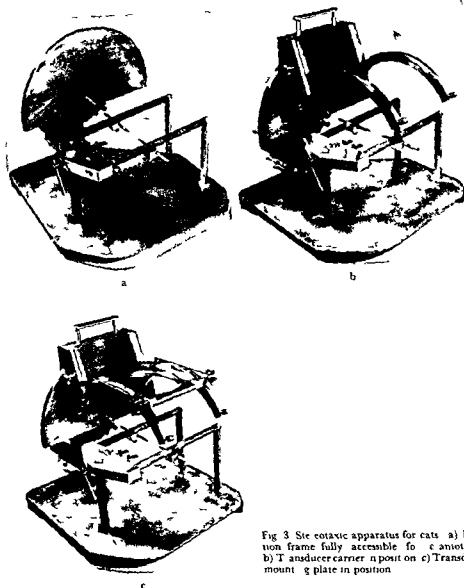


Fig 3 Stereotaxic apparatus for cats. a) Fixation frame fully accessible for craniotomy b) Transducer carrier in position c) Transducer mounting plate in position

the surface of the hemispheres but even to identify the position of the sagittal sinus to a matter of thousandths of an inch (fortieths of a millimeter). Further it has been possible to measure with similar accuracy the distance from the top of the lateral ventricle to the surface of the cortex above it.

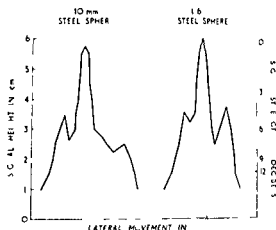


Fig 2 Echo amplitude with lateral scan at level of focus (diameter 10 cm focal length transducer 10 cm) showing the slight effect obtained by altering size of target sphere

beyond the variable funds. It was however essential to identify the position of the focus with accuracy. To do this biologically is very difficult. It was however realised that ultrasonic pulse techniques could be used for this purpose by the simple device of using a steel sphere as target. The bowl transducer is connected to a standard Sperry reflectoscope or echo encephalograph and the steel sphere is supported by a fine wire attached on the far side.

When the center of the sphere corresponds to the center of the focus, the rays all strike the surface of the sphere normally and are reflected back on their track. With the slightest displacement the angulation ceases to be optimum and the echo signal falls greatly. Strangely enough, there is hardly any effect on the accuracy if a sphere of 1.6 mm diameter is replaced by one 10.0 mm in diameter (Fig 2).

The extreme precision of this measurement will explain why the focussing can be so good that LELA has produced lesions as small as 50 nerve cells.

The use of the focused transducer and the reflectoscope had proved so satisfactory in calibration that it was decided to use it during the course of an animal operation. It is possible to obtain large echo signals from a very small structure at the focus, but large structures elsewhere in the beam part gave no detectable signals. By restricting observation to the signals obtained from the focal area it was possible to map out the anatomy of the upper surface of the brain at the first attempt, using a British flow detector. The pulse length was however so long that no deeper structure could be detected. It was thought necessary to employ a special damped transducer to obtain short enough pulses.

Very recently however the Sperry reflectoscope became available and it was found possible with this to obtain short enough pulses from the standard undamped bowl transducer. Two cats have been operated upon with the latest equipment and in each case it has been possible not merely to identify

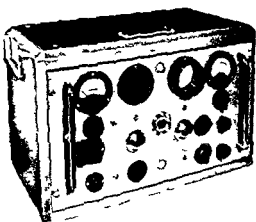


Fig. 6 Ultrasonic power generator for lesions making

antero posterior plane and by a mounting plate that slides over the curved arms to give lateral angulation. These movements are arranged to produce no shift of the focus relative to the semicircular plate (Fig. 3b and c).

Into the recess in the mounting plate can be put a pointer that indicates the position of the focus 15 cm from the center of the 15 cm diameter circle. All the transducers are adjusted to have their foci at the same point relative to the recess. If necessary the pointer can be introduced first to indicate the site of the focus and a series of readings taken on the scales that indicate the position of the focus according to Horsley Clark Cartesian co-ordinates. If the position of the sagittal sinus is known relative to the ear bars the brain size can be determined (Figs 4 and 5).

Alternatively the transducer can be inserted and the sinus located ultrasonically. In the complete equipment a parallelogram pantograph will be attached to the baseplate and to the transducer plate and the other end will move a pointer over the teledeltos paper. In this way a magnified tomogram will be produced from which the site of the tissue to be destroyed can be determined. The transducer is moved to bring the focus to the site and its cable is then connected to a power generator to produce the lesions. Each lesion will be recorded automatically on the same teledeltos paper.

The results of stereotaxic surgery in Parkinsonism using the Bennett apparatus are so good that it is not suggested that ultrasound should be used to attack the globus pallidus. The scope foreseen for the new technique is immediately in neurophysiology and later in tractotomy of the cord, the reduction in size of gliomata of the dominant hemisphere and in attacking tumors in the pons and other surgically inaccessible sites. Only time will show the value and limitations of this new technique.

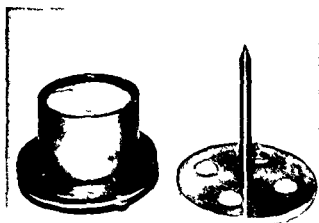


Fig 4 Pointer and transducer for stereotaxic apparatus. Center of curvature of concave transducer has the same relation to the mount as the pointer tip. Aperture in transducer is for saline circulation.



Fig 5 Transducer in position in the mounting plate.

The application of this degree of precision to the localization of an electrode within the brain stem is obvious. There are however other commoner applications. The new equipment, when complete, will permit the automatic recording of magnified coronal or sagittal cross sections of the brain or spinal cord through the unopened dura.

Electronically it is a simple matter to select only those echo signals that occur at the focus to amplify them and make them record on teledeltos paper. It is already possible to obtain suitable signals from the cortex and ventricles but with further developments it may well be possible to detect the interfaces between grey and white matter.

Technique. While performing the craniotomy only the semicircular transducer plate is in position (Fig 3a). When sufficient access has been obtained the frontal sinuses, if opened, are sealed with bone wax and a sponge rubber gasket makes a water tight seal between the skull and under surface of a plate with a central aperture.

A saline reservoir is provided by using nylon film and rings of clear perspex (lucite) to construct a bath of sufficient height. The nylon is clamped to the edge of the opening in the plate so that degassed saline can fill the space between the dura and the transducer.

The transducer is supported by a carrier that provides angulation in the

- DUSSEK K. T. Über die Möglichkeit hochfrequente mechanische Schwingungen als diagnostisches Hilfsmittel zu verwenden. *Z. Neurol.* 174 (1942) 153
- FRY W. J. Neurosonic surgery. In *Ultrasound in biology & medicine* Ed E. Kelly p. 99. American Institute of Biological Sciences, Washington 1957
- GORDON D. An apparatus for producing lesions in small animals with focused ultrasound. In *Ultrasound as a diagnostic & surgical tool* Ed D. Gordon p. 233. E & S Livingstone, Edinburgh 1964
- LELE P. P. and BASALAI L. A simple method for production of trackless focal lesions with focused ultrasound. In *Ultrasound as a diagnostic & surgical tool* Ed D. Gordon p. 185. E & S Livingstone, Edinburgh 1964
- MEYERS R., FRY F. J., FRY W. J., EGGLETON R. C. and SCHULTZ D. F. Determination of topological human brain representations and modifications of signs and symptoms of some neurologic disorders by the use of high level ultrasound. *Neurology* 10 (1960) 271

Acknowledgements

This work was made possible through the Clinical Research Fund of the North West Metropolitan Board of the National Health Service. Technical assistance from Dr H C Grant in performing the neurohistologic investigations and from the Sperry Products Co for the modified reflectoscope have been invaluable, thanks are also due to the Paddington General Hospital staff for animal operation facilities.

SUMMARY

Highly focused ultrasonic transducers have been developed using ceramic piezo electric materials which can be employed to produce sharply defined trackless focal lesions in the central nervous system. Ways have been found to use the same transducers with an echo technique to establish the internal anatomy of the brain with high accuracy. Steel spheres in water baths permit the accuracy of focusing of the transducer to be established. The size of the steel sphere is unimportant. Automatic recording of the anatomy in cross section in enlarged form is being planned.

ZUSAMMENFASSUNG

Stark fokussierte Ultraschallstrahler sind unter Verwendung von keramischen piezo-elektrischem Material mit dem man scharf umschriebene narbenlose fokale Veränderungen im ZNS erzeugen kann entwickelt worden. Es wurden Wege gefunden dieselben Strahler bei Echo Technik zu verwenden um die innere Gehirnanatomie mit grosser Genauigkeit bestimmen zu können. Stahlkugeln im Wasserbad gestatten eine genaue Fokussierung der Strahler. Die Grösse der Stahlkugeln ist nicht von Bedeutung. Automatische Registrierung von anatomischen Querschnitten in vergrösserter Form ist geplant.

RÉSUMÉ

Des matériaux céramiques piézo électriques ont permis de fabriquer des transducteurs ultrasoniques très focalisés que l'on peut utiliser pour créer des lésions focales à limites nettes dans le système nerveux central. On a trouvé le moyen d'utiliser ces mêmes transducteurs par une technique d'écho pour établir avec une haute précision l'anatomie interne du cerveau. La précision de la focalisation du transducteur peut être appréciée au moyen de sphères d'acier placées dans l'eau. Le diamètre de la sphère d'acier est sans importance. L'auteur a le projet de faire des enregistrements automatiques en coupes agrandies de régions anatomiques.

REFERENCES

- ARSLAN M. An improved technique of the ultrasonic irradiation of the vestibular apparatus by Ménière's disease. In *Ultrasound as a diagnostic & surgical tool* Ed. D. Gordon p. 288 E. & S. Livingstone Edinburgh 1964.
- BALLANTINE Jr. H. T., HUETER T. F., NAUTA W. J. H. and SOSA D. M. Focal destruction of nervous tissue by focused ultrasound. Biophysical factors influencing its application. *J. exp. Med.* 104 (1956) 337.

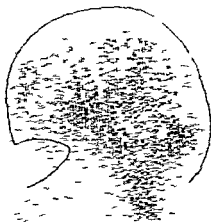


Fig 1 Dilatation de la partie intracrânienne de la grande citerne (meso-citerne) sans atrophie cérébelleuse vérifiée par encephalographie gazeuse fracturée. Forte radioactivité du pôle postérieur de la fosse postérieure

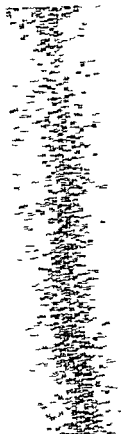


Fig 2 Atrophie médullaire diffuse vérifiée par myelographie gazeuse. Homogénéisation du contraste scintigraphique sur toute l'étendue du rachis (5 h après injection de 200 microcuries de RISA)

superposable dans les cas d'obstacle partiel. Le methiodal et la RISA marquent en effet un arrêt complet devant un obstacle incomplet alors que le contraste lourd (lipiodol) montre la persistance d'un passage au niveau de tels obstacles partiels. Dans un cas nous avons constaté d'autre part que la diffusion de la sérum albumine était bloquée devant un obstacle cervical également incomplet dans ce cas le contraste aérien franchissait cet obstacle en délimitant parfaitement l'opacité tumorale (meningiome cervical).

Les atrophies cérébrales corticales sont bien objectivées par l'importance de la radioactivité des espaces pericrâniens. Il en est ainsi pour les atrophies diffuses et pour les atrophies localisées. Le scintigramme latéral de la fosse postérieure est assez variable car on observe une radioactivité toujours importante au niveau des citernes pre-bulbopontiques avec une diffusion très inconstante dans la grande citerne. Les cas de megaciterne non pathologique

SCINTIGRAPHIE CISTERNALE

par

CH. M. GROS, A. WACKENHEIM, C. VROUNOS et M. SUBIRANA

Nous avons présenté ailleurs nos premiers résultats de scintigraphie cisternale obtenue par scanning avec le nucléographe de Siemens. Actuellement nous disposons de 60 examens scintigraphiques tant du canal rachidien que des cisternes intracrâniennes après injection lombaire de 200 microcuries de sérum albumine humaine marquée à l' ^{131}I .

L'examen scintigraphique, bien que soumis à des servitudes techniques résultant de la longueur du temps d'enregistrement et de l'imprécision morphologique inhérente aux méthodes actuelles, semble néanmoins devenir un examen de routine. Les neurologues et neurochirurgiens sont encore peu orientés vers ce type d'examen en raison de la multiplicité des autres moyens d'investigation radiologique mis à leur disposition.

Notre matériel est très homogène quant à la technique d'application. Nous avons toujours procédé aux scintigrammes 5 heures après injection lombaire. Il est évident que l'exploration fonctionnelle et morphologique approfondie devrait comprendre des enregistrements répétés dans le temps. Dans ce travail, nous tenons à préciser quelques points particuliers observés sur ce matériel de 60 cas.

Des examens scintigraphiques confrontés avec les données du contraste hydrosoluble nous ont permis de constater qu'ils avaient un comportement

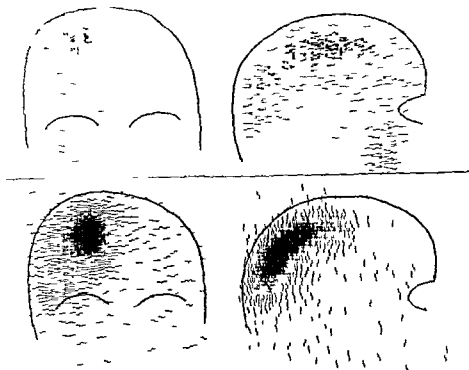


Fig 4 Hématome péri-crânien droit du nourrisson (injection par la fontanelle antérieure) En haut Grande cavité parasagittale s'étendant dans la fosse cérébrale moyenne En bas (Dix jours après ponction évacuatrice) Persistance d'une cavité paréto-occipitale Les parties frontale et basale de l'hématome ont disparu

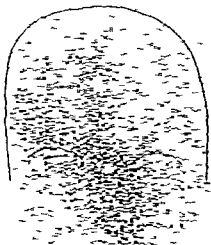


Fig 5 Masse expansive frontale gauche (glioblastome) Exclusion de la cisternographie gauche Déviation des cisternes sagittales vers la droite

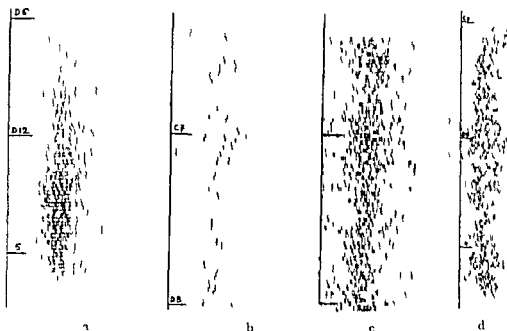


Fig. 3 Forte diminution de la radio-activité cervico dorsale vraisemblablement en rapport avec la position en procubitus pendant l'examen a) Forte radio-activité du segment lombaire b) Faible radio-activité cervico dorsale (conditions d'enregistrement identiques qu'en a) c) Enregistrement de toutes les impulsions de la région cervico dorsales d) Elargissement de l'image scintigraphique des régions dorsolombo sacrée avec faux arrêt au niveau de C7 (injection lombaire) Ce trouble de la diffusion constaté 5 h après l'injection semble dû à la diffusion latérale du radio élément

se caractérisent par une forte activité de la région occipitale postérieure et ne peuvent pas être interprétés comme signe d'atrophie cérébelleuse. L'étendue de la tente du cervelet est toujours bien dessinée.

Les cas d'atrophie médullaire sont moins explicites. Dans un cas d'atrophie médullaire segmentaire vérifiée chirurgicalement, nous avons observé une hyperactivité nettement localisée dans le segment atrophique. Dans un cas d'atrophie médullaire diffuse vérifiée par myélographie gazeuse, nous avons observé une nette homogénéisation du noircissement sur l'ensemble du canal rachidien.

Dans 4 de nos 60 cas, il existait une très nette diminution de la radio-activité cervico dorsale qui pose a priori le problème d'un rétrécissement du canal rachidien ou d'une hypertrophie diffuse du cordon médullaire. Dans aucun de ces 4 cas, nous n'avons pu vérifier l'une de ces hypothèses. Cette répartition hétérogène semble être en rapport avec la moindre quantité du liquide céphalo rachidien dans la région dorsale en position de procubitus, que nous avons fait adopter à nos malades dans cette première série d'examen.

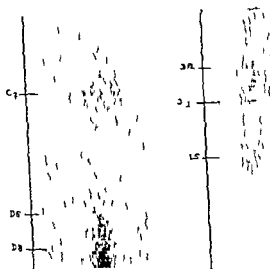


Fig. 7 Suspicion d'arachnoïdite spinale après méningite purulente (malade du Professeur G. ARNOULD, Nancy). A gauche Arrêt à la hauteur de D6 marquant un blocage qui est incomplet car on note une certaine activité au niveau de C7. A droite Nettoyage de l'activité au niveau de la queue de cheval.

s'avère très utile pour la délimitation beaucoup plus précise et plus élégante que la méthode pneumographique. Cette dernière nécessite en effet de nombreux clichés dans les différentes positions et souffre des rapports hydroaériques alors que le radioélément diffuse dans l'épanchement proprement dit en réalisant un mélange homogène. Les contrôles scintigraphiques après ponction ou intervention permettent de suivre l'extension du volume de la cavité. Dans deux cas nous avons été frappés par l'extension de ces épanchements péricérébraux du nourrisson vers la base du crâne au niveau du pôle antérieur de la fosse cérébrale moyenne.

Nous n'insistons pas sur la facilité du diagnostic scintigraphique de déviation du plan sagittal médian lorsqu'il s'agit de processus expansifs hémisphériques d'une certaine taille. Les modifications scintigraphiques directes sous forme de zone froide ou chaude sont bien entendu plus difficiles à reconnaître tant de face que de profil. L'exclusion de certaines cisternes viendra toutefois renforcer les possibilités de diagnostic.

La scintigraphie cisternale s'avère particulièrement intéressante dans les cas de blocage arachnoïdien. La diffusion du radioélément se fait toujours très nettement dans les cisternes basales. Le blocage de ces cisternes s'accom-

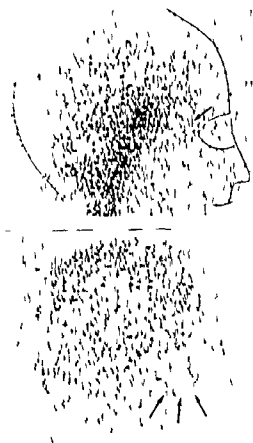


Fig. 6 Rhinorrhée cérébro-spinale spontanée par fistule de la partie antérieure droite de la lame criblée. *En haut* L'alignement de quelques symboles indique le siège de la fistule (→) sur le scintigramme de la 5e h. *En bas* Après 24 h le radio élément intracrânien a diffusé dans les cisternes basales antérieures et parasagittales. Il existe en outre un renforcement de la radio activité dans la région ethmoïdale par l'accumulation de l'CR radioactif (→)

Dans 5 cas nous observons un élargissement anormal du scintigramme rachidien. Cet élargissement est particulièrement prononcé dans la région lombaire. Dans 1 de ces cas la diffusion du radio élément est arrêtée à la hauteur de C7. Il s'agit d'un faux arrêt, la myélo radio cinématographie ayant démontré l'absence d'obstacle avec des signes de protrusion discale cervicale. Le faux arrêt enregistré à la 5e heure est probablement en rapport avec la diffusion latérale du radio élément. Il semble d'ailleurs que dans 3 autres cas d'élargissement scintigraphique du canal rachidien il s'agit de diffusion latérale (radiculaire?) du radio élément. Dans une seule de nos 5 observations de dilatation scintigraphique transversale du canal rachidien lombaire nous avons pu constater une image sacro-radiculographique de dilatation du fourreau sous arachnoïdien lombaire avec kystes radiculaires. L'exploration scintigraphique des arachnoïdites spinales s'avère particulièrement intéressante, car elle permet de localiser des zones lacunaires d'hypo activité ainsi que les blocages.

Dans les cas d'épanchements sanguins péri-cérébraux du nourrisson (nous avons étudié trois malades), l'injection du radio élément par le bregma

schen Subtentoriale Tumoren der Hemisphären des Kleinhirns zeigen die Verschiebung der Mittellinie nach der gegensätzlichen Seite in Szintillogramm. Ebenso kann die Ausweitung der Cysten bei Kleinhirnatrophie und Stenosen bei Arachnoiditis erkannt werden. Fisteln zwischen dem Gehirn und dem Gesichtsschädel zeigen die radioaktive Hyperaktivität in der Linie der Fistel und möglicherweise in den Lufthöhlen des Gesichtsschädels. Die Füllung des Subduralraumes mit radioaktiven Stoffen ist die Methode der Wahl für die Aufzeiherung der Ausdehnung der subduralen Hamatome im Kindesalter.

BIBLIOGRAPHIE

- ATKINSON J R and FOLTZ E L Intraventricular RISA as a diagnostic aid in pre and post operative hydrocephalus *J Neurosurg* 19 (1967) 159
- BAGGIO G F et MORGANDO E Myeloscintigraphie Riv Pat nerv ment B4 (1963) 285
- — et SICURO A Notre expérience dans le diagnostic avec le scintillographie du canal rachidien *In Radioisotopes et Système nerveuse* Ed Fischgold et Planiol Masson et Cie 1964
- BAUER I K and JHULE T Myelography by means of I 131 The myeloscintigram *Neurology* 3 (1953) 341
- BELL R L Isotope transfer test for diagnosis of ventriculo-subarachnoidal block *J Neurosurg* 14 (1957) 674
- Isotope transfer test in the diagnosis and treatment of hydrocephalus *Int J appl Radiat* 5 (1959) 89
- Anatomic contour myelography in infants *A nucl Med* 3 (1962) 288
- and HERTSCH G L Automatic contour scanner for myeloscintigram *Int J appl Radiat* 7 (1959) 19
- DI CHIRO G Anatomy of the brain and basic principles of brain scanning *Progress in medical radioisotope scanning* US Department of Commerce Washington DC 20230 pages 347-370
- RISA encephalography and conventional neuroradiologic methods *Acta radiol Suppl* 201 (1961)
- New radiographic and isotopic procedures in neurological diagnosis *J Amer med Ass* 188 (1964) 574
- Anatomic three-dimensional brain scanning *In Radioisotopes et Système nerveuse* Ed Fischgold et Planiol Masson et Cie 1964
- FRAMES P M and MATTHEWS W B RISA ventriculography and RISA-cisternography *Neurology* 14 (1964) 185
- GIOL S N and FRENCH L A Systemic absorption and urinary excretion of Rihsa from subarachnoid space *Neurology* 5 (1957) 555
- ROS CH M et WACKENHEIM A La scintigraphie des cisternes intracrâniennes (cisterno-scintigraphie) Images normales et pathologiques *J de radiol d électrol et de méd nucléaire* 1965 sous presse
- — VROUSOS C et SUBIRANA M La scintigraphie des espaces sous arachnoidiens du canal rachidien *J de radiol d électrol et de méd nucléaire* 1965 sous presse
- LISS F M and SMAGIN B I The use of the scanning method for more accurate localization of spinal cord tumors *Medical Radiol* 5 (1960) 57
- MFALEY J RISA-encephalography *J Neurosurg* 19 (1962) 934
- MIGLIORE A PAOLETTI P e VILLANI R L'impiego degli isotopi radioattivi nello studio della dinamica liquorale *Riv Neurol* 31 (1961) 37

précise d'un arrêt de la diffusion que nous avons observé dans un cas suspect d'arachnoidite basale.

L'étude radiologique des rhinorrhées céphalorachidiennes est toujours particulièrement difficile. Les radioisotopes permettent naturellement de confirmer la radio-activité de l'écoulement après injection lombaire du radio élément. L'étude scintigraphique nous a permis de déterminer en outre le siège approximatif de la fistule. La densité des symboles est toutefois difficile à reconnaître au niveau du trajet fistuleux en raison de l'importance de la radio-activité des cisternes basales. Après 24 heures, nous avons observé une nette hyperactivité de la face, en rapport avec l'envahissement des cavités ethmoïdo-sinuses par la RISA du liquide céphalo-rachidien.

RÉSUMÉ

Les obstacles dans le canal rachidien sont facilement mis en évidence par la scintigraphie des espaces sous arachnoïdiens. En dehors de ces obstacles on rencontre des images très intéressantes de rétrécissement du canal rachidien. Lorsque le radioélément diffuse latéralement dans les poches radiculaires on peut observer des ralentissements de la diffusion qui simulent des arrêts. Dans les tumeurs hémisphériques sous-tentorielles la déviation contro latérale du plan sagittal médian est repérée sur le scintigramme. La dilatation cisternale des cas d'atrophie cérébrale, les arrêts d'hyperactivité et sténoses des arachnoïdites spinales sont également bien visibles. Les fistules liquidiennes cranio-faciales se caractérisent d'une part par l'hyperactivité du trajet fistuleux et d'autre part par la radio-activité secondaire des cavités pneumatiques de la face. La sous duréographie est l'examen de choix pour délimiter les cavités d'hématome sous dural du nourrisson.

SUMMARY

Obstructions in the vertebral canal are readily demonstrated by scintiscanning of the subarachnoid spaces. In addition to such obstruction interesting evidence of narrowing of the spinal canal may be encountered. When the radio-element diffuses laterally in the root sleeves a slowing of the diffusion simulating arrest may be observed. In subtentorial tumours of the hemispheres the contralateral deviation of the median sagittal plane is shown on the scintigram. Cisternal dilatation in patients with cerebral atrophy, arrested hyperactivity and stenoses in spinal arachnoiditis are also well demonstrated. Craniofacial fistulas are characterized on the one hand by hyperactivity of the fistular outline and on the other hand by secondary radio-activity of the facial air cavities. Subdurography is the examination of choice for delineating the cavities of subdural hematomas in infants.

ZUSAMMENFASSUNG

Verschlüsse des Wirbelkanals können leicht durch Scintillographische Untersuchung des Subarachnoidalraumes erkannt werden. Auch wichtige Information über eine Verengung dieses Raumes kann festgestellt werden. Die Diffusion des radioaktiven Elementes lateralwärts in die Ärmel der Nervenwurzeln geht langsam von statten und kann Verschluss vortau-

PALENCEPHALOGRAPHY

by

C G DE GUTIERREZ MAHONEY and C CUEVAS VERDU

Palencephalography is a method which can be applied for neurological diagnosis in the same manner as electroencephalography, echoencephalography or other non specific types of localizing measures. The term originates from the Greek *ταλσα* which can be translated to mean oscillation, pulsation or vibration. Attempts are being made through the analysis of the records acquired through palencephalography to approach a pathologic as well as a topographic diagnosis.

More than a decade ago a series of studies was made by the school of BARCIA GONZALEZ which followed the thesis of CALVO in 1950 concerning the vascular structures of cerebral tumors. They directed their studies to an interpretation of the vibrations which were recorded from various parts of the head with a microphone and they gave the name palencephalogram to the record obtained. After determining the appearance of the normal record they first studied the tracings in patients with intracranial tumors and intracranial hematomas. Later they studied the conditions found with abnormalities of the circulatory system such as arteriovenous fistulae, arteriosclerosis and hypertension, they also studied the records of psychotics. Since this work has not been corroborated by published reports from any other clinics we have undertaken the present study which has dealt principally with intracranial tumors, subdural hematomas, intracerebral hematomas and arteriovenous fistulae. We have in

- — Radioisotopic method for evaluating the patency of the Spitz Holter valve J Neurosurg 19 (1962) 605
- PERRYMAN C R, NOBLE P R and BRADON F H Myelogrammy: a useful procedure for localization of spinal block lesions Amer J Roentgenol 80 (1958) 104
- PINTO I Mielocintilogramma Contribuição à mielografia isotópica com ^{99}Tc nos bloqueios do espaço subaracnoideu I teste de concurso 1962 Rio de Janeiro Edit Impregrafica
- MACHADO O e PINTO COELHO A Mielocintilogramma Primeiros resultados Comunicação no 11 Congresso da Sociedade Brasileira de Neurocirurgia Porto Alegre Rio G do Sul 7—10 de setembro de 1960
- RIFSELBACH R, DI CHIRO G, IREIREICH F and RATTI D Subarachnoidal distribution of drugs following lumbar injection determined by autoradiography and external scanning New Engl J Med 267 (1962) 1273
- SWEET W H et coll The formation flow and absorption of cerebrospinal fluid newer concepts based on studies with isotopes Res Publ Ass nerv ment Dis 34 (1954) 101
- and LOCKSLEY H B Formation flow and reabsorption of cerebrospinal fluid in man Proc Soc exp Biol (N Y) 84 (1953) 397
- WACKENHEIM A, VROUSOS C et SUBIRANA M La scintigraphie des espaces sous arachnoïdiens du canal rachidien Quelques pages méd. scientifi. litt 150 (1964) 10
- — — La scintigraphie rachidienne Revus d'ONO 1965 sous presse
- WACKENHEIM A L'exploration du canal rachidien par la radiocartographie J de médecine de Besançon 3 (1965) 211
- Le diagnostic topographique de l'hématome péricérébral du nourrisson par la radiocartographie J de médecine de Besançon 1 (1966) 33

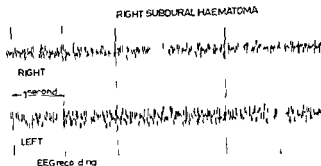


Fig 3 Palencephalogram of a right subdural hematoma showing diminution of amplitude as compared with normal left side

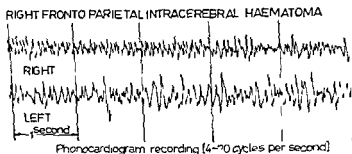


Fig 4 Palencephalogram (recorded with a phonocardiograph) of a right intracerebral hematoma showing diminution of amplitude as compared with opposite side

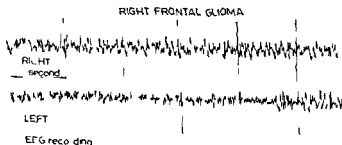


Fig 5 Palencephalogram of a right frontal glioblastoma. Note greater amplitude and distortion of waves (slowing and irregularity) as compared with left side

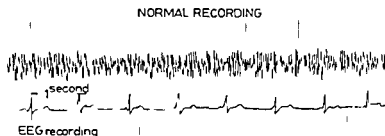


Fig 1 Normal palencephalogram recorded with electroencephalograph showing fusiform configuration of tracing with a frequency of 18 to 20 per sec in relation to cardiac activity (T.K.G.)

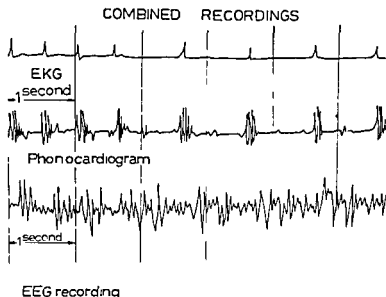


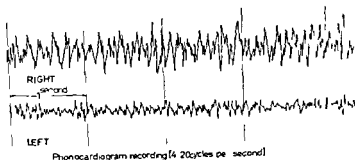
Fig 2 Normal palencephalogram recorded with electroencephalograph for comparison with the different configuration of the EKG and phonocardiogram showing their time relationships

some measure found comparable results, but do not feel that we can be as categorical in our report at this time as they have been.

The technique consists in the application of a microphone to various parts of the head and the recording of the vibration by means of a phonocardiograph or by electroencephalography. It is most important that the patient be at ease during the recording since emotional states cause artifacts due to an increase in the heart rate which can result in an increase of the frequency, amplitude and configuration of the waves. In addition to being quiet the patient should not swallow nor should there be any movement of his teeth, as these activities cause a high wave to be recorded. Records are run from various parts of the head and over comparable positions of both hemispheres.

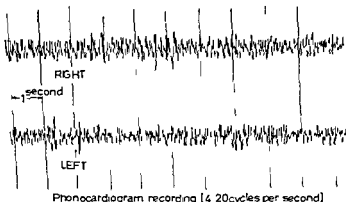
The vibrations are recorded as tracings of waves which are rhythmical

RIGHT OCCIPITAL ARTERIOVENOUS MALFORMATION before operation



Phonocardiogram recording [4 20 cycles per second]
Fig 8 Palencephalogram of a right occipital arteriovenous malformation (recorded with phonocardiograph) demonstrating increased amplitude and slowing of frequency as well as distortion of configuration of waves as compared to left side

RIGHT OCCIPITAL ARTERIOVENOUS MALFORMATION after operation



Phonocardiogram recording [4 20 cycles per second]
Fig 9 Palencephalogram of same case as in fig 8 after operation showing recovery toward normal pattern by diminution of amplitude and less distortion of waves compared with fig 8. The frequency is the same as the left side and the distortion is minimal

tumors meningiomas and arteriovenous malformations. We have also noted that there is a greater regularity to the amplitude of the waves with meningiomas than with these other processes which show a more variable spiky character.

These characteristics can best be considered by the presentation of typical tracings associated with various types of intracranial pathology as seen in Figs 1 to 9.

LEFT PARIETAL METASTATIC ADENOCARCINOMA



Fig 6 Talencephalogram of a left parietal metastatic bronchogenic adenocarcinoma showing greater amplitude slowing and irregularity of waves compared with right side

LEFT PARIETAL PARASAGITAL MENINGIOMA

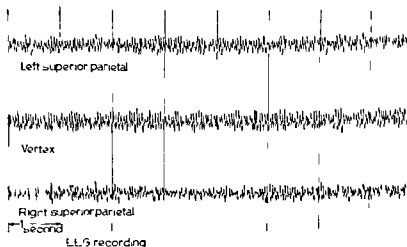


Fig 7 Talencephalogram of a left parietal parasagittal meningioma showing some increase of amplitude compared with right side. Note absence of fusiform morphopology on left side compared to right. There is no distortion of the morphopology of the tracing as seen in that of glioblastoma in fig 5

are related to the cardiac cycle, have a frequency of 5 to 20 cycles per second and an amplitude which is variable, being high in the frontal regions, of medium grade in the mid temporal and parietal regions and low in the occipital region. The frequency is also highest in the frontal region, reaching 20 per second, and is about 10 in the other regions.

We have found that the amplitude is the more diagnostic feature of the record, and with a subdural hematoma the amplitude is depressed over the site of the hematoma. This is also true with intracerebral hematomas. On the other hand the amplitude with gliomas is increased, as it also is with metastatic

RAPID BRAIN SCANNING WITH TECHNETIUM 99m

by

P V HARPER R A FINK D B CHARLESTON R N BECK K A LATHROP
and J P EVANS

Brain scanning for the diagnosis and localization of focal neurological disease is a well established adjunctive procedure in modern clinical practice. All forms of scanning however are limited on one hand, by the radiation dosage to the patient from the administered isotope and on the other by the prolonged scanning time and relatively poor resolution of the resulting picture. Nevertheless the innocuous nature of the procedure as compared to angiography and pneumography appears to warrant continued efforts to overcome these limitations. The present report describes preliminary results of a combined attack on various aspects of this problem.

The limitations of scanning are obviously reciprocal in nature. By doubling the isotope dosage one may reduce the scanning time to half or by sharpening the resolution of the collimator detector one may improve the resulting picture at the expense of sensitivity. In our minds the prolonged time especially when multiple views are required represents the most serious practical limitation to brain scanning. This is especially true in patients with brain tumors who are frequently very ill disoriented and unable to cooperate. The factors considered in the present approach were (1) improvement of

SUMMARY

Palencephalography is a non specific method of cerebral localization which depends on picking up the non audible vibrations from the head by means of a microphone and recording them as tracings with an electroencephalograph. The method has been useful in localizing intracranial tumors hematomas cysts abscesses and arteriovenous malformations.

ZUSAMMENFASSUNG

Palencephalographie ist eine unspezifische Methode für die Gehirnlokalisierung die auf den Empfang der unhörbaren Vibrationen des Kopfes mit Hilfe eines Mikrophones und deren Aufzeichnung in Form von Kurven mit einem Elektroencephalograph beruht. Diese Methode ist bei der Lokalisierung von intrakraniellen Tumoren Hämatomen Zysten Abszessen und arteriovenösen Missbildung von Nutzen gewesen.

RÉSUMÉ

La palencephalographie est une méthode non spécifique de localisation cérébrale basée sur la réception des vibrations inaudibles de la tête par un microphone et leur enregistrement sous forme de tracé par un électro-encéphalographie. Cette méthode a été utile pour localiser des tumeurs intracrâniennes des hématomes des kystes des abcès et des malformations artérioveneuses.

REFERENCES

- CALVO W. Angiotectónica de los tumores encefalomedulares. Tesis Doctoral. Madrid 1950.
- y BARCIA SALORIO J. L. La palencefalografía. Med. esp. 36 (1956) 481.
- BARCIA CAYANES J. J., CALVO W. y BARCIA SALORIO J. L. Un nuevo método de exploración del encéfalo: la palencefalografía. Rev. esp. Oto-neuro-oftal. 15 (1956) 31.
- und BARCIA SALORIO J. L. Die Palencephalographie in der Diagnose der Glioblastome des Grosshirns. Acta neurochir. (Wien) Suppl. 6 (1959) 119.
- — La palencefalografía en el diagnóstico de los meningiomas. Rev. esp. Oto-neuro-oftal. 19 (1960) 1.
- — Palencephalography in the diagnosis of intracranial hematomas. Second European Congress of Neurological Surgery 1963. International Congress Series No. 60 p. 104. Ixcerpta Medica Foundation, New York.
- — y BARCIA SALORIO D. Un nuevo método para el estudio de la dinámica vascular cerebral: la palencefalografía. Med. esp. 48 (1962) 1.
- DE CORTIÉRRIZ MAHONEY C. G. y CUEVAS VERDU C. La palencefalografía. Un nuevo método para explorar el cerebro. Rev. esp. Oto-neuro-oftal. 24 (1963) 75.

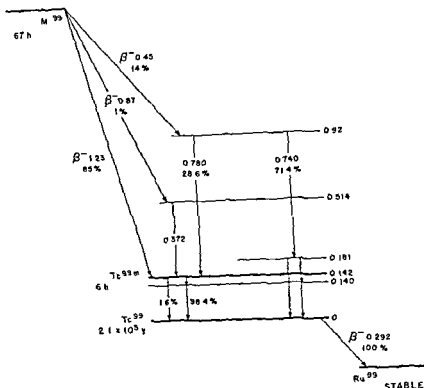


Fig 3 Decay scheme of molybdenum 99

ity for specific gamma energies. The shape of the collimator field of view has been introduced as a design parameter making it possible to design collimators which provide spatial resolution that is approximately independent of the distance from the collimator face to the midline of the patient's head (BECK 1964). All scans presented in this study were performed with such collimators using 1 inch focal length and 1 inch diameter of view.

In addition, the time wasted in scanning 'empty space' beyond the patient's head is minimized by an interrupted light beam system which consists of small light bulbs in the center holes of collimators on one side of the patient's head focused on photodiodes in the center holes of the opposite collimators. Signals from this system reverse the scan direction and produce marks on the film record to outline the patient's head.

The system utilizes no background erase, count down, 'contrast enhancement' or rate meter circuitry involving a time lag. Thus, it is possible to scan



Figs 1 and 2 Brain scanner designed at the Argonne Cancer Research Hospital showing opposed pairs of detectors, plastic sling for head and the four channel electronic assembly and scan control console on right with patient in position for lateral scans and for frontal and occipital scans respectively

mechanical design to permit rapid and more efficient scanning, (2) the use of an optimized detector collimator assembly to increase the detection sensitivity and resolution, and (3) the use of ^{99}Tc as pertechnetate as the radioisotope to reduce radiation dosage to the patient and to increase the available number of detectable photons.

The scanning system used in this study was designed and constructed at the Argonne Cancer Research Hospital under the supervision of two of the authors (R. N. B. and D. B. C.) who were in daily consultation with a third (P. V. H.). Although a theoretical study (BECK 1961) had indicated the efficacy of gamma energies below 200 keV, and that the optimum energy is closer to 100 keV (HARPER et coll. 1964) isotopes such as ^{99}Tc (140 keV) were not in use for brain scanning when the detectors were designed. The instrument was therefore designed as a research tool with detector shielding adequate for gamma energies up to at least 364 keV (^{131}I). Many of the techniques incorporated in this system were developed in a pilot study which resulted in the construction of a small animal scanner (BECK & CHARLESTON 1964).

The ACRH brain scanner (Figs 1 and 2) was designed to produce simultaneous left and right lateral scans of conventional quality (or a p. and p. scans) in as little as 90 seconds. This short scanning time is made possible by a combination of factors. The time is reduced by a factor of approximately four by use of four scintillation detectors arranged in opposing pairs which scan both sides of the patient's head simultaneously.

Since good spatial resolution requires that collimator septa be thick enough to permit only negligible penetration of gamma rays, these detectors have been designed to accept interchangeable collimators which have maximum sensitiv-

(HVL in lead 0.026 cm) The daughter activity of ^{99m}Tc is technetium 99, whose radioactivity is negligible, being $3.3 \times 10^{-6} \mu\text{Ci}$ per millicurie of ^{99m}Tc destroyed or $3.3 \times 10^{-5} \mu\text{Ci}$ per millicurie of ^{99}Mo destroyed. Technetium 99 decays by emitting a soft (0.29 MeV) beta to stable ruthenium 99.

Technetium 99m generators are currently available from Brookhaven National Laboratory at reasonable cost (Fig. 4). The daughter isotope is eluted from the generator with 0.1 N HCl. This solution may be sterilized and used directly with or without neutralization or processed further if desired (HARPER et al. 1964).

The distribution of pertechnetate in the body is superficially very similar to that of iodide. It is distributed rapidly in the extracellular space and is selectively localized in the stomach, salivary glands and thyroid from which it may be displaced by chemical competition by I^- , or more effectively by ClO_4^- . The brain tumor ratio is almost identical to that of neohydrin (McAFEE & FUEGGER 1964) and it is selectively excluded from the cerebrospinal fluid. Studies in mice show 90% excretion of intravenously administered pertechnetate in the first 24 hours with a considerably slower excretion rate of the remaining fraction. Human studies show that approximately one half of the injected ^{99m}Tc activity is excreted in the first 48 hours after intravenous administration of the material as pertechnetate. Unlike radiiodide, intestinal excretion of the ^{99m}Tc activity forms a substantial fraction of the total excretion. These studies are being published in detail elsewhere.

In the present study, pertechnetate was used as an extracellular space tag similar to gallium 68 EDTA (ANGER & GOTTSCHALK 1963). While satisfactory brain scans may be obtained after oral administration of the isotope, higher blood levels and higher count rates are achieved with intravenous administration. After intravenous injection of pertechnetate, ^{99m}Tc has a disappearance curve from the blood with an initial rapid component whose half time is approximately 15 minutes. This probably represents equilibration with the extracellular space. The remaining ^{99m}Tc has a blood disappearance half time of approximately 3 hours. These two components are of approximately equal magnitude. Injection of 1.0 gm NaI with the pertechnetate does not significantly alter this pattern. While administration of the isotope alone gives satisfactory brain scans, it has been our practice to give 1.0 gm of NaI to reduce the specific localization in the stomach, thyroid and salivary glands. It is possible that the administration of perchlorate would be more efficient as 1.0 gm perchlorate abolishes this localization completely, making more isotope available for the scan. The radiation dosage from the usual scanning dose of 10 to 12 mCi of ^{99m}Tc assuming complete retention and uniform distribution is approximately 100 mrad to the total body and approximately 3,000 mrad

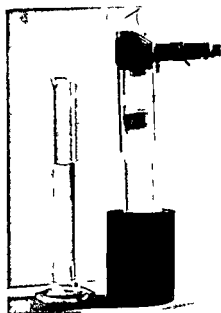


Fig. 4. Technetium 99m generator as prepared by Hot Lab Division Brookhaven National Laboratory, Upton, Long Island, New York.

at high speed (2.5 cm/sec) without producing 'scalloping'. Artifacts such as line and spot structure are minimized by using a small index width between scan lines and by recording bell shaped spots which overlap smoothly (CHARLESTON & BECK 1964).

The reduction of the radiation dosage to the patient by choice of a more suitable radioactive material has probably made the largest contribution to the present method, although without the concurrent improvements in the scanning mechanism, much of this advantage would be lost. The advantage of a short effective half time in reducing the radiation dosage to the patient is obvious, and this factor has led to the very general use in brain scanning of neohydrin tagged with mercury 203 or 197. The rapid excretion of the agent is the controlling factor in this case. To reduce the effective half time by using a material of short physical half life introduces severe logistical problems which in certain cases, including the present study, are met by using a generator or 'cow' from which the short lived daughter isotope is eluted or 'milked' from a longer lived parent. Gallium 68 is produced in this way from germanium 68 (YANO & ANGER 1964). Similarly technetium 99m, whose half life is 6 hours, is produced from 2.8 day molybdenum 99 (Fig. 3).

Technetium 99m has the additional advantage that it produces no primary particle radiation so that the energy deposited in tissue is small. The E_β is 0.014 MeV and includes the effects of conversion electrons and soft γ and fluorescent photons. The I_γ is 0.56 R/hr at 1 cm. The principal 140 keV γ (0.92/disintegration) penetrates tissue well (HVL 4.5 cm) and is shielded easily.



Fig. 6 Ninety-second lateral scan of same patient as in fig. 5 1/4 inch scale (Reprinted from *Nucleonics* Vol. 22 pp. 50-54 January 1964 with permission of McGraw-Hill and Company)

showed no abnormal uptake but a lesion was in fact discovered on radio logical surgical or postmortem study of the patient. Scans were considered technically unsatisfactory when not interpretable for technical reasons. The definite categories were those in which the clinical correlation was precise. They include those patients in whom neuroradiologic procedures or operative intervention denoted with clarity the presence or absence of a lesion. In several patients suspected lesions were confirmed at post mortem examination. The probable categories contain scans of patients in whom on clinical grounds the presence or absence of lesions was known with a fair degree of certainty although operative or autopsy confirmation was not obtainable. These results are summarized below.

Category	Definite	Probable	Total
Positive	63	5	68
Negative	78	10	88
Falsely positive	2	4	6
False negative	8	2	10
Technically unsatisfactory			10
			182

In this series 38 patients had neoplasms of the brain verified either by an unequivocal neuroradiologic examination, a positive operative approach, or a confirmatory post mortem examination. The correlation between the scan interpretations and verified neoplasms is shown on the following page.



Fig. 5. Fifteen minute lateral scans of patient with a glioblastoma of the left parietal lobe. 1/16 inch index 10 mCi $^{99m}\text{TcO}_4^-$ (Reprinted from *Nuclear Medicine* Vol. 22 pp. 50-54 January 1964 with permission of McGraw Hill and Company.)

to the stomach which is the target organ. It has been our practice to begin scanning 15 minutes after injection of the isotope, allowing time for equilibration between the intravascular and extravascular compartments. The usual scanning time for each pair of lateral or frontal occipital scans is 10 to 15 minutes, so that the whole procedure takes about one hour per patient, including injection, set up time and developing.

Results

The method described above was used to make brain scans on 175 patients from August 1, 1963 through July 1, 1964. Several patients were scanned more than once making a total of 182 runs, or 738 scans (4 or more scans for each patient). Scans were classified into five main categories: positive, negative, false positive, false negative and technically unsatisfactory, and each category was further subdivided into definite and probable. Scans were called positive when abnormalities in distribution of the radioactivity corresponded to radiological, operative, or autopsy findings. Negative scans were those with no evidence of abnormal uptake, and were in agreement with clinical findings for absence of any focal lesion. A scan was classified as false positive when abnormal concentration of the isotope suggested a focal lesion which was not found on subsequent radiological or operative study of the patient. A false negative scan



Fig 8 Anterior scan and right carotid angiogram in a patient with a huge chromophobe adenoma invading the right frontal lobe

disturbances probably representing the so called Munchausen syndrome. Although the scan indicated a parasellar localization of the isotope, no organic cause for this has yet been determined. The other patient in this group was an elderly man with signs and symptoms of an agitated depression. His scan was rather unequivocally positive in the right parasellar region. Although there were no definite neurological signs, angiography and encephalography were performed, both with negative results.

Probable false positive scans were considered to be present in 4 patients since no full follow up was available. The first of these was an elderly man with diabetic neuropathy and seizures. The patient had a moderate degree of hypertension and clinically was suspected of having a possible intracerebral hemorrhage. The scan revealed an area of abnormal uptake in the left anterior frontal region. No other neurodiagnostic procedures could be performed before the patient expired. True correlation was impossible as autopsy was not permitted. The second patient in this probably false positive category was a woman with hyperthyroidism and ophthalmoplegia of unknown cause. The scan suggested an area of increased uptake in the midline temporo occipital region. No ancillary tests were performed and the cause of the ophthalmoplegia was never documented. The patient is currently being followed in the outpatient department. The third patient was a woman with a history of migraine headache and numerous psychogenic problems. A diagnosis of multiple



Fig. 7. Anterior scan in patient with a subdural hematoma (chronic)

Total number of patients with brain neoplasms scanned	38
Positive scans of patients in tumor group	31
Negative scans of patients in tumor group	
Foramen magnum tumor	4
Multiple small cerebral metastases (pancreas)	
Probable parietal glioma—biopsy specimen revealed gliosis only	
Posterior fossa cholesteatoma	
Per cent positive scans in patients of tumor group	89.4%

Lesions other than neoplasms demonstrated by brain scanning were as follows

Vascular accidents	5
Skull lesions (1 osteoma, 2 metastases, 1 depressed fracture)	4
Postoperative changes	3
Subdural hematoma	2
Arteriovenous malformations	2
Focal atrophy (confirmed by pneumography)	1
Multiple sclerosis with focal lesion	1
Thalamotomy lesion (electrical)	1
Cranioplasty (tantalum)	1

Representative scans are shown in Figs 5 through 11

Review of the false positive and false negative scans revealed two cases where the results were definitely false positive. The first patient was a middle aged woman with bizarre and diffuse complaints of headache and dizziness with no definite neurological findings. Electroencephalography, roentgenograms of the skull, and further neurological evaluation, revealed no definite objective findings. Subsequent history showed that the patient had severe psychiatric



Fig 8 Anterior scan and right carotid angiogram in patient with a huge chromophobe adenoma invading the right frontal lobe

disturbances probably representing the so called Munchausen syndrome. Although the scan indicated a parasellar localization of the isotope no organic cause for this has yet been determined. The other patient in this group was an elderly man with signs and symptoms of an agitated depression. His scan was rather unequivocally positive in the right parasellar region. Although there were no definite neurological signs angiography and encephalography were performed both with negative results.

Probable false positive scans were considered to be present in 4 patients since no full follow up was available. The first of these was an elderly man with diabetic neuropathy and seizures. The patient had a moderate degree of hypertension and clinically was suspected of having a possible intracerebral hemorrhage. The scan revealed an area of abnormal uptake in the left anterior frontal region. No other neurodiagnostic procedures could be performed before the patient expired. True correlation was impossible as autopsy was not permitted. The second patient in this probably false positive category was a woman with hyperthyroidism and ophthalmoplegia of unknown cause. The scan suggested an area of increased uptake in the midline temporo occipital region. No ancillary tests were performed and the cause of the ophthalmoplegia was never documented. The patient is currently being followed in the outpatient department. The third patient was a woman with a history of migraine headache and numerous psychogenic problems. A diagnosis of multiple



Fig. 7. Anterior scan in patient with a subdural hematoma (chronic).

Total number of patients with brain neoplasms scanned	33
Positive scans of patients in tumor group	31
Negative scans of patients in tumor group	
Foramen magnum tumor	} 1
Multiple small cerebral metastases (pancreas)	
Probable parietal glioma (biopsy specimen revealed gliosis only)	
Posterior fossa cholesteatoma	
Percent positive scans in patients of tumor group	89.4 %

Lesions other than neoplasms demonstrated by brain scanning were as follows:

Vascular accidents	5
Skull lesions (1 osteoma, 2 metastases, 1 depressed fracture)	4
Postoperative changes	3
Subdural hematomas	2
Arteriovenous malformations	2
Local atrophy (confirmed by pneumoencephalography)	1
Multiple sclerosis with focal lesion	1
Thalamotomy lesion (electrical)	1
Cranioplasty (tantalum)	1

Representative scans are shown in Figs 5 through 11.

Review of the false positive and false negative scans revealed two cases where the results were definitely false positive. The first patient was a middle aged woman with bizarre and diffuse complaints of headache and vertigo with no definite neurological findings. Electroencephalography, roentgenograms of the skull, and further neurological evaluation revealed no definite objective findings. Subsequent history showed that the patient had severe psychiatric



Fig. 10 Right lateral scan and lateral view of late arterial phase obtained by right carotid angiography in a patient with a small astrocytoma of the right occipital lobe. The only symptom was that of seizures.

The two probable false negative scans were two cases of astrocytoma removed (presumably subtotally) up to 10 years prior to scanning. One was in the left parietal region and the other was in the left temporal region.

Discussion

While the apparent diagnostic accuracy of existing methods of brain scanning has not been greatly improved in the present study, the rate at which the scans can be carried out has been greatly increased and the radiation dosage to the patient has been greatly reduced. Although this technique is not completely transferable to other scanning systems, modification of collimators and scan speed permit a substantial reduction in scanning time. In fact, it has been possible by a relatively minor modification to increase the scan speed of our Picker Magna Scanner to 420 cm/min. We have yet to explore in detail the possible gains obtainable with higher resolution.

It should be emphasized that the scan pictures shown here are smoothed primary photographic records without contrast enhancement or background subtraction. It was our thought that the further processing of these film records by closed circuit television or flying spot scanning for contour enhancement, contrast enhancement and background subtraction under the control of the observer might lead to greater ease in interpretation. That the primary records are so easily interpreted seems remarkable, one factor certainly being the very large amount of information recorded in scans consisting of 300 000



Fig. 9 Left lateral and anterior scans and axial view of left carotid angiogram in a patient with a left sphenoid wing meningioma.

sclerosis made elsewhere was not confirmed at the University of Chicago Clinics. Although her scan suggested an area of increased uptake in the midline fronto-central region, no neurodiagnostic studies were performed. During the three months the patient has been followed as an out-patient no clinical evidence of a mass lesion has developed. The final patient in this group was a middle-aged man with psychosis and dementia thought probably to represent a presenile type of degeneration. The patient had no localizing signs on neurological examination. Evidence for an area of increased uptake in the right parasellar region was seen on the scan. The patient refused carotid angiography, and is at present lost to follow-up.

There were 10 cases of false-negative scans. Of these, eight fell into the definite, and two into the probable, category. Of the definite false negatives, three patients gave clinical and radiologic evidence of encephalomalacia in the right cerebral hemisphere, of varying duration, all longer than one year. There was one patient with multiple small metastases from a pancreatic carcinoma. One patient had a history of trauma and lowering level of consciousness, the scan revealed no focal uptake, but following a rapid clinical decompensation a large left subdural hematoma was evacuated. There was one patient who had on neurodiagnostic evaluation a mass lesion in the left parietal region, but this was not confirmed at biopsy. It was felt clinically that the patient probably harbored an astrocytoma diffusum, but histological evidence was never obtained in a non-equivocal manner. Of the remaining two patients, one gave evidence of a bilateral cholesteatoma involving both the posterior and middle cranial fossae with a history of previous surgery. The remaining patient had, one day prior to the performance of the scan, undergone a thalamotomy for Parkinson's disease. The scan failed to reveal evidence of a lesion.

Acknowledgements

The authors gratefully acknowledge the essential contributions of Paul Eidelberg Charles R. Breback Bernard W. Frommes John J. Stupka and Alexander Simla to the design and painstaking construction of the brain scanner and the care with which the scans were done by Miss Rose Lee Seslar.

SUMMARY

A conventional brain scanning system is described in which multiple improvements have resulted in a very substantial increase in performance. Preliminary clinical results in 170 patients indicate no appreciable sacrifice in diagnostic accuracy with a considerable reduction in scan time.

ZUSAMMENFASSUNG

Konventionelle cerebrale Szintigraphie ist infolge einer vielseitigen Verbesserung nunmehr wesentlich leichter durchzuführen. Vorläufige klinische Resultate von 170 Patienten zeigen keine wahrnehmbare Einschränkung der diagnostischen Sicherheit, jedoch eine beträchtliche Reduktion der Untersuchungszeit.

RÉSUMÉ

Description d'un appareil classique de scintigraphie cérébrale dont les performances ont été très améliorées par de nombreux perfectionnements. Les résultats préliminaires sur 170 malades montrent que la précision du diagnostic n'a pas été appréciablement diminuée malgré une réduction importante de la durée du balayage.

REFERENCES

- ANGER H. O. and GOTTSCALK A. Localization of brain tumors with the positron scintillation camera. *J. nucl. Med.* 4 (1963) 326.
- ANGER H. O. Scintillation camera with multichannel collimators. *J. nucl. Med.* 5 (1964) 515.
- BECK R. N. A theoretical evaluation of brain scanning systems. *J. nucl. Med.* 2 (1961) 314.
- Collimators for radioisotope scanning systems. *Proceedings of the IAEA Symposium on Medical Radioisotope Scanning*, Athens, Greece, April 1964, Vol. I, p. 211.
- and CHARLESTON D. B. A small animal scanning system. *Int. J. appl. Radiat.* 15 (1964) 101.
- CHARLESTON D. B. and BECK R. N. Techniques which aid in the quantitative interpretation of scan data. *Proceedings of the IAEA Symposium on Medical Radioisotope Scanning*, Athens, Greece, April 1964, Vol. I, p. 574.
- HARPER I. V., BECK R., CHARLESTON D. and LATHROP K. A. Optimization of a scanning method using Tc^{99m} . *Nucleonics* 22 (1964) 50.
- LATHROP K. A., MCCARDLE R. J. and ANDROS C. The use of Tc^{99m} as a clinical scanning agent for thyroid, liver and brain. *Proceedings of the IAEA Symposium on Medical Radioisotope Scanning*, Athens, Greece, April 1964, Vol. II, p. 33.
- MCCAFFE J. G. and FLUEGER G. F. Tumor to brain concentration ratios mouse ep. ndymoma. In *Scintillation Scanning in Clinical Medicine*, Ed. QUINN J. L. III, p. 213. W. B. Saunders Company, Philadelphia 1964.
- YANO I. and ANGER H. O. A gallium-68 positron cow for medical use. *J. nucl. Med.* 5 (1964) 482.

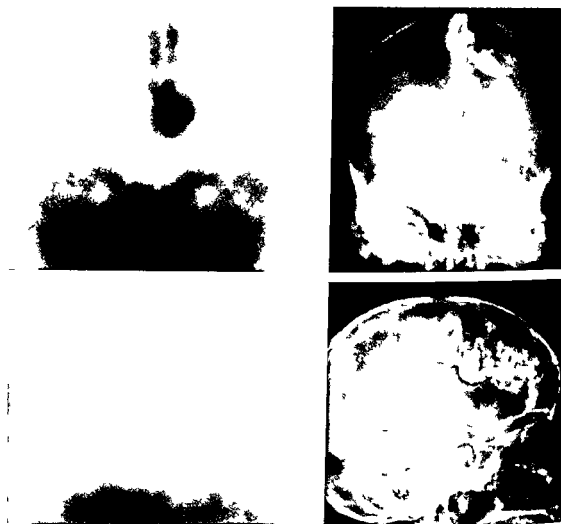


Fig. 11. *Top view:* Frontal scan and carotid angiogram of patient with a large arteriovenous malformation: the scan was performed as an incidental procedure and angiography was performed only after the scan films had been examined. *Lower view:* Lateral scan and angiogram.

to 500 000 counts. This is many times the number of counts usually collected with currently available scanning systems, and approaches the rate of information collection of the camera type detectors (which, incidentally, work very effectively with ^{99}Tc) (ANGER 1964). It would appear that the limitations of conventional scanning systems have not yet been reached. By the use of multiple head detectors moving rapidly it should be possible to approach or equal the sensitivity of a camera detector while maintaining the resolution possible with the focused collimator systems. It may be that some combination of these systems, either separately or in hybrid form, will ultimately prove to be the most satisfactory.

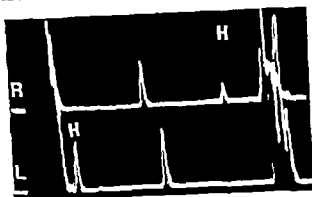


Abb. 1 Echoencephalogramm eines 15-jährigen Jungen mit Verdacht auf epidurales Hämatom links 21 mm vor dem Endecho kommt bei der Ableitung von rechts (R) ein Haematomecho (H) u. Darstellung das an der Grenzfläche Gehirn Dura Blutung entsteht Auch von links (L) ist das Haematomecho (H) zu erkennen Außerdem Verschiebung des Mittlechos von links nach rechts um 5 mm Echoencephalographische Diagnose epidurales Hämatom links temporal Bestätigung durch Carotangiographie

weniger Minuten auf Grund der Verschiebung des Mittlechos lokalisieren. Ausnahmen bildeten nur die doppelseitigen Hämatome. Lediglich in 2 Fällen mit multiplen Kontusionen und gleichzeitig bestehenden ausgedehnten Kopfschwellenhämatomen war die Lage des Mittlechos nicht zu beurteilen.

Neben der Mittlechoverlagerung können in vielen Fällen von der Grenzfläche Hirngewebe/Hämatom besondere Reflexionen abgeleitet werden, die wir als Haematomecho bezeichnen. Als erste machten TER BRAAK, GRANDIA & DE VLIJGER auf diese Reflexion aufmerksam. Einige Autoren haben dagegen das Haematomecho nicht nachweisen können (JEPPSON) oder bezweifeln

Tabelle 1

Verhalten des Mittlechos nach Schädel-Hirnverletzung (314 Patienten)

Verletzung	Gesamtzahl	Mittlecho normal	Mittlecho verlagert	Mittlecho nicht zu beurteilen
Contusion	141	141	—	—
Contusion cereb.	9	4?	48	2
Extracerebral	81	11	70	—
Hämatom				

ECHOENCEPHALOGRAPHISCHE UNTERSUCHUNGS- ERGEBNISSE BEI SCHÄDEL-HIRNVERLETZUNGEN*

von

E. KAZNER und W. SCHIEFER

Unter 1 250 Patienten, die in den letzten Jahren an unserer Klinik mit der temporalen Echoencephalographie nach LEASELL untersucht wurden, waren mehr als 300 Schädel-Hirnverletzte. Wir verwendeten einen Echo-Encephalographen Typ USM 1 nach KRAUTKRAMER der Firma Siemens-Reiniger AG. Die Echogramme wurden mit einer Polaroid-Land-Camera für die Dokumentation fixiert.

Die speziellen Vorteile der Echo-Methode in der frühen Phase der Schädel-Hirnverletzung sind die Leichtigkeit und Schnelligkeit in der Anwendung. Besondere Aufmerksamkeit widmeten wir der Erkennung posttraumatischer Komplikationen.

Tabelle 1 zeigt das Verhalten des Mittelechos nach Schädel-Hirnverletzungen. Bei einfachen Gehirnerschütterungen fand sich das Mittelecho immer an normaler Stelle. Ein großer Teil der Hirnkontusionen entwickelte in den ersten Tagen nach dem Trauma eine Massenverschiebung mit entsprechender Mittelechoverlagerung, maximal bis zu 5 mm. Der echoencephalographisch nachweisbare, spätere Rückgang dieser Verlagerung bestätigte die Diagnose einer Kontusion. Alle Blutungen im Bereich einer Hemisphäre ließen sich innerhalb

* Herrn Prof. Max Schneider zum 60. Geburtstag gewidmet

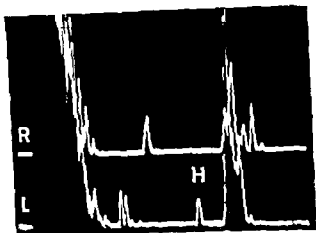


Abb 3 Echogramm einer 16-jährigen Patientin mit Verdacht auf raumfordernde intrakranielle Blutung. Mittellechoverschiebung von rechts nach links um 7,5 mm. Man erkennt zusätzlich bei der Ableitung von links mit nach temporo-praezentral gerichtetem Ultraschallstrahlenbündel 18 mm vor dem Endecho eine Reflexion (H). Echoencephalographische Diagnose: epidurales Haematom rechts temporo-praezentral.

und die Aufnahme mit um 30 Grad nach links gedrehtem Kopf bestätigte die echoencephalographische Diagnose. Bei der Operation wurde das atypisch lokalisierte weit nach occipital reichende Haematom erfolgreich ausgeräumt.

Anfangs haben wir nach der Echoencephalographie zur Sicherheit immer noch angiographiert. In Not Situationen läßt sich aber wie der nächste Fall zeigt hierauf verzichten. Abbildung 3 zeigt das Echobild eines 16-jährigen Mädchens, das 12 Stunden nach einem Motorradunfall mit sekundärer Bewußtlosigkeit und Streckkrämpfen aufgenommen wurde. Die Erweiterung der linken Pupille schien für eine linksseitige Blutung zu sprechen. Das Echogramm wies aber eine deutliche Mittellechoverschiebung nach links auf und bei Ableitung von links mit nach temporo-praezentral gerichtetem Ultraschallstrahlenbündel tauchte eine Reflexion (H) auf, sodaß wir ein in dieser Region gelegenes epidurales Haematom vermuteten (Abb 3). Ohne weitere Diagnostik erfolgte die operative Ausräumung der Blutung. Der erhebliche Zeitgewinn hat hier sicher zu dem günstigen Ausgang beigetragen.

Insgesamt konnten wir 28 epidurale Haematome mit Ultraschall untersuchen. Bei allen temporalen, temporo-parietalen, temporo-occipitalen und temporo-praezentralen Blutungen fand sich neben der Massenschiebung das erwähnte Haematomecho. Nur die frontalen, temporo-basalen und occipitalen Haematome, die bei der üblichen Untersuchungstechnik nicht direkt

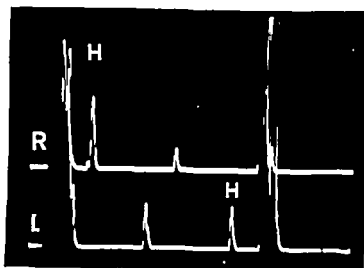


Abb. 2 Echoencephalographische Diagnose eines epiduralen Hämatoms rechts temporo occipital bei einem 8-jährigen Jungen mit klinischer Beschwerdefreiheit. Man erkennt das Hämatomecho H, das von beiden Seiten her ableitbar ist. Daneben Verlagerung des M-Echos von rechts nach links.

dessen Signifikanz (LITHANDER). Unsere Untersuchungsergebnisse, die im folgenden durch einige Fallberichte erläutert werden, lassen jedoch kaum Zweifel an der Existenz derartiger Reflexionen zu.

Bei einem typischen *Epiduralhaematom* auf der linken Seite zeigt sich im Echoencephalogramm bei der Beschallung von rechts (R) eine Verlagerung des Mittelschalls zur gleichen Seite und zusätzlich eine Reflexion (H), die dem Endecho vorausgeht. Bei Beschallung von links (L) wird dieses Echo (H) sofort nach dem Mittelschall sichtbar (Abb. 1). Der Abstand zwischen diesem Hämatomecho und dem Endecho entspricht der angiographisch und bei der Operation festgestellten Ausdehnung der Blutung. Zweifellos handelt es sich bei dem sogenannten Hämatomecho um eine an der Grenze zwischen Gehirnoberfläche, Dura und Blutung entstandene Reflexion.

Der nächste Fall läßt den Wert der Echo-Methode noch eindeutiger erkennen. Ein 8-jähriger Junge wurde 2 Tage nach einem Schädeltrauma zu uns eingewiesen. Bei der Aufnahme war er wach, der neurologische Befund bis auf ein Spreizphänomen im rechten Fuß normal. Nach dem EEG wurde eine Kontusion im rechten Schläfenlappen angenommen. Im Echoencephalogramm fanden wir aber eine Verlagerung des Mittelschalls von rechts nach links um 8 mm und eine von beiden Seiten ableitbare Reflexion (H), sodaß wir ein epidurales Hämatom rechts temporooccipital diagnostizierten (Abb. 2). Im r.p. Phlebogramm sah man eine Verlagerung der Vena cerebri interna nach links.

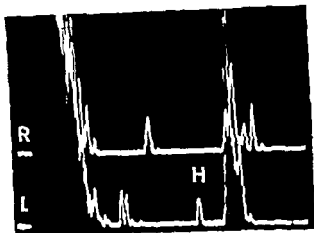


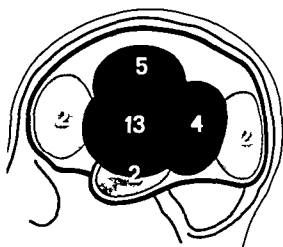
Abb. 3 Echogramm einer 16-jährigen Patientin mit Verdacht auf raumfordernde intrakranielle Blutung. Mittellinienverschiebung von rechts nach links um 7,5 mm. Man erkennt zuätzlich bei der Ableitung von links mit nach temporo-praezentral gerichtetem Ultraschallstrahlenbündel 18 mm vor dem Endecho eine Reflexion (H). Echoencephalographische Diagnose: epidurales Haematom rechts temporo-praezentral.

und die Aufnahme mit um 30 Grad nach links gedrehtem Kopf bestätigte die echoencephalographische Diagnose. Bei der Operation wurde das atypisch lokalisierte, weit nach occipital reichende Haematom erfolgreich ausgeräumt.

Anfangs haben wir nach der Echoencephalographie zur Sicherheit immer noch angiographiert. In Notsituationen läßt sich aber wie der nächste Fall zeigt hierauf verzichten. Abbildung 3 zeigt das Echobild eines 16-jährigen Mädchens, das 12 Stunden nach einem Motorradunfall mit sekundärer Bewußtlosigkeit und Streckkrämpfen aufgenommen wurde. Die Erweiterung der linken Pupille schien für eine linksseitige Blutung zu sprechen. Das Echogramm wies aber eine deutliche Mittellinienverschiebung nach links auf und bei Ableitung von links mit nach temporo-praezentral gerichtetem Ultraschallstrahlenbündel tauchte eine Reflexion (H) auf, sodaß wir ein in dieser Region gelegenes epidurales Haematom vermuteten (Abb. 3). Ohne weitere Diagnostik erfolgte die operative Ausräumung der Blutung. Der erhebliche Zeitgewinn hat hier sicher zu dem günstigen Ausgang beigetragen.

Insgesamt konnten wir 28 epidurale Haematome mit Ultraschall untersuchen. Von allen temporalen, temporo-parietalen, temporo-occipitalen und temporo-praezentralen Blutungen fand sich neben der Massenverschiebung das erwähnte Haematomecho. Nur die frontalen, temporo-basalen und occipitalen Haematome, die bei der üblichen Untersuchungstechnik nicht direkt

Abb 4 Echoencephalographische Befunde bei 28 epiduralen Hämatomen. Alle temporo-occipitalen, temporo-occipitalen, temporo-parietalen und temporo-präzentralen Blutungen riefen eine Mittelechoverlängerung und ein Hämatomecho hervor (dunkelgrau). Nur die frontalen, temporo-basalen und occipitalen Hämatome zeigten eine Mittelechoverlängerung ohne Hämatomecho, da diese Blutungen nicht direkt vom Ultraschallstrahl erfaßt werden (hellgrau).



vom Ultraschall erfaßt werden, zeigten kein Hämatomecho. Die richtige Seitenlokalisation ergab sich aber auch hier durch die Mittelechoverlängerung (vgl. Schraubild in Abb. 4).

Das klinische Bild des epiduralen Hämatoms hat manche Ähnlichkeit mit dem des akuten subduralen Hämatoms. Hier können oft die echoencephalographischen Befunde zur Differenzialdiagnose beitragen. Beim akuten subduralen Hämatom gelingt es nämlich gelegentlich zwar auch eine Reflexion von der Blutansammlung zu erhalten. Diese ist aber nach unseren Beobachtungen nie so signifikant wie beim Epiduralhämatom.

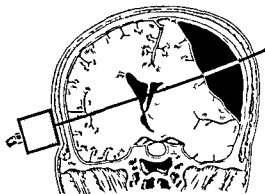
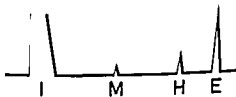


Abb 5 Schematische Darstellung der Schrägbeschallungstechnik beim chronischen subduralen Hämatom. Bei weitgehend senkrechtem Auftreffen des Ultraschalls auf die Hämatomoberfläche erhält man eine deutliche Reflexion von dieser Grenzfläche (H). Das Mittelecho (M) hat bei dieser Technik eine sehr geringe Amplitude oder verschwindet ganz.



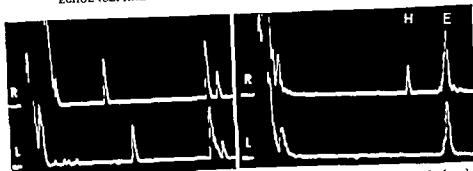


Abb 6 Links 11 mm von links nach rechts verlagertes Mittelecho spricht für raumfordernden Prozeß links Rechts bei der Schrägbeschallung Reflexion (H) 25 mm vor dem Endecho bei rechts (R) aufgesetztem Prüfkopf Echoencephalographische Diagnose chronisches subdurales Haematom links mit 25 mm Durchmesser







Abb 7 Doppelseitiges chronisches subdurales Haematom Links Mittelecho im Bereich der Norm Rechts Ergebnis der Schrägbeschallung Haematoreflexionen (H) beiderseits vor dem Endecho

Zur Erkennung des *chronischen subduralen Haematoms* hat sich uns (SCHIEFER HAZNER & BRUCKNER 1963) eine besondere Beschallungstechnik bewahrt (siehe schematische Darstellung in Abb 5) Bei der üblichen horizontalen Beschallung läßt sich bei einseitigen Haematomen zwar die Mittelechoverlagerung feststellen Das meist parietal gelegene Haematom wird aber nur erfaßt wenn das Ultraschallstrahlenbündel die Grenzfläche zwischen Hirngewebe und Blutung weitgehend senkrecht trifft Deshalb richten wir bei Verdacht auf eine derartige Erkrankung den Ultraschall schrag nach oben Bei Vorliegen eines subduralen Haematoms wird dann auf dem Bildschirm ein charakteristisches Haematomecho (H) sichtbar

Abbildung 6 zeigt einen solchen Fall Ein 41-jähriger Mann wurde bei uns 8 Wochen nach einem Schädel-Hirntrauma mit Verdacht auf subdurales Haematom aufgenommen Das Echogramm wies eine 11 mm Massenverschiebung von links nach rechts auf Bei der Schrägbeschallung wurde von rechts hier eine Reflexion (H) sichtbar die ein 25 mm dickes Haematom anzeigte

Tabelle 2

Echoencephalographische Befunde bei 81 extracerebralen Blutungen

		<i>M-Echo normal</i>	<i>M Echo shifted</i>	<i>Hematoma Echo</i>	<i>Midline- Displacement (mm)</i>
<i>extradural Hematoma</i> 28		-	28	22	7,4
<i>acute subdural Hematoma</i> 23		-	23	9	7,3
<i>chron subdural Hematoma</i> 16		-	16	15	8,2
<i>chron subdural Hematoma doublesided</i> 14		11	3	10	
		11	70	56	

Die Diagnose wurde durch Angiographie und anschließende Operation bestätigt.

Auch doppelseitige chronische Subduralhämatome, die ja meist keine Verschiebung des Mittelechos hervorrufen, können durch die Schallbeschränkung oft dennoch nachgewiesen werden. Sowohl von links als auch von rechts erhält man Hämatomechos (H), die dem Endecho (E) vorauslaufen und die Hämatomdicke erkennen lassen (Abb. 7).

JEPSSON glaubt, daß es sich bei den Hämatomechos um Reflexionen von Knochenvorsprüngen an der Innenseite der Schädelskalotte handeln könnte. Dieser Einwand läßt sich durch den nächsten Fall einfach entkräften. In Abbildung 8 sind die Echogramme eines 59-jährigen Mannes mit einem chronischen subduralen Hämatom über der linken Hemisphäre zusammengestellt. Vor der Operation zeigte sich ein Hämatomecho (H) 25 mm vor dem Endecho (E). Die bei der Operation gemessene Dicke der Blutung betrug 2,5 cm. 8 Tage später ließ sich durch die Reflexion H noch ein Resthämatom von 12 mm Durchmesser nachweisen. Daraufhin wurde am folgenden Tage nachpunktiert und gleichzeitig der Liquorraum von lumbal her mit phys. Kochsalzlosung aufgefüllt. Im Echoencephalogramm war während dieser

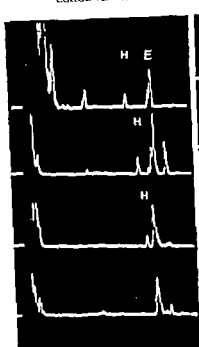


Abb 8 Chronisches subdurales Haematom links bei einem 59-jährigen Mann. Von oben nach unten (alle Echogramme sind mit der Schrägbeschallungstechnik erstellt): Untersuchung vor der Operation: Hematomecho H in 25 mm Abstand vom Endecho E. 8 Tage später liegt noch ein 12 mm dickes Resthaematom vorangeregt durch das Haematomecho H. Am folgende Tage Aspirat von dem Resthaematom. Dabei wandert das Haematomecho H in Richtung auf das Endecho. Bei ambulanten Kontrollen 4 Wochen später ist kein Haematomecho mehr nachweisbar.

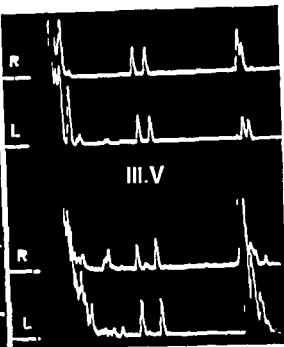






Abb 9 22-jährige Patient mit schweren gedecktem Schädel Hirntrauma. Oben: Echogramm 24 Tage nach der Verletzung. Es zeigt eine beginnende Ventrikelerweiterung. Das gedoppelte Mittellecho (III V) entsteht an den Seitenwänden des 3. Ventrikels, dessen Weite sich sofort ablesen läßt. Unten: weitere 18 Tage später hat der Abstand der beiden vom 3. Ventrikel stammenden Reflexen deutlich zugenommen. Diagnose: erheblicher posttraumatischer Hydrocephalus internus.

Manipulation ein Wandern des Haematomechos (H) auf das Endecho zu zu beobachten (3. Kurve von oben). Bei einer ambulanten Kontrolluntersuchung 1 Monat später fehlte diese zusätzliche Echo. In solchen Fällen kann zumindest auf die Kontrollangiographie nach Entleerung eines subduralen Haematoms verzichtet werden.

Tabelle 2 faßt unsere echoencephalographischen Befunde bei insgesamt 81 extracerebralen Haematomen zusammen. Alle 67 einseitigen Blutungen wurden mit Hilfe des Echo-Impuls Verfahrens richtig seitenlokalisiert. Die durchschnitt

Tabelle 2

Echoencephalographische Befunde bei 81 extracerebralen Blutungen

		<i>M-Echo normal</i>	<i>M Echo shifted</i>	<i>Hematoma Echo</i>	<i>Midline - Displacement (mm)</i>
<i>extradural Hematoma</i> 28		-	28	22	7,4
<i>acute subdural Hematoma</i> 23		-	23	9	7,3
<i>chron subdural Hematoma</i> 16		-	16	15	8,2
<i>chron.subdural Hematoma doublesided</i> 14		11	3	10	
		11	70	56	

Die Diagnose wurde durch Angiographie und anschließende Operation bestätigt.

Auch doppelseitige chronische Subduralhämatome, die ja meist keine Verschiebung des Mittelechos hervorrufen, können durch die Schlägbeschallung oft dennoch nachgewiesen werden. Sowohl von links als auch von rechts erhält man Hämatomechos (H), die dem Endecho (E) vorausseilen und die Hämatomdicke erkennen lassen (Abb. 7).

JEPSSON glaubt, daß es sich bei den Hämatomechos um Reflexionen von Knochenvorsprüngen an der Innenseite der Schädelskuppe handeln könnte. Dieser Einwand läßt sich durch den nächsten Fall einfach entkräften. In Abbildung 8 sind die Echogramme eines 59-jährigen Mannes mit einem chronischen subduralen Hämatom über der linken Hemisphäre zusammengestellt. Vor der Operation zeigte sich ein Hämatomecho (H) 25 mm vor dem Endecho (E). Die bei der Operation gemessene Dicke der Blutung betrug 2,5 cm. 8 Tage später ließ sich durch die Reflexion H noch ein Resthämatom von 12 mm Durchmesser nachweisen. Daraufhin wurde am folgenden Tage nachpunktiert und gleichzeitig der Liquorraum von lumbal her mit phys. Kochsalzlösung aufgefüllt. Im Echoencephalogramm war während dieser

konnte eine zusätzliche Reflexion des sogenannte Haematomecho aufgefangen werden. Dies ermöglichte oft die genaue Diagnose. Auch die meisten chronischen subduralen Haematome wurden bei Anwendung einer besonderen Beschallungstechnik durch ein Haematomecho erkannt.

SUMMARY

Echo-encephalography has become indispensable for the quick recognition of complications in cerebral trauma on account of its great speed, its reliability and the facility of repeated control examinations. In all 314 cases of skull injury were investigated. Some cases of contusion but all those of unilateral haematomas produced a displaced midline echo. An additional reflection was registered, the so-called haematoma echo, wherever an epidural haematoma was sounded vertically by ultrasonic waves. This phenomenon frequently permits accurate diagnosis. Equally, most of the chronic subdural haematomas were recognisable by means of a special ultrasonic technique.

RÉSUMÉ

En raison de sa rapidité, de sa fidélité et de la possibilité de la répéter, l'écho encéphalographique est devenue indispensable pour faire en temps utile le diagnostic des complications des traumatismes crâniocérébraux. Les auteurs ont examiné 314 traumatisés crâniens. Ils ont trouvé un déplacement de l'écho médian dans une partie des contusions et dans tous les hématomes unilatéraux. Dans tous les cas où les ultrasons abordent l'hématome extradural perpendiculairement sur une grande surface, on a constaté une réflexion supplémentaire appelée l'écho d'hématome. Ceci permet souvent le diagnostic exact. La plupart des hématomes sous-duraux chroniques ont aussi pu être identifiés par un écho d'hématome grâce à une technique spéciale.

LITERATUR

- AMBROSE, J. Pulsed ultrasound. Illustrations of clinical applications. *Brit J Radiol* 3 (1964) 165.
- BRAAK, J. W. G. ter, GRANDIA, W. A. M. and DE VLIETTER, M. Echo-encephalography as an aid in the diagnosis of the subdural and extradural haematomas. In: A. Biedmond et coll. Recent Neurology Research, S. 37. Amsterdam 1959.
- DREISE, M. J. and NETSKY, M. G. The clinical use of echo-encephalography. *Virginia Med Monthly* 90 (1963) 539.
- FRIEDMAN, G. und TIMM, F. Zuverlässigkeit und Fehlermöglichkeiten der Echo-Enzephalographie bei supratentoriellen raumfordernden Prozessen. *Med Welt* (1964) 689.
- JEFFERSON, A. Clinical experiences with echoencephalography. *Acta neurochir. (Wien)* 10 (1967) 397.
- JEPPESEN, S. T. Echo-encephalography III. Further studies on the sources of the midline echo and a clinical evaluation. *Acta chir. scand.* 119 (1960) 455.
- ~ Echo-encephalography IV. The midline echo: an evaluation of its usefulness for diagnosing intracranial expansivities and an investigation into its sources. *Acta chir. scand. Suppl.* 212 (1961).

liche Massenverschiebung im Echogramm betrug 7—8 mm, ein signifikanter Unterschied zwischen den einzelnen Blutungsformen war dabei nicht erkennbar. Bei 3 doppelseitigen chronischen Subduralhämatomen fand sich eine geringe Mittelechoverlagerung, bedingt durch die unterschiedliche Größe der Blutungen. Die übrigen zeigten ein normales Mittelecho.

Bei den 81 extracerebralen Hämatomen konnten wir 56 mal Reflexionen von der Blutung, sogenannte Hämatomechos registrieren. Von 23 akuten subduralen Blutungen wiesen nur 9 eine solche Reflexion auf, dagegen von 28 Epiduralhämatomen 22. Bei 30 chronischen Subduralblutungen fanden wir ein Hämatomecho sogar in 25 Fällen, bei den einseitigen Hämatomen fast immer. Wir halten das Hämatomecho bei den epiduralen und chronischen subduralen Blutergüssen für ein sehr zuverlässiges diagnostisches Hilfsmittel.

Neben den posttraumatischen intrakraniellen Blutungen sind es vor allem die Folgezustände schwere gedeckter Schädel Hirnverletzungen, bei denen die Echoencephalographie wertvolle Befunde liefert. Genauso, wie wir bei den infratentoriellen Prozessen schon vor der Luftfüllung echoencephalographisch die Weite der 3. Hirnkammer bestimmen können, ist dies auch bei Hirn atrophischen Vorgängen nach Hirnverletzungen möglich. Von einem Ansatzpunkt direkt über der Ohrmuschel beschallt man den 3. Ventrikel und erhält von dessen seitlichen Wänden getrennte Reflexionen, deren Abstand uns die Weite der 3. Hirnkammer angibt. Abbildung 9 demonstriert einen solchen Fall. Man erkennt im Echoencephalogramm deutlich den großer werdenden Abstand der beiden vom 3. Ventrikel stammenden Echos. Die Diagnose eines zunehmenden Hydrocephalus internus kann damit ohne eingreifendere Untersuchungen sicher gestellt werden.

Wenn auch die echoencephalographischen Befunde nur im Rahmen der gesamten klinischen Symptomatologie bewertet werden dürfen, so hat diese Methode inzwischen doch zunehmende Bedeutung in der neurologischen Diagnostik gewonnen. Sie ist gerade für die rechtzeitige Erkennung der Früh- und Spatkomplikationen nach Schädel Hirnverletzungen wegen der Schnelligkeit in der Anwendung, der beliebigen Wiederholbarkeit und ihrer Zuverlässigkeit unentbehrlich geworden.

ZUSAMMENFASSUNG

Für die rechtzeitige Erkennung von Komplikationen nach Schädel Hirnverletzungen ist die Echoencephalographie wegen ihrer Schnelligkeit beliebigen Wiederholbarkeit und Zuverlässigkeit unentbehrlich geworden. Es wurden 314 Schädelverletzte untersucht. Bei einem Teil der Kontusionen und allen einseitigen Blutungen fand sich eine Verlagerung des Mittelechos. Bei allen vom Ultraschall weitgehend senkrecht getroffenen epiduralen Hämatomen

FROM THE DEPARTMENTS OF RADIOLOGY AND NEUROSURGERY OF THE HOSPITAL
OF THE UNIVERSITY OF PENNSYLVANIA AND THE DEPARTMENT OF NEUROLOGY
OF THE CHILDREN'S HOSPITAL PHILADELPHIA PENN U S A

BRAIN SCANNING OF CHILDREN USING BODY SECTION TECHNIQUES AND PERTECHNETATE ^{99}Tc

by

D E Kuhl F W Pitts and S H Tucker

Radionuclide scanning is now widely accepted as an effective yet relatively atraumatic method for studying the adult brain. In spite of this experience in brain scanning of children is limited.

This is a report of our 6 months experience (1964) in rapid brain scanning of children using pertechnetate ^{99m}Tc and tomographic separation of the brain images. We chose the scanning agent pertechnetate ^{99}Tc to keep radiation exposure of the child low even when we gave large doses of radionuclide to increase the count rate. With high count rate fine resolution collimation could be used the scan speed was increased and multiple high quality images were obtained in an acceptable period of time. Tomographic scanning was used to demonstrate the radioactive brain in cross section. We explored the use of transverse section scanning in order to improve the description of lesion extent in three dimensions. We predicted that this body section scanning technique should increase the accuracy of detecting lesions of the base of the brain and in the posterior fossa by reducing the obscuring effect of the images of overlying radioactive muscle and blood pools.

- KAZNER E und SCHIEFER W Das Ultraschall Echo Verfahren (Echoencephalographie) eine Methode zur frühzeitigen Erkennung raumfordernder intrakranieller Prozesse Med Wschr 18 (1964) 27
- KIKUCHI S und ITO K Ultrasonic diagnosis of intracranial disease Rinsho Geka (Tokyo) 18 (1963) 376
- LEKSELI L Echo encephalography I Detection of intracranial complications following head injury Acta chir scand 110 (1955/56) 301
- LIETHANDER B The clinical use of echo encephalography Acta psychiatr neurol scand 35 (1960) 241
- Clinical and experimental studies in echo encephalography Acta psychiatr neurol scand Suppl 159 (1961)
- MULIER H R Zur Echoencephalographie ihre Indikation beim Schadel Hirn Trauma Schweiz med Wschr 94 (1964) 119
- SCHIEFER W KAZNER E und BRUCKNER H The diagnostic possibilities offered by echoencephalography Excerpta Med International Congress Series No 60 Sec Europ Congress Neurol Surgery Rome April 18—20 1963
- — Die Echoencephalographie ihre Anwendungswiese und klinischen Ergebnisse Fortschr Neurol Psychiatr 31 (1963) 457
- — Die Echo Encephalographie Diagnostische Möglichkeiten Dtsch med Wschr 89 (1964) 1394
- TANAKA K ITO K and ISHIIKAWA S Ultrasonic Diagnosis of Brain tumor Sogo Igaku (Tokyo) 18 (1961) 297
- — Ultrasonic diagnosis of intracranial disease Shinkai Kenkyu no Shunpo (Tokyo) 7 (1963) 335
- VILIEGER M DE and RIDDI R H J Use of Echoencephalography Neurology 9 (1959) 216

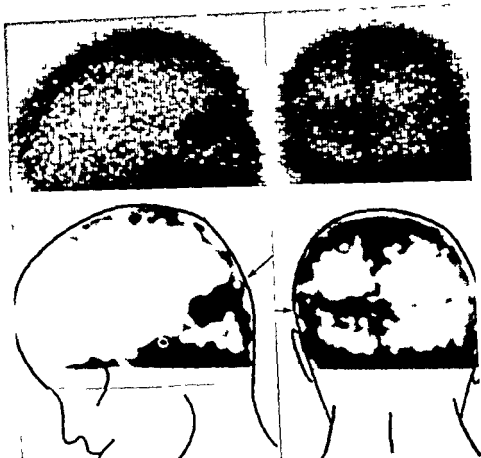


Fig. 1. Left cerebellar astrocytoma of 13-year-old child: rectilinear scanning. The top views were generated from data on paper tape as matrices of elements, each representing a measurement of $0.25\text{ cm} \times 0.25\text{ cm}$ over the patient. The lower views are the same scans modified with contrast enhancement and a glass diffusion filter.

For ordinary rectilinear scanning, two opposed scintillation detectors scan both sides of the head simultaneously. Each detector has a sodium iodide crystal 2 inches thick and 3 inches in diameter. The collimators used for rectilinear scanning are designed for lower energy photons and have a $1/2$ inch diameter of view at the focal length of 3 inches (Kuhl, in press). Pulse height analysis is used to count photons in a 50 keV window centered on the 140 keV photopeak. Count rates over the head vary from 100 to 500 counts per second. The scan speed is 2 cm/sec and the line spacing is 0.25 cm.

At the time of scanning, two channels of counting and positional data

Radioactive agent The brain scanning agent most widely used in the United States at present is chlormerodrin ^{203}Hg , introduced by BLAU & BENDER (1960, 1962). The radioactive label ^{203}Hg has a 279 keV photon emission, an average beta energy of 0.10 MeV, and a 47.9 day physical half-life. Unfortunately, the compound has the undesirable property of concentrating in the renal cortex. GREENLAW & QUARF (1962) estimated that 75 % of the administered dose leaves the body with a biologic half-life of 5 hours, while the remaining 25 % remains in the kidneys, disappearing with a biologic half-life of 8.2 days. In the absence of an effective blocking agent to abolish renal concentration, the usual dose of 10 microcuries per kg body weight delivers a radiation dose of 25 to 30 rad to the kidneys of a child.

Because of this kidney dose chlormerodrin labeled with the shorter-lived ^{197}Hg was considered for use in children. ^{197}Hg has a 77 keV photon emission, an average 'beta' energy of 0.077 MeV, and a physical half-life of only 2.7 days. Earlier reports by SODEE (1963, 1964), FEINDEL et coll (1964), and RHOTON et coll (1964) estimated that equal microcuries of chlormerodrin ^{197}Hg should deliver only 1 % to 10 % of the renal radiation dose of chlormerodrin ^{203}Hg . Using the more recent nuclear spectral data of HARRIS & ROHRER (1964), we estimate that the ^{197}Hg label reduces the renal dose to about 20 % of that expected with the ^{203}Hg label, on an equal microcurie basis. This is still a significant advantage in favor of chlormerodrin ^{197}Hg , but it is an advantage that cannot be fully realized, due to scatter problems associated with counting the 77 keV photon emission (HARRIS et coll 1963, Ross et coll 1964).

The brain scanning agent pertechnetate ^{99}Tc , introduced by HARPER et coll (1964), has properties particularly advantageous for use in children. The compound is easily recovered each day from a molybdenum ^{99}Mo generator (STANG & RICHARDS 1964). It has a 140 keV photon emission, an average 'beta' energy of only 0.014 MeV, and a physical half-life of only 6 hours. The photon energy is very near the optimum for brain scanning predicted by BECK (1961). There is no preferential concentration in the kidneys. The small concentration in the thyroid gland is prevented by iodide premedication. Because of the low energy dissipation in tissue and the short half-life, the radiation exposure to the patient is very low, even when the radionuclide is used in large amounts. At present we administer 200 microcuries per kg body weight for high count rate brain scanning of either children or adults. The total body radiation dose is approximately 120 millirad.

Instrumentation and technique The theory and operation of the scanning system used in this study has been described in detail elsewhere (KUIL 1963, 1964).

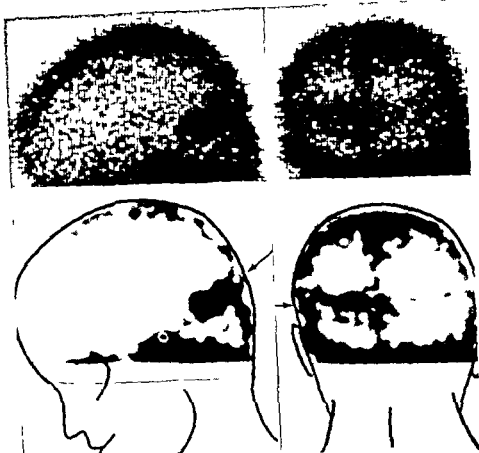


Fig. 1. Left cerebellar astrocytoma of 13-year-old child: rectilinear scanning. The top views were generated from data on paper tape as matrices of elements, each representing a measurement of $0.95 \text{ cm} \times 0.25 \text{ cm}$ over the patient. The lower views are the same scans modified with contrast enhancement and a gaussian diffusion filter.

For ordinary rectilinear scanning, two opposed scintillation detectors scan both sides of the head simultaneously. Each detector has a sodium iodide crystal 2 inches thick and 3 inches in diameter. The collimators used for rectilinear scanning are designed for lower energy photons and have a $1/2$ inch diameter of view at the focal length of 3 inches (KUNITZ, in press). Pulse height analysis is used to count photons in a 50 keV window centered on the 140 keV photopeak. Count rates over the head vary from 100 to 500 counts per second. The scan speed is 2 cm/sec. and the line spacing is 0.25 cm.

At the time of scanning, two channels of counting and positional data

Radioactive agent The brain scanning agent most widely used in the United States at present is chlormerodrin ^{203}Hg , introduced by BLAU & BENDER (1960, 1962). The radioactive label ^{203}Hg has a 279 keV photon emission, an average beta energy of 0.10 MeV, and a 47.9 day physical half-life. Unfortunately, the compound has the undesirable property of concentrating in the renal cortex. GREENLAW & QUARF (1962) estimated that 75 % of the administered dose leaves the body with a biologic half-life of 5 hours, while the remaining 25 % remains in the kidneys, disappearing with a biologic half-life of 8.2 days. In the absence of an effective blocking agent to abolish renal concentration, the usual dose of 10 microcuries per kg body weight delivers a radiation dose of 25 to 30 rad to the kidneys of a child.

Because of this kidney dose, chlormerodrin labeled with the shorter-lived ^{197}Hg was considered for use in children. ^{197}Hg has a 77 keV photon emission, an average "beta" energy of 0.077 MeV, and a physical half-life of only 2.7 days. Earlier reports by SODEF (1963, 1964), FEINDEL et al. (1964), and RHOTOX et al. (1964) estimated that equal microcuries of chlormerodrin ^{197}Hg should deliver only 1 % to 10 % of the renal radiation dose of chlormerodrin ^{203}Hg . Using the more recent nuclear spectral data of HARPIS & ROHRER (1964), we estimate that the ^{197}Hg label reduces the renal dose to about 20 % of that expected with the ^{203}Hg label, on an equal microcurie basis. This is still a significant advantage in favor of chlormerodrin ^{197}Hg , but it is an advantage that cannot be fully realized, due to scatter problems associated with counting the 77 keV photon emission (HARRIS et al. 1963, Ross et al. 1964).

The brain scanning agent pertechnetate ^{99m}Tc , introduced by HARPER et al. (1964), has properties particularly advantageous for use in children. The compound is easily recovered each day from a molybdenum ^{99}Mo generator (STANG & RICHARDS 1964). It has a 140 keV photon emission, an average beta energy of only 0.014 MeV, and a physical half-life of only 6 hours. The photon energy is very near the optimum for brain scanning predicted by BECK (1961). There is no preferential concentration in the kidneys. The small concentration in the thyroid gland is prevented by iodide premedication. Because of the low energy dissipation in tissue and the short half-life, the radiation exposure to the patient is very low, even when the radionuclide is used in large amounts. At present we administer 200 microcuries per kg body weight for high count rate brain scanning of either children or adults. The total body radiation dose is approximately 120 millirad.

Instrumentation and technique The theory and operation of the scanning system used in this study has been described in detail elsewhere (KUHIL 1963, 1964).

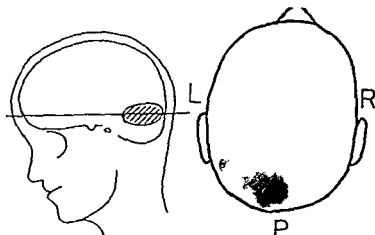


Fig 3 Transverse section scanning of left cerebellar astrocytoma which is the same tumor as shown in fig 1. Section image of the transverse venous sinus is shown on either side of the tumor. Scanning time 10 min.

In a restless child we give 1 to 4 ml of paraldehyde intramuscularly, deep in the buttocks immediately before scanning.

Brain scanning is begun 15 minutes after injection of the radionuclide. This early time of scanning is convenient when a large number of patients are to be studied. Also it is our impression that detection effectiveness is more favorably influenced by the high early count rate than by improving the tumor to blood radionuclide concentration ratio by later scanning.

The routine examination is a four view, rectilinear survey (anterior, posterior, right lateral and left lateral) and a transverse section scan through the base of the brain. If localizing signs are prominent the section level is chosen through the region of particular interest. The total scanning time for each patient is one hour.

Results

Diagnostic accuracy. In the past six months (1964) we have studied 38 children of less than 13 years of age with pertechnetate ^{99m}Tc and this scanning system. The report of each examination included a narrative interpretation and a classification of the results as definitely abnormal, probably abnormal, probably normal, or definitely normal.

Among the children in the total group 20 had a final diagnosis of a brain lesion established by consideration of clinical findings, electroencephalography, neuroradiography, surgical exploration, or autopsy, as shown below.

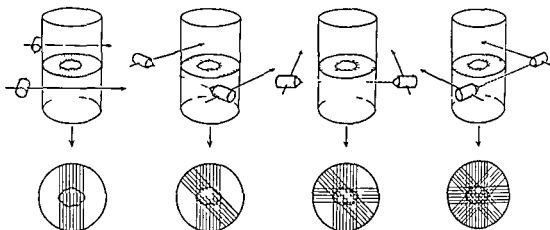


Fig 2 Transverse section scanning. A pair of detectors scan the circumference of the head from many different directions. The resulting record displays the radioactivity in a thin cross section of brain.

are alternately recorded in binary code on perforated paper tape at spatial sampling intervals of 0.25 cm. Later, the tapes are read at 300 characters per second to control the raster and the beam brightness of an oscilloscope so as to generate the pictures rapidly on Polaroid film. During this playback processing, the contrast is under the control of the operator. Each paper tape is stored as a permanent record for possible future reference to the undistorted data. In some instances, interpretation has been facilitated by the additional use of glass diffusion filters and closed circuit television for viewing the polaroid pictures (Fig 1).

For section scanning, an entirely different scanning pattern is required (Fig 2). The transverse section scan is analogous to the axial transverse tomograph and represents the radioactivity in a cross section of the brain approximately 1 or 2 cm thick. The collimators used for section scanning are also of lower energy design, but have a diameter of view of 1/2 inch at a more distant focal length of 4.5 inches. The pair of detectors makes a sequence of tangential scans at angular intervals of 7.5 degrees around the complete circumference of the patient's head, at the level of the cross section desired. The scan speed is 2 cm/sec. When the picture is generated from the data on the paper tape bands of increased film exposure, corresponding to radioactivity, converge and overlap on the film to represent the image of radioactive structures in the transverse section (Fig 3). One complete transverse section image requires approximately 10 minutes of scanning time.

During the study, soft music is played on a radio and the room is darkened to encourage sleep. Sedation is seldom required for child cooperation. With a

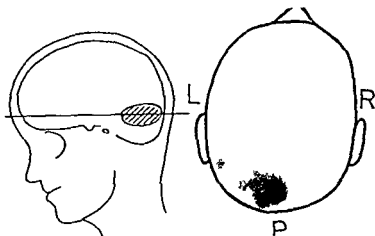


Fig 3 Transverse section scanning of left cerebellar astrocytoma which is the same tumor as shown in fig 1. Section image of the transverse venous sinus is seen on either side of the tumor. Scanning time 10 min.

In a very restless child we give 1 to 4 ml of paraldehyde intramuscularly deep in the buttocks immediately before scanning.

Brain scanning is begun 15 minutes after injection of the radionuclide. This early time of scanning is convenient when a large number of patients are to be studied. Also it is our impression that detection effectiveness is more favorably influenced by the high early count rate than by improving the tumor to blood radionuclide concentration ratio by later scanning.

The routine examination is a four view rectilinear survey (anterior, posterior, right lateral and left lateral) and a transverse section scan through the base of the brain. If localizing signs are prominent the section level is chosen through the region of particular interest. The total scanning time for each patient is one hour.

Results

Diagnostic accuracy. In the past six months (1964) we have studied 38 children of less than 13 years of age with pertechnetate ^{99m}Tc and this scanning system. The report of each examination included a narrative interpretation and a classification of the results as definitely abnormal, probably abnormal, probably normal or definitely normal.

Among the children in the total group 20 had a final diagnosis of a brain lesion established by consideration of clinical findings, electroencephalography, neuroradiography, surgical exploration or autopsy, as shown below.



Fig. 4 Detectable concentration of pertechnetate in straight sinus and deeper vasculature (arrow) of a three year old child this should not be misinterpreted as abnormal

	Lesion	Location	Number of cases
Tumor (total 17)	Astrocytoma	Optic chiasmal	2
		Hypothalamic	2
		Thalamic	1
		Cerebellar	1
		Pontine	1
	Cranio-pharyngioma	Hypothalamic	2
	Ependymoma	Temporal	1
	Pinealoma (scanned during a course of radiotherapy to tumor)	Pineal	1
	Sarcoma	Temporal	1
Non tumor (total 8)	Subdural hematoma	Frontal	1
	Intracerebral hematoma	Frontal	1
	Focal inflammation	Temporal	2
		Cerebellar	1
	Abscess	Frontal	1
	Angiomatosis	Hemispheric	2

The interpretations of the scan results of all 20 correctly localized the lesions. Of these, 18 had been classified as definitely abnormal and 2 probably as normal.

Of the children in the total group 12 were finally considered to have no tumour or vascular brain lesion on the basis of examinations other than the scanning. The scan results of 10 of these children had been interpreted as

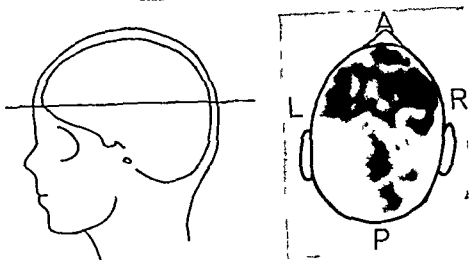


Fig 5 Angi matosis (Sturge Weber) of right hemisphere and left frontal lobe of an 11 month old child in transverse section

normal (7 definitely normal 3 probably normal) Scan results were interpreted as abnormal in 2 children who are now presumed to have no brain lesion (one definitely abnormal one probably abnormal) These false positive studies were done early in the series In each we misinterpreted the image of normal deep vascularity frequently demonstrated with this scanning technique (Fig 4)

Six children in the total group remain incompletely diagnosed the scan results of three were classified as definitely abnormal two probably abnormal and one probably normal

Section scan results A transverse section scan was included in the examination of 18 of the 20 children subsequently diagnosed as having brain lesions The section records of 15 of the 18 cases demonstrated the lesion

In these 15 cases, the combination of section and rectilinear records provided an unusually complete description of lesion extent Sometimes the lesion topography of a single section record was information unavailable by any other current study method (Fig 5) The improved tumour topography was of particular value to us for neurosurgical planning and design of portals for radiotherapy

The section scan was the only good evidence of localization in the examinations of three children one with an optic glioma and two with focal inflammation in the temporal lobe In each of these cases the image of diseased brain

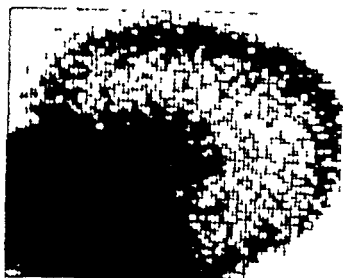
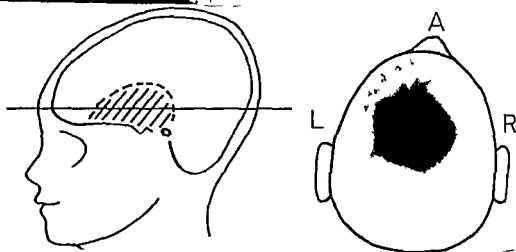


Fig. 6 Large glioma arising from optic chiasm of 4 year old child. The lateral rectilinear scan (upper left) demonstrates the tumor which is large and extends above the temporal muscle. The transverse section image of the tumor is shown below.

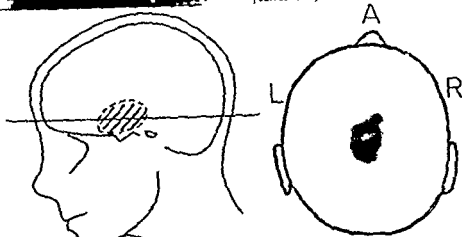


was obscured in the rectilinear scan by images of overlying temporal or occipital muscles. With rectilinear scanning a lesion arising low in the brain can be detected effectively above, or even through, these muscles, if the lesion is large (Fig. 6), situated laterally, or very radioactive. On the other hand, a small midline lesion in this region can be missed (Fig. 7). This interference is reduced with the transverse section method, since the lesion image can be demonstrated separate from that of the surrounding wall of muscle (Fig. 7).

The section recordings failed to demonstrate a frontal subdural hematoma, a craniopharyngioma, and a pinealoma, all of which were correctly localized on the rectilinear scans. The section level was incorrectly chosen for detection of the craniopharyngioma. We could not distinguish the transverse section image of the pinealoma from the expected normal image of the straight sinus and other adjacent deep vasculature.



Fig. 7. Small glioma arising from optic chiasm of 18 month-old child. The tumor cannot be distinguished from overlying temporal muscle in the lateral rectilinear scan (upper left). The tumor is demonstrated in the transverse section scan (below) which separates its image from the surrounding muscle image.



Section studies were done also on 8 of the 12 children subsequently considered to have no brain lesions. All but one of these section examinations were reported as normal. The incorrectly diagnosed study was done early in the series and accounted for one of the two false positive results reported above. The section image of the deep vasculature was misinterpreted.

Discussion

From this 6 month experience (1964) we conclude that pertechnetate ^{99m}Tc is the current agent of choice for brain scanning of children. This is because the radiation dose to the child is low yet there is a potentiality for producing multiple high quality images in a short period of time using high count rate fast scanning.

Since the radiation dose is low, we have been encouraged to introduce serial scanning at 6 month intervals for follow up examination of patients who have received radiotherapy to the brain. Also, we now rescans at shorter intervals to follow the response of inflammatory brain disease to antibiotic treatment.

With our present method, diagnostic accuracy is good. It is apparent, however, that images of vascular anatomy are demonstrated that we are not accustomed to evaluating. With increasing experience in interpreting these images, their delineation eventually may prove to be of diagnostic advantage rather than liability.

Our recent experience indicates that transverse section scanning does add additional valuable information about the anatomic distribution of most intracranial lesions. When the lesion is so situated that its image is easily confused with overlying muscle, the transverse section scan may be crucial for diagnosis. Because of this, we expect that body section scanning technique should increase the accuracy of detecting lesions of the posterior fossa, a region of predilection in children. We have yet to demonstrate this advantage, however, since there was a fortuitous scarcity of posterior fossa lesions in our material.

The introduction of pertechnetate ^{99m}Tc for brain scanning has implications that will influence instrument design. For example, the complexity of our present research scanning system could be reduced considerably by adapting its design to a very light weight detector system. The lower energy photon of ^{99m}Tc (140 keV) requires much less heavy shielding than higher energy emitters more commonly in use at present.

Advances in instrument design should also influence the useful application of section scanning. With the introduction of even more efficient detecting devices, it may be possible to perform routine multiple layer transverse section scanning at narrow separation intervals as the principal scanning examination. If so, we would approach for the first time a true three dimensional representation of brain disease.

Acknowledgements

The authors thank Miss Sandra Betz, R.N. and Mrs Martha Gubry, R.N. who performed the scanning studies reported in this paper. This investigation was supported by U.S. Public Health Service Research Grant No. C-4456 from the National Cancer Institute, U.S. Atomic Energy Commission Contract No. AT(30-1) 3175 and U.S. Public Health Service Research Career Program Award CA 14 020 from the National Cancer Institute.

SUMMARY

High count rate brain scanning was performed on 38 children using short lived pertechnetate ^{99m}Tc to minimize radiation dose. Four rectilinear views and a transverse section scan were performed during one hour. The section scans improved the outlining of lesion extent and aided detection of brain disease otherwise hidden by radioactive muscle. All 20 confirmed brain lesions (12 tumor 8 benign) were correctly localized. Two false positives resulted from misinterpreting normal vasculature.

ZUSAMMENFASSUNG

Um die Strahlendosis zu verringern wurde bei 34 Kindern scanning des Gehirns mit hoher Zahlgeschwindigkeit unter Verwendung von kurzstrahlendem Pertechnat ^{99m}Tc durchgeführt. Vier geradlinige Ansichten und ein Querschnitt scan werden während einer Stunde angefertigt. Das Schnitt scan verbesserte die Möglichkeit der Abgrenzung von ausgedehnten Veränderungen und erleichtert die Aufdeckung einer Gehirnerkrankung die ansonsten von radioaktiver Muskulatur überlagert wird. Alle 20 nachgewiesenen Gehirnveränderungen (12 Tumore 8 benign) wurden korrekt lokalisiert. Zwei fälschlicherweise als positiv gedeutete Befunde beruhten auf Fehlbeurteilung normaler Gefäßsysteme.

RÉSUMÉ

Les auteurs ont fait chez 34 enfants des scintigraphies cérébrales avec un taux de comptage élevé en utilisant un pertechnetate ^{99m}Tc de courte période pour diminuer la dose de radiation. En une heure on fait quatre scintigrammes perpendiculaires et une coupe transversale. Les scintigrammes en coupe améliorent la délimitation de la tumeur et ont facilité la détection d'affections cérébrales qui dans d'autres conditions techniques sont cachées par la radio-activité des muscles. Les 20 lésions cérébrales confirmées (12 tumeurs 8 bénignes) avaient été correctement localisées. Deux cas faussement positifs étaient dus à une mauvaise interprétation de vaisseaux normaux.

REFERENCES

- BECK R. A. A theoretical evaluation of brain scanning systems. *J. nucl. Med.* 2 (1961) 314.
 BLAU M. and BENDER M. A. Clinical evaluation of ^{203}Hg Neohydrin and ^{131}I albumin in brain tumor localization. *J. nucl. Med.* 1 (1960) 106.
 — — Radiomeric cury labeled Neohydrin. New agent for brain tumor localization. *J. nucl. Med.* 3 (1967) 83.
 FEINDEL W., YAMAMOTO L. and RUMIN N. Comparison of radioactive iodinated serum albumin (RISA) and radioactive mercury 203 for brain scanning. *J. Neurosurg.* 21 (1964) 1.
 — — McRAE D. L. and ZAVALLI J. Contour brain scanning with iodine and mercury compounds for detection of intracranial tumors. *Amer. J. Roentgenol.* 92 (1964) 177.
 GREENLAW R. H. and QUARF E. M. Retention of Neohydrin ^{203}Hg as determined with total body scintillation counter. *Radiology* 78 (1962) 970.
 HARPER P. A., BECK R., CHARLESTON D. and LATHROP K. A. Optimization of a scanning method using ^{99m}Tc . *Nucleonics* 22 (1964) 50.

- HARRIS C C BELL P R SETTERFIELD M M and JORDAN J C Some important considerations in the use of low energy gamma emitters in scanning, *J nucl Med* 4 (1963) 183
- and ROHRER R H Letter to Editor *J nucl Med* 5 (1964) 317
- KUIHL D E and EDWARDS R Q Image separation radioisotope scanning *Radiology* 80 (1963) 653
- KUIHL D E Section scanning, for image separation In *Progress in Medical Radioisotope Scanning* USAEC TID 7673 (1963) 171
- and EDWARDS R Q Cylindrical and section radioisotope scanning of the liver and brain *Radiology* 83 (1964)
- A clinical radioisotope scanner for cylindrical and section scanning In *Proceedings of the Symposium on Medical Radioisotope Scanning* IAEA Athens 1964 (In press)
- Influence of collimator design photon energy and radiation dose on detection effectiveness in liver scanning *Phys in Med Biol* (In press)
- RHOTOY A L CARLSSON A M and FERPOCOSSIAN M M Posterior fossa tumors Localization with radioactive mercury (^{197}Hg or ^{203}Hg) labeled Chlormerodrin *Arch Neurol* 10 (1964) 521
- — — Brain scanning with Chlormerodrin ^{197}Hg and Chlormerodrin ^{203}Hg *Arch Neurol* 10 (1964) 369
- ROSS D A SETTERFIELD M M JORDAN J C HARRIS C C and BELL P R Low energy gamma emitters in scanning, and other clinical applications *Int J appl Radiat* 15 (1964) 497
- SODEL D B A new scanning isotope Mercury 197 A preliminary report *J nucl Med* 4 (1963) 335
- Letter to Editor *J nucl Med* 5 (1964) 74
- Letter to Editor *J nucl Med* 5 (1964) 187
- STANG L G and RICHARDS P Tailoring the isotope to the need *Nucleonics* 22 (1964) 46

NOVEL IMMERSION SCANNER AND DISPLAY SYSTEM FOR ULTRASONIC BRAIN TOMOGRAPHY

by

D M MAKOW W WYSLOUZIL D N WHITE and J BLANCHARD

At the present time the one dimensional ultrasonic pulse position or A display method to detect midline displacements is gaining ground among neuroradiologists and neurosurgeons. To date only the midline echo can be shown reliably and this only when the operator has considerable skill and knowledge.

A complete two dimensional horizontal or coronal cross section of the head promises to give a greater amount and more reliable information about the position of the ventricular structures in the brain as can be seen from the bronze model of the skull shown in Fig 1. To obtain a cross section a compound scanning technique is used combining reversible scanning and circular movement around the head. Two different methods may be considered in the development of a compound scanner for echoencephalography — the contact or the immersion method.

A contact scanner (DE VLIJGER et coll 1963 GREATORREY & IRELAND 1964) has the advantage of small size and mobility as it can be moved to the patient. However maintenance of a satisfactory and continuous transducer contact with the skull is difficult and so is the reproducibility of the transducer position with respect to the skull.

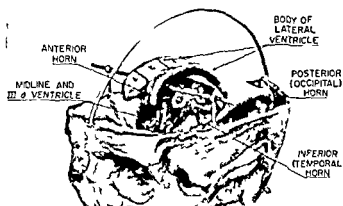
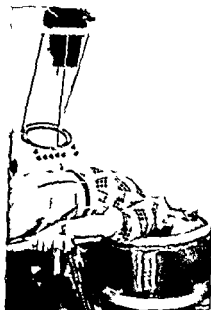


Fig 1 (above) Bronze model of ventricles showing their relative position in the head

Fig 2 (right) Photograph of equipment used in the investigation



In the immersion scanner, water used as the coupling medium provides satisfactory contact at all times. The relative position of the head and transducer can be fixed, thus freeing the operator from the patient. Mobility however is limited and in some cases the patient will find it difficult to dip his head in water.

About two years ago, we decided to explore the immersion technique first and to develop a suitable display system. The results obtained to date are summarized in this paper.

Description of apparatus

Fig 2 shows a water tank and the display system. The water tank rotates while the transducer is scanning back and forth. The combined movement provides a compound scanning motion of the head. The patient is lying on his back on a stretcher above the tank with his head bent downwards and immersed in water.

An electronic system has been developed which permits a 360° display of echoes from tissue interfaces on the face of a cathode ray tube, shown in Fig 2. These echoes appear in positions which correspond to the location of the reflecting tissues in the brain. The source of radiation, the transducer, moves on the circumference of a circle with the target in its center. This is unlike radar PPI displays, also used in diagnostic work (REID & WILD 1955). Thus the position of the source and target of a conventional radar display is completely reversed.

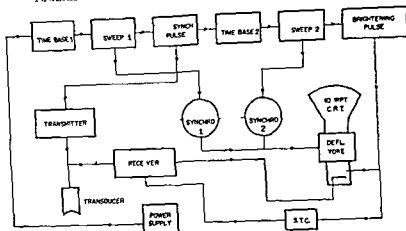


Fig 3 Block diagram of transmitter receiver and display system

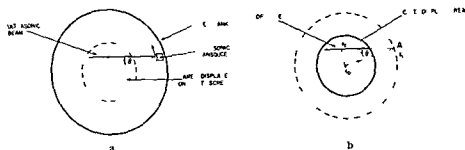


Fig 4 Diagram to illustrate correspondence of path of ultrasonic pulse and electron sweep
a) The relative positions of the transducer, the ultrasonic beam in the water tank and area displayed on the CRT screen b) CRT's screen area sweep corresponding to the position of the ultrasonic beam

In addition to the circumferential movement the reversible scanning motion with respect to the radial direction is superimposed on the transducer. The resulting position of the ultrasonic beam must then be faithfully reproduced on the CRT with a suitable sweep.

Most of the two dimensional or B scan display systems used in ultrasonic diagnoses are limited to a sector of the circle (DONALD & BROWN 1961 HOWRY 1955 DE VILIEGER et coll 1953) and a complete display could be obtained only by suitable superposition of the individual sectors (HOWRY 1955). Recently an electro mechanical (GORDON 1962) and an electronic display with electrostatic beam deflection for a contact scanning system (GREATOREX & IRELAND 1964) were proposed. The display system described in the following uses electromagnetic deflection.

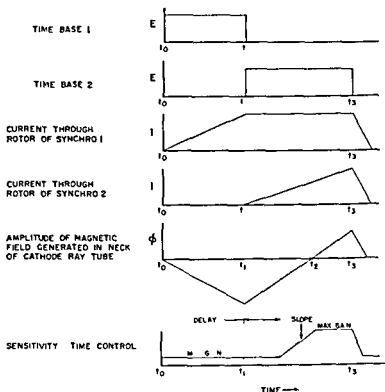


Fig 5 Waveforms illustrating the generation of the sweep and sensitivity time controls

The block diagram of the transmitter receiver and the display system is shown in Fig 3. The transmitter generates a 1 microsecond voltage pulse across a barium titanate transducer which then rings at 2 Mc/s. The angle of the beam is ± 2.2 degrees and the beginning of the far field coincides approximately with the position of the skull in the tank. Echoes are received by the same transducer then connected to a receiver tuned to 2.0 Mc/s with a bandwidth of 1 Mc and 80 db gain. When an echo is received, the potential of the cathode of the CRT with respect to its grid is lowered, permitting the electron beam to excite a spot on the phosphorescent screen. The receiver gain can be adjusted to vary with the timing of the received echoes, thus amplifying more the weak echoes from the inside of the head, and less the strong echo from the skull.

In the following the operation of the display system will be described which positions the electron beam in synchronism with the instantaneous position of the transducer. The electron beam is normally undeflected and at the center of the screen. At the time t_0 (see Fig 4) a sweep waveform from Sweep 1 is applied to the rotor of Synchro 1 (Figs 3 and 5). The resulting three phase

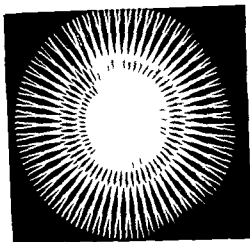


Fig. 6. Photograph of display illustrating the superposition of individual sweeps. A low PRF was used to separate consecutive sweeps.

current is applied to the yoke of the CRT which deflects the electron beam magnetically towards the point A on the perimeter of the CRT. This point corresponds to the position of the face center of the transducer which is synchronized with the movement of the rotor of Synchro 1.

At the time t_1 the electron beam has reached position A. The trailing edge of Time Base 1 waveform is used to generate a synch pulse at the time t_1 . This pulse is in turn used to trigger the transmitter as well as the Time Base 2 which then is applied to Sweep 2. The resulting current energizes the rotor of Synchro 2. The rotors of the two synchros are coupled together so that the beam in absence of the additional scanning movement would always be deflected from A towards the center when A travels along the circumference of the circle. The stator of Synchro 2 is coupled to the transducer and rocks back and forth with the scanning action of the transducer. The resulting three phase currents of Synchro 2 are added to those of the Synchro 1 at that time and generate a suitable magnetic field in the yoke of the CRT which deflects the electron sweep in a direction corresponding to the instantaneous direction of the transducer. The superposition of the sweep lines as seen on the screen when the intensity is adjusted suitably is shown in Fig. 6.

At the time t_2 the electron beam reaches a point equivalent to the distance from the center to A. The time required to traverse this distance equals the propagation time of the ultrasonic pulse from the transducer to the center of the tank and back. The sweep will usually be continued beyond the center of

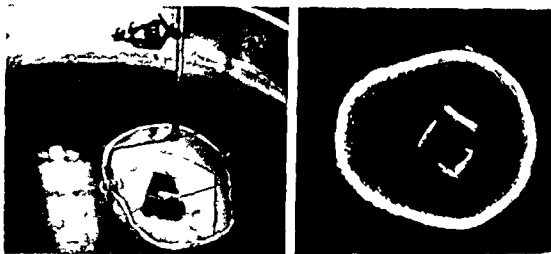


Fig 7 Human skull cap with metal target submerged in water tank and corresponding CRT display showing outline of skull and target

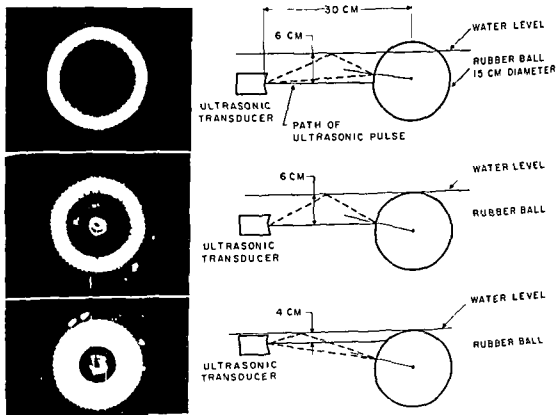
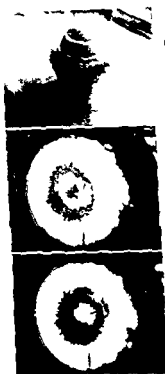


Fig 8 CRT display of a rubber ball showing ghosts due to reflections from the water surface at various depths and angles of incidence



PHOTOGRAPH OF RUBBER BALL
WITH FRINGE OF HAIR

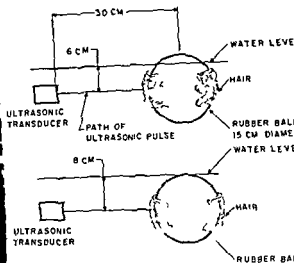


Fig 9 The effect of hair like compound placed around the ball at different depths and no

the screen. The presentation on the screen can be expanded or compressed appropriately changing the slope of the Sweep 1 and Sweep 2 waveform. A brightening pulse is generated at the time t_1 so that the electron beam is visible after t_1 and not visible when it is deflected from centre to point A (Fig 4).

Experimental results

The evaluation of the scanner and display system performance is in progress and some results have been obtained. The tests carried out to date are designed to study the effects of skull attenuation curvature and position tank effects of multiple reflections from tank bottom and water surface. In the presence of hair, the feasibility of detecting the third ventricle, cornu, referred to as the midline, and the temporal ventricles of an average adult skull cap immersed in water with a metallic object inside is shown.

A skull cap immersed in water with a metallic object inside is shown in Fig 7. The adjoining picture shows a photograph of the compound

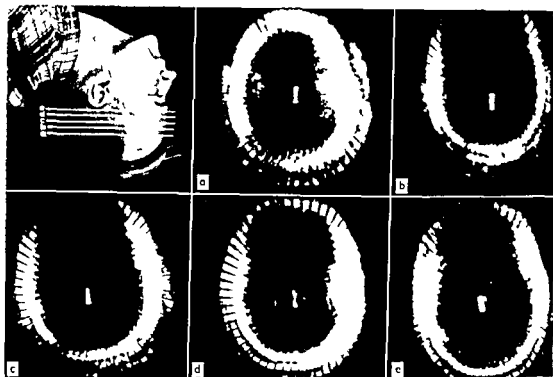


Fig 10 Five images of horizontal head cross sections of a 40 year old male indicated in top left corner. Position of forehead is at top

obtained. The missing edges of the square could be caused by the oblique incidence on the skull in front of the metallic object.

Fig 8 shows the effect of reflections from the water surface obtained with a rubber ball as the target. The dashed line indicates a possible path for a reflection from water surface. For certain immersion depths a ghost in the center of the picture or a thickening of the walls of the ball is apparent. In the third picture both effects are present. Similar effects may be expected when reflections from the tank bottom are present. Reflections from water surface were not found troublesome, possibly because the angle of the skull with respect to the surface was less than 90 degrees. The bottom of the tank was too far away to cause echoes to fall within the image of the skull.

The effect of stiff hairlike compound placed around the ball is shown in Fig 9. A depth dependent ghost in the center is also present here, as a result of multiple reflections from this compound and water surface. In addition a thickening of the wall and an irregular outline is seen, the former probably the result of scatter from this compound and reflections from the water surface. In actual practice human hair, when confined closely by a retainer, did not

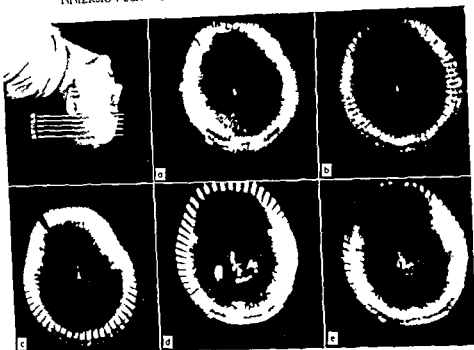


Fig 11 Five images of horizontal head cross sections of a 27 year old male indicated in top left corner. Position of forehead is at top

cause much deterioration on the skull outline and did not produce ghosts inside the image

In Fig 10 five horizontal cross sections are shown, obtained at levels indicated on the profile of an adult male aged 45 at the top left corner. These levels varied by one centimeter: the cross section A was 4.5 cm from the top of the head and the cross section E is 8.5 cm. The midline echo was obtained in each case and has left an imprint twice: each time the transducer was scanning the left and the right temporal region. On cross section D the echo to the left of the midline could have come from the lateral ventricles. The differences in intensity and thickness of the skull outline can be explained by the positioning of the head with respect to the tank: as depth gain control decreases the amplifier gain further from the center of the display. The double outline of the skull in some regions is probably due to multiple reflections within the skull wall.

Fig 11 shows similar cross sections. The subject was an adult male aged 27. Also here in cross section D there are echoes near the midline, particularly marked in this case. These echoes have been repeatedly observed in subsequent trials and are believed to originate from the lateral ventricles.

Acknowledgements

Thanks are extended to Dr L. E. Howlett for encouragement and interest in this work and to Mr R. R. Reel, Mr A. Zuidhof and Mr S. K. Keays for assistance in testing and construction.

SUMMARY

An immersion scanner and display system are described which provide a 360 degree ultrasonic image of a head cross section. Effects of multiple reflections from water surface, oblique incidence and presence of hair were studied. Five head cross sections of male adults aged 45 and 27 are shown. In all cases investigated, it was possible to obtain an image of the midline.

ZUSAMMENFASSUNG

Ein Immersionscanner und display System wodurch ein 360° Ultraschallbild eines Schadelquerschnittes erzeugt wird werden beschrieben. Effekte von multiplen Reflexen von der Wasseroberfläche, schrägem Einfall und Gegenwart von Haaren wurden studiert. Fünf Schadelquerschnitte von männlichen Erwachsenen im Alter von 45 und 27 Jahren werden gezeigt. In allen untersuchten Fällen war es möglich eine Abbildung der Mittellinie zu erhalten.

RÉSUMÉ

Description d'un scanner à immersion donnant une image ultrasonique sur 360° d'une coupe de la tête. Les auteurs ont étudié les effets des réflexions multiples par la surface de l'eau, de l'incidence oblique et de la présence de cheveux. Ils présentent cinq coupes de la tête d'hommes adultes âgés de 45 et de 27 ans. Dans tous les cas examinés, il a été possible d'obtenir une image de la ligne médiane.

REFERENCES

- DONALD I. and BROWN I. G. Demonstration of tissue interfaces within the body by ultrasonic echo sounding. *Brit. J. Radiol.* 31 (1961) 339.
- GORDON D. An ultrasonic tomograph for medical diagnosis. *Proc. San Diego Symposium for Bio Medical Engineering*, 2 (1962) 20.
- GREATOREN C. A. and IRELAND H. J. D. An experimental scanner for use with ultrasound. *Brit. J. Radiol.* 37 (1964) 179.
- HOWRY D. H. Techniques used in ultrasonic visualization of soft tissue structures of the body. *IRE Convention Record* (1955) pt 9, 73.
- LITHANDER B. Clinical and experimental studies in echo encephalography. *Acta psychiat. scand.* 36 (1961) 159.
- KEID J. M. and WILD J. J. Ultrasonic echo ranging for tissue diagnostic studies. *IRE Convention Record* (1955) pt 9, 68.
- D. VLIJGER M., DE STREEK A., MOLIN C. E. and VAN DER VIN C. Ultrasound for two dimensional echo encephalography. *Ultrasonics* 1 (1963) 148.

EVALUATION OF FIVE HUNDRED PSYCHIATRIC IN PATIENTS BY MIDLINE ECHOENCEPHALOGRAPHY

by

W M MCKINNEY J F TOOLE W T SHARP E A MACMILLAN J W
GIBSON and B D SOUTH

I hear beyond the range of sound
I see beyond the range of sight
New earths and skies and seas around
And in my day the sun doth pale this light
Thoreau

Diagnosis of unsuspected space occupying brain lesions in psychiatric patients is difficult. A review of reported autopsied psychiatric patients revealed that up to 17% had brain tumor (2) and up to 79% had subdural hematoma (1). Patients in psychiatric hospitals in the United States comprised 51%, (712 174 patients) of the daily hospital census in 1962 (4). An estimated one out of every ten persons is now suffering from some form of mental illness.

Midline echoencephalography offers a safe rapid screening procedure for these patients. FORD & AMBROSE reported an overall accuracy for midline shift in 93.8% of one thousand cases (3).

This is a preliminary report of five hundred ambulatory psychiatric in patients who were screened at the Veterans Administration Hospital Salisbury North Carolina.

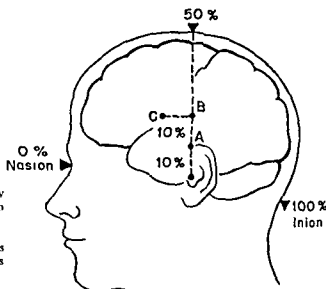


Fig. 1. Coordinate system. At fifty percent of the distance from nasion to inion a measurement is taken connecting the external auditory meatuses. Ten percent of this measurement is used for placement of standard positions A, B, and C for midline determinations by the coordinate system.

Materials and Methods. Ultrasonic instruments consisted of a Biosonar 200 by Sonomedic, and a modified Ekoline 20 by Smith Kline Instruments. Polaroid ten second film was used for recording. Selected cases were studied by averaging multiple exposures on the same film by sweeping with intensity modulation on a modified Ekoline 20 (5). Aquasonic 100 Gel (Parker Laboratories, Inc., Irvington, New Jersey) was used for conduction.

For standardization in repeated examinations and correlation of results a coordinate system (5) was used for placement of a 2.25 mc/cycle transducer. Midlines were determined at standard positions A, B, and C (Fig. 1).

Head diameters at these positions were measured by calipers to determine the theoretic midline for comparison with ultrasonic midline.

EEG, skull films, and neurologic evaluation by three neurologists were performed on all patients with shifts and borderline shifts and further studies were done as indicated.

Patients were ambulatory and are shown with relation to age, sex, and psychiatric diagnosis (Fig. 2).

Results

In some patients skull thickness and various other factors prevented interpretable tracings in all three positions (position A, 418 patients, position B, 451 patients, position C, 171 patients). One or more satisfactory tracings were obtained in all patients.

The average midline by ultrasonic and external measurement with calipers

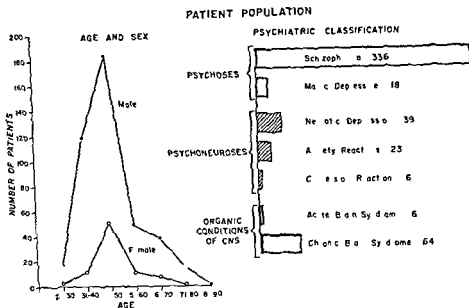


Fig 2 Patient population. Patients are shown with relation to age, sex and psychiatric classification.

in all three positions correlated within one mm (Fig 3). The average measurement connecting the external auditory canals at 50% of the distance from nasion toinion was 36.3 cm.

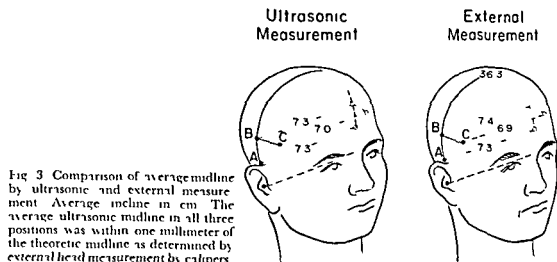
There was no significant shift to right or left with handedness (see Table).

Twenty-five cases were selected for further study. Nineteen cases with normal and borderline shifts were evaluated with insufficient evidence to proceed to further contrast studies. Six abnormal midline shifts were found and are shown with correlation studies (Fig 4). Two cases were proved to have brain tumor. None had calcified pineals.

Discussion

The use of midline echoencephalography to screen large population groups for organic brain lesions would seem of value since it is a rapid, safe procedure. Psychiatric patients offer a very large population group in which organic disease may exist and be difficult to diagnose. This study was to determine the usefulness of this procedure on a mass screening basis.

A system for examination is most important in reproducing results, correlation of data, and later follow-up. The coordinate system used is simple for routine examinations. By pathologic correlations usually the echogram in the A



position will give echoes from the walls of the third ventricle, in the B position, from the walls of the third ventricle and septum pellucidum, and in the C position, from the septum pellucidum more anteriorly. This provides three determinations of the midline for greater accuracy and establishes a plane to aid in localization. Frontal lesions may shift only the C position without abnormal shifts in positions A or B. The difficulty in obtaining a more anterior position is reflected in our results with only 171 C positions obtained. This may be due to increased skull thickness and curvature as well as other factors. Therefore, frontal lesions may well have been missed in the remaining 329 patients. This is a serious limitation of the current method. In difficult cases with numerous echoes near the midline, averaging the strongest echo by multiple exposures using B mode was of value. Compound scanning by ultrasound may well offer a better screening technique and replace midline echoencephalography in the near future.

Table
Effect of handedness on midline

Handed	Shift	Position (shift in mm)		
		A	B	C
Left (39)	Right	1.1 (9)	0.9 (16)	1.1 (7)
	Left	1.4 (19)	1.1 (11)	1.2 (6)
Right (461)	Right	1.2 (129)	1.0 (153)	1.4 (64)
	Left	1.3 (186)	1.1 (15)	1.4 (67)

(dominance (by handedness) did not affect slight shifts within normal limits)

Position of Midline Shift	Skull Film (no calcified peduncles)	EEG	Neurological	PEG	ART	Diagnosis
B	O	O	X	X		Cerebral atrophy
C	O	X	X	X	X	Recurrent Oligodendroglioma
B	O	X	O	Permissives not obtained for further studies		
A	O	X	O	X	X	Astrocystoma
C	O	X	X	X		Cerebral atrophy
A	O	X	X		X	Postoperative aneurysm

O Normal

X Abnormal

Fig 4 Correlation studies of six abnormal midlines. None of the patients had calcified peduncles. Two had brain tumors.

The ultrasonic instrumentation had been calibrated for echoencephalography. It was of interest and reassuring to find maximum error of only one mm on comparison of midline by ultrasound and external head measurements.

The question of slight shift within the limits of normal (3 mm) being related to dominant hemisphere (as determined by handedness) would appear not true from our data. The shift may be to either side.

The small number of brain tumors and the fact that no subdurals were found as compared with autopsy series was of interest. This may reflect the selection of the ambulatory patients of the hospital as well as limitations in current technique.

The procedure was inexpensive, rapid, and tolerated well by the patients. Until better techniques become available, midline echoencephalography would appear to be a useful diagnostic tool for screening psychiatric patients.

Acknowledgements

The authors wish to express their appreciation to A. Patel, M.D., for his assistance in neurologic evaluation; Mrs. Betty Poul for her untiring efforts in assisting with examinations; preparation of the manuscript; and useful suggestions; and to the numerous members of The Veterans Administration who aided in this research project.

Supported by USPHS HE07672 and NB 5206.

SUMMARY

Five hundred ambulatory psychiatric patients were screened by midline echoencephalography for unsuspected organic brain lesions. A coordinate system for examination was used. Average ultrasonic midline and theoretic midline by external head measurement correlated within one millimeter. Handedness did not correlate with slight shift to right or left.

ZUSAMMENFASSUNG

Es wurden 500 Patienten wegen nicht verdächtiger organischer Gehirnveränderungen mit Mittellinien echoencephalographie untersucht. Für die Untersuchung wurde ein Koordinatensystem erwendet. Die durchschnittliche Ultraschall Mittellinie und die theoretische Mittellinie von den Schädelmessungen stimmten innerhalb der Grenzen eines Millimeters überein. Rechts- oder Linkshändigkeit hatte keinen Zusammenhang mit geringer Rechts- oder Linksverschiebung.

RÉSUMÉ

Cinq cents malades psychiatriques ont subi un examen écho encéphalographique de la ligne médiane pour rechercher des lésions cérébrales organiques. Les auteurs ont utilisé un système de coordonnées pour cet examen. La ligne médiane écho encéphalographique a coïncidé à moins d'un millimètre avec la ligne médiane théorique déterminée par des mesures externes de la tête. La dextérité ou la gaucherie sont sans rapport avec un léger décalage à droite ou à gauche de la ligne médiane écho encéphalographique.

REFERENCES

- 1 ALLEN A. M., MOORE M. and DAVIS B. B. Subdural hemorrhage in patients with mental disease. *New Engl J Med* 223 (1950) 324.
- 2 DAVIDOFF L. M. and IERRARO A. Intracranial tumor among mental hospital patients. *Amer J Psychiat* 8 (1929) 599.
- 3 FORD R. and AMBROSE J. Echoencephalography. The measurement of the position of midline structures in the skull with high frequency pulsed ultrasound. *Brain* 86 (1963) 189.
- 4 LASKER A. D. and MAHONEY I. What are the facts about mental illness in the United States. Compiled by The National Committee Against Mental Illness Inc. Washington D. C. 1964.
- 5 MCKINNEY W. M. The value of B mode determination of midline in echoencephalography. Presented American Academy of Neurology, April 1964.

SCINTILLOGRAPHY OF INFANTILE SUBDURAL EFFUSIONS AND ITS CLINICAL APPLICATION

by

JOHN MEALEY JR and JOHN A CAMPBELL

Progress in the treatment of persistent subdural collections of fluid in infancy must be based on further knowledge of various pathogenetic factors influencing the course of this disease. The most common neurosurgical therapy is excision of the subdural membranes when present to eliminate the presumably restrictive effects of these membranes on the developing brain (5). It has also been suggested that removal of subdural membranes and their abnormally permeable blood vessels could prevent recollections of fluid (4, 7). Usually a conventional contralateral craniotomy is done if subdural membranes are found by exploratory burr holes. Recently persistent reaccumulations of subdural fluid and the eventual clinical outcome have been related more to the disproportion between a contracted poorly expansile brain and a larger skull than to the postulated effects of retained subdural membranes (8, 11).

The role of neuroradiology in the study and management of subdural effusions in infancy has not been established clearly. Since a definitive diagnosis can be made in these cases by a needle puncture contrast procedures such as lumbar encephalography and ventriculography have not been found necessary as a rule or even desirable (5). Subdural air encephalography can visualize

SUMMARY

Five hundred ambulatory psychiatric patients were screened by midline echoencephalography for unsuspected organic brain lesions. A coordinate system for examination was used. Average ultrasonic midline and theoretic midline by external head measurement correlated within one millimeter. Handedness did not correlate with slight shift to right or left.

ZUSAMMENFASSUNG

Es wurden 500 Patienten wegen nicht verdächtigter organischer Gehirnveränderungen mit Mittellinien echoencephalographie untersucht. Für die Untersuchung wurde ein Koordinatensystem erwendet. Die durchschnittliche Ultraschall Mittellinie und die theoretische Mittellinie von den Schädelmessungen stimmten innerhalb der Grenzen eines Millimeters überein. Rechts- oder Linkshändigkeit hatte keinen Zusammenhang mit geringer Recht- oder Linksverschiebung.

RÉSUMÉ

Cinq cents malades psychiatriques ont subi un examen écho encéphalographique de la ligne médiane pour rechercher des lésions cérébrales organiques. Les auteurs ont utilisé un système de coordonnées pour cet examen. La ligne médiane écho encéphalographique a coïncidé à moins d'un millimètre avec la ligne médiane théorique déterminée par des mesures externes de la tête. La droiterie ou la gaucherie sont sans rapport avec un léger décalage à droite ou à gauche de la ligne médiane écho encéphalographique.

REFERENCES

- 1 ALLEN A. M., MOORE M. and DALY B. B. Subdural hemorrhage in patients with mental disease. *New Engl. J. Med.* 223 (1950) 324.
- 2 DAVIDOFF I. M. and IERRARO A. Intracranial tumor among mental hospital patients. *Amer. J. Psychiat.* 8 (1929) 599.
- 3 LORD R. and AMBROSE J. Echoencephalography. The measurement of the position of midline structures in the skull with high frequency pulsed ultrasound. *Brain* 86 (1963) 189.
- 4 LASKER A. D. and MAHONEY I. What are the facts about mental illness in the United States. Compiled by The National Committee Against Mental Illness, Inc. Washington D. C. 1964.
- 5 MCKINNEY W. M. The value of B mode determination of midline in echoencephalography. Presented American Academy of Neurology, April 1964.

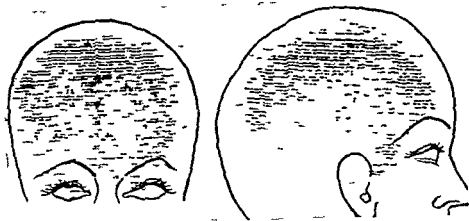


Fig 1 Frontal and lateral dot scans after a right subdural injection of RISA ($25 \mu\text{c}$) large communicating hematoma

investigative procedure. The subdural scans have been found useful as guides in the neurosurgical management of these patients. The characteristics of subdural effusions as delineated on the scans appear to have etiologic and prognostic relevance when correlated with the other clinical data.

Material and methods. Seventeen of the 25 infants (Table 1) had presumably traumatic effusions or chronic subdural hematomas. Subdural taps revealed bilateral hematomas in all but one patient. Twenty-eight of the total of 33 left and right sided hematomas were visualized by scanning. In the other 8 patients subdural effusions followed bacterial meningitis with *Hemophilus influenzae*, the most common known causative organism. In 7 out of 8 patients with post-infectious effusions the lesions were bilateral, totalling 15 in number of which 11 were scanned.

All the patients had previous treatment with multiple taps over varying intervals prior to receiving percutaneous subdural injections of RISA just lateral to the anterior fontanelle. The dose of RISA was $20 \mu\text{c}$ to $30 \mu\text{c}$ depending on the infant's head size and weight. Potassium iodide solution administered before the radioactive injection blocked the uptake of RISA by the thyroid gland.

In most infants the head was scanned 4 to 6 hours after the subdural injections using an automatic commercially available scintillation scanner. These modifications in the original technique in terms of earlier (rather than at 24 hours after injection) scanning with a more sophisticated apparatus have greatly improved the quality of the scans. Print out recordings and photoscans were obtained simultaneously. A three by two-inch sodium iodide crystal and 31 hole fine focusing collimator were used. Typical control settings were: rectilinear scan speed 20–24 cm per minute, line spacing 0.3 cm, time constant $1/8$ second, and dot factor 9. The discriminator window was set at 314 keV.

The procedures were carried out under light barbiturate sedation. Frontal and lateral scans were performed routinely and usually completed within an hour. For the frontal projection the infants were supine with the head flexed on the chest to give a frontobregmatic rather than a true anteroposterior scan. The infants were positioned on their sides with the injected hematoma uppermost for the lateral views.

Table 1

Type and distribution of subdural effusions in 25 infants

Type	Number of patients		Total left and/or right hemispherical effusions	
	Bilateral	Unilateral	Number	Number scanned
Post traumatic				
Communicating (left right)	6	—	12	12
Lateralized	10	1	21	16
Total	16	1	33	28
Post infectious	7	1	12	11

the intracranial extent of infantile effusions, however, it has never been widely practised despite its usefulness in delineating the fluid collections and brain. These attitudes almost certainly have arisen in part because of the morbidity inherent in time consuming air contrast studies in these infants who frequently are severely ill. The larger volumes of air which must be exchanged to outline adequately the more extensive subdural effusions are often poorly tolerated.

In 1962 it was shown that the size and location of subdural effusions could be accurately visualized by radioactive scanning (6). For this procedure small amounts of radioiodinated (^{125}I) human serum albumin (RISA) were injected percutaneously into the subdural space. The labeled albumin was distributed uniformly throughout the subdural fluid collections where it remained in high concentration. The activity of RISA in the subdural fluid was 800 to 150 times greater than that measured in the plasma at 4 and 24 hours, respectively. Favorable activity ratios of this magnitude made feasible the precise representation of a subdural effusion *in situ* as a gamma ray image. This procedure was found to be safe, convenient, and practicable, and did not interfere with a therapeutic regimen of serial subdural taps.

The radiation dose associated with subdural scanning has been measured and is within acceptable levels. As calculated from experimental data 30 μC of RISA injected into the subdural space of an infant weighing 7 kg provides a total body dose (beta and gamma radiation) of 0.334 rad (10). However, in practice as soon as scanning is completed, nearly all of the injected radioactive material can be recovered by aspiration of subdural fluid. Thus, local and whole body irradiation hazards can be virtually eliminated.

This is a report of our experiences with subdural scintiscanning in 25 infants observed during the past 2 years. No morbidity was associated with this in

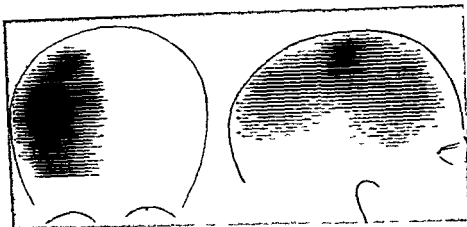


Fig. 3 Frontal and lateral photoscans after injection of RISa (30 μ c) into the right subdural space show a lateralized hematoma over the entire fronto-parieto-occipital convexity.

disproportion. The marked cerebral attenuation associated with these infantile subdural hematomas caused a pathophysiological free continuity between the left and right subdural spaces under the inferior margin of the falx.

The histories in these 6 cases revealed many similarities. These common findings described below seemed in many ways to distinguish clinically infants with diffuse bilateral communicating hematomas from infants whose scans showed more localized subdural effusions. Craniocerebral trauma was poorly documented in all 6 patients, probably dating to the time of delivery (or earlier) in 5. One infant proved to have a linear skull fracture. Measurements of head circumference were not remarkable. These infants as a group did not thrive normally following birth. Ages at the time of admission to the hospital and establishment of a definitive diagnosis ranged from 6 weeks to 4 months, averaging 2.7 months. The infants generally were symptomatic for periods of a few days to several weeks prior to hospitalization.

Lateralized subdural effusions. The scans of the other 19 infants showed subdural effusions in 18 that were noncommunicating and confined to a hemispherical space. These radioisotopic investigations revealed no significant differences between the traumatic effusions (11 patients) and the effusions which followed infection (8 patients). Many scans demonstrated generalized collections of fluid over the entire cerebral convexity (Fig. 3). Somewhat more limited effusions were also noted parasagittally over the uppermost frontoparietal aspects of the cerebral hemispheres (Fig. 4). However, in about half the scans

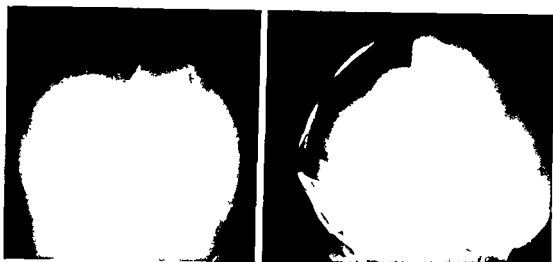


Fig 2 Roentgenograms (brow down) after unilateral injection of air into the subdural space show the bilaterality and extent of the lesion and the size of the cerebral hemispheres

Results

A remarkable diversity in the size and form of subdural effusions was disclosed. From the scans the effusions could be classified (Table 1) either as diffuse collections that freely communicated across the midline or as lesions that remained lateralized to the right or left subdural space. Twenty craniotomies were performed in 14 infants. These direct surgical observations confirmed that scanning gave an accurate representation of the size, configuration, and location of subdural fluid collections. The results of subdural scanning and subdural pneumoencephalography agreed in the 3 patients in which both procedures were done. The scans and the surgical observations were not completely congruous in only one case. This infant had a postmeningitic, anteriorly situated, unilateral subdural effusion of fairly typical serosity which was well demonstrated on the scan. However, at surgery an encapsulated collection of thick pus was found adjacent and posterior to the site of the effusion. This localized subdural empyema was not visualized in the scans.

Diffuse bilateral communicating subdural effusions. Scanning after unilateral subdural injections of RISA in 6 infants revealed massive generalized subdural effusions which were bilaterally continuous. These lesions were presumably of traumatic origin. The intracranial extent of this type of hematoma as depicted by scanning is seen in Fig 1 with analogous views of a subdural pneumoencephalogram shown in Fig 2. Although the effusions are symmetrical, their dimensions are greatest over the superior and parasagittal aspects of the cerebral hemispheres; the area of maximum craniocerebral

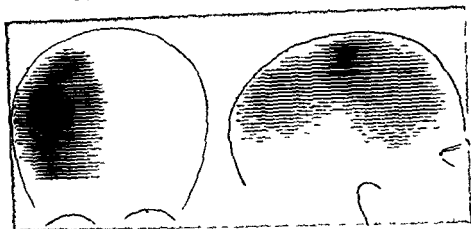


Fig 3 Frontal and lateral photoscans after injection of RISA (30 μ c) into the right subdural space show a lateralized hemispheric area over the entire fronto-parieto-occipital convexity

disproportion. The marked cerebral attenuation associated with these infantile subdural hematomas caused a pathophysiological, free continuity between the left and right subdural spaces under the inferior margin of the falx.

The histories in these 6 cases revealed many similarities. These common findings described below seemed in many ways to distinguish clinically infants with diffuse bilateral communicating hematomas from infants whose scans showed more localized subdural effusions. Craniocerebral trauma was poorly documented in all 6 patients, probably dating to the time of delivery (or earlier) in 5. One infant proved to have a linear skull fracture. Measurements of head circumference were not remarkable. These infants as a group did not thrive normally following birth. Ages at the time of admission to the hospital and establishment of a definitive diagnosis ranged from 6 weeks to 4 months, averaging 2.7 months. The infants generally were symptomatic for periods of a few days to several weeks prior to hospitalization.

Lateralized subdural effusions. The scans of the other 19 infants showed subdural effusions in 18 that were noncommunicating and confined to a hemicranial space. These radioisotopic investigations revealed no significant differences between the traumatic effusions (11 patients) and the effusions which followed infection (8 patients). Many scans demonstrated generalized collections of fluid over the entire cerebral convexity (Fig 3). Somewhat more limited effusions were also noted parasagittally over the uppermost, frontoparietal aspects of the cerebral hemispheres (Fig 4). However, in about half the scans

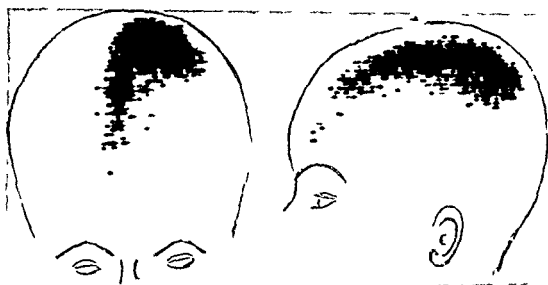


Fig 4 Frontal and lateral photoscans after injection of RISN (30 μ c) into the left subdural space. Lateralized hematoma is chiefly parasagittal in location.

more focal varieties were noted, predominantly anterior or posterolateral. The sixteen traumatic effusions that were scanned showed 8 generalized hematomas and an equal number of more limited collections of fluid. Fig 5 shows an example of a persistent subdural hematoma that was principally frontal in location. The photoscans and lateral skull roentgenogram are superimposed for orientation.

In the post infectious group, 6 scans in 4 patients showed fairly generalized subdural fluid collections, and 5 effusions were made more localized. One patient in this group showed a large effusion over the left cerebral hemisphere which was continuous with a focal collection of fluid over the right frontal pole. This was the only example of partial communication between the left and right hemicranial subdural spaces in the 25 infants studied. The next two illustrations are examples of more limited types of post infectious subdural effusions. In Fig 6 the scans show a laterally placed collection of subdural fluid. Most of the lesion is in the parietal area with some parasagittal frontotemporal extension anteriorly. Fig 7 shows the lateral scan of a similar type of post meningitic subdural effusion. The post operative skull roentgenogram has been superimposed on the scan to show the location of the parietal bone flap turned down in this infant. In both of these patients (Figs 6 and 7) successive daily paracenteses lateral to the anterior fontanelles suggested progressively smaller reaccumulations of subdural fluid. It was only after subdural scanning that the posteriorly situated, unresolved reservoirs of fluid were disclosed.

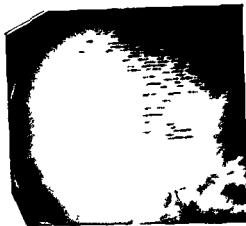


Fig 5 Lateral photostatic scan showing a subdural hematoma over the right frontal hemisphere with some extension along the Sylvian fissure

From the clinical histories the 11 infants with separate lateralized subdural hematomas differed as a group in several ways from the 6 infants whose diffuse bilateral hematomas were in free communication. Precipitating craniocerebral trauma was well documented or established in 8 patients. A history of injury was not verified in only 3 patients and 2 of these presented with an abnormal increase in head size. These 11 infants were older when first seen. Postnatal progress was entirely satisfactory as a rule until the onset of the definitive illness. Ages at admission ranged from 7 weeks to 12 months averaging 5.6 months. Only one child was admitted before the age of 3 months, a battered neglected baby who at 7 weeks of age more nearly resembled clinically the type of infants seen with massive communicating hematomas. However, the generalized bilateral hematomas in this infant were separate.

The patients with post-infectious subdural effusions were well until the onset of their acute illness. A post-meningitic etiology was established definitely in 7 and was probable in the other. Average age at admission was 5.6 months.

Clinical outcome

Table 2 summarizes the surgical results in the 25 infants with subdural effusions who were studied by radioactive scanning. In the 6 infants in group I whose scans showed such extensive lesions it did not seem probable that staged bilateral craniotomies could successfully overcome the craniocerebral disproportions and obliterate the subdural spaces. In fact, one of this group had previously been subjected to these procedures prior to his being included in this study with massive recurrent hematomas. Consequently bilateral subdural pleural or peritoneal shunting procedures were carried out and proved

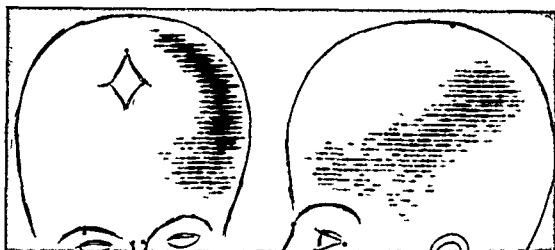


Fig. 6 Frontal and lateral photocopies after injection of RISA (30 μ c) into the left subdural space in a focal type of post meningitic effusion

satisfactory in preventing reaccumulations of subdural fluid. The patency and function of these systems were also tested in several patients by injecting RISA subdurally and probe counting or scanning over the thorax or abdomen. Only one of these children was normal in the period of followup. The other 5 in this group were obviously defective with one or more manifestations of severe brain damage, such as gross mental retardation, frequent convulsions, blindness, and marked spasticity. One infant who was probably only moderately retarded and seemed otherwise to be doing well 2 months after discharge from the hospital died suddenly in his crib from unknown cause.

In the 11 infants with other types of subdural hematomas (group II) the initial results were more gratifying. Six hematomas in 4 infants resolved with repeated subdural taps. These lesions were bilateral in 2 patients, and scanning showed in one a focal anterior and in the other a thin generalized subdural collection of fluid. Fourteen craniotomies were carried out in 9 infants. The subdural fluid and membranes were removed and the dura was tailored where feasible to approximate the brain more closely, reducing the size of the subdural space. All the infants with persistent hematomas had preoperative subdural scans. These were used to plan the position of the cranial bone flaps. A large central craniotomy was performed for example in the patient whose hematoma is outlined in Fig. 3. In contrast, for the lesion shown in Fig. 5 a more limited frontal craniotomy via a coronal scalp flap proved entirely satisfactory. There were 2 operative deaths, one from shock and hypothermia, and the other from fulminating sepsis. In retrospect both fatalities were preventable. Eight of the 11 patients in this group appeared to be doing well at

Table 2
Surgical results in 25 infants with subdural effusions

Definitive treatment	Groups		
	I	II	III
Subdural taps	0	4(6)	7(2)
Burr holes	0	0	4(7)
Craniotomies	0	9(14)	5(6)
Shunts	6	0	0
Deaths	1	2	0
Good in final results	1	8	8

Group I = communicating subdural hematomas 6 patients
 Group II = lateralized subdural hematomas 11 patients
 and Group III = postmeningitic subdural effusions 8 patients

Figures in parentheses indicate the total number of hemispheric effusions treated individually in each category

the most recent followup. Only the battered infant referred to above has obvious mental and motor deficits.

The 8 patients in group III the postmeningitic effusions all had good initial results following treatment. Effusions in two infants were successfully treated with subdural taps. Seven effusions in 4 patients resolved after drainage through burr holes. Six craniotomies were carried out in the 5 patients whose scans showed larger or persistent subdural effusions. The surgical application and technique in this group were essentially the same (Fig. 7) as that described for the lateralized subdural hematomas.

Comment

Our extended experience substantiates the earlier contention that subdural scanning is a practical new diagnostic method which can aid in the individual surgical management of persistent subdural effusions in infancy. Previously subdural pleural shunts have been advocated as treatment for chronic subdural hematomas in infants presenting with enlarged heads and in whom large volumes of subdural fluid continued to reaccumulate following repeated aspirations (9). The distended subdural spaces were visualized roentgenographically by subdural air injections. Subdural peritoneal drainage has been used by others initially for large recurrent hematomas and subsequently as a primary operation (2). The surgical indications for the latter were not given

Fig. 7 Lateral photoscan after injection of RISAN (23 μ c) into the left subdural space in a predominantly parietal post meningitic effusion. Radiolucent areas demarcate the inferior aspect of the bone flap.



Internal drainage was used here as the procedure of choice and successfully resolved all of the large hematomas described in the infants in group I. Subdural scans provided specific indications for shunting procedures for this type of communicating hematoma and the coexistent, marked craniocerebral disproportion. The bad clinical outcome in 5 of these cases reflected directly the primary influence of underlying brain damage. The good result in one child, who is normal at 2 years of age, argues against any deleterious effects attributable to retained subdural membranes. The severe clinical sequelae in this group contrast sharply with the satisfactory initial results of treatment in infants with lateralized hematomas. These observations emphasize the value of subdural scanning in the prognosis of subdural hematomas in infancy, as an adjunct to the clinical appraisal.

In the lateralized subdural hematomas and post meningitic effusions radioactive assessment, *in situ*, also proved very helpful in treatment. It seemed reasonable to delay craniotomy in the smaller collections of subdural fluid and seek to resolve these by more conservative methods. In some cases, guided by the scans, a more aggressive program of subdural aspirations was carried out, via the metopic, lambdoidal, and inferior coronal sutures as well as adjacent to the anterior fontanelles. Eight subdural fluid collections were dried up with taps. In none of these was the volume of fluid removed extreme. Scans in two infants confirmed the relatively small size of the hematomas. In 3 patients who had burr holes over localized varieties of post meningitic effusions shown on the scans the fluid components of these lesions had resolved. The residual membranes were not removed. Thus our present surgical orientation to infantile subdural fluid collections is not necessarily dependent on the presence or character of the subdural membranes. Treatment is more directed



Fig. 8. Aborted fetus at 3.5 months (crown-rump length 9.5 cm) with calvarium and dura removed. A subdural hematoma overlays the right hemisphere. Translucent membranes extend over most of the cerebral convexities. A smaller clot over the left Sylvian area is not clearly visible. (Courtesy of Dr. WILLIAM E. DEMMY.)

at overcoming the craniocerebral disproportion and obliterating the enlarged subdural space. In the lateralized traumatic and post meningitic effusions that do not respond to the simpler measures described above good results follow evacuation of the fluid (and part of the membranes) and dural tailoring via craniotomy. Subdural scanning gives unique aid in this regard in planning the type of cranial bone flap.

The significant differences in histories and morbidity in the two groups of subdural hematomas reported here emphasize the different pathogenic mechanisms in this disease. There is a striking similarity between our results predicated by observations on the scans and the clinicopathological studies in a surgical series of 24 infants with chronic subdural hematomas reported recently by CHRISTENSEN & HUSBY (1). The prognosis in their cases was correlated with the condition of the brain and specific pernicious effects from retained subdural membranes were largely discounted. These authors classified most of their patients into those with pre- and perinatal head injuries and infants with probable postnatal trauma. Cases in the former groups were seen earlier (mean age 4 months with the perinatal lesions) and had uniformly bad results following treatment. This experience is duplicated in 5 of 6 patients

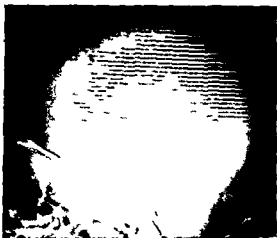


Fig. 7 Lateral photoscan after injection of RISAN (23 μ c) into the left subdural space in a predominantly parietal post meningitic effusion. Radiolucent areas demarcate the inferior aspect of the bone flap.

Internal drainage was used here as the procedure of choice and successfully resolved all of the large hematomas described in the infants in group I. Subdural scans provided specific indications for shunting procedures for this type of communicating hematoma and the coexistent, marked craniocerebral disproportion. The bad clinical outcome in 5 of these cases reflected directly the primary influence of underlying brain damage. The good result in one child, who is normal at 2 years of age, argues against any deleterious effects attributable to retained subdural membranes. The severe clinical sequelae in this group contrast sharply with the satisfactory initial results of treatment in infants with lateralized hematomas. These observations emphasize the value of subdural scanning in the prognosis of subdural hematomas in infancy, as an adjunct to the clinical appraisal.

In the lateralized subdural hematomas and post meningitic effusions radioactive assessment, *in situ*, also proved very helpful in treatment. It seemed reasonable to delay craniotomy in the smaller collections of subdural fluid and seek to resolve these by more conservative methods. In some cases, guided by the scans, a more aggressive program of subdural aspirations was carried out, via the metopic, lambdoid and inferior coronal sutures as well as adjacent to the anterior fontanelles. Eight subdural fluid collections were dried up with taps. In none of these was the volume of fluid removed extreme. Scans in two infants confirmed the relatively small size of the hematomas. In 3 patients who had burr holes over localized varieties of post meningitic effusions shown on the scans the fluid components of these lesions had resolved. The residual membranes were not removed. Thus our present surgical orientation to infantile subdural fluid collections is not necessarily dependent on the presence or character of the subdural membranes. Treatment is more directed

RÉSUMÉ

Présentation de 25 nouveaux cas de gamma-encéphalographie d'épanchements sous-duraux chez des nourrissons après injection de RISA dans l'espace sous-dural. Ces scintigrammes ont été classés et confrontés avec l'histoire clinique et l'effet du traitement. Cette nouvelle technique s'est montrée utile pour guider le traitement chirurgical de ces malades. L'analyse de nos cas nous fait penser que les renseignements tirés du scintigramme sous-dural sont applicables au pronostic et à l'étiologie des hématomes sous-duraux chroniques du nourrisson.

REFERENCES

- 1 CHRISTENSEN E and HUSBY J. Chronic subdural hematoma in infancy. *Acta neurol scandinav* 39 (1963) 373
- 2 COLLINS W F and PLECI G L. Peritoneal drainage of subdural hematomas in infants. *J Pediat* 58 (1961) 482
- 3 DEMEYER W E. Department of Neurology, Indiana University Medical Center. Personal communication 1964
- 4 GITLIN D. Pathogenesis of subdural collections of fluid. *Pediatrics* 16 (1955) 345
- 5 INGRAHAM F D and MATSON D D. *Neurosurgery of infancy and childhood* p 191. Charles C Thomas, Springfield, Ill 1954
- 6 MEALEY J JR. Gamma ray image of subdural effusions. Scanning after injection of radio-iodinated serum albumin into subdural space and its clinical application. *J Neurosurg* 19 (1962) 934
- 7 PEET M M and HAHN E A. Subdural hematoma in infants. *J Amer med Assoc* 98 (1932) 1851
- 8 RABE E F, FLYNN R E and DODGE P R. A study of subdural effusions in an infant. With particular reference to the mechanisms of their persistence. *Neurology* 12 (1962) 19
- 9 RANSOHOFF J. Chronic subdural hematoma treated by subdural pleural shunt. *Pediatrics* 70 (1957) 561
- 10 REESE I C. Radiation physicist, Department of Radiology, Indiana University Medical Center. Personal communication 1964
- 11 SILLMAN K and RANSOHOFF J. Subdural hematoma in children. The fate of children with retained membranes. *J Neurosurg* 18 (1961) 175

presented here with radioactive studies showing extensive communicating subdural hematomas. Their cases with probable postnatal head trauma presented after 6 months of age on the average, occasionally had increased head circumference, and had generally good results after treatment. These reported data are identical to our experience in the 11 infants with lateralized subdural hematomas shown by scanning.

Other observations on the prenatal incidence of subdural hematomas have been made at this medical center by Dr WILLIAM E. DEMIER in studies of human fetal teratology (3). A number of aborted fetuses have shown fairly typical hematomas on gross neuropathological examination. Head injury incident to uterine expulsion through a tight cervical os cannot be excluded with certainty as the acute traumatic etiology in some of these specimens. However, in other fetuses more chronic appearing hematomas with translucent membranes have been demonstrated grossly (Fig. 8). Histological studies of this material are in progress to determine more exactly the age and pathomorphology of these lesions. These observations suggest tentatively the occurrence of subdural hematomas in the viable fetus, in utero, as early as the end of the first trimester of pregnancy. Pathogenetic mechanisms remain obscure. More specifically, possible correlation of these data with the poor prognosis found in infants with extensive subdural hematomas presenting soon after birth (group I) is an attractive hypothesis.

Acknowledgement

This work was supported in part by U.S.P.H.S. Grants H 6308 and CA 06145 from the National Institutes of Health, Bethesda, Maryland.

SUMMARY

Further experiences with gamma ray scanning of subdural effusions after injection of RISA into the subdural space are reported in 25 infants. Scans were classified and correlated with the clinical histories and responses to treatment. This new procedure proved valuable as a practical guide in the surgical management of these patients. Analysis of our material suggested that information gained from subdural scanning is relevant to the prognosis and etiology of chronic subdural hematomas in infancy.

ZUSAMMENFASSUNG

Die Mitteilung berichtet über die Erfahrung mit der Gammastrahlen Scan Methode an 25 Kindern nach Einspritzung von RISA in subdurale Ergüsse. Die Scans wurden tabuliert entsprechend den klinischen Befunden und entsprechend den therapeutischen Resultaten. Diese neue Methode erwies sich nützlich zur Bestimmung des chirurgischen Vorgehens in diesen Fällen. Die Analyse unseres Materiales erweist, dass die Methode wertvoll für die Prognose und für die Abklärung der Ursachen der subduralen Hämatome im Kindesalter ist.

SCINTISCANNING OF CEREBRAL NEOPLASMS BY RADIOACTIVE MERCURY (NEOHYDRIN ^{203}Hg)

by

F MORELLO G P GIORDANO, C ALVISE and R SCIASCIA

Our experience with radioisotopic diagnosis of cerebral neoplasms is relatively short, but we wish to report our results from the use of radioactive mercury

In 1960 BLAU & BENDER used Neohydrin ^{203}Hg as a new detector for localizing cerebral tumours, this detector has been suggested by an Oak Ridge group as an ideal tracer for gammascan techniques. Subsequently BRINAMAN, WEGST & KAHN (1962), CROLL, BRADY & HAND (1962), MCGINNIS, EYLER, DU SAULT & KRISTEN (1963) and SKLAROFF, POLAKOFF, LIN & CHARLES (1963) submitted their observations.

The advantages of Neohydrin ^{203}Hg over serum albumin labelled ^{131}I (RISA) are not due to a higher specificity, but to more suitable physiological and biological characteristics of the ^{203}Hg as compared with RISA.

The average life of ^{203}Hg is 45 days with a single gamma output of 208 KeV and low energy beta radiation. The single gamma ray of ^{203}Hg can easily be

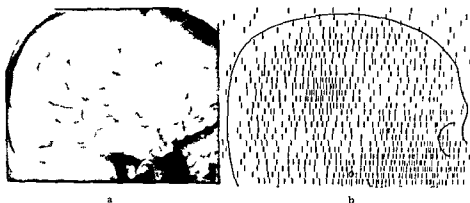


Fig 1 Right temporo-parietal glioblastoma. a) The capillary phase angiogram in the capillary phase shows a number of newly formed vessels arranged coil-like. b) Corresponding scan

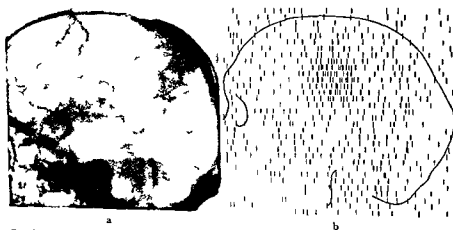


Fig 2 Left fronto-parietal glioblastoma. a) The venous capillary phase angiogram shows a number of arterio-venous shunts. b) Corresponding scan

collimated and the scatter problems are minimal. The low energy of beta particles of ^{203}Hg reduces the irradiation to the patient.

The disadvantage of the rather long physical average life of ^{203}Hg is partly corrected by incorporating ^{203}Hg with a compound having a short biological average life. Neohydrin ^{203}Hg (3-chloro mercury 2-methoxypropylurea) in fact is quickly excreted: 50% of the dose is discharged during the first 8 hours and the remainder within an average time of 3 days. After 5 hours the hematologic radioactivity is 10 to 16% of the administered dose and falls to 4.1% after 24 hours.

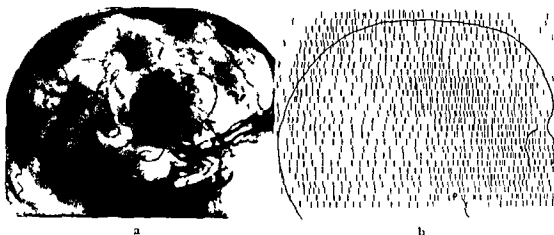


Fig 3 Right fronto-parietal glioblastoma after partial surgery. a) The carotid angiogram shows pathologic circulation due to residual neoplasm. b) Corresponding scan

Consequently the total irradiation dose to the patient is on the whole less than with R I S A

The experimental findings show an improvement of the $\frac{\text{target}}{\text{non target}}$ rate on the side of Neohydrin ^{203}Hg . Radiation dose for the kidney 10 % of the Neohydrin ^{203}Hg is taken up by the kidney, with a biological average life of 28 days. The radiation dose for the kidney, the average dose being $10 \mu\text{Ci/kg}$, seems to be 35 to 40 rad. When administering mercurial diuretics (sterdy mercurhydrin) the day before scan, urinary secretion during the following 48 hours increases from 11 to 32 % and the radiation dose to the kidney decreases to about 15 to 25 rad.

In short, the quick hematic clearance and the efficiency of collimation and screening of the ^{203}Hg monoenergetic gamma rays seem to offer a better means for demonstration of cerebral tumours, with a safer radiation dose.

Up to now, results have been significant but not exceptional.

Technique of the examination In order to keep down the renal uptake of the isotope we have given an intramuscular injection with 1 ml of sterdy Neohydrin, or a similar detector having the property of reducing the renal uptake of the isotope, 24 hours before endovenous injection of $10 \mu\text{Ci/kg}$ of Neohydrin ^{203}Hg (maximum dose $700 \mu\text{Ci}$), carrying out scan 2 to 4 hours later. We have employed an automatic scanner simultaneously performing the dotscan and the photoscan (19 holes focusing collimator with 25 cm lead screening, collimation depth 5 to 7 cm, collimator head distance 1 to 3 cm. Sodium iodide crystal activated with Thallium 50 KeV spectrometric window focused

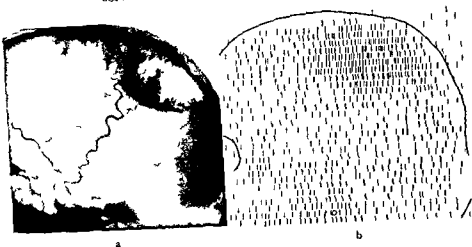


Fig. 4. Left parietal meningioma. a) Structural alterations of the cranium. selective catheterization of the external carotid shows impregnation of the contrast medium through the tumour. b) Corresponding scan.

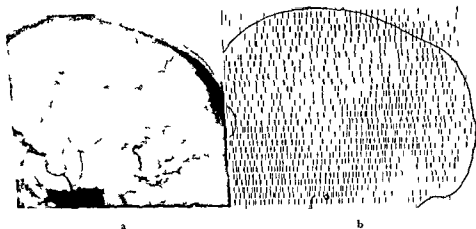


Fig. 5. Left occipital meningioma. a) Round osteolytic zone in the occipital region on arteriography of the external carotid. b) Pathologic halo-like ruculation. c) Corresponding scan.

on the 230 KeV photopeak of ^{203}Hg). The scan is carried out in the two a.p. and lateral projections. Reference marks: external auditory meatus, mastoid apex, head summit, glabella, a.p. pupils, occipital tuberosity, zygomatic root. Time: 30 to 40 minutes for each projection.

Material. The scintiscanning was carried out on 22 patients with brain neoplasm. All the cases had been previously submitted to carotidography.

in order to compare the two methods as to results. After these examinations, all the patients were submitted to surgery, with the exception of one case, a patient with astrocytoma in whom the scintiscanning was carried out after a necessarily partial operation.

Histologically, the cases were classified as follows: 11 glioblastomas, 4 meningiomas, 3 astrocytomas, 2 neurinomas, and 2 brain metastases. The seat of these brain neoplasms was almost always supratentorial.

Results

Our cases were too small in number to permit a percentage computation of the results for the various histologic types. The overall percentage of positivity was 80 %. The higher storage of the radioisotope was found in the less differentiated tumours. Extremely high concentration was noted in glioblastomas (Figs 1, 2, 3), meningiomas (Figs 4, 5), and metastases; in astrocytomas the concentration was moderate. The findings were negative in acoustic neuromas. In our examinations, no disturbances were noted.

In the literature referring to the use of Neohydrin ^{203}Hg , high percentages of positive results have been noted. BLAU & BENDLER (1960) reported 85 % (100 cases), BRINKMAN *et coll.* (1962) 65 % (92 cases), CROLL *et coll.* (1962) 70 % (17 cases), and SKLAROFF *et coll.* (1962) 83 % (20 cases).

Conclusions

Although our experience is still rather limited we feel that the radioisotopic method is a sound diagnostic test which may be useful as a complement to the traditional angiographic and pneumographic examinations, though it does not claim to replace them.

Although at present the best results are obtained in highly vascularized neoplasms, a satisfactory demonstration is also achieved in tumours with relatively moderate circulation. The method can also give some information on the nature of the tumour. With some locations, the topographic indications are sufficiently clear for clinical purposes whereas with others the result is not so satisfactory.

SUMMARY

In the diagnosis of intracranial neoplasms the authors have made use of scintiscanning as an aid to the traditional neuroradiological examinations. As a tracer they employed radioactive mercury (Neohydrin ^{203}Hg). To demonstrate and record the radioactivity they used an automatic scanner and scintiscans and photocans were carried out. Positive results were noted in glioblastomas, meningiomas, metastases and astrocytomas.

ZUSAMMENFASSUNG

Zur Diagnose von intracranialen Neoplasmen wurde unterstützend zu den traditionellen neurologischen Untersuchungen Szintigraphie durchgeführt. Als tracer kam radioaktives Quecksilber (Neohydrin ^{203}Hg) zur Verwendung. Für die Demonstration und Aufzeichnung der Radioaktivität verwendeten die Autoren einen automatischen Scanner; es wurden Scintigramme und Photoscans angefertigt. Positive Ergebnisse erhielt man bei Glioblastomen, Meningeomen, Metastasen und Astrocytomen.

RÉSUMÉ

Les auteurs ont utilisé la scintigraphie comme complément des examens neuroradiologiques traditionnels pour le diagnostic des néoplasies intracrâniennes. Ils ont employé comme traceur le mercure radioactif (Neohydrine ^{203}Hg) et pour la détection et l'enregistrement de la radioactivité un scanner automatique. Ils ont obtenu des résultats positifs dans des glioblastomes, des méningiomes, des métastases et des astrocytomes.

REFERENCES

- BLAU M. and BENDER M. Clinical evaluation of Hg^{203} neohydrin and J^{131} albumin in brain tumor localization. *J. Nucl. Med.* 1 (1960) 106.
- — Radiomercury (Hg^{203}) labelled neohydrin: a new agent for brain tumor localization. *J. Nucl. Med.* 3 (1963) 83.
- BRINKMAN C., WEGST A. and KAHN E. Brain scanning with mercury 203 labelled neohydrin. *J. Neurosurg.* 8 (1962) 644.
- CROLL M. M., BRADY L. and HAND B. M. Brain tumor localization using Mercury 203 . *Radiology* 78 (1962) 635.
- DI CUNEO G. R. I. S. A. encephalography and conventional neuroradiological methods: a comparative study. *Acta radiol. Suppl.* 201 (1961).
- MCCORMACK F. Personal communication.
- MCGINNIS K. D., EYLER W. R., DU SALIT L. and KRISTEN K. Mercury 203 brain scanning: method of clinical classification. *Radiology* 80 (1963) 264.
- PLANOL T. Diagnostic des lésions intracérébrales par les radioisotopes (gammaencephalographie). Masson Ed. Paris 1959.
- SCHLESINGER E. B., DE BOYES S. and TAVERAS J. Localization of brain tumors using radio-iodinated human serum albumin. *Amer. J. Roentgenol.* 87 (1962) 449.
- SJOGREN S. E. Experiences in localization of brain tumors by means of duodo 131 fluorescein. *Acta radiol.* 40 (1953) 356.
- SALAROFF D., GOLAKOFF P. L., LIN P. and CHARRAS D. Cerebral scanning with radioactive chloromerodrin (Neohydrin). *Neurology* 13 (1963) 79.

ISOTOPE ENCEPHALOMETRY A SIMPLIFIED AND RAPID SCANNING PROCEDURE

by

KARE MYHRE

During the last 10 years, about 1 000 patients have been examined by isotope encephalometry. An automatic scanner was provided 1 year ago. According to the procedure formerly used the patient was examined in a supine position, 2 hours and 24 hours after an intravenous injection of 150 to 200 μ Ci of radioactive, iodinated serum albumin. A transparent plastic plate of rectangular shape was positioned on either side of the head partly to stabilize the head and partly to define the fields to be examined. Twelve spots on one side of the cranial vault were selected and marked on one of the plates. The positions from one plate were transferred to the other one by means of a 'back pointer', so that exactly corresponding positions could be ascertained. A difference in activity of 10 % or more between corresponding spots was regarded as a positive finding. This indicated either a tumor, an abscess, or a hemorrhage. A clue with regard to aetiology could be obtained by comparing the findings at 2 hours with those at 24 hours or by repeating the examination 3 weeks later.

Of approx. 1 000 cases examined, 535 were available for evaluation. A tabular compilation is presented below showing the number of the different types of brain tumor found in this material.

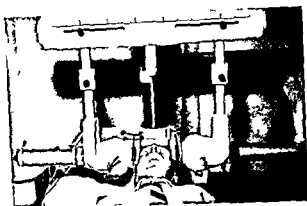


Fig 1 Automatic scanner for isotope encephalometry

Type	Number	Found
Glioblastoma multiforme	81	67
Astrocytoma	20	10
Oligodendroglioma	12	5
Metastases	23	18
Meningeoma	38	25
Meningeosarcoma	4	3
Medulloblastoma	1	1
Ependymoma	1	0
Totals	180	129

It is evident that slow growing tumors such as astrocytomas and oligodendrogliomas frequently escape detection.

The automatic scanner (from Friscke Hoepfner, Germany) is ordinarily equipped with only one scintillation counter. A supporting arm for 2 scintillation counters was constructed in Norway (Fig 1). The two counters move in a vertical plane on opposite sides of the head with the patient in a supine position. The speed is 2 to 3 mm/sec and the distance between horizontal scanning lines is 10 mm. The scanner is equipped with a magnetic and photoelectric recorder and a mechanical printer. The photoelectric record is made inside a square light tight box with the film in a frame beneath the top. With the patient resting upon the box, a roentgenogram of the organ to be examined can be made on the same film as the photorecord. The background is subdued by adjustments of the current to a decharging tube.

A useful unit of the scanner is the differential scaler. A deliberate number of pulses per second may be fed to this scaler. These pulses are automatically subtracted from those counted, thus permitting small differences in activity to



Fig 2 Roentgenogram of the skull with a black area representing a tumor

be recorded. This is of especial value in the scan of a voluminous organ such as the liver.

The unit can be used to subtract the counts of one scintillation counter from those of the other one. Fig 2 shows a film of the skull with a black area corresponding to a tumor. The elimination of background is obvious. The picture was made by superimposing the photoelectric record on a roentgenogram and making an exposure with a Polaroid camera. With negative findings the scan must be repeated and this time the former subtractend is now subtractor.

When interest is focused mainly on brain scans, a rapid scan can be made using a simple electronic circuit. Two scintillation counters with separate ratemeters are used, often combined with two pulse height analyzers. The currents from the ratemeters counteract each other by means of an electronic device. When equal activities are present no current is produced. A difference in activity of 10% or more results in a current shown by deflection of the pen of a recorder. The zero line is adjusted by a potentiometer to the center of the paper. The deviations to either side of the zero line indicate the side location of the isotope concentrating process. If the recorder runs at the same speed as the counters, the exact location is easily disclosed.

A similar principle may be used in photoelectric recording. The tube can be turned in two opposite directions by means of an electromagnet, depending upon the prevailing current. The rectangular, oblique light imprints on the film will accordingly be different.

Addendum

The photoscan has recently been modified. Instead of one discharging tube two tubes are used, each of them connected to separate units consisting of a counter and a ratemeter. When the currents from the units are brought in opposition by a device, the prevalent current will discharge the tube to the unit registering the strongest activity. As only one half of the film 40×40 cm is assigned to each tube, a black area on either the upper or the lower part of the film will disclose the exact position of a process in the brain. The use of the two units independently and simultaneously will reduce the scan time of symmetrical organs to half that required when only one unit is used.

SUMMARY

A commercial scanner equipped with two units each consisting of a counter, a ratemeter and a discharging tube has been used. The currents from the units are put in opposition and the prevalent current is demonstrated either by deflecting the pen of a recorder to the left or right of the zero line or by activating a discharging tube. As only one half of the film 40×40 cm is assigned to each tube, the position of a black area will indicate the exact location of the process in the brain.

ZUSAMMENFASSUNG

Ein im Handel befindlicher Scanner wird mit zwei Komponenten, jede bestehend aus einem Zähler, einem Mittelwertmesser und einem entladenden Röhrchen, ausgerüstet. Wenn die Ströme der beiden Komponenten gegeneinander gerichtet sind, wird entweder der vorher schende Strom den Feder eines Aufzeichners nach einer von zwei Seiten verschoben oder das entladende Röhrchen aktiviert. Da nur die eine Hälfte des Filmes 40×40 cm von jedem Röhrchen beleuchtet wird, kann die Position einer geschwartzten Fläche eine Anzeige für die genaue Lokalisation eines Prozesses im Gehirn geben.

RESUME

Un appareil commercial pour balayage linéaire est équipé avec deux assemblages. Chaque assemblage comprend un compteur, un intégrateur et un tube à décharges. Les courants des deux assemblages sont mis en opposition et le courant dominant est démontré ou par un enregistreur dont la plume se déplace à l'une ou l'autre direction ou par le décharge d'un des deux tubes. Par le fait que seulement un demi-part du film est assigné à chaque tube, un endroit noir sur le film indique la localité exacte d'un processus cérébral.

SCANNING WITH POSITRON-EMITTING ISOTOPES IN CEREBROVASCULAR DISEASE

by

ROBERT G. OJEMANN, SAUL ARONOW and WILLIAM H. SWEET

Most reports on brain scanning have been limited to the use of this procedure in the diagnosis of intracranial tumors. Relatively little attention has been directed towards its value in the assessment of patients with cerebrovascular disease.

During the past 8 years more than 4,000 brain scans have been performed at the Massachusetts General Hospital using the positron emitting isotopes ^{45}As and ^{64}Cu . In this group there were 54 scans on 48 patients with confirmed diagnoses of aneurysm, arteriovenous malformation, subarachnoid hemorrhage or intracerebral hemorrhage (Table 1) and 146 scans of patients with a history and clinical findings which pointed to the likelihood of occlusive cerebral vascular disease, e.g. either the sudden onset of a neurologic deficit followed by stabilization or some degree of recovery, or transient attacks of neurologic deficit presumably on an ischemic basis (Table 2). The important findings are summarized in this report. Detailed analyses of our results are reported elsewhere (28, 29).

Method

Several previous reports have discussed our use of positron emitting isotopes for localization of focal intracranial lesions (2, 24, 28, 29, 35). Two isotopes,

^{54}As as sodium arsenate and ^{64}Cu chelated with DTPA (diethylenetriamin pentacetic acid) have been used most frequently

Localization with positron emitting radioisotopes utilizes the peculiar physical properties of the positron electron annihilation process. This reaction yields a pair of oppositely directed gamma rays which are recorded when they hit a pair of detectors in time coincidence. This record is called a positrocephalogram (PCG). In addition, the difference in total gamma activity between one side of the head and the other may be recorded. This unbalance scan, or asymmetrogammagram (AGG), indicates the asymmetry of a concentration of activity which is right or left sided. The two scans, PCG and AGG are printed simultaneously by mechanical printers directly connected to the moving detector heads so that a full sized lateral picture is immediately available. An a p view may also be obtained. The radioisotope is administered by intravenous injection and the scan is performed about one hour after injection.

Scans are interpreted by describing the locus of the concentration and the degree of abnormality is reported on a 1 to 4 scale. 1 indicates a definitely abnormal scan, 2 probably abnormal scan, 3 probably normal, and 4 a definitely normal scan. For statistical purposes 1 and 2 are called abnormal, 3 and 4 are normal. No clinical interpretation is given of the abnormal scan, although the character of the concentration of the printed markings may present a useful diagnostic clue.

In order to correlate scan abnormality and neurologic status an arbitrary division into a Mild, Moderate and Severe clinical deficit has been made. In general, patients with a severe deficit had complete or nearly complete hemiplegia or homonymous hemianopsia or evidence of severe sensory impairment or aphasia when the dominant hemisphere was involved or severe disturbance of mentation. Patients with lesser degrees of clinical dysfunction (28) were placed in the moderate and mild groups.

Results

Aneurysm and subarachnoid hemorrhage Review of the literature has revealed that scans using all types of isotopes had been reported in 58 patients with known intracranial aneurysms (3, 5, 6, 7, 8, 10, 12, 17, 18, 22, 23, 30, 31, 32, 33, 35, 36, 37). Twenty one of these were abnormal. The largest previous series was reported by PLAMOL & GAUTHIER (31) who used radioactive iodinated serum albumin and demonstrated 3 positive studies in 13 cases of arterial aneurysm.

Fourteen of our patients had a history of subarachnoid hemorrhage associated with some degree of neurologic deficit due to cerebral injury and demonstra

Table 1

Radioisotopic scans in patients with aneurysm arteriovenous malformation subarachnoid hemorrhage and intracerebral hemorrhage

Disease category	¹¹³ As		⁶⁴ Cu		Total
	Abnormal	Normal	Abnormal	Normal	
Aneurysm					
With subarachnoid hemorrhage and neurologic deficit	8	3	1	2	14
With subarachnoid hemorrhage and third nerve palsy	0	1	0	2	3
Without subarachnoid hemorrhage	3	0	1	0	4
Arteriovenous malformation	3	1	0	1	5
Intracerebral hemorrhage	12	5	4	7	28
Total	26	10	6	12	54

tion of an aneurysm on arteriography. Eight of 11 arsenic and 1 of 3 copper scans were abnormal. The aneurysms ranged in size from 2×3 mm to 17×14 mm. In no case was the outline of the aneurysm demonstrated. The positive scans instead demonstrated increased concentration in the cerebral tissue adjacent to the aneurysm or in the tissue supplied by the vessel harboring the aneurysm. Subsequent studies of many of these cases showed intracerebral hemorrhage and/or infarction. Fig. 1 illustrates such a case where cerebral infarction followed rupture of a middle cerebral aneurysm. However, infarction and hemorrhage could not be differentiated on the scan.

Three patients with aneurysms of the internal carotid artery had subarachnoid hemorrhage, but a third nerve palsy was their only neurologic abnormality. All had normal scans (1 arsenic and 2 copper).

Four abnormal scans were obtained on 3 patients who had demonstrated aneurysms but no hemorrhage. Two of these patients had been admitted for evaluation of seizures, and their positive arsenic scans led to additional diagnostic studies. In one, isotopic localization was in the left temporal area, and the arteriogram revealed a large middle cerebral arterial aneurysm. In the other, isotopic concentration indicated abnormality in the left temporal parietal region, and a calcified lesion removed at operation proved to be an aneurysm on pathologic examination. This scan is illustrated in Fig. 2. The third patient had a 3×4 cm aneurysm of the basilar artery which was almost completely filled with thrombus. In this case the area of increased concentration seen in the scan may have represented the large thrombosed aneurysm, the compressed tissue, or both.

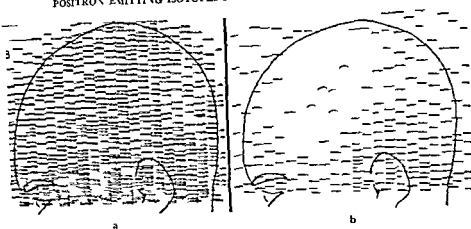


Fig 1 Ruptured middle cerebral aneurysm with associated infarct on in cerebral tissue supplied by this vessel a) Postrocephalogram (PCG) Increased concentration in the inferior frontal parietal area b) Asymmetrical Mammogram (AGG) Straight abnormality in the frontal parietal area The diffuse distribution of the straight symbols indicates the head is slightly off to the left side the localized area of absence of these marks and the presence of the curved marks indicates a definite right-sided abnormality

Arteriovenous malformation Fifty of 73 reported scans were abnormal in patients with arteriovenous malformation (1, 3 5 7 8 10 11 12 15, 17, 21 22 25 26 27 30 31 32 34 35 37) Again the largest group was reported by PLANIOL & GAUTHIER With RISA 24 of 28 scans were abnormal (31) In our series (Table 1) the 3 patients with intracerebral arteriovenous malformations had abnormal arsenic studies The normal arsenic study was in a patient with an epidural extracranial malformation The patient with the normal copper study had no symptoms referable to the malformation which measured $1 > 3$ cm and was an incidental finding at arteriography

Spontaneous intracerebral hemorrhage In the literature 25 of 39 intracerebral hematomas were associated with an increased isotopic concentration (3 5 6 7 8 10 11 14 15 17 18 21 22 26 27, 30 31 35) We have evaluated 23 patients with spontaneous intracerebral hemorrhage principally due to hypertension with 28 scans

In the group of patients with severe neurologic deficit at the time of the scan 9 of 12 arsenic but only 1 of 4 copper studies were abnormal (Table 3) Seven of the patients with abnormal arsenic scans had putaminal hemorrhages (16) Normal arsenic studies were found in 2 patients with putaminal hemorrhages and in 1 patient with a cerebellar hemorrhage In all but one abnormal study the area of localization delineated the site of pathology which had been

Table 1

Radioisotopic scans in patients with aneurysm, arteriovenous malformation, subarachnoid hemorrhage and intracerebral hemorrhage

Disease category	¹¹³ As		⁶⁴ Cu		Total
	Abnormal	Normal	Abnormal	Normal	
Aneurysm					
With subarachnoid hemorrhage and neurologic deficit	8	3	1	2	14
With subarachnoid hemorrhage and third nerve palsy	0	1	0	2	3
Without subarachnoid hemorrhage	3	0	1	0	4
Arteriovenous malformation	3	1	0	1	5
Intracerebral hemorrhage	12	5	1	7	28
Total	26	10	6	12	54

tion of an aneurysm on arteriography. Eight of 11 arsenic and 1 of 3 copper scans were abnormal. The aneurysms ranged in size from 2×3 mm to 17×14 mm. In no case was the outline of the aneurysm demonstrated. The positive scans instead demonstrated increased concentration in the cerebral tissue adjacent to the aneurysm or in the tissue supplied by the vessel harboring the aneurysm. Subsequent studies of many of these cases showed intracerebral hemorrhage and/or infarction. Fig. 1 illustrates such a case where cerebral infarction followed rupture of a middle cerebral aneurysm. However, infarction and hemorrhage could not be differentiated on the scan.

Three patients with aneurysms of the internal carotid artery had subarachnoid hemorrhage, but a third nerve palsy was their only neurologic abnormality. All had normal scans (1 arsenic and 2 copper).

Four abnormal scans were obtained on 3 patients who had demonstrated aneurysms but no hemorrhage. Two of these patients had been admitted for evaluation of seizures, and their positive arsenic scans led to additional diagnostic studies. In one, isotopic localization was in the left temporal area, and the arteriogram revealed a large middle cerebral arterial aneurysm. In the other, isotopic concentration indicated abnormality in the left temporal parietal region, and a calcified lesion removed at operation proved to be an aneurysm on pathologic examination. This scan is illustrated in Fig. 2. The third patient had a 3×4 cm aneurysm of the basilar artery which was almost completely filled with thrombus. In this case the area of increased concentration seen in the scan may have represented the large thrombosed aneurysm, the compressed tissue, or both.

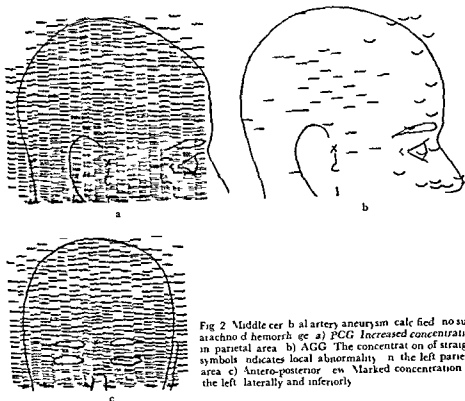


Fig 2 Middle cerebral artery aneurysm calcified no subarachnoid hemorrhage a) PCG Increased concentration in parietal area b) AGG The concentration of straight symbols indicates local abnormality in the left parietal area c) Antero-posterior view Marked concentration on the left laterally and inferiorly

10 12 13 15 17 19 20 22 23, 24 32 33, 34, 35 36) For the most part these reports do not draw conclusions about the diagnostic value of scanning in these disorders. RUSHTON (33) discusses 22 patients thought to have had either a thrombotic or embolic stroke. In 9 patients where the lesion was at least six weeks old at the time of the scan no abnormality was seen. In 13 patients the onset of symptoms had occurred less than six weeks before the study, and in 4 increased isotopic concentration occurred in the appropriate brain region.

In our series 86 patients had a clinical diagnosis of cerebral infarction and a neurologic deficit at the time of the scan which persisted with little or no improvement (Table 2). In the group with a severe neurologic deficit 11 of 12 ⁶⁷As scans were abnormal (Table 4) while only 3 of 8 ⁶⁴Cu chelate studies were positive. The area of increased concentration was in good agreement with that suspected on the basis of the clinical picture. Fig 3 demonstrates an abnormal arsenic scan from this group and illustrates the clear degree of

Table 2

Radioisotopic scans in patients with cerebral vascular occlusive disease

Disease category	No. of cases	⁷⁵ As		⁶⁴ Cu		Total cases
		Abnormal	Normal	Abnormal	Normal	
Thrombosis permanent deficit						86
Intracranial occlusion	71	31	15	9	13	
Carotid occlusion	15	10	1	—	4	
Thrombosis temporary deficit	25	7	8	1	9	25
Transient ischemic attacks						22
Carotid region	15	2	10	—	3	
Vertebral basilar region	7	1	3	1	2	
Embolism						
Permanent deficit	9	—	6	—	3	13
Temporary deficit	1	—	1	—	3	
					Total	116

suspected on the basis of the clinical examination or determined at arteriography or operation.

The temporal relationship between onset of symptoms and the radioisotopic study was evaluated. During the first week after onset of symptoms, considering all degrees of deficit together, only 5 of 10 arsenic and 1 of 6 copper scans were abnormal. None of these was classified as '1' (definitely abnormal). During the second and third weeks after hemorrhage, all scans were abnormal (3 copper and 7 arsenic). Four of the arsenic studies were classified as '1'.

Multiple serial scans in 3 patients confirmed the superiority of ⁷⁵As over the ⁶⁴Cu chelate. They also demonstrated an increasing degree of abnormality from the first to the second week after onset.

In 2 patients tissue samples taken during operative removal of the hematoma indicated that the cerebral tissue immediately adjacent to the hematoma contained 5 to 20 times more isotope than the hematoma itself. This was true for both the ⁷⁵As and the ⁶⁴Cu chelate.

Cerebral thrombosis. A number of reports have described small numbers of patients who were scanned following cerebral infarction (2, 3, 4, 5, 6, 7, 8, 9,

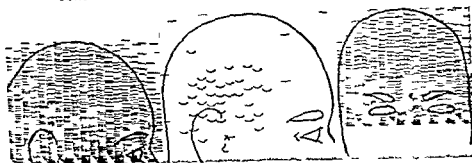


Fig 3 Abnormal arsenic scan permanent deficit thrombosis of the middle cerebral artery Left PCG Posterior temporal parietal concentration Cerebral AGG Concentration of curved marks indicates right sided unilateral Right lateral inferior concentration

Embolism In 13 cases with a clinical diagnosis of cerebral embolism the 7 arsenic and 6 copper scans were normal. Nine patients had permanent deficits of which 4 were severe and 5 moderate. The time from onset of symptoms to scan ranged from one day to 2 years. Four other patients had temporary deficits followed by recovery. The reason for this striking lack of abnormality was not apparent from the clinical or pathologic evaluation.

Discussion

Radioisotopic scans utilizing ^{74}As are abnormal in a high percentage of patients having a neurologic deficit and subarachnoid hemorrhage from an aneurysm. The area of increased isotopic concentration is located in the region adjacent to the aneurysm or in the area of brain tissue supplied by the parent vessel. The abnormality is due to the presence of hemorrhage or infarcted cerebral tissue. Failure of the scan to demonstrate the aneurysm was documented also in the normal studies of three patients whose third nerve palsy was the only symptom of an internal carotid artery aneurysm. Presumably little or no cerebral damage had occurred. The use of the radioisotopic scan in the evaluation of patients with seizures is emphasized. In two instances positive studies led to further diagnostic procedures and appropriate therapy.

We have been confronted occasionally by a patient with multiple aneurysms but no arteriographic evidence to indicate which aneurysm had bled. Clinical examinations either were inconclusive or pointed to an aneurysm subsequently found not to be the source of hemorrhage. Since most abnormal arsenic scans correctly localize the area adjacent to or in the territory of the vessel harboring the ruptured aneurysm, it may be possible to utilize this diagnostic procedure in determining which of the aneurysms has ruptured.

In patients with intracerebral hemorrhage scanning with ^{74}As is a valuable

Table 3

Radioisotopic scans in patients with spontaneous intracerebral hemorrhage

Deficit at scan	¹¹³ As		⁶⁴ Cu		Total
	Abnormal	Normal	Abnormal	Normal	
Severe	9	3	1	3	16
Moderate	2	1	2	3	8
Mild	1	1	1	1	4
Total	12	5	4	7	28

Table 4

Radioisotopic scans in patients with permanent neurologic deficits following cerebral infarction

Deficit at scan	¹¹³ As		⁶⁴ Cu		Total
	Abnormal	Normal	Abnormal	Normal	
Severe	11	1	3	5	20
Moderate	23	13	3	9	48
Mild	10	2	3	3	18
Total	44	16	9	17	86

unbalance (AGG) associated with a more diffuse increase in concentration on the coincidence scan. This finding was apparent in a number of the abnormal studies.

In patients with arteriographic evidence of carotid occlusive disease, 10 of 11 arsenic scans were abnormal. These scans usually showed a larger, more diffuse area of abnormality than did those of patients with intracranial occlusive disease. All 4 patients studied with copper had normal studies.

An analysis of the correlation between onset of deficit and time of scan revealed a high percentage of abnormal studies during the first four weeks after onset, followed by a gradual decrease in the percentage of abnormal studies.

Twenty-five patients had a neurologic deficit at the time of the scan, but there was recovery of function over subsequent weeks or months. Within this group there were 19 patients with a mild deficit. Only 5 had abnormal scans. In contrast, in the group of patients whose mild deficit persisted 10 of 12 scans were abnormal.

Transient ischemic attacks. In this group of 22 patients, 15 had symptoms in the carotid territory and 7 symptoms in the vertebral/basilar system. In each group there were only two 'probably abnormal' studies.

SUMMARY

Scanning with ^{24}As and ^{64}Cu has been evaluated in cerebral vascular disease. A high percentage of ruptured intracranial aneurysms have increased concentration. The aneurysm itself is not demonstrated but changes in adjacent cerebral tissue are seen. Scans of arteriovenous malformations also appear abnormal. All hypertensive intracranial hemorrhages were localized with ^{24}As during the second and third weeks after onset. Permanent neurologic deficit associated with cerebral infarction due to thrombotic occlusion usually produces an abnormal arsenic scan during the first 4 weeks after onset. Transient ischemic attacks or temporary neurologic deficits usually yield normal scans. All scans of embolism were negative. The ^{64}Cu chelate showed a much lower percentage of abnormal isotope concentrations than arsenate.

ZUSAMMENFASSUNG

Scanning mit ^{24}As und ^{64}Cu wurde bei zerebralen Gefässerkrankungen angewendet. Ein hoher Prozentsatz von rupturierten intrakraniellen Aneurysmen zeigen erhöhte Konzentration. Das Aneurysma selbst wird nicht dargestellt, jedoch können die Veränderungen des umgebenden Gewebes gesehen werden. Scans von arteriovenösen Missbildungen erscheinen auch normal. Alle hypertensiven intrakraniellen Blutungen wurden mit ^{24}As in der zweiten und dritten Krankheitswoche lokalisiert. Dauernder neurologischer Ausfall ergibt beim thrombotisch bedingten zerebralen Infarkt in den ersten vier Krankheitswochen gewöhnlicherweise ein abnormes Arsen Scan. Vorübergehende ischämische Attacken und temporäre neurologische Ausfälle ergeben gewöhnlich normale Scans. Alle Scans bei Embolie waren negativ. Scanning bei Verwendung von ^{64}Cu ergab einen viel geringeren Prozentsatz von abnormaler Isotopenkonzentration als bei Anwendung von ^{24}As .

RESUME

Les auteurs ont étudié la scintigraphie par ^{24}As et ^{64}Cu dans les affections vasculaires cérébrales. Un grand nombre des anévrysmes intracrâniens rompus présentent une concentration augmentée. L'anévrysme lui-même n'est pas mis en évidence, mais on voit les lésions du tissu cérébral adjacent. Les scintigraphies de malformations artério-veineuses sont elles aussi normales. Toutes les hémorragies intracrâniennes donnant une hypertension intracrânienne ont été localisées par ^{24}As dans les deuxièmes et troisièmes semaines après leur début. Le déficit neurologique permanent du ramollissement cérébral par occlusion thrombotique se traduit habituellement par une scintigraphie à l'arsénite anormale pendant les quatre premières semaines après le début. Les accidents ischémiques transitoires ou les déficits neurologiques passagers donnent habituellement des scintigrammes normaux. Tous les scintigrammes d'embolies ont été négatifs. Le chélate de ^{64}Cu a eu une proportion de concentrations isotopiques anormales bien moindre que l'arsénite.

REFERENCES

1. ASKENASY H. M., ANBAR M., LAOR Y., LEWITZ L. Z., KOSARY I. Z. and GUTTMAN S. The localization of intracranial space-occupying lesions by fluoroborate ions labelled with fluorine 18. *Amer. J. Roentgenol.* 88 (1967) 350.
2. BARNALL H. J., BENDA I., BROWNELL C. L. and SWEET W. H. Positron scanning with copper-64 in the diagnosis of intracranial lesions: partition of copper-64 versenate in and excretion from the body. *J. Neurosurg.* 15 (1958) 411.

able diagnostic aid in localizing the site of the lesion. Twelve of 17 arsenic scans were abnormal while only 4 of 11 copper studies had an increased concentration. In no specific area does hemorrhage appear to be more likely to produce an abnormal scan.

FEINDEL and co-workers (15) concluded in one case of intracerebral hemorrhage that 'uptake was mainly on the basis of the recent bleeding or the edema of the adjacent brain tissue about the clot'. In our study of two patients, one given ^{75}As and ^{64}Cu and the other ^{64}Cu , concentration of the radioisotopes in the cerebral tissue adjacent to the clot was several times that found within the hematoma itself.

Another fact to be noted is that all copper and arsenic scans were abnormal during the second and third weeks after hypertensive intracerebral hemorrhage. During the first week there was a high percentage of normal studies, indicating that the alteration of the tissue surrounding the hematoma may induce further changes in the surrounding tissue and result in an increased concentration of isotope. This could prove to be an important point in assessing the time of surgical therapy in these lesions. Removal of the hematoma within the first week after onset of symptoms may be indicated since its continued presence appears to alter the surrounding tissue.

Over 90 % of the patients with a severe, persistent neurologic deficit due to thrombotic infarction will have an abnormal arsenic scan. ^{64}Cu chelates localize poorly in these regions. Even when the neurologic deficit is mild we find that 83 % of the scans are abnormal if the deficit is going to persist, in contrast to the 26 % abnormality in cases where the mild neurologic deficit is only temporary. On the basis of this data, it might be possible to make some assessment of the prognosis from the radioisotopic scan. When a neurologic deficit is present and an abnormal arsenic scan is in good agreement with the suspected area of involvement, the deficit will be likely to persist. On the other hand, if the scan is normal there is a better chance of full recovery. If a copper scan is abnormal with any degree of deficit, the deficit probably will be permanent. In patients with carotid occlusive disease when carotid surgery is being considered, the radioisotopic brain scan could be of assistance in indicating the extent of cerebral injury. If one finds an abnormal scan in a patient thought to have cerebral embolism or transient ischemic attacks, care should be exercised in following the patient closely for development of tumor.

Acknowledgements

This work was aided by grants from U.S. Atomic Energy Commission under contract No. AT (30-1) 1242, USPHS grants HF 04769 and NB 04348 and a fellowship grant from the Medical Foundation of Boston, Inc.

- 23 MCGINNIS K. D. EYLER W. R. DESAULT L. and KRISTEN K. Mercury 203 brain scanning *Radiology* 80 (1963) 264
- 24 MEALEY J. JR. BROWNELL G. L. and SWEET W. H. Radioarsenic in plasma, urine, formal tissues and intracranial neoplasms: distribution and turnover after intravenous injection in man. *Ann. Arch. Neurol. Psychiat.* 81 (1959) 310
- 25 MERCHIE G. et MOUCINETTE R. Exploration des lésions intracranéennes par les isotopes radioactifs la gammaencéphalographie. *Acta clin. belg.* 17 (1967) 284
- 26 MOUCINETTE R. La Gammaencéphalographie. *Rev. Med. Liège* 18 (1963) 278
- 27 MURRAY R. L. Scintillation scanning of the brain with mercury 203 neohydrin: technical considerations and clinical evaluation. *S. Med. J.* 56 (1963) 914
- 28 OJEMANN R. G. ARONOW S. A. and SWEET W. H. Scanning with positron emitting radioisotopes: occlusive cerebral vascular disease. *Arch. Neurol.* 10 (1964) 218
- 29 — — — Scanning with positron emitting radioisotopes: aneurysm, arteriovenous malformation and intracerebral hemorrhage. *J. Neurosurg.* 22 (1965) 489
- 30 PAUL W. and BOTTERELL E. H. An appraisal of As 74 for localization of brain tumors. *J. Nucl. Med.* 4 (1963) 1
- 31 PLANIOL T. and GAUTHIER G. Gamma-encephalographie. *Bull. schweiz. Akad. med. Wiss.* 18 (1963) 425
- 32 RHODY R. B. and NOWLIS G. R. The use of radioactive iodinated serum albumin in the localization of intracranial lesions. *J. Neurosurg.* 14 (1957) 413
- 33 RUSHTON J. G. SVEN H. J. and BALDES E. J. Localization of brain lesions by means of RISA. *Pediatrics* 29 (1957) 478
- 34 SKLAROFF D. POLAKOFF P. P. LEN P. M. and CHARKES V. D. Cerebral scanning with radioactive chlormerodrin (neohydrin). *Neurology* 13 (1963) 79
- 35 SWEET W. H. MEALEY J. JR. ARONOW S. and BROWNELL G. L. Localization of focal intracranial lesions by scanning of rays from positron emitting isotopes. In: *Clinical Neurosurgery. Proc. of the Congress of Neurological Surgeons, Miami Beach 1959*. R. K. Thompson and I. J. Jackson. Ed. Williams and Wilkins Co. Baltimore 7 (1961) 159
- 36 TOCUS E. C. OKITA G. T. EVANS J. P. and MULLAN S. The localization of octoiodo-fluorescein I¹³¹ in human brain tumors. *Cancer* 15 (1962) 153
- 37 WEST H. J. The localization of brain tumors by photoscanning. *Harper Hosp. Bull.* 20 (1962) 117

- 3 BAZAN C JR, OVLERTON M C, WILSON M, BEINTJES L B, SNODGRASS S R, SHEFFEL D D and SCHNEIDER M. Diagnosis of intracranial neoplasms by scintiscanning. *Iowa State J Med* 59 (1963) 1079
- 4 BENDER M A and BLAU M A. Versatile high contrast photoscanner for the localization of human tumors with radioisotopes. *Int J appl Radiat* 4 (1959) 154
- 5 BOTTERELL E H, LOUGHEED W M, MORLEY T P and LASKER R R. Use of radioactive arsenic (As^{74}) in the diagnosis of supratentorial brain tumors. *Canad med Ass J* 85 (1961) 1321
- 6 BRINKMAN C A, WEGST A V and KAHN F A. Brain scanning with mercury 203 labeled neohydrin. *J Neurosurg* 19 (1962) 644
- 7 BROWNELL G I and SWEET W H. Scanning of positron emitting isotopes in diagnosis of intracranial and other lesions. *Acta radiol* 46 (1956) 425
- 8 COWAN G A B, LEDORUK S O, LEINDEL W, STRATFORD J G. Localization of intracranial lesions using radioactive iodinated human serum albumin and an automatic scanner. *J Canad Ass Radiol* 11 (1960) 15
- 9 CROLL M N, BRADY L W and HAND B M. Brain tumor localization utilizing mercury 203 . *Radiology* 78 (1962) 685
- 10 DI CUNEO G. RISA encephalography and conventional neuroradiologic methods. *Acta radiol* (1961) Suppl 201
- 11 DUGER G S and PEPPIE I D. The reliability of radioisotopic encephalography. *Neurology* 13 (1963) 1042
- 12 DUNBAR H I and RAY B S. Localization of brain tumors and other intracranial lesions with radioactive iodinated human serum albumin. *Surg Gynec Obstet* 98 (1954) 433
- 13 DUNBAR H I. Experience in brain scanning. Presented at the Symposium on Brain Visualization by Means of Radioisotope Scanning, Philadelphia 1963
- 14 FARRER P A and McRAE J. Radioactive arsenic in the diagnosis of intracranial tumours. *Aust Ann Med* 12 (1963) 93
- 15 LEINDEL W, ROVIT R L and STEPHENS NEWSHAM L. Localization of intracranial vascular lesions by radioactive isotopes and an automatic contour brain scanner. *J Neurosurg* 18 (1961) 811
- 16 LISHNER C M. Clinical syndromes in cerebral hemorrhage. In: Pathogenesis and treatment of cerebrovascular disease. William S Fields, Ed. Seventh Annual Scientific Meeting of the Houston Neurologic Society, pp 318-342. C C Thomas Springfield Illinois 1961
- 17 GROS C, GONSETTE R, VLAHOVITCH B et GARRY BOBO J. La perméabilité des vaisseaux cérébraux. *Acta Neurol Belg* 60 (1960) 481
- 18 CURDJIAN E S, WEBSTER J I, LISSNER H R, HARDY W G and LINDNER D W. Radioactive iodinated human serum albumin in the diagnosis of intracranial mass lesions. *Neurology* 7 (1957) 392
- 19 LAZERTE G D and KNOPP L M. Radioactive mercury brain scan. *Northwest Med J* 62 (1963) 945
- 20 MAGALOTTI M F and HUMMON I F. Localization of intracranial lesions by radioactive isotopes (DII) (RISA). *Amer J Roentgenol* 83 (1960) 135
- 21 MASTROPAOLO C e D'ACQUINO T. Utilità della gammacencefalografia nella diagnosi delle lesioni cerebrali. *Minerva nucleare* 7 (1963) 153
- 22 McAFEE J G and TAYLOR D R. Comparison of radioisotope scanning with cerebral angiography and air studies in brain tumor localization. *Radiology* 77 (1961) 207

Origine des signaux dans les techniques ambulatoires Les signaux recueillis au cours de ces explorations sont émis par des générateurs différents

Les figures de l'E E G proviennent du cortex hémisphérique au contact de la voûte et non de la tumeur, l'œdème cérébral joue le rôle majeur dans l'apparition des ondes lentes

Les molécules radioactives pénètrent plus dans le tissu tumoral que dans le tissu cérébral sain le rayonnement gamma des molécules radioactives provient essentiellement du tissu d'œdème, c'est en tout cas par l'intermédiaire des vaisseaux que les émetteurs gamma pénètrent dans ce que d'une manière imprécise nous appelons la lésion tumorale

L'écho median ultra sonore se réfléchit sur des interfaces encore discutées, il n'y a pas un écho, mais des échos l'observateur doit identifier l'écho réfléchi par une formation anatomique repoussée de l'autre côté de la ligne médiane septum pellucidum, citerne interhémisphérique 3^e ventricule épiphyse? difficile à dire¹

Si les générateurs des signaux sont différents en E F G G F G et Echo-graphie un facteur leur est pourtant commun l'œdème, qui entoure la tumeur favorise les ondes lentes la fixation sélective de l'émetteur gamma et le passage de l'hémisphère dans l'hémicrâne opposé

Applications cliniques

Nous allons envisager l'emploi de ces techniques ambulatoires de plusieurs points de vue 1) diagnostic positif de tumeur cérébrale 2) diagnostic étiologique — nature de la lésion occupant de l'espace et 3) diagnostic précoce

La première question porte sur l'existence d'une formation occupant de la place Sur 110 lésions expansives (dont 98 vérifiées à l'intervention) l'E E G est franchement positif 100 fois le G E G est franchement positif 99 fois, et l'Echo est franchement positif 80 fois Le fond d'oeil ne montre une stase papillaire que 47 fois Dix fois l'E E G se révèle négatif ou à la limite du normal, comme suit

	G E G	Echo M
1 Ménégome tot orbital	+	0
2 Ménégome en plaque	+	0
3 Ménégome pariétal	+	0
4 Cistome crânien	+	0
5 Lymphosarcome fosse temp	+	0
6 Tuberculome par sagittal	+	6 mm
7 Abcès purulent	+	15 mm
8 Cistostomie	+	0
9 Cistome pédiculaire	+	35
10 Récidive	—	11
	+	0

EXPLORATIONS TECHNIQUES AMBULATOIRES DANS LE DIAGNOSTIC DES TUMEURS CÉRÉBRALES HÉMISPHERIQUES

par

THI PLANIOT, J. METZGER, M. DAVID et H. FISCHGOLD

Le diagnostic pré opératoire d'une tumeur cérébrale hémisphérique implique des examens de contraste iodés ou gazeux. Le diagnostic positif et le diagnostic étiologique exprimés en termes de probabilité, ne suffisent plus, le neurochirurgien a besoin de connaître le siège exact de la néoformation, son volume et ses rapports avec les structures intracérébrales.

Pour intervenir ou s'abstenir, il demande des informations aussi précises que possible sur l'histologie de la néoformation.

Enfin on évitera l'inflation des examens de contraste, entraînés de quelques risques et pas mal de désagréments, en pratiquant les trois techniques ambulatoires : 1) LEEG, 2) les radio isotopes, gammacéphalographie ou scanning, et 3) l'échographie de la ligne médiane par ultrasons. A. Restent la thermographie et la palléncéphalographie dont on nous parlera ici, et la rhéocéphalographie qui décourage beaucoup d'entre nous parce qu'on en a parlé trop tôt !

Enfin, la tomographie à ultrasons B dont vous avez aux Etats Unis une première expérience pleine de promesses.

PLANIOL et METZGER ont comparé les conclusions préopératoires du GEG et de l'angiographie dans 275 cas de TCH il résulte de cette confrontation que sur 225 diagnostics de nature, le GEG s'est montré 43 fois erroné sur 157 diagnostics étiologiques, l'angiographie s'est montrée erronée 17 fois

Des informations sur la nature et l'histologie des néoformations deviennent donc de plus en plus significatives si on ajoute à la radiographie standard le GEG sans oublier un bon interrogatoire et l'examen clinique

Le nombre des TCH devant lesquelles le neurochirurgien reste hésitant avant l'arteriographie tend donc à baisser si on utilise les explorations ambulatoires et complémentaires énumérées

La troisième question est si on peut par les techniques énumérées reconnaître une tumeur cérébrale au début Il devient évident que nous sommes actuellement en état de faire le diagnostic de TCH par l'EEG, le GEG et l'Echo avant l'apparition de la stase papillaire Ceci marque un grand progrès réalisé au cours des 20 dernières années et prouve que le diagnostic des tumeurs hémisphériques se fait déjà à une phase beaucoup plus précoce qu'il y a 10 ou 15 ans

Un diagnostic précoce devient possible aussi du fait que la sémiologie neurologique s'est raffinée et l'expérience des praticiens élargie ils pensent à une tumeur plus tôt qu'autrefois et s'inquiètent devant toute épilepsie tardive et devant tout déficit neurologique psychique ou sensoriel

Sur les trois techniques laquelle est la plus précoce ou la plus tardive?

EEG Sur une série de 63 néoformations, BUISSON-FÉREY a noté que les abcès les hématomes intra-cérébraux et les glioblastomes s'accompagnent d'un EEG évocateur avant la fin du 1er mois d'évolution clinique, plus le processus évolue rapidement (même bénin comme l'abcès) plus les anomalies électriques sont précoces

Les méningiomes peuvent montrer un tracé non évocateur ou normal après une évolution de mois ou d'années (voir le Tableau)

Le GEG fournit par contre des signes plus précoces que EEG dans les méningiomes de la convexité plus de 80 % montrent un foyer GEG net au cours de la première année d'évolution clinique

Mais la nature de la lésion imprime nettement son cachet ainsi 40 % des astrocytomes resteront jusqu'à la fin négatifs au GEG

Si l'on reprend les 110 TCH dont nous avons déjà parlé on trouve EEG négatifs 10 GEG négatifs 11 Echo négatifs 30, Fond d'œil négatifs 63

Du point de vue du diagnostic précoce EEG et GEG paraissent d'une sensibilité équivalente et l'Echo franchement plus tardif, le fond d'œil reste

Neuf fois la négativité de l'E L G se trouvait compensée par un G E G positif et deux fois par un déplacement très significatif de la ligne médiane, les cinq premiers cas appartiennent aux tumeurs lentement évolutives ou propres du crâne, l'E L G négatif ne constitue pas une surprise et la radiographie standard du crâne reste pour ces cas l'examen ambulatoire de choix.

Onze fois le G E G se montre négatif

	E L G	Echo M
1 Astrocytome temporal	J	15
2 Astrocytome temporal	J	25
3 Astrocytome temporal	J	26
4 Oligodendrogliome	+	6
5 Gliome kystique frontal	+	0
6 Métastase isolée	J	0
7 Métastase thalamique pedonc.	J	6
8 Tumeur thalamique	+	16
9 Tumeur thalamo pedonculaire	+	11
10 Absces temporal	+	3
11 Hématome intra-cérébral	+	2

J = ondes delta polymorphes en foyer très évocatrices d'une lésion localisée

Trois fois pour des astrocytomes — notion bien connue, les trois fois l'E E G évocateur (Δ delta) et des déplacements énormes de l'Echo M redressent le diagnostic, trois fois l'E L G et de gros déplacements corrigent le G E G négatif dans les tumeurs thalamiques ou pedonculaires profondes, quatre fois l'Echo M se montre normal ou son déplacement peu significatif avec un E E G positif, sur ces quatre derniers cas nous ne notons que deux tumeurs.

L'Echo négatif 30 fois sur 110, apparaît comme le procédé le moins fidèle et de ce fait comme une exploration en retard sur l'E E G et le G E G, mais sur 30 résultats négatifs, 27 proviennent de tumeurs paramédianes ou bilatérales (métastases). Le flux du cerveau empêche certaines encoconvolutions de se déplacer dans l'hémicrâne opposé, mais ne les empêche pas d'émettre des ondes delta polymorphe ou de fixer les radioisotopes plus que le cerveau sain.

La seconde question est la nature de la neoformation L'E E G manque de spécificité mais réfléchit l'évolution rapide ou lente de la neoformation très anormal pour l'abcès il peut rester normal pour le méningiome.

Le G E G tel que nous l'utilisons à la *Pitté* indique souvent la nature du processus expansif. Dans la technique de Madame PLANIOL, l'examen répété pendant 2 ou 3 jours consécutifs révèle un foyer d'hyperactivité gamma

1) immédiat dans les angiomes, 2) précoce dans les méningiomes, 3) tardif dans les glioblastomes, et 4) très tardif dans les métastases.

PLANIOL et METZGER ont comparé les conclusions pré opératoires du G E G et de l'angiographie dans 275 cas de T C H il résulte de cette confrontation que sur 225 diagnostics de nature le G E G s'est montré 43 fois erroné sur 157 diagnostics étiologiques l'angiographie s'est montrée erronée 17 fois

Des informations sur la nature et l'histologie des néoformations deviennent donc de plus en plus significatives si on ajoute à la radiographie standard le G E G sans oublier un bon interrogatoire et l'examen clinique

Le nombre des T C H devant lesquelles le neurochirurgien reste hésitant avant l'artériographie tend donc à baisser si on utilise les explorations ambulatoires et complémentaires énumérées

La troisième question est si on peut par les techniques énumérées reconnaître une tumeur cérébrale au début Il devient évident que nous sommes actuellement en état de faire le diagnostic de T C H par l'E E C le G E G et l'Echo avant l'apparition de la stase papillaire Ceci marque un grand progrès réalisé au cours des 20 dernières années et prouve que le diagnostic des tumeurs hémisphériques se fait déjà à une phase beaucoup plus précoce qu'il y a 10 ou 15 ans

Un diagnostic précoce devient possible aussi du fait que la séméiologie neurologique s'est raffinée et l'expérience des praticiens élargie ils pensent à une tumeur plus tôt qu'autrefois et s'inquiètent devant toute épilepsie tardive et devant tout déficit neurologique psychique ou sensoriel

Sur les trois techniques laquelle est la plus précoce ou la plus tardive ?

E E G Sur une série de 65 néoformations BUISSON FEREY a noté que les abcès les hématomes intra-cérébraux et les glioblastomes s'accompagnent d'un E E G évocateur avant la fin du 1er mois d'évolution clinique, plus le processus évolue rapidement (même bénin comme l'abcès) plus les anomalies électriques sont précoces

Les méningiomes peuvent montrer un tracé non évocateur ou normal après une évolution de mois ou d'années (voir le Tableau)

Le G E G fournit par contre des signes plus précoces que E E G dans les méningiomes de la convexité plus de 80 % montrent un foyer G E G net au cours de la première année d'évolution clinique

Mais la nature de la lésion imprime nettement son cachet ainsi 40 % des astrocytomes resteront jusqu'à la fin négatifs au G E G

Si l'on reprend les 110 T C H dont nous avons déjà parlé on trouve E E G négatifs 10 G E G négatifs 11 Echo négatifs 30 Fond d'œil négatifs 63

Du point de vue du diagnostic précoce E E G et G E G paraissent d'une sensibilité équivalente et l'Echo franchement plus tardif le fond d'œil reste

Neuf fois la négativité de l'E L G se trouvait compensée par un G E G positif et deux fois par un déplacement très significatif de la ligne médiane, les cinq premiers cas appartiennent aux tumeurs lentement évolutives ou propres du crâne, l'E L G négatif ne constitue pas une surprise et la radiographie standard du crâne reste pour ces cas l'examen ambulatoire de choix.

Onze fois le G L G se montre négatif

	I L G	Echo M
1 Astrocytome temporal	Δ	15
2 Astrocytome temporal	Δ	25
3 Astrocytome temporal	Δ	16
4 Oligodendrogliome	+	6
5 Gliome kystique frontal	+	0
6 Métastase isolée	Δ	0
7 Métastase thalamique pedonc	Δ	6
8 Tumeur thalamique	+	16
9 Tumeur thalamique pedonculaire	+	11
10 Absces temporal	+	3
11 Hématome intra-cérébral	+	2

Δ = ondes delta polymorphes en foyer très évocatrices d'une lésion localisée

Trois fois pour des astrocytomes — notion bien connue, les trois fois l'E E G évocateur (Δ delta) et des déplacements énormes de l'Echo M redressent le diagnostic, trois fois l'E L G et de gros déplacements corrigent le G E G négatif dans les tumeurs thalamiques ou pédonculaires profondes, quatre fois l'Echo M se montre normal ou son déplacement peu significatif avec un L E G positif, sur ces quatre derniers cas nous ne notons que deux tumeurs.

L'Echo négatif 30 fois sur 110, apparaît comme le procédé le moins fiable et de ce fut comme une exploration en retard sur l'E L G et le G E G, mais sur 30 résultats négatifs, 27 proviennent de tumeurs peu médianes ou bilatérales (métastases). Le flux du cerveau empêche certaines circonvolutions de se déplacer dans l'hémicrâne opposé, mais ne les empêche pas d'émettre des ondes delta polymorphes ou de fixer les radioisotopes plus que le cerveau sain.

La seconde question est la nature de la néoformation. L'E E G manque de spécificité mais reflète l'évolution rapide ou lente de la néoformation très anormal pour l'abcès il peut rester normal pour le méningiome.

Le G E G tel que nous l'utilisons à la *Pitié* indique souvent la nature du processus expansif. Dans la technique de Madame PLANIOL, l'examen répété pendant 2 ou 3 jours consécutifs révèle un foyer d'hyperactivité gamma 1) immédiat dans les angiomes, 2) précoce dans les méningiomes 3) tardif dans les glioblastomes, et 4) très tardif dans les métastases.

PLANIOL et METZGER ont comparé les conclusions pré opératoires du G E G et de l'angiographie dans 275 cas de T C H il résulte de cette confrontation que sur 225 diagnostics de nature le G E G s'est montré 43 fois erroné sur 157 diagnostics étiologiques l'angiographie s'est montrée erronée 17 fois

Des informations sur la nature et l'histologie des néoformations deviennent donc de plus en plus significatives si on ajoute à la radiographie standard le G E G sans oublier un bon interrogatoire et l'examen clinique

Le nombre des T C H devant lesquelles le neurochirurgien reste hésitant avant l'artériographie tend donc à baisser si on utilise les explorations ambulatoires et complémentaires énumérées

La troisième question est si on peut par les techniques énumérées reconnaître une tumeur cérébrale au début Il devient évident que nous sommes actuellement en état de faire le diagnostic de T C H par l'E E G le G E G et l'Echo avant l'apparition de la stase papillaire Ceci marque un grand progrès réalisé au cours des 20 dernières années et prouve que le diagnostic des tumeurs hémisphériques se fait déjà à une phase beaucoup plus précoce qu'il y a 10 ou 15 ans

Un diagnostic précoce devient possible aussi du fait que la séméiologie neurologique s'est raffinée et l'expérience des praticiens élargie ils pensent à une tumeur plus tôt qu'autrefois et s'inquiètent devant toute épilepsie tardive et devant tout déficit neurologique psychique ou sensoriel

Sur les trois techniques laquelle est la plus précoce ou la plus tardive ?

E E G Sur une série de 63 néoformations BUISSON FEREY a noté que les abcès les hématomes intra-cérébraux et les glioblastomes s'accompagnent d'un E E G évocateur avant la fin du 1er mois d'évolution clinique plus le processus évolue rapidement (même bénin comme l'abcès) plus les anomalies électriques sont précoces

Les méningiomes peuvent montrer un tracé non évocateur ou normal après une évolution de mois ou d'années (voir le Tableau)

Le G E G fournit par contre des signes plus précoces que E E G dans les méningiomes de la convexité plus de 80 % montrent un foyer G E G net au cours de la première année d'évolution clinique

Mais la nature de la lésion imprime nettement son cachet ainsi 40 % des astrocytomes resteront jusqu'à la fin négatifs au G E G

Si l'on reprend les 110 T C H dont nous avons déjà parlé on trouve E E G négatifs 10 G E G négatifs, 11 Echo négatifs 30 Fond d'œil négatifs 63

Du point de vue du diagnostic précoce E E G et G E G paraissent d'une sensibilité équivalente et l'Echo franchement plus tardif le fond d'œil reste

Tableau

On considère précoce l'enregistrement pratiqué après le début clinique au cours des 14 premiers jours pour les abcès du premier mois pour l'hématome intracérébral et le glioblastome des six premiers mois pour l'astrocytome de la première année pour le méningiome SP = Stas papillaire

cc	34	Γ	Lap au debut	Sans S P	31 avec S P				
					0	1	II	III	IV
8	5		Abscs	< 14j				2 1	1 4
7	3		Hématome I Cer	< 1m				2 3	2
19	9		Glioblast	< 1m	1		3 2	4 1	3 5
10	6		Astrocyt	< 6m		1	1 1	2 1	1 3
9	6		Mening	< 1an		2 1	1 2	2	1
12	5		Metastases		1	1	1	3 1	4 1

normal dans plus de la moitié des 110 tumeurs au moment où les autres explorations physiques ambulatoires sont déjà positives, la même conclusion se dégage des études de TONNIS

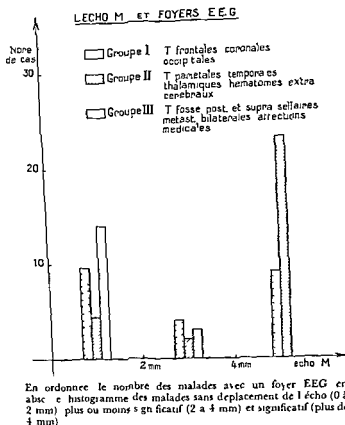
Mais sur 110 tumeurs examinées à une période évolutive donnée, ce ne sont pas les mêmes malades qui ont un EEG et un GEG négatif, ou un GEG et un Echo négatif, fait significatif, sur cette série de 110 sujets il n'y en a eu aucun avec EEG, GEG et Echo négatifs à la fois

EEG et GEG attestent en pourcentage la même précocité diagnostique sur les 110 tumeurs, mais en considérant les trois explorations physiques à la lumière des cas individuels le type histologique joue un rôle fondamental, nous venons de voir que le méningiome, compatible longtemps avec un tracé EEG normal, se révèle dès le début par un foyer gamma caractéristique, tandis que l'astrocytome assez rapidement positif en EEG, peut échapper au GEG jusqu'à la fin de l'évolution enfin le glioblastome même négatif en EEG et GEG au moment des premières manifestations cliniques accuse un virage positif si on répète l'examen après quelques semaines les signes cliniques accusant aussi une progression rapide

En pratiquant donc à titre systématique, en plus de la radiographie sans substance de contraste et de l'examen oculaire, les trois techniques physiques citées, nous disposons d'une grande probabilité pour faire un diagnostic précoce avant de le préciser par les substances de contraste

Pour conclure nous allons revenir sur l'échographie médiane, c'est la technique la plus récente qui, malgré sa simplicité apparente, pose le plus de problèmes et soulève le plus de difficultés

Difficultés qui proviennent du fait que la recherche de l'Echo M se termine



dans quelques minutes le film polaroïde objective un écho — dégagé parmi beaucoup d'autres avec la sonde appliquée sur un point choisi assez arbitrairement sur le crâne — écho obtenu sous un angle qu'on suppose perpendiculaire à l'interface explorée

Mais cette interface anatomiquement inconnue (car c'est cette interface qu'on cherche) varie avec le déplacement et l'angulation de la sonde, l'Echo M reste donc malgré le film polaroïde l'exploration complémentaire la plus subjective

Subjectivisme qui ne trouve sa correction que dans l'habileté et l'expérience clinique de l'observateur

MIKOL met dans un histogramme (voir diagramme) les résultats de l'Echo médian dans 69 cas avec foyers EEG évocateurs

Sur 23 tumeurs frontales, coronales ou occipitales seulement 9 ont déplacé l'écho de 4 mm ou plus 10 ne l'ont pas déplacé du tout

Par contre sur 29 tumeurs pariétales, temporales, thalamiques ou hématomas extracérébraux, 25 ont déplacé l'Echo médian d'une manière très significative.

Le facteur qui intervient dans la positivité de l'Echo paraît plutôt anatomique et mécanique, l'Echo a toute chance de constituer un signe de diagnostic précoce pour les tumeurs (temporales, thalamiques etc.) non gênées dans leur expansion par la faux du cerveau.

Mais quand l'Echo a coté du G E G, redresse la conclusion d'un E E G normal pour certaines néoformations à évolution lente comme le méningiome, et quand il compense un G E G normal pour certains astrocytomes ou tumeurs profondes, nous le considérons comme bien venu, malgré son subjectivisme et ses limitations.

Conclusion

Tout sujet âgé de plus de 25 ans, accusant des crises convulsives, des céphalées ou des signes déficitaires d'apparition récente, doit être exploré par des techniques ambulatoires : radio du crâne, fond d'œil, L E G, G L G et Echo M.

L'intégration de ces résultats à la clinique, évite ou justifie les examens de contraste auxquels on demande la véritable radio-anatomie lésionnelle.

Du fait de l'utilisation de l'E E G, du G L G et de l'Echo, le fond d'œil ne fournit des résultats positifs que dans un pourcentage de plus en plus réduit de cas.

Les résultats de ces trois examens ambulatoires, se laissent ainsi formuler :

L F G	+	} Tumeur pratiquement certaine les examens de contraste s'imposent
G L C	+	
Lcho	+	
L L G	-	} Tumeur peu probable attendre et répéter les examens ambulatoires surtout L L G & LCHO en fonction de l'évolution clinique
G E G	-	
Lcho	-	
L E G	-	} Méningiomes oligodendrogliomes tumeurs propres du crâne angiographie de la carotide interne et externe
C L C	+	
Lcho	+	
L E G	+	} T. coronale occipitale paramédianes ou médianes bilatérales examens de contraste
G E G	+	
Lcho	-	
E E G	+	} Astrocytomes tumeurs profondes de petit volume médianes examens de contraste
G L G	-	
Lcho	+	

Pour les trois dernières éventualités, seuls les examens de contraste vont lever le doute, G E G et E E G ayant fourni des indications topographiques assez variables.

Les techniques physiques d'examen ambulatoire exploitent des particularités lésionnelles et des signaux de provenance différentes d'où leur caractère complémentaire.

La probabilité pour que les 3 explorations physiques ambulatoires restent négatives sur le même malade atteint d'une néoformation hémisphérique paraît de ce fait réduite.

Si la néoformation évolue rapidement (glioblastome) ou infiltre le parenchyme cérébral (astrocytome) l'EEG devient positif d'une manière assez précoce.

Le GEG s'avère positif dès le début clinique pour certains types histologiques comme le méningiome mais peut rester négatif jusqu'à la fin pour d'autres types comme l'astrocytome. Il est précoce dans le glioblastome.

Enfin les facteurs mécaniques qui agissent sur l'écho médian lui impriment un caractère diagnostique plutôt tardif même si la topographie de la néoformation paraît favoriser les déplacements en masse du cerveau.

RÉSUMÉ

Les techniques ambulatoires de recherche des tumeurs cérébrales, en particulier l'EEG, le GEG et l'écho M, permettent d'établir les indications des examens radiographiques avec moyen de contraste. Si ces 3 techniques sont positives, la tumeur cérébrale est pratiquement certaine et les examens avec moyen de contraste sont indiqués. Si elles sont négatives, la tumeur est peu probable. Quand leurs résultats sont discordants, elles renseignent cependant souvent sur le siège et la nature de la tumeur et les examens avec moyen de contraste préciseront le diagnostic.

SUMMARY

Alternating techniques for the investigation of cerebral tumours, especially EEG, GEG and the M echo, make it possible to establish indications for radiographic examinations with contrast media. If all three techniques give positive results, the presence of a tumour is almost certain and examination with contrast media is indicated. If they are all negative, it is not likely that a tumour is present. When their results are conflicting, they can nevertheless often give information regarding the site and nature of the tumour and the examination with contrast medium will help to establish the diagnosis.

ZUSAMMENFASSUNG

Verschiedene Techniken für ambulatonische Untersuchungen von Gehirntumoren, besonders EEG, GEG und das M Echo, machen es möglich, Indikationen für Kontrastmitteluntersuchungen aufzustellen. Falls alle drei Techniken positive Resultate geben, ist das Vorhandensein eines Tumors fast sicher und eine Untersuchung mit Kontrastmittel ist empfehlenswert. Falls alle drei negativ sind, ist es nicht anzunehmen, dass ein Tumor vorhanden ist. Wenn ihre Resultate widersprechend sind, können sie trotzdem oft Informationen über den Platz und die Natur des Tumors geben und Untersuchungen mit Kontrastmittel helfen eine Diagnose aufzustellen.

Par contre sur 29 tumeurs pariétales, temporales, thalamiques ou hématomas extracérébraux, 25 ont déplacé l'Echo median d'une manière très significative

Le facteur qui intervient dans la positivité de l'Echo paraît plutôt anatomique et mécanique, l'Echo a toute chance de constituer un signe de diagnostic précoce pour les tumeurs (temporales, thalamiques etc) non gênées dans leur expansion par la fixation du cerveau

Mais quand l'Echo a coté du G E G, redresse la conclusion d'un E E G normal pour certaines néoformations à évolution lente comme le méningiome, et quand il compense un G E G normal pour certains astrocytomes ou tumeurs profondes, nous le considérons comme bien venu, malgré son subjectivisme et ses limitations

Conclusion

Tout sujet âgé de plus de 25 ans, accusant des crises convulsives, des céphalées ou des signes déficitaires d'apparition récente, doit être exploré par des techniques ambulatoires radio du crâne, fond d'œil, E E G, G E G et Echo M

L'intégration de ces résultats à la clinique, aide ou justifie les examens de contraste auxquels on demande la véritable radio anatomie lésionnelle

Du fait de l'utilisation de l'E E G, du G E G et de l'Echo, le fond d'œil ne fournit des résultats positifs que dans un pourcentage de plus en plus réduit de cas

Les résultats de ces trois examens ambulatoires, se laissent ainsi formuler

L E G +	}	Tumeur pratiquement certaine les examens de contraste s'imposent
G E G +		
Lcho +		
L E G -	}	Tumeur peu probable attendre et répéter les examens ambulatoires surtout EEG & ECHO en fonction de l'évolution clinique
G E G -		
Echo -		
L E G -	}	Méningiomes oligodendrogliomes tumeurs propres du crâne angiographie de la carotide interne et externe
G E G +		
Lcho +		
L E G +	}	T coronale occipitale paramédianes ou métastases bilatérales examens de contraste
G E G +		
Lcho -		
E E G +	}	Astrocytomes tumeurs profondes de petit volume médianes examens de contraste
G E G -		
Echo +		

Pour les trois dernières éventualités seuls les examens de contraste vont lever le doute, G E G et E E G ayant fourni des indications topographiques assez valables

DIAGNOSIS OF BRAIN TUMOR USING ULTRASOUND

by

KENJI TANAKA and KAZUFUMI ITO

Since the first report by DUSSIK (1942) the problem of the application of ultrasound in neurosurgery has been studied by FRENCH et coll (1950 1951) BOLT & HUETER (1951) LERSELL (1955) GORDON (1959) JEFFERSON (1959) DE VLIJGER & RIDDER (1959) JEFFSSON (1960) LITHANDER (1961) and TAYLOR et coll (1961) We reported on this subject at the Second I C A Congress at Cambridge Mass in 1956 and at the Third I C A Congress in Stuttgart Germany in 1959 (TANAKA 1959)

We present here an account of the ultrasonic diagnosis of brain tumors by the reflection method

Technical equipment An ultrasonic apparatus Model SSD 2 developed by the Japan Radio Co of Tokyo has been used in this work The echoes are displayed on the Braun tube by A scope indication

The transducers used were provided with barium titanate (1 and 2.25 megacycles and piezoelectric quartz crystals (5 and 10 megacycles) The diameters of the transducer are 30 10 and 3 mm The following types of transducers were used 1 and 2.25 megacycles of 10 mm diameter for examination through the intact skull 5 and 10 megacycles of 3 or 10 mm diameter for direct application to the brain (Fig 1)

BIBLIOGRAPHIE

- FISCHGOLD H et GASTAUT H Rayons X, radioisotopes et EEG dans l'épilepsie Masson et Cie, Paris 1960
- et DREYFUS BRISAC C Savoir interpréter un électroencéphalogramme Editions De Visscher (Les 3 dernières éditions de ce petit livre destiné aux praticiens sont état l'une après l'autre des différentes techniques complémentaires à l'EEG) 1964
- PLANIOL T METZGER J et DAVID M Intérêt de l'association gamma encéphalographie — angiographie carotidienne pour le diagnostic de nature des néoformations intracrâniennes Neuro chirurgie 10 (1964) 23

DIAGNOSIS OF BRAIN TUMOR USING ULTRASOUND

by

Kenji TANAKA and Kazufumi ITO

Since the first report by Dussik (1942) the problem of the application of ultrasound in neurosurgery has been studied by French et coll (1950-1951) Bolt & Hueter (1951) Lemsell (1955) Gordon (1959) Jefferson (1959) De V Lieger & Ridder (1959) Jeppsson (1960) Lithander (1961) and Taylor et coll (1961). We reported on this subject at the Second ICA Congress at Cambridge Mass in 1956 and at the Third ICA Congress in Stuttgart Germany in 1959 (Tanaka 1959).

We present here an account of the ultrasonic diagnosis of brain tumors by the reflection method.

Technical equipment An ultrasonic apparatus Model SSD 2 developed by the Japan Radio Co. of Tokyo has been used in this work. The echoes are displayed on the Braun tube by A scope indication.

The transducers used were provided with barium titanate (1 and 2.25 megacycles) and piezoelectric quartz crystals (1 and 10 megacycles). The diameters of the transducer are 30, 10 and 3 mm. The following types of transducers were used: 1 and 2.25 megacycles of 10 mm diameter for examination through the intact skull; 5 and 10 megacycles of 3 or 10 mm diameter for direct application to the brain (Fig. 1).

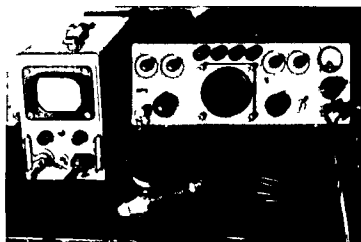


Fig 1 Ultrasonic diagnosing apparatus (right) and its monitor (left)

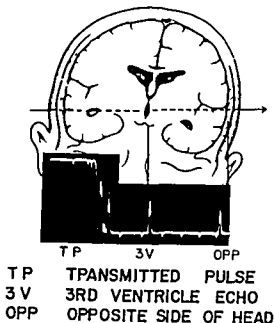


Fig 2 Normal pattern of intracranial echo at the temporal region

Examination technique and findings

For examination through the scalp, liquid paraffin is applied to the surfaces of the transducer and scalp as a coupling medium. The transducer is held by hand and it is desirable to shave off the hair in order to make a good contact. Standard examination is performed through the temporal and frontal regions of the head.

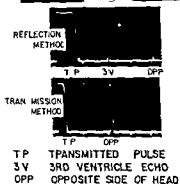
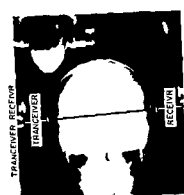


Fig 3 Verification of third ventricle echo. The encephalogram shows the direct path of the ultrasonic beam

Midline echo The examination through the temporal region is easier because the temporal bone is thin. When the transducer is placed just in front of and over the ear the echo originating from the third ventricle wall is detected as a midline pulsating echo. These pulsations are synchronous with the heart beat (Fig 2). When the transducer is applied in this position, ultrasound does not pass the falx cerebri or pineal gland.

Experimentally, using a brain specimen in a water tank, a thin steel blade was inserted into the third ventricle and the midline echo was then detected with greater ease.

Furthermore, the direction of the ultrasonic beam is measured using reflection and transmission methods. The third ventricle echo, being at the midline, is best obtained when the transducer is applied just above and ahead of the external ear using the reflection method. The direction of the ultrasound beam was confirmed by radiography applying the transmission from the same point. On this occasion, encephalography revealed that the ultrasonic beam of the transducer passes through the third ventricle (Fig 3).

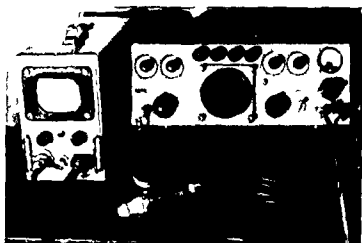
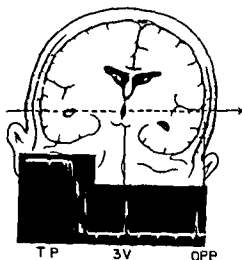


Fig 1 Ultrasonic diagnosing apparatus (right) and its monitor (left)



TP	TRANSMITTED PULSE
3V	3RD VENTRICLE ECHO
OPP	OPPOSITE SIDE OF HEAD

Fig 2 Normal pattern of intracranial echo at the temporal region

Examination technique and findings

For examination through the scalp, liquid paraffin is applied to the surfaces of the transducer and scalp as a coupling medium. The transducer is held by hand, and it is desirable to shave off the hair in order to make a good contact. Standard examination is performed through the temporal and frontal regions of the head.

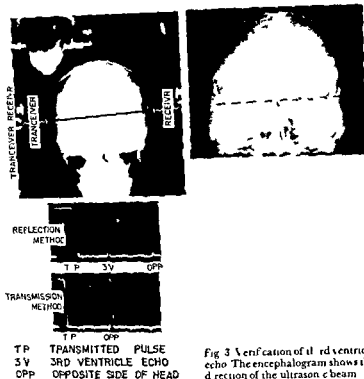


Fig 3 Verification of third ventricle echo. The encephalogram shows the direction of the ultrasonic beam

Midline echo The examination through the temporal region is easier because the temporal bone is thin. When the transducer is placed just in front of and over the ear the echo originating from the third ventricle wall is detected as a midline pulsating echo. These pulsations are synchronous with the heart beat (Fig 2). When the transducer is applied in this position, ultrasound does not pass the falx cerebri or pineal gland.

Experimentally, using a brain specimen in a water tank, a thin steel blade was inserted into the third ventricle and the midline echo was then detected with greater ease.

Furthermore, the direction of the ultrasonic beam is measured using reflection and transmission methods. The third ventricle echo, being at the midline, is best obtained when the transducer is applied just above and ahead of the external ear using the reflection method. The direction of the ultrasound beam was confirmed by radiography, applying the transmission from the same point. On this occasion, encephalography revealed that the ultrasonic beam of the transducer passes through the third ventricle (Fig 3).

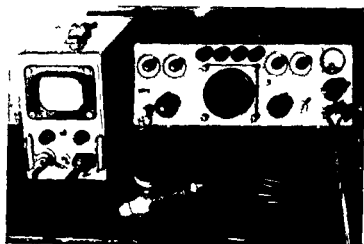


Fig 1 Ultrasonic diagnosing apparatus (right) and its monitor (left)

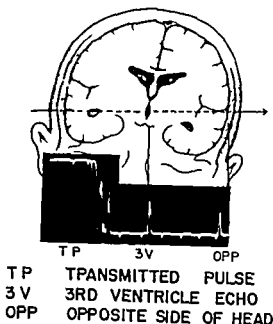
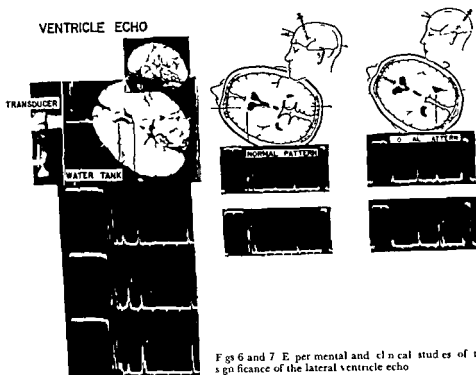


Fig 2 Normal pattern of intracranial echo at the temporal region

Examination technique and findings

For examination through the scalp liquid paraffin is applied to the surfaces of the transducer and scalp as a coupling medium. The transducer is held by hand, and it is desirable to shave off the hair in order to make a good contact. Standard examination is performed through the temporal and frontal regions of the head.



Figs 6 and 7 Experimental and clinical studies of the significance of the lateral ventricle echo

the frontal region. With regard to the question of structures responsible for the echoes registered the writers have carried out the following experiments to clarify this problem.

By using a human brain in a water tank and pulsed ultrasound through the frontal region to the occipital area a distinct reflection wave was detected when a rubber tube (3 mm in diameter) was inserted into the anterior horn of the lateral ventricle (Fig 6).

Clinically patients with burr holes for ventriculography in the frontal and occipital region were examined. When the rubber tube was inserted into the anterior horn and posterior horn by ventricular puncture the pulsating echoes were detected more distinctly from the examination through the frontal region (Fig 7).

Acoustic impedance of normal brain and tumor tissue

It has been a question whether the difference of the acoustic impedance between brain tumor tissue and normal brain tissue is too small to cause sufficient reflection of the ultrasonic wave.

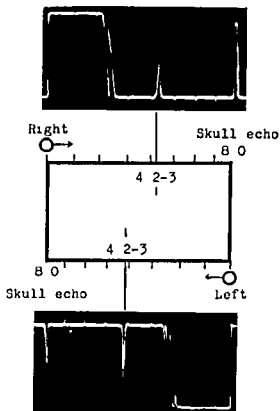


Fig 4

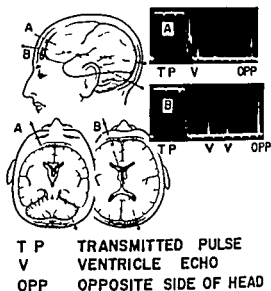


Fig 5

Figs 4 and 5 Normal patterns of third ventricle echo and of intracranial echoes in the frontal region

The third ventricle echo is detected at 4 2—4 3 with the time marker (dividing by 8) set to the beginning of the first echo. If the ventricle is deviated by more than 0 2 mark, we can be convinced of a shift of this ventricle (Fig 4).

As already reported (TANAKA 1962, TANAKA et al 1961, 1962, 1963), many echoes which pulsate synchronously with the heart beat are observed from within the brain. A great part of these echoes are probably due to the ventricle walls. Continuous records of these pulsating echoes, especially the third ventricle echo, were made on the cathode ray screen for the analysis of these phenomena. As the method of recording, both time position indication and continuous record of echo height were used. In hydrocephalic patients the pulsations are approximately 180° out of phase with each other.

The lateral ventricles For this examination the beam was passed from the frontal region to the occipital area, with a finding of some pulsating echoes from within the brain (Fig 5). In some cases we found pulsating echoes through



Fig 8 Normal pattern of intracranial echo midline locator at the temporal region

respectively in fresh specimens. From the results of these experiments, the acoustic impedance of brain tumor tissue is greater than that of normal tissue. Thus it is theoretically possible that the border between brain tissue and tumor tissue will cause a reflection (Table 1).

Furthermore, the tumor echo pattern is complicated and the ultrasonic attenuation is different. In addition to the diagnosis of brain tumors by echo

Table 4
Results of ultrasonic diagnosis of brain tumor

Location of tumor	Number of cases examined	Number of correctly diagnosed cases
Cerebral hemispheres	55	53
Chiasmatic region	18	14
Rostral brain stem	8	3
Caudal brain stem	5	0
Cerebellum	11	9
Fourth ventricle	1	0
Cerebello-pontine angle	13	1
Total	111	80

Table 1

Acoustic impedance of normal brain specimen and brain tumor tissues

	Velocity, c cm/sec $\times 10^3$	Density ρ g/cc	Acoustic impedance zc $\times 10$
Cerebrum	1.16	1.036	0.151
Astrocytoma (grade II)	1.66	1.034	0.171
Retinoblastoma	1.60	1.046	0.167
Meningioma	1.64	1.050	0.172
Meningioma (fibroblastic)	1.64	1.040	0.171
Meningioma (meningotheliomatous)	1.66	1.048	0.173
Metastatic cancer (adenocarcinoma)	1.59	1.058	0.168

Table 2

Ultrasonic attenuation on brain tumor compared with normal brain

	5 megacycle	10 megacycle
Meningioma	+ 2.75	+ 5.15
Neurinoma	- 2.5	- 4.5
Chromophobe adenoma	- 1.0	- 1.53
Astrocytoma	0	0
Glioma (unclassified)	- 1.75	- 5.0
Medulloblastoma	- 1.75	- 6.1
	db/cm	db/cm

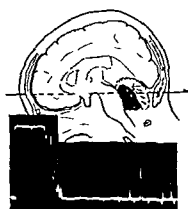
Table 3

Ultrasonoechograms checked by radiograms on 92 patients

Ultrasonoechography	Checked by neuroradiology	
Displacement of third ventricle echo 56 cases	Median structures shifted	53 cases
	No shift of median structures	3 cases
No displacement of third ventricle 36 cases	Median structures shifted	0 cases
	No shift of median structures	36 cases

The acoustic impedance of a substance is defined as the product of the density of the substance and the velocity of sound in it. The velocity of sound from fresh specimens was measured with a clamp transducer.

The acoustic impedances for normal brain tissue, meningioma and glioma were found to be 1.51×10^5 , $1.71-1.73 \times 10^5$ and $1.67-1.71 \times 10^5$ g/cm²/sec



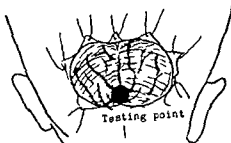
TP T OPP

TP TRANSMITTED PULSE

T TUMOUR ECHO

OPP OPPOSITE SIDE OF HEAD

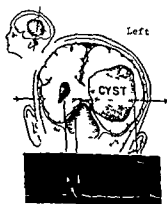
a



TUMOR ECHO

b

Fig 12 Case of medulloblastoma occupying the fourth ventricle (found and removed at operation)
 a) Ultrasonic examination through the temporal route. The third ventricle echo is large and not displaced. At examination through the frontal route abnormal echoes were detected just before the opposite side of the occipital region. b) Surgical exploration. At first no abnormality but abnormal echoes were detected on ultrasonic examination of the brain at the posteromedian part at the depth of 4 cm the echoes were regular and continuous.



TP V CE

TP TRANSMITTED PULSE

V VENTRICLE ECHO

CE CYSTIC ECHO

Fig 13 Case of choroid plexus papilloma. Ultrasonic examination through the right temporal route. The third ventricle echo is displaced to the right. At examination through the left temporal route a cystic echo was detected adjacent to the third ventricle echo.

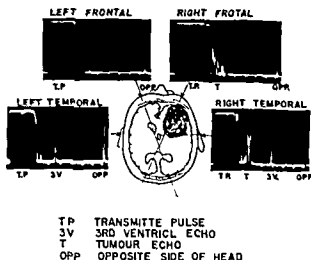


Fig. 9

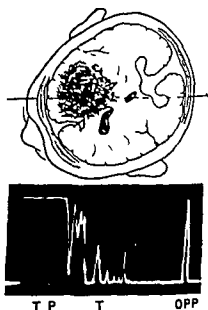


Fig. 10

Fig. 9 Case of meningioma. The ultrasonic examination was performed through the temporal route. The third ventricle echo is shifted to the left and the right frontal examination resulted in abnormal irregular echoes adjacent to the transmitted pulse at a depth of 8 cm.

Fig. 10 Case of glioblastoma. Examination through right temporal region showed abnormal irregular echoes adjacent to transmitted pulse at 8 cm depth and through fronto-parietal region right side less ultrasonic attenuation and tumor echoes at 6–7 cm depth.

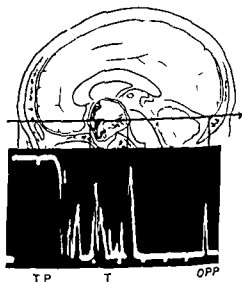


Fig. 11 Case of craniopharyngioma. Examination through the temporal route. Third ventricle not displaced. Examination through the bilateral frontal route showed abnormal irregular echoes at a depth of 6–7 cm.

TP TRANSMITTED PULSE
T TUMOUR ECHO
OPP OPPOSITE SIDE OF HEAD

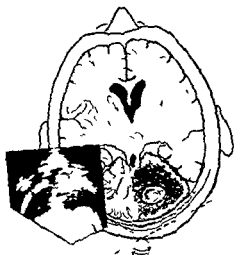


Fig. 16 Ultrasonotomogram of a cerebellar tumor showing outside border of cerebellum and tumor echoes including a cystic pattern

Results

Comparison between the third ventricle echo and midline structure displacement The third ventricle as the source of the midline echo ascertained by examination through the above mentioned temporal route was first pointed out by TANAKA et coll (1973, 1974)

The use of the ultrasonic echo method to measure the position of the third ventricle will be described in the following

In 89 cases (97 %) of a series of 92 cases confirmed by conventional neuro radiologic investigation the presence or absence of the third ventricle displacement was predicted correctly and in 3 cases (cerebellar tumor, pituitary adenoma and thalamus tumor) the location of the third ventricle was predicted incorrectly by ultrasonic examination (Table 3)

The A scope indication method is useful for clinical diagnosis but some times the analysis of the echo patterns is not easy. Therefore in order to determine the accurate position of the third ventricle the writers have been engaged in research on a midline locator by means of ultrasound

The midline locator requires slight modification of the standard ultrasonic apparatus, a sensitivity time control circuit is adapted to it and the pass-band of this locator is narrowed. The third ventricle echo is detected more readily with this midline locator than with the standard apparatus. A barium titanate transducer which is 10 mm in diameter and has a frequency of 2.25 megacycles is suitable for detection of the third ventricle through the skull (Fig. 8)

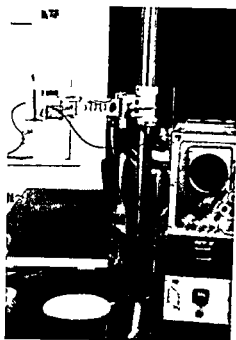
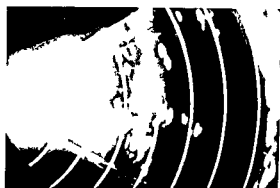


Fig. 14 Apparatus for ultrasonotomography used in the diagnosis of a brain tumor



a



b

Fig. 15 Ultrasonotomograms a) Horizontal section of a living human head showing the ventricular pattern. The third ventricle is in the midline b) Distinct irregular pattern in a case of temporal meningioma. third ventricle shifted

patterns, the observation of the degree of ultrasonic attenuation in the brain is sometimes important. Meningiomas show increased attenuation while glioma shows a decreased attenuation in almost all cases. Results of ultrasonic attenuation on brain tumor tissue compared with normal brain tissue are shown in Table 2.

ZUSAMMENFASSUNG

Es wird die klinische Bedeutung von Ultraschall Diagnostik von Hirntumoren mittels der Pulsmethode vorgeführt. Es wurde der Standard Ultraschallapparat (Aloka Modell SSD-2 A scope Methode) verwendet und die passenden Frequenzen waren 1—10 Megacyklen. Der akustische Widerstand des normalen Gehirns und der von Hirntumoren wird gemessen. Positives Tumorecho konnte in 80 von 111 Patienten mit Hirntumoren erhalten werden. Es war operativ und autopsisch verifiziert werden konnte. Ein Mittellinien Lokalisator und Kontakt Sektor Tomographie wurden ebenfalls studiert.

RÉSUMÉ

L'auteur montre l'intérêt clinique du diagnostic des tumeurs cérébrales par les ultrasons avec la méthode des impulsions. Il a utilisé l'appareil ultrasonique standard (Aloka Model SSD 2 A scope indication method) et les fréquences convenables étaient de 1 à 10 mégacycles. L'auteur a mesuré l'impédance acoustique du cerveau normal et des tumeurs cérébrales. Il a trouvé des échos de tumeur dans 80 cas sur 111 cas de tumeur vérifiés par opération ou par autopsie. Il a aussi étudié un localisateur de ligne médiane et un dispositif de tomographie.

REFERENCES

- BOLT R. H. and HLETER T. F. Ultrasonic method for outlining the cerebral ventricles. *J. acoust. Soc. Amer.* 23 (1951) 160.
- DUSSIK K. T. Über die Möglichkeit Hochfrequente Mechanische Schwingungen als diagnostisches Hilfsmittel zu verwenden. *Z. ges. Neurol. Psychiat.* 174 (1942) 153.
- FRENCH L. A., WILD J. J. and NEAL D. D. Detection of cerebral tumors by ultrasonic pulses. *Cancer* 3 (1950) 705.
- — The experimental application of ultrasonics to the localization of brain tumors. *J. Neurosurg.* 8 (1951) 198.
- GORDON D. Echoencephalography. *Brit. Med. J.* 1 (1959) 1500.
- JEFFERSON A. Some experiences with echo-encephalography. *J. Neurol. Psychiat.* 22 (1959) 83.
- JEFFERSON S. Echo-encephalography III. *Acta chir. scand.* 119 (1960) 455.
- LEKSELL I. Echo-encephalography I. *Acta chir. scand.* 110 (1955/56) 301.
- LITLANDER B. Clinical and experimental studies in echo-encephalography. *Acta psychiat. scand.* (1961) Suppl. 159.
- TANAKA K. Ultrasonic diagnosis of brain tumor. *VOLT*, January 1962.
- ITO K., ISHIKAWA S., ABE Y. and WAGAI T. Diagnosis of brain tumors using ultrasound. *Jap. J. clin. Med.* 21 (1963) 2195.
- — and UEMATSU S. Ultrasonoechography in children. *J. Pediat. Practice* 25 (1962) 976.
- — and ISHIKAWA S. Ultrasonic diagnosis of brain tumor. *Medicine* 18 (1961) 297.
- KIKUCHI Y. and UCHIDA R. Ultrasonic diagnosis of intracranial diseases. Report to Scientific Research of Ministration of Education Japan 1953-1954 (Japanese).
- — Ultrasonic diagnosis of brain tumor. *Proc. Third Internat. Cong. Acoust. Stuttgart* p. 1191, 1953.
- TAYLOR J. C., NEVILL J. A. and HAYMONS B. Ultrasonic in the diagnosis of intracranial space-occupying lesions. *Lancet* 3 (1961) 1197.
- WILFINGER M. DE and RIDDER H. J. Use of echoencephalography. *Neurology* 9 (1959) 216.

Diagnosis and localization of the brain tumor In 300 cases of suspected brain tumor confirmation of the site of the tumor had been obtained by operation and/or autopsy in 111 patients. Of these cases, the pathologic diagnoses were glioma in 44 patients, meningioma in 13, neurinoma in 13, pituitary adenoma in 9, metastatic tumor in 8, craniopharyngioma in 6, cholesteatoma in 2, tuberculoma in 2, plexus papilloma in 2, and other tumors in 5.

Tumor echoes were positive in 80 of the 111 patients. Of 111 with tumors 55 had cerebral tumors and 53 of these had a positive echo. In 30 cases of infratentorial tumors, 10 cases were correctly diagnosed (Table 4).

Our findings in some of these cases are illustrated in Figs 9 to 13.

Ultrasonotomography of the brain

As stated in a foregoing section, the A scope indication method is useful for various clinical diagnoses but sometimes the analysis of the echo patterns is not easy. Therefore, in order to determine the accurate positions of the brain tumors we made our studies with ultrasound tomographies.

In the case of brain tomography, a B scope indication method is not completely successful as the convex form of the skull and the large attenuation of the skull are barriers to ultrasonic propagation.

The present writers have therefore been studying the application of contact scanning to overcome this difficulty. The principle is as follows. A transducer is placed directly on the surface of the scalp in the desired plane. Ultrasonic energy is emitted radially from the transducer to scan the plane section of the brain. On the cathode ray tube screen the direction of a time base is varied in synchronization to the direction of the axis of the transducer. The information of the axis is picked up electrically by a resolver and sent to the deflection coil of the cathode ray tube (Fig. 14).

Efforts to improve the apparatus and its resolving power are in progress. Some patterns obtained by ultrasonotomography are shown in Figs 15 and 16. A new phase in the diagnosis of brain lesions should soon be at hand.

SUMMARY

The clinical value of ultrasonic diagnosis of brain tumors by means of the pulse method is presented. The standard ultrasonic apparatus (Aloka Model SSD 2, A scope indication method) was used and suitable frequencies were 1 to 10 megacycles. The acoustic impedance of the normal brain and of brain tumor were measured. Tumor echoes were positive in 80 out of 111 patients with brain tumor verified by operation and autopsy. A midline locator and ultrasonotomography were also studied.

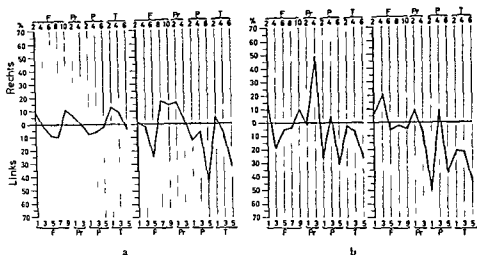
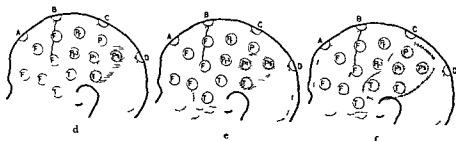


Abb 1 Gamma encephalographische Verlaufuntersuchungen bei einem Kranken mit nem Glioblastom (operative Therapie)
a) Vor Operation b) 7 Monate nach der Operation c) 9 Monate nach der Operation (d-f entsprechen a-c)



VERLAUFSUNTERSUCHUNGEN BEI HIRNTUMOREN MIT RADIOAKTIVEN ISOTOPEN

von

SIGURD WENDE

Die Gamma-Encephalographie mit RISA (radioaktives jodiertes Serum-Albumin) erlaubt es, Beginn und Ablauf der Strahlen-Einwirkung auf das Gehirn zu erfassen. Gamma-encephalographische Verlaufsuntersuchungen geben ferner Aufschluss über das Wachstum eines Hirntumors. Gleichzeitig kann durch diese Verlaufsuntersuchungen der Erfolg einer operativen Therapie oder einer Strahlen-Behandlung bestimmt werden.

Unsere Untersuchungsergebnisse lassen sich in 3 Gruppen zusammenfassen:

In der 1. Gruppe handelt es sich um Kranke, bei denen nur eine operative Behandlung erfolgte.

Die Abb. 1a zeigt den gamma-encephalographischen Befund eines Patienten mit einem parieto-temporo-occipital gelegenen Glioblastom. Die Geschwulst konnte operativ weitgehend entfernt werden, der Kranke verliess im guten Zustand die Klinik. Bei einer Kontroll-Untersuchung 7 Monate nach der Operation hatte sich die neurologische Symptomatik nicht verändert. Im Gamma-Encephalogramm war jedoch eine Grössenzunahme der Isotopen-Anreicherung zu verzeichnen (Abb. 1b), die für ein Rezidiv und für ein

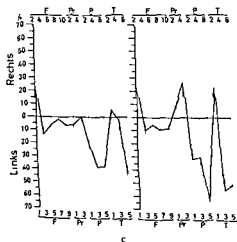
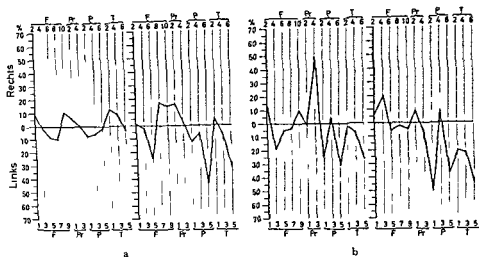
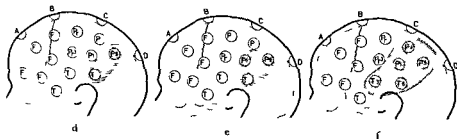


Abb 1 Gamma encephalographische Verlaufuntersuchungen bei einem Kranken mit einem Glioblastom (operative Therapie): a) Vor Operation b) 7 Monat nach der Operation c) 9 Monate nach der Operation (d-f entsprechen a-c)



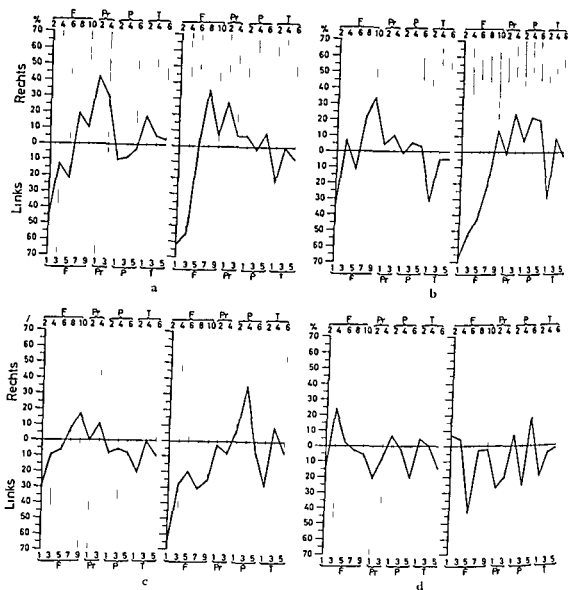


Abb 2 Gamma encephalographische Verlaufsuntersuchungen bei einer Kranken mit einem Glioblastom (guter Erfolg der Strahlen Therapie reversibles Hirnodem) a) Vor Strahlen Therapie b) Nach Bestrahlung von 2 500 R c) Nach 5 000 R d) 9 Wochen nach der Strahlungsbehandlung

weiteres Tumor Wachstum spricht. Wiederum 2 Monate später, also 9 Monate nach der Operation kam es dann zu einer schnell einsetzenden Verschlechterung des Allgemeinzustandes des Patienten. Die Isotopen Untersuchung bestätigte das rasche Tumor Wachstum (Abb 1c). Dabei ist nicht nur eine Grossenzunahme der Isotopen Speicherung festzustellen sondern es liegt auch eine verstärkte Aufnahme der radioaktiven Substanz im Tumor Gebiet vor.

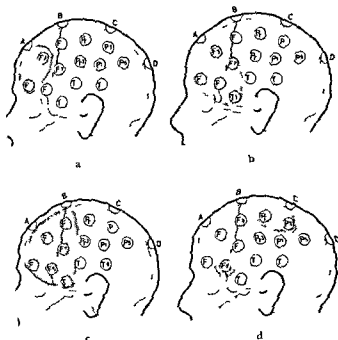


Abb 3 a—d entsprechen Abb 2 a—d

An dem Beispiel eines weiteren Kranken soll die 2. Gruppe geschildert werden, bei der nach einer reversiblen Permeabilitäts-Störung der Blut-Hirn-Schranke ein guter Erfolg der Strahlen-Therapie zu verzeichnen ist.

Bei einer Kranken mit einem Glioblastom frontal war mit dem Gamma-Encephalogramm vor der Röntgen-Therapie Lokalisation und Ausdehnung der Geschwulst genau abzugrenzen (Abb. 2a). Nach einer Bestrahlung von 2000 R hatte sich der Bezirk der pathologischen Isotopen-Speicherung vergrößert (Abb. 2b). Im klinischen Zustand war eine massige Verschlechterung eingetreten. Eine weitere Größenzunahme der Isotopen-Anreicherung war nach 5000 R zu beobachten (Abb. 2c). Durch die Röntgen-Therapie trat also eine umschriebene verstärkte Permeabilitäts-Störung der Blut-Hirn-Schranke im Tumor-Gebiet und in seiner Umgebung auf. 9 Wochen nach der Strahlen-Behandlung war die Kranke bei einer Kontroll-Untersuchung weitgehend beschwerdefrei. Auch das Gamma-Encephalogramm hatte sich bis auf noch nachweisbare Tumor-Reste wieder normalisiert (Abb. 2d).

Bei der 3. Gruppe von Hirntumor-Patienten lässt sich mit dem Gamma-Encephalogramm der Einfluss der Röntgen-Therapie auf die Geschwulst

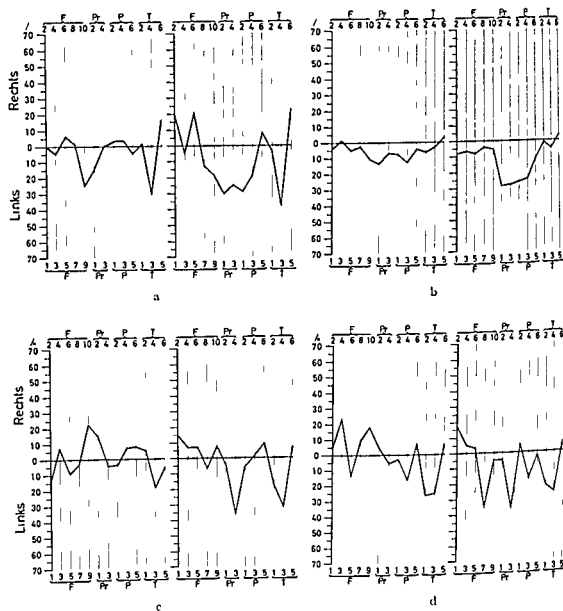


Abb 4 Gamma encephalographische Verlaufsuntersuchungen bei einer Kranken mit einem Oligodendrogliom (Rückbildung des Hirntumors unter Strahlen Therapie Grosszunahme der Geschwulst 10 Wochen nach der Behandlung) a) Vor Strahlenbehandlung b) Nach 2 500 R c) Nach 5 000 R d) 10 Wochen nach der Strahlenbehandlung

ebenfalls beweisen, eine vorübergehende Permeabilitäts Störung der Blut Hirn Schranke ist jedoch nicht erkennbar

Abb 4a gibt das Gamma Encephalogramm einer Kranken mit einem Oligodendrogliom vor Therapie Beginn wieder Nach einer Bestrahlung von 2 500 R hatte sich der Hirntumor zurückgebildet (Abb 4b) Nach 5 000 R

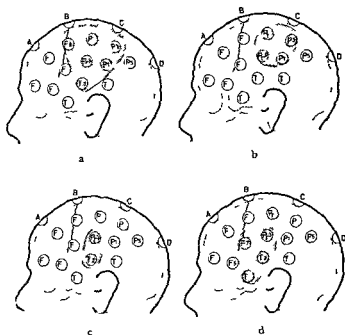


Abb 5 a—d entsprechen Abl 4 a—d

war eine weitere Rückbildung der pathologischen Isotopen Anreicherung zu verzeichnen (Abb 4c) Aber schon 10 Wochen nach der Strahlen Therapie machte sich wieder eine Verschlechterung der neurologischen Symptomatik bemerkbar Das Gamma Encephalogramm bewies die Grossenzunahme des Tumors (Abb 4d)

Auch bei dieser Gruppe von Patienten geht also der Befund der Isotopen Untersuchung mit dem klinischen Befund parallel Allerdings ist hier eine durch die Strahlen Therapie ausgeloste Permeabilitats Störung der Blut Hirn Schranke nicht zu beobachten

Zur Frage des Zusammenhanges zwischen Malignitat einer Geschwulst und Speicherung der radioaktiven Substanz im Tumor Gebiet sei folgende Untersuchung angeführt

Bei dem Kranken bestand ein Astrocytom das 2 1/2 Jahre nach der ersten Operation nochmals operativ behandelt wurde Die erste Gamma Encephalographie bewies die Tumor Ausdehnung sie zeigte auch die ausgeprägte Isotopen Aufnahme im Geschwulst Bereich Es liess sich ein Impuls Überwiegen von fast 60 % erkennen (Abb 6a)

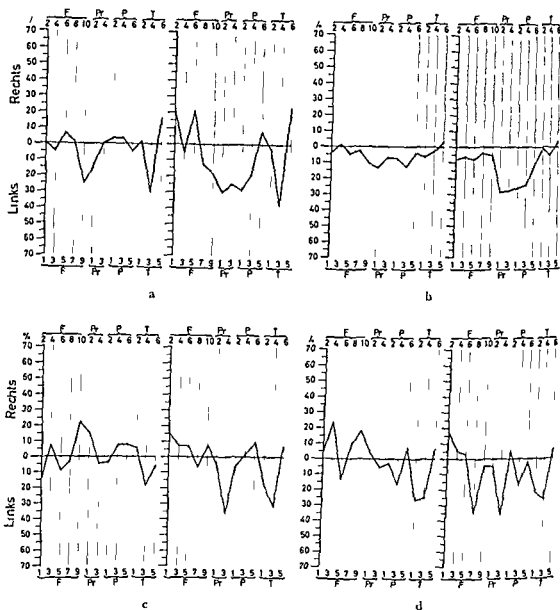


Abb 4 Gamma encephalographische Verlaufuntersuchungen bei einer Kranken mit einem Oligodendrogliom (Rückbildung des Hirntumors unter Strahlen Therapie Grossenzunahme der Geschwulst 10 Wochen nach der Behandlung) a) Vor Strahlenbehandlung b) Nach 2 500 R c) Nach 5 000 R d) 10 Wochen nach der Strahlenbehandlung

ebenfalls beweisen, eine vorübergehende Permeabilitäts Störung der Blut Hirn Schranke ist jedoch nicht erkennbar

Abb 1a gibt das Gamma Encephalogramm einer Kranken mit einem Oligodendrogliom vor Therapie Beginn wieder Nach einer Bestrahlung von 2 500 R hatte sich der Hirntumor zurückgebildet (Abb 4b) Nach 5 000 R

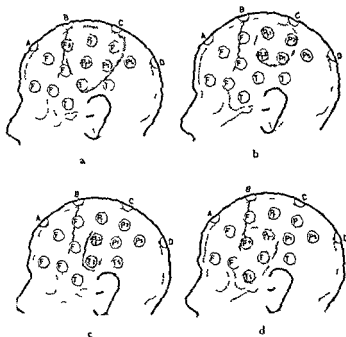


Abb 3 a d entsprechen Abb 4 a-d

war eine weitere Rückbildung der pathologischen Isotopen Anreicherung zu verzeichnen (Abb 4c) Aber schon 10 Wochen nach der Strahlen Therapie machte sich wieder eine Verschlechterung der neurologischen Symptomatik bemerkbar Das Gamma Encephalogramm bewies die Grossenzunahme des Tumors (Abb 4d)

Auch bei dieser Gruppe von Patienten geht also der Befund der Isotopen Untersuchung mit dem klinischen Befund parallel Allerdings ist hier eine durch die Strahlen Therapie ausgeloste Permeabilitäts Störung der Blut Hirn Schranke nicht zu beobachten

Zur Frage des Zusammenhanges zwischen Malignität einer Geschwulst und Speicherung der radioaktiven Substanz im Tumor Gebiet sei folgende Untersuchung angeführt

Bei dem Kranken bestand ein Astrocytom das 2 1/2 Jahre nach der ersten Operation nochmals operativ behandelt wurde Die erste Gamma Encephalographie bewies die Tumor Ausdehnung sie zeigte auch die ausgeprägte Isotopen Aufnahme im Geschwulst Bereich Es liess sich ein Impuls Über wiegen von fast 50 % erkennen (Abb 6a)

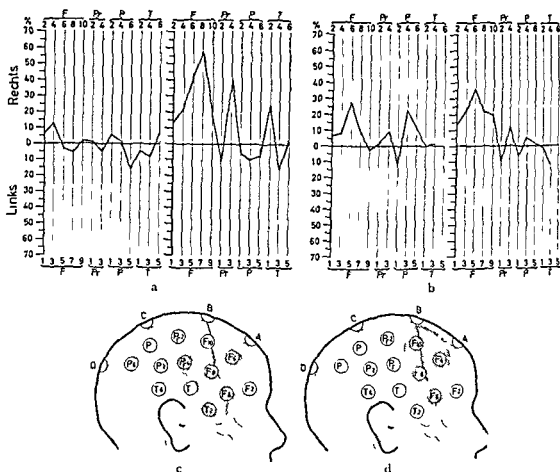


Abb 6 Abnahme der Speichungs Intensität bei einem Astrocytom trotz zunehmender Malignisierung der Geschwulst a) Vor der ersten Operation b) Vor der zweiten Operation (c und d entsprechen a und b)

Vor der zweiten Operation wurde die Gamma Encephalographie wiederholt. Der Tumor war auch jetzt abgrenzbar. Die Intensität der Isotopen-Speicherung war jedoch nicht so ausgeprägt wie bei der ersten Untersuchung, die Differenz Prozent Kurven wiesen nur ein Impuls Überwiegen von 45 % auf (Abb 6b).

Bei dem Vergleich der histologischen Präparate konnte aber eindeutig nachgewiesen werden, dass der Tumor erheblich in Malignität zugenommen hatte.

Es ist daraus abzuleiten, dass das Gamma Encephalogramm bei bösartigen Tumoren zwar die Grossenausdehnung der Geschwulst und das Vorliegen eines Rezidivs anzeigt, zum Grad der Malignität kann jedoch auf Grund der Isotopen Untersuchung nicht Stellung genommen werden.

ZUSAMMENFASSUNG

Durch die Gamma Encephalographie lässt sich die Ausdehnung einer Hirngeschwulst und ihr allmähliches Wachstum exakt bestimmen. Der Therapie Erfolg bei der Bestrahlung bösartiger Hirntumoren kann durch die Gamma Encephalographie objektiviert werden. Die Intensität der Isotopen Speicherung im Tumor Gebiet geht nicht mit der Malignität der Hirngeschwulst parallel.

SUMMARY

Gamma encephalography enables the extent of a cerebral tumour and its gradual increase to be determined. The effectiveness of radiotherapeutic measures in cerebral malignant neoplasms can also be checked by this method. The storage of isotopes within a brain tumour and its degree of malignancy are not correlated.

RESUME

La gamma encephalographie permet de déterminer exactement l'extension et la croissance progressive d'une tumeur cérébrale. Elle permet d'objectiver le résultat thérapeutique de l'irradiation des tumeurs cérébrales malignes. L'intensité de la fixation de l'isotope dans le territoire tumoral n'est pas parallèle à la malignité de la tumeur cérébrale.

LITERATUR

- PLANIOL TH. Diagnostik des Läsions intracranien par les radio isotopes. Masson & Cie Paris 1959
- Diagnostik des recidives de tumeurs intracranien par la gamma encéphalographie. Neuro-chirurgie 8 (1962) 14
 - La gamma encéphalographie. Rev. Prat. 13 (1963) 625
- WENDE S. Radioisotope in neurologisch-neurochirurgischer Diagnostik. Habilitationsschrift Freie Universität Berlin 1962
- Technik und Wert der Gamma Encephalographie. Fortschr. Röntgenstr. 98 (1963) 466
 - Das radiologisch ausgelöste Hirnödem und seine Verhütung I. Teil: Tierexperimentelle Untersuchungen. Fortschr. Röntgenstr. 98 (1963) 589
 - Das radiologisch ausgelöste Hirnödem und seine Verhütung II. Teil: Untersuchungen an Hirntumorpacienten. Fortschr. Röntgenstr. 98 (1963) 594
 - Neuroradiologische Untersuchungen mit radioaktiven Substanzen. Röntgenpraxis 17 (1964) 175

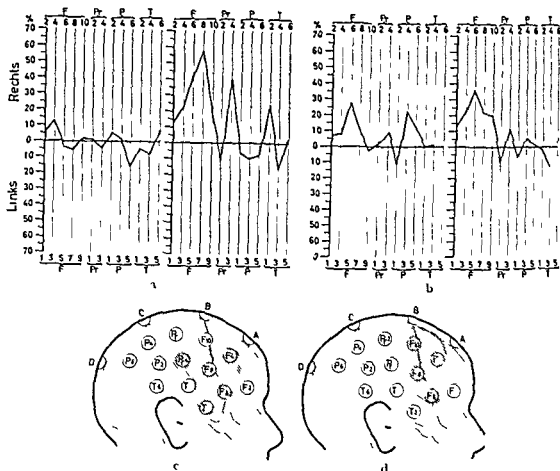


Abb 6 Abnahme der Speicherungs Intensität bei einem Astrocytom trotz zunehmender Malignisierung der Geschwulst a) Vor der ersten Operation b) Vor der zweiten Operation (c und d entsprechen a und b)

Vor der zweiten Operation wurde die Gamma Lucenthographie wiederholt. Der Tumor war auch jetzt abgrenzbar. Die Intensität der Isotopen Speicherung war jedoch nicht so ausgeprägt wie bei der ersten Untersuchung, die Differenz Prozent Kurven wiesen nur ein Impuls Überwiegen von 15%, auf (Abb 6b).

Bei dem Vergleich der histologischen Präparate konnte aber eindeutig nachgewiesen werden, dass der Tumor erheblich in Malignität zugenommen hatte.

Es ist daraus abzuleiten, dass das Gamma Lucenthogramm bei bösartigen Tumoren zwar die Grossenausdehnung der Geschwulst und das Vorliegen eines Rezidivs anzeigt, zum Grad der Malignität kann jedoch auf Grund der Isotopen Untersuchung nicht Stellung genommen werden.

ZUSAMMENFASSUNG

Durch die Gamma Encephalographie lässt sich die Ausdehnung einer Hirngeschwulst und ihr allmähliches Wachstum exakt bestimmen. Der Therapie Erfolg bei der Bestrahlung bosartiger Hirntumoren kann durch die Gamma Encephalographie objektiviert werden. Die Intensität der Isotopen Speicherung im Tumor Gebiet geht nicht mit der Malignität der Hirngeschwulst parallel.

SUMMARY

Gamma encephalography enables the extent of a cerebral tumour and its gradual increase to be determined. The effectiveness of radiotherapeutic measures in cerebral malignant neoplasms can also be checked by this method. The storage of isotopes within a brain tumour and its degree of malignancy are not correlated.

RÉSUMÉ

La gamma encéphalographie permet de déterminer exactement l'extension et la croissance progressive d'une tumeur cérébrale. Elle permet d'objectiver le résultat thérapeutique de l'irradiation des tumeurs cérébrales malignes. L'intensité de la fixation de l'isotope dans le territoire tumoral n'est pas parallèle à la malignité de la tumeur cérébrale.

LITERATUR

- PLANIGOL TH. Diagnostic des lésions intracrâniennes par les radio isotopes. Masson & Cie Paris 1959
- Diagnostic des récidives de tumeurs intracrâniennes par la gamma encephalographie. Neuro-chirurgie 8 (1962) 14
 - La gamma encéphalographie. Rev. Prat. 13 (1963) 3625
- WENDE S. Radioisotope in neurologisch-neurochirurgischer Diagnostik. Habilitationsschrift. Freie Universität Berlin 1962
- Technik und Wert der Gamma Encephalographie. Fortschr. Röntgenstr. 98 (1963) 466
 - Das radiologisch ausgeloste Hirnodem und seine Verhütung. I. Teil. Tierexperimentelle Untersuchungen. Fortschr. Röntgenstr. 98 (1963) 589
 - Das radiologisch ausgeloste Hirnodem und seine Verhütung. II. Teil. Untersuchungen an Hirntumorpatienten. Fortschr. Röntgenstr. 98 (1963) 594
 - Neuroradiologische Untersuchungen mit radioaktiven Substanzen. Röntgenpraxis 17 (1964) 175

STUDIES IN ULTRASONIC ECHO- ENCEPHALOGRAPHY II

An objective technique for the A scan presentation of the
cerebral midline structures

by

D. NALDRETT WHITE and J. B. BLANCHARD

While echoencephalography using an A scan presentation for examination of the cerebral midline structures is a remarkably attractive technique because of its speed and simplicity and safety, some of us working in the field have been concerned by its lack of objectivity and by our lack of ability to identify with certainty the origin of most of the multiplicity of echoes that can be seen on the oscilloscope. The need for some objective control is all the more important in view of the plethora of high amplitude echoes that, with patience, can be evoked at almost any depth from the transducer, particularly on the near side of the midline. Such a need appeared to us to become all the greater after an initial experience with this technique (8) had shown that observer bias and poor experimental technique had greatly exaggerated the reliability of the examination. We believe firmly that it is only a matter of time before compound scanning of the brain is sufficiently developed to give satisfactory tomograms of the ventricular system (7). When this development has taken place the position of A scan echoencephalography will have to be reconsidered. At such a time it would appear to us that the only justification there could be for the continuation of a method that gives so much less information than will be

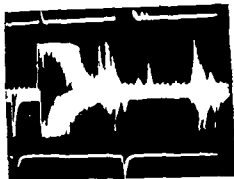


Fig 1 Time exposure of A scan echoencephalogram from patient shown by cerebral angiography to have no displacement of the cerebral midline taken from point perpendicular to centre of incisura in the falx cerebri and above the foramen of Munro. Position of cerebral midline at intersection of the start of the central deflections in top and bottom traces which are of transmission impulses across the skull. The start of the lower transmission pulses is denoted by the small deflection in line with the initial deflections in the other three traces. The larger deflection to the left of this is an artefact. (Read from left to right.) No high amplitude echo can be seen in the two central traces at the site of the cerebral midline.

available with compound scanning would be its much greater simplicity and the smaller cost of the equipment. Under these circumstances it is possible to envisage the time when equipment for A scan echoencephalography will be widely available even in small hospitals and doctors' offices and possibly also in mobile units capable of examining large segments of the healthy population. It would thus be used as a screening device to pick up cases with significant shift of the cerebral midline structures both from the population at large and from patients with indefinite symptoms such as headache who might be suffering from unilateral cerebral disease.

If this situation were to come to pass then it is obvious that the technique must be reasonably simple and quick but more important it must be made quite objective free from observer bias and preferably capable of giving a graphic record which could be readily interpreted by any informed person. We feel that the technique as it has been developed up to the present time lacks true objectivity. We feel moreover that while individual workers may, with experience, acquire much skill and reliability with the technique that if it is to have any future application once the difficulties of compound scanning of the brain have been solved then it must be capable of being used by relatively unskilled workers and in their hands be able to give some readily interpretable graphic record. We therefore determined to try to evolve a technique that was not only objective but was capable of being recorded in a graphic form which could be interpreted by any person familiar with the method.

The identification of the M echo

Initially we were concerned with the source of the M echo as well as the other high amplitude echoes seen in the A scan. The results of these investigations will be reported later elsewhere. The purpose of this paper is to describe

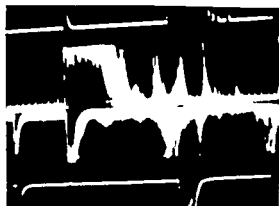


Fig. 2 Time exposure A scan from a subject with a 3-5 mm shift of the third ventricle to the left. Taken from the same position and using the same conventions as in fig. 1.



Fig. 3 Time exposure A scan from the same patient as in fig. 2 taken one week later from the same position and using the same conventions.

in endeavour to evolve a technique that would both reliably and consistently identify the M echo from other echoes and measure its position with respect to the mid line of the cranial contents.

There seem to be few properties upon which most authorities are agreed which are peculiar to and characteristic of, the M echo and which distinguish it from other echoes. JEPSSON (5) stresses that a true M echo has the double peaked shape of an M. Not every other worker agrees that such is the case and some workers have stated it often is seen as a single high peak with twin shoulder peaks at lower amplitude on either side. While we would agree that the M echo usually has one or other of these characteristic shapes its pattern on the oscilloscope is, in our experience, so evanescent that we have been unable to photograph this consistently. Thus we have been unable to use the shape of the M echo as a means of identification. It is probably this factor more than any other that enables the skilled worker to identify one echo out of the multiplicity appearing on the oscilloscope as the M echo. However since, in our hands at least, it has proved impossible to record this shape graphically with any consistency, we have been unable to use this property as a means of identifying the M echo.

JEPSSON (5) also stresses, as have subsequent workers, the fact that the M echo pulsates. However without special techniques involving moving films or other recording devices, it is difficult to provide a graphic trace identifying pulsating echoes and separating them from those that are stationary. It is possible however that this property of the M echo could be used for its more certain identification in the way developed by EIFFERT (2) and EDLER (1).



Fig. 4 Time exposure A scan from patient with no displacement of his midline taken from a point just behind the vertical plane passing through the anterior margin of the p pna and at level just above the p pna. Two clear cut high amplitude echoes in the midline.

Most workers do seem agreed that the M echo is the echo of highest amplitude and the most persistent of those seen across the length of an A scan. We decided to test the validity of this belief by means of time exposures taken during the elicitation of the M echo by scanning. Under these circumstances it would be expected that the highest amplitude echoes would stand out above the lower amplitude echoes and moreover the persistent high amplitude echoes would be clearly distinguished from the evanescent high amplitude echoes coming from varying and differing positions across the scan by forming a more intense image on the negative.

At first we investigated the echoes that were to be found from a scan performed by a transducer placed 5 cm above the mid point of the line joining the external canthus of the orbit and the external auditory meatus. At this position the transducer would be perpendicularly above the foramen of Munro and approximately at the mid point in the incisura of the falx cerebri and it is at this position that one would expect to find and indeed does find radiologically the greatest degree of shift of the cerebral mid line with various unilateral intracranial lesions. However it was found that the time exposures rarely if ever allowed the identification of a single echo as being of highest amplitude and greatest persistence and when they did they often were seen in a position not corresponding to the position of the cerebral mid line as determined by pneumography or angiography.

Fig. 1 shows that in a patient who was known to have no shift of the cerebral mid line structures the most persistent echoes of highest amplitude were found to the near side of the midline both with scans from the left and right temporal regions and no high amplitude echo was distinguishable from the site of the true midline. Perhaps the most damning feature of this procedure was its complete lack of reproducibility from day to day or even hour to hour.

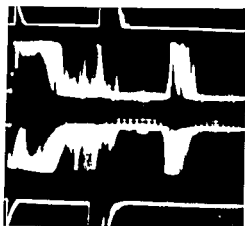


Fig. 5. Same conditions as in fig. 4 from another patient. The highest amplitude and most persistent echoes are in the midline.

Fig. 2 shows a time exposure from a patient shown by pneumography to have a slight midline shift to the left. By the convention used in our display system and to be described below, the M echoes should have appeared on the upper echo trace 1.5–2 mm to the left of the intersection of the two transmission pulses and that on the lower echo trace the same amount to its right. No echoes will be noted at these sites and when the time exposure was repeated a week later (Fig. 3) a very different outline was obtained, this time showing a high amplitude and persistent echo on the lower trace from the right hand transducer to be at the site of the theoretical midline but no corresponding echo on the upper trace from the left hand transducer but instead one well to the left of the midline.

Our complete inability to obtain reliable and reproducible results with time exposures was paralleled by our inability to obtain reliable scans from this position by the conventional techniques. This experience is in accord with that of most other workers who are agreed that while occasional scans can be made from the preauricular position these are the exception and most scans in this area merely produce a confusing complexity of high amplitude echoes. It is unfortunate that this is the case since if ultrasonic scanning of the cerebral midline structures is to be developed into a sensitive investigative tool evidence of the earliest and greatest shifts would be expected to be obtained from scans of the structures in the centre of the incisure of the falx where shifts would be expected to be maximal.

We next investigated the position just above and behind the anterior and superior margin of the pinna. It is from this position that most investigators are agreed that reliable identification of the M echo can almost always be made. From this position the transducer when perpendicular to the skull would be expected to radiate a beam whose central axis passes close to the pineal gland

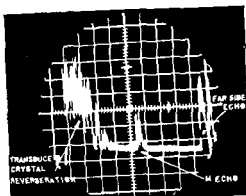


Fig. 6. A typical A-scan across the temporal regions of the head.

and the posterior part of the third ventricle. Here our results were more gratifying and from this position in every case we were able by means of exposures to demonstrate a maximal echo which was single and reproducible with repeated examinations and which we believe to be the M echo (Fig. 4). The M echo did not always stand out so well as in Fig. 4; more often other echoes were seen on either side of it, especially the near side. But in every case one echo alone, which we identify as the M echo, was distinguishable from these other echoes by its greater amplitude and its greater persistence, the latter of course causing more intense exposure of the photographic negative at its site (Fig. 5). It is interesting that echoes are seen in Fig. 5 symmetrically on either side of the M echo, which naturally raises the possibility that they are originating from the two lateral ventricles.

Localisation of the M echo with respect to the midline

Having found what appeared to be a satisfactory, reliable, reproducible and graphic method of identifying the M echo, we then turned our attention to the problem of measuring the position of the M echo in relation to the theoretical cerebral midline. Various investigators have endeavoured to make this measurement. FORD & AMBROSE (3) in their series of patients checked each representation to make sure that when the distance represented on the oscilloscope from one transducer to the far side of the skull was equal, then the sum of the two midline echoes would equal the distance across the skull. This method in our opinion is not exact. Firstly, the mass of echoes associated with the crystal of the transducer is such that in our experience any echoes from the near side of the skull are completely obliterated. The only constant feature of this mass of echoes (Fig. 6) is their onset, which we presume to correspond topographically with the site of the transducer face, which is, of course, in contact with the scalp.

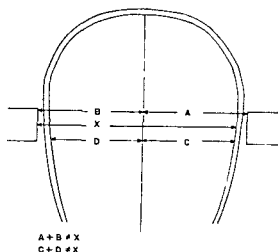


Fig 7 In measuring the position of the midline neither $A+B$ nor $D+C$ equals X

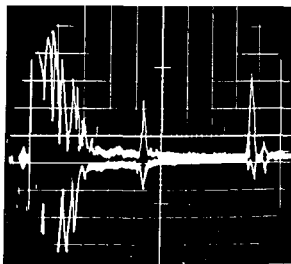


Fig 8 Two superimposed M echoes using a comparator

and external to the outer table of the skull. Secondly, the echoes from the far side of the skull characteristically consist of a pair of echoes which we have assumed (though this has never been proved) to represent the inner and outer tables of the skull.

Thus, we believe that the method described by FORD & AMBROSE cannot properly measure the skull diameter but measures the distance from the crystal face to the inner or outer table of the far side of the skull (X in Fig 7) and then endeavours to equate this distance with either the sum of the distances from the transducer face to the midline on each side ($A+B$ Fig 7) or the sum of the distances from the midline to the inner or outer tables on each side ($D+C$, Fig 7). Since the scalp in the temporal region is about 3 mm thick and the skull another 3 mm thick, we believe that this method, even under the most favourable conditions, either overestimates the sum of the two distances, or underestimates the measurement of the apparent skull diameter by the thickness of the skull and scalp on one side. If there is any uncertainty in identifying either the outer or inner tables of the skull on the opposite side, then these errors may be either increased or decreased. This may be important since it is not always easy to elicit these far side echoes in the characteristic paired fashion that would make the identification of the echo from either the outer or inner table of the far side certain.

A better method would appear to be that suggested by Smith & Kline Instruments, the manufacturers of the Echoline machine. They advise that the scalp

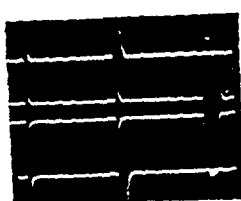


Fig 9 False M-echo across a tank filled with water only. Top and bottom traces are transmission pulses between the two transducers. The two echo traces obtained with a comparator show apparently a reflection from some midline structure which is not present.

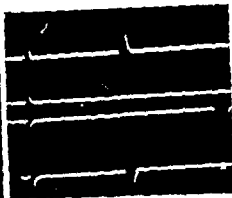


Fig 10 Same as in fig 9 but with the left hand transducer removed from contact with the water bath. Disappearance of both M-echoes. Top and bottom traces are transmission pulses obtained with both transducers applied to the tank.

on the far side of the skull be identified by moving it with a finger until the echo from it distal to the twin echoes from the far side of the skull is identified and its position then marked on the oscilloscope or a scale. The true midline will then lie along the scan halfway between this mark and the onset of the crystal reverberation. While this is undoubtedly an accurate method to our mind it has the disadvantage of showing the operator probably before he attempts to elicit the M echo just where a midline echo would be expected to lie or alternatively where a displaced M echo might be sought. Such a method therefore lays itself open to the occurrence of observer bias which as we have already mentioned we fear might easily develop with this technique (8).

Gordon (4) attempted to overcome these difficulties by introducing a comparator unit which enabled the echoes from the two receivers to be represented on the oscilloscope simultaneously the one below the other and inverted in form (Fig 8). When the two traces on the oscilloscope were properly adjusted the first crystal echo from one transducer would appear exactly above that from the other and the echoes from each far side of the skull would be similarly aligned. Under these circumstances the two M echoes should be seen exactly above each other if the midline structures were undisplaced. Such a representation would appear to be an ideal method of easily detecting shifts in the midline. However in our hands the comparator unit has not proved to be a very reliable tool. Firstly the relay that is needed to switch rapidly from one receiver unit to the other proved unreliable and electrically noisy. Secondly and much the

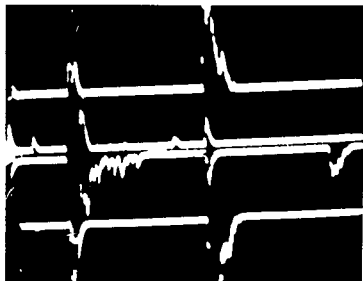


Fig. 11 Two apparent M echoes superimposed above each other (middle traces) and thus presumably coming from a surface equidistant from each transducer in left and right temporal areas respectively i.e. from the midline. Top and bottom traces are transmission pulses across the skull to show position of a midline echo.



Fig. 12 Angiogram from the patient whose echoencephalogram was shown in Fig. 11.

more important drawback, is the fact that with two transducers on opposite sides of the skull at the same time as the transmission pulse is jittered to one transducer, some of this energy is also conveyed to the transducer which is meant to be inactive by means of 'cross talk' in the jittering relay. Thus, at the time the active transducer is receiving echoes from its own pulse it also receives, as a straight transmission pulse, the cross induced energy from the other transducer on the opposite side of the skull. This induced transmission pulse will be received by the active transducer at the same distance along the X axis of the oscilloscope as echoes from the mid point between the two transducers. Thus each transducer is capable of recording a false midline echo which in fact is a straight transmission pulse from the opposite transducer which has been activated by cross talk across the jittering relay. This false echo with the comparator is demonstrated (Fig. 9) by a scan across an otherwise empty, water filled bath apparently showing a midline echoing surface. As soon as one transducer is removed from contact with the side of the tank (Fig. 10) both M echoes disappear but the false side echo remains for the transducer in contact with the side of the tank. The two transmission pulses were superimposed by a double exposure for reference and, of course, were obtained with the two transducers applied to the tank. That this error can falsify M echo determinations from the human skull is shown by Fig. 11 where two apparent

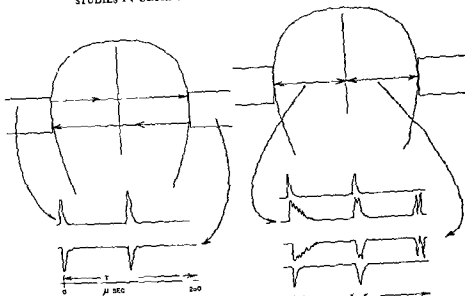


Fig 13

Fig 14

Fig 13 A transmission pulse one way across the skull

Fig 14 The one way transmission pulse travels the same distance as an echo pulse to the true midline and back to the transducer. Thus both transmission pulses and both M echo pulses will all lie the same distance along the time base when the midline is undisturbed.

M echoes are superimposed so it might be concluded that the midline was not displaced. Fig 12 shows the angiogram from the same patient and the gross displacement present of his midline structures. Thus we do not feel that the comparator as developed by GORDON, is of any help in identifying the M echo and indeed is positively misleading in that it gives rise to low amplitude pulses simulating echoes from the midline.

Both LITHANDER (6) in 1960 and JEPSSON (5) in 1961 chose another method to try and indicate the position where the true midline might be expected and to eliminate the tedium of measurements from deflections whose true significance or position were unclear. They superimposed a third oscilloscope tracing upon the two traces each representing echoes from beams entering from either side of the skull. This third trace was obtained not by recording the echoes received from pulses of ultrasound sent out by the same transducer as was the case with the two conventional echo traces but used one probe as a transmitter and the other as a receiver so that the linear deflection of this trace represented the time taken for the sound to traverse one way across the skull and thus would equal the time taken for a sound impulse to arrive at the true midline and to

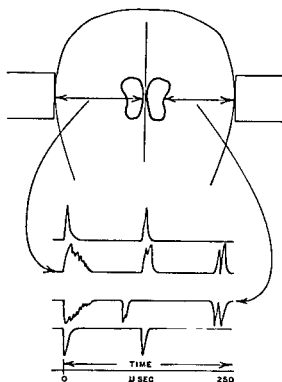


Fig. 15

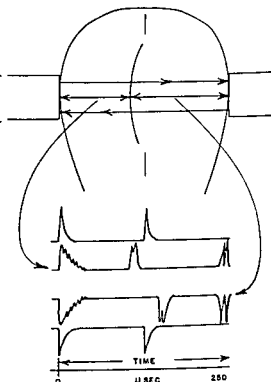


Fig. 16

Fig. 15 Echoes from different structures will give echo pulses which neither lie at the same distance along the time base as the transmission pulses nor symmetrically before and after the transmission pulses

Fig. 16 In shifts of the mid line the two M echo pulses are seen symmetrically an equal time before and after the two transmission pulses

be reflected back to the original transmitting transceiver. Thus, true shifts of the midline should be apparent with LITHANDER's control trace by showing symmetrical displacement of the conventional midline echoes, one on each side of the control deflection.

Equipment and technique

In our endeavour to increase the objectivity of the technique we have used both GORDON's and LITHANDER's methods with slight modifications.

We have modified LITHANDER's method so that instead of a single transmission pulse we superimpose two on our photographs. The first is seen in the top trace and is the transmission from left transducer to right hand receiver; the other is seen in the bottom trace from right transducer to left receiver (Fig. 13). The two middle traces are our echo traces, the top one being from the left

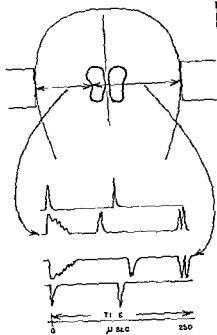


Fig 17

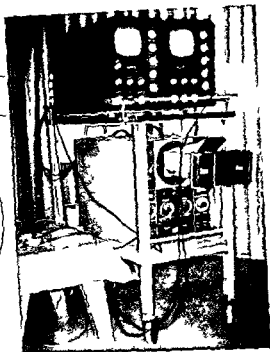


Fig 18

Fig 17 A false M echo which is probably recorded from both echoes at high amplitude from a single paramedian interface

Fig 18 Lay out of the equipment used

hand transducer also acting as a receiver and the lower from the right hand transducer (Fig 14). Thus in any case where the midline structures are not displaced the M echoes from them will lie in the same line as the line intersecting the onset of the two transmission pulses always providing that in every case the initial echoes from the crystals are, in all four traces accurately aligned above each other.

It will be seen that the advantage of this method is that it should enable one to say quite definitely whether two echoes on the middle traces are coming from one and the same object. Thus, Fig 15 if the echo on one side was recorded from a lateral ventricle (say) and on the other side from the midline this would be immediately apparent because while the echo on the lower echo trace is displaced towards the transducer that on the upper echo trace is in the midline. Thus they cannot be coming from the same structure. On the other

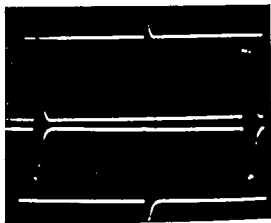
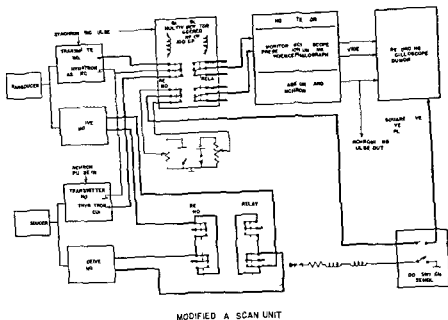


Fig. 19. Absence of cross talk between the two transmitters which are scanning across a water tank in the same way as shown in figs. 9 and 10.

hand, if the midline is displaced (Fig. 16) and echoes are obtained from it on either side, this will be immediately apparent by showing a shift of the two echo traces by an equal amount to either side of the intersecting transmission pulses. The only source of error that is possible with this control (Fig. 17) is the situation where both transducers record echoes from an identical reflecting surface which is not part of the midline structures. We hoped that this would be an unlikely occurrence not only because the greater degree of attenuation of the echo coming from the far side of the midline might make it hard to receive such echoes at high amplitude, but also because we thought many such reflecting surfaces might be curved and therefore liable to give rise to echoes of greatly different strength depending whether these were evoked from the concave or the convex surfaces.

Our other modification is the use of two separate flow detectors. If one detector only is used we found that it was impossible to avoid the appearance of a straight transmission pulse in the position of the M echo without the expense and difficulty of elaborate coaxial shielding and switching. Only if two separate flow detectors are employed and their activity alternately displayed on a common presentation system do we feel that it is possible to avoid completely any possibility of cross talk between the two transducers by means of straight transmission pulses which will, of course, give rise to false M echoes. The layout of our equipment is shown in Fig. 18 and the absence of cross talk in Fig. 19, using the same water bath which in Fig. 9 showed the false M echo where no reflecting surface was present due to transmission pulses between the two transceivers. Fig. 20 shows the wiring diagram of our equipment. A simple foot switch enables us to change from using each transducer alternately as both transmitter and receiver for intra cerebral echoes to a transmission system in which the pulse from the left to the right temporal transducer is represented



MODIFIED A SCAN UNIT

Fig 20 Diagram of the modification of the comparator with transmission pulse control

at the top of the trace and that from the right to the left temporal transducer at the bottom. The presentation system is adjusted so that these two transmission pulses are exactly superimposed and approximately in the midline of the oscilloscope.

The presentation system is monitored on to a second oscilloscope to which a camera is connected. The examination is carried out in two parts, each being recorded by the camera on a separate single exposure. Firstly, with one transducer applied to the skull just behind the vertical line passing through the front of the pinna and at a level just above the pinna, a time exposure is taken for about one minute during which time the operator endeavours to elicit and hold on the oscilloscope echoes of maximal amplitude. The procedure is then repeated with the second transducer at the homologous area on the opposite side and a further time exposure made on the same film. After these exposures have been made two transmission pulses are superimposed on the same polaroid negative. This polaroid photograph is then developed and examined for the presence of a single echo of maximal amplitude and persistence (Figs 4 and 5) in each echo trace. The approximate position of these maximal

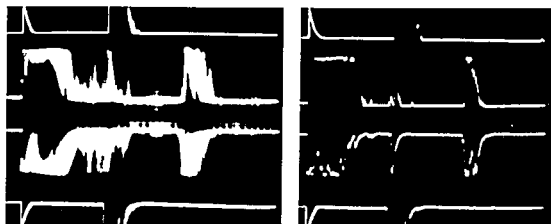


Fig 21 Time exposure and instantaneous exposure which are considered satisfactory and fulfil the five separate criteria enumerated in the text. The scan shows an undisplaced M echo from a patient shown by pneumography to have no displacement of the midline structures.

echoes is then noted with respect to the line intersecting the two transmission pulses.

The whole procedure is then repeated but this time no time exposure is made. Instead we endeavour to display on the trace high amplitude echoes in the same position as the maximal echoes seen in the time exposure. When such echoes are being displayed satisfactorily an instantaneous exposure is made, first on the one side, then on the other, and finally the two transmission pulses are also superimposed on the same negative. The photograph is developed and examined to see that the following criteria have been fulfilled.

Firstly, all four initial crystal deflections must be aligned. Secondly, the echoes from the far side of the skull in the two echo traces must be superimposed. Thirdly, the M echo deflections must (1) lie each in the same position as the maximal echoes demonstrated in the time exposure, (2) be of adequate amplitude and sharpness with a clean take off from the baseline, and (3) lie either in the line intersecting the two transmission pulses or symmetrically to either side of it (Fig 21). If the photograph does not fulfil all these criteria the examination is immediately repeated until a satisfactory picture is obtained. It is for this reason that we use polaroid film so that no delay occurs in repeating an unsatisfactory examination. The instantaneous photograph is taken, of course, to allow accurate measurement of the M echo pulses at their take off from the baseline. This cannot be seen accurately in the time exposures where the contours of the maximal echoes are blurred, especially at their bases.

It will be noted that both in the time exposure and the instantaneous photographs we display the echoes from each side separately and not simultaneously as could easily be done. We do this in order to try and eliminate all

observer bias since we found that when the two echoes were displayed simultaneously the operator often tried to manipulate the transducers so that the high amplitude echoes lay directly above and below each other as they do when both arise from undisplaced midline structures. We wanted our operators to elicit the most persistent maximal amplitude echoes no matter where they lay along the scan only thus did we feel we could make the test truly objective and free from observer bias. Moreover when the instantaneous exposures were being made it is not always easy to display satisfactory echoes of sufficient amplitude from both sides simultaneously.

Acknowledgements

This work was supported by grants from the Medical Research Council of Canada. The authors wish to express their gratitude to Dr. David Makow of the Applied Physics Division and Mr. Ross Smyth of the Radio and Electrical Engineering Division of the National Research Council of Canada for technical help and advice.

SUMMARY

An attempt has been made to design a technique for A scan echo-encephalography which is objective and reproducible and which provides an easily read graphic record. This has been achieved by using time exposures to identify the maximal and most persistent echo which is considered the M echo. The position of the M echo is then recorded with instantaneous exposures and transmission pulses are used to determine its position with relation to the theoretical midline. The M echo however can only reliably be elicited from the midline structures in the region of the posterior margin of the third ventricle.

ZUSAMMENFASSUNG

Es wurde versucht eine objektive, wiederholbare und leicht lesbare Registriermethode für die A Scan Echo-encephalographie zu entwickeln. Dies konnte bewirkt werden, indem man Zeitaufnahmen machte, die das Maximalecho, das am längsten andauerte, registrierte, dieses wird dann kurz als M-echo bezeichnet. Die Lokalisation des M echos wird später mit Momentaufnahmen festgehalten und man benutzt dann die Transmissionimpulse um dessen Lage in Bezug zur theoretischen Mittellinie zu ermitteln. Ein gutes M echo wird jedoch nur von den in der Mitte liegenden Strukturen, die hinter dem dritten Ventrikel liegen, hervorgebracht.

RÉSUMÉ

Les auteurs ont essayé de mettre au point une technique d'écho-encéphalographie A qui soit objective, reproductible et qui donne un enregistrement graphique facile à lire. Ils y sont parvenus en utilisant des durées d'exposition permettant d'identifier l'écho maximal et le plus persistant qui est considéré comme l'écho M. La position de l'écho M est ensuite enregistrée.

par une exposition instantanée et on utilise des impulsions de transmission pour déterminer sa position par rapport à la ligne médiane théorique. Ce n'est cependant que dans la région de la partie postérieure du troisième ventricule que l'on peut déduire sûrement l'écho M des structures de la ligne médiane.

REFERENCES

- 1 EDLER I. Ultrasound cardiography. *Acta med scand Suppl* 170 1961
- 2 EFFERT Von S. Der derzeitige Stand der Ultraschallkardiographie. *Arch Kreisf Forsch* 30 (1959) 213
- 3 FORD R. and AMBROSJ J. Echoencephalography. *Brain* 86 (1963) 189
- 4 GORDON D. Echo encephalography: ultrasonic rays in diagnostic radiology. *Brit med J* 1 (1959) 1500
- 5 JEPSSON S. Echoencephalography IV. The midline echo: an evaluation of its usefulness for diagnosing intracranial expansivities and an investigation into its sources. *Acta chir scand Suppl* 272 1961
- 6 LITHANDER B. A control method for echo encephalography. *Acta psychiat scand* 35 (1960) 235
- 7 MAKOW D. M., WHITE D. N., WYSLOUZIL W. and BLANCHARD J. B. A novel immersion scanner and display system for ultrasonic brain tomography. *Acta radiol Suppl* (this volume)
- 8 WHITE D. N., CHILSBROUGH J. C. and BLANCHARD J. B. Studies in ultrasonic echoencephalography. I. *Neurology* 15 (1965) 81

HIRNDURCHBLUTUNGSMESSUNG MIT ISOTOPEN UND IHR KLINISCHER WERT

von

O. WILCKE

Die bisher entwickelten Methoden zur Bestimmung der Hirndurchblutung mit Isotopen lassen sich in 2 Gruppen einteilen

1) In Methoden, die eine quantitative Bestimmung des cerebralen Blutvolumens bezwecken

2) In Methoden zur qualitativen Bestimmung der Hirndurchblutung

Die quantitativen Methoden basieren auf dem Prinzip der Methode von KETY & SCHMIDT und ermöglichen durch den einfachen und schnelleren Nachweis der radioaktiven Isotope die Bestimmung des cerebralen Blutvolumens, des Herzminutenvolumens und auch des Sauerstoffverbrauchs des Hirns (NYLIN, MUNCK-LASSEN, HEDLUND u. a.). Die hierzu notwendige Punktion der Carotiden und Venae jugulares stellt jedoch eine erhebliche Belastung für den Patienten dar, so dass die Methode zur klinischen Routineuntersuchung ungeeignet ist. Bei den anderen quantitativen Isotopen-Methoden (THOMPSON, OLDENDORF, HORTEN) werden nach Bestimmung des Gesamtblutvolumens aus dem Verlauf der über dem Schädel registrierten Aktivitätskurven durch Bestimmung des Volumenindex Zahlenwerte gewonnen, die auf das cerebrale



Abb 1 Apparat zur qualitativen Bestimmung der Hirndurchblutung

Blutvolumen schliessen lassen. Alle diese Methoden sind mit erheblichem Zeitaufwand verbunden und haben eine gewisse Fehlerbreite, so dass sich nur aus dem Querschnitt einer grosseren Untersuchungsreihe Aussagen machen lassen. Für die klinischen Belange wichtige Aussagen über die regionalen Zirkulationsverhältnisse oder die unterschiedliche Durchblutung beider Hirnhälften oder auch über kurzfristige Veränderungen der Hirnzirkulation lassen sich mit diesen Methoden nicht machen.

Eigene Methode

Zur schnellen klinischen Information über die cerebralen Durchblutungsverhältnisse haben wir eine qualitative Methode entwickelt, bei der in einem Arbeitsgang sowohl die Zirkulationszeit, als auch die Gesamtdurchblutung jeder Hirnhälfte bestimmt wird. Wir verwenden 50—100 μ c ^{51}Cr Hippuran und bestimmen nach Injektion in die Cubitalvene die Zirkulationszeit mit Hilfe von 2 Szintillationszählern, die über der Cirotis und, tangential zum Schadel, über dem Confluens sinuum angesetzt werden (Abb 1). Gleichzeitig wird mit 2 weiteren bifrontal aufgesetzten Szintillationszählern der Durchfluss der Radioaktivität durch jede Hirnhälfte gemessen. Die besondere Anordnung der Zähler, sowie entsprechende Bleiabschirmungen und trapezförmige Kollimatoren ermöglichen eine strenge Trennung beider Hirnhälften. Durch die Verwendung von Einkanalanalysatoren wird durch Aus-

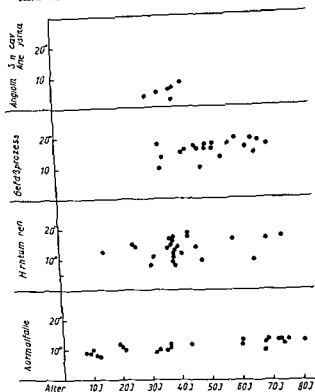


Abb 2 Zirkulationszeit bei Normalfällen Hirntumoren arteriosklerotischen Gefäßprozessen und Angiomen oder Cavernösen Sinus cavernosus Aneurysmen

blendung des Gammasppektrums die Streustrahlung aus dem Körper unterdrückt und nur die Direktstrahlung einer Hirnhälfte erfasst. Die Registrierung erfolgt über Vorverstärker und Ratemeter mit einem Vierfachsreiber. Die Zeitkonstante der Ratemeter zur Bestimmung der Zirkulationszeit beträgt 0,3 sec, die des Schreibers bis zum Vollausschlag 1 sec. Um ein übersichtliches Kurvenbild über den Hemisphären zu erhalten, hat sich hier die Ratemeter-Einstellung auf eine Zeitkonstante von 1–3 sec als nützlich erwiesen. Die Untersuchung dauert wenige Minuten und kann leicht ambulant durchgeführt werden.

Ergebnisse

Die Zirkulationszeit gemessen am Aktivitätsmaximum über der Carotis bis zum Aktivitätsmaximum über dem Confluens sinuum beträgt bei dieser Messung (Abb 2) bei Normalpersonen 7–12 sec. Bei Patienten mit Hirn-

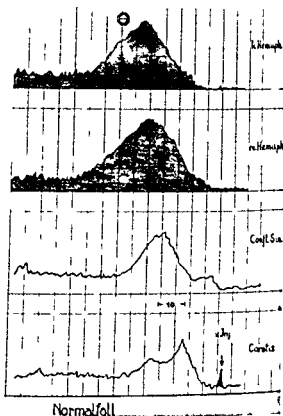


Abb 3 Normalfall = i.v. Injektion Zirkulationszeit 10 sec Gleicher Kurvenverlauf über der rechten und linken Hemisphäre

tumoren sind die Zirkulationszeiten deutlich verlängert und es wurden, besonders wenn Hirndruck besteht, Zeiten bis 23 sec gemessen. Auch bei Patienten mit klinisch nachgewiesenen, sklerotischen Gefäßprozessen ist die Zirkulationszeit verlängert, während erwartungsgemäss bei Angiomen und Sinus cavernosus Aneurysmen die Zirkulationszeit verkürzt ist.

Im Normalfalle (Abb 3) findet sich ein gleicher Kurvenverlauf über beiden Hemisphären sowie eine normale Zirkulationszeit von etwa 10 sec. Sowohl beim ersten Durchfluss der Radioaktivität durchs Hirn, als auch im weiteren Verlauf nach Gleichverteilung in der Blutbahn, finden sich über beiden Hemisphären gleich hohe Kurvenverläufe, die einer seitengleichen Verteilung der Aktivität entsprechen. Bei Hirntumoren finden sich meist Differenzen in der Durchblutung beider Hirnhälften (Abb 4). Bei stark durchbluteten Tumoren, wie Meningiomen, bleibt auch dem ersten Durchfluss der Radioaktivität durchs Hirn die Aktivität über der Tumorseite höher. Die Zirkulationszeit ist bei Meningiomen häufig normal. Erst bei klinisch erkennbaren Hirndrucksymptomen ist die Zirkulationszeit verlängert. Bei Glioblastomen findet sich fast stets eine verlängerte Zirkulationszeit. Für gliomatöse Tumoren ist die verlängerte Zirkulationszeit und das langsamere Absinken der Kurve

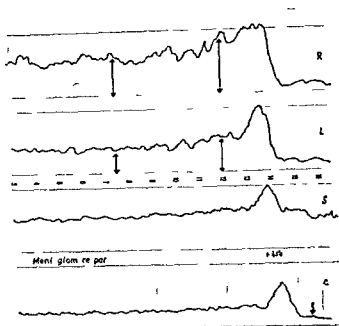


Abb 4 Meni glom re par Normale Zirkulationszeit (70 sec). Entsprechend dem Blutreichtum des Tumors ist die Radioaktivität über der rechten Hemisphäre anhaltend höher als über der linken

über der Tumorseite auf eine gleichbleibende Höhe typisch (Abb 5). Sehr charakteristisch ist das Bild bei sklerotischen Gefäßprozessen (Abb 6), wo die verlängerte Zirkulationszeit mit nur geringen Ausschlägen über beiden Hirnhälften stets die Diagnose ermöglicht. Angiome sind durch eine verkürzte Zirkulationszeit und anhaltende Erhöhung der Radioaktivität über der Angiomseite gekennzeichnet. Bei Carotis Sinus cavernosus Aneurysmen (Abb 7) zeigt die verkürzte Zirkulationszeit den arterio-venösen Kurzschluss an. Bleibt im weiteren Verlauf die Aktivität über beiden Hirnhälften gleich hoch, so ist darauf zu schließen, dass die gesunde Seite die Blutversorgung der Aneurysmaseite mit übernimmt. Anderenfalls bleibt die Aktivität über der Aneurysmaseite zunächst niedriger als über der gesunden Seite. Auch beim frischen Hirntrauma kann diese qualitative Hirndurchblutungsmessung wichtige diagnostische Hinweise geben (Abb 8), indem bei Vorliegen eines Hirnodems oder eines subduralen Hämatoms die betroffene Seite sich durch eine schlechtere Durchblutung und damit durch entsprechend flachen Kurvenverlauf darstellt.

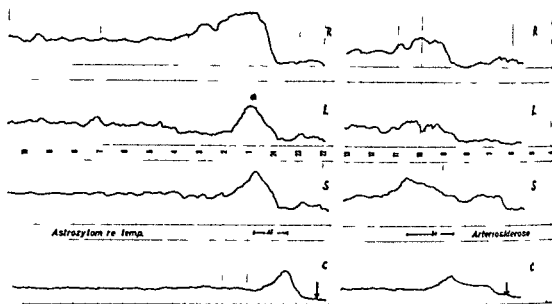


Abb 5 Astrocytom rechts temporal Verlangerte Zirkulationszeit (15 sec) Die Zirkulation ist auf der Tumorseite verlangsamt

Abb 6 Arteriosklerosis cerebri Verlangerte Zirkulationszeit (70 sec) Der niedrige Kurvenverlauf über beiden Hemisphären zeigt die mangelhafte Durchblutung

Besprechung der Ergebnisse

Unter Verzicht auf quantitative Auswertungen ermöglicht diese qualitative Method zur Registrierung der cerebralen Zirkulationsverhältnisse schnell und mit grosser Sicherheit diagnostische Aussagen. Sie ist daher besonders für die poliklinische Untersuchung eine wesentliche diagnostische Hilfe, zumal sie schnell auszuführen und mit keiner Belastung für den Patienten verbunden ist. Aus der Kombination der Zirkulationszeit des Hirns und der kurvenmässig dargestellten Durchblutungsgrösse der beiden Hirnhälften ergeben sich wesentliche diagnostische Hinweise. Eine verlängerte Zirkulationszeit weist stets auf eine mangelhafte Hirndurchblutung hin. Diese kann entweder durch einen sklerotischen Gefässprozess oder durch eine intrakranielle Drucksteigerung bedingt sein. Bei sklerotischen Gefässprozessen ermöglicht der flache, sehr charakteristische Kurvenverlauf über den Hemisphären stets die Diagnose, während für Hirntumoren die Differenz in der Durchblutung beider Hirnhälften und damit der unterschiedliche Kurvenverlauf typisch ist. In gewissen Grenzen sind hierbei artdiagnostische Aussagen möglich. Mit grosser Sicherheit weist eine verkürzte Zirkulationszeit auf einen arterio-venösen Kurzschluss im Sinne eines Angioms oder eines Carotis Sinus cavernosus Aneurysmas hin. Hier ist der über den Hemisphären registrierte Kurvenverlauf

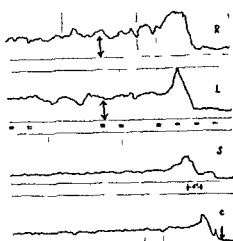


Abb 7 Carotid-sphenoidal Aneurysma links. Verkürzte Zirkulationszeit (6 sec) Spitze weniger hoch über der linken Hemisphäre (arterio-venöser Kurzschluss). Im weiteren Verlauf lässt die gleiche hohe Radioaktivität über beiden Hemisphären das aufschließen, dass die linke Hemisphäre von der rechten Carotis mit versorgt wird.

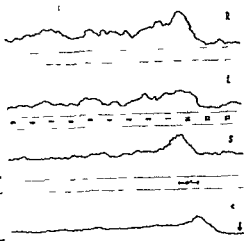


Abb 8 Subduales Hamatom links. Flacher Kurvenverlauf über der Hamatomseite.

für jedes der beiden Krankheitsbilder typisch. Der besondere Wert dieser Methode liegt damit neben der Tumordiagnostik vor allem in der Möglichkeit Gefäßprozesse verschiedener Ätiologie sicher zu erkennen und gegenüber Hirntumoren abzugrenzen. Bei älteren Patienten für die eine Carotis Angiographie gefährvoll sein kann, ist damit die Möglichkeit gegeben, durch diese sehr einfache Untersuchung ein anschauliches Bild über die Zirkulationsverhältnisse des Hirns zu gewinnen.

ZUSAMMENFASSUNG

Es wird eine Methode beschrieben, bei der nach intravenöser Injektion von wenigen μC eines radioaktiven Stoffes in einem Untersuchungsang sowohl die Zirkulationszeit des Hirns als auch die qualitative Durchblutung beider Hirnhälften registriert wird. An Hand von Beispielen werden die diagnostischen Möglichkeiten zur Erkennung von Hirntumoren und cerebralen Gefäßprozessen verschiedenen Ursprungs dargestellt.

SUMMARY

The intravenous injection of a few millicuries of a radioactive substance makes it possible to assess simultaneously the circulation time of the brain as well as the relative circulation in either hemisphere. Examples are given to demonstrate the diagnostic possibilities in cerebral tumours and in vascular conditions of varying origin.

RÉSUMÉ

Description d'une méthode permettant après injection intraveineuse de quelques μCi d'un corps radioactif de déterminer en une seule séance le temps de circulation cérébrale et la qualité de l'irrigation des deux moitiés du cerveau. Des exemples illustrent la possibilité de diagnostiquer des tumeurs cérébrales et des processus vasculaires cérébraux d'origines diverses.

LITERATURE

- HEDLUND S, LJUNGGREN K, BERGGREN B and BRUNDELL P O. Scintillation detectors for determination of cerebral blood flow. *Acta radiol. Therapy Phys Biol* 2 (1964) 51.
- HORTON G E and JOHNSON JR P C. The application of radioisotopes to the study of cerebral blood flow: comparison of three methods. *Angiology* 15 (1964), 70.
- KETY S S and SCHMIDT C I. The determination of cerebral blood flow in man by the use of nitrous oxide in low concentration. *Amer J Physiol* 143 (1945) 53.
- LASSEN N A. Cerebral blood flow and oxygen consumption in man. *Physiol Rev* 39 (1959) 138.
- HOEDT RASMUSSEN K, SORESENSEN S C, SKINHOJ E, CRONQVIST S, BODFORSS B, LAG E and INGVAR D H. Regional cerebral blood flow in man determined by krypton⁸⁵. *Neurology* 13 (1963) 719.
- MUNCK O. Use of radioactive Krypton⁸⁵ for the determination of blood flow. *Radioactive Isotope in Klinik und Forschung* Bd V (1963) Verlag Urban & Schwarzenberg, München Berlin S 127—137.
- NYLIN G, HEDLUND S and REGNSTRÖM O. Cerebral circulation studies with labelled red cells in healthy males. *Acta radiol* 55 (1961) 281.
- SILFVERSKIÖLD B P, LOFSTEDT S, REGNSTRÖM O and HEDLUND S. Studies on cerebral blood flow in man using radioactive labelled erythrocytes. *Brain* 83 (1960) 293.
- OLDENDORF W H and CRANDALL P H. Bilateral cerebral circulation curves obtained by intravenous injection of radioisotopes. *J Neurosurg* 18 (1961) 19.
- CRANDALL P H, NORDYKE R A and ROSE A S. A comparison of the arrival in the cerebral hemispheres of intravenously injected radioisotope. *Neurology* 10 (1960) 223.
- PITLYK P J, KERR I W, TAUNE W N, SEDLACK R E and SVEN H J. Localisation of brain tumors with iodine 131 polyvinylpyrrolidone. *Arch Neurol* 9 (1963) 437.
- TAUNE W N, PITLYK P J, SEDLACK R E, KERR I W and SVEN H J. Localisation of brain tumor with ^{131}I labelled polyvinylpyrrolidone. *J Nucl Med* 4 (1963) 185.
- THOMPSON S W. A radioisotope method for studying cerebral circulation. *Arch Neurol* 5 (1961), 580.
- WILCKE O. Eine einfache Methode zur Bestimmung der Hirndurchblutung mit Radioisotopen. *Acta neurochir* 12 (1964) 31.
- und ZEH H. Klinische und experimentelle Untersuchungen zur Bestimmung der Zirkulationszeit des Hirns mit radioaktiven Isotopen. *Zbl Neurochir* 4 (1963) 145.

THERMOGRAPHY IN THE DIAGNOSIS OF CEREBROVASCULAR OCCLUSIVE DISEASE

by

ERNEST H. WOOD and RICHARD P. HILL

Thermography is a relatively new medical procedure used to record the radiant heat emitted by the human skin. A thermogram is a graphic recording of spontaneous infrared radiation that is obtained by scanning the skin surface. Because heat emission of the body is automatic and the thermograph provides an atraumatic means of collecting heat for measurement, the method constitutes a simple, painless and harmless technique for determining the skin temperature and indirectly the cutaneous blood supply.

Previous clinical uses of thermography have been concerned principally with the detection of increased skin temperatures. Such abnormal radiant emissions have been found to occur with superficial neoplasms (WILLIAMS et coll 1961; BARNES & GERSHON COHEN 1963), some deep tumors (BARNES & GERSHON COHEN 1963), infections (WILLIAMS et coll 1961), over the sites of placental implantation (JOHNSON 1964) and in connection with various other conditions associated with increased blood supply to the skin. Decreased radiant heat emissions have been shown to occur with impaired blood flow in the extremities (BARNES 1963). Only recently have alterations in the heat of



Fig. 1 Direct facial thermography. Patient seated in a comfortable chair and head immobilized. The motor driven heat detecting device is directed toward the patient's head and the upper portion of the face is scanned automatically. On table at left are accessories including a calibrated heat reference source (front), a manual bolometer (middle central and middle right), a thermal resistor (middle left), a semiquantitative graphic recorder of thermographic scanning data (rear).

the skin of the forehead been correlated with changes in cerebral circulation (Wood 1964).

It is the purpose of this paper to describe the practical methods that have been found most useful in applying thermography to clinical problems and to review the anatomic basis for its effectiveness. Other aims are to assess the reliability of thermography as a means of surveying patients for the presence or absence of carotid artery disease, to compare the method with other accepted diagnostic procedures, and to suggest further clinical investigations for the evaluation and utilization of thermal data.

General considerations

Thermography makes use of a high resolution scanning device (Fig. 1) that records skin temperature information and presents the data photographically.

The final products of thermography are a print and a negative that are available for immediate inspection through use of the Polaroid method. The thermogram is a composite dark (cool) and light (warm) image formed by parallel lines, each of which comprises approximately 350 point recording of thermal data (Fig. 2).

Technically, thermography is carried out simply and without preparation of the patient except for exposure of the part to be examined to cool dry air in a draft free room. The ambient temperature should be maintained between 70° and 72° F (or approximately 21° and 22° C). Exposure of the skin for 10 to 20 minutes under these standard conditions serves to

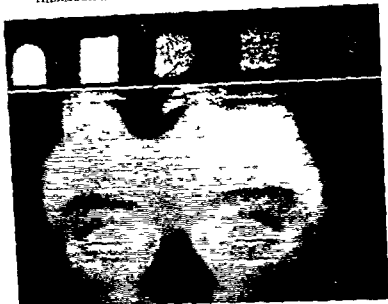


Fig. 2. No. 1. The thermogram. Infrared radiation spontaneously emitted by skin of upper face is recorded and presented photographically as a light (warm) and dark (cool) pattern. The nose, cheeks and avascular corneas of the eyes are cool as are the hair-insulated eyebrow, eyelash and scalp areas. The calibrated heat reference sources at top of figure represent from the scale: left approximately 98.6, 97.5, 93, 91 and 90.5 degrees Fahrenheit (37.3, 33.3, 33.9, 33.3 and 32.5 degrees Centigrade).

remove perspiration and otherwise create stable conditions to assure accurate measurement of cutaneous infrared emissions. Bedridden patients and others who cannot cooperate for direct scanning as shown in Fig. 1 can be examined in the horizontal position through the use of a front coated heat reflecting mirror.

In the average case, symmetry or asymmetry of the heat emission patterns of the two sides of the forehead will be clearly manifested under the standard conditions described above. In order to assure the demonstration of minor changes, two primary thermograms after simple air cooling usually are made. Each tracing is taken at an instrument setting of intermediate sensitivity. The brightness of the light source is varied for each primary examination to provide one light and one dark scan; a meter on the thermograph denotes during scanning what degree of photographic change can be expected.

Thermograms can be made with many different combinations of sensitivity and brightness as indications warrant. In the present study, additional thermograms have been made to determine the rate of skin heat recovery after cooling to subambient levels. Simple cold compresses applied to the forehead constitute one of a variety of satisfactory methods of producing further cooling of the skin. The forehead temperature is evenly reduced five degrees below the average air-cooled primary readings (usually to about 88° F or 31° C). A hand-held infrared radiometer or bolometer (Fig. 1) or the thermograph itself may be used to make certain that the secondary wet-cooled forehead temperatures are the same on the two sides. With the thermograph then directed only towards the orbital and supraorbital regions, re-

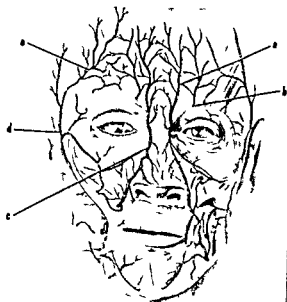


Fig 3 Superficial dissection of face. Arterial vascular supply of soft tissues is from both internal carotid and external carotid systems. While the latter is by far larger, the medial supraorbital areas are supplied by the frontal (a) and supraorbital (b) branches of the ophthalmic artery. Although anastomoses are present between the two sides between the frontal and angular (c) arteries and between the supraorbital artery and the frontal branches (e) of the superficial temporal artery (d), the temperature of the forehead is basically related to the ophthalmic artery flow on each side.

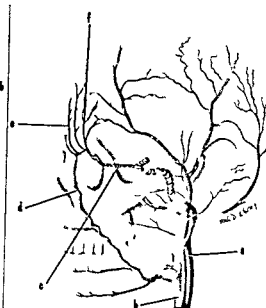


Fig 4 External and internal carotid system in relation to bony landmarks. The extracranial extensions of the frontal (e) and supraorbital (f) arteries over the superior rim of the orbit are shown together with their deeper relationships to the ophthalmic artery (c) and the carotid system. As an early large branch of the internal carotid artery (a), the ophthalmic artery is primarily dependent for its blood flow on the parent vessel. In the presence of occlusion of the internal carotid artery, the ophthalmic frontal and supraorbital arterial flow is reduced. Collateral circulation superficially is through frontal anastomoses with the angular artery (d), a branch of the external carotid artery (b), and through supraorbital anastomoses with the superficial temporal artery (e). Profoundly, the main collateral circulation is from the internal maxillary artery to the ophthalmic artery.

scanning is carried out continuously (usually for 20 minutes) until heat emission has returned to the primary (air cooled) level on one or both sides. In the present series, no patient with an entirely normal primary thermogram has been shown to have abnormal findings after secondary wet cooling. In occasional cases, however, secondary wet cooling has demonstrated not only delayed recovery of skin heat on the side of deficient circulation, but also has made more readily discernible the insufficiency patterns described below.

Normal facial thermograms vary according to fixed heat emission patterns. The nose, cheeks, ears, and the avascular corneas of the eyes are cool, as are the hair-insulated eyebrow, eyelash, and scalp areas. The anterior portion of the forehead is warm; heat normally is trapped by folds at the canthi and along the free margins of the eyelids. Essentially symmetrical facial thermograms were found almost without exception in examining large numbers of healthy individuals of all ages.

Anatomically the medial supraorbital integument is supplied almost exclusively by branches of the internal carotid artery (Fig 3). The frontal and supraorbital arteries are terminal extensions of the ophthalmic artery, the latter being the first sizable branch of the internal carotid artery (Fig 4). The fact that the integumentary and anterior ocular branches of the ophthalmic artery provide the only surface display of the internal carotid artery constitutes the basis for the facial thermogram being an index of the blood flow through the carotid artery.

The anterior ocular branches of the ophthalmic artery also may reflect carotid artery blood flow. The inner canthus is supplied by branches of the medial palpebral and dorsal nasal arteries. The anterior ciliary arteries and a branch of the supraorbital artery also contribute warmth to the medial canthus. In contrast to the medial supraorbital integument which is supplied almost entirely by the internal carotid artery, the medial palpebral commissure is also reached by the terminal angular branch of the external carotid artery. Because of the dual blood supply, the inner canthus does not provide an index of internal carotid artery blood flow as often as the supraorbital skin. In occasional cases, however, the asymmetry of infrared radiation from the medial canthus and exposed surfaces of the globes is quite striking.

An abnormal facial thermogram develops most frequently when there is asymmetrical radiant heat emission from the two medial supraorbital portions of the forehead owing to a deficient cutaneous blood supply which in turn is secondary to impaired carotid artery blood flow (Fig 5). In support of this anatomic explanation of the thermographic phenomena are changes that can be induced by vascular compression. Mechanical compression of the common carotid or internal carotid artery in young healthy subjects will produce a thermographic pattern identical to that found following surgical ligation or in patients with atheromatous occlusion. In addition, compression of the frontal and supraorbital arteries against the bony rim of the orbit will produce forehead patterns similar to those caused by carotid occlusion.

Material

The present investigation is based on the analysis of the thermograms and case records of a large number of patients with cerebrovascular occlusive disease in whom the anatomic nature of the pathologic process was established by angiography, operation or necropsy. In addition, attention has been given to the thermographic changes associated with generalized vascular alterations, salient anatomic variations and severe local abnormalities of circulatory physiology caused by non-occlusive vascular lesions. The most significant thermographic findings have occurred in patients with extra-cranial lesions of the carotid arteries, many of which are amenable to surgical treatment.

Unilateral occlusion of the internal carotid artery was the most frequently encountered lesion producing an abnormal thermogram among all of the cases that have been studied (Fig 6). As noted above, patients who had undergone surgical ligation of the internal carotid artery or common carotid artery exhibited parallel thermographic changes. Patients with external carotid artery ligation had essentially normal thermograms. Unilateral atherosclerotic occlusion

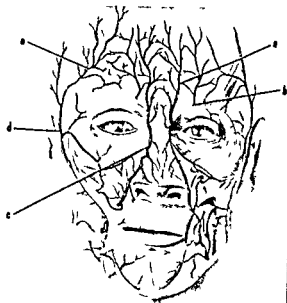


Fig 3 Superficial dissection of face. Arterial vascular supply of soft tissues is from both internal carotid and external carotid systems. While the latter is by far larger, the medial supraorbital artery is supplied by the frontal (a) and supraorbital (b) branches of the ophthalmic artery. Although anastomoses are present between the two sides between the frontal and angular (c) arteries and between the supraorbital artery and the frontal branches (e) of the superficial temporal artery (d), the temperature of the forehead is basically related to the ophthalmic artery flow on each side.

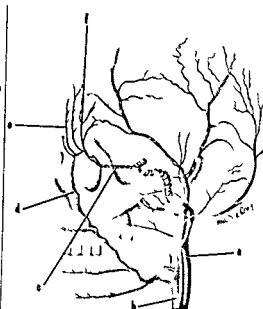


Fig 4 External and internal carotid system in relation to bony landmarks. The extracranial extensions of the frontal (e) and supraorbital (f) arteries over the superior rim of the orbit are shown together with their deeper relation hips to the ophthalmic artery (c) and the carotid system. As an early large branch of the internal carotid artery (a), the ophthalmic artery is primarily dependent for its blood flow on the parent vessel. In the presence of occlusion of the internal carotid artery, the ophthalmic frontal and supraorbital arterial flow is reduced. Collateral circulation superficially is through frontal anastomoses with the angular artery (d) a branch of the external carotid artery (b) and through supraorbital anastomoses with the superficial temporal artery (g). Profoundly the main collateral circulation is from the internal maxillary artery to the ophthalmic artery.

scanning is carried out continuously (usually for 20 minutes) until heat emission has returned to the primary (air cooled) level on one or both sides. In the present series, no patient with an entirely normal primary thermogram has been shown to have abnormal findings after secondary wet cooling. In occasional cases, however, secondary wet cooling has demonstrated not only delayed recovery of skin heat on the side of deficient circulation, but also has made more readily discernible the insufficiency patterns described below.

Normal facial thermograms vary according to fixed heat emission patterns. The nose, cheeks, ears, and the avascular corneas of the eyes are cool, as are the hair-insulated eyebrow, eyelash, and scalp areas. The anterior portion of the forehead is warm; heat normally is trapped by folds at the canthi and along the free margins of the eyelids. Essentially symmetrical facial thermograms were found almost without exception in examining large numbers of healthy individuals of all ages.



Fig 6 Left internal carotid artery occlusion. The thermogram discloses an area of cool supraorbital skin on the left side. Angiography disclosed complete occlusion of the internal carotid artery at its origin.

static role of the circle of Willis in its attempt to preserve cerebral circulation following occlusion of both middle and both anterior cerebral arteries from the stenotic side usually can be demonstrated at angiography. Associated with the cerebral steal on the still patent internal carotid artery is a reduction of outward blood flow in (or steal from) the ophthalmic artery. The circumstances are somewhat analogous to the steal (or bypass) phenomenon associated with an arteriovenous fistula in the cavernous sinus or a large angioma of the brain with an arteriovenous shunt (Fig 7).

In patients with bilateral asymmetrical atherosclerosis who have had surgical restoration of the carotid lumen to normal size on the stenotic side, the dark supraorbital patch associated with the stenosis disappears, follow-up angiography indicates that the repaired artery then is capable of supplying its own ophthalmic branch as well as the opposite cerebral hemisphere. Inasmuch as the majority of such patients present themselves with symptoms and neurological signs referable only to the fully occluded side, a thermographic change contralateral to clinical manifestations should lead to a diagnosis of bilateral carotid insufficiency with the objective of instituting treatment to improve circulation on the still patent side. Thus far, an opportunity to perform thermography in a patient with complete obstruction of both internal carotid arteries has not presented itself.

Proximally stenosis or occlusion of the orifice of the common carotid artery by atherosclerosis, dissecting aortic aneurysm or other diseases have been



Fig. 1. Right sided carotid occlusion. Right supraorbital area darkened in territory supplied by frontal and supraorbital arteries owing to complete obstruction of the internal carotid artery with resultant reduced vascular supply to the surface. Calibrated reference sources and hand bolometer readings disclosed that on the normal left side the skin temperature was 94°F (34.4°C) while on the abnormal right side it was 91°F (33.8°C).

or stenosis of the common or internal carotid artery has produced, without exception, an ipsilateral patch of cool supraorbital skin demonstrable in the thermogram. Patients with marked carotid artery kinking and with sizable atherosclerotic plaques that were symptom producing exhibited similar changes. Since beginning this study, we have not encountered any patients with normal thermograms who later were found to have carotid artery occlusion or stenosis by angiography or at operation.

It has also been shown that patients who have had a successful surgical carotid artery repair with reestablishment of good blood flow, as shown by angiography, have developed a normal thermogram. If attempted surgical restoration of the vessel lumen fails, or if a strong blood flow is not maintained postoperatively, the thermogram will remain abnormal. There has been insufficient experience with patients receiving anticoagulants to state whether thermography is useful in evaluating the effectiveness of such medical treatment.

Bilateral asymmetrical carotid atherosclerosis causes more complex changes in the thermogram than occur with a unilateral lesion. In patients with occlusion on one side and carotid stenosis on the other, the cooler supraorbital skin at thermography is found on the side of the stenosis. The best explanation appears to be twofold. First, the occlusive lesion is more mature, and well developed collateral circulation often is found for the ophthalmic artery and its branches through the facial soft tissue anastomoses. Second, is the homeo-



Fig 6 Left internal carotid artery occlusion. Thermogram discloses an area of cool supraorbital skin on the left side. Angiography disclosed complete occlusion of the internal carotid artery at its origin.

static role of the circle of Willis in its attempt to preserve cerebral circulation. Filling of both middle and both anterior cerebral arteries from the stenotic side usually can be demonstrated at angiography. Associated with the cerebral demand on the still patent internal carotid artery is a reduction of outward blood flow in (or steal from) the ophthalmic artery. The circumstances are somewhat analogous to the steal (or bypass) phenomenon associated with an arteriovenous fistula in the cavernous sinus or a large angioma of the brain with an arteriovenous shunt (Fig 7).

In patients with bilateral asymmetrical atherosclerosis who have had surgical restoration of the carotid lumen to normal size on the stenotic side the dark supraorbital patch associated with the stenosis disappears. Follow-up angiography indicates that the repaired artery then is capable of supplying its own ophthalmic branch as well as the opposite cerebral hemisphere. Inasmuch as the majority of such patients present themselves with symptoms and neurological signs referable only to the fully occluded side, a thermographic change contralateral to clinical manifestations should lead to a diagnosis of bilateral carotid insufficiency with the objective of instituting treatment to improve circulation on the still patent side. Thus far an opportunity to perform thermography in a patient with complete obstruction of both internal carotid arteries has not presented itself.

Proximally stenosis or occlusion of the orifice of the common carotid artery by atherosclerosis, dissecting aortic aneurysm or other diseases have been



Fig. 7. Arteriovenous malformation of left cerebral hemisphere. The thermogram (a) discloses a large area of forehead coolness in left medial supraorbital region. Left orbit and anterior convexity of the globe are cooler than the right. The angiogram (b) reveals enlargement of internal carotid and its middle cerebral extension supplying a large angioma of the convexity which exhibits shunting of contrast material into the venous system. No filling of left ophthalmic artery or anterior cerebral artery.

associated with abnormal facial thermograms. In some instances, corrective intrathoracic surgical procedures have been undertaken.

Distally, abnormal thermograms have not been found in association with occlusive lesions above the clinoid level. Thus, occlusion of the carotid siphon, of the middle cerebral artery or of various cerebral branch arteries have not caused thermographic changes.

Generalized cerebral atherosclerosis and scattered small plaques have not been found responsible for specific thermographic patterns although an overall coolness of skin temperature often is found in bolometer readings. The generalized vasal alterations produced by fever, coma or the lack of standard conditions for the examination frequently obscure a local vascular disorder. Thermographic studies after the inhalation of carbon dioxide or oxygen and studies involving the pharmacologic effects of a host of drugs are under way, but are beyond the scope of this paper.

Comment

It is apparent from the foregoing data that thermography provides a ready means of evaluating carotid artery circulation by assessing the blood flow in

the small group of branches that constitute the only extension of the internal carotid artery to the body surface. Thermography plays its chief role in detecting lesions that produce a reduction in flow in the internal carotid artery by narrowing of the common carotid at its orifice or by compromising the lumen of the internal carotid artery in the neck. The abnormal thermogram is most often associated therefore with lesions in locations accessible for surgical correction. Thermography as described in this paper is primarily a technique for the analysis of carotid blood flow and might more properly be called *carotid thermography*.

Semiquantitative tracings can be made of the multitude of bolometric readings executed by the thermograph (Woon 1964). The value of precise quantitative heat determinations separate from the photographic display is not yet clear and more experience will be required to find the proper niche for such data. The postoperative studies of pressure and flow, and of angiographic changes after carotid obstruction, suggest that there is so much variation from case to case that quantitative readings and clinical effects may be very difficult to reconcile (ODOM et coll 1962). It is necessary to keep in mind that the vascular supply of the skin provides only one parameter for deducing the complex manifestations of carotid disease (ALLEN & MUSTIAN 1962).

Calibrated reference sources have been used to collect quantitative data 1) at the time of clinical thermography (Figs 1 and 2) 2) in conjunction with infrared radiometer readings taken directly from the facial skin and 3) with clinical thermopiles and thermal resistors. The facial skin temperatures of many hundreds of normal individuals and patients have been determined in these ways. On the average the temperature of the medial integument of the forehead is 93.5 F (34.2° C). Occasionally normal individuals are found with skin temperatures 2 F (1.1 C) above and as much as 3 F (1.7 C) below the average level; greater deviations are rare. Differences between the two sides usually are small as evidenced by thermograms (Fig 2). On the other hand the values obtained by attaching thermopiles or thermal resistors to the skin or by hand held bolometers are not as reliable as those of the thermograph in detecting asymmetry because the sensitivity and resolution of the more simple instruments are lower. The average measured variation between right and left using the manual bolometer was 0.6 F (0.3 C) in the large series studied. Manual bolometer temperature differences of 1.8 F (1.0 C) were found to be significant in all cases. Although it is common for patients with carotid insufficiency to exhibit a variation of as much as 3 F (1.7 C) and occasionally more between the two sides of the forehead nevertheless it is doubtful that ordinary thermal resistors and simple bolometers can substitute for the thermograph in clinical work. The delicate display

provided by the thermograph allows a visual comparison of the two sides and the detection of subtle relative changes that cannot be approached by other instruments. Although no normal thermogram has been found in the presence of carotid occlusion or symptomatic stenosis, it is to be expected that exceptions will be encountered with further experience. The rare cases with falsely positive thermograms were benefited by definitive angiographic diagnosis and in each instance angiography provided a clear explanation of the thermographic changes (Fig. 7).

At the time of thermography, each patient had a thorough clinical examination by a qualified neurologist. Procedures popular in the past to help determine the presence or absence of carotid disease also were carried out, including ophthalmodynamometry, the clinical assessment of pulsations and aneurysms detected, and radioactive isotope studies in selected cases. Thermography was more reliable by far than the other procedures as a method of surveying patients for the presence or absence of carotid disease. Personal experience with carotid compression tests has been limited since the opinion prevailed among the physicians who attended these patients that compression maneuvers carry some risk. Thermography, however, was more successful in the cases described here than carotid compression in the hands of others who have described their experiences in the literature (TOOLE & BEVILACQUA 1963).

SUMMARY

Thermography is a superior method of surveying patients for the presence or absence of carotid artery insufficiency. The procedure appears to be more reliable than isotope circulation studies, ophthalmodynamometry, the carotid compression test (with or without electroencephalography) and the clinical evaluation of carotid pulses and bruits. Thermography has been used successfully to aid in the selection of patients requiring angiography and to evaluate the effectiveness of therapy. Reversal of the thermographic patterns after treatment serves as an index of the effectiveness of therapy.

ZUSAMMENFASSUNG

Thermographie ist eine gute Methode um die Anwesenheit oder Abwesenheit von Carotisinsuffizienz zu zeigen. Sie scheint zuverlässiger als Isotopzirkulationsstudien, Ophthalmodynamomessungen, Carotiskompressionsteste (mit oder ohne Elektroenzephalographie) und als klinische Auswertung des Carotispulses und des Carotisturses zu sein. Thermographie ist mit Erfolg bei der Auswahl von Patienten die Angiographie erfordern und um die Effektivität der Behandlung auszuwerten verwendet worden. Eine thermographisch registrierte Verbesserung nach der Behandlung dient als Effektivitätstest der Behandlung.

RESUME

La thermographie est la meilleure methode de dépistage de l'insuffisance carotidienne elle parait plus fidele que les études isotopiques de circulation l'ophtalmodynamométrie l'épreuve de compression carotidienne (avec ou sans électro-encéphalographie) et que l'étude clinique du pouls et des bruits carotidiens. La thermographie a été utilisée avec succes pour contribuer a poser les indications de l'angiographie et pour juger l'efficacité des traitements. L'amélioration des thermogrammes apres traitement sert de test de l'efficacité des traitements.

REFERENCES

- ALLEN J N and MUSTIAN V M Origin and significance of vascular murmurs of the head and neck *Medicine* 41 (1962) 227
- BARNES R B Thermography of the human body *Science* 140 (1963) 870
- and GERSHON COHEN J Clinical thermography *J Amer med Ass* 185 (1963) 949
- — Thermomastography *J Albert Einstein Med Center* 2 (1963) 107
- JOHNSON P M Personal communication (1964)
- ODOM G L, WOODHALL B, TINDALL G T and JACKSON J R Changes in distal intravascular pressure and size of intracranial aneurysm following common carotid ligation *J Neurosurg* 19 (1967) 41
- TOOLE J F and BEVILACQUA J E The carotid compression test *Neurology* 13 (1963) 601
- WILLIAMS K L, WILLIAMS F J L and HANDLEY R S Infra red thermometry in the diagnosis of breast disease *Lancet* 281 (1961) 1378
- WOOD E H Thermography in the diagnosis of cerebrovascular disease: Preliminary report *Radiology* 83 (1964) 540

FROM THE NEURORADIOLOGY SECTION OF THE RADIOLOGY DEPARTMENT (M
ELKIN) AND THE NEUROLOGY DEPARTMENT (R KATZMAN AND L SCHEINBERG)
OF THE ALBERT EINSTEIN COLLEGE OF MEDICINE, BRONX, NEW YORK, U.S.A

GAMMA ENCEPHALOGRAMS IN EXTRACEREBRAL HEMATOMAS

by

L ZINGESSLER, S MANDELL and M SCHECHTER

The potentialities of gamma encephalography are still being explored as work progresses in pharmacologic and electronic spheres relating to scanning and as clinical experience accumulates. The purpose of this paper is to report our experience with the use of gamma encephalography (rectilinear scanning) in the evaluation of patients who have sustained head trauma. In previous scanning series extracerebral hematomas have been labelled only false positives, meaning that they presented on radioactive brain scans as lesions that might be confused with neoplasms. Other workers have dealt specifically with extracerebral hematomas. The ability to localize extracerebral hematomas depends on a difference between count rates from the lesion itself and adjacent areas. This is a function of both the isotope employed and the chemical and physical properties of the labelled compound. Radioactive iodine labelled compounds such as diiodofluorescein and serum albumin do get into subdural fluid though usually there is less radioactivity in this compartment than in the peripheral venous blood (MOORE 1958, DUNBAR et coll 1954, FEINDEL et coll 1963). Scanning with ^{64}Cu has seldom demonstrated an extracerebral hematoma. ^{113}As by virtue of its concentration in subdural membrane enables demonstration of subdural hematomas (SWEET et coll 1961, MEALY 1963). When radioactive mercury labelled chlormerodrin is used, epidural and subdural hematomas appear on the brain scan (in the



Fig 1 A p scan of a patient with bilateral chronic subdural hematomas



Fig 2 A p scan of patient with bilateral subacute subdural hematomas. Left subdural appears thicker than right but is thinner in reality

frontal projection) is an increase in the normal vascular rim. Radioactive mercury labelled chlormerodrin has shown the best results in the demonstration of extracerebral hematomas to date as has been noted by McGIVIS et coll (1963) and by MEALY (1963) among others.

A tabulated summary of the literature on the demonstration of extracerebral hematomas using radioactive isotopes is presented below.

Our experience with the interpretation of gamma encephalograms using radioactive mercury is derived from two sources (1) scans of patients who have sustained trauma and those who have not and (2) comparison of count

Y	Author	Diagnostic agent	Lesions	Results
1951	ASHKE AZI et coll	Diodofluorescein	8 chronic subdurals	Little or no localization
1952	PEYTON et coll	Diodofluorescein	1 chronic subdural	Localized
1953	MOORE et coll	RISA	several subdural hem	Only one localized due to isotope in adjacent edematous brain
1954	DUNBAR & RAY	RISA	4 unilateral subdurals	Localized due to leakage into adjacent brain
1957	RIDDY & NOLAN	RISA	1 patient with bilateral subdurals	Not localized
1961	FEINDEL et coll	RISA	3 subdurals	Localized
1961	SLEET et coll	Cu ⁶⁴	1 hemipneural	Not localized
		As	3 subdurals	Not localized
1962	BRINKMAN et coll	Hg ²⁰³	8 subdurals	7 localized
			2 subdurals	Localized
1963	MEALY	RISA	Localization site	injection into subdural cavity
1963	MEALY	Hg ²⁰³	3 subdurals	Localized
1963	McGIVIS et coll	Hg ²⁰³	19 subdurals	Localized

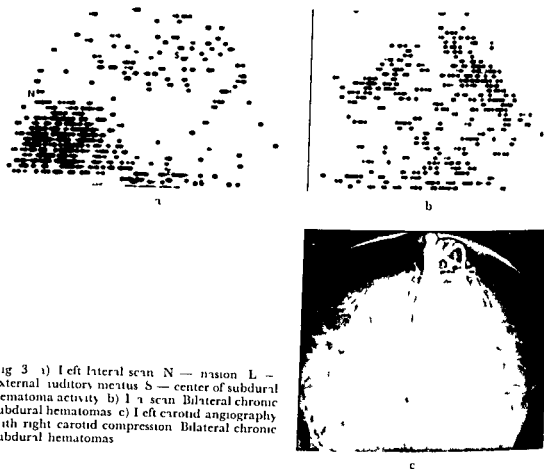


Fig 3 a) Left lateral scan N — nasion L — external auditory meatus S — center of subdural hematoma activity b) 1 p scan Bilateral chronic subdural hematomas c) Left carotid angiography with right carotid compression Bilateral chronic subdural hematomas

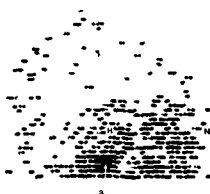
rates of samples of extracerebral hematomas collected at the time of surgery with peripheral venous blood

There are no false negatives in our scanning series, i.e. none of the cases which we are asked to scan turned out to have an extracerebral hematoma when the scan was entirely negative

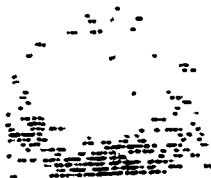
Six patients with extracerebral hematomas had positive scans. In the first case (Fig 1) scanning demonstrated the presence of bilateral, chronic subdural hematomas. In the second case (Fig 2) scanning demonstrated bilateral subacute subdural hematomas, but although the 1 p scan suggested that the subdural hematoma on the left was thicker than that on the right, in actuality the right sided collection was thicker. Left sided periorbital ecchymoses probably accounted for the discrepancy. In the third case (Fig 3) the 1 p scan was entirely negative. Only the lateral and p 1 scans indicated the presence of bilateral chronic subdural hematomas which were posteriorly situated. In the next case (Fig 4), a patient with bilateral subacute subdural hematomas in which the left subdural hematoma was thicker than the one on the right,



Fig 4 A p scan of a patient with bilateral subdural hematomas. The one on the right is overshadowed by the left sided subdural.



a



b

Fig 5 a) Right lateral scan of a patient with an epidural hematoma adjacent to the temporal lobe. N — nas on white a row — external auditory meatus. H — center of the hematoma. b) A p scan of the patient with the right sided epidural hematoma.

scanning clearly demonstrated the left subdural hematoma. The one on the right is not as obvious. The interpretation of the scan of a patient with bilateral subdural hematomas is often difficult because of the fact that comparison of the two sides is crucial in evaluation of the a p and p a scan and one side may overlie the other. In the next case (Fig 5) scanning demonstrated what angiographically seems to be an epidural hematoma. There is no surgical confirmation of this lesion. No operation was performed because the patient was doing well clinically. In the next case (Fig 6) scanning demonstrated a subgaleal hematoma. This was clinically evident although it had reached maximum size some weeks before and was regressing in size. Angiography and encephalography were entirely negative.

Our false positive cases were as follows: (1) bilateral heavy vascular rim, (2) aneurysm of left internal carotid artery, (3) peripheral infarct, and

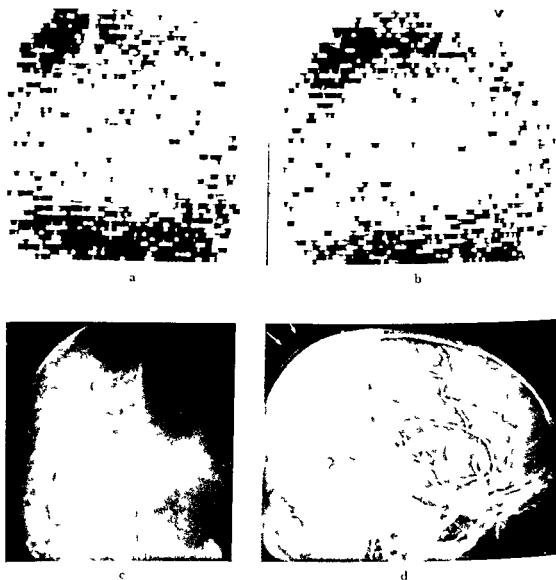


Fig 6 a) Ap scan of a patient with a subgaleal hematoma in the right parietal area b) Right lateral scan of the patient with the subgaleal hematoma c) Right carotid angiogram. No intracranial hematoma d) Lateral view right carotid angiogram. The subgaleal hematoma is indicated by the arrows

(4) peripheral metastatic tumor. We have learned there are certain pitfalls in the diagnosis of extracerebral hematomas using scanning with radioactive mercury. Injury to the soft tissues — ecchymoses of the face and subgaleal hematomas — lead to an abnormal concentration of radioactive isotopes in these areas. Paget's disease and renal disease are often associated with a heavy concentration of activity around the periphery of the brain

scan and for this reason they enter into the differential diagnosis of bilateral subdural hematomas. Infarcts and tumours may simulate subdural hematomas if they are peripherally located. Our first false positive case (Fig 7) is such only in the sense that the 2½ hour scan showed a heavy vascular rim bilaterally when there was no history of renal disease or Paget's disease. The scan performed after 24 hours no longer showed this heavy vascular rim so we dismissed the diagnosis of bilateral extracerebral hematomas. The 24 hour scan was performed because we had realized at this time that the collections which were extracerebral would be seen better after 24 hours since the blood was being cleared of mercury while the extracerebral collections retained a relatively high radioactive mercury content. We have no good explanation for the next false positive scan (Fig 8) where the pathology was an aneurysm of the left internal carotid artery. Scanning suggested a right subdural hematoma. Perhaps spasm on the left with diminished blood flow there reduced the normal vascular rim there, leading to misinterpretation of a normal vascular rim on the right side as a subdural hematoma. Spasm was not present angiographically however. The patient at autopsy had no evidence of blood either in the subarachnoid or subdural spaces on the right. The next two patients had scans which suggested subdural hematomas. One had an infarct and one had a peripherally situated tumor.

We have alluded to the fact that we have counted samples of extracerebral collections removed at the time of operation and compared the count rate to peripheral venous blood removed at the same time. The results are summarized below.

It appears as if the ratio of counts in extracerebral hematoma to counts in peripheral venous blood increases as the time interval increases between the administration of the isotope and the operative procedure. This means then that while blood is being cleared of the radioactive isotope the extra

Patient	Radioisotope	Time interval between administration and operation	Ratio in cts/min/ml between hematoma and peripheral venous blood as percentage	Lesion
G	²⁰¹ Hg	6 days	Left 141	Bilateral chronic
I	²⁰¹ Hg	20 hours	Right 105	subdural
D	Hg	10 hours	Left 435	Bilateral chronic
O	²⁰¹ Hg	6 hours	Right 457	subdural
	Cr (tagged RBC)	4 days	117	Chronic subdural
S	²⁰¹ Hg	4 ½ hours	9	Subacute subdural
H	²⁰¹ Hg	3 hours	29	
B	Hg	2 ½ hours	7	Acute subdural
R	Hg	1 hour	9	Acute subdural
			5	Acute subdural
			10	Acute subdural

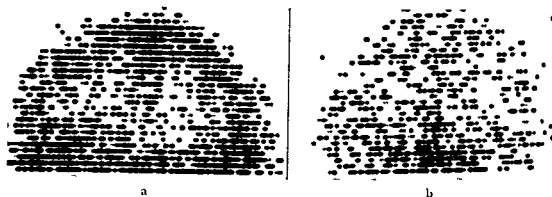


Fig 7 a) Ap brain scan performed at 2 1/2 hours in a patient with no lagett's disease, renal disease or extracerebral hematomas. The vascular rim is exceptionally prominent. b) Ap scan after 24 hours. Vascular rim no longer prominent.

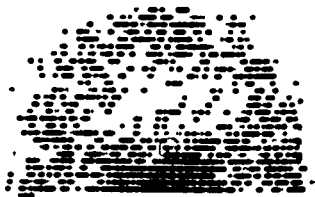


Fig 8 Ap scan of a patient with an intracranial internal carotid aneurysm on the left. The vascular rim is more prominent on the right than the left.

cerebral hematoma is being cleared much more slowly. Case 4 (labelled 0) is of particular interest as this patient received ^{51}Cr labelled red cells about four days before receiving radioactive mercury. Note that the differential counting indicated that there seemed to be some leakage of fresh blood into the subacute subdural hematoma, but that there was much more radioactive mercury present in the subdural collection than radioactive chromium.

An inquiry into the pathologic mechanisms involved in the production of the positive scan in patients with extracerebral hematomas is the next step in our discussion. When a patient is given a diagnostic dose of radioactive mercury approximately 80% of the radioactive mercury that is intravascular is found in the plasma. Roughly 20% is bound to red cells, bound meaning

that the mercury cannot be washed off with saline. About 98 % of the mercury in plasma is complexed with protein. Using an electrophoretic technique we have found that approximately 11 % of the protein bound mercury in plasma is complexed with albumin, 5 % with alpha one globulin, 67 % with alpha two globulin, 13 % with beta globulin and 4 % with gamma globulin. Other workers have indicated that mercury is attached to the sulfhydryl groups of protein molecules.

Chronic subdural hematomas are richer in protein, especially albumin (CITLIN 1955) than plasma. The membranes of chronic subdural hematomas contain blood vessels. Physical laws govern the diffusion of mercury through the semipermeable membranes of the subdural hematomas and while the plasma level of radioactive mercury is regressing, a relative increase in the amount of radioactive mercury within the subdural collection is noted.

The vessel wall is the only barrier in the acute subdural hematoma yet enough radioactive mercury gets into the acute extracerebral hematoma to increase the vascular rim or cap of the rectilinear scan, enabling diagnosis of this condition. Our patients with acute extracerebral hematomas came to surgery much sooner than those with chronic extracerebral hematomas yet significant count rates were found within these acute subdural collections due to both diffusion and probably to continued bleeding. Further work involving the administration of both chromium tagged red cells and radioactive mercury needs to be done to support this last contention.

Acknowledgement

This work was supported in part by a Special Traineeship (B.T. 937) from the National Institute of Neurologic Diseases and Blindness, Public Health Service.

SUMMARY

Rectilinear scanning using radioactive mercury labelled chlormerodrin may safely be used as a screening device in the evaluation of patients with a history of trauma. There are no false negative scans in our series. False positive scans were encountered and the causes are discussed. Use of a technique involving the administration of ^{51}Cr labelled red cells in addition to chlormerodrin labelled with radioactive mercury may be used to elucidate the pathogenesis of subdural hematomas since the count rates of the two isotopes in the extracerebral collection can be differentiated.

ZUSAMMENFASSUNG

Geradlinige Szintigraphie mit radioaktivem Queck Silber gemerktem Chlormerodrin kann als primäre Untersuchung von Patienten mit Trauma Anwendung finden. Unsere Serie umfasst keine falschen negativen Szintigramme, jedoch wurden falsche positive gefunden. Die Ursachen hierfür werden besprochen. Es können ^{51}Cr gemerkte rote Zellen

zusätzlich zu radioaktivem Quecksilber gemerktem Chlormerodrin verabreicht werden um die Pathogenese der subduralen Hämatome zu beleuchten da die Zählgeschwindigkeit dieser zwei Isotopen in der extracerebralen Ansammlung differenziert werden können

RÉSUMÉ

La scintigraphie rectiligne utilisant la Chlormerodrin marquée au mercure radioactif peut être employée sans danger comme méthode de dépistage chez les malades ayant des antécédents traumatiques. Il n'y a pas de scintigraphies faussement négatives dans notre série. Il y a des scintigraphies faussement positives dont les auteurs examinent les causes. Pour élucider la pathogénie des hématomes sous duranx on peut associer à la Chlormerodrin marquée au mercure radioactif l'administration de globules rouges marqués au ^{51}Cr car on peut distinguer le comptage des deux isotopes dans la collection extra-cérébrale.

REFERENCES

- ASHKINAZI M, DAVIS L and MARTIN J. An evaluation of the technic and results of the radioactive di-iodo fluorescein test for the localization of intracranial lesions. *J Neurosurg.* 8 (1951) 300.
- BRINKMAN C A, WEGST A V and KAHN E A. Brain scanning with mercury 203 labelled Neohydryn. *J Neurosurg.* 19 (1962) 644.
- DUNBAR H S and RAY B S. Localization of brain tumors and other intracranial lesions with radioactive iodinated human serum albumin. *Surg Gynec Obstet* 98 (1954) 433.
- FEINDEL W, ROVIT R L and STEPHENS NEWSHAM L. Localization of intracranial vascular lesions by radioactive isotopes and an automatic contour brain scanner. *J Neurosurg.* 18 (1961) 811.
- GITLIN D. Pathogenesis of subdural collections of fluid. *Pediatrics* 16 (1955) 34.
- MCGINNIS K D, EYLER W R, DUSAULT L and KRISTIN K. Mercury 203 brain scanning. A method of clinical classification. *Radiology* 80 (1963) 264.
- MEALY J. Gamma ray image of subdural effusions scanning after injection of radio-iodinated serum albumin into subdural space and its clinical application. *J Neurosurg.* 19 (1963) 934.
- Radioisotopic localization in subdural hematomas. *J Neurosurg.* 20 (1963) 770.
- MOORE G F. Diagnosis and localization of brain tumors. A clinical and experimental study employing fluorescent and radioactive tracer methods. Charles C Thomas Springfield Ill. 1953.
- PEYTON W T, MOORE G E, FRENCH L A and CHOU S N. Localization of intracranial lesions by radioactive isotopes. *J Neurosurg.* 9 (1952) 432.
- PLANIOL T. Diagnostic des lésions intra-cranienues par les radio isotopes (gammaencephalographie). Masson et Cie Paris 1959.
- RHODY R B and NOWLIS G R. The use of radioactive iodinated serum albumin in the localization of intracranial lesions. *J Neurosurg.* 14 (1957) 413.
- SWEET W H, MEALY J, ARANOW S and BROWNELL G L. Localization of focal intracranial lesions by scanning of rays from position emitting isotopes. *Clin Neurosurg.* 7 (1961) 159.

EXPERIENCES WITH SH 617 L MYELOGRAPHY

by

A. BACIOCCO, A. GALLUZZO and S. SASSAROLI

After the introduction of lumbar myelography with water soluble contrast media whose usefulness has been widely recognized, it seemed desirable that a contrast medium possessing similar properties for total myelography should be evolved.

Experimental attempts (FUNKLISCH & OBEL 1960, SASSAROLI & BACIOCCO 1961) with the aim of evolving such a contrast medium have not been successful. We can therefore understand the interest aroused by the introduction of the SH 617 L medium which has been referred to as resorbable and suitable for cisternal and lumbar introduction. We have had an opportunity to try SH 617 L in a series of eighteen myelographies using both techniques. Our conclusions from the use of this contrast medium may be stated in the following.

In the amounts of SH 617 L suggested by the producer the absorption of roentgen rays by the medium is clearly lower if compared with pantopaque and kindred contrast media including the water soluble ones. The best results are achieved when the medium is introduced as close as possible to the lesion.

No symptoms were noted during or immediately after the examination. After 8 to 30 hours all the patients showed an irritative meningeal reaction with fever lasting a few days. Because of this the neurologist could always determine which contrast medium had been used. Invariably the cerebrospinal

zusätzlich zu radioaktivem Quecksilber gemerktem Chlormerodrin verabreicht werden um die Pathogenese der subduralen Hämatome zu beleuchten da die Zählgeschwindigkeit dieser zwei Isotopen in der extracerebralen Ansammlung differenziert werden können

RÉSUMÉ

La scintigraphie rectiligne utilisant la Chlormerodrin marquée au mercure radioactif peut être employée sans danger comme méthode de dépistage chez les malades ayant des antécédents traumatiques. Il n'y a pas de scintigraphies faussement négatives dans notre série. Il y a des scintigraphies faussement positives dont les auteurs examinent les causes. Pour élucider la pathogénie des hématomes sous-duraux on peut associer à la Chlormerodrin marquée au mercure radioactif l'administration de globules rouges marqués au ^{51}Cr car on peut distinguer le comptage des deux isotopes dans la collection extra-cérébrale.

REFERENCES

- ASHKANAZY M, DAVIS L and MARTIN J. An evaluation of the technique and results of the radioactive diiodo fluorescein test for the localization of intracranial lesions. *J Neurosurg* 8 (1951) 300.
- BRINKMAN C A, WEGST A V and KAHN E A. Brain scanning with mercury 203 labelled Neohydryn. *J Neurosurg* 19 (1962) 644.
- DUNBAR H S and RAY B S. Localization of brain tumors and other intracranial lesions with radioactive iodinated human serum albumin. *Surg, Gynec Obstet* 98 (1954) 433.
- FEINDEL W, ROVIT R L and STEPHENS NEWSHAM L. Localization of intracranial vascular lesions by radioactive isotopes and an automatic contour brain scanner. *J Neurosurg* 18 (1961) 811.
- GITLIN D. Pathogenesis of subdural collections of fluid. *Pediatrics* 16 (1955) 345.
- MCGINNIS K D, ELLER W R, DUBAULT L and KRISTEN K. Mercury 203 brain scanning. A method of clinical classification. *Radiology* 80 (1963) 264.
- MEALY J. Gamma ray image of subdural effusions scanning after injection of radio-iodinated serum albumin into subdural space and its clinical application. *J Neurosurg* 19 (1967) 934.
- Radioisotopic localization in subdural hematomas. *J Neurosurg* 20 (1963) 770.
- MOORE G E. Diagnosis and localization of brain tumors. A clinical and experimental study employing fluorescent and radioactive tracer methods. Charles C Thomas Springfield Ill 1953.
- PEYTON W T, MOORE G E, FRENCH L A and CHOW S N. Localization of intracranial lesions by radioactive isotopes. *J Neurosurg* 9 (1952) 432.
- PLANIOL F. Diagnostic des lésions intra-craniennees par les radio isotopes (scintiscintigraphie). Masson et Cie Paris 1959.
- RHODY R B and NOWLIS G R. The use of radioactive iodinated serum albumin in the localization of intracranial lesions. *J Neurosurg* 14 (1957) 413.
- SWEET W H, MEALY J, ARANOW S and BROWNELL G L. Localization of focal intracranial lesions by scanning of rays from positron emitting isotopes. *Clin Neurosurg* 7 (1961) 159.

ZUSAMMENFASSUNG

Ein gewisse Anzahl von myelographischen Untersuchungen wurden mit einem neuen resorbierbaren Kontrastmittel bezeichnet SH-617 L ausgeführt. Das neue Kontrastmittel bietet zwar einige Vorteile, ist jedoch anderen Kontrastmitteln bei weitem nicht vorzuziehen.

RESUMÉ

Un nombre limité de myélographies ont été faites avec un nouveau moyen de contraste résorbable appelé SH-617 L. Ce nouveau produit présente certains avantages mais il est loin d'être préférable aux autres moyens de contraste.

REFERENCES

- ARNELL S. Weitere Erfahrungen über Myelographie mit Abrodil. *Acta radiol.* 25 (1944) 408.
 CATALANO D. e PESCE L. Mielografia con nuovo mezzo di contrasto idrosolubile e riassorbibile. *Riv. ital. Radiol. clin.* 3 (1964) 382.
 DECKER K. *Klinische Neuroradiologie*. Georg Thieme, Stuttgart, 1960.
 DENSTAD T. The resorption of abrodil in myelography. *Acta radiol.* 32 (1949) 428.
 FUNKQUIST B. and OBEL N. Tonic muscle spasms and blood pressure changes following the subarachnoid injection of contrast media. *Acta radiol.* 53 (1960) 337.
 LINDBLOM K. Lumbar myelography by abrodil. *Acta radiol.* 1 (1946) 27.
 LIDGREN E. *Handbuch der Neurochirurgie*. Band 2. Springer Verlag, Berlin, 1954.
 RUGGIERO G. *Technique Neuroradiologique. Traité de Technique Chirurgicale*. Tome 3. Masson, Paris, 1961.
 SASSAROLI S. e BAGGIOCCO A. Iniezione sperimentale di mezzo di contrasto idrosolubile negli spazi liquorali encefalici del cane. *Nuntius Radiol.* 12 (1961) 1060.
 VÖGLER E. und WALCHER W. Versuche mit einem neuen Kontrastmittel für die subarachnoidale Myelographie. *Fortschr. Röntgenstr.* 22 (1963) 493.
 WELLAUER J. *Die Myelographie Mit Positiven Kontrastmitteln*. Georg Thieme, Stuttgart, 1961.



Fig. 1



2a



2b



2c

Fig. 1 (left) Lumbar myelogram. Defect on anterior surface of dura at level of L2-L3.

Fig. 2 a) and b) Total obstruction to contrast medium at level of T4-T5 (A neurinoma was found at operation). c) Photograph taken during operation. The contrast medium is closely spread on the spinal cord at level of lesion.

fluid presented pleocytosis and an increased protein content. The irritative phenomena disappeared after a few days. This aseptic meningitis and related signs were especially strong in the normal myelographies; the irritative symptoms were milder when a total obstruction was present, possibly because of less extensive spreading of the substance.

The resorption of the contrast medium was slow. After 4 to 5 weeks it was much less noticeable, and only after 9 to 10 weeks was it no longer identifiable.

All the symptoms of the spinal compression showed a tendency to exacerbation. In one case, during the surgical exposure, we could observe the contrast medium closely spread like a thin film on the surface of the spinal cord (Fig. 2c).

We are unable definitely to evaluate the properties of SH 617 L, but in our view this contrast medium is in no way superior to the pantopaque and kindred substances.

SUMMARY

A limited number of myelographies have been carried out with a new resorbable contrast medium called SH 617 L. The new medium offers some advantages but it is far from being preferable to other contrast media.



Fig 1 a) Lumbar route myelography. Complete block at D2 without other elements of diagnostic value. b) After urea the contrast medium flows beyond the obstacle and outlines the cord which is enlarged up to the level of the fifth cervical vertebra due to an intramedullary glioma.

of 60 drops per minute. With this technique we have not observed side effects except for mild headache in a few cases. Half an hour after the termination of the urea perfusion the patients were re-examined and new films taken after repeated tilting of the table in order to observe whether changes had occurred in the images of the block.

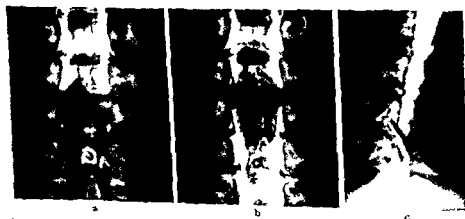


Fig 2 Suboccipital route myelography. Complete block probably due to an extramedullary lesion at the level of space C5-C6. b) and c) After urea the classical picture of C5-C6 intervertebral disc herniation appears.

FROM THE NEURORADIOLOGICAL SECTION (A. CALABRO) OF THE NEUROSURGICAL
DEPARTMENT (DIRECTOR I. CASTELLANO) OF OURR AND THE NEURORADIOLOGICAL
SECTION (F. SMALTINO) OF THE NEUROLOGICAL CLINIC OF THE UNIVERSITY
(DIRECTOR PROF. V. LONGO), NAPLES, ITALY

UREA IN POSITIVE CONTRAST MYELOGRAPHY

by

A. CALABRO and F. SMALTINO

In recent years the use of hypertonic urea solutions has been introduced in neuroradiology as a means of lessening cerebral edema and intracranial hypertension. This renders encephalographic examinations less dangerous, better tolerated and of increased pictorial quality. TURBULL in 1962 said "Personal observation during a cervical cordotomy demonstrated that with urea the cord does shrink and the spinal theca becomes slack", and in 1963 JOYNER & FREEMAN demonstrated that the administration of hypertonic urea in the dog exerts an anti edema effect on the spinal cord. This fact suggested to us the possibility of applying this effect in positive myelography, in the hope that a reduction of swelling might change a complete block into a partial one. If this were to be obtained, an improved definition of contour and size of the lesion could ensue and thus allow clarification of its anatomical relationships with the cord and its envelopes.

Methods We have selected cases of complete myelographic block of the spinal space, where the image could not be modified either by extension flexion or by axial rotation movements of the spinal column. Urea, in a 30 % glucose solution, was then injected intravenously in doses of 0.8 g/kg at a rate



Fig 1 a) Lumbar route myelography. Complete block at D⁹ without other elements of diagnostic value. b) After urea the contrast medium flows beyond the obstacle and outlines the cord which is enlarged up to the level of the fifth cervical vertebra due to an intramedullary glioma.

of 60 drops per minute. With this technique we have not observed side effects except for mild headache in a few cases. Half an hour after the termination of the urea perfusion the patients were re-examined and new films taken after repeated tilting of the table in order to observe whether changes had occurred in the images of the block.



Fig 2 a) Sacral route myelography. Complete block probably due to an extramedullary lesion at the level of space L⁵-C⁶. b) and c) After urea the classical picture of C²-C⁶ intervertebral due herniation appears.

Fig. 3 a) Suboccipital route myelography. Complete block at cervical level. On the left side the opaque column stops at the level of the C6-C7 intervertebral space while on the right it does not go beyond the C5-C6 intervertebral space. b) After urea the contrast medium passes over the obstacle and shows that the cord is swollen from the level of C6 to the inferior surface of D1.



A total of 9 cases were studied during a period of 6 months, ending in March 1964. In 6 cases the block was caused by vertebral tumours, either primary or metastatic. In these cases the administration of urea did not cause any modification in the myelographic block. In the other 3 cases the administration of urea caused significant changes as briefly described below.

Case reports

Case 1 In this case the presence of an intramedullary glioma was verified at a subsequent surgical operation. By performing myelography by the lumbar route the flow of the opaque column appeared to be arrested completely at the level of the second thoracic vertebral body (Fig. 1a). After infusion of urea the contrast medium flowed beyond the obstacle and showed the classical picture of an intramedullary lesion (Fig. 1b).

Case 2 The contrast medium injected by the suboccipital route appeared immovably blocked at the level of the intervertebral space between C5 and C6 (Fig. 2a). The images of this block of flow seemed to be those of an extramedullary space occupying lesion. The picture persisted after the patient had been standing for a long time and despite repeated movements of flexion, extension and rotation of the neck. After urea the contrast fluid by passed the obstacle and outlined the typical image of herniation of the C5-C6 intervertebral disc (Fig. 2b).

Case 3 In this case the contrast medium injected by the suboccipital route was arrested asymmetrically at the cervical level (Fig. 3a). Changes of position and movements did not modify this picture. After urea the contrast medium flowed beyond the obstacle and showed that the cord below was enlarged. The considerable enlargement of the cord was interpreted as being due to an intramedullary growth and this opinion proved to be correct when an intramedullary glioma (Fig. 3b) was found at a surgical intervention.

Conclusions

Although the number of cases studied by us is small as yet the use of hypertonic urea solutions as an adjunct to myelographic procedures seems justified in some cases where the usual technique reveals the existence of a complete block which is difficult to interpret diagnostically

SUMMARY

When a complete block is present at a positive contrast myelography it is sometimes difficult to locate an expansive lesion with respect to its relationships with the spinal cord or its coverings. In some cases urea has been found to change a block from a complete into an incomplete one making it possible to use the modifications thus obtained for establishing a more precise diagnosis.

ZUSAMMENFASSUNG

Bei Anwesenheit eines totalen Blocks ist es mit positiver Kontrastmyelographie manchmal schwierig eine expansive Veränderung mit Hinsicht auf ihre Beziehung zum Rückenmark und seinen Häuten zu lokalisieren. In einigen Fällen fand man, dass Urea einen kompletten in einen inkompletten Block verwandeln kann. Durch diese Modifikation wird es möglich die Diagnose zu verbessern.

RESUMÉ

Quand il y a un blocage complet à la myélographie par moyen de contraste positif il est parfois difficile de localiser une tumeur par rapport à la moelle ou à ses enveloppes. Dans certains cas on a constaté que l'urée transforme un blocage complet en blocage incomplet permettant d'utiliser des modifications pour établir un diagnostic plus précis.

REFERENCES

- ENGST R and HALGE T. Urea as an aid in encephalography. *Acta radiol* 1 (1963) 565
 JOYNER J and FREEMAN L W. Urea and spinal cord trauma. *Neurology* 13 (1963) 69
 TURNBULL F. *Clinical Neurosurgery* 8 (1962) 241. The Williams and Wilkins Company
 Baltimore 1962

FROM THE SECTION ON NEURORADIOLOGY (DIRECTOR DR GIOVANNI DI CHIRO),
MEDICAL NEUROLOGY BRANCH OF THE NATIONAL INSTITUTE OF NEUROLOGICAL
DISEASES AND BLINDNESS, NATIONAL INSTITUTES OF HEALTH,
BETHESDA, MARYLAND, U S A

OBSERVATIONS ON THE CIRCULATION OF THE CEREBROSPINAL FLUID

by

GIOVANNI DI CHIRO

I believe that most of us have been taught that the cerebrospinal fluid (CSF) slowly circulates (Fig 1), passing from the ventricular system, through the foramen of Magendie and the lateral clefts of Luschka, to the subarachnoid spaces at the base of the brain, and from there ascending towards the convexity of the brain where the greater part of its absorption occurs. A lesser portion of the fluid descends along the posterior aspect of the spinal cord and then, in front of the cord, returns towards the mainstream. The principal site of production of this fluid is the choroid plexus, the portals through which most of the fluid passes from the subarachnoid spaces into the blood are the granulations of Pacchioni. Even a superficial perusal of the literature will however, show that our actual knowledge on the production and absorption of the CSF and in particular on its circulation, is still in a state of considerable controversy and doubt. This is due mainly to the fact that the CSF pathways and the fluid contained within them represent a system particularly difficult to study (BOWSER 1960). To obtain reliable information on this system one has, in fact, to avoid opening it, so as not to change the hydrodynamic conditions under

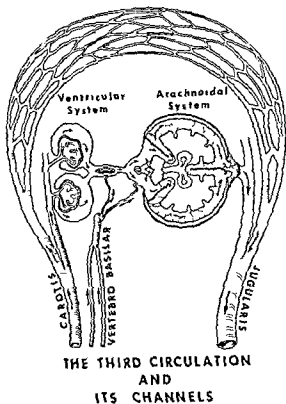


Fig 1 Routes followed by cerebrospinal fluid (Modified from LUSHING)

which it normally subsists. The subarachnoid cavities are in addition peculiarly susceptible to the irritation caused by the presence of foreign bodies. This markedly limits the possibility of obtaining valuable data by using extraneous tracers. Finally, the results of animal experimentation on the CSF system should cautiously be extrapolated to the human. The advent of radio active isotopes in biology has allowed the study of the CSF system closer to its natural status and to accumulate a great deal of new information. A certain number of previously broadly accepted concepts have been reappraised and new value has been given to concepts of early workers which had been shelved for many years.

Limiting ourselves to the kinetics of the CSF and the factors regulating this movement, it is obvious that a net transfer (flow) of fluid out of the ventricles into the subarachnoid space must take place. Obstructions of ventricular

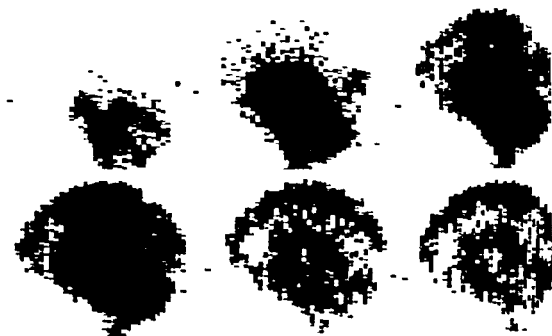


Fig. 2. Lateral serigraphic radio iodinated serum albumin cisternograms at 1, 3, 6, 12, 20 and 24 hours.

outflow, in fact, invariably result in hydrocephalus. Dyes injected into the lateral ventricles make their appearance in the cisterna magna within a few minutes (DANDY & BLACKFAN 1914, RISER 1929) and may be detected in the lumbar fluid after 10 minutes (SOLOMON THOMPSON & PFEIFFER 1922). Pulsations of the fluid synchronous with respiration and cardiac systole have been stressed (O'CONNELL 1943) as an important factor for the maintenance of the CSF circulation and coughing, sneezing and straining considerably affect its motion (RISER 1929). SEITZ (1928) regarded vascular contractions as the major factor in the circulation of the fluid. This latter view has received support from the clinical observations of DOTT & GILLINGHAM (1958) on the formation of pouches along the course of the major cerebral arteries in cases of localized obstructions of the subarachnoid space. Most of us have observed pulsatile movements in the CSF pathways at fluoroscopy during Pantopaque myelography and in cineradiography of myelography and encephalography. The pulsations of the choroid plexuses and their volume changes at each heart beat are considered responsible by BERING (1955) for this to and fro motion of the CSF. With the filling of the choroid plexuses the ventricular content increases and fluid is actively pumped out of the ventricles. The emptying of the choroid plexuses results in a diminution of volume of the ventricular content and the fluid changes direction. Thus the pumping action of the choroid plexus would cause

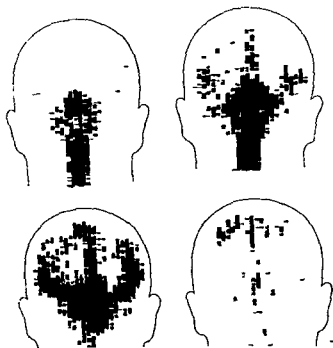


Fig. 3. Sagittal seriographic radio-labeled serum albumin in cerebrospinal fluid at 1, 3, 6 and 24 hours.

an ebb and flow pattern of motion out of the ventricles and a slow progression of the CSF through the subarachnoid spaces towards the surface and the convexity of the cerebral hemispheres. Despite all these observations and theories no direct evidence has been offered that flow in a given direction actually exists in the CSF system. In fact the present trend is to consider unlikely that any complicated circulation takes place in the subarachnoid space and that production and absorption of the CSF and its various constituents occur everywhere though not at the same rate in the fluid pathways. If this is true because the fluid gets in and out of the system at every point no mainstream flow may exist in the CSF cavities. The observations of various investigators on the ascending of drugs injected into the spinal subarachnoid space would tend to confirm this view. WESTON (1921) injected phenol sulfonephthalein in patients; SACHS, WILKINS & SAMS (1930) trypan blue in dogs; KOSTER et coll. (1938) procaine in patients; EICHLER, LINDER & SCHMEISER (1951) radiosodium in dogs; and FUNKQUIST (1961) methiodal in dogs. With all these different substances the movement upwards into the spinal subarach



Fig 4 Activity spreads towards convexity mainly through anterior cisternal pathways

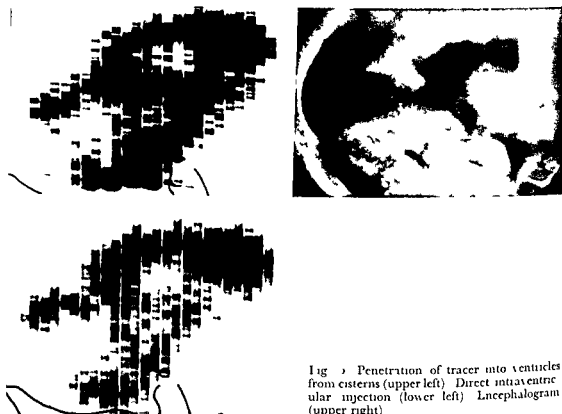


Fig 5 Penetration of tracer into ventricles from cisterns (upper left) Direct intraventricular injection (lower left) Cisternogram (upper right)

noid space was proven to be a very slow process. SACHS and co workers reached the conclusion that movements in the spinal subarachnoid space are only due to simple diffusion and denied the existence of any direct fluid circulation in the spinal subarachnoid space. HASSON (1933) suggested that no cranial or cephalad flow of the spinal fluid exists but that this fluid moves only in a transverse direction.

In 1962 we (RIESELBACH et coll.) used scintillation detection to study the subarachnoid distribution of the drugs injected intrathecally. In 8 patients (6

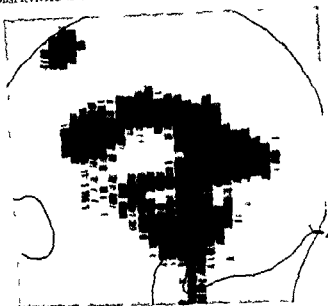


Fig 6 Tracer out into basal cisterns soon after intraventricular injection

with meningeal leukemia and 2 with medulloblastoma) ^{199}Au was injected intrathecally and taking advantage of the 10 % gamma emission of this isotope external scintillation scanning was performed to determine the intracranial distribution of the radionuclide. In these early experiments we were impressed by the constantly similar distribution pattern of the endocranial radioactivity. We also noted that the barotage of fluid at the injection and the positioning of the patient (even Trendelenburg) had no effect on the upward spreading of the radioactivity. One factor which proved to be important and able to influence the rate of ascent of the isotope was the amount of fluid injected. The larger the volume of solvent the faster the activity moved upwards towards the basal cisterns. This data paralleled similar findings in monkeys using ^{131}I rose bengal and methiodal (RIESELBACH et coll 1962). We were able to obtain in one patient an autoradiography of a brain slice which showed a strikingly analogous activity distribution with the scans which had been done in vivo. Microscopical examination of brain tissue revealed gold particles within macrophages throughout the subarachnoid space. We then passed on to use in neurological patients another tracer namely radio iodinated serum albumin (DI CHIRO 1964 1965; DI CHIRO & REAMES 1964; DI CHIRO, REAMES & MATTHEWS 1964) which we have been injecting intrathecally (isotope

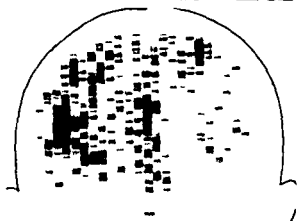


Fig. 7 No air was visible at encephalography but at scintillography a pool of tracer was seen on right convexity. At surgery a huge arachnoidal cyst was found at the site (see specimen).

cisternography) and intraventricularly (isotope ventriculography). The diagnostic value of the isotope cisternography and isotope ventriculography is now established. The present report, however, is not mainly concerned with these diagnostic aspects, but with the possible applications to the physiology of the movement of the CSF. Keeping this in mind we have used, in some patients, ^{131}I tagged autologous CSF. Here the only foreign substance injected in the system is the tagging isotope. The distribution pattern and the rate of flow of the tagged autologous CSF is analogous to the one observed with the radioiodinated serum albumin (Fig. 2). At one hour the basal cisterns are well filled with activity, at three the activity has reached the Sylvian fissures, at 12 it is over the convexity. Generally at 24 hours high activity is present along the superior longitudinal sinus (Fig. 3). The ascending of the fluid takes place mostly through the anterior subarachnoid pathways (Fig. 4) — cisterns in front of the brain stem, suprasellar, subfrontal, prefrontal spaces — and the Sylvian fissures. These are the highways of the CSF circulation. In the posterior subarachnoid spaces (supracerebellar, occipital, posterior parietal) very little activity is seen. At 24 to 48 hours, the injected tagged albumin is predomi-

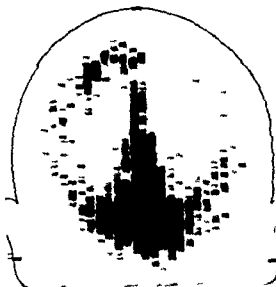


Fig. 8 Partial block of CSF pathways at left tentorial notch. Activity reaches cranium mainly through right routes.

namely, often exclusively recognized in the parasagittal area, along the superior longitudinal sinus. Though recently the so called Key and Retzius-Weed (WEED 1914) hypothesis (i.e. that the largest resorption of CSF occurs through the arachnoid granulations) has been challenged by many investigators and in particular by HOWARTH & COOPER (1955) and KISS & SÄTTLER (1956), there is no doubt from our studies that a significant part of the CSF streams toward the region where these granulations abound. Occasionally the activity penetrates into the ventricular system after intrathecal injection in such an amount as to be recognized pictorially in the scans through the familiar morphology of the ventricles (Fig. 5). When the tracer is injected within the ventricles the passage into the cisterna magna takes place in a few minutes (Fig. 6). Afterwards the spreading from the cisterna magna to the hemispheric convexity is analogous to the one observed in cisternography. As expected, individual variations play an important role. We have constantly observed, for instance, that in children the spreading of activity is faster than in adults. We would like to point out that most of our patients were epileptics. Many of them had neuroradiological studies within normal limits.

Quantitative determinations by head scanning of the amount of the intrathecally injected material which has reached the endocranium and of the amount which has remained in the lumbar area are at best gross. Our judge-

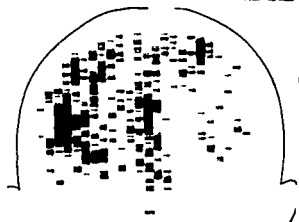


Fig 7 No air was visible at encephalography but at scintillography a pool of tracer was seen on right convexity. At surgery a huge arachnoidal cyst was found at the site (see specimen)

cisternography) and intraventricularly (isotope ventriculography). The diagnostic value of the isotope cisternography and isotope ventriculography is now established. The present report, however, is not mainly concerned with these diagnostic aspects, but with the possible applications to the physiology of the movement of the CSF. Keeping this in mind we have used, in some patients, ^{131}I tagged autologous CSF. Here the only foreign substance injected in the system is the tagging isotope. The distribution pattern and the rate of flow of the tagged autologous CSF is analogous to the one observed with the radioiodinated serum albumin (Fig 2). At one hour the basal cisterns are well filled with activity, at three the activity has reached the Sylvian fissures, at 12 it is over the convexity. Generally at 24 hours high activity is present along the superior longitudinal sinus (Fig 3). The ascending of the fluid takes place mostly through the anterior subarachnoidal pathways (Fig 4) — cisterns in front of the brain stem, suprasellar, subfrontal, prefrontal spaces — and the Sylvian fissures. These are the highways of the CSF circulation. In the posterior subarachnoid spaces (supracerebellar, occipital posterior parietal) very little activity is seen. At 24 to 48 hours the injected tagged albumin is predom-

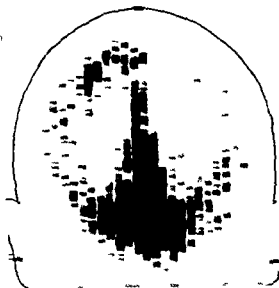


Fig 8 Partial block of CSF pathways at left tentorial notch. Activity reaches convexity mainly through right routes.

nantly often exclusively recognized in the parasagittal area along the superior longitudinal sinus. Though recently the so called Key and Retzius-Weed (WEED 1914) hypothesis (i.e. that the largest resorption of CSF occurs through the arachnoid granulations) has been challenged by many investigators and in particular by HOWARTH & COOPER (1955) and KISS & SÄTTLER (1956) there is no doubt from our studies that a significant part of the CSF streams toward the region where these granulations abound. Occasionally the activity penetrates into the ventricular system after intrathecal injection in such an amount as to be recognized pictorially in the scans through the familiar morphology of the ventricles (Fig. 5). When the tracer is injected within the ventricles the passage into the cisterna magna takes place in a few minutes (Fig. 6). Afterwards the spreading from the cisterna magna to the hemispheric convexity is analogous to the one observed in cisternography. As expected, individual variations play an important role. We have constantly observed for instance that in children the spreading of activity is faster than in adults. We would like to point out that most of our patients were epileptics. Many of them had neuroradiological studies within normal limits.

Quantitative determinations by head scanning of the amount of the intrathecally injected material which has reached the endocranium and of the amount which has remained in the lumbar area are at best gross. Our judge

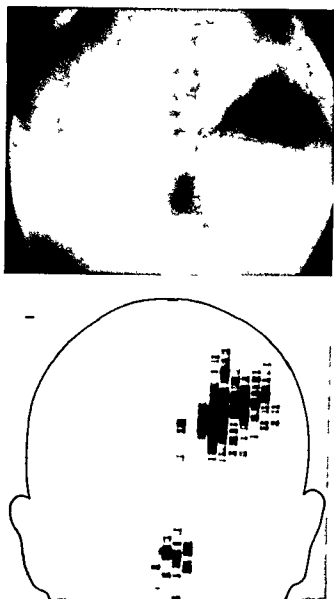


Fig 9 Spontaneous ventriculostomy with porencephalic cyst communicating both with lateral ventricle and subarachnoidal spaces Upper view Axial transverse encephalogram Lower view Isotope cisternogram

ment is that $1/5$ to $1/3$ (20 to 35 microcuries) of the hundred microcuries introduced by lumbar puncture eventually reach the endocranium. The lumbosacral 'cul de sac' — as judged by external scintillation scanning—remains 'hot' for at least 48 hours.

When using radio iodinated serum albumin, as we do in most instances, the albumin concentration has varied in our ventriculo- and cisternograms from a

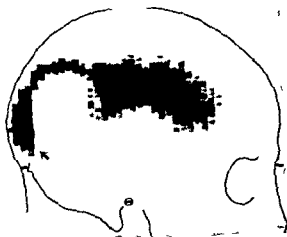


Fig 10 Flocked (arrow) ventriculo-cisternal shunt.

minimum of 10 mg per ml (before adding the diluting Elliott's B solution) to a maximum of about 50. No appreciable distribution differences have been noted within this range of albumin concentration. We generally work with preparations containing a specific activity of 500 microcuries per ml. The total amount of fluid injected is 5 to 10 ml, i.e. 1/15 to 1/30 of the commonly estimated 130 to 150 ml amount of CSF in adults. As detected previously with gold-labeled albumin also demonstrated that an increase in the volume of injected fluid increases the rate of upward movement of the tracer.

This report is not, as noted above, concerned with the diagnostic applications of isotope ventriculography and cisternography. However, some pathologic cisterno- and ventriculograms may be pertinent to emphasize some of our physiological observations. Thus the injected radioactive material reaches every spot bathed by the CSF itself. This is not always the case of the injected air in encephalography (Fig 7). Whenever and wherever a block to the free movement of the CSF exists, the radioactive material follows other open routes to reach the hemispheric convexities (Fig 8). In fact, in such instances, the radioactivity spreading through the open pathways is in higher concentration—vicarious function—than in cases in which no block exists. The amount of radioactivity immediately proximal to a block is larger than normally seen—prestenotic dilatation of the subarachnoid pathways—this observation being in agreement with what Dorr & Gillingham (1958) observed at surgery. The labeled fluid passes through spontaneous (Fig 9) and surgical shunts (Fig 10).

The motion of the injected tagged albumin is undoubtedly more than a mere mixing effect or simple diffusion—at least from the cisterna magna up

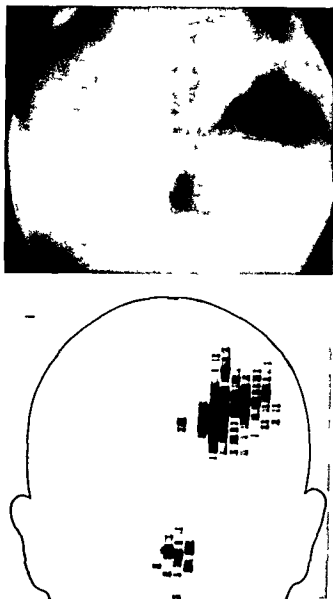


Fig 9 Spontaneous ventriculostomy with porencephalic cyst communicating both with lateral ventricle and subarachnoidal spaces. Upper view: Axial transverse encephalogram. Lower view: Isotope cisternogram.

ment is that $1/5$ to $1/3$ (20 to 35 microcuries) of the hundred microcuries introduced by lumbar puncture eventually reach the endocranium. The lumbosacral cul de sac — as judged by external scintillation scanning—remains 'hot' for at least 48 hours.

When using radio iodinated serum albumin, as we do in most instances, the albumin concentration has varied in our ventriculo- and cisternograms from a

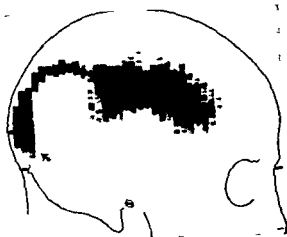


Fig 10 Blocked (arrow) ventriculo-cisternal shunt

minimum of 10 mg per ml (before adding the diluting Elliott's B solution) to a maximum of about 50. No appreciable distribution differences have been noted within this range of albumin concentration. We generally work with preparations containing a specific activity of 500 microcuries per ml. The total amount of fluid injected is 5 to 10 ml, i.e. 1/15 to 1/30 of the commonly estimated 130 to 150 ml amount of CSF in adults. As detected previously with gold-labeled albumin also demonstrated that an increase in the volume of injected fluid increases the rate of upward movement of the tracer.

This report is not, as noted above, concerned with the diagnostic applications of isotope ventriculography and cisternography. However, some pathologic cisterno- and ventriculograms may be pertinent to emphasize some of our physiological observations. Thus the injected radioactive material reaches every spot bathed by the CSF itself. This is not always the case of the injected air in encephalography (Fig 7). Whenever and wherever a block to the free movement of the CSF exists, the radioactive material follows other open routes to reach the hemispheric convexities (Fig 8). In fact, in such instances the radioactivity spreading through the open pathways is in higher concentration—vicarious function—than in cases in which no block exists. The amount of radioactivity immediately proximal to a block is larger than normally seen—prestenotic dilatation of the subarachnoid pathways—this observation being in agreement with what DOTT & GILLINGHAM (1958) observed at surgery. The labeled fluid passes through spontaneous (Fig 9) and surgical shunts (Fig 10).

The motion of the injected tagged albumin is undoubtedly more than a mere mixing effect or simple diffusion—at least from the cisterna magna up

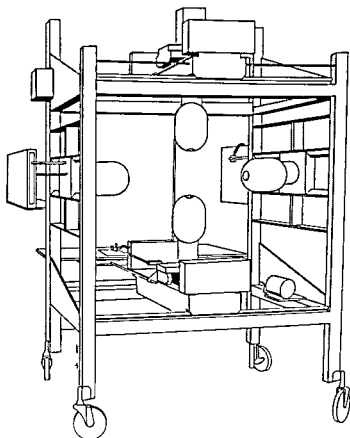


Fig 11 Four probe scanner

We are confronted, in my opinion, with a 'transport' or 'sweeping' phenomenon, possibly with an ebb and flow component but definitely with a net forward progression. This may be a product of vascular pulsations, choroid plexuses pulsations, or may be caused by the *vis a tergo* of the newly formed fluid. We wish to stress at this point that the movement of the tagged fluid through the cerebrospinal pathways is not affected by the movements or the positioning of the patient. The same distribution pattern has been noted in patients kept supine and with the head lower than the feet and in other patients who, after the lumbar puncture, have freely moved and walked around the room.

In three patients we have attempted to carry out an isotope cisternography using 500 microcuries of Technetium 99m (pertechnetate — $^{99m}\text{TcO}_4$). The radioactivity never ascended towards the endocranium but spread freely from the lumbar region into the blood stream. Already one hour after the intrathecal injection of the pertechnetate one could demonstrate by head scanning the high activity in the salivary glands which one finds after the intravenous in

jection of the same isotope. This was also the case in a patient in whom we injected 500 microcuries of Technetium 99m intraventricularly. This confirms the observations of other investigators (HOWARTH & COOPER 1949, SWEET et coll 1954) of how critical is the molecular size when studying the CSF with tracers. Tracers with small molecular size leave the CSF at the closest point and do not follow in any significant amount the CSF in its flow. Therefore the observations made by others on the circulation of the CSF with radiosodium (EICHLER, LINDEP & SCHMEISER 1951) and the method suggested by CROW, KEOGH & NORTHFIELD (1956) for the localization of CSF fistulae also with radiosodium, have little value.

Isotope ventriculography and cisternography will offer additional information on the problem of the normal and abnormal CSF circulation when already available technical refinements are applied to these procedures. With four probes (Fig. 11) the scanning time will be markedly reduced and we will be able to study the movement of the tagged fluid simultaneously in the three dimensions. With the gamma cameras and with the future cine registration and television monitoring, fast recordings of the activity spreading will be possible. With the technique of image separation or radioactive tomography (KAHL 1964) we will be able to evaluate how often a cisterno-ventricular backflow of fluid occurs and how significant this is. With tomography we will also probably be able to establish whether it is true that the spinal fluid moves in two streams in the spinal canal — descending behind the cord and ascending in front of it. New ideas in the field of tracers for isotope ventriculography and cisternography are also worth pursuing, though it is our present opinion that serum albumin and in particular the autologous CSF tagged with iodine have many advantages. Tagging the albumin with an isotope better suited for scanning work than ^{131}I may be a lead worth following.

Conclusions

1. With the techniques of isotope ventriculography and cisternography we may pictorially appraise the movement of the CSF in living humans.
2. Our observations, especially when using tagged autologous CSF, are made under almost ideal conditions, i.e. a closed system with no foreign substance in the physiological system.
3. The CSF begins to leave the ventricular system very rapidly — within minutes.
4. At least a part of the lumbo-sacral CSF ascends to the basal cisterns. Thus upward movement takes place in about 1 hour, possibly faster in children.
5. The fluid arriving in the basal cisterns from the ventricular system or the

spinal canal ascends toward the convexity of the brain following a constant pattern, through the anterior and Sylvian subarachnoid pathways in 4 to 8 hours

6 At 24 to 48 hours after the intraventricular or intrathecal injection, the tagged albumin 'crowds' in the parasagittal area, while little or no activity is evident in the rest of the CSF pathways

7 When a normal path is blocked the fluid moves along other open channels which, as vicariously functioning, let a larger amount of activity pass through than normally

8 The particle size of the tracers to be used to study the CSF flow is of critical importance. Small molecules move freely out of the CSF cavities at the closest point and therefore do not follow the mainstream. Other factors than particle size, such as electrical charge and lipid solubility, possibly play an important role in this respect

9 It is probably true that the CSF is formed everywhere and resorbed everywhere in the CSF cavities. It is also true, however, that possibly due to the vascular and choroid plexuses pulsations, plus the 'vis a tergo' of the newly produced fluid, at least a portion of this fluid moves in a current like fashion

SUMMARY

With the techniques of isotope cisternography and isotope ventriculography we have been able to ascertain that at least part of the cerebrospinal fluid moves in a flow within the fluid pathways in living humans. This flow has been mapped by serial scans. These observations give a better understanding of the normal and abnormal dynamics of the cerebrospinal fluid circulation.

ZUSAMMENFASSUNG

Mit der Technik der Isotopen Cisternographie und Ventrikulographie konnten wir beweisen, dass wenigstens ein Teil der Cerebrospinalflüssigkeit sich in den Liquorraumen des lebenden Menschen flussartig bewegt. Dieser Fluss wurde mit Seriencans ermittelt. Diese Beobachtungen tragen zu einem besseren Verständnis der normalen und abnormalen Dynamik der Liquorzirkulation bei.

RÉSUMÉ

L'auteur a pu, par les techniques de cisternographie isotopique et de ventriculographie isotopique, montrer qu'une partie au moins du liquide céphalo-rachidien se déplace en un courant dans les voies liquidiennes chez l'homme vivant. Ce courant a été étudié par des scintigraphies en série. Ces observations permettent de mieux comprendre la dynamique normale et pathologique de la circulation du liquide céphalo-rachidien.

REFERENCES

- BERNG JR E A Studies on the role of the choroid plexus in tracer exchanges between blood and CSF *J Neurosurg* 12 (1955) 385
- BOWSHIER D Cerebrospinal fluid dynamics in health and disease Charles C Thomas Springfield 1960
- CROW H J, KEOGH C and NORTHFIELD D W C The localisation of cerebrospinal fluid fistulae *Lancet* 271 (1956) 325
- DANDY W E and BLACKFAN K D Internal hydrocephalus *Amer J Dis Child* 8 (1914), 406
- DI CHIRO G Anatomical three-dimensional brain scanning *In* Radio-isotopes et affections du système nerveux central Ed T Plantol Masson & Cie Paris 1960
- DI CHIRO G Movement of the cerebrospinal fluid in human beings *Nature* 204 (1964) 290
- New radiographic and isotopic procedures in neurological diagnosis *J Amer med Ass* 188 (1964) 524
- and REAMES P M Isotopic localization of cranio-rasal cerebrospinal fluid leaks *J Nucl Med* 5 (1964) 316
- and MATTHEWS JR W B RISA ventriculography and RISA-cisternography *Neurology* 14 (1964) 185
- DOTT N M and GILLINGHAM F J Mechanical aspects of the cerebrospinal fluid circulation physiological pathological surgical *In* Ciba Foundation Symposium on The Cerebrospinal Fluid Editors C E W Wolstenholme and C M O'Connor Little Brown and Co Boston 1958
- EICHLER O, LINDER F and SCHMEISER K Über die Bildung von Liquor im Lumbalraum nachgewiesen mit Radionatrium *Klin Wschr* 29 (1951) 9
- FLAUGELST B Cervical myelography with watersoluble contrast medium experimental study in dogs *Acta radiol* 56 (1961) 237
- HASTY G B So-called circulation of the cerebrospinal fluid *J Amer med Ass* 101 (1933) 821
- HO ARTH F and COOPER E R A Departure of substances from the spinal theca *Lancet* 2 (1949) 937
- The fate of certain foreign colloids and crystalloids after subarachnoid injection *Acta anat* 25 (1955) 112
- KISS F and SATTLER J Struktur und Funktion der Pacchionischen Granulationen *Anat Anz* 103 (1946) 273
- KOSTER H, SHAPIRO A and LEIKENSOHN A Concentration of procaine in cerebrospinal fluid of human being after subarachnoid injection *Arch Surg* 37 (1938) 603
- LUHL D E Scanning the brain in cross section *J Nucl Med* 5 (1964) 371
- O'CONNELL J E A The vascular factor in intracranial pressure and the maintenance of the cerebrospinal fluid circulation *Brain* 66 (1943) 204
- RIESELBACH R E, DI CHIRO G, FREIREICH E J and RALL D P Subarachnoid distribution of drugs after lumbar injection *New Eng J Med* 267 (1962) 1273
- RISER M M J Les liquides céphalo-rachidiens *Physiologie et exploration du système ventriculo-méningé* Masson et Cie Paris 1929
- SACHS E, WILKINS H and SAMS C F Studies on cerebrospinal circulation by a new method. *Arch Neurol* 23 (1930) 130
- SEPP E D e Dynamik der Blutzirkulation im Gehirn *J Springer* Berlin 1928

- SOLOMON H C THOMSON I J and PREIFFER H M Circulation of phenolsulphonephthalein in the cerebro spinal system J Amer med Ass 79 (1922), 1014
- SWEET H H, BROWNELL G SCHOLL J A BOWSER D R BENDA Ph and STICKLEY E E The formation flow and absorption of cerebrospinal fluid newer concepts based on studies with isotopes Research Publ Ass nerv ment Dis 34 (1954) 101
- WEED L H Studies on the cerebrospinal fluid III The pathways of escape from the subarachnoid spaces with reference to the arachnoid villi J med Res 26 (1914) 51
- WESTON P G Phenolsulphonephthalein absorption from subarachnoid space in paresis and dementia praecox Arch Neurol 5 (1921) 58

RADIOLOGICAL ASPECTS OF SPINAL CYSTICERCOSIS

by

JAIME DORFSMAN

Cysticercosis of the central nervous system is well known in places such as Latin America India Russia some Mediterranean areas and other countries. This type of cysticercosis may be either cerebral (DORFSMAN 1963) spinal or a combination of both. Cerebral forms are the most frequent and best known. The diagnosis is relatively simple when using encephalography and/or ventriculography in combination with the cerebrospinal fluid laboratory tests (DORFSMAN 1963). Spinal cysticercosis is the rarest form of this disease. It is difficult to determine the real incidence of this form mainly because postmortem studies of the vertebral column are often ignored. However, we have an approximate idea based on our clinical series the ratio being one hundred cerebral to one spinal. On the other hand the ratio in our series of cerebral cysticercosis to the remainder of cerebral lesions which produce intracranial hypertension is 1 to 3. These approximate figures give us a good idea of the high frequency of cerebral cysticercosis and the rarity of spinal cysticercosis. The reason for this difference is not known though some hypotheses have been advanced to explain this discrepancy. The literature concerning spinal cysticercosis is very scanty (CABIESES et coll 1959) and we have no knowledge of any work which specifically describes the radiological changes in this disease.



Fig 1 Multiple lumbar intradural extramedullary filling defects caused by vesicles of cysticercus. One of them (arrow) was the only one among all cases which was seen to move in different positions (L 5 and L 4)



Fig 2 Single intradural extramedullary vesicle of cysticercus (arrow) associated with irregularities and fragmentation of the contrast medium in the lower cervical region

The present paper is based on the study of seven such cases, all of them sub arachnoid, we have not seen any intramedullary cases, although this type has been described elsewhere (CABIESER et coll 1959). The localization was as follows: one cervical, two in the cervico thoracic region, one thoracic (Th 10) and three in the lumbar region. The clinical picture in all cases was a more or less advanced cord or radicular compression, and in none save one was it possible to make the etiological diagnosis using only the clinical findings. The only case which was diagnosed clinically as spinal cysticercosis had cerebral cysticercosis as well. Conventional films of the vertebral column showed no abnormalities related to the disease. Myelography was performed in every case. Five demonstrated intradural extramedullary filling defects variable in size and more or less spherical in shape. In four cases these defects were multiple (Fig 1), being associated with adjacent irregularities and fragmentation of the column of contrast medium (Fig 2). The fifth case had a single defect which in turn produced a complete obstruction at C 2 (Fig 3). Four of these cases were diagnosed radiologically as probable, intradural extramedullary tumors, one of them suggesting the possibility of vascular malformation. The other case was the only one diagnosed clinically and radiologically as spinal



Fig 3 Complete obstruction at C 2 (external puncture) due to an intramedullary vesicle



Fig 4 Arachnoiditis with small vesicles of cysticercosis. Fragmentation and irregularities of the contrast medium with complete obstruction at Th 12



Fig 5 Expanded process at Th 1 diagnosed as possible intramedullary tumor (Courtesy of P. BELTRAN)

cysticercosis The remaining two cases showed only marked irregularities deformities and fragmentation of the column of contrast medium with complete obstruction in one at Th 9 and in the other at Th 12 (Fig 4). These two cases were diagnosed as non specific arachnoiditis. In all cases spinal fluid was taken during myelography; the laboratory tests reported in each of them an inflammatory process of the type usually seen in cysticercosis. In four cases the cysticercosis reaction was positive. In the remaining three cases this reaction was not performed. All cases were verified surgically demonstrating in all of them vesicles with multiple cysts localized in the subarachnoid space and associated with a severe adjacent arachnoiditis. In the two cases where no myelographic filling defects were seen and only an arachnoiditis was demonstrated, some of the vesicles were bound to the arachnoidal reaction and others were located distal to the site of obstruction. This explains why the vesicles were not shown during the myelography.

Although the myelographic diagnosis of these lesions is non specific from the experience acquired in these seven cases we can suggest that in places

where cysticercosis is a common disease, the presence in the myelogram of single or multiple, intradural extramedullary defects associated with an adjacent arachnoiditis, or arachnoiditis alone, would strongly indicate the possibility of spinal cysticercosis, which can be easily corroborated by the cerebrospinal fluid studies, specifically the cysticercosis reaction. With these two studies (myelography and cerebrospinal fluid tests) it will be possible to make the correct topographic and etiologic pre-operative diagnosis in practically all of the cases. When making the radiological diagnosis of this disease, other multiple intradural extramedullary lesions such as neurofibromas, meningiomas and metastasis should also be borne in mind.

Another case was seen after this study had been completed, myelography suggested an intramedullary tumor (Fig. 5), but at operation a single intradural, extramedullary vesicle of cysticercus was encountered, well attached to the dorsal aspect of the cord, and was easily separated by blunt dissection.

SUMMARY

The myelographic changes of spinal cysticercosis are described on the basis of 8 observed cases. The appearances were not specific. In almost all cases the pre-operative diagnosis could be made with the aid of the spinal fluid laboratory tests.

ZUSAMMENFASSUNG

Es werden die myelographischen Veränderungen bei spinaler Cysticercosis an Hand von 8 beobachteten Fällen beschrieben. Die Befunde waren nicht spezifisch. In fast allen Fällen konnte die Diagnose mit Hilfe der Laboruntersuchungen gestellt werden.

RÉSUMÉ

Description d'après 8 cas des signes myélographiques de la cysticercose médullaire. Les images ne sont pas spécifiques. Dans presque tous les cas les examens de laboratoire du liquide céphalo rachidien ont permis de faire le diagnostic pré opératoire.

REFERENCES

- CABIESER F. et coll. Cysticercosis of the spinal cord. *J. Neurosurg.* 16 (1959) 357.
 DORFSMAN J. The radiological aspects of cerebral cysticercosis. *Acta radiol. (Diagnosis)* 1 (1963) 836.

SYPHONAGE TECHNIQUE FOR REMOVAL OF PANTOPAQUE

by

B S EPSTEIN and J A EPSTEIN

Pantopaque myelography is in many quarters a standard procedure in the investigation of diseases of the vertebral column the spinal cord and its coverings. While there is some question as to whether or not Pantopaque can remain safely within the subarachnoid space it is generally held that its removal is advisable. At present this is accomplished by aspiration through the lumbar puncture needle as described by KUBIK and HAMPTON in 1941. The movement imparted to fluid within the spinal canal by the Valsalva maneuver of straining or coughing (EPSTEIN 1944 REITMAN 1941) also is used to facilitate its removal (SCOTT & FURLOW 1944). Not infrequently the patient complains of considerable pain during this part of the examination so much so that the procedure has to be discontinued. The apprehension in the minds of patients and physicians as to the rigors of myelography should not be underestimated.

The present study is concerned with the position of the needle tip in the spinal canal its relationship to nerve roots the configuration of the spinal canal and the withdrawal of Pantopaque by means of the creation of a syphon (EPSTEIN 1964). Experience with this technique in 40 consecutive myelographic examinations has shown that Pantopaque can be syphoned off quite completely and with little or no pain.

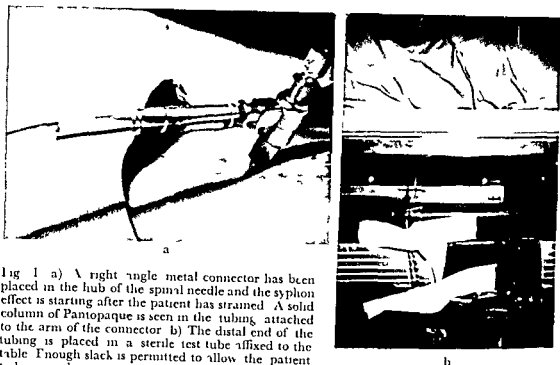


Fig 1 a) A right angle metal connector has been placed in the hub of the spinal needle and the syphon effect is starting after the patient has strained. A solid column of Pantopaque is seen in the tubing attached to the arm of the connector b) The distal end of the tubing is placed in a sterile test tube affixed to the table. Enough slack is permitted to allow the patient to be moved.

The aspiration of Pantopaque from the lumbar subarachnoid space is facilitated when the tip of the spinal needle is at or close to the midline and somewhat above or below the level of an intervertebral disc. A relationship exists between the configuration of the spinal canal and the ease of instillation and removal of Pantopaque (EPSTEIN et coll 1964). Quite often the introduction of a lumbar puncture needle into a lumbar canal with an anteroposterior diameter of less than 1.2 cm is difficult, and removal of Pantopaque is more likely to be troublesome and painful. On the other hand, a wide canal usually permits easy introduction and aspiration of the contrast material. Intrusions of discal material or spondylotic spurs into canals of wider dimensions may be without clinical significance while similar lesions can be productive of severe disturbances in patients with narrow canals (EPSTEIN et coll 1962, VERBIEST 1954).

Whether the lumbar spinal canal is normal in width and configuration or narrowed, intrusion of a nerve root into the lumen of the needle tip will interrupt the flow of Pantopaque while it is being aspirated. This occurs even with the needle tip placed in the midline but is more likely to take place when the canal is narrowed. Even the gentlest aspiration may be quite painful, and the patient often complains of exquisitely localized radicular pain at that time. If the needle tip is situated laterally the possibility of intraluminal

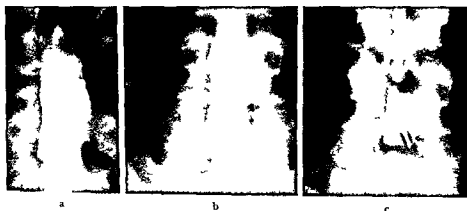


Fig 2 a) The tip of the lumbar puncture needle is situated far in the left lateral recess at the fourth interspace. The canal is of normal dimensions. b) The syphon tube is connected directly to the hub of the needle. Flow is taking place. A nerve root is seen close to the needle tip. c) After rotation of the needle syphonage proceeded satisfactorily. Only a few droplets of Pantopaque remain.

intrusion of a nerve root is increased and painful unsuccessful attempts at aspiration follow. Manipulating and twisting the needle often produces nothing more than added discomfort and may be accompanied by bleeding into the subarachnoid space. Furthermore, the needle tip must be placed as close as possible to the floor of the canal for the successful removal of Pantopaque. Otherwise only clear cerebrospinal fluid or fluid mixed with Pantopaque is withdrawn.

During the past six months we have employed a syphon method for the removal of Pantopaque. A syphon effect is created when a sterile polythene tube is attached to the hub of the lumbar puncture needle by way of either a three way stopcock or a right angle metal connector. This is preferred to direct attachment of the tube because it reduces the height of the apparatus. Syphonage also is improved if the lumbar puncture needle used is as short as possible. The distal tip of the drainage tube is placed in a sterile container about 30 cm below the level of the spinal canal. A valve may be placed in the system to interrupt the flow at times. The system should be air tight so that the syphon action is not interrupted by air bubbles. Flow is started by having the patient strain or take a series of deep breaths. Occasionally it is necessary to aspirate gently from the distal end of the system. Usually the flow continues nicely once the head of the fluid column is below the level of the needle tip. Manipulation of the position of the Pantopaque is greatly facilitated by the use of image intensification. This permits the radiologist to minimize the quantity of fluid removed by keeping the Pantopaque column at the tip of the needle. So long as the

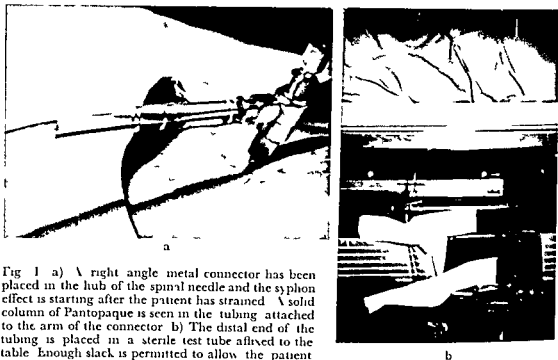


Fig. 1 a) A right angle metal connector has been placed in the hub of the spinal needle and the siphon effect is starting after the patient has strained. A solid column of Pantopaque is seen in the tubing attached to the arm of the connector. b) The distal end of the tubing is placed in a sterile test tube affixed to the table. Enough slack is permitted to allow the patient to be moved.

The aspiration of Pantopaque from the lumbar subarachnoid space is facilitated when the tip of the spinal needle is at or close to the midline and somewhat above or below the level of an intervertebral disc. A relationship exists between the configuration of the spinal canal and the ease of installation and removal of Pantopaque (EPSTEIN et coll 1964). Quite often the introduction of a lumbar puncture needle into a lumbar canal with an anteroposterior diameter of less than 1.2 cm is difficult, and removal of Pantopaque is more likely to be troublesome and painful. On the other hand, a wide canal usually permits easy introduction and aspiration of the contrast material. Intrusions of discal material or spondylotic spurs into canals of wider dimensions may be without clinical significance while similar lesions can be productive of severe disturbances in patients with narrow canals (EPSTEIN et coll 1962, VERBIEST 1954).

Whether the lumbar spinal canal is normal in width and configuration or narrowed, intrusion of a nerve root into the lumen of the needle tip will interrupt the flow of Pantopaque while it is being aspirated. This occurs even with the needle tip placed in the midline, but is more likely to take place when the canal is narrowed. Even the gentlest aspiration may be quite painful, and the patient often complains of exquisitely localized radicular pain at that time. If the needle tip is situated laterally the possibility of intraluminal

space because the patients immediately mentioned that pain could be felt on the affected side radiating to the lower extremity, the buttock or the perineum. If the flow of cerebrospinal fluid was free the Pantopaque was injected under image intensification control. Eleven of these patients had narrowed canals with the sagittal diameters less than 1.3 cm in diameter at the level of the spinal tap. Four patients had normal spinal canals. The removal of Pantopaque by syphonage was successful in 11 patients without delay. In 3 the needle tip became occluded by a nerve filament. The needle was rotated to disengage the obstruction whereupon syphonage continued. In one patient the needle tip rested in the subdural space and no return was obtained. The arachnoid became depressed as the needle was advanced. Withdrawal and reinsertion one interspace lower was followed by rapid syphonage.

The quantity of fluid removed by syphonage is quite variable. If one is careful to permit the syphon to function only when Pantopaque is being removed the procedure may be performed with removal of about 20 or 25 ml of clear cerebrospinal fluid. Often this is not within the control of the radiologist because a needle with a relatively long bevel will permit passage of a considerable quantity of cerebrospinal fluid towards the end of the procedure. For this reason we prefer a relatively short bevelled needle. The control of the position of the Pantopaque column often is rather unpredictable. Only an examiner who has observed the vagaries of a Pantopaque column towards the end of the syphonage can understand how vexing the removal of the last drop can be. However the fact that Pantopaque can be removed quickly relatively completely and often without pain makes the procedure worth while.

SUMMARY

A syphonage technique is described which has been used successfully for the removal of Pantopaque from narrow as well as from wide canals with the needle tip placed centrally or laterally.

ZUSAMMENFASSUNG

Eine Aspirations-Technik die bei der Entfernung von Pantopaque aus engen wie auch aus weiten Kanälen erfolgreich war wird beschrieben. Die Lage der Nadelspitze war zentral oder lateral.

RESUME

Description d'une technique de syphonage utilisée avec succès pour retirer le Pantopaque de canaux étroits ou larges. L'extrémité de l'aiguille étant placée au centre ou latéralement.

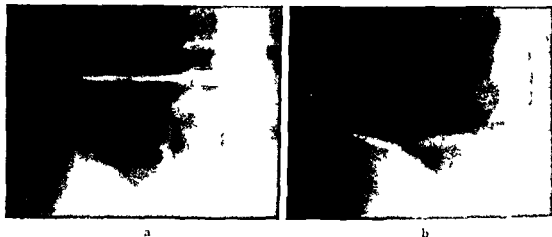


Fig 3 a) The syphonage is beginning and a solid column of Pantopaque is seen in the tubing b) Towards the end of the procedure droplets of Pantopaque are interspersed with cerebrospinal fluid. Practically complete evacuation was obtained.

level of the spinal needle is completely immersed in Pantopaque its passage is uniform. This can be watched either through the image intensifier or by inspecting the transparent polythene tube. Towards the end of the procedure the bevel becomes only partly immersed, so that an emulsion of cerebrospinal fluid and Pantopaque passes through the tube. When the last droplets are marshalled to the needle tip it is not uncommon to observe a beaded arrangement of drops of Pantopaque and cerebrospinal fluid.

This procedure has been successful in 38 out of 40 consecutive patients in whom from 10 to 35 ml of Pantopaque had been injected into the subarachnoid space. Adequate removal was attained in that less than approximately 0.25 ml of Pantopaque or a few tiny globules remained in the canal in 14 patients. In four about 0.5 ml persisted because the globules could not be marshalled to the tip of the needle. In two patients the needle tip was occluded by a nerve root and replacement of the needle was required. This was done by partly withdrawing the needle and reinserting it into the same interspace after checking the position and direction of the needle with the image intensifier.

In 25 patients the needle tip was at or close to the midline and in 24 of these the Pantopaque was syphoned off quickly and painlessly. Of these, 18 had spinal canals which were normal in configuration. In 7 the sagittal diameter of the canal at the level of insertion of the needle was between 1.0 and 1.3 cm. In one patient a nerve filament occluded the orifice of the needle and some manipulation was required to free the tip. In 15 patients the needle tip was off center, often close to the lateral margins of the spinal canal. We could usually predict this as soon as the needle tip entered the subarachnoid

EMBRYOLOGIC ORIGIN OF SPINAL MALFORMATIONS

by
W. JAMES GARDNER

In acquired disease states the terms early and mild as well as severe are almost synonymous whereas the opposite is true in congenital disorders. In the investigation of a disease process it is usually begun with the study of mild cases and progress to the severe cases is followed unintentionally in the study of certain cases of the central nervous system. The accumulated experience has led to the recognition of syringomyelia as representing the mild extreme of a spectrum of which its severe form is responsible for myelomeningocele and diastematomyelia.

The cavity of syringomyelia consists fundamentally of a canal of the cord (hydromyelia). This dilatation is usually fully enclosed in a dilated portion of the bony canal also constitutes an essential feature of diastematomyelia. Klippel Feil syndrome and of posterior lumbosacral agenesis (hemivertebrae) and of posterior lumbosacral agenesis (hemivertebrae). In each of these conditions the dilated tube of the spinal cord contains neural tissue within a dilated tubular structure, the relationship

REFERENCES

- EPSTEIN B S The removal of Pantopaque from the lumbar spinal canal by means of siphonage To be published in Radiology
- The effect of increased intraspinal pressure on the movement of iodized oil within the spinal canal Amer J Roentgenol 52 (1944), 196
- EPSTEIN J A and LAVINE L The effect of anatomic variations in the lumbar vertebrae and spinal canal on cruda equina and nerve root syndromes Amer J Roentgenol 91 (1964) 1055
- EPSTEIN J A, EPSTEIN B S and LAVINE L Nerve root compression associated with narrowing of the lumbar spinal canal J Neurol, Neurosurgery Psychiat 25 (1962) 163
- KUBIK C S and HAMPTON A O Removal of iodized oil by lumbar puncture New Engl J Med 224 (1941) 455
- REITMAN H On movements of fluid inside the cerebrospinal space Acta radiol 22 (1941) 455
- SCOTT W G and FURLOW L T Myelography with Pantopaque and a new technic for its removal Radiology 43 (1944) 241
- VERBIEST H Radicular syndrome from developmental narrowing of lumbar vertebral canal J Bone Jt Surg 36 B (1954) 230

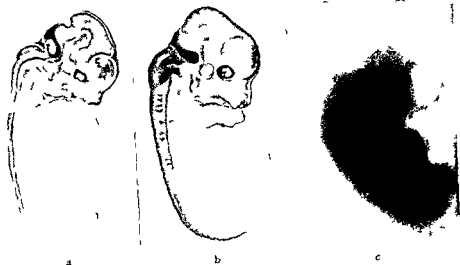


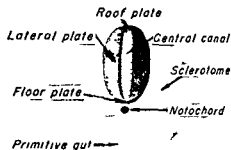
Fig. 2. Pig embryos 18 mm (a) and 26 mm (b) corresponding in development to the sixth and eighth week in the human, reduced to same overall length in order to better depict the increased distention of the neural tube in the older embryo. This degree of hydrocephalus and hydromyelia phylogenic in embryonal life is obstructive until the sixth week when fluid is just beginning to push through attenuating areas in the rhombic roof. It is communicating at the eighth week by which time the entire subarachnoid space has been dissected open. Neural tubes outlined with precipitated crystals of Prussian blue. Section overstained on of the neural tube at the sixth week (a) will result in posterior rupture (myelomelia) of the less mature caudal somites to constitute the embryonic foreunner of myelomelia. The escape of fluid from the neural tube interferes with the dissection of the subarachnoid space. Overdistention occurring after the development of the subarachnoid space (b) may cause the meninges to bulge posteriorly without rupturing because the skin being more mature is tougher. Compensation may then occur and the infant will be born with a meningocele covered with intact skin. If separation of the lateral plates of the neural tube also has occurred, diastematomyelia will be present beneath the meningocele. A sixth week human embryo (c) photographed in transmitted light by transillumination. The fluid-filled portions are lighter and correspond to the dark areas (a).

(a and b: Courtesy Carnegie Institution of Washington.)

Hydromyelic theory. Two hundred years ago MORGAGNI (1769) was unencumbered with the knowledge that the sac of a myelomelia consists of an open neural tube and therefore must represent failure of closure of the embryonal neural groove. From his observations he naively concluded that these watery tumors of the vertebrae result from the pressure of fluid descending from the hydrocephalic head through the tube of the spine and pressing the bones asunder. More than a century later VON RECKLINGHAUSEN (1886) disputed this hydromyelic mechanism. Because his microscope revealed an open portion of the neural tube within the sac he believed it to be the result of failure of closure. Von Recklinghausen's belief since has been repeatedly confirmed albeit by investigators whose observations were based on this preconceived idea. It is



Photomicrograph of
16-somite human embryo



Photomicrograph
shown diagrammatically



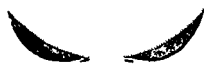
Dilatation of neural tube
Stage 1



Separation of roof and floor plates
Stage 2



External rupture
Stage 3



External and internal rupture
Stage 4

Fig 1 Effect of overdistention of neural tube on surrounding germ layers. Because the roof and floor plates as seen in the photomicrograph and the diagram are thin with little reinforcing tissue they will yield readily in response to overdistention of the lumen. At stage 1 if overdistention becomes compensated the roof and floor plates though stretched remain intact and syringomyelic symptoms develop in adulthood. At stage 2 the continuity of the roof and floor plates is interrupted. If compensation then occurs the lateral plates may close separately to form two hemicords and diastematomyelic symptoms develop in adolescence. Above the diastematomyelia is hydromyelia. At stage 3 if the neural tube ruptures through the overlying ectoderm (posterior myeloschisis) compensation cannot occur and myelocle is obvious at birth the open everted spinal cord may be split (diastematomyelia) and cephalad to it the cord is hydromyelic. If as shown in stage 4 the floor and roof plates rupture (posterior and anterior myeloschisis) the fetus dies in utero with a gut fistula presenting in a myeloschi is.

(Photomicrograph Courtesy E. C. SENSENIG, Carnegie Institution of Washington)



Fig. 4. Syringomyelia stage 1: the patient's symptoms developed at the age of 11 years. A dilated tube of neural tissue (a) was found within the dilated tube of bone (b).

ure of closure of the neural plate (myelochisis) can be reproduced by slitting open the closed neural tube. It is further supported by the work of HOLTZER (1952) who demonstrated that the diameter of the developing spinal canal of the embryo is determined by the diameter of the neural tube that it encloses. He found that migrating precartilaginous cells respond in a discriminatory and stereotyped fashion to the presence of any neural tissue by maintaining a characteristic distance from the neural tissue. The precartilaginous cells are deployed in such a fashion that a lumen will eventually be formed in the cartilage whose size is a function of the enclosed nerve bundle. HOLTZER did not point out that if transverse stretching of the precartilaginous sclerotomes occurs because of overdilatation of the neural tube these paired cell masses may fail to unite not only posteriorly but anteriorly as well resulting in combined anterior and posterior spina bifida (complete hemivertebrae Fig. 1). Furthermore such transverse stretching of the sclerotomes will result in their longitudinal shortening and approximation so that these cell masses

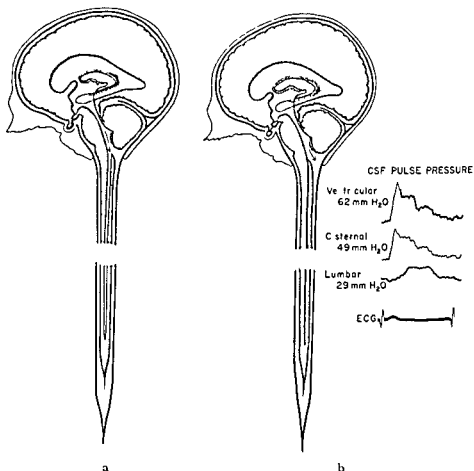


Fig. 3 Cerebrospinal fluid spaces represented diagrammatically. a) Until the foramina perforate the central canal constitutes a long diverticulum of the fourth ventricle. Its lumen receives the pulse waves of the ventricular fluid (arrow) generated by the pulsations of the choroid plexus. b) After the foramina perforate the ventricular fluid pulse waves are shunted into the subarachnoid space (arrow) and the central canal is compressed to vestigial remnant. Recordings are from Bering (1955).

now fitting that Morgagni's disruption hypothesis receive similar consideration, particularly since von Recklinghausen's theory does not explain how a tube that has never closed becomes overdistended. On the other hand, Morgagni's theory of rupture from overdistention will explain every feature of the distorted anatomy not only of myelocoele, but also of related malformations, such as meningocele, diastematomyelia, syringomyelia and Klippel-Feil syndrome (GARDNER 1964).

Embryology. This 200 year old hydromelic theory gains support from FOWLER's (1953) demonstration that the microscopic appearance attributed to full



Fig. 4. Syngomelia stage I: the patient's symptoms developed at the age of 11 years. A dissection of the spinal canal (a) was found within the dilated tube of bone (b).

ure of closure of the neural plate (myeloschisis) can be reproduced by slitting open the closed neural tube. It is further supported by the work of HOLTZER (1952) who demonstrated that the diameter of the developing spinal canal of the embryo is determined by the diameter of the neural tube that it encloses. He found that migrating precartilaginous cells respond in a discriminatory and stereotyped fashion to the presence of any neural tissue by maintaining a characteristic distance from the neural tissue. The precartilaginous cells are deployed in such a fashion that a lumen will eventually be formed in the cartilage whose size is a function of the enclosed nerve bundle. HOLTZER did not point out that if transverse stretching of the precartilaginous sclerotomes occurs because of overdistention of the neural tube, these paired cell masses may fail to unite not only posteriorly but anteriorly as well, resulting in combined anterior and posterior spina bifida (complete hemivertebrae, Fig. 1). Furthermore, such transverse stretching of the sclerotomes will result in their longitudinal shortening and approximation so that these cell masses



Fig. 1. Diastematomyelia, stage 2. a) From this patient, 5 years old when examined, a meningocele had been removed at birth. Symptoms of diastematomyelia developed at the age of 12 years. Operation then disclosed a divided spinal cord at the level of the bony spur, as well as hydromyelia of stage 1. Dilatation, shortening, fusion, scoliosis and partial hemivertebrae constituting Klippel-Feil syndrome of the lumbar spine are seen. b) Same patient as in (a). The dilatation of the cervical canal indicates that hydromyelia involved this level as well. The a.p. diameter at C1 was 30 mm, at C2 24 mm. c) and d) Similarity to the Klippel-Feil syndrome is better shown in these films of the lumbar spine of another adolescent with diastematomyelia. This patient, in addition to the vertebral changes, had the fused ribs frequently encountered in the short neck syndrome. (c and d, Courtesy GEORGE E. MARR and ALFRED UHLEIN, W. B. Saunders Company.)

may coalesce longitudinally to form fused vertebrae. Thus, the stretching that interferes with normal fusion in the transverse axis of the spine may be accompanied by shortening with abnormal fusion (tethering) in its long axis. Overdistention will explain other skeletal distortions as well, such as fused ribs and scoliosis to constitute the full-blown picture of Klippel-Feil syndrome.

Occurring prior to the development of the subarachnoid space, overdistention of the neural tube also will cause a coalescence of neuroectoderm with mesoderm, cutaneous ectoderm or endoderm and result in fusion (tethering) of the neural tube to these surrounding cell layers. Subsequent splitting off of these coalesced cell masses by the dissecting subarachnoid space will explain the glial cell nests in the meninges which COOPER and KERNOHAN (1951) found in the adult with syringomyelia as well as in the infant with myelocoele. It also will account for other types of hamartomas either in the spinal cord or in surrounding structures. An example is the occurrence of gut epithelium in the bony spur of diastematomyelia. This line of reasoning appeals to the mechanically oriented mind of the surgeon. It affords an explanation of such vague entities as dysraphia and dysplasia. It makes it unnecessary to

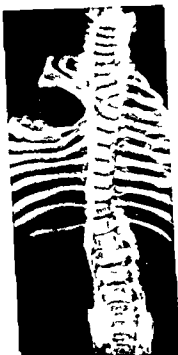


Fig 6 Film of the skeleton of an infant with myelocle. In addition to the midline bony spur there is fusion of L 1 and 2 widening and shortening of the spinal canal with scoliosis hemivertebrae and fused ribs all features of Klippel Feil syndrome (Courtesy A H CAMERON Oliver and Boyd Ltd)

involve such hypothetic considerations as retardation of the blastophore (CAMERON 1937) accessory neuroenteric canal (BREMER 1932) or any of the earlier theories that SAUNDERS (1943) has summarized in his review of the subject

A fact usually overlooked by the clinician is that the embryonal neural tube is a single cavity which constitutes the anlage of the ventricles and the central canal of the cord. Distention of this tube, that is hydrocephalus and hydro myelia (hydrocephalomyelia) is a normal state in embryonic life (Fig 2). This physiologic distention becomes compensated as the ventricular fluid filters through the attenuating rhombic roof to dissect open the subarachnoid space. As pointed out by WEED (1917) if for any reason the roof of the fourth ventricle does not become adequately permeable during the critical sixth to eighth week period a sufficient quantity of fluid will not filter through it to properly dissect open the developing subarachnoid space. In this event even though the roof subsequently perforates to form the foramina, communicating hydrocephalus may prevail. Thus in 1917 WEED explained not only the mechanism of congenital hydrocephalus both obstructive and communicating and why both forms frequently co exist but his illustrations also show

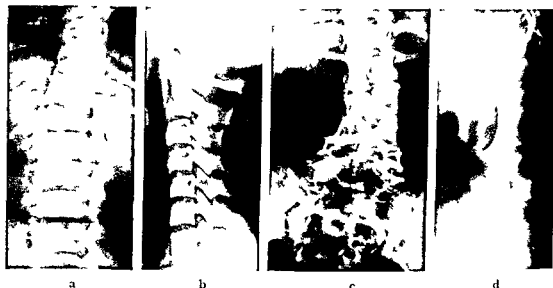


Fig. 5 Diastematomyelia stage 2. a) From this patient 5 years old when examined a meningocele had been removed at birth. Symptoms of diastematomyelia developed at the age of 12 years. Operation then disclosed a divided spinal cord at the level of the bony spur as well as hydromyelia (cf stage 1). Dilatation shortening fusion scoliosis and partial hemivertebrae constituting Klippel Feil syndrome of the lumbar spine are seen. b) Same patient as in (a). The dilatation of the cervical canal indicates that hydromyelia involved this level as well. The a.p. diameter at C1 was 30 mm at C2 24 mm. c) and d) Similarity to the Klippel Feil syndrome is better shown in these films of the lumbar spine of another adolescent with diastematomyelia. This patient in addition to the vertebral changes had the fused ribs frequently encountered in the short neck syndrome (c and d. Courtesy GEORGE L. MARR and ALFRED UHLLIN, W. B. Saunders Company.)

may coalesce longitudinally to form fused vertebrae. Thus, the stretching that interferes with normal fusion in the transverse axis of the spine may be accompanied by shortening with abnormal fusion (tethering) in its long axis. Overdistention will explain other skeletal distortions as well, such as fused ribs and scoliosis to constitute the full-blown picture of Klippel Feil syndrome.

Occurring prior to the development of the subarachnoid space overdistention of the neural tube also will cause a coalescence of neuroectoderm with mesoderm, cutaneous ectoderm or endoderm and result in fusion (tethering) of the neural tube to these surrounding cell layers. Subsequent splitting off of these coalesced cell masses by the dissecting subarachnoid space will explain the glial cell rests in the meninges which COOPER and KERNOHAN (1951) found in the adult with syringomyelia as well as in the infant with myelocoele. It also will account for other types of hamartomas either in the spinal cord or in surrounding structures. An example is the occurrence of gut epithelium in the bony spur of diastematomyelia. This line of reasoning appeals to the mechanically oriented mind of the surgeon. It affords an explanation of such vague entities as dysraphia and dysplasia. It makes it unnecessary to

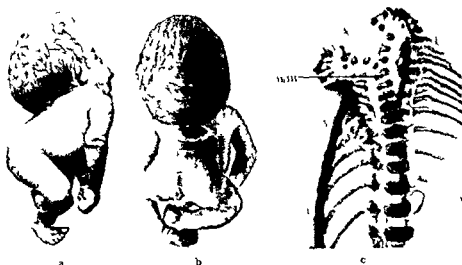


Fig. 8. a) and b) Stillborn fetus with severe Klippel-Feil syndrome and myelocoele. c) After removal of head in Klippel-Feil syndrome the marked disruption of the vertebral halves suggests an almost explosive force with its lumen. (Courtesy A. FELLNER and H. STERNBERG, Springer Verlag.)



Fig. 9. a) Skeleton of Klippel-Feil syndrome in an adult. b) Film of this skeleton shows the tremendous distention of the cervical canal. The neurological picture of Klippel-Feil syndrome is syringomyelia. (Courtesy A. FELLNER and H. STERNBERG, Springer Verlag.)

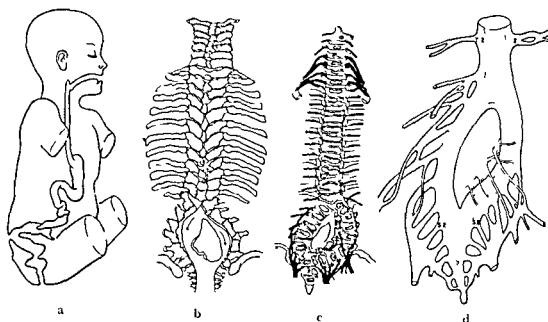


Fig 7 If the roof plate ruptures into the amniotic sac (stage 3) and the floor plate simultaneously ruptures into the primitive gut (stage 4) the result is a gut fistula (a) presenting posteriorly between the two halves of the split spinal canal (b and c) and the cord (d). The diastematomyelic cord (stage 2) was hydromyelic (stage 1).

clearly that hydrocephalus developing in embryonal or fetal life must be accompanied by hydromyelia. Therefore, if hydrocephalus with hydromyelia is present in postnatal life, and particularly if the outlets of the fourth ventricle are found unperforated, as is true in many cases of syringomyelia, diastematomyelia, meningocele, and myelocele, this represents not a new condition, but the pathologic persistence of a state that is normal in the embryo. That Weed's views are not widely accepted is a striking example of the time lag so often separating laboratory demonstration and clinical acceptance.

The central canal of the cord takes off from the floor of the fourth ventricle at the level of the obex. In the normal adult with patent fourth ventricle foramina, the central canal is narrow if not entirely closed. Conversely, in individuals in whom the foramina have failed to perforate, the central canal is dilated (GARDNER 1964). This reciprocal relationship suggests that normally the central canal narrows because the foramina open, and conversely, if the foramina do not open, the central canal dilates. This is logical, for if the foramina fail to open, even though filtration is adequate to maintain normal intraventricular pressure, the central canal will continue to receive the thrust of the ventricular fluid pulse generated by the beating of the choroid plexus. On the other hand, when the foramina open this waterhammer

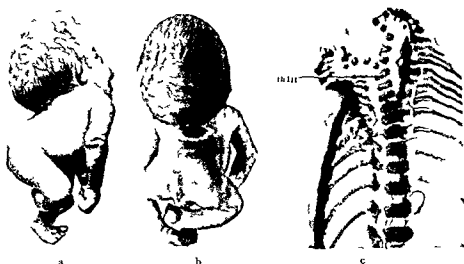


Fig 8 a) and b) Stillborn fetus with severe Klippel-Feil syndrome and nuchal cyst c) After removal of head in Klippel-Feil syndrome the marked disruption of the vertebral arches suggests an almost complete fusion of the cervical vertebrae with its lumen (Courtesy A. FELLER and H. STERNBERG, Springer Verlag)



Fig 9 a) Skeleton of Klippel-Feil syndrome in an adult b) Film of this skeleton shows the tremendous distention of the cervical canal. The neurologic picture of Klippel-Feil syndrome is syringomyelia (Courtesy A. FELLER and H. STERNBERG, Springer Verlag)

effect is shunted past the central canal into the subarachnoid space. Hence force exerted on the outer surface of the spinal cord will tend to compress and close off its lumen (Fig. 3).

The normally dilated central canal of the embryonic cord shrinks as the physiologic hydrocephalus becomes compensated. Because of this same compensatory process, a pathologic overdistention of the central canal may be reduced to normal. Despite such reduction the stretched sclerotomes having taken a set still may proceed to form a dilated spinal canal. Therefore, a spinal cord of normal diameter within a dilated canal, as in the cases reported by WALKER (1944), is no indication that the cord was not overdistended in embryonal life. By the same token, a normal degree of distention of the neural tube during the precartilaginous stage followed by overdistention at a later stage may result in a hydromyelic spinal cord within a bony canal of normal diameter. Thus is explained the findings of WELLS, SHILLINE, and BLIGH (1959) that when syringomyelic symptoms develop after age 30 the cervical canal usually is of normal diameter, whereas, in the more severe cases in which symptoms develop before age 30 it usually is dilated.

The skeletal features of the Klippel Feil syndrome consist of varying degrees and combinations of dilatation, shortening, bifid states, fusion of the vertebral column, scoliosis, and deformities of the rib cage. Until now Klippel Feil and short neck syndrome have been considered synonymous. However any or all of these skeletal deformities may be present at the level involved by myelocle, meningocele, diastematomyelia, tethered cord or syringa (Figs 4-9, GARDNER 1964). The one feature of Klippel Feil syndrome present in all of these congenital malformations is dilatation of the vertebral canal, which fact certainly supports the premise that the neural tube was overdistended in the sclerotome stage.

SUMMARY

Syringomyelia, diastematomyelia, meningocele, and myelocle with their accompanying skeletal changes are the result of varying degrees of overdistention of the neural tube in embryonic life. The defect responsible for this overdistention is inadequate permeability of the rhombic roof.

ZUSAMMENFASSUNG

Syringomyelie, Diastematomyelie, Meningocele und Myelocle mit ihren begleitenden Skelettveränderungen sind das Ergebnis von verschiedenen Graden von Überstreckung des Neuralrohres während des embryonalen Lebens. Das Ergebnis dieser Überstreckung ist insuffiziente Permeabilität des Daches des Rautenhirns.

RÉSUMÉ

La syringomyélie la diastématomyélie la ménincocele et la myélocéle ainsi que les malformations squelettiques qui les accompagnent sont le résultat de divers degrés de surdistension du tube neural au cours de la vie embryonnaire. Le défaut cause de cette surdistension est une perméabilité insuffisante du toit du rhombencéphale.

REFERENCES

- BERINC E A JR Choroid plexus and arterial pulsation of cerebrospinal fluid demonstration of choroid plexuses as cerebrospinal fluid pump Arch Neurol Psychiat (Chic) 73 (1955) 165
- BREMER J L Dorsal intestinal fistula accessory neuroenteric canal diastematomyelia Arch Path 54 (1952) 132
- CAMERON A H Arnold Chiari and other neuro-anatomical malformations associated with spina bifida J Path Bact 73 (1957) 195
- COOPER I S and KEROHAN J W Heterotopic glial nests in subarachnoid space histopathologic characteristics mode of origin and relation to meningeal gliomas J Neuropath exp Neurol 17 (1958) 255
- FELLER A and STERNBERG H Zur Kenntnis der Fehlbildungen der Wirbelsäule die anatomischen Grundlagen des Kitzhalses (Klippel-Feilschen Syndroms) Virchow's Arch Path Anat 285 (1932) 112
- FOWLER J Responses of chick neural tube in mechanically produced spina bifida J exper Zool 123 (1953) 115
- GARNER W J Diastematomyelia and Klippel Feil syndrome relationship to hydrocephalus syringomyelia meningocele meningomyelocele and meningocele Cleveland Clin Quart 31 (1964) 19
- HOLTZER H Experimental analysis of development of spinal column I Response of precartilage cells to size variations of spinal cord J exper Zool 121 (1952) 121
- MARR G E and LITTLE A D Polymyelia and compression of spinal cord and not of cauda equina by congenital anomaly of third lumbar vertebra Surg Clin N Amer (1944) 963
- MORGAGNI J B The seats and causes of diseases investigated by anatomy 3 vols Translated by Benjamin Alexander A Millar and T Cadell London 1769
- ON RECKLINGHAUSEN F Untersuchungen über die Spina bifida Arch f path Anat 105 (1886) 243 373
- SPENGLER E C Contr Embryol Carnegie Instn 33 (1949) Fig 1 Plate 2
- SANDERS R L and DE C H Combined anterior and posterior spina bifida in living neonatal human female Anat Rec 87 (1943) 255
- WALKER A E Dilatation of vertebral canal associated with congenital anomalies of spinal cord Amer J Roentgenol 52 (1944) 571
- WELLS L H Development of cerebro-spinal spaces in pig and in man Contr Embryol Carnegie Instn 5 (1917) 1
- WELLS C E C SPILLANE J D and BLIGH A S Cervical spinal canal in syringomyelia Brain 87 (1964) 23

effect is shunted past the central canal into the subarachnoid space. Hence the force exerted on the outer surface of the spinal cord will tend to compress and close off its lumen (Fig. 3).

The normally dilated central canal of the embryonic cord shrinks as the physiologic hydrocephalus becomes compensated. Because of this same compensatory process, a pathologic overdistention of the central canal may be reduced to normal. Despite such reduction the stretched sclerotomes having taken a set still may proceed to form a dilated spinal canal. Therefore, a spinal cord of normal diameter within a dilated canal, as in the cases reported by WALKER (1944), is no indication that the cord was not overdistended in embryonal life. By the same token, a normal degree of distention of the neural tube during the precartilaginous stage followed by overdistention at a later stage may result in a hydromyelic spinal cord within a bony canal of normal diameter. This is explained in the findings of WELLS, SHILLINE, and BLIGH (1959) that when syringomyelic symptoms develop after age 30 the cervical canal usually is of normal diameter, whereas in the more severe cases in which symptoms develop before age 30 it usually is dilated.

The skeletal features of the Klippel Feil syndrome consist of varying degrees and combinations of dilatation, shortening, bifid states, fusion of the vertebral column, scoliosis, and deformities of the rib cage. Until now Klippel Feil and short neck syndrome have been considered synonymous. However, any or all of these skeletal deformities may be present at the level involved by myelocoele, meningocele, diastematomyelia, tethered cord or syringomyelia (Figs 4-9, GARDNER 1964). The one feature of Klippel Feil syndrome present in all of these congenital malformations is dilatation of the vertebral canal, which fact certainly supports the premise that the neural tube was overdistended in the sclerotome stage.

SUMMARY

Syringomyelia, diastematomyelia, meningocele, and myelocoele with their accompanying skeletal changes are the result of varying degrees of overdistention of the neural tube in embryonic life. The defect responsible for this overdistention is inadequate permeability of the rhombic roof.

ZUSAMMENFASSUNG

Syringomyelie, Diastematomyelie, Meningocele und Myelocoele mit ihren begleitenden Skelettveränderungen sind das Ergebnis von verschiedenen Graden von Überstreckung des Neuralrohres während des embryonalen Lebens. Das Ergebnis dieser Überstreckung ist insuffiziente Permeabilität des Daches des Rautenhirns.



Fig 1 Thoracic myelogram Vertical beam decubitus view using Pantopaque 15. Herniated calcified thoracic disc at Th 6-7



Fig 2 Lateral cervical myelogram with Pantopaque 30. Evaluation of the ventral cord margin difficult with standard technique (top). With the high kV technique the ventral cord margin is visible (below).

the visibility of the cord in the lateral view with both Pantopaque 22 % and 30 %. (Fig 2) This was more apparent with Pantopaque 30 %. However one could obtain the same visibility with average techniques using Pantopaque 22 % with preservation of bony detail. This tends to be lost with higher kilovoltage techniques.

Pantopaque 22 % is slightly more difficult to follow fluoroscopically over the foramen magnum. However with experience and the use of image intensification it presents no problem. Because Pantopaque 22 % has a lower specific gravity it flows more slowly over the dorsal spinal kyphosis. This is a distinct advantage in myelography of the thoracic spine. It is however less desirable in the cervical region.

The optimal amount of contrast material for the lumbar region will cover three intervertebral disc spaces in the prone position and also cover the L4-5 and L5-S1 disc spaces in the erect position. An amount of 12 ml of contrast material is sufficient in the vast majority of patients.

In lumbar myelography it is desirable to demonstrate the roots and con-

ADVANTAGES OF A LESS DENSE PANTOPAQUE CONTRAST MATERIAL FOR MYELOGRAPHY

by

E. RALPH HEINZ, RAY A. BRINKER and JUAN M. TAVERAS

Pantopaque, 30 % iodinated ethyl phenyl undecanoate, has been used widely since RAMSEY et coll. made their initial report in 1944. Recently there has been a trend toward using greater volumes of contrast material to better fill the subarachnoid space. With larger volumes of Pantopaque 30 % the subtle differences in density are obscured.

Material and Methods A new form of Pantopaque, consisting of 15 % iodinated oil, was provided by Lafayette Pharmaceutical Inc. A total of 132 consecutive myelographies were performed with patients randomly allocated.

The important myelographic aspects in the cervical region are the demonstration of the spinal cord, the roots and the root sleeves. Pantopaque 15 % was tried initially in this study and was acceptable in most cases. However, in cases of severe spondylosis the anatomic details were often difficult to observe, due to insufficient density.

It was our impression that high kilovoltage technique definitely increased



Fig. 6. Lumbar myelograms with Pantopaque 15%. The displaced nerve roots are well shown.

possible to simplify the choice of contrast material by using Pantopaque 22%. If a given concentration of Pantopaque is too dilute in appearance it can be made more concentrated by adding Pantopaque 30%. Conversely, a dense concentration of Pantopaque may be diluted by the addition of Pantopaque 15%.

The conus medullaris can be shown by using large amounts of Pantopaque 15% (up to 20 ml). This structure is usually obscured when Pantopaque 30% is used (Fig. 7).

The number of thoracic myelographies performed is too small for statistical analysis. Since large volumes are necessary to perform a proper examination of the thoracic region 20 ml was arbitrarily used in this study and it proved to be suitable in every case. Frontal fluoroscopic spot films were greatly facilitated because the larger volume tended to move more as a column even in the difficult Th6—Th7 area of dorsal spinal kyphosis. Lateral films with the patient in the prone position were routinely included. This was accomplished by pooling the large Pantopaque column at the C3—Th3 region by frontal fluoroscopy. The cassette for the lateral views should be positioned and the films taken 5 seconds after raising the head of the table 10 degrees. Thus the Pantopaque is flowing over the Th5—Th12 area as the film is exposed (Fig.



Fig. 3 Lateral cervical myelogram with Pantopaque 22 % using 30 ml. The ventral and dorsal margins of cervical and upper thoracic cord are well shown.

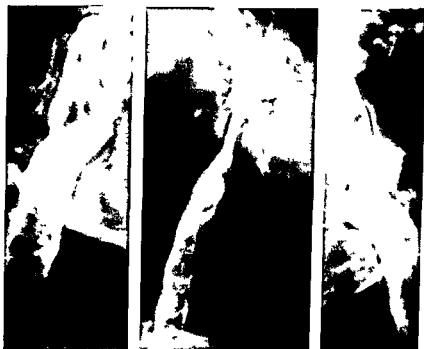


Fig. 4 Lateral and oblique films with Pantopaque 22 % using 30 ml. Excellent demonstration of the basilar artery despite the lower concentration of Pantopaque.

sleeves as well as a double contour on the ventral side of the column when there is unilateral disc protrusion (Figs 5 and 6). Pantopaque 15 % is not as satisfactory as the water soluble material to demonstrate the cranial equine roots but it does represent a slight improvement over Pantopaque 30 %.

Several lumbar myelograms done utilizing Pantopaque 22 % indicate that it is intermediate between Pantopaque 15 % and 30 %. Since Pantopaque 22 % seems optimal for use in the cervical and dorsal regions it may be



Fig 8 Lumbar myelogram with 15 ml of Pantopaque 15 Frontal view The conus medullaris and cauda equina are visible This requires a greater volume of Pantopaque than the usual lumbar myelogram

The appearance of the cord in the lateral projection (cord lateral) was evaluated the appearance was then evaluated in the anteroposterior diameter (cord anteroposterior) and then the nerve roots and nerve sleeves were evaluated Excellent visibility was rated at 100 % good at 75 %, fair at 50 % and poor at 25 % The average was then listed for the varying concentrations of Pantopaque and quantities of material used (Table 1)

In the cervical region Pantopaque 22 % using either 12 ml or 20 ml was considerably better in all respects than using 30 % Pantopaque The use of 20 ml of Pantopaque 22 % resulted in considerably better analysis of lesions in the cervical region

In the lumbar region the films were analyzed again using nerve root visibility root sleeve visibility and double density as criteria Specifically, we

Table 1

Evaluation of cervical myelograms The numbers are averages 100 being excellent visibility of details Cord lateral refers to appearance of the spinal cord in the lateral prone projection cord a p to the anteroposterior view Concentrations of Pantopaque indicated on left side of table

Pantopaque		Cord lateral	Cord a p	Nerve roots	Nerve sleeves
22	12 ml	69	84	53	56
"	20 ml	83	75	75	83
30	12 ml	56	71	56	64
30	20 ml	54	58	58	54

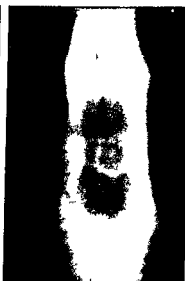


Fig 6 Lumbar myelogram with Pantopaque 15. Lateral view (left) shows double contour at L4 to 5 and the frontal (right) unilateral extradural impression. Herniated nucleus pulposus.

Fig 7 Thoracic myelogram. Lateral prone view. The large column of contrast (20 ml) is positioned at the lordotic cervical curve.

8) This technique is considerably aided by the lighter, and correspondingly slower flowing, Pantopaque 22 %. Finally, lateral decubitus films, with vertical and horizontal beam direction, were exposed (see Fig 1).

Discussion

One of the most difficult problems in Pantopaque myelography is evaluation of the cervical cord dimension in the lateral view. The sagittal cord diameter is critically important when the transverse diameter of the cord is widened. Using larger volumes of Pantopaque 22 % one can define the ventral and dorsal margins of the cord in every case (Figs 3 and 4). Thus, the differential diagnosis of intramedullary cord disease or ventral extramedullary lesions such as spondylosis, cervical disc, or a ventrally placed meningioma, can be made.

When larger quantities of Pantopaque 30 % are used, the ventral margin of the cord is often not seen. High kilovoltage technique facilitated the demonstration of the cord margins but the bony margins so important for correlation are less distinct (Fig 2).

Evaluation of cases All of the myelograms were reviewed by the authors without knowledge of which concentration of Pantopaque had been used.



Fig 8 Lumbar myelogram with 15 ml of Pantopaque 15 Frontal view The conus medullaris and cauda equina are visible This requires a greater volume of Pantopaque than the usual lumbar myelogram

The appearance of the cord in the lateral projection (cord lateral) was evaluated the appearance was then evaluated in the anteroposterior diameter (cord anteroposterior) and then the nerve roots and nerve sleeves were evaluated Excellent visibility was rated at 100 % good at 75 % fair at 50 %, and poor at 25 % The average was then listed for the varying concentrations of Pantopaque and quantities of material used (Table 1)

In the cervical region Pantopaque 22 % using either 12 ml or 20 ml was considerably better in all respects than using 30 % Pantopaque The use of 20 ml of Pantopaque 22 % resulted in considerably better analysis of lesions in the cervical region

In the lumbar region the films were analyzed again using nerve root visibility root sleeve visibility and double density as criteria Specifically we

Table 1

Evaluation of cervical myelograms The numbers are averages 100 being excellent visibility of details Cord lateral refers to appearance of the spinal cord in the lateral prone projection cord a p to the anteroposterior view Concentrations of Pantopaque indicated on left side of table

Pantopaque	Cord lateral	Cord a p	Nerve roots	Nerve sleeves
22 12 ml	69	84	33	56
22 20 ml	83	75	75	83
30 12 ml	56	71	56	64
30 20 ml	54	58	58	54

Table 2

Evaluation of lumbar myelograms The same principles of evaluation were applied as in table 1

Pantopaque	Nerve root visibility	Root sleeve visibility	Double density
15 ° 9 ml	50	32	36 °
15 ° 15 ml	67	64	75 °
30 ° 9 ml	46	54	70 °
30 ° 15 ml	53	64	20

were interested in learning if Pantopaque 15 % resulted in improved root sleeve filling. However, visibility of the root sleeves was the same with Pantopaque 30 % and Pantopaque 15 % (Table 2). Extradural impressions on the Pantopaque column were more frequently seen with Pantopaque 15 %. Smaller extradural impressions could be detected more readily utilizing Pantopaque 15 % because of the greater spectrum of contrast recorded.

Thoracic myelography has been facilitated by large volumes of Pantopaque. Frontal fluoroscopic spot films are done in the usual manner. There is better filling as a result of a large column. Lateral films taken in the horizontal direction in the midthoracic region are impossible with small volumes of contrast material. With larger volumes and the slower flow of Pantopaque 22 % excellent films may be obtained defining the ventral subarachnoid space in the sagittal plane. With the method described the time required for an optimal thoracic myelogram can be greatly reduced. Removal of the large volumes described presents little, if any, additional difficulty over existing methods. The importance of a well centered spinal needle with the bevel directed either cephalad or caudad cannot be overemphasized.

Acknowledgement

Drs Heinz and Brinker undertook this study as Special Fellows NB 973 02 and NB 974 07 National Institute of Neurological Diseases and Blindness NIH

SUMMARY

Larger volumes of Pantopaque add considerably to the ease of performance and diagnostic accuracy of myelography. These larger volumes require less concentrated contrast material than Pantopaque 30 %. Optimal volume in the cervical region is Pantopaque 22 % in 15 to 20 ml quantities. In the lumbar region 12 ml of Pantopaque 15 % is ideal while 20 ml of Pantopaque 22 % is used in the thoracic region.

ZUSAMMENFASSUNG

Die Verwendung von grosseren Mengen Pantopaque erleichtern die Diagnosestellung bei der Myelographie. Infolge der grosseren Kontrastmenge kann die Konzentration von Pantopaque unter 30 gehalten werden. Für die Cervicalregion ist die optimale Menge 15 bis 20 ml 22 Pantopaque. In der Lumbalregion genügen 12 ml 15 Pantopaque während in der Thorakalregion 20 ml 22 Pantopaque verwendet wird.

RÉSUMÉ

L'emploi d'une quantité plus importante de Pantopaque facilite l'exécution de la myélographie et augmente sa précision diagnostique. Ces grandes quantités permettent d'utiliser un moyen de contraste moins concentré que le Pantopaque à 30°. Pour la région cervicale on utilisera 15 à 20 ml de Pantopaque à 22° pour la région lombaire 12 ml de Pantopaque à 15° et pour la région dorsale 20 ml de Pantopaque à 22°.

REFERENCES

- DI CIURO G. and FISHER R. L. Contrast radiography of the spinal cord. *Arch. Neurol.* 11 (1964) 125.
MALIS L., NEWMAN C. M. and WOLF B. S. Full-column technique in lumbar disc myelography. *Radiology* 60 (1953) 18.
RANNEY G. H., FRENCH J. D. and STRAIN W. H. Iodinated organic compounds as contrast media for radiographic diagnosis. Pantopaque Myelography. *Radiology* 43 (1944) 236.
SCHULTZ E. H. JR. Cervical disc disease simulating intramedullary neoplasm by myelography. *Amer. J. Roentgenol.* 91 (1964) 1051.
STRAIN W. H., PLATT J. T. and WARREN S. L. Iodinated organic compounds as contrast media for radiographic diagnosis. I. Iodinated aracyl esters. *J. Amer. chem. Soc.* 64 (1942) 1436.

PANTOPAQUE ARACHNOIDITIS

Experimental study of blood as a potentiating agent and
corticosteroids as an ameliorating agent

by

W J HOWLAND and J L CURRY

This study was initiated to investigate the reasons for the occasional development of severe arachnoiditis following myelography with ethylodiphenylundecylate (Pantopaque, Myodil). There are numerous reports in the literature of signs and symptoms of severe arachnoiditis with operative (2, 7, 8, 10, 12) or autopsy (1, 3, 5, 9) confirmation of severe meningeal inflammation. The idea occurred to us that subarachnoid bleeding during the course of needle positioning might produce an added irritant factor which would occur in only occasional patients and that this might explain the occasional development of severe arachnoiditis. Review of the literature available to us has not disclosed any previous investigation of this possibility. SARISIAN in 1956 suggested that a bloody tap should be considered a contraindication to the injection of oil intrathecally, evidently basing this recommendation on the possibility of emulsification of oil. JAEGER's studies of the harmful effects of emulsified oils were cited.

Because of difficulties encountered in ascertaining whether or not subarachnoid bleeding had occurred in human clinical material, it was decided to

evaluate the effect of blood mixed with Pantopaque in the subarachnoid space of dogs. Initial studies of this problem (4) prompted us to expand these investigations. Following the publication by SEHCAL et coll (1962) of successful treatment of chronic symptomatic pantopaque arachnoiditis with subarachnoid injections of corticosteroids we decided to investigate the possibility of prevention of arachnoiditis in experimental animals.

Material and Methods A total of 24 mongrel dogs in good clinical condition were used. In all dogs, the contrast material was injected into the cisterna magna through a posterior midline puncture with a 20 gauge infant spinal needle using aseptic technique. The injection was made with the animal in a 60° caudal tilt and the neck flexed. The neck was extended immediately upon completion of the injection. In this position almost all of the contrast material flowed slowly along the subarachnoid space to the lumbar region over a period of approximately one hour. The injection was made slowly after preliminary withdrawal of 5 ml of spinal fluid. Roentgenograms were obtained at intervals until the contrast medium reached the lumbar region. The animal was maintained under light pentobarbital anesthesia during this period.

Two dogs were injected with 3 ml of blood alone. Four were injected with 3 ml of Pantopaque. Six were injected with 3 ml of Pantopaque and 3 ml of blood. Six more dogs were injected with 3 ml of Pantopaque and 20 mg of methylprednisolone acetate and six were injected with 3 ml of Pantopaque plus 3 ml of blood plus 20 mg of methylprednisolone acetate. The blood was withdrawn from the animal's leg vein immediately prior to injection and mixed with the Pantopaque or the Pantopaque and corticosteroids in the syringe and injected before clotting had occurred.

The dogs were sacrificed 6 to 8 weeks following injection with the exception of two animals which had to be sacrificed earlier. Films were exposed at the time of sacrificing the animals. These films were compared with the initial roentgenograms to estimate the amount of Pantopaque absorbed from the subarachnoid space in this interval.

Complete central nervous system autopsies were performed. Following fixation inflammatory response was graded grossly and microscopically by two examiners without knowledge of the material that the animal had received.

Results

Injection of blood The two animals which received only blood showed no significant clinical symptoms. There was minimal nuchal rigidity in both animals after the injection but this rapidly disappeared and these animals



Fig 1 Subarachnoid injection of Pantopaque γ lone Smooth symmetrical distribution of the oil column

Fig 2 Same dog as in fig 1 8 weeks later Most of the opaque oil has been absorbed

remained in good health until the time of sacrifice. Autopsies showed no significant abnormality of the spinal cord and microscopic studies were also normal.

Injection of Pantopaque Clinically these four animals showed very little difference from the animals which received only blood. No obvious neurologic deficiencies developed during the period of observation and they were all in excellent health when sacrificed.

Roentgenograms made at the time of injection showed a smooth symmetrical oil column (Fig 1). At autopsy, 6 to 8 weeks later, films showed the Pantopaque to be dispersed in small droplets and globules. Comparison of the roentgenograms made at the time of injection and at the time of sacrifice showed that over one half of the Pantopaque had been absorbed (Fig 2).



Fig 3 a) Subarachnoid injection of Pantopaque mixed with blood. The oil is fragmented into globules with uneven dispersion. b) Same dog 8 weeks later. A considerable volume of the oil remains and is most concentrated in the lower cervical region.

Grossly the spinal cord and meninges showed multiple small areas of oily material with slight to moderate arachnoid thickening. Much of the Pantopaque remained free within the subarachnoid space. The microscopic appearance was one of mild chronic inflammatory reactive change about small encysted oil droplets.

Injection of blood mixed with Pantopaque. Clinically all of these animals had severe reactions. The day following injection there was severe nuchal rigidity and apathy. All dogs went through an initial period where food and water were refused. All of these dogs were febrile for the first few days following injection. Three of the six animals developed definite paralysis of the extremities and in one this progressed to complete paralysis of the hind limbs. This paraplegic dog was sacrificed on the 18th post injection day. The others gradually recovered their appetite and became afebrile. Three of these six dogs ap-



Fig 1 Subarachnoid injection of Pantopaque and lone Smooth symmetrical distribution of the oil column

Fig 2 Same dog as in fig 1 8 weeks later Most of the opaque oil has been absorbed

remained in good health until the time of sacrifice. Autopsies showed no significant abnormality of the spinal cord and microscopic studies were also normal.

Injection of Pantopaque Clinically these four animals showed very little difference from the animals which received only blood. No obvious neurologic deficiencies developed during the period of observation and they were all in excellent health when sacrificed.

Roentgenograms made at the time of injection showed a smooth symmetrical oil column (Fig 1). At autopsy, 6 to 8 weeks later, films showed the Pantopaque to be dispersed in small droplets and globules. Comparison of the roentgenograms made at the time of injection and at the time of sacrifice showed that over one half of the Pantopaque had been absorbed (Fig 2).

Table
Summary of Pantopaque arachnoiditis

	Blood alone	Pantopaque alone	Pantopaque and blood	Pantopaque and MPA	Pantopaque blood MPA
Number of animals	2	4	6	6	6
Average gross inflammation (0-4+)	0	2	3.7 (1D)	1.3	1.9 (1D)
Average microscopic inflammation (0-4+)	0	2.3	3.0	1.6	2.2
Average amount Pantopaque remaining	—	46	16	43	52

inflammation induration of the arachnoid. This was most striking in the lower cervical region (Fig. 4). Grossly some oily material was associated with the visible lesions and it was difficult to find any oil free in the subarachnoid space.

Microscopically the inflammatory areas were seen to occur about cystic spaces. No bacteria could be identified (Fig. 5).

Injection of Pantopaque and methylprednisolone acetate. Clinically none of these animals showed any significant reaction except for minimal transient nuchal rigidity and post anesthesia lethargy. All animals remained in good health until the time of sacrifice without development of any neurological abnormality.

Roentgenograms obtained at the time of injection showed the Pantopaque column to be less smooth and symmetrical when compared to Pantopaque alone. There was more tendency for the oil to disperse into globules. Roentgenograms made at the time of sacrifice showed a similar appearance. Although less than half of the Pantopaque remained, this was essentially the same as with animals receiving Pantopaque without corticosteroids (Table).

Grossly and microscopically there were many small areas of meningeal inflammation very similar to that seen with Pantopaque alone although generally somewhat less.

Injection of Pantopaque blood and methylprednisolone acetate. Clinically two of the six animals had a moderately severe reaction with temperature elevation, apathy and refusal to eat. Both of these developed some paralysis of the hind limbs and one died 19 days following injection. The other four showed surprisingly little clinical abnormality.

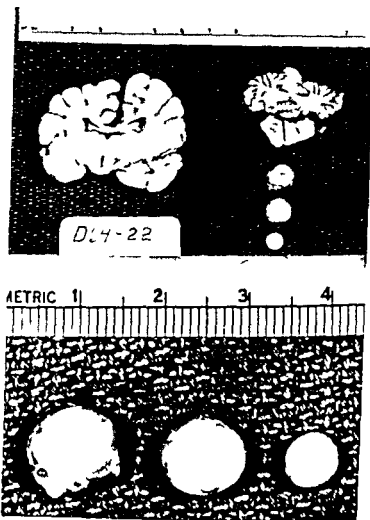


Fig 4 Postmortem specimens of dog sacrificed 8 weeks after subarachnoid instillation of Pantopaque mixed with blood. Inflammatory reaction surrounding oil droplets in the cervical cord region (lower left) at this level subarachnoid inflammatory reaction was usually most intense

peared to be in good clinical condition at the time of sacrifice 6 to 8 weeks following injection

In all of these animals, roentgenograms obtained at the time of injection showed the Pantopaque column to be broken into many large globules and poorly dispersed in the subarachnoid space (see Fig 3a). At the time of sacrifice, roentgenograms showed a similar appearance and considerably more Pantopaque remained in the subarachnoid space than in the dogs injected with Pantopaque alone (see Fig 3b).

Autopsy in all of these animals revealed moderately severe to very severe

Discussion

A potentiating action of blood in the production of Pantopaque arachnoiditis was remarkably consistent in this small series. Each of the six animals in which blood mixed with Pantopaque was injected showed a moderately severe or very severe inflammatory reaction which was consistently more than that produced by Pantopaque alone. This occurred in spite of the lack of significant inflammatory reaction produced by blood alone.

The results of addition of corticosteroids are not as clear cut. Certainly this did not give complete protection from the inflammatory response produced either by Pantopaque or Pantopaque mixed with blood. Comparing the overall inflammatory response as judged by gross inspection and microscopic examination, there was very little difference between the animals which received Pantopaque alone and those which received Pantopaque and methylprednisolone acetate. However, when the two groups of animals which received Pantopaque and blood are compared, there does appear to be a significant difference. All six of the animals which received Pantopaque and blood developed severe arachnoiditis, whereas only two of the six which received Pantopaque and blood and methylprednisolone acetate developed severe arachnoiditis.

A potentiating action of blood traumatically introduced into the subarachnoid space suggests a logical explanation for the severe arachnoiditis occasionally encountered following Pantopaque myelography. Therefore, it may be inadvisable to introduce Pantopaque into the subarachnoid space if there is evidence of gross bleeding when the spinal puncture is performed. It also seems equally important to be extremely careful to avoid subarachnoid bleeding during the removal of the Pantopaque.

In an effort to prevent arachnoiditis, the instillation of methylprednisolone acetate into the subarachnoid space at completion of Pantopaque myelography seems worthy of further investigation, especially if subarachnoid bleeding occurs during removal of the oil.

The reason for the potentiating action of blood in the production of Pantopaque arachnoiditis is not known. Various possible decomposition products produced by the mixture of these two substances have been investigated. There is no significant difference in free phenol levels in the spinal fluid. To the present time, we have not been able to ascertain any consistent difference in free iodine levels in the spinal fluid produced by the mixture of blood and Pantopaque. Blood does not act as an emulsifying agent for Pantopaque in the presence of spinal fluid.

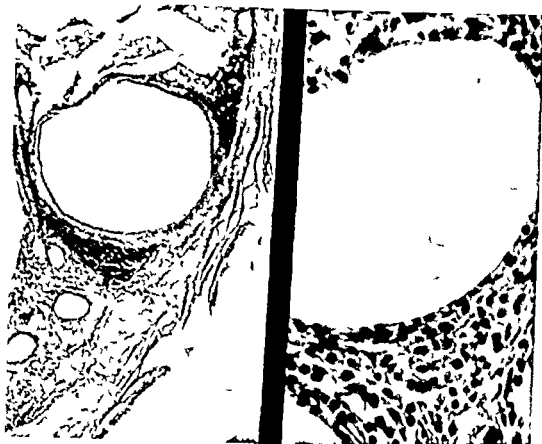


Fig 5 Low (left $\times 40$) and high (right $\times 500$) power photomicrographs (hematoxylin and eosin) of lower cervical cord segment from dog sacrificed 8 weeks after intrathecal injection of Pantopaque blood mixture. The most intense inflammatory reaction is in close proximity to the oil droplets.

Roentgenograms at the time of injection showed the oil to be dispersed in globules in much the same manner as when the corticosteroid was not added. Roentgenograms made at the time of autopsy showed considerable residual Pantopaque but not as much as in the animals who received Pantopaque and blood without methylprednisolone acetate.

The animal which died 19 days following the injection showed severe arachnoiditis in the cervical region and this appeared to be the cause of death. There were other areas of arachnoiditis of less severe degree in more caudal portions of the arachnoid. One other animal showed severe arachnoiditis in the cervical region with many localized areas of involvement. However, the other four animals that received methylprednisolone acetate in addition to the Pantopaque and blood showed minimal inflammatory changes.

- 4 HOWLAND W J and CURRY J L Pantopaque arachnoiditis experimental study of blood as a potentiating agent *Radiology* 80 (1963) 489
- 5 HURTEAU E F BAND W C and SINCLAIR E Arachnoiditis following the use of iodized oil *J Bone Jt Surg* 36A (1954) 393
- 6 JAEGER R Cited by Sarkisian
- 7 MASON M B and RAAF J Complications of pantopaque myelography *J Neurosurg* 19 (1962) 302
- 8 PEACHER W G and ROBERTSON R C L Pantopaque myelography results comparison of contrast media and spinal fluid reaction *J Neurosurg* 2 (1945) 220
- 9 SARKISIAN S S Spinal cord pseudotumor A complication of pantopaque myelography *U S Armed Forces Med J* 7 (1956) 1683
- 10 SCHURR P H McLAURIN R L and INGRAHAM F D Experimental studies on the circulation of the cerebrospinal fluid *J Neurosurg* 10 (1953) 515
- 11 SEIGAL A D GARDNER W J and DOHN D F Pantopaque arachnoiditis *Cleveland Clin Quart* 29 (1967) 177
- 12 STEINHAUSEN T B et coll Iodinated organic compound as contrast media for radiographic diagnoses *Radiology* 43 (1944) 230

Acknowledgement

This investigation was supported by the James Picker Foundation on recommendation of the Committee on Radiology, National Academy of Sciences, National Research Council.

SUMMARY

Experimental studies of pantopaque arachnoiditis in 24 dogs were conducted. Pantopaque alone caused mild arachnoiditis; blood alone produced no significant reaction; a mixture of blood and Pantopaque produced severe arachnoiditis. When methylprednisolone acetate was added to the blood and Pantopaque mixture, only two of six animals developed severe arachnoiditis. The studies suggest that Pantopaque should not be injected intrathecally if gross bleeding is present. The use of intrathecal corticosteroids should be considered if subarachnoid bleeding has occurred.

ZUSAMMENFASSUNG

Es wurden experimentelle Studien von Pantopaque bedingter Arachnoiditis in 24 Hunden durchgeführt. Pantopaque allein verursacht nur leichte Arachnoiditis. Blut allein erzeugt keine nennenswerte Reaktion. Eine Mischung von Blut und Pantopaque erzeugt eine schwere Arachnoiditis. Wenn der Pantopaque Blutmischung Methylprednisolonacetat zugesetzt wurde, entwickelte sich nur bei zwei von 6 Hunden eine ernsthafte Arachnoiditis. Aus diesen Studien geht hervor, dass Pantopaque nicht intrathekal injiziert werden sollte, wenn eine massive Blutung vorhanden ist. Injektion von intrathekalen Corticosteroiden sollte erwogen werden, wenn eine subarachnoidale Blutung aufgetreten ist.

RESUME

Les auteurs ont fait une étude expérimentale de l'arachnoidite au pantopaque sur 24 chiens. Le Pantopaque seul cause une arachnoidite légère. Le sang seul ne produit pas de réaction importante. Le mélange de sang et de l'antopaque donne lieu à une arachnoidite grave. Après addition d'acétate de méthylprednisolone au mélange de sang et de Pantopaque, deux chiens seulement sur six ont présenté une arachnoidite grave. D'après ces travaux, il semble qu'on ne devrait pas injecter de Pantopaque dans l'espace intradural quand il y a une hémorragie importante. On devrait envisager l'administration de corticostéroïdes par voie intradurale dans les cas où il s'est produit une hémorragie sous arachnoidienne.

REFERENCES

1. BERING, E. A. Notes on the retention of pantopaque in the subarachnoid space. *Amer J Surg* 80 (1950) 455.
2. DAVIES, F. L. Effects of unabsorbed radiographic contrast media on central nervous system. *Lancet* 2 (1956) 747.
3. ERICKSON, T. C. and VAN BAREN, H. J. Late meningeal reaction to ethyl iodophenylundylate used in myelography. *J Amer med Ass* 153 (1953) 636.

mobility of the thoracic spine and to the lesser frequency of disc herniations it has less clinical implications than in the cervical spine

Movements of the cervical spinal cord can be found in every individual providing there is enough space available in the spinal canal. On the contrary, adequate movements of the thoracic spinal cord exist only in approximately 50 % of normal subjects. This was found to be in correlation with the degree of permeability of the posterior arachnoidal space. In 117 normal individuals this space was adequately filled with gas in 50 % of cases, in 25 % the filling was incomplete, and in 25 % it did not fill at all. This seems to be due to individual differences in the density of the arachnoidal trabeculae. An analysis of 169 subjects showed that in older individuals this space filled better and more frequently than in younger ones. The differences are statistically significant and they seem to indicate that the trabecular tissue becomes thinner and finally disappears as it undergoes relatively early senile involution. These pneumographic correlations have been confirmed by anatomic studies (JIROUT FISCHER & NADVORNÍK). Our studies showed a definite correlation between the degree of filling of the posterior thoracic arachnoidal space and the extent of mobility of the spinal cord. In the great majority of cases — over 80 % — in which this space filled well, the mobility of the spinal cord was adequate whereas in cases in which this space was not permeable mobility was absent. Thus our findings seem to indicate that a decrease or absence of the movements of the thoracic spinal cord in older individuals may be more often regarded as pathologic than in young subjects. These facts must be borne in mind in the evaluation of abnormal conditions.

Whenever an abnormal position of the spinal cord is found, it is advisable to examine such a condition more thoroughly. The patient should be turned to a position which would enhance the shift of the spinal cord to the opposite wall of the spinal canal. It should then be possible to differentiate a pathologic immobilization of the spinal cord, for instance by a neoplasm or arachnoidal adhesions from an artefact caused by the position of the patient before the procedure.

The immobilization of the spinal cord in cases of meningocele is mainly due to its extravertebral position and sometimes to arachnoidal adhesions. In an 11 year-old boy the spinal cord entered into an anterior meningocele at the level of the upper thoracic spine. At this level the cord was immobilized whereas the nearby segments had good mobility.

In the Arnold Chiari malformation the upper cervical spinal cord may be immobilized on account of a very low protrusion of the cerebellar tonsils or by the arachnoidal adhesions frequently connected with this anomaly. In other patients a backward shift of the cord in the supine position disclosing

MOBILITY OF THE SPINAL CORD UNDER ABNORMAL CONDITIONS

by

JAN JIROUT

Through our previous pneumographic studies, the existence of the movements of the spinal cord in the anteroposterior direction resulting from changes of the position of the body was assessed. The extent of this mobility under normal conditions has been measured in large groups of individuals, and this has made it possible to evaluate the mobility under abnormal conditions.

It seems that a pathologic increase in mobility, if it exists at all, is rare. It is not certain that the considerable mobility of the thoracic spinal cord observed in some individuals can be regarded as abnormal. A relative increase in the mobility of an atrophic segment of an otherwise immobile thoracic spinal cord is also rare.

It appears, therefore, that it is practically only the decrease in mobility which is of clinical interest.

Developmental narrowing of the cervical spinal canal as frequently seen in normal individuals, is an obvious cause of decreased mobility of the spinal cord. In a group of 280 patients a narrowing of the sagittal diameter of the cervical canal to less than 12 mm was found in 16%. In these cases there was thus practically no possibility for the spinal cord to move. Considerable narrowing of the thoracic spinal canal is much less frequent. Owing to the lesser

the cord dorsally and prevent it from moving forward when the patient is in the prone position

Fixation of the spinal cord by metastatic medulloblastomas can be readily detected. The upper cervical cord is deformed and loses its normal mobility if pressure from the intracranial space is exercised in the direction of the axis of the brain stem. The resulting dorsal dislocation, dorsal bulging and fixation of the cord in this pathologic position in supra- and infratentorial brain tumors was described previously (Jirout 1959).

In angiomas not only changes in the position of the spinal cord but also differences in the filling of the venous channels due to postural changes may be observed. These variations make a correct diagnosis of the nature of these lesions possible. Similarly in syringomyelia the level of maximal dilatation of the spinal cord may vary according to the position of the patient.

On the whole the observation of displacements of the spinal cord due to postural changes of the patient constitutes in our opinion an extremely valuable help in the diagnosis of pathologic processes in the spinal canal.

Slides demonstrating the mobility of the cord were shown at the Symposium.

SUMMARY

The previous pneumographic assessment of the existence and normal range of the movements of the spinal cord has made it possible to evaluate changes under abnormal conditions. A pathologic increase in the mobility is rare; a decrease in mobility is of major clinical interest. The possible artefacts are discussed. The diagnostic importance of evaluation of the mobility of the spinal cord in developmental disturbances, in neoplasms, in arachnoidal adhesions and in discopathies is also stressed.

ZUSAMMENFASSUNG

Der früher gelieferte pneumographische Nachweis des Vorhandenseins und der Grösse der Bewegungen des Rückenmarkes hat es ermöglicht Veränderungen unter abnormalen Bedingungen zu studieren. Eine pathologische Erhöhung der Beweglichkeit ist selten, die Abnahme der Beweglichkeit ist jedoch von grösserem klinischen Interesse. Mögliche Artefakte werden besprochen. Es wird die diagnostische Bedeutung des Studiums der Mobilität des Rückenmarks bei Entwicklungsstörungen, Neoplasmen, arachnoidalen Adhäsionen und Discopathien hervorgehoben.

RÉSUMÉ

Des travaux antérieurs ayant établi l'existence et l'étendue normale des mouvements de la moelle épinière permettent d'en apprécier les modifications dans des conditions anormales. L'augmentation pathologique de la mobilité de la moelle est rare; la diminution de sa mobilité présente un grand intérêt clinique. L'auteur examine les artefacts possibles. Il souligne l'importance diagnostique de l'appréciation de la mobilité de la moelle épinière dans les troubles du développement, les néoplasmes, les adhérences arachnoïdiennes et dans les discopathies.

a wide anterior arachnoidal space, practically settles the problem of the differential diagnosis of some types of this developmental malformation from neoplasms of the upper cervical region (J JIROUT 1958)

Spondylotic spurs or disc protrusions are a frequent cause of immobility of the cervical spinal cord, especially if the spinal canal is narrow. The decrease or absence of natural movements is a valuable sign of a close contact between the anterior aspect of the spinal cord and the pathologic structures. A protrusion or herniation of a thoracic disc prevents the spinal cord from shifting ventrally when the patient is in the prone position. A disc herniation of considerable size not only causes an immobilization of the cord but also changes its form and position. The cord is stretched and bent over the protruding mass lesion like a violin string.

Gas myelography makes it possible to differentiate these conditions from similar findings due to the retractional effect of the arachnoidal adhesions. Immobilization of the spinal cord is an indirect sign of arachnoidal adhesions. Nevertheless, in evaluation of these findings, we must bear in mind that clinically asymptomatic adhesions frequently occur. They are either of congenital origin or residual arachnoidal adhesions after inflammatory processes of the meninges or of the neighbouring tissues, for instance in connection with lung tuberculosis.

Examination of the mobility of the spinal cord is a valuable adjunct whenever a mass lesion is suspected. The immobilized segments of the cord adjacent to the tumor may be readily distinguished from those whose normal mobility is still preserved. These findings are most valuable in cases in which clinical symptoms are inconclusive. In tumors, an absence of physiologic movements of the spinal cord can be expected whenever the mass lesion attains a sufficient size to prevent the cord from shifting. We observed that at the level of an extramedullary tumor situated dorsally the mobility of the thoracic spinal cord is decreased, while in other parts it may be well preserved. On the other hand, a ventrally situated tumor causes stretching of the cord and impairment of the mobility of the whole spinal cord. Similar findings may be seen in extradural tumors. In intramedullary neoplasms, the mobility of the spinal cord depends entirely on the size of the mass lesion. If it is small the mobility may be well preserved. In tumors of the upper lumbar spine the question may arise, whether there is any connection with the spinal cord. If the neoplasm is without any connection with the lower end of the spinal cord the mobility of these segments remains unimpaired. On the other hand, an intramedullary lesion growing caudally necessarily causes immobilization of the caudal end of the cord. The extramedullary tumors on the ventral aspect of the upper cervical spinal cord or in the foramen magnum displace

the cord dorsally and prevent it from moving forward when the patient is in the prone position

Fixation of the spinal cord by metastatic medulloblastomas can be readily detected. The upper cervical cord is deformed and loses its normal mobility if pressure from the intracranial space is exercised in the direction of the axis of the brain stem. The resulting dorsal dislocation, dorsal bulging, and fixation of the cord in this pathologic position in supra- and infratentorial brain tumors was described previously (JIROLT 1959).

In angiomas not only changes in the position of the spinal cord but also differences in the filling of the venous channels due to postural changes may be observed. These variations make a correct diagnosis of the nature of these lesions possible. Similarly, in syringomyelia the level of maximal dilatation of the spinal cord may vary, according to the position of the patient.

On the whole the observation of displacements of the spinal cord due to postural changes of the patient constitutes in our opinion an extremely valuable help in the diagnosis of pathologic processes in the spinal canal.

Slides demonstrating the mobility of the cord were shown at the Symposium.

SUMMARY

The previous pneumographic assessment of the existence and normal range of the movements of the spinal cord has made it possible to evaluate changes under abnormal conditions. A pathologic increase in the mobility is rare; a decrease in mobility is of major clinical interest. The possible artefacts are discussed. The diagnostic importance of evaluation of the mobility of the spinal cord in developmental disturbances, in neoplasms, in arachnoidal adhesions, and in discopathies is also stressed.

ZUSAMMENFASSUNG

Der früher gefeierte pneumographische Nachweis des Vorhandenseins und der Grösse der Bewegungen des Rückenmarkes hat es ermöglicht Veränderungen unter abnormalen Bedingungen zu studieren. Eine pathologische Erhöhung der Beweglichkeit ist selten; die Abnahme der Beweglichkeit ist jedoch von grosserem klinischen Interesse. Mögliche Artefakte werden besprochen. Es wird die diagnostische Bedeutung des Studiums der Mobilität des Rückenmarks bei Entwicklungsstörungen, Neoplasmen, arachnoidalen Adhäsionen und Discopathien hervorgehoben.

RÉSUMÉ

Des travaux antérieurs ayant établi l'existence et l'étendue normale des mouvements de la moelle épinière permettent d'en apprécier les modifications dans des conditions anormales. L'augmentation pathologique de la mobilité de la moelle est rare; la diminution de sa mobilité présente un grand intérêt clinique. L'auteur examine les artefacts possibles. Il souligne l'importance diagnostique de l'appréciation de la mobilité de la moelle épinière dans les troubles du développement, les néoplasies, les adhérences arachnoïdiennes et dans les discopathies.

a wide anterior arachnoid space, practically settles the problem of the differential diagnosis of some types of this developmental malformation from neoplasms of the upper cervical region (J JIROUT 1958)

Spondylotic spurs or disc protrusions are a frequent cause of immobility of the cervical spinal cord, especially if the spinal canal is narrow. The decrease or absence of normal movements is a valuable sign of a close contact between the anterior aspect of the spinal cord and the pathologic structures. A protrusion or herniation of a thoracic disc prevents the spinal cord from shifting ventrally when the patient is in the prone position. A disc herniation of considerable size not only causes an immobilization of the cord but also changes its form and position. The cord is stretched and bent over the protruding mass lesion like a violin string.

Gas myelography makes it possible to differentiate these conditions from similar findings due to the retraction effect of the arachnoid adhesions. Immobilization of the spinal cord is an indirect sign of arachnoid adhesions. Nevertheless, in evaluation of these findings, we must bear in mind that clinically asymptomatic adhesions frequently occur. They are either of congenital origin or residual arachnoid adhesions after inflammatory processes of the meninges or of the neighbouring tissues, for instance in connection with lung tuberculosis.

Examination of the mobility of the spinal cord is a valuable adjunct whenever a mass lesion is suspected. The immobilized segments of the cord adjacent to the tumor may be readily distinguished from those whose normal mobility is still preserved. These findings are most valuable in cases in which clinical symptoms are inconclusive. In tumors, an absence of physiologic movements of the spinal cord can be expected whenever the mass lesion attains a sufficient size to prevent the cord from shifting. We observed that at the level of an extramedullary tumor situated dorsally the mobility of the thoracic spinal cord is decreased, while in other parts it may be well preserved. On the other hand, a ventrally situated tumor causes stretching of the cord and impairment of the mobility of the whole spinal cord. Similar findings may be seen in extradural tumors. In intramedullary neoplasms, the mobility of the spinal cord depends entirely on the size of the mass lesion. If it is small the mobility may be well preserved. In tumors of the upper lumbar spine the question may arise, whether there is any connection with the spinal cord. If the neoplasm is without any connection with the lower end of the spinal cord the mobility of these segments remains unimpaired. On the other hand, an intramedullary lesion growing caudally necessarily causes immobilization of the caudal end of the cord. The extramedullary tumors on the ventral aspect of the upper cervical spinal cord or in the foramen magnum displace

CONGENITAL TUMOURS OF THE SPINAL CORD

by

G LOMBARDI and A PASSERINI

Nineteen congenital tumours of the spinal cord corresponding to 4.8 % of the 347 spinal tumours operated on up to the end of 1963 have been recorded. The distribution by type was 10 lipomas, 5 dermoids, 3 epidermoids and 1 teratoma.

Lipomas accounted for 2.90 % of tumours of the spinal cord which is well above the 1 % reported by other workers (EHNI & LOVE 1945; EPSTEIN 1962). They were observed in 6 women and 4 men. Larger series than the one now reported reveal the same non significant difference. Six lipomas were intradural and 4 extradural—a distinction important in several respects.

Intradural lipomas It is thought that these are derived from lipoid cells in the pia mater or from fatty transformation of connective tissue. Histologic examination reveals adult adipose tissue with no evidence of embryonal fat cells; no trace of glial tissue is evident either, which confirms the mesenchymal origin of the tumour. The signs and symptoms to which these lipomas give rise are generally very slowly progressive, at times interrupted by spontaneous remission. The tumours are at least at first extramedullary but they develop such intimate connexions with the cord as to appear and behave

REFERENCES

- JIROUT J. Changes in the size of the subarachnoidal spaces after insufflation of air. *Acta radiol* 46 (1956) 81
- Pneumographic investigation of the cervical spine. *Acta radiol* 50 (1958) 221
 - Myelographic syndrome of caudad dislocation of the brain stem. *Brit J Radiol* 32 (1959) 188
 - The mobility of the cervical spinal cord under normal conditions. *Brit J Radiol* 32 (1959) 744
 - Die Beweglichkeit des Halsrückenmarks unter normalen und pathologischen Umständen. *Trans of 1st Inter Congress of Radiol G Thieme Stuttgart 1960* 445
 - Contribution à l'étude pathogénique et diagnostique de la malformation d'Arnold Chiari. *Ann Radiol* 4 (1961) 691
 - Mobility of the thoracic spinal cord under normal conditions. *Acta radiol* 1 (1963) 729
 - Pnevmonyelografija. *Stát zdrav náklad Prague 1964*
 - and KUNC Z. Traumatic herniation of the thoracic intervertebral disc. *Acta neurochir* 8 (1960) 88
 - FISCHER J. und NADVORNIK F. Anatomische und pneumographische Studien des hinteren Arachnoidalraumes der normalen Brustwirbelsäule. *Fortschr Geb Röntgenstrahlen* 104 (1964) 89

tumours erosion of the pedicles and increase in the interpedicular distance, with or without arcuate indentation of the dorsal aspect of the vertebral bodies. Only in the case of the teratoma and in one case of epidermoid were the changes very extensive.

Calcification was observed in 2 cases. The relative incidence in congenital tumours (10 %) is distinctly higher than in the total of 347 tumours of the spinal cord (1.6 %). There is frequent mention in the literature of the concomitant presence of other malformations of the cord or spine or both, but the authors observed these in 2 cases only, in one case a malformed cord extended right down to the sacrum where it ended in a lipoma within an occult meningocele and in the other there was vertebral schisis at the same level as an intramedullary dermoid. The bone changes of congenital tumours do not differ in tumour type but their incidence does. Analysis reveals that in lipomas especially if extradural bone changes are infrequent (4 out of 10) while the reverse is the rule in dermoids, epidermoids and teratomas (8 out of 9 cases).

Myelography. Myelography was performed in 18 cases. The contrast medium indicated the tumour site and its position with reference to the spinal cord and the dura in every case but yielded no information as to type. The examination disclosed definitive block in 15 cases (83 %). The cerebrospinal pathways were clear in 3 cases of lipoma.

Conclusions

Congenital tumours represented 5 % of all the tumours of the spinal cord. The largest group was that of the lipomas followed in descending order by dermoids, epidermoids and a teratoma. The age at diagnosis was however in the reverse order beginning with the teratoma and ending with the lipomas, the extradural variety being last of all. Congenital tumours were found more often in the distal parts of the cord, 7 lying in the conus medullaris.

Bone changes in the lipomas were relatively infrequent but the rule in the other types. Association with other malformations of the spine and cord was rare in the present series. Myelography located the tumours but did not disclose their nature.

SUMMARY

Nineteen congenital tumours of the spinal cord were studied. Bone changes were observed in 12 cases (63 %) and were infrequent only in extradural lipomas. Calcifications were observed in 2 cases. Other associated malformations of the spine and cord as well as the value of myelography are discussed.

as intramedullary tumours even at operation. Their distribution was dorsal in one case, dorsolumbar in 3 cases, and lumbar and sacral in one case each, they may also be found in the cervical region. The growths nearly always occupy the dorsal aspect of the spinal cord, as in the present cases. The average age of the group was 36 years.

Extradural lipomas These are often associated with an angiomatous component as in 3 of the 4 cases. It is thought that they arise from bipotential mesenchymal cells about the adult capillaries that may develop into either blood vessels or fat (Elli & Love 1945). These tumours present a more acute clinical symptomatology than intradural lipomas and, being clearly demarcated from the surrounding areas of extrathecal fat, can usually be easily removed. They may be present anywhere along the spine but have a distinct preference for the dorsal region, the site of all the 4 cases. Extradural lipomas are observed later in life than the intradural variety, the average age of our patients being 51 years.

The *dermoids*, *epidermoids* and *teratomas* form a group of allied tumours that have often been confused, probably because of their gross similarity.

Dermoids Dermoids are demarcated by a capsule of well differentiated stratified squamous epithelium and contain hair, sebaceous glands and other appendages of the skin. All 5 cases were intradural and 4 were intramedullary. Their locations were 2 dorsal, 2 in the conus medullaris, and one lumbar. The average age of the patients was 21 years and 4 of the 5 were males.

Epidermoids The tumour capsule encloses a mass of desquamated cells containing keratohyaline. Known also as pure cholesteatomas or pearly tumours, they occur much more frequently in the brain than in the spinal cord. Thirty one cerebral and 5 cranial epidermoids were operated on during the same period. The 3 epidermoids of the spinal cord were in the conus medullaris or in the cauda equina. The average age of the patients, all males, was 12 years.

Teratomas These are derived from the three germ layers and may be distinguished from dermoids by the presence of muscle, cartilage and other mesodermal tissues. The tumours have a definite predilection for the distal parts of the spine, especially for the sacrococcygeal region, when they occur in this situation they usually extend into the pelvis also and cause obstructive symptoms attributable to the rectum and ureters. The teratoma observed in a 5 month old female child was lumbosacral and calcified. This tumour has a predilection for females and sometimes becomes malignant.

Bone changes were present in 12 cases (63 %). These were mostly confined to one or two vertebrae and were of the type usual in very slow growing

CONTRAST EXAMINATION OF THE SPINAL EPIDURAL SPACE

by

W. LUYENDIJK and A. E. VAN VOORTHUISEN

The epidural or peridural spaces which lie between the dura mater and the walls of the vertebral canal may be examined in the lumbosacral region by means of peridurography. The dural sac tapers below into the filum durae matris spinalis which lies in the sacral canal. The peridural space contains spinal nerves and blood vessels embedded in areolar connective tissue and fat and is connected with the paravertebral and presacral connective tissue via the intervertebral foramina. Connective tissue in these openings attaches the spinal nerves and blood vessels to the walls of the foramina (Charpy's ligament). Furthermore, the peridural space is connected with the subcutaneous tissue via the sacral hiatus.

The size and shape of the peridural space is determined by the manner of attachment of the dural sac to the walls of the spinal canal, for example by the spinal nerves. According to some authors the connective tissue on the ventral aspect of the dural sac is denser than elsewhere and may also provide some degree of fixation to the corresponding wall of the spinal canal. There is no suggestion in the literature of any fixation to the dorsal wall.

Peridurography is performed by the injection into the peridural space

ZUSAMMENFASSUNG

Neunzehn angeborene Tumoren des Rückenmarkes wurden untersucht. In zwölf Fällen (63 %) wurden Knochenveränderungen gefunden, nur in extraduralen Lipomen waren diese selten. Verkalkungen wurden in zwei Fällen festgestellt. Begleitende Missbildungen der Wirbelsäule und des Rückenmarkes sowie der Wert der Myelographie werden besprochen.

RÉSUMÉ

Les auteurs ont étudié dix-neuf tumeurs congénitales de la moelle. Des signes osseux ont été observés dans 12 cas (63 %) ils ne sont rares que dans les lipomes extraduraux. Il y avait des calcifications dans 2 cas. Les auteurs examinent l'association de ces tumeurs avec d'autres malformations du rachis ou de la moelle et la valeur de la myélographie.

REFERENCES

- LIHM G. and LOWE J. G. Intraspinal lipomas. Report of cases, review of literature and clinical and pathologic study. *Arch. Neurol. Psychiat.* 53 (1945) 1.
ESTLIN B. S. *The Spine*. Lea and Febiger, Philadelphia 1962.
LOMBARDI G. and PASSERINI A. Spinal cord diseases. A radiologic and myelographic analysis. Williams and Wilkins, Baltimore 1964.

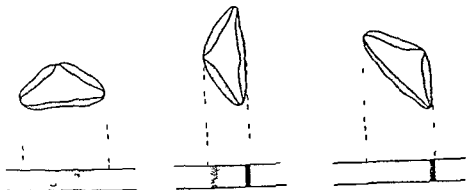


Fig 2 Contrast medium in the peridural space (dotted areas) in a p (p a) lateral and oblique projections. White line in midline of a p projection corresponds with the dorsomedian dural fold. A lighter central area separates the wider dorsal from a narrow ventral contrast band in the lateral view while one of the dorsolateral contrast bands appears as a narrow strip in the oblique film.

the intradural pressure is lowered and due to this dorsomedian fixation forms a median fold this can be observed at operations in the lumbosacral area. The same thing occurs when the pressure in the peridural space is elevated for example when contrast medium is injected, the ventral and both dorsolateral aspects of the dural sac will be expanded so that the sac is moulded into a more or less triangular cross section with the dorsomedian fold lying superiorly.

This was clearly shown by post mortem studies following the injection of a barium gelatine mixture into the sacral hiatus. Roentgenograms demonstrated a distribution of the contrast medium identical to that obtained in clinical examinations. The vertebral column was then removed, sectioned and examined roentgenographically and by means of dissection. This study confirmed the expansion of the contrast medium with formation of the dorsomedian dural fold at the lower lumbar levels (Fig 1). The projection of the peridural contrast medium in a p (or p a) lateral and oblique views is illustrated in Fig 2. The contrast medium in the lateral peridurograms is spread in a thin layer between the dural sac and the ventral wall of the spinal canal (Fig 3). This indicates that the peridural space lies in a more or less frontal plane between the dural sac and the ventral wall of the spinal canal and that its dorsoventral dimension is narrow. This distribution is not uniform dorsal to an intervertebral disk it is small but behind a vertebral body it is usually larger increasing at every segment toward the centre of the latter.

The dorsal aspect usually has a sharp borderline with a lighter central zone dorsal to which it passes into the wider dorsal contrast band. It is thus obvious that at the level of the lighter mid zone the dimension of the peridural space

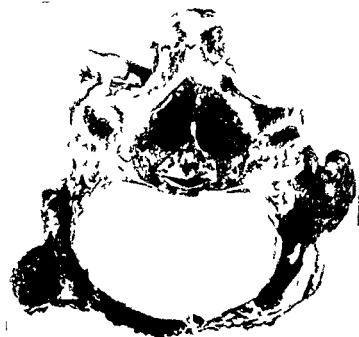


Fig. 1 Autopsy in a 2 year old child. Barium Indian ink gelatine mixture injected peridurally. Cross section of vertebral column at level of lumbosacral disk. Dorsomedian dural fold clearly demonstrated after some of the peridural gelatine mass has been removed. The dural sac is moulded into a triangular form.

through the sacral hiatus of 20 ml of a water soluble contrast medium, generally sodium diatrizoate. No blood or cerebrospinal fluid must have escaped from the needle during the previously performed Valsalva manoeuvre. Furthermore, the midline position of the tip of the needle not above the level of S3—4 must have been checked by a post and lateral roentgenograms. These precautions will ensure that the contrast medium is not injected into the subarachnoid space (*vide infra*). The medium usually reaches the upper lumbar or lower dorsal region. It is absorbed in 30 to 45 minutes and excreted by the kidneys.

Normal appearances of the lumbar peridural space

The shape of the peridural space is determined by the manner in which the dural sac is attached to the walls of the spinal canal. The attachment is effected on the ventrolateral aspect by the spinal nerves but anatomic and surgical investigations revealed that the sac in the lumbosacral region appears to have another point of fixation in the median plane on its dorsal aspect where it is attached to the vertebral arches. The sac more or less collapses if



Fig 4 Female aged 32 with low back pain radiating to both legs Diminished reflexes especially of Achilles tendon on right side A.P. peridurogram Central contrast column with light midline peripheral extensions of the contrast medium beyond the intervertebral foramina excepting on right side at level of L5-S1 (1)



Fig 5 Male aged 40 with low back pain radiating into left leg hypotonia of left quadriceps and diminished left patellar reflex Peridurogram oblique Dorsolaterally located contrast medium lying in same direction as central beam In front the conning medium is partially interrupted at L3-L4 (confirmed by a protruding disk)

the central ray (Fig 5) this strip at the side of the vertebral bodies is bordered by a lighter zone by which it is separated from a wide band of medium intensity.

The periradicular situated contrast medium often extends into the paravertebral areas and there is apparently no discontinuity between the peridural space and the paravertebral regions Charpy's ligament not acting as a barrier



Fig. 3 Female aged 29 with left radicular ischialgia and diminished reflexes on same side. Lighter midzone between the ventral and the broader dorsal contrast band in lateral peridurogram: ventral contrast band interrupted at L 4—5 (B) and dorsal contrast band curved backward (Operation: Large protruding disk at L 4—5 mainly on left side.)

is small. With the localization of the dural sac within the spinal canal and its anchoring by the spinal nerves to the lateral regions of the spinal canal in mind, there is justification for considering the compressed dural sac responsible for the central zone.

It may be assumed from the width and intensity of the dorsal contrast band that the peridural space is larger in size in the dorsal than in the ventral region of the spinal canal although its exact dimensions cannot be evaluated from lateral peridurograms alone.

An a.p. peridurogram usually reveals a central contrast column (Fig. 4), denser in the lateral than in the central zone. A further continuation of the contrast medium along the spinal nerves can be seen passing through the intervertebral foramina (periradicularly) and running laterally and caudally. A narrow strip is usually evident in the mid zone of the central contrast column and, as already explained, is due to the median fold of the dural sac in the dorsal region of the peridural space (*plica mediana dorsalis*). The 45 degree oblique peridurograms usually reveal a relatively narrow intense, sharply outlined strip along the side of the vertebral laminae that lie in the same direction as

care must be exercised because the dural sac may extend to an abnormally low level

Painful cramps occurred in only 6 cases of the present material, all of which recovered completely. No other complications were encountered.

The recommendation having been made that lumbar puncture should be performed only after peridurography the question has arisen whether the peridurally injected contrast medium may bring about changes in the composition of the lumbar spinal fluid. An investigation was therefore performed in two groups of cases. In the first group of 13 cases the composition of the spinal fluid was examined at various times before and after the peridurography. In the second group of 8 cases the same procedure was carried out twice after the peridurography. This study revealed no essential changes in the spinal fluid. A slight increase in the total protein content was demonstrated in about a third of the cases but with the exception of one case no changes in the cell content were established.

Present investigation

The investigation was performed in 600 cases. The examination was unsuccessful in a number of cases (7.5 %) the sacral canal being either too narrow or the hiatus could not be entered because of abnormal ossification in some of the cases while in others the puncture needle entered a vein and the contrast medium was injected intravenously. In a few cases the investigation was unsuccessful because of a deformity of the roof of the sacral canal either it was not ossified or the hiatus was unusually high. In the remaining unsuccessful cases the contrast medium rose insufficiently high into the lumbar region and a large part escaped through the sacral foramina.

It is to be expected that in a number of pathologic conditions of the lumbar spinal and sacral canal changes will take place in the normal size and shape of the peridural space. It need hardly be stated that this applies to prolapse of the intervertebral disk, developmental narrowing of the lumbosacral vertebral canal, peridural and/or periradicular adhesions and sacral perineural cysts. These abnormalities often result in ischialgia of a radicular character together or without other radicular signs. Evidence of either the orthotic cauda syndrome or compression of the cauda equina fibres is sometimes present. Although the clinical signs of disk prolapse are sometimes so definite that there is no great need for radiologic investigation with contrast medium, there are cases in which the latter is of great importance. Peridurography is indicated when the diagnosis is still uncertain after clinical neurologic and supplementary radiologic examinations have been performed. The cases in the present material

It is assumed in the literature that a barrier effect increases with increasing age, so that according to some authors (e.g. BROMAGE 1954) there is even a chance of complete impermeability. This is of importance with regard to effecting peridural anaesthesia. The peridurograms were used to make a study of the communication between the peridural space and the paravertebral area in the various age groups. No definite evidence of an increased barrier effect in older subjects was found. The impression was obtained, however, that in the lumbar and lumbosacral intervertebral foramina the barrier effect increases somewhat at more advanced ages, although this does not hold to any extent for the anterior sacral foramina.

Complications It is necessary, as has been mentioned, by taking suitable precautions, to avoid introducing the contrast medium into the subarachnoid space. Reports in the literature and our own experience (in patients and experimental animals) have shown that this false injection may produce, shortly after its exhibition, intense painful cramps that may be accompanied by a state of severe shock.

Urografin 60% was injected into the subarachnoid space in 14 cats weighing from 2.5 to 3.5 kg. It generally produced cramps but this appeared to depend upon the dose. No cramps were observed after the injection of 0.1 ml Urografin. When 0.2 ml or more was injected severe cramps which caused the death of the animal occurred. These could be prevented by an intraperitoneal injection of 120 to 240 mg Nembutal during the period of paroxysm; the cramps stopped and the cats recovered completely. There appeared to be a certain interval of time between the subarachnoid injection and the moment the cramps occurred. The length of this interval depended upon the amount of material injected. 0.2 ml caused cramps after about 15 minutes whereas 0.3 ml produced the paroxysm after 2 to 3 minutes. Another difference was observed when the results of suboccipital and lumbar injections were compared: the cramps after suboccipital injection started in the fore limbs and the neck whereas lumbar injection produced paroxysms starting in the hind limbs, the tail and the caudal part of the rump.

Different amounts of methylglucamine (146.25 mg/ml) were also injected into the subarachnoid space in another series of cats. No cramps could be produced by this solvent.

Prompt intravenous infusion with a small dose of sodium Pentothal continued during the entire period of any tendency to symptoms produces complete alleviation. The chances of this complication are reduced by not performing a lumbar puncture for at least two, preferably three weeks, prior to peridurography.

The precautions mentioned previously reduce the chance of entering the caudal end of the dural sac or the radicular sheaths or perineural cysts originating from them to a minimum. The possibility of structural anomalies within the vertebral and sacral canal must be taken into account in the presence of marked signs of status dysraphicus. Under such circumstances the greatest



Fig 7 Male aged 63 with low back pain radiating into front of right thigh and calf. Dysbasia and patella reflexes diminished. Normal aortic pulsation on both sides. Peridurography. Indentations of dorsal contrast band at L4 and L5. Operative narrowing of vertebral canal at cranial ridges of arches of L4 and L5.



Fig 8 Female aged 45 with right radicular sciatic paraparesis of right peritibial muscles and some urinary incontinence. Peridurography. Contrast column interrupted at L4--5 especially on right side (IIla). Round contrast filled and contrast free areas. Operation. Protruding disk at L4--5. Dural sac compressed by cranial ridge of arch of L4. Perineural cysts of 2nd and 3rd sacral nerves.

veins peridural and/or periradicular adhesions spina bifida occulta, hypertrophy of the ligamentum flavum sacral perineural cysts and spondylolysis.

The composition of these groups was selected wherever possible so as to exclude conditions complicated by other abnormalities. The problem presented by this formation of pure groups is that the material for some conditions was very limited and so might preclude reliable statistical treatment. In

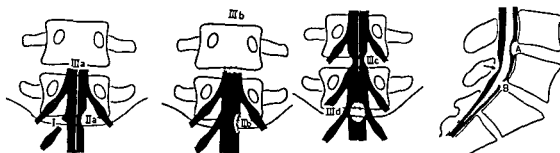


Fig. 6. Schematic representation of basic changes.

except for about a hundred cases during the early period of the study, were treated according to these principles. Peridurography was carried out in the accepted group of cases when there was any suggestion of radicular ischaemia, in order to collect data.

A number of basic patterns that either alone or in various mutual combinations represent radiologic abnormalities were established for a closer study of peridurograms. These patterns were derived from both a.p. and lateral peridurograms. Each basic change was indicated by a code number (in the a.p. film I, IIa, IIb, IIIa, IIIb, IIIc, IIId, and in the lateral film A and B). This has made it possible to analyse every identified peridurographic abnormality in terms of one or more basic changes and to indicate it with a code number or a combination of such numbers (Fig. 6).

In addition to the changes produced by combinations of these basic patterns, several others characteristic of particular abnormalities appear. An indentation of the dorsal contrast band is observed at the site of the malformation in cases of developmental narrowing of the vertebral canal (Fig. 7). A marked increase in the width of the ventral contrast band, more or less triangular in shape, also appears at the site of the displaced vertebra in spondylolisthesis. Perineural cysts in the sacral canal may be evident in the a.p. peridurogram either as more or less rounded, contrast filled or contrast free areas in the sacral contrast column, the latter being more frequent than the former (Fig. 8).

The frequency of the different basic patterns was determined as part of a detailed study of the peridurographic changes that accompany the conditions studied. This was calculated according to the number of levels at which peridurographic alterations were observed. Only those cases in which confirmation at operation was possible were included in the group of conditions that were studied in more detail. These conditions consisted of prolapsed intervertebral disk, protruding disks with osteochondroticipping of the bone, developmental narrowing of the lumbar vertebral canal, dilated peridural

summarized as III but this does not obtain. This should probably be ascribed to the fact that a disk prolapse with a predominantly lateral localization is often accompanied by a threshold formation extending over the entire width of the affected intervertebral disk. The difference became more accentuated when the comparison was limited to a subgroup in which operation demonstrated strikingly large prolapses.

If comparison be made with a group of prolapsed disks with osteochondrotic bone lipping only small differences are observed. A markedly higher frequency is found only for IIIc (40.7 %) which statistically is on the borderline of significance. Basic patterns IIb and IIId are not present in this group. The importance to be attached to this fact is hard to estimate without indulging in speculation.

In the group of developmental narrowing of the lumbar vertebral canal the highest frequencies are found for basic patterns I, IIIa, IIIb, IIIc and A. The characteristics of this group become more marked after elimination of the basic patterns due to complicating changes.

Basic pattern I appears to have a lower frequency than in the two preceding groups (46.2 %). This difference is significant as is the combination of I with IIa (51 %). The frequency of combination I with IIb on the contrary is not significantly different for either group. If this comparison be extended significantly higher values are found for IIIa and IIIb (28.2 and 48.7 % resp.) but for IIa an appreciably lower figure (7.7 %) which differs significantly from both preceding groups is reached. To a lesser degree a similar difference which is however not significant can be demonstrated for B. If compared with disk prolapses with osteochondrotic bone lipping this difference in the frequency of B is significant however.

Since the developmental narrowing of the vertebral canal usually occurs over the entire width of the vertebral lamina the frequent occurrence of IIIa, IIIb and IIIc is even less surprising than the lower frequency of I, IIa and B. In addition to these differences attention has also been given to abnormalities of the dorsal contrast band at the level at which the vertebral arch exerts pressure and in particular to the dorsal indentation, which is considered of great importance. The presence of this abnormality almost certainly points to a developmental narrowing of the vertebral canal.

The fourth group that is considered to be sufficiently large to allow a more detailed analysis comprises peridurographic changes associated with peridural and/or periradicular adhesions as compared with the group of prolapsed disks. The process of elimination was again applied. In general corresponding frequencies could be established for many basic patterns. A significant difference is evident for basic pattern IIb (22.9 %) while no great importance may

Table

The more frequent basic patterns and their mutual combinations in four groups of abnormalities studied in greater detail. The figures give the percentile frequencies. Values of 11%, and higher in bold type, frequencies which differ significantly in italics

Abnormality	I	IIa	IIb	IIIa	IIIb	IIIc	I + IIa	I + IIb	I + IIIc	A	B
Disk prolapse	73.8	33.0	8.7	1.9	10.7	23.3	30.1	5.0	20.1	35.0	27.2
Disk prolapse with osteochondrotic bone spurs	70.1	37.1	11.1	3.7	—	40.7	29.6	7.1	33.3	35.9	40.7
Developmental narrowing of the vertebral canal	46.2	7.7	7.7	28.2	48.7	30.8	5.1	2.6	28.2	30.8	12.8
Peridural/periradicular adhesions	60.4	33.3	22.9	1.2	16.7	16.7	22.9	14.6	16.7	29.2	22.9

view of the method used, an exception was made in a number of groups. The groups comprising developmental narrowing of the lumbar vertebral canal and of the peridural and/or periradicular adhesions were thus given more detailed study not only in the 'pure' cases but also in those with complications, in the latter an elimination procedure was applied by which the frequency of the entire group was reduced by subtracting those which could be considered as caused by complicating abnormalities.

The results of the peridurographic analysis of the various groups were compared, especially with the group of disk prolapses, and the differences were examined statistically for significance (see Table).

In the group of uncomplicated prolapsed disks, the highest frequencies were found for I (73.8%), IIa (33.0%), IIIc (23.3%), A (35.0%) and B (27.2%). Of the other basic patterns only IIb and IIIb stood out with values of about 10%. The most frequently seen combinations were I with IIa (30.1%) and I with IIIc (20.1%), as well as I, IIa and IIIc with A and B.

Basic patterns A and B were never present as single abnormalities when the x-ray peridurogram presented no changes.

The peridurographic alterations seem to be independent of the disk from which the prolapse developed. Appreciable differences appear, however, to exist between prolapsed disks with a lateral location and those which have no predominantly lateral localization. As could be expected, in the former group I and II are outstanding, with significant values for I (82.6%) and IIa (13.1%).

In the second group the same might be expected for the basic changes

summarized as III, but this does not obtain. This should probably be ascribed to the fact that a disk prolapse with a predominantly lateral localization is often accompanied by a threshold formation extending over the entire width of the affected intervertebral disk. The difference became more accentuated when the comparison was limited to a subgroup in which operation demonstrated strikingly large prolapses.

If comparison be made with a group of prolapsed disks with osteochondrotic bone lipping, only small differences are observed. A markedly higher frequency is found only for IIIc (40.7 %) which statistically is on the borderline of significance. Basic patterns IIIb and IIId are not present in this group. The importance to be attached to this fact is hard to estimate without indulging in speculation.

In the group of developmental narrowing of the lumbar vertebral canal the highest frequencies are found for basic patterns I, IIIa, IIIb, IIIc, and A. The characteristics of this group become more marked after elimination of the basic patterns due to complicating changes.

Basic pattern I appears to have a lower frequency than in the two preceding groups (46.2 %). This difference is significant as is the combination of I with IIa (51 %). The frequency of combination I with IIb, on the contrary, is not significantly different for either group. If this comparison be extended significantly higher values are found for IIIa and IIIb (28.2 and 48.7 % resp.) but for IIa an appreciably lower figure (7.7 %) which differs significantly from both preceding groups is reached. To a lesser degree a similar difference which is however not significant can be demonstrated for B. If compared with disk prolapses with osteochondrotic bone lipping, this difference in the frequency of B is significant, however.

Since the developmental narrowing of the vertebral canal usually occurs over the entire width of the vertebral lamina, the frequent occurrence of IIIa, IIIb and IIIc is even less surprising than the lower frequency of I, IIa and B. In addition to these differences, attention has also been given to abnormalities of the dorsal contrast band at the level at which the vertebral arch exerts pressure and in particular to the dorsal indentation which is considered of great importance. The presence of this abnormality almost certainly points to a developmental narrowing of the vertebral canal.

The fourth group that is considered to be sufficiently large to allow a more detailed analysis comprises peridurographic changes associated with peridural and/or periradicular adhesions as compared with the group of prolapsed disks. The process of elimination was again applied. In general corresponding frequencies could be established for many basic patterns. A significant difference is evident for basic pattern IIb (22.9 %) while no great importance may

Table

The more frequent basic patterns and their mutual combinations in four groups of abnormalities studied in greater detail. The figures give the percentile frequencies. Values of 11% and higher in bold type; frequencies which differ significantly in italics

Abnormality	I	IIa	IIb	IIIa	IIIb	IIIc	I+IIa	I+IIb	I+IIIc	A	B
Disk prolapse	73.8	33.0	8.7	4.9	10.7	23.3	30.1	5.8	20.4	35.0	27.2
Disk prolapse with osteochondrotic bone lipping	70.4	37.1	11.1	3.7	—	<u>40.7</u>	29.6	7.4	33.3	35.9	40.7
Developmental narrowing of the vertebral canal	<u>46.2</u>	<u>7.7</u>	7.7	<u>28.2</u>	<u>48.7</u>	30.8	<u>5.1</u>	2.6	28.2	30.8	<u>12.8</u>
Peridural/periradicular adhesions	60.4	33.3	<u>22.9</u>	4.2	16.7	16.7	22.9	14.6	16.7	29.2	22.9

view of the method used, an exception was made in a number of groups. The groups comprising developmental narrowing of the lumbar vertebral canal and of the peridural and/or periradicular adhesions were thus given more detailed study not only in the 'pure' cases but also in those with complications, in the latter an elimination procedure was applied by which the frequency of the entire group was reduced by subtracting those which could be considered as caused by complicating abnormalities.

The results of the peridurographic analysis of the various groups were compared, especially with the group of disk prolapses, and the differences were examined statistically for significance (see Table).

For the group of uncomplicated prolapsed disks, the highest frequencies were found for I (73.8%), IIa (33.0%), IIIc (23.3%), A (35.0%) and B (27.2%). Of the other basic patterns only IIb and IIIb stood out with values of about 10%. The most frequently seen combinations were I with IIa (30.1%) and I with IIIc (20.4%), as well as I, IIa and IIIc with A and B.

Basic patterns A and B were never present as single abnormalities when the a.p. peridurogram presented no changes.

The peridurographic alterations seem to be independent of the disk from which the prolapse developed. Appreciable differences appear, however, to exist between prolapsed disks with a lateral location and those which have no predominantly lateral localization. As could be expected, in the former group I and II are outstanding, with significant values for I (82.6%) and IIa (13.4%).

In the second group the same might be expected for the basic changes

required to study this phenomenon. Marked abnormalities as were already evident peridurographically, were present in all these cases however at nearby levels at surgical exploration. No case in which peridurography had revealed changes was found to be normal at operation. Restricting the cases to those with peridurographic findings at levels at which surgery revealed none — as against adjacent areas in the vertebral canal — the following may be emphasized.

Only basic pattern A was evident in some cases in which the alteration was probably still within the limits of normal variation. It is essential in individual cases that this basic pattern when present alone be interpreted with extreme care. Basic pattern IIIc was evident in 3 cases but was not very distinct. Surgery in all the cases revealed marked quantities of fat especially predually. This finding was noted in the surgical report which is exceptional. It therefore seems most probable that the fat explains the peridurographic abnormality. Peridurographic changes at one side of the vertebral canal in which the contrast medium had not risen normally because of unilateral obliteration of the peridural space at a lower level were described in some other cases. The value of the peridurographic findings is evidently very dubious.

Apart from six other cases in which only slight peridurographic changes together with normal distribution of the contrast medium were evident three other cases with definite unilateral abnormalities (basic pattern I) in which contrary to expectation operation provided no explanation must be recorded.

In summary it may be stated that myelography was inadequate in a number of cases in which peridurography was able to provide reliable information. This is undoubtedly dependent upon the special limitations caused by the dural sac. In addition peridurography offers diagnostic possibilities in numerous conditions that cannot or cannot adequately be demonstrated by myelography (e.g. peridural adhesions, developmental narrowing of the vertebral canal). On the other hand a number of peridurographic abnormalities have to be interpreted critically which means that the method to be of use unquestionably requires more experience than myelography.

SUMMARY

Peridurography a method of examination that indicates the shape and size of the peridural space at the lumbosacral level of the spinal canal is described. It was found that it could be superior to myelography. The method is particularly important in cases of disk prolapse, peridural adhesions, osseous stenosis of the vertebral canal and perineural sacral cysts.

be attached to the higher frequency of IIb (16.7%). The frequency of the combination of I with IIb reveals no significant difference when compared with the other groups, in this group, B of the single lateral basic patterns is present when no abnormalities are evident in the γ p peridurogram at the same level.

Basic patterns A and B are less frequently seen in the subgroup of the uncomplicated cases. This holds particularly for A, for which the difference with the disk prolapse group is significant.

The most striking frequencies of the basic patterns and their combinations for the four groups described are evident from the Table presented.

Sacral perineural cysts for the greater part appeared to be located at the second and the third sacral nerves and varied in size from γ pea to γ pigeon's egg. Apart from the peridurographic changes already described, the diagnosis may sometimes be made radiologically without contrast media if the cysts have produced pressure atrophy of the sacrum. A communication between the perineural cysts and the subarachnoid space could sometimes be established.

Finally, γ group of exceptional cases must be mentioned. These cases include γ number of tumours, originating from intradural, vertebral and paravertebral tissue, three cases of epidural cysts, and γ case of spondylolysis, as well as γ case of subdural haematoma.

The results of peridurographic and myelographic examination could be compared in 72 cases. Forty-eight of these were operated upon so that the radiologic and surgical findings could also be compared. In 35 of them the myelography and the peridurography gave different results. The operative findings did not agree with the results of the myelographic investigation, but in all but 4 cases there was agreement with the peridurographic findings. In 3 of them a second abnormality at a lower level had blocked off the peridurally injected contrast medium, in the fourth case γ slight abnormality (IIb) was evident for which no surgical finding was reported. The inadequacy of the myelographic investigation, apart from 18 out of 31 cases of disk prolapse, especially concerned developmental narrowing of the vertebral canal, peridural and/or periradicular adhesions, and dilated peridural veins.

In all of the cases that were treated surgically, the peridurographic method provided insufficient information in only 29%. This, without exception, can be ascribed to other abnormalities cranial to the involved level, such as a very prominent disk prolapse, developmental narrowing of the vertebral canal, or, as in reoperation, extensive peridural adhesions. These anomalies preclude further ascent of the contrast medium.

On the other hand it is doubtful whether at the level at which surgery revealed no pathologic findings changes were really evident at peridurography. Such cases have actually been encountered (4%) and further analysis is

- CELDEREN CHR Fin Orthotisches (Lordotisches) Kaudasyndrom Acta Psychiat scand 23 (1948) 57
- GOLLNITZ G Erfahrungen mit der Peridurographie Nervenarzt 22 (1951) 444
- GOTZE J Zwischenfälle nach Injektion in den Periduralraum Chirur 23 (1952) 1/6
- GROENENDIJK H J De peridurale anaësthesie Diss Groningen 1954
- HASNAEIS P R M J The weak back Diss Nijmegen 1959 Ed Elsevier Amsterdam London New York, Princeton
- HAUSLER G Leber die Indikation zur Luftmyelographie und Peridurographie beim lumbalen Bandscheibenvorfall Nervenarzt 21 (1950) 297
- HEILE Zur Darstellung des epiduralen Raumes Zbl Chir 40 (1913) 110
- HERBERT J J, PAILLOT J et FAIDHERBE P L'exploration lipiodolée de l'espace epidural dans les sciaticques et les lombalgies Mém Acad Chir 76 (1950) 584
- JUNGE H Peridurographie Dtsch med Wschr 74 (1949) 682
- Zwischenfälle und Gefahren bei periduraler Kontrastdarstellung Nervenarzt 23 (1952) 345
- KARLEN A Komplikationen bei intraduraler Per Abrodil Myelographie Acta chir scand 87 (1942) 182
- Todesfall an Fett Knochenmarkembolie und Uramie nach intraduraler Per Abrodil myelographie Acta chir scand 87 (1942) 496
- KNUTSSON F Experiences with epidural contrast investigation of the lumbosacral canal in disk prolapse Acta radiol 22 (1941) 694
- Epidurale Kontrastfüllung des Lumbosacralkanales bei Discusprolaps (Perabrodil) Acta radiol 22 (1941) 694
- KRAMER W Canalografie Het röntgenologisch zichtbaar maken van het vertebraalkanaal door het epiduraal inspuiten van snel resorbierbare contrastmiddelen Med Maandbl 3 (1950) 718
- LANSCHÉ W E and FORD L T Correlation of the myelogram with clinical and operative findings in lumbar disc lesions J Bone Jt Surg 42A (1960) 193
- LOEW F Zur Diagnose des lumbalen Bandscheibenvorfalls mittels Kontrastfüllung des Periduralraums Zbl Neurochir 9 (1949) 307
- LUYENDIJK W Canalography as a diagnostic aid in a case of compression of the cauda equina Folia psychiat neerl 56 (1953) 488
- Congenital extradural cyst Acta chir neerl 7 (1955) 23
- Canalografie Thesis Leiden 1962
- and DEL PRADO E A Peridurography in the lumbosacral region Camara Radiologica (1958) 27
- PADBERG G Perineurale wirtelkysten Ned T Geneesk 103 (1959) 2054
- PENZHOLZ H Gefahren der Peridurographie mit Perabrodil Zbl Neurochir 11 (1951) 260
- RITTER L Fehldiagnosen und Gefahren der Peridurographie Fortschr Röntgenstr 75 (1951) 346
- ROSENFELD W Die röntgenologische Darstellung des Periduralraumes und ihre diagnostische Bedeutung Nervenarzt 21 (1950) 304
- SARPYNER W A Congenital stricture of the spinal canal J Bone Jt Surg 27 (1945) 70
- SICARD J A et FORESTIER J Méthode radiographique d'exploration de la cavité épurale par le lipiodol Rev neurol 28 (1921) 1264
- TARLOV I M Perineural cysts of the spinal nerve roots Arch Neurol Psychiat 40 (1938) 1067
- Sacral nerve root cysts pathogenesis and clinical significance J nerv ment Dis 117 (1953) 156

ZUSAMMENFASSUNG

Peridurographie ist eine Methode die die Form und Grösse des Periduralraumes der Lumbosakralgegend aufzeigt. Es wurde gefunden dass die Methode der Myelographie in gewissen Fällen überlegen ist, sie ist von besonderer Bedeutung beim Diskprolaps bei periduralen Verklebungen, knöcherner Stenose des Wirbelkanales und bei perineuralen Sakralzysten.

RÉSUMÉ

Description de la péridurographie, méthode d'examen qui montre la forme et les dimensions de l'espace épidural dans la région lombo-sacrée du canal rachidien. Elle peut être supérieure à la myélographie. Elle est particulièrement utile dans les cas de prolapsus discal, d'adhérences épidurales, de sténose osseuse du canal vertébral et de kystes sacrés périméuraux.

BIBLIOGRAPHY

- ABBOT K. H., RETTER R. H. and LEIMBACH W. H. The role of perineural sacral cysts in the sciatic and sacroccocygeal syndromes. A review of the literature and report of nine cases. *J Neurosurg* 14 (1957) 5.
- ALBRECHT K. und DRESSLER W. Die Kontrastdarstellung des Periduralraums (Peridurographie). *Fortschr. Röntgenstr.* 72 (1950) 6.
- BROMAGE P. R. *Spinal epidural analgesia*. F. & S. Livingstone, London, 1954.
- BUCHHOLZ H. W. und HAUSLER G. Über die hohe Peridurographie. *Zbl. Neurochir.* 11 (1951) 328.
- CATHÉLIN I. *Les injections épidurales par ponction du canal sacré et leurs applications dans les maladies des voies urinaires*. Bailière et Fils, Paris, 1903.
- CLOWARD R. B. and BUCK P. C. Spinal extradural cyst and kyphosis dorsalis juvenilis. *Amer. J. Roentgenol.* 38 (1937) 681.
- CRAMER H. Beitrag zur Kontrastfüllung des Periduralraums mit 35^o viskosem Perabrodil durch den Sakralkanal. *Dtsch. med. Wschr.* 75 (1950) 769.
- DAVIS H. Spinal extradural cyst. Case report and tabulation of previously reported cases. *J. Neurosurg.* 6 (1949) 251.
- DECKER H. G. and LIVINGSTON K. E. Spinal extradural cyst. *J. Neurosurg.* 6 (1949) 248.
- DUTTMAN G. Die röntgenologische Darstellung des Periduralraumes und ihre diagnostische Bedeutung. *Arch. klin. Chir.* 264 (1950) 450.
- ELAUT L. und VERDONK G. Anatomische Beobachtungen zur epiduralen und transsakralen Anästhesie. *Zbl. Chir.* 61 (1934) 12.
- ESPADALER J. M., SALERS R. et SOLE J. Diverticules paravertébraux intrasacrés. *Rev. neurol.* 98 (1958) 316.
- FORESTIER J. Le trou de conjugaison vertébral et l'espace épidural. Thèse de Paris. Ed. Jouve, Paris, 1922.
- FREGNANI L., DE MARCO G. e FABBRI I. L. *La peridurografia*. Ed. Minerva med., 1962.
- LUNDAQUIST B. and OBEL N. Tonic muscle spasms and blood pressure changes following the subarachnoid injection of contrast media. *Acta radiol.* 53 (1960) 337.

LES HEMANGIOMES DU RACHIS CERVICAL

par

C J MELOT J BRIHAYE L JEANMART et C GOMPEL

La symptomatologie radiologique des hemangiomes vertebraux est bien connue et pratiquement pathognomonique striation longitudinale du corps, legere deformation eventuelle de celui ci aspect parfois ponctue des pedicules et des lames lorsqu'ils sont entrepris Il est aise de les reconnaitre Nous nous proposons d'etudier ici certaines lesions du rachis etiquetees hemangiomes dont l'aspect radiologique est different et prete a confusion Il s'agit de tumeurs developpees au niveau de la colonne cervicale constituant des cas limites d'interpretation difficile s'accompagnant de complications graves

Les hemangiomes vertebraux sont le plus souvent localises aux niveaux dorsaux et lombaires et preferentiellement a la charniere dorsolombaire Cette rarete relative de l'hemangiome cervical est illustree par les statistiques de SCHIMMORL (584 cas dont 32 localisations cervicales) de HOLTA (40 cas dont deux cervicaux) de TOPFER de STETTBACHER (104 cas dont 5 cervicaux) de SHERMAN et WIENER (14 cas dont 1 cervical)

Cette disposition s'expliquerait par la vascularisation rachidienne Celle ci est assuree par deux plexus intra et extra rachidiens qui communiquent largement par les trous de conjugaison par les espaces situes entre les lames et au travers des corps vertebraux Cette vascularisation n'est pas d'egale

- LIWISIN A. I. Kontrastdarstellung des Periduralraums mit Perabiodil zum Nachweis des hinteren Bandscheibenvorfalles (Peridurographic) *Chirurg* 22 (1951), 247
- VERBIEST H. A radicular syndrome from developmental narrowing of the lumbar vertebral canal *J. Bone Jt. Surg.* 36B (1954), 230
- Further experiences on the pathological influence of a developmental narrowness of the bony lumbar vertebral canal *J. Bone Jt. Surg.* 37B (1955), 576
- VINKE T. H. and WHITE E. H. Congenital narrowing of the lumbosacral space *Surg. Gynec. Obstet.* 76 (1943), 531



Fig 1 Cas 1 a) Hémangiome de C4—C5. Aspect de la lésion lors de son dépistage radiologique
b) Tomographie. Rétrécissement du canal médullaire en C2—C3

L'amélioration se poursuit durant 8 mois environ puis la quadriplégie réapparaît progressivement sans que l'image radiologique ne soit modifiée.

Une traction continue est réinstallée durant 10 mois, en outre, au cinquième mois de traction et sans que celle-ci ne soit interrompue, une large intervention décompressive cervicale est réalisée. Elle est associée à la mise en place d'une greffe osseuse prélevée à la crête iliaque allant de C6 à la protubérance occipitale externe et immobilisant la colonne cervicale. L'intervention chirurgicale permet de constater un épaississement des éléments vertébraux responsables d'un notable rétrécissement du canal rachidien. Dès la traction installée, les troubles neurologiques régressent progressivement, en même temps que le segment pathologique du rachis s'allonge et se redresse.

La radiothérapie est reprise dès la fin du traitement par traction, la dose totale administrée s'élevant à 2 700 R profonds.

L'amélioration des troubles neurologiques se poursuit peu à peu en même temps que la recalcification des lésions. Le greffon est parfaitement toléré. La décalcification des vertèbres sus et sous-jacentes au bloc a cependant progressé (Fig. 3).

Revue 4 ans plus tard, la patiente conserve quelques troubles neurologiques et une immobilisation gênante du cou par la greffe osseuse. Elle se déplace seule et peut vaquer à ses occupations sans trop de peine.

2. Deuxième observation. La patiente, âgée de 45 ans, est admise pour un syndrome quadriparétique évolutif (1963).

À l'âge de 22 ans, il avait été pris dans un éboulement de la mine dont il fut retiré quadriplégique. Les radiographies de la colonne cervicale ne mirent cependant aucune lésion osseuse en évidence. La récupération s'installa après deux mois et fut lente. Elle permit

importance au niveau des divers segments rachidiens. Elle augmente progressivement à partir des premières vertèbres cervicales et présente son maximum au niveau de la charnière dorso lombaire. Elle décroît brusquement au niveau des vertèbres sacrales (REBOUV).

En 1933, HENLEY et WHITAKER décrivent le premier cas intéressant une vertèbre cervicale, l'avis GISCHEGLER et KEASBEY en 1935, rapportent le premier cas d'hémangiome cervical prouvé histologiquement et ayant provoqué une compression médullaire avec paralysie. Les corps des 4e, 5e et 6e vertèbres cervicales étaient atteints par le processus. SCHLEZINGER et UNGAR, JACOBOWICZ, GHORMLEY et ADSON, HOLTA, et BROBECK décrivent chacun une observation d'hémangiome d'une ou plusieurs vertèbres cervicales. Enfin GURI, BIEMOND, COCCHI, GUNTERT, ROBINS et LOUNTAIN ont rapporté depuis 1918, les observations de cinq cas d'hémangiomes cervicaux ayant entraîné, une compression médullaire, complication dont nous n'avons retrouvé que 11 cas rapportés actuellement au niveau cervical. Un angiome des tissus mous du cou peut présenter une extension intraspinal. PIGOTT et HUTTON l'ont prouvé par artériographie.

Exposé des cas

1. Première observation. À l'âge de 39 ans, cette patiente ressent un craquement douloureux de la colonne cervicale lors d'une flexion forcée de la nuque au cours d'une séance de gymnastique. Les radiographies montrent une cyphose cervicale haute, une décalcification et une déformation de C2 et de C3 dans leur totalité. La trabéculatation est grêle et relâchée. Elle se présente sous la forme d'un réseau à larges mailles. Le disque intercalaire n'est pas visible. Les apophyses épineuses, les lames sont partiellement soudées. L'inclinaison de l'apophyse odontoïde est exagérée vers l'avant. La texture de l'atlas est conservée. C4 et C5 sont assez peu calcifiées, mais leurs limites sont nettes; les apophyses articulaires supérieures de C4 sont atteintes par le même processus que celui décrit en C2—C3. Le corps de C4 est décalé vers l'arrière par rapport à C5. Les rebords des corps de ces vertèbres portent des ostéophytes. La largeur de l'espace pré-vertébral est normale (Fig. 1).

La tomographie sagittale (Fig. 1 b) confirme la description ci-dessus. Elle définit en plus un rétrécissement notable du canal médullaire en C2—C3. Le bord postérieur des corps de C2—C3 forme une voûture importante à convexité postérieure.

Deux ans plus tard, après s'être cogné la tête contre un mur, la patiente développe une quadriplégie spastique. Des contrôles radiographiques mettent en évidence une accentuation de la lésion. Le processus s'est étendu vers le bas aux corps de C4—C5 et vers le haut à l'atlas. L'espace pré-vertébral est élargi (Fig. 2). L'examen du reste du squelette (colonne dorsale, lombaire, crâne, épaules) ne met pas de lésion en évidence.

L'étude du métabolisme phosphocalcique s'avère normale. La biopsie de la lésion est en faveur du diagnostic d'angiome osseux.

Durant un an, un traitement par traction discontinue au moyen d'une mentonnière puis par traction continue au moyen d'un étrier de CAUTIONNEAU est appliqué avec un résultat favorable. Il est complété par de la radiothérapie (dose profonde de 1 200 R) qui amène une certaine recalcification des lésions vertébrales.



Fig. 4. Cas 2. Hémangiome de C2—C3.



Fig. 5. Cas 2. Temps artériel de l'angiographie vertébrale. Il n'y a pas de foyer évident de sclérose pathologique de la lésion vertébrale qui paraît mieux visualisée que sur les clichés standards.

L'investigation biologique ne mit en évidence qu'un taux élevé des phosphatases alcalines: 118 unités Bodansky pour 100 ml lors d'un premier examen et 96 unités lors d'un contrôle une semaine plus tard. Le liquide céphalo rachidien était de composition normale. La vitesse de sédimentation était de 2 mm en une heure.

Un traitement par R_x fut instauré en même temps qu'un collier en plastique soutenait et immobilisait la colonne cervicale. 2 500 R profonds furent délivrés en deux séries de 29 et 11 séances respectivement.

Des contrôles radiographiques et neurologiques furent faits au cours des mois suivants et ne montrèrent aucune modification notable des lésions bien que le patient manifeste une amélioration clinique discrète.

Discussion

Nos deux cas posent de nombreux problèmes tant au sujet de l'interprétation radiologique que de l'interprétation histologique. Ils donnent lieu en conséquence à discussion quant à l'origine de la symptomatologie clinique et radiologique et encore au point de vue du traitement.

Considérations radiologiques. Lors d'un angiome, il existe habituellement une diminution légère de l'opacité générale du corps vertébral. L'aspect le plus



Fig 2 Cas 1 Deux ans après l'examen représenté par fig 1 l'espace pré vertébral est élargi



Fig 3 Cas 1 Radiographie 4 ans après la laminectomie décompressive et pose d'un greffon de C6 à la protubérance occipitale externe

finalement une reprise satisfaisante des activités professionnelles 3 ans après l'accident Six mois avant son hospitalisation le patient rate une marche d'escalier et tombe de sa hauteur Cette chute bénigne entraîne l'installation brutale de la quadriplégie en même temps que le patient accuse une sensation fugace de courant électrique dans le dos et le membre supérieur gauche La récupération des troubles moteurs se réinstalle une fois encore et débute par le membre supérieur droit pour gagner ensuite le membre inférieur droit Elle n'est cependant que très lentement progressive et relativement peu importante

Au moment de son hospitalisation le patient se plaint toujours d'une raideur de la nuque L'examen met en évidence une quadriparésie spastique à prédominance hémiplegique gauche Les déficits sensitifs rappellent le syndrome de Brown Séquard Il existe des troubles sphinctériens

Les radiographies de la colonne cervicale montrent que C2 est fortement déformé en particulier au niveau de son apophyse épineuse qui est fortement tuméfiée (Fig. 4) La trabéculisation se présente sous la forme d'un réseau irrégulier à mailles très lâches Ce processus s'étend à l'extrémité supérieure du corps de C3 Le disque C2—C3 n'est pas visible Les corps des lames les apophyses épineuses de C2—C3 sont soudés

Les tomographies n'apportent pas d'élément diagnostique supplémentaire

Une angiographie vertébrale droite ne met pas de foyer de vascularisation pathologique en évidence avec certitude (Fig. 5) bien qu'il existe un certain degré de dolichoartère au niveau cervical Il n'y a pas de foyer évident de vascularisation pathologique de la lésion vertébrale qui paraît cependant mieux visualisée que sur les clichés standards

Une iodo ventriculographie montre simplement un ralentissement du produit de contraste au niveau du segment cervical supérieur

Une biopsie de l'apophyse épineuse de C2 est pratiquée et à l'examen anatomo-pathologique on observe des plaques de remaniement fibreux de la trame médullaire et de nombreuses formations vasculaires limitées par un simple endothélium

secondaires et l'augmentation d'activité des ostéoclastes le phénomène initial. La relation entre angiomatose et ostéolyse massive a été soulignée par GORHAM et STOUT en 1933. Ils ont pu étudier les préparations microscopiques de 8 parmi 24 cas qui avaient été précédemment décrits comme des ostéolyses massives. Chacune des huit coupes leur a permis d'infirmer ce diagnostic primitif et de le remplacer par celui d'hémangiome osseux vertébral.

Plus récemment TICKER étudiant les lymphangiectasies a relevé les difficultés qui surviennent au moment de différencier parmi les angiomatoses les hémangiomatoses des lymphangiomatoses. Il démontre également les aspects d'ostéolyse massive qui s'y apparentent.

La possibilité de la localisation vertébrale d'une dysplasie fibreuse a été également envisagée. Cette éventualité a été signalée par LEDOUX LEBARD et SULTAN reprise ultérieurement par JENSEN. Selon LEDOUX LEBARD la dysplasie fibreuse pourrait se présenter sous l'aspect d'un type pseudo angiomatoux et d'un type pseudo pagétique. Dans la première éventualité des stries verticales caractéristiques se retrouvent ainsi que de petites images en logettes. Parfois se produit une soufflure du corps et de l'arc postérieur. L'examen radiologique systématique du squelette est indispensable à la recherche d'une autre localisation. Cette étude évite une biopsie qui peut être hémorragique. La vertèbre pseudopagétique se présente sous un aspect en cadre des zones de destruction et d'éburnation peuvent alterner. Le diagnostic est guidé par l'appréciation de l'âge et du sexe du patient et par la recherche d'une autre localisation squelettique. Néanmoins lorsque cette localisation est monostotique seule une biopsie permet de résoudre le dilemme. D'une manière générale les examens de laboratoire au cours de la dystrophie fibreuse décelent une augmentation des phosphatases alcalines, celles-ci dont le taux normal est de 4 passent à 17 à 22 unités Bodanski.

Les images que nous avons décrites dans nos deux cas incitent encore à discuter l'éventualité de tumeur primitive ou secondaire de tumeur à myéloplaxe d'enchondrome de métastase d'ostéose fibro kystique para thyroïdienne de Recklinghausen de myélome localisé de maladie de Hodgkin de réticulose bénigne ou maligne de leucémie. Bien souvent la biopsie permettra seule d'éclaircir le problème.

L'aspect de bloc présent dans nos deux cas est aussi à discuter. S'agit-il d'un bloc primitif ou secondaire? La question de l'intégrité de l'espace intervertébral au cours des hémangiomes est diversement interprétée par les auteurs. Classiquement BROBECK (1950) considère que l'espace est intact, pourtant en 1919 TROMMER décrivait un hémangiome de D5-D6 ayant infiltré et détruit le disque intervertébral. REBOUL et coll. posent la question de savoir si la disparition du disque est une conséquence de l'angiome ou le résultat de

caractéristique cependant est constituée par la présence de stries verticales longitudinales bien appréciables de profil, sur la vue de face se présente habituellement une texture aréolaire. Le cortex du corps vertébral peut être légèrement mal défini, mais il est habituellement intact, (SHERMAN, REBOUL) Dans nos cas, le réseau trabéculaire est riche, il n'y a pas de striation longitudinale ni de disposition aréolaire à petites mailles caractéristique.

Cet aspect rappelle plutôt la disposition locale décrite par certains auteurs au cours du lymphangiome. COHEN et CRAIG ont présenté un cas de lymphangiome du rachis cervical dont l'aspect est proche de celui visible chez nos malades, tant par sa situation que sa texture. Le diagnostic différentiel n'a pu être résolu qu'après biopsies multiples et même vérification nécropsique. La tumeur s'était progressivement étendue de C2 à C6. Elle se caractérisait par une apparence bulleuse du tissu spongieux. Cette lésion pourrait correspondre à une simple malformation, à un néoplasme, à une infection. Elle pourrait encore être secondaire à l'obstruction de vaisseaux lymphatiques. Une autre éventualité a été envisagée, celle d'une ostéolyse massive ou maladie de Gorham.

Les ostéolyses ont été liées à des troubles neurologiques ou neurosympathiques apparus dans le cadre d'une ostéoarthropathie réténue, syringomyélique ou lepreuse, à des syndromes neuroendocriniens complexes et à des polyarthrites ou à des rhumatismes chroniques progressifs, à des phénomènes post-traumatiques dans lesquels le phénomène vasomoteur serait le fait essentiel (LERICHE).

KUFMAN a décrit un cas d'ostéolyse cervicale au contact d'une adénopathie ayant guéri par lymphadénectomie.

Le problème très touffu de l'ostéolyse massive a été étudié particulièrement par GORHAM et STOUT, ils ont schématisé la topographie squelettique d'après une série de 18 cas. Le degré de résorption osseuse correspondant au niveau de la colonne cervicale est modéré. Cette affection se développe habituellement dans l'enfance. 13 de leurs patients avaient moins de 21 ans. L'ostéolyse progressive est toujours associée à une angiomatose de vaisseaux sanguins ou lymphatiques qui en paraissent responsables. Pour JOHNSON et McLURE, l'ostéolyse massive représente une variation d'angiomatose. Elle présente deux états pathologiques au moins. Au début de l'affection se produit une prolifération capillaire intra-osseuse comparable à celle vue distalement à une fistule congénitale artério-veineuse. Plus tard, l'angiome devient fibreux, une angiosclérose complète est cependant rare et une calcification n'a pas été observée. Pour ABELL et BADLEY, la prolifération vasculaire locale et l'hypertrophie secondaire servent à l'origine d'un déséquilibre de l'antagonisme entre ostéoblaste et ostéoclaste. Pour d'autres, les anomalies vasculaires servent

stade, certains troubles de la sensibilité peuvent être présents, qui prennent une topographie radiculaire à un stade d'évolution ultérieure la symptomatologie est celle d'une compression médullaire. Pourtant il est impossible de dresser un tableau clinique précis de l'hémangiome vertébral dont les conséquences symptomatiques multiples et variées sont fonction directe du degré d'extension de l'angiome et de l'importance des lésions osseuses. Elles ne sont en réalité pas différentes de toute affection tumorale de la colonne vertébrale.

L'évolution de la maladie est capricieuse et imprévisible. Le plus généralement elle n'entraîne aucune complication et reste bénigne. Ce n'est que très rarement que les troubles nerveux apparaissent. Il semble qu'on puisse observer des poussées évolutives suivies de périodes de repos surtout chez les patients âgés.

FOSTER et HUEBLEIN ont classifié les angiomes vertébraux en quatre groupes : (1) asymptomatiques (2) symptomatiques (douleur sans atteinte neurologique) (3) entraînant des signes de compression médullaire dus à l'extension de l'hémangiome dans l'espace épidural (4) accompagnées de fracture pathologique de la vertèbre avec ou sans signes médullaires.

Cette classification rejoint celle de REBOUL et coll. qui envisagent quatre formes : latentes, patentes, compliquées ou associées (à d'autres angiomes viscéraux, cutanés ou osseux extra-vertébraux).

La symptomatologie clinique apparaît lorsque l'hémangiome affleure la surface osseuse et atteint la moelle (HOLTA). Celle-ci peut être lésée par la propagation de l'hémangiome dans le canal spinal par pression due à la tuméfaction du corps vertébral ou des arcs par tassement de la vertèbre envahie par l'hémorragie épidurale.

Considérations thérapeutiques. Ces deux observations traitées différemment l'une de l'autre nous amènent à discuter du problème thérapeutique. Celui-ci est en fait fonction de plusieurs facteurs parmi lesquels la déformation de l'axe vertébral et la compression du cordon médullaire sont les plus importants.

L'hémangiome vertébral surtout cervical peut se développer sous forme d'une lésion ostéoclastique prédominante entraînant une ou plusieurs vertèbres. Cette altération de l'architecture osseuse entraîne alors des modifications plus ou moins graves de la statique vertébrale sous forme de courbures anormales à court rayon de tassement ou de subluxation.

Si le malade est vu avant que les altérations osseuses ne soient trop prononcées et n'entraînent de troubles neurologiques importants, il peut être traité par radiothérapie seule pour autant que la précaution élémentaire de protéger la colonne par un collier de soutien soit prise. La radiothérapie en

phenomenes arthrosiques favorises par la presence de cet angiome JAFFE decrit des modifications plus ou moins importantes de l'espace intervertebral surtout lorsque deux vertebres voisines sont angiomeuses. L'analyse de notre premier cas montre que les espaces intervertebraux ont subi un renvoiement profond aboutissant a la formation d'un bloc reunissant quatre vertebres cervicales.

Ces problemes ont particulierement ete mis au point par DESEZE d'une part, par MARCHANT et coll d'autre part. Enfin, l'etude tomographique et pneumomyelographique d'un bloc vertebraal cervical a ete effectuee par BOUTE, NIQUET et CARON. L'hypothese de la degenerescence hemangiomeuse de malformations vertebrales a ete retenue par certains auteurs. L'aspect fusionne de deux ou plusieurs vertebres resulterait du developpement d'un angiome au niveau d'un bloc vertebraal d'origine congenitale. Leurs arguments ne nous ont pas paru convaincants, nous pensions plutot que le developpement de l'angiome est primitif et que son extension entraine la formation d'un bloc osseux s'etendant a plusieurs segments. DESEZE reconnait le bloc congenital au parallelisme des plateraux de l'extremite superieure et inferieure du bloc, a la regularite parfaite et a la rectitude des limites anterieures et posterieures du bloc, a la persistance d'une image discale, a la synostose des arcs posterieurs des lames et des apophyses epineuses a la diminution de la hauteur des trous de conjugaison ainsi qu'a leur forme arrondie. MARCHANT insiste sur la presence de trous de conjugaison arrondis, leur surface laisse supposer que les racines qui y passent sont greles. Il s'agirait embryologiquement d'un defaut de segmentation.

Dans les blocs acquis, la diminution de hauteur des corps vertebraux porte surtout sur leur partie anterieure et se caracterise par une convergence en avant des plateraux, par une voussure anterieure a la jonction des deux vertebres synostoses, a une angulation a sommet dorsal de la limite posterieure du bloc vertebraal, a l'absence de toute image discale, a l'absence de soudure des arcs posterieurs, a la divergence des apophyses epineuses a la forme allongee des trous de conjugaison. Ils s'accompagnent souvent d'intercedents infectieux qui sont a rechercher.

Lorsque ces criteres sont appliques a nos cas, il parait s'agir plutot de blocs secondaires que de blocs congenitaux. La preuve en est donnee par une radiographie anterieure de notre cas 2 qui montre l'absence de bloc vertebraal anterieur, 23 ans avant le debut de l'hemangiome.

Considerations cliniques. Au point de vue de la symptomatologie clinique la premiere plainte emise par le patient consiste en une douleur locale, associee a un spasme musculaire et a une rigidite segmentaire de la colonne. Deja, a ce

RÉSUMÉ

Les hemangiomes vertébraux classiques sont aisément reconnaissables par leur aspect radiologique. Leur symptomatologie clinique est absente, fruste ou sévère. Les statistiques montrent que leurs localisations au niveau du rachis cervical sont rares. Leur aspect radiologique prête souvent à confusion. Le choix s'impose fréquemment entre hémangiome, lymphangiome, ostéolyse, blocs primitifs ou secondaires, dysplasie fibreuse, néoplasies primitives ou secondaires, etc. Ils entraînent fréquemment des complications cliniques extrêmement graves, telles des quadriplégies. La thérapeutique soulève de nombreux problèmes. Bien souvent des biopsies même répétées prêtent à discussion et ne permettent pas d'établir un diagnostic précoce. Ces considérations sont étayées par l'exposé de deux cas particulièrement complexes.

SUMMARY

The classic hemangiomas of the vertebral column are readily recognized from their radiographic appearances. Clinical symptoms are either absent, mild or severe. Statistically they seldom occur at the cervical level. They are often difficult to distinguish roentgenographically from lymphangioma, osteolysis, primary or secondary blocks, fibrous dysplasia and primary or secondary neoplasms. They often cause severe clinical complications such as quadriplegia and their treatment can be difficult. Biopsy, even if repeated several times, does not always lead to a definite diagnosis. Two difficult cases are described.

ZUSAMMENFASSUNG

Die klassischen vertebrealen Hamangiome sind radiologisch leicht erkennbar. Eine klinische Symptomatologie mag nicht vorhanden sein, aber kann auch mild oder ernstlich sein. Statistisch werden sie selten auf dem Niveau der cervikalen Wirbelsäule lokalisiert. Es ist oft schwer auf dem radiologischen Wege eine Differentialdiagnose zwischen Lymphangiomen, Osteolysen, primären oder sekundären Blocken und zwischen fibrosen Dysplasien, primären oder sekundären Neuplasmen festzustellen. Die Hamangiome sind oft mit schweren klinischen Komplikationen sowie mit Quadriplegie begleitet. Die Therapie bietet zahlreiche Probleme. Die Biopsie, auch mehrmals wiederholt, gibt keine klare Indikation und ermöglicht keine definitive Diagnose. Zwei besonders schwierige Fälle werden beschrieben.

BIBLIOGRAPHIE

- ABELL J. M. et BADCLYF C. E. A propos d'un cas d'ostéolyse essentielle. *J. Amer. med. Ass.* (1961) 177.
- BIEMOND A. Un cas d'hémangiome vertébral extramedullaire et intramedullaire. *Acta neurol. belg.* 51 (1951) 497.
- BONTE G., NIOULET C. et CARON J. Etude tomographique et pneumomyélographique d'un bloc vertébral cervical. *J. Radiol. Electrol.* 38 (1957) 806.
- BACBECK O. Haemangioma of vertebra associated with compression of the spinal cord. *Acta radiol.* 34 (1950) 235.
- BLEY I. C. and CAPP C. C. Primary hemangioma of bone. *Amer. J. Roentgenol.* 23 (1930) 1.
- COLCHI L. Zur Diagnose und Therapie der Wirbelhaemangiome. *Strahlentherapie* 92 (1953) 368.
- COHEN J. and CRAIG J. M. Multiple lymphangiectases of bone. *J. Bone Jt. Surg.* 37 A (1955) 83.

effet paraît jouer un rôle efficace en déclenchant une certaine recalcification de la lésion

En plus des altérations osseuses rappelées ci dessus, l'hémangiome vertébral peut se développer sous forme d'une lésion plus ou moins expansive, entraînant un accroissement de volume de la vertèbre et par conséquent une réduction des diamètres du canal rachidien

Il peut en résulter une compression du sillon durai qui se rencontre aussi lorsque la statique de l'axe de la colonne vertébrale sont gravement altérés

Il nous paraît évident que la radiothérapie devient inopérante lorsque les troubles neurologiques sont provoqués par l'une ou l'autre de ces deux causes et qu'elle doit être précédée soit par une décompression chirurgicale du canal rachidien, associée ou non à une fixation de la colonne, soit par une traction continue

Il ne faut cependant pas se crâcher que le blocage par greffe du segment cervical entraîne une impotence fonctionnelle fort gênante. Par ailleurs l'abord de ces vertèbres fragiles n'est pas sans risque d'aggravation du tableau neurologique et doit se faire avec infiniment de précautions et de douceur. Pour notre second malade par exemple, bien qu'il existe une quadriparésie, nous n'avons recouru qu'à la seule radiothérapie, parce que l'analyse cytochimique du liquide céphalo rachidien était normale et que d'autre part la myélographie avait montré un simple retard du transit du produit opaque. En outre, une lente amélioration clinique était en cours.

Il nous paraît donc qu'aucune attitude thérapeutique ne peut être fixée d'avance. Celle-ci sera fonction de l'image radiologique, des troubles subjectifs (forme douloureuse) et de l'examen neurologique.

Conclusion

L'hémangiome vertébral correspond à une lésion lentement évolutive qui peut s'étendre progressivement à plusieurs vertèbres. Il se complique souvent, au niveau cervical, d'une inflexion anormale de la colonne. En outre, des traumatismes bénins peuvent occasionner des subluxations et des contusions médullaires. Enfin, la distension de la vertèbre par le processus néoplasique peut aggraver la compression de la moelle.

Le traitement à base de radiothérapie seule ou combinée soit à une traction continue, soit à une décompression du canal rachidien avec, ou sans fixation du segment vertébral, dépendra du tableau radiologique ou neurologique.

RESUME

Les hémangiomes vertébraux classiques sont aisément reconnaissables par leur aspect radiologique. Leur symptomatologie clinique est absente, fruste ou sévère. Les statistiques montrent que leurs localisations au niveau du rachis cervical sont rares. Leur aspect radiologique prête souvent à confusion. Le choix s'impose fréquemment entre hémangiome, lymphangiome, ostéolyse, blocs primitifs ou secondaires, dysplasie fibreuse, néoplasies primitives ou secondaires, etc. Ils entraînent fréquemment des complications cliniques extrêmement graves, telles des quadriplégies. La thérapeutique soulève de nombreux problèmes. Bien souvent, des biopsies même répétées prêtent à discussion et ne permettent pas d'établir un diagnostic précoce. Ces considérations sont étayées par l'exposé de deux cas particulièrement complexes.

SUMMARY

The classical hemangiomas of the vertebral column are readily recognized from their radiographic appearances. Clinical symptoms are either absent, mild or severe. Statistically, they seldom occur at the cervical level. They are often difficult to distinguish roentgenographically from lymphangioma, osteolysis, primary or secondary blocks, fibrous dysplasia and primary or secondary neoplasms. They often cause severe clinical complications such as quadriplegia and their treatment can be difficult. Biopsy, even if repeated several times, does not always lead to a definite diagnosis. Two difficult cases are described.

ZUSAMMENFASSUNG

Die klassischen vertebralen Hamangiome sind radiologisch leicht erkennbar. Eine klinische Symptomatologie mag nicht vorhanden sein, aber kann auch mild oder ernstlich sein. Statistisch werden sie selten auf dem Niveau der cervikalen Wirbelsäule lokalisiert. Es ist oft schwer auf dem radiologischen Wege eine Differentialdiagnose zwischen Lymphangiomen, Osteolysen, primären oder sekundären Blocken und zwischen fibrösen Dysplasien, primären oder sekundären Neuplasmen festzustellen. Die Hamangiome sind oft mit schweren klinischen Komplikationen sowie mit Quadriplegie begleitet. Die Therapie bietet zahlreiche Probleme. Die Biopsie auch mehrmals wiederholt, gibt keine klare Indikation und ermöglicht keine definitive Diagnose. Zwei besonders schwierige Fälle werden beschrieben.

BIBLIOGRAPHIE

- ABELL J. M. et BADGLEY C. E. A propos d'un cas d'ostéolyse essentielle. *J. Amer. med. Ass.* (1961) 177.
- BIEMOND A. Un cas d'hémangiome vertébral extramedullaire et intramedullaire. *Acta neurol. belg.* 51 (1951) 497.
- BONTE G., VIOLET C. et CARON J. Etude tomographique et pneumomyélographique d'un bloc vertébral cervical. *J. Radiol. Electrol.* 38 (1957) 806.
- BROBECK O. Haemangioma of vertebra associated with compression of the spinal cord. *Acta radiol.* 34 (1950) 235.
- BLICK P. C. and CAPP C. C. Primary hemangioma of bone. *Amer. J. Roentgenol.* 23 (1930) 1.
- COCCHI L. Zur Diagnose und Therapie der Wirbelhaemangiome. *Strahlentherapie* 92 (1953) 368.
- COHEN J. and CRAIG J. M. Multiple lymphangiectases of bone. *J. Bone Jt. Surg.* 37 A (1955) 585.

- DE SEZE S et RYCKEWAERTS A Maladie des os et des articulations I Lammarton, Paris 1959
- FOSTER D B and HUEBLEIN G W Hemangioma of vertebrae associated with compression of the cord Arch Neurol Psychiat 47 (1942) 19
- GESCHICKTER R K and HENKLEY L I Tumors of blood vessels Amer J Cancer 23 (1935) 368
- GORHAM L W and STOUT A P Massive osteolysis J Bone Jt Surg 37 (1955) 984
- GORRILEY R K and ANDSON A W Hemangioma of vertebrae J Bone Jt Surg 23 (1941) 887
- CUNERT W Beitrag zur kasuistic und Rontgenologie der Wirbelsaenlenhemangiome Radiol clin 24 (1955) 167
- GURI J P Tumors of vertebral column Surg Gynec Obstet 87 (1948) 583
- HANEY I S and WHITAKER P H Hemangioma of spine Brit Med J 2 (1953) 775
- HOLTA O Hemangioma of the cervical vertebra with fracture and compression myelomalacia Acta radiol 23 (1942), 423
- JACOBOWITZ S Beitrag zur Klinik und Therapie des Wirbelsaenlenhemangiomes Helv med Acta 16 (1949) 574
- JAFFE H J Tumors and tumorous conditions of the bones and joints Lea et Febiger Philadelphia 1959
- JENSENS P Localisation vertébrale de la maladie de Jaffé Lichtenstein et angiomes vertébraux J Radiol Electrol 35 (1954) 644
- JOHNSON P M and MCLUR J G Observations on massive osteolysis Radiology 71 (1958) 28 43
- KAUFMAN R Ostéolyse et tuberculose Presse med 67 (1959) 1
- LEDOUX LEBARD G et SULTAIN C Les localisations vertébrales de la dysplasie fibreuse des os ou maladie de Jaffé Lichtenstein J Radiol Electrol 34 (1953) 349
- LERICHE R A propos des ostéolyses d'origine indéterminé Mém Acad Chir 63 (1937) 418
- MARCHAND J H CLEMENT G BARAG N et SANTACOSTINI N Etude radiologique des blocs cervicaux J Radiol Electrol 38 (1957) 550
- PIGOTT I and HUTTON C F Angioma of the neck with intraspinal extension Brit J Radiol 37 (1964) 72
- REBOUL J, POUYANNE L, DELORME C et LEDIASCOUX H Etude radioclinique et thérapeutique de l'angiome vertébral Ann Radiol 1 (1958) 857
- ROBBINS L R and FOUNTAIN E N Hemangioma of cervical vertebrae with spinal cord compressions New Engl J Med 1 (1958) 258 685
- SCHLEZINGER N S and UNCER H Hemangioma of vertebra with compression myelopathy Amer J Roentgenol 42 (1939) 192
- SCHMORL G Die pathologische Anatomie der Wirbelsaenbe Verh dtisch orthop Ges Kongress 21 (1927) 3
- SCHERMAN R S and WIENER D The roentgen diagnosis of hemangioma of bone Amer J Roentgenol 86 (1961) 1146
- SHOFFNER C E and ALLEN R P Lymphangioma of bone Radiology 76 (1961) 449
- STETTINBACHER A Beitrag zur Klinik und Therapie des Wirbelsaenlenhemangioms Helv med Acta 16 (1949) 574
- TOPFER D I Ueber ein infiltrierend wachsendes Hemangiom der Haut Frankfurt Z Path 36 (1928) 337
- FROMMER B Zur Lehre der Hamangiome der Wirbelsaule Frankfurt Z Path 22 (1919) 313
- TUCKER A S Lymphangiectasis benign and malignant Amer J Roentgenol 91 (1964)

LA MYELOBULBOGRAPHIE GAZEUSE DANS LES MYELOPATHIES CRONIQUES

par

J METZGER PH ENGEL D DILENCE et J ABOLKER

On connaît mal la cause de certaines myélites ou de myélopathies provoquant des paraplegies ou des quadriplegies chroniques. Nous pensons qu'il s'agit de maladies mécaniques d'origine rachidienne liées à une sténose du défile crano cervical ou du canal cervical.

Pendant plusieurs années l'un de nous (J. A.) a opéré un certain nombre de ces malades sur des données cliniques sans examen de contraste. Depuis deux ans nous avons adapté la méthode de LINDGREN de myelographie gazeuse totale pour visualiser le bulbe, mesurer les dimensions du canal, mettre en évidence les sténoses et enfin montrer par une étude dynamique la réalité des traumatismes que subit le neuraxe lors des mouvements de la tête.

Chaque intervention est donc maintenant précédée et suivie d'une myélobulbographie gazeuse.

La technique

Nous pratiquons essentiellement des tomographies sagittales en balayage hypocycloïde, le seul permettant d'obtenir de bonnes images de la région cervico-dorsale. Avec l'appareillage utilisé qui comporte une table mobile pour la recherche du plan de coupe, le coefficient d'agrandissement est toujours le même, égal à 1,35 et tous les clichés sont de ce fait comparables.

En général deux aiguilles sont utilisées l'une sous occipitale pour retirer le liquide céphalo rachidien l'autre lombaire pour injecter l'air. Une fois la soustraction du liquide terminée l'aiguille sous occipitale est retirée et de l'air est injecté par voie lombaire sous une pression correspondant à environ 40 cm d'eau au manomètre de Claude ce qui permet une véritable myélobulbographie gazeuse (Fig. 1).

Nous voyons en effet non seulement la moelle mais aussi le tronc cérébral ou sa partie inférieure le 4ème ventricule la cisterna pré pontique, la grande citerne et le vermis.

Grâce à l'aiguille lombaire conservée en place l'hyperpression est supprimée dès que la prise des clichés est faite.

Quand une malformation entraîne une sténose de trou occipital rendant la ponction sous occipitale dangereuse il est utile de faire précéder cette dernière d'une étude de la grande citerne. Dans ces cas on pratique la myélographie gazeuse totale uniquement par voie lombaire. Cette méthode dite de reflux consiste à injecter 7 à 8 ml d'air toutes les cinq minutes en contrôlant au manomètre de Claude la pression qui s'élève après l'insufflation à 55 cm d'eau pour retomber à chaque fois à 35 cm environ en 5 minutes.

La myélographie gazeuse montre sur les tomoscographies sagittales médiane et para-médianes la tête étant dans ce premier temps en position indifférente le cordon bulbo-médullaire limité par des colonnes d'air antérieure et postérieure correspondant à l'espace sous-arachnoïdien et qui dans certaines conditions s'amincissent et disparaissent. Or normalement cet espace sous-arachnoïdien forme un coussin hydraulique qui protège la moelle de tout contact direct traumatisant avec les parois ostéo-ligamentaires du canal rachidien.

Dans plusieurs de nos cas nous avons pratiqué des mensurations mais l'aspect des colonnes d'air antérieure et postérieure est souvent plus significatif que les dimensions du canal et du cordon médullaire.

Signalons qu'une myélographie gazeuse pratiquée chez des malades ayant déjà eu un examen par huile iodée est de lecture difficile du fait d'images d'adhérences et de superpositions gênantes.

Étude dynamique. Elle donne des renseignements complémentaires intéressants dans les cas de sténose. Les tomoscographies sont pratiquées après avoir placé la tête du patient en flexion puis en déflexion pour mettre en évidence le comportement du cordon médullaire au cours de ces différents mouvements. Dans les sténoses cervicales les mouvements produisent des micro-agressions sur le nerf et sur les racines et ces traumatismes chroniques peuvent jouer un rôle déterminant dans la pathogénie d'une partie des maladies chroniques de la moelle cervicale et du bulbe.

Cette étude dynamique prolonge quelque peu la durée de l'examen et c'est la raison qui fait préférer l'injection d'air à celle d'oxygène dont la résorption est un peu trop rapide.

Resultats

Dans 48 cas, la myélobulbographie a mis en évidence 21 cas de sténose pure et 27 cas de sténose constitutionnelle du canal cervical, compliquée d'arthrose.

Sténoses cervicales pures, constitutionnelles, sans arthrose

Nous avons réuni sous ce titre tous nos cas de rétrécissement du calibre du canal rachidien n'ayant pas présenté d'arthrose ou de malformation osseuse associées. Elles peuvent se classer de la façon suivante.



Fig 1 Myelobulbographie gazeuse en flexion. Espace sous-arachnoïdien bien visible autour du bulbe et de la moelle. Quelle que soit l'étendue des mouvements, la moelle est protégée de tout contact avec le canal par un large espace sous-arachnoïdien.



Fig 2 Myelobulbographie en flexion. Sténose du canal cervical étroit sur toute sa hauteur. Espace sous-arachnoïdien mince en avant, presque disparu derrière la moelle de C2 à C7. Femme de 50 ans. Paraplégie spino-médullaire chronique progressive.

Sténoses du défile occipito-cervical et du canal cervical (10 cas) Certaines formes comportent une sténose dysmorphique globale du canal cervical et du défile crano-cervical. Le rétrécissement s'étend du trou occipital jusqu'à la charnière cervico-dorsale. Le canal rachidien s'élargit alors dans la région dorsale supérieure.

La myelobulbographie gazeuse montre dans 70 % des cas une moelle plaquée en avant contre le plan vertébro-discal tandis qu'une mince colonne d'air est encore visible en arrière. Dans les autres cas c'est l'inverse : la moelle

En général deux aiguilles sont utilisées : l'une sous occipitale pour retirer le liquide céphalo-rachidien, l'autre lombaire pour injecter l'air. Une fois la soustraction du liquide terminée, l'aiguille sous occipitale est retirée et de l'air est injecté par voie lombaire sous une pression correspondant à environ 10 cm d'eau au manomètre de Claude : ce qui permet une véritable myélobulbographie gazeuse (Fig. 1).

Nous voyons en effet non seulement la moelle mais aussi le tronc cérébral ou sa partie inférieure : le 4^{ème} ventricule, la citerne pré pontique, la grande citerne et le vermis.

Grâce à l'aiguille lombaire conservée en place, l'hyperpression est supprimée dès que la prise des clichés est faite.

Quand une malformation entraîne une sténose de trou occipital rendant la ponction sous occipitale dangereuse, il est utile de faire précéder cette dernière d'une étude de la grande citerne. Dans ces cas on pratique la myélographie gazeuse totale uniquement par voie lombaire. Cette méthode dite de 'reflux' consiste à injecter 7 à 8 ml d'air toutes les cinq minutes en contrôlant au manomètre de Claude la pression qui s'élève après l'insufflation, à 55 cm d'eau pour retomber à chaque fois à 35 cm environ en 5 minutes.

La myélographie gazeuse montre sur les tomographies sagittales médiane et para-médianes la tête étant dans ce premier temps en position indifférente : le cordon bulbo-médullaire limite par des colonnes d'air antérieure et postérieure correspondant à l'espace sous-arachnoïdien et qui dans certaines conditions s'amincissent et disparaissent. Or normalement cet espace sous-arachnoïdien forme un coussin hydraulique qui protège la moelle de tout contact direct traumatisant avec les parois ostéo-ligamentaires du canal rachidien.

Dans plusieurs de nos cas nous avons pratiqué des mensurations mais l'aspect des colonnes d'air antérieure et postérieure est souvent plus significatif que les dimensions du canal et du cordon médullaire.

Signalons qu'une myélographie gazeuse pratiquée chez des malades ayant déjà eu un examen par huile iodée est de lecture difficile du fait d'images d'adhérences et de superpositions gênantes.

Étude dynamique Elle donne des renseignements complémentaires intéressants dans les cas de sténose. Les tomographies sont pratiquées après avoir placé la tête du patient en flexion puis en déflexion pour mettre en évidence le comportement du cordon médullaire au cours de ces différents mouvements. Dans les sténoses cervicales les mouvements produisent des micro-agressions sur le nerf et sur les racines et ces traumatismes chroniques peuvent jouer un rôle déterminant dans la pathogénie d'une partie des maladies chroniques de la moelle cervicale et du bulbe.

Cette étude dynamique prolonge quelque peu la durée de l'examen et c'est la raison qui fait préférer l'injection d'air à celle d'oxygène dont la résorption est un peu trop rapide.

Resultats

Dans 48 cas, la myélobulbographie a mis en évidence 21 cas de sténose pure et 27 cas de sténose constitutionnelle du canal cervical, compliquée d'arthrose.

Sténoses cervicales pures, constitutionnelles, sans arthrose

Nous avons réuni sous ce titre tous nos cas de rétrécissement du calibre du canal rachidien n'ayant pas présenté d'arthrose ou de malformation osseuse associées. Elles peuvent se classer de la façon suivante :



Fig 5 Myelobulbographie Homme de 60 ans Paraplegie progressive et syndrome cérébelleux à gauche Canal cervical et outre à partir de C2 Mince colonne d'ar antérieure et postérieure. Après Contrôle postopératoire C1 à D2 Résection sous occipitale et laminectomie de C1 à D2 Reconstitution d'un espace sous-arachnoïdien de dimensions normales



Fig 6 Myelobulbographie Sténose du défilé cranio cervical Disparition quasi totale de l'espace sous arachnoïdien et de la grande cisterna Un épéron ligamentaire et dur mé en supprime l'entonnoir cranio-cervical habituel Femme de 46 ans Paraplegie progressive et troubles de la voix

L'étude dynamique dans ces cas montre le rôle défavorable de la flexion qui réduit le diamètre antéro-postérieur du canal et l'amincissement encore plus considérable ou la disparition de l'espace sous arachnoïdien (Figs 2 et 3)

Ces myélobulbographies permettent en outre de comprendre l'utilité des laminectomies étendues qui peuvent aller de C1 à D2 avec ouverture en arrière du trou occipital

La myélographie gazeuse de contrôle (Fig 4) est effectuée trois semaines après l'intervention et montre la reconstitution de l'espace sous arachnoïdien identique à celui des myélographies gazeuses normales Cette libération de la moelle bien visible rend évident le mécanisme par lequel s'obtiennent les bons résultats qui suivent les opérations

Sténoses du canal cervical avec aspect normal de la région du trou occipital (6 cas)
Chez ces malades le rétrécissement du canal rachidien se manifeste en dessous



Fig. 3. Même examen que fig. 2. Déflexion. L'espace sous arachnoïdien antérieur disparaît. La moelle se plaque contre le plat du disco vertébral. Le bulbe est coincé entre l'épui et le ligament occipito odontoidien en avant et l'arc postérieur de l'atlas qui a fortement avancé dans le mouvement de déflexion.



Fig. 4. Même malade. Myélobulbographie six semaines après l'opération. L'espace sous arachnoïdien est reconstitué. Amélioration rapide de la marche. Reprise du travail au même mois.

apparut pliquée contre les arcs. On observe également, quand le calibre du canal en C^5-C^6 s'abaisse à 9—10 mm (pour une moyenne normale de 13 à 15 mm), une absence totale des colonnes d'air antérieure et postérieure. Dans deux cas où il existe une courbure anormale du rachis, la moelle prend la corde, plaquée contre l'une des parois du canal tandis que du côté opposé subsiste une colonne d'air très large, nous sommes ainsi amenés à constater que les mensurations, souvent intéressantes, ont d'autres fois une valeur assez relative.

La myélographie gazeuse met toujours en évidence une moelle à l'étroit sur toute la hauteur du canal. Le bulbe est également gêné dans un défilé crânio cervical rétréci entre une odontoïde souvent doublée d'un ligament croisé très épais et un arc postérieur d'atlas trop court.



Fig 10 Meme examen que fig 9 Flexion La moelle se tend pendant la corde à sautoir supérieure Un filet d'air est visible entre le cordon médullaire et le bourrelet arthrosique C5—C6



Fig 11 Myelobulbographie post opératoire Laminectomie C1—D7 Reconstitution de larges espaces sous arachnoïdiens antérieur et postérieur Meme malade que dans figs 9 et 10 Amélioration de la marche dans les premiers mois

2 Un rétrécissement du défilé crano cervical par gros ligament croisé occipito odontoidien (1 cas) Le ligament croisé épaissi fait saillie devant le bulbe et la moelle réduisant l'espace sous arachnoïdien (Fig 7) Le trou occipital est en outre congénitalement étroit

3 Un rétrécissement de défilé crano cervical par gros ligament postérieur (2 cas) Le gros ligament occipito alioïdien postérieur forme un éperon dur menant invisible sur les clichés simples mais évident par myélographie gazeuse surtout en déflexion Il détermine une saillie supprimant en partie la grande citerne (Fig 8)

Stenoses cervicales constitutionnelles compliquées d'arthrose

Les becs ostéophytiques de l'arthrose cervicale occasionnent parfois par leur importance un rétrécissement susceptible de provoquer des compressions et des traumatismes répétés de la moelle au cours des mouvements Cependant le plus souvent les mensurations nous ont montré que ce qu'on appelle les



Fig 7



Fig 8



Fig 9

Fig 7 Myelobulbographie. Sténose du défilé cranio cervical par gros ligament croisé. ce dernier épaissi fait saillie devant le bulbe et la moelle réduisant l'espace sous arachnoïdien. Femme de 40 ans. Syndrome cérébello pyramidal.

Fig 8 Myelobulbographie. Sténose du défilé cranio cervical par gros ligament postérieur occipito atloldien. L'éperon dure mérien (invisible sur le cliché sans contraste) supprime l'entonnoir. Femme de 36 ans. Quadriparesie évoluant depuis 4 ans.

Fig 9 Myelobulbographie. Déflexion. Sténose du canal cervical et petite arthrose C₅-C₆. Disparition de l'espace sous arachnoïdien postérieur. Ligament jaune refoulant la moelle contre le bourrelet arthrosique en C₅-C₆. Homme de 39 ans. Paraplegie progressive.

de C2 (Fig 5), tandis que la partie supérieure conserve l'aspect habituel en entonnoir, ouvert vers le haut, prolongé par la grande citerne.

Sténoses du défilé cranio cervical (5 cas) Cette sténose est caractérisée par

1. Un rétrécissement d'origine essentiellement osseuse (2 cas). L'etrottesse du trou occipital et le raccourcissement de l'arc de l'atlas peuvent être isolés ou complétés par une hypertrophie ligamentaire. Ceci entraîne une disparition quasi totale de l'espace sous arachnoïdien et de la grande citerne, un éperon ligamentaire et dure mérien supprime l'entonnoir cranio cervical. Il en résulte une souffrance du bulbe (Fig 6). Il s'agit d'une malformation que la radiographie standard permet de soupçonner, normalement le diamètre osseux antéro postérieur du trou occipital mesure environ 35 mm, dans nos cas, nous avons trouvé des dimensions de l'ordre de 25 à 27 mm (dimensions réelles après rectification de l'agrandissement de 1,35 du système de tomographie).

graphie gazeuse montre la disparition totale des espaces sous arachnoidiens a différents niveaux (Fig 12)

Il existe enfin des myélopathies a l'absence de toute sténose quand l'arthrose est tres importante. Chez ces malades les dimensions des becs osteophytiques revetus d'un ligament épaissi expliquent a elles seules la souffrance de la moelle (avec un canal cervical normalement large)

La mobilité de la tete est invoquée depuis longtemps comme l'un des mecanismes de la souffrance medullaire dans les myelopathies arthrosiques nous avons pu mettre ce mécanisme en évidence de façon systématique et il constitue a notre avis également la cause principale des myelopathies dans les stenoses pures

Conclusion

Les myelites ou myélopathies chroniques forment un chapitre mal défini de la neurologie. Faute de mieux on invoque souvent une sclérose en plaques et le malade reste condamné a une paraplégie progressive qui se complete souvent d'une impotence des membres supérieurs

La myélobulbographie gazeuse et les résultats des interventions montrent qu'un certain nombre de ces paraplégies progressives sont des maladies mecaniques susceptibles de bénéficier d'un traitement chirurgical

Les sténoses constitutionnelles sans arthrose (21 cas) portent sur le défilé occipito cervical et le canal cervical (10 cas), le canal cervical seul (6 cas) et le défilé crano cervical seul (5 cas). Ces sténoses sont dues non seulement a la dimension du canal osseux visible sur la radiographie standard mais aussi a l'hypertrophie des ligaments mis en évidence grace a la myélobulbographie

Les stenoses cervicales compliquées d'arthrose (27 cas) ont comme cause déclenchante des signes cliniques l'hypertrophie des rebords des corps vertébraux revetus de ligaments épaissis

Dans toutes ces éventualités les examens en flexion et déflexion mettent en évidence les facteurs et les mouvements traumatisants de la moelle

Lors des controles post opératoires la myélobulbographie gazeuse a permis de constater l'importance de ces facteurs a l'origine de la myelopathie chronique. La reconstitution d'un espace sous arachnoidien coincide avec la régression du syndrome clinique

RÉSUMÉ

La myélobulbographie en balayage tomographique hypocycloïde avec agrandissement constant permet de voir et de mesurer les dimensions du canal rachidien, des espaces sous-arachnoidiens et du cordon médullaire. Elle montre parfaitement les protrusions et les épaiss-



Fig 12 Myelobulbographie. Homme de 41 ans. Paraparesie à prédominance gauche depuis un an après voyage pénible en voiture. Astéréognosie transitoire de la main gauche. *1 gauche*. Canal cervical très étroit, compliqué d'arthrose. Becs ostéophytiques postérieurs en C4—C5 C5—C6 et C6—C7. Réduction très importante du calibre du canal rachidien cervical. *1 droit*. Contrôle postopératoire. Reconstitution des espaces arachnoidiens antérieur et postérieur. La moelle est maintenant à une large distance des becs ostéophytiques postérieurs. Amélioration postopératoire.

myélopathies arthrosiques sont en réalité des stenoses constitutionnelles du canal décompensées par l'arthrose.

À la période de début, l'examen radiologique standard ne met en évidence que des becs ostéophytiques discrets. La myélographie gazeuse montre un épaississement du ligament commun vertébral postérieur au même niveau, avec disparition de la colonne d'air intérieure.

L'étude dynamique fait apparaître en déflexion une empreinte de la sangle ligamentaire sur la face antérieure du cordon médullaire (Fig 9). La colonne d'air réapparaît en flexion (Fig 10).

Les myélographies post-opératoires montrent la formation de vastes espaces sous arachnoidiens antérieur et postérieur qui mettent le bulbe et la moelle à distance du plan vertébral et à l'abri des mouvements traumatisants (Fig 11).

D'autres fois, le rétrécissement du canal aggravé par d'importants becs ostéophytiques est déjà évident sur les radiographies standards, la myélo-

graphie gazeuse montre la disparition totale des espaces sous arachnoidiens à différents niveaux (Fig 12)

Il existe enfin des myélopathies et l'absence de toute sténose quand l'arthrose est très importante. Chez ces malades, les dimensions des becs ostéophytiques revêtus d'un ligament épaissi expliquent à elles seules la souffrance de la moelle (avec un canal cervical normalement large)

La mobilité de la tête est invoquée depuis longtemps comme l'un des mécanismes de la souffrance médullaire dans les myélopathies arthrosiques nous avons pu mettre ce mécanisme en évidence de façon systématique et il constitue à notre avis également la cause principale des myélopathies dans les sténoses pures

Conclusion

Les myélites ou myélopathies chroniques forment un chapitre mal défini de la neurologie. Faute de mieux on invoque souvent une sclérose en plaques et le malade reste condamné à une paraplegie progressive qui se complète souvent d'une impotence des membres supérieurs

La myélobulbographie gazeuse et les résultats des interventions montrent qu'un certain nombre de ces paraplegies progressives sont des maladies mécaniques susceptibles de bénéficier d'un traitement chirurgical

Les sténoses constitutionnelles sans arthrose (21 cas) portent sur le défilé occipito cervical et le canal cervical (10 cas) le canal cervical seul (6 cas) et le défilé crano cervical seul (5 cas). Ces sténoses sont dues non seulement à la dimension du canal osseux visible sur la radiographie standard mais aussi à l'hypertrophie des ligaments mis en évidence grâce à la myélobulbographie

Les sténoses cervicales compliquées d'arthrose (27 cas) ont comme cause déclenchante des signes cliniques l'hypertrophie des rebords des corps vertébraux revêtus de ligaments épaissis

Dans toutes ces éventualités les examens en flexion et déflexion mettent en évidence les facteurs et les mouvements traumatisants de la moelle

Lors des contrôles post opératoires la myélobulbographie gazeuse a permis de constater l'importance de ces facteurs à l'origine de la myélopathie chronique la reconstitution d'un espace sous arachnoïdien coïncide avec la régression du syndrome clinique

RÉSUMÉ

La myélobulbographie en balayage tomographique hypocycloïde avec agrandissement constant permet de voir et de mesurer les dimensions du canal rachidien des espaces sous arachnoïdiens et du cordon médullaire. Elle montre parfaitement les protrusions et les épais

sissements ligamenteux arthrosiques. Mise au point pour l'étude des myélopathies méxpliques elle met en évidence les sténoses du canal cervical, montre les traumatismes provoqués sur la moelle par la flexion et la déflexion. Les myélobulbographies post-opératoires montrent la disparition de la sténose et des traumatismes qu'elle provoque.

SUMMARY

Tomographic myelography in hypocycloid scanning, with a constant enlargement, enables us to demonstrate and measure the size of the vertebral canal, the subarachnoid space and the spinal cord. It clearly shows disc protrusions and the thickening of ligaments in arthrosis. It has been perfected in order to allow the study of unexplained myelopathies and demonstrates stenosis of the cervical canal and spinal cord damage brought about by flexion and deflexion. Postoperative myelobulbographies show disappearance of the stenosis and of the damage caused by it.

ZUSAMMENFASSUNG

Die Casmyelobulbographie mit hypocycloider Tomographie und steter Vergrößerung erlaubt den Spinalkanal, die Subarachnoidalräume, das Rückenmark zu sehen und zu messen. Sie zeigt genau die Diskusvorwölbungen und die arthrosischen Ligamentenverdickungen. Die Untersuchung der unerklärlichen Myelopathien ergibt, dass man die Stenose des Cervikalkanals und die daher auf der Medulla bei Flexion und Deflexion verursachten Traumatismen nachweisen kann. Die postoperative Myelobulbographien zeigen Verschwinden der Stenose und der Traumatismen, die sie reizt.

BIBLIOGRAPHIE

- ABOULKER J., DAVID M., METZGER J., ISCHIGOLD H., LIEVRE J. A., CILLA P., FANEL P., MESSIMY R. et IRADAT P. Myélopathies chroniques par sténoses du trou occipital et du canal cervical. A paraître en *Revue Neurologique*.
- METZGER J., DAVID M., ENGEL P., BODSON G., JOURNIER J. J., LICHTENBERG R. et THIBAUT A. Etude tomographique et myélographique des phénomènes de chaudière au niveau du bulbe et de la moelle cervicale. *La Radiographie des Formations Intracrâniennes*. Journée du 23 Septembre 1963, Strasbourg, Masson Ed. 1963, p. 89.
- BREIG A. *Biomechanics of the central nervous system*. Almqvist and Wiksell, Stockholm, 1960.
- CLARKE E. and LITTLE J. H. Cervical myelopathy. *Neurology* 5 (1955) 861.
- DI CHIRO G. Contrast Radiography of the spinal cord. *Arch. Neurol.* 11 (1964) 125.
- ISCHIGOLD H., LICHTENBERG R., DOYON D. et METZGER J. Etude radiographique des lésions de la chaudière occipitocervicale. *Röntgen Europ.* 6 (1963) 204.
- JRENKEL V. K. Myelorradiometry in diseases of spinal cord. *Med. Radiol. (Moskva)* 7 (1962) 11.
- GIRARD P. T., GARDE A. et DEVIC M. Contribution à l'étude anatomique des manifestations médullaires observées au cours des discarthroses. *Rev. Neurol.* 90 (1954) 48.
- JIROUT J. Pneumographic investigation of cervical spine. *Acta radiol.* 50 (1958) 221.

- JIROULT J The mobility of the cervical spinal cord under normal conditions Brit J Radiol 32 (1959) 744
- KAHN E A The role of the dental ligaments in spinal cord compression and the syndrome of lateral sclerosis J Neurosurg 4 (1947) 191
- KHILNANI M T and WOLF B S Transverse diameter of cervical spinal cord on pantopaque myelography J Neurosurg 20 (1963) 660
- LINDGREN E Radiologic examination of brain and spinal cord Acta radiol Suppl 151 (1957) p 139
- METZGER J et DILLENCE D Etude tomographique de la region occipito-cervicale 5 Cours International de Tomographie Minerva med 1964 p 210
- NORDQVIST I The sagittal diameter of the spinal cord and subarachnoid space in different age groups A roentgenographic postmortem study Acta radiol Suppl 227 (1964)
- PORTER E C Measurement of cervical spinal cord in pantopaque myelography Amer J Roentgenol 76 (1956) 270
- RIDD J D Effects of flexion extension movements of the head and spine upon the spinal cord and the nerve roots J Neurol Neurosurg Psychiat 3 (1960) 214
- ROTH G Myelographie gazeuse par refoulement Une nouvelle methode J Radiol Electrol 43 (1962) 831

BIOMECHANICAL ASPECTS OF SPONDYLOTIC MYELOPATHY

by

L. PENNING and P. VAN DER ZWAAG

According to BRAIN (1956), cervical spondylotic myelopathy is the most common disease of the spinal cord during and after middle age. A difficult feature of this myelopathy is its diagnosis. Roentgenographic demonstration of cervical spondylosis is no argument in favor of the diagnosis as it is common during and after middle age. In syringomyelia spondylosis may even be more severe.

In establishing diagnostic criteria and a concise concept of the genesis of spondylotic myelopathy is wanted, one has to prove that the spondylosis really is the cause of the myelopathy. We agree with many authors that the only reliable diagnostic criterion is the demonstration of cord compression by means of cerebrospinal fluid manometry and myelography. In typical cases both will show a block of the cerebrospinal fluid pathways if head and neck are in the extended position, in the flexed position free flow of the cerebrospinal fluid and contrast medium is reestablished. Mere demonstration of a protruding disc by myelography is not specific for the disease (McRAE 1956).

A brief summary of the hypotheses underlying the diagnostic phenomena may be given. Although KAPLAN & KENNEDY in 1949 found that the manometric block in extension of the cervical spine was more or less typical of

spondylotic myelopathy and is seen already in an early stage of the disease a satisfying explanation could not be given. TAYLOR & BLACKWOOD (1948) showed bulging of the ligamenta flava into the spinal canal if the neck was extended.

In 1953 TAYLOR suggested that the bulging ligamenta flava would contribute to the production of cervical myelopathy by compressing the cord in the extended position of the neck, thus at the same time offering an explanation for the finding of KAPLAN & KENNEDY. ALEXANDER *et coll.* (1958) myelographically measured a reduction of 50 % of the sagittal diameter of the spinal canal on extension of the neck. NUGENT (1959) reported similar findings. STOLTMAN & BLACKWOOD (1964) observed in specimens of the extended cervical column that at the level of C 2, 3 and 4 the spinal cord occupied all space available in the spinal canal.

ARNOLD (1955) and MAYFIELD (1955) made a valuable contribution by suggesting that subjects with a constitutionally small cervical spinal canal would be predisposed to spondylotic myelopathy. Measurements by BOYSEN (1954) had already shown that the sagittal diameter of the cervical spinal canal is subjected to remarkably wide variations, the maximal diameter being nearly 2 times as large as the minimal diameter. Spondylotic bars, protruding discs and so on should have a far more pathologic influence on the spinal cord if it had practically no room to give way. The theory of ARNOLD and MAYFIELD was supported by WOLF *et coll.* (1956), ALEXANDER *et coll.* (1959), NUGENT (1959) and others. In the selected material of the neurosurgical clinic (in which compression of the cord was proved by myelography) we found an average diameter of the bony spinal canal (spondylotic narrowing not included) of 12.8 mm as opposed to a normal average of 17 mm with a range of 12–22 mm (BELS & PENNING 1964).

Other factors that contribute to a crowding of the lumen of the cervical spinal canal in extension are the step formation (HADLEY 1956) of the vertebral bodies, the folding of the dura mater and the thickening of the spinal cord (BREIG 1960). PENNING (1961) showed that especially in cases of vertebral retrolisthesis the spinal canal is considerably narrowed in extension by a bony pincer formed by the body of the retrolisthetic vertebra and by the lamina of its underlying neighbour. In the constitutionally shallow spinal canal this pincer mechanism might be responsible for intermittent compression of the spinal cord causing a slow development of myelopathic symptoms. On the other hand the pincer mechanism might be responsible for acute neurological signs in cases of forcible hyperextension as reported by FENDER (1952) and SIMONDS (1953) in intubation for anaesthesia, in tonsillectomy and in tooth extraction. TAYLOR & BLACKWOOD (1948) and LOGUE (1956) explained

BIOMECHANICAL ASPECTS OF SPONDYLOTIC MYELOPATHY

by

L. PENNING and P. VAN DER ZWAAG

According to BRAIN (1956), cervical spondylotic myelopathy is the most common disease of the spinal cord during and after middle age. A difficult feature of this myelopathy is its diagnosis. Roentgenographic demonstration of cervical spondylosis is no argument in favor of the diagnosis as it is common during and after middle age. In syringomyelia spondylosis may even be more severe.

In establishing diagnostic criteria and concise concept of the genesis of spondylotic myelopathy is wanted, one has to prove that the spondylosis really is the cause of the myelopathy. We agree with many authors that the only reliable diagnostic criterion is the demonstration of cord compression by means of cerebrospinal fluid manometry and myelography. In typical cases both will show a block of the cerebrospinal fluid pathways if head and neck are in the extended position, in the flexed position free flow of the cerebrospinal fluid and contrast medium is reestablished. Mere demonstration of a protruding disc by myelography is not specific for the disease (McRAE 1956).

A brief summary of the hypotheses underlying the diagnostic phenomena may be given. Although KAPLAN & KENNEDY in 1949 found that the manometric block in extension of the cervical spine was more or less typical of

Table 1

Sagittal diameter (in mm) of the subarachnoidal space and spinal cord measured on the myelograms of the flexed cervical spines of 20 adult cadavers at the levels C₁—C₇

Subarachnoidal space							
C ₁	C ₂	C ₃	C ₄	C ₅	C ₆	C ₇	Measured and Spread
14—0	13—19	11—17	11—17	10—18	10—18	10—18	Mean value
17	15 1/2	14	13 1/2	13	12 1/2	12 1/2	
Spinal cord							
8—12	8—12	8—11	7—10 1/2	7—10	7—10	6—9	Spread
9 1/2	9 1/2	9	9	8 1/2	8 1/2	8	Mean value

load only or even by its own weight. Increasing the load to 350 g results in a negligible further lengthening of the cord. This means that the cord (once stretched (and this is presumably the case in the maximally flexed cervical spine) will exert a certain force on bulging discs, spondylotic bars, etc. REID (1960) measured in cadavers the forces to lift the cord 3 mm off the anterior border of the spinal canal in the maximally flexed neck. These amounted to from 400 to 1 000 g. This is in fair agreement with the considerations of BREIG.

Methods and material

In order to obtain further information about functional anatomic aspects of cervical spinal canal and cervical cord and their significance in the pathogenesis of spondylotic myelopathy we made cervical myelograms in 23 cadavers in flexion and extension of the cervical spine especially in lateral projection. The ages of 20 adult cadavers varied from 14 to 84 years; there were 10 men and 10 women who had died of non-neurological diseases with the function of the spinal cord presumably intact. In addition two newborns and a child of 4 years of age were examined; the child had died after surgical intervention for medulloblastoma cerebelli. As a contrast medium a saturated lead acetate solution was used. The solution was introduced into the spinal subarachnoid space by suboccipital puncture. As a rule 40—60 ml was injected. The mechanism of movement of the cervical vertebrae in these cadavers appeared to be identical with the mechanism of movement during life. This was controlled by the method introduced by one of us (LENNING 1960). The films were made at a target film distance of 150 cm with the film alongside the shoulder; the radiological enlargement factor is estimated to be about 1.2.

Results

In extension of the cervical spine the dorsal and ventral borders of the subarachnoid space of the spinal canal are folded (Fig. 1). The folding of the dorsal border is due to folding of the dura mater and of the ligamenta flava. This is most evident in the region of C₃—7. Slight folding was noticed in four

those cases by assuming a rupture of the anterior longitudinal ligament with pathologic dorsal shift of a vertebra, followed by immediate reposition.

Although mechanical factors seem to play an important role in the genesis of myelopathy, other factors may also be responsible, especially vascular factors. MAIR & DRUCKMAN (1953) investigated in some detail four cases of cord compression by a herniated disc. The distribution of the lesions in these cases appeared to be identical with the area of supply of the anterior spinal artery, except for the sparing of the anterior columns. According to these authors the lesions are caused by compression and distortion of the anterior spinal artery by the protruding disc material. LOGUL (1957) called this theory attractive because it explains the development of symptoms above the level of compression, such as spasticity of the muscle groups of the arm in a low disc lesion, at C5-6 or even C6-7. Several authors (CLARKE & ROBINSON 1956, NUGENT 1959, TAYLOR 1964, and others) have stressed the important role of vascular factors. It is felt however that mechanical compression of the cord might imply compression of its intrinsic vessels including the anterior spinal artery. Compression of the spinal ramus of the vertebral arteries in the intervertebral foramina and compression and atherosclerosis of the vertebral arteries may add to the onset and progression of the disease. NUGENT (1959) suggested that 'connective tissue factors' might contribute to the development of a myelopathy, often adhesions between dura and arachnoid as well as between arachnoid and pia are found. It seems possible that these adhesions may carry collateral blood vessels and have a reparative function.

In contradiction to the theory that extension and hyperextension of the neck are the significant movements that contribute to the genesis of spondylotic myelopathy, some authors believe that flexion and hyperflexion are to be blamed. As shown by O'CONNELL (1956), the spinal canal lengthens in flexion and shortens in extension, implying changes in position and the form of the spinal cord. BREIG (1961), in his monograph concerning 'biomechanics of the central nervous system', states that the cord shows a plastic adaptation to the changes in form of the spinal canal and not a shift in axial direction as suggested by O'CONNELL (1956), nor an elastic displacement of all parts of the cord towards a certain point in the midcervical region as found by SMITH (1956). According to BREIG the cord is compressed axially in extension and drawn out in flexion. The cross-sectional area increases and decreases in extension and flexion, respectively. In flexion of the neck an axial tension appears in the spinal cord. If the cord is hyperelongated, as may be the case in cervical hyperkyphosis, hyperangulation, bulging discs and spondylotic ridges, etc., neurological damage might result. BREIG demonstrated that *in vitro* the isolated, suspended spinal cord is extended to its maximal length by a small

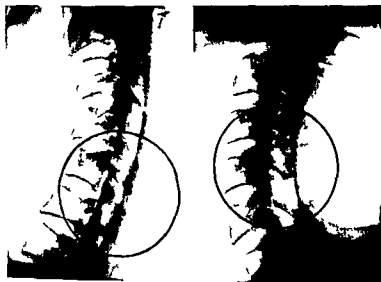


Fig. 2. Cervical myelograms with the neck in flexion and extension. In extension far less contrast agent surrounds the cord in the region C3—6.

direction (Table 1). In one specimen (man 84 years) the sagittal diameter proved to be smallest at C2—1.4 mm, increasing caudally to 18 mm at C7.

At C5 the mean sagittal diameter in flexion is 16 mm. In midposition the sagittal diameter of the subarachnoid space is largest. A small folding may be present due to bulging of the flaval ligaments, discs, etc. therefore two values for the diameter must be given. It ranges from 8—10 to 17—19 mm with a mean value of 12 1/2—14 mm (measurements at the level of C5).

Table 2

Sagittal diameter (in mm) of the bony spinal canal, subarachnoid space and spinal cord of the cervical spine in flexion, midposition and extension, measured on the myelograms of 20 adult cadavers at the level of C5.

Bony spinal canal			Midposition			Extension		
min	max	mean	min	max	mean	min	max	mean
12 1/2	0	16 1/2	12 1/2	20	16 1/2	12 1/2	20	16 1/2
Subarachnoid space								
10—12	18	13	8—10	17—19	12 1/2—14	8 1/2—10 1/2	12—1	11—13
Spinal cord								
7	10 1/2	8 1/2	7—7 1/2	11	9—9 1/4	8—8 1/2	11	9—9 1/2



Fig. 1. Cervical myelograms with the neck in flexion, midposition and extension. 63 year old male cadaver. In extension the folding of the walls of the spinal canal is clearly visible; the walls of the spinal cord are slightly undulated. In flexion dura and spinal cord are stretched. The spinal cord in flexion is smaller than in extension and follows the shortest possible route through the spinal canal.

preparations. In the two newborns and the child folding was practically absent. The folding of the ventral border must be ascribed to step formation of the vertebral bodies and folding of the dura, in elderly persons bulging of discs, spondylotic ridges and retrolisthesis contribute to the folding.

In flexion of the cervical spine the dorsal border of the spinal canal is straight, due to stretching of the flaval ligaments and of the dura. The ventral border as a rule is straight, but may be slightly undulated because of some step formation of the vertebral bodies. As bulging of discs are flattened out in flexion, no significant impression on the contrast column is visible, the same is true for retrolisthesis. In larger bulging of discs and spondylotic ridges, impressions on the ventral border of the spinal cord are noted.

As the midposition of the cervical spine varies from subject to subject a description of the normal configuration of the spinal canal cannot be given. It assumes the characteristics, though to a lesser degree of the flexed spinal canal in the kyphotic or stretched type, and of the extended spinal canal in the lordotic type.

The sagittal diameter of the flexed spinal canal (spinal subarachnoidal space) is largest at the foramen magnum and decreases gradually in the caudal

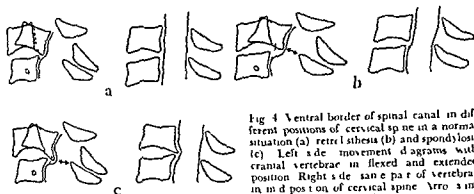


Fig. 4 Ventral border of spinal canal in different positions of cervical spine in a normal situation (a) retraction (b) and spondylosis (c) Left side movement diagrams with cranial vertebrae in flexed and extended position Right side same part of vertebrae in different position of cervical spine Arrows indicate bony pincers mechanism

pressed away from the cervical region in extension and flows in during flexion (Fig. 2)

As to the position of the spinal cord in the spinal canal in different positions of the neck we find that in extension the cord is more or less clenched between the ventral and dorsal borders of the spinal canal dependent on its constitutional width. The difference between the sagittal diameter of the subarachnoid space and of the spinal cord at the level of C4-5 and C5-6 in the extended spine varies from 0-3 mm. For the wider spinal canal (bony sagittal diameter at C6 more than 16 mm) the mean value is 3.5 mm. For the smaller canal (bony sagittal diameter less than 17 mm) 1.7 mm.

In flexion the cord always has a stretched appearance apparently following the shortest possible route through the spinal canal (Fig. 3). In lordosis the cord contacts the ventral border of the spinal canal in the C5-6 or even the C4-7 region. In the more cranial region the cord is free from the wall or contacts the ventral border (C2-3 region) of the spinal canal.

Discussion

Analysing the results of the myelographic examinations we note two basic phenomena that may be of significance in the understanding of the genesis of spondylotic myelopathy: 1) narrowing of the subarachnoid envelope around the spinal cord in extension of the neck, and 2) stretching of the cord in flexion of the neck.

As to the narrowing of the subarachnoid space, the myelograms confirm that folding of the dorsal wall of the spinal canal is a physiological phenomenon in the adult. In our youngest specimens (cervical spines of a girl of 14 and a male of 33) however, folding was less evident, as it also was in the newborns.



Fig. 3 Position of the spinal cord in several flexed spines (drawings after the myelogram). The cord invariably follows the shortest possible route through the spinal canal.

In extension the spinal subarachnoidal space proves to be the smallest with values of 7–10 mm to 12–15 mm and a mean value of 11–13 mm.

The spinal cord has a maximum sagittal diameter at the level of the foramen magnum and atlas and gradually decreases in the caudal direction. An indication of the intumescencia cervicalis in the sagittal plane is visible in infants and newborns only.

Measured at the level of C5 the cord has a sagittal diameter of 7–10 1/2 mm (mean value 8 1/2 mm) in flexion (Table 2). In extension the cord may show slightly undulating borders, with some variation in diameter; the mean diameter was 9–9 1/2 mm. As a rule the cord is smallest at the levels of the bulging ligamentum flavum and intervertebral discs. In midposition of the cervical spine the cord measured 7–11 mm with a mean value of 9–9 1/4 mm. These values are in fair agreement with the values found by ELLIOT (1946) and JIROUT (1959).

Comparing the measurements of the spinal canal in flexion and extension with the measurements of the spinal cord it is evident that the cord has less surrounding subarachnoidal space in extension than in midposition and flexion, especially in the intervertebral regions. As a rule the sagittal diameter of the subarachnoidal space here is 1–2 mm smaller in extension than in flexion while the cord is 1/2–1 mm broader. Our myelograms clearly show that the contrast agent surrounding the cord in the C3–7 region is much less in extension than in flexion. We may conclude that the cerebrospinal fluid is

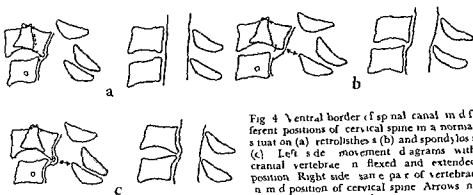


Fig 4 Ventral border of spinal canal in different positions of cervical spine in a normal situation on (a) retrolisthes (b) and spondylosis (c) Left side movement diagrams with cranial vertebrae in flexed and extended position Right side same pair of vertebrae in mid position of cervical spine Arrows indicate bony piners mechanism

pressed away from the cervical region in extension and flows in during flexion (Fig 2)

As to the position of the spinal cord in the spinal canal in different positions of the neck we find that in extension the cord is more or less clenched between the ventral and dorsal borders of the spinal canal dependent on its constitutional width. The difference between the sagittal diameter of the subarachnoidal space and of the spinal cord at the level of C4—5 and C5—6 in the extended spine varies from 0—3 mm for the wider spinal canal (bony sagittal diameter at C5 more than 16 mm) the mean value is 3.5 mm for the smaller canal (bony sagittal diameter less than 17 mm) 1.7 mm.

In flexion the cord always has a stretched appearance apparently following the shortest possible route through the spinal canal (Fig 3). In lordosis the cord contacts the ventral border of the spinal canal in the C5—6 or even the C4—7 region. In the more cranial region the cord is free from the wall or contacts the ventral border (C2—3 region) of the spinal canal.

Discussion

Analysing the results of the myelographic examinations we note two basic phenomena that may be of significance in the understanding of the genesis of spondylotic myelopathy: 1) narrowing of the subarachnoidal envelope around the spinal cord in extension of the neck and 2) stretching of the cord in flexion of the neck.

As to the narrowing of the subarachnoidal space the myelograms confirm that folding of the dorsal wall of the spinal canal is a physiological phenomenon in the adult. In our youngest specimens (cervical spines of a girl of 14 and a male of 33) however folding was less evident as it also was in the newborns.

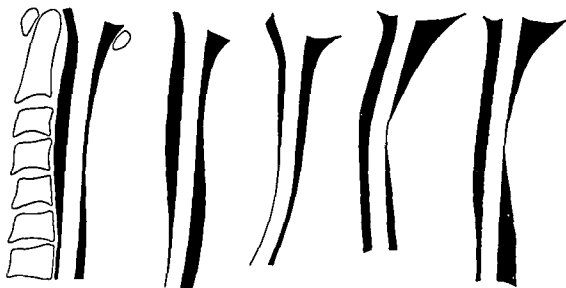


Fig. 3 Position of the spinal cord in several flexed spines (drawings after the myelograms). The cord invariably follows the shortest possible route through the spinal canal.

In extension the spinal subarachnoidal space proves to be the smallest with values of 7–10 mm to 12–15 mm and a mean value of 11–13 mm.

The spinal cord has a maximum sagittal diameter at the level of the foramen magnum and then gradually decreases in the caudal direction. An indication of the *intumescentia cervicalis* in the sagittal plane is visible in infants and newborns only.

Measured at the level of C5 the cord has a sagittal diameter of 7–10 1/2 mm (mean value 8 1/2 mm) in flexion (Table 2). In extension the cord may show slightly undulating borders, with some variation in diameter; the mean diameter was 9–9 1/2 mm. As a rule the cord is smallest at the levels of the bulging ligamenta flava and intervertebral discs. In midposition of the cervical spine the cord measured 7–11 mm with a mean value of 9–9 1/4 mm. These values are in fair agreement with the values found by ELLIOT (1946) and JIKOUT (1959).

Comparing the measurements of the spinal canal in flexion and extension with the measurements of the spinal cord it is evident that the cord has less surrounding subarachnoidal space in extension than in midposition and flexion, especially in the intervertebral regions. As a rule the sagittal diameter of the subarachnoidal space here is 1–2 mm smaller in extension than in flexion while the cord is 1/2–1 mm broader. Our myelograms clearly show that the contrast agent surrounding the cord in the C3–7 region is much less in extension than in flexion. We may conclude that the cerebrospinal fluid is

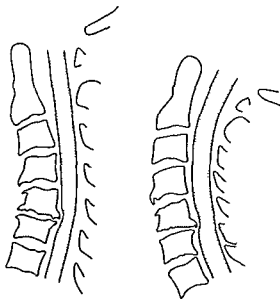


Fig 6 For legend see opposite page



Fig. 5 Films of the cervical spine of a 62 year old electrotechnician with slowly progressing weakness of the right arm and both legs of 3 months duration. After a forced hyperextension during maxillary sinus puncture a complete paralysis of right arm and both legs developed. Left extension position: retrolisthesis C3-4 and C4-5 with bony pincers of 10 mm. postural manometry: total block in extension, normal findings in flexion. pantopaque myelography: stop at C3-4 in extension. After laminectomy C4 and C5 and nearly complete recovery followed.

and the child. Perhaps a certain loss of elasticity of the flaval ligaments plays a role, as suggested by TAYLOR (1951), PAYNE & SHILLANE (1957), and others. The maximal narrowing in our cases, 10%, as compared with the situation in flexion, occurred in a male specimen, aged 81.

Fig. 6. Cervical spine of a 51 year old woman with weakness and ataxia of lower limbs of three weeks duration. Right extension position: retrolisthesis C5-6 with bony pincer of 11 mm diameter. postural manometry: no stop in extension. pantopaque myelography: no stop. Diagnosis: compression of cord in extension is improbable. Left flexion position: important degree of kyphosis. The spondylotic ridges C4-6 protrude into the spinal canal. Spine fusion in moderate extension was performed (C3-7) with considerable improvement. Drawings show the two ways in which the spinal cord could be affected by spondylosis and retrolisthesis C5-6: the possibility of cord compression in extension was rejected because of normal findings in postural manometry and myelography.

such protrusions may obstruct the blood flow in the spinal arteries in the maximally flexed spine. A protrusion spondylotic bar etc. must however reach considerable dimensions to have a height of 3 mm on the ventral border of the flexed spine. As pointed out before and shown in Fig. 4 protrusions have a tendency to flatten if the spine is flexed.

From a diagnostic point of view the pathogenetic value of a certain degree of spondylosis and a certain degree of hyperkyphosis of the flexed cervical spine is difficult to evaluate. Firstly, in children and adults the cervical spine may assume an important kyphotic curvature in flexion apparently without ill effects on the cord. Secondly, myelographic demonstration of protrusions is difficult in the flexed spine (at least with pantopaque, gasmyelography offers distinct advantages) moreover a reliable criterion in assessing the pathogenetic quality of the protrusion is lacking. The test of KAPLAN & KENNEDY in this context is useless as the cord and subarachnoidal space are not compressed but impressed.

We tend to support the hypothesis of REID and of BREIG that stretching of the cord may play a role in the production of chronic myelopathy, but in the meantime its usefulness, at least clinically, is doubtful. In Fig. 6 the case of a patient is shown where we considered the diagnosis of impression of the cord in flexion and adequate therapeutic measures were taken.

Our studies give no support to the wellknown theory of KAHN (1947) postulating that free movement of the spinal cord posteriorly away from a protruding disc is prevented by the tethering function of the ligamenta dentculata resulting mechanically in an area of primary stress in the vicinity of the attachments of the ligaments to the meridian of the cord. As the cord in flexed spine follows the shortest possible route through the spinal canal the tethering function of the dentate ligaments in an antero-posterior direction cannot be of much importance. According to KEY & RETZIUS (1875) the dentate ligaments become shorter in the cranial direction. As a consequence the spinal cord in the C2/3 region should lie ventrally in the spinal canal. The myelograms however prove the contrary. Moreover the relative free antero-posterior mobility of the cord within the spinal canal was shown by JIROULT (1959) and recently by STOLTMANN & BLACKWOOD (1964).

SUMMARY

The mechanical theories explaining the genesis of spondylotic myelopathy offer two different viewpoints: compression of the spinal cord in extension and impression of the cord in flexion. On the basis of myelographic experiments in cadavers we conclude that both theories may

The folding of the ventral wall of the spinal canal is due not only to slackening of the dura but also to the normal backward gliding movement of the vertebral bodies in relation to their underlying neighbours. As a consequence, disc protrusions on the ventral border of the spinal canal will cause an increased narrowing effect on the spinal canal in extension, whereas their effect in flexion is decreased (Fig. 4). Disc protrusions are most evident, myelographically, in extension. Perhaps this explains why the surgeon is sometimes disappointed at the operation, because as a rule the spine then is in the flexed position.

The myelograms confirm that, if compression of the cord occurs, it occurs at first in extension. The need for 'postural' manometry and 'postural' myelography should be emphasized. Although the myelograms show that in extension the subarachnoidal space in the midcervical region may be practically obliterated, pathological manometric readings in extension in normal subjects were not noted by KAPLAN & KENNEDY. As an explanation the small bore of the lumbar puncture needle is held responsible, if only more cerebrospinal fluid could pass through the cervical region than through the needle, the test would give normal results. Good correlation between the results of postural manometry and myelography were reported by BRAHAM & HERZBERGER (1956), CLARKE & ROBINSON (1956), TENG (1960) and others. It proves that the test of KAPLAN & KENNEDY is valuable in differentiating spondylotic myelopathy from other myelopathies. A clinical example is given in Fig. 5.

In 2 of the 12 cases of KAPLAN & KENNEDY with pathological manometric readings a block in flexion was found, with normal results in extension. The cases were not verified surgically. An explanation could not be given. Our myelographic investigations too do not contribute to a better understanding. We can only refer to the case of CLARKE & LITTLE, where intermittent cord compression at the level of C2/3 occurred on flexion of the spine. In our opinion, a similar occurrence is only possible in anterolisthesis of a cervical vertebra, as opposed to retrolisthesis where compression takes place in extension (PENNING 1961, 1964).

In the flexed cervical spine the spinal cord invariably follows the shortest possible route through the spinal canal. This proves that a certain amount of stretching is present, completely in accordance with the observations of REID (1960) and BRIGG (1960). Pressure of the cord against the ventral border of the spinal canal is mainly to be expected in the C5-6 or C4-7 region, the extent and force being dependent on the degree of kyphosis of the cervical spine in flexion. After converting the given values of REID it becomes evident, that the pressure of the cord against a spondylotic bar of 3 mm height on the ventral border of the spinal canal averages about 1 000 mm Hg. This exceeds the blood pressure of the spinal arteries many times. It is obvious then that

- JIRJCT J The mobility of the cervical spinal cord under normal conditions *Brit J Radiol* 32 (1959) 744
- KAHN E A The role of the dentate ligaments in spinal cord compression and the syndrome of lateral sclerosis *J Neurosurg* 4 (1947) 191
- KAPLAN L and KENNEDY F Effects of head posture on manometrics of cerebrospinal fluid in cervical lesions: new diagnostic test *Brain* 73 (1950) 337
- LODGE V Cervical spondylosis *Modern Trends in Neurology* second series Hoeber New York 1957
- MAIR W G P and DRUCKMANN R The pathology of spinal cord lesions and their relation to clinical features in protrusions of the cervical intervertebral disc *Brain* 76 (1953) 40
- MAYFIELD F H Neurosurgical aspect of cervical trauma In *Clinical Neurosurgery* Vol II Williams & Wilkins Baltimore 1955
- MURRAY D L Asymptomatic intervertebral disc protrusions *Acta radiol* 46 (1956) 9
- NUGENT G R Clinicopathologic correlations in cervical spondylosis *Neurology* 9 (1959) 273
- O'CONNELL J E A Involvement of the spinal cord by intervertebral disk protrusions *Brit J Surg* 43 (1955) 225
- PAYNE E E and SPILLANE J D The cervical spine: an anatomical study of 70 specimens with special reference to the problem of cervical spondylosis *Brain* 80 (1957) 571
- PENNING L Functional radiologic investigation of degenerative and traumatic diseases of the lower cervical motor segments Summary of thesis *J belge Radiol* 44 (1961) 531
- PENNING L Some aspects of plain radiography of the cervical spine in chronic myelopathy *Neurology* 12 (1962) 513
- REID J D Effects of flexion extension movements of the head and spine upon the spinal cord and nerve roots *J Neurol Neurosurg Psychiat* 23 (1960) 214
- SMITH C G Changes in length and position of the spinal cord with changes in posture in the monkey *Radiology* 66 (1956) 259
- SPILLANE J D and LLOYD G H T Spastic paraplegia in late adult life with degeneration and protrusion of cervical discs *Lancet* 2 (1951) 653
- — The diagnosis of lesions of the spinal cord in association with osteoarthritic disease of the cervical spine *Brain* 75 (1952) 177
- STOLTMANN H F and BLACKWOOD W The role of the ligamenta flava in the pathogenesis of myelopathy in cervical spondylosis *Brain* 87 (1964) 45
- SYMMONDS C Interrelation of trauma and cervical spondylosis in compression of spinal cord *Lancet* 1 (1953) 451
- TAYLOR A R and BLACKWOOD W Paraplegia in cervical injuries with normal radiographic appearance *J Bone Jt Surg* 30B (1948) 245
- TAYLOR A R The mechanism of injury to the spinal cord in the neck without damage to the vertebral column *J Bone Jt Surg* 33B (1951) 543
- Mechanism and treatment of spinal cord disorders associated with cervical spondylosis *Lancet* 1 (1953) 717
- TEO P Spondylosis of cervical spine with compression of spinal cord and nerve roots *J Bone Jt Surg* 42A (1960) 392
- WOLF B S KJILNANT M and MALIN L Sagittal diameter of the bony cervical canal and its significance in cervical spondylosis *J Mt Sinai Hosp* 23 (1956) 283

be valid though only compression in extension can be proven in the clinical case. Before assuming impression of the cord in flexion, compression in extension should be ruled out by postural manometry and myelography.

ZUSAMMENFASSUNG

Die mechanischen Theorien zur Erklärung der Genese der spondylotischen Myelopathie bieten zwei verschiedene Ansichten: Kompression des Rückenmarks in Extension und Kompression in Flexion. Auf Grund von myelographischen Versuchen an der Leiche mögen beide Theorien ihre Gültigkeit haben, obwohl nur die Kompression in Extension klinisch geprüft werden kann. Bevor man sich für die Impression des Rückenmarks in Flexion entscheidet, sollte die Kompression in Extension mittels Manometrie und Myelographie ausgeschlossen werden.

RÉSUMÉ

Les théories mécaniques expliquant la pathogénie de la myélopathie par arthrose vertébrale comportent deux hypothèses différentes: compression de la moelle épinière en extension et impression de la moelle en flexion. L'expérimentation myélographique sur le cadavre nous fait conclure que les deux théories peuvent être vraies, bien qu'on ne puisse prouver dans les cas cliniques que la compression en extension. Avant d'admettre l'impression de la moelle en flexion, on devrait éliminer par manométrie posturale et myélographie la possibilité de la compression en extension.

REFERENCES

- ALEXANDER M. D., DAVIS C. H. and FIELD C. H.: Hypertension injuries of the cervical spine. *Arch Neurol Psychiat* 79 (1958) 146.
- ARNOLD J. G.: Spondylochoondrosis of the cervical spine. *Ann Surg* 141 (1955) 872.
- BEAS J. W. F. and PENNING L.: Ergebnisse neurochirurgischer Behandlung von ausgewählten Fällen spondylotischer Myelopathie. *Neurochirurgia* 7 (1964) 7.
- BOYSEN E.: The cervical spinal canal in intraspinal expansive processes. *Acta radiol* 42 (1954) 101.
- BRAHAM J. and HERZBERGER E.: Cervical spondylosis and compression of the spinal cord (cit. Ectors). *J Amer med Ass* 161 (1956) 1560.
- BRAIN W. R.: Spondylosis: the known and the unknown. *Lancet* (1954) 687.
- Some aspects of the neurology of the cervical spine. *J Fac Radiol* 8 (1956) 74.
- BRIIG A.: Biomechanics of the central nervous system. Almqvist & Wiksell, Stockholm 1961.
- CLARKE E. and ROBINSON P. A.: Cervical myelopathy: a complication of cervical spondylosis. *Brain* 79 (1956) 483.
- ELLIOT H. C.: Spinal cord diameters. *Anat Rec* 93 (1945) 287.
- FENDER F. A.: A new hazard in cervical laminectomy. *J Amer med Ass* 149 (1952) 227.
- HADLEY L. A.: The spine. *Anatomico-Radiographic Studies: Development and the Cervical Region*. Charles C. Thomas, Springfield, Ill. 1956.

- JIROUT J. The mobility of the cervical spinal cord under normal conditions. *Brit J Radiol* 32 (1959) 744
- KAPIN E. A. The role of the dentate ligaments in spinal cord compression and the syndrome of lateral sclerosis. *J Neurosurg* 4 (1947) 191
- KAPLAN L. and KENNEDY F. Effects of head posture on manometrics of cerebrospinal fluid in cervical lesions: new diagnostic test. *Brain* 73 (1950), 337
- LOGIE V. Cervical spondylosis. *Modern Trends in Neurology* second series Hoeber New York 1957
- MAIR W. G. P. and DRUCKMANN R. The pathology of spinal cord lesions and their relation to clinical features in protrusions of the cervical intervertebral disc. *Brain* 76 (1953) 70
- MAYFIELD F. H. Neurosurgical aspect of cervical trauma. In *Clinical Neurosurgery* Vol II Williams & Wilkins Baltimore 1955
- MURRAY D. L. Asymptomatic intervertebral disc protrusions. *Acta radiol* 46 (1956), 9
- MURRAY G. R. Clinicopathologic correlations in cervical spondylosis. *Neurology* 9 (1959) 273
- O'CONNELL J. E. A. Involvement of the spinal cord by intervertebral disk protrusions. *Brit J Surg* 43 (1955) 225
- PAYNE E. E. and SPILLANE J. D. The cervical spine: an anatomical study of 70 specimens with special reference to the problem of cervical spondylosis. *Brain* 80 (1957) 571
- PENNING L. Functional radiologic investigation of degenerative and traumatic diseases of the lower cervical motor segments. Summary of thesis. *J belge Radiol* 44 (1961) 551
- PENNING L. Some aspects of plain radiography of the cervical spine in chronic myelopathy. *Neurology* 12 (1962) 513
- REID J. D. Effects of flexion extension movements of the head and spine upon the spinal cord and nerve roots. *J Neurol Neurosurg Psychiat* 23 (1960) 214
- SMITH C. G. Changes in length and position of the spinal cord with changes in posture in the monkey. *Radiology* 66 (1956) 259
- SPILLANE J. D. and LLOYD G. H. T. Spastic paraplegia in late adult life with degeneration and protrusion of cervical discs. *Lancet* 2 (1951) 653
- — The diagnosis of lesions of the spinal cord in association with osteoarthritic disease of the cervical spine. *Brain* 75 (1952) 177
- STOLTMAN H. F. and BLACKWOOD W. The role of the ligamenta flava in the pathogenesis of myelopathy in cervical spondylosis. *Brain* 87 (1964) 45
- SYMONDS C. Interrelation of trauma and cervical spondylosis in compression of spinal cord. *Lancet* 1 (1953) 451
- TAYLOR A. R. and BLACKWOOD W. Paraplegia in cervical injuries with normal radiographic appearance. *J Bone Jt Surg* 30B (1948) 245
- TAYLOR A. R. The mechanism of injury to the spinal cord in the neck without damage to the vertebral column. *J Bone Jt Surg* 33B (1951) 543
- Mechanism and treatment of spinal cord disorders associated with cervical spondylosis. *Lancet* 1 (1953) 717
- TENG P. Spondylosis of cervical spine with compression of spinal cord and nerve roots. *J Bone Jt Surg* 42A (1960) 392
- WOLF B. S. KHILNANI M. and MALIS L. Sagittal diameter of the bony cervical canal and its significance in cervical spondylosis. *J Mt Sinai Hosp* 23 (1956) 283

DOUBLE CONTRAST MYELOGRAPHY

by

LOMAZ REZENDE

Myelography has been much discussed, both as regards the method of the examination and the best contrast medium, since it was introduced by DANCE in 1919. The author favours lumbar puncture with air or gas as a negative contrast medium. The entire subarachnoid space may thus be studied and the examination repeated as often as desired without fear of complications such as arachnoiditis and granulomata.

We have devised a method, based on physical laws, of performing myelography with two contrast media in cases of complete or partial block of the spinal canal. The upper and lower poles of the lesion, preferably with the aid of tomography, may thus be demonstrated in a single film.

The technical details may be varied. The examination may commence with lumbar pneumomyelography with the patient seated (7, 8), followed by the injection of a positive contrast medium by the suboccipital route. Alternatively the suboccipital injection of gas or air (4, 5, 6, 7, 8) with the patient in the Trendelenburg position may be followed by the lumbar injection of a positive contrast medium (Pantopaque (1, 9) Myodil, Ethiodan). The author has employed the latter method in 5 cases.

The main advantages of the method appear to be: 1) The positive contrast

Awarded the Austregésilo Prize in 1964 by the National Academy of Medicine, Rio de Janeiro, Brasil.



Fig 1 Double contrast myelography before tomography. Positive contrast injected in the lumbar region. Almost total block at level of Th 5. Air introduced by suboccipital route in the Trendelenburg position. The air column delineates the spinal cord and reveals obstructions at level of Th 4.



Fig 2 The delineation of the spinal cord and the tumour are improved by tomography.

medium is used only once and in a small quantity 2) precision is obtained in determining the limits of the block in the spinal canal since the exact size of the lesion will be demonstrated in a single film 3) despite tomography the method is practical and inexpensive a median section in profile sometimes suffices 4) the Trendelenburg position may be avoided at least for part of the time in old people or in those with cardiac or pulmonary disease (3, 4, 5).

As disadvantages it may be mentioned that suboccipital puncture is necessary and this by itself represents a dangerous procedure. The second obvious disadvantage is the use of positive contrast media.

Case report

A white female aged 59 who at the end of 1962 had weakness while walking and had fallen to the ground several times. The condition progressively deteriorated. There was no sphincter involvement. She was admitted in March 1963 with crural paraplegia.

Physical examination suggested spinal cord compression characterized by spastic paraplegia with possible sensory loss below Th 8. Roentgen examination revealed slight osteoarthritis in the thoracic spine. Double contrast myelography disclosed a juxta medullary expansive lesion about 2 cm in size posteriorly at the level of Th 5. At operation (laminectomy) a

spherical tumour was found lying posterolaterally and displacing the spinal cord anteriorly and slightly to the right. A histologic examination of the specimen proved it to be a meningioma.

Postoperative course. Uneventful recovery. The patient started to walk again about 1 month later.

SUMMARY

The author describes a technique for myelography with double contrast media (negative and positive) performed with or without tomography.

ZUSAMMENFASSUNG

Der Verfasser beschreibt die Durchführung der Myelographie mit doppeltem (negativem und positivem) Kontrastmedium mit oder ohne Tomographie.

RÉSUMÉ

L'auteur décrit une technique de myelographie avec double contrast (négatif et positif) sans ou avec tomographie.

REFERENCES

1. BULL J and McKISSOCK W. *ANA Atlas of Positive Contrast Myelography*. Grune & Stratton, New York and London 1962.
2. DANDY W E. Roentgenography of the brain after the injection of air into the spinal canal. *Ann Surg* 70 (1919) 397 (Quoted by LINDGREN and ROTH).
3. JACOBSEN H H and YLLISTED K. Localized atrophy of the spinal cord. *Acta radiol* 50 (1958) 211.
4. LINDGREN E. Radiologic examination of the brain and spinal cord. *Acta radiol Suppl* 151 (1957) 139.
5. ODÉN S. Diagnosis of spinal tumours by means of gas myelography. *Acta radiol* 40 (1953) 301.
6. KLEFENBERG G and SALTZMAN G F. Gas myelographic studies in syringomyelia. *Acta radiol* 52 (1959) 123.
7. ROTH G. Myelographie gazeuse par refoulement. Une nouvelle méthode. *J Radiol Electrol* 43 (1962) 831.
8. ROTH M. Gas myelography by the lumbar route. *Acta radiol New series* 1 (1963) 53.
9. WIEDENMANN O und DECKLER K. *Spinale Tumoren in Klinische Neuroradiologie*. Georg Thieme Verlag, Stuttgart 1960.

LE FOURREAU DURAL LOMBO SACRE

Etude radio anatomique

par

G SALAMON R LOUIS et G GUFRINEL

Le fourreau dural lombo sacre represente l'enveloppe dure meniee des racines de la queue de cheval. Il s'etend du cone terminal jusqu'aux premieres vertebres sacrees.

D'apres les auteurs classiques la moelle se termine a la hauteur de L2 alors que le fourreau dural se termine en S2. En fait de nombreuses variations peuvent interesser ce segment de la dure mere. Les travaux anatomiques qui concernent cette region sont deja fort anciens (KEY & RETZIUS 1870 CHIPAULT 1885).

Trois elements ont contribue a mieux faire connaitre ce segment des formations intra rachidiennes. D'une part la possibilite d'y injecter des substances iodées huileuses ou hydro solubles. D'autre part la connaissance de hernies discales lombaires et enfin la possibilite d'un traitement chirurgical.

L'importance de cette pathologie radiculaire qu'un examen assez simple permet de soupçonner a donc mis l'accent sur un segment du systeme nerveux central peu étudie jusque la.

On dispose a l'heure actuelle de confrontations anatomiques (dissections, corrosions de pieces plastiques, coupes de rachis congeles) et radiologiques.

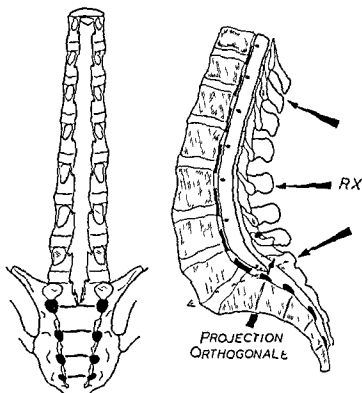


Fig. 1 Schéma de face et de profil du cul de sac duril lombo sacré. On retiendra de face l'aspect festonné du cul de sac chaque émergence radriculaire déterminant une véritable évagination de la dure mère. Sur le cliché de profil on conçoit la discordance qui peut exister entre le système de référence anatomic et la référence orthogonale par rapport au rachis et la référence radiologique.

(examens myélographiques par myélographie gazeuse, lipiodol ou methiodal) qui permettent d'avoir une idée très précise sur la topographie du cul de sac duril et des racines.

Les examens radiologiques les plus précis sont constitués par des myélographies aux hydro-solubles. En effet, leur résorption rapide permet d'injecter des quantités assez importantes pour obtenir un moule satisfaisant de l'ensemble du cul de sac. La faible opacité de ces produits donne une image satisfaisante des racines et de leur émergence.

Nous avons sélectionné 150 myélographies normales, et pour chacune d'elles, nous avons étudié le niveau de terminaison, la forme du cul de sac, le niveau d'émergence des racines et leurs types morphologiques. Les données anatomiques nous ont été fournies soit par des dissections, soit par des moulages aux résines plastiques avec corrosion des pièces, soit, enfin par injection du



Fig 2 Myelographie du méthodol. Aspect normal. Incidences de face 3/4 et profil. On retrouve sur ces clichés l'aspect festonné du cul-de-sac correspondant aux émergences radiculaires. L'incidence de profil met en évidence les saillies au niveau des espaces inter-vertébraux provoquées par le disque et son surtout ligamentaires.

cul de sac et radiographies des coupes horizontales de 1 centimètre d'épaisseur permettant ainsi d'avoir une vue axiale du fourreau.

Nous avons utilisé les renseignements de dissections du cul de sac chez 75 sujets (Figs 3 6 7 8 9 15).

Nous avons ainsi pu préciser le mode de terminaison, la forme du cul de sac et l'émergence des racines et comparer ces résultats à ceux des examens myelographiques. Après ouverture du cul de sac, nous avons pu observer la disposition intra-durale des racines et leur mobilité aux mouvements de flexion ou d'extension du rachis (Fig 9).

Dans d'autres cas, l'injection d'une résine plastique mélangée à du sulfate de baryum a permis d'obtenir par corrosion de véritables moules radiopaques du cul de sac (Figs 4 et 5).

Enfin, sur des rachis entiers, les espaces sous-arachnoïdiens ont été injectés de minium. Les pièces ainsi congelées ont été coupées en tranches d'épaisseur

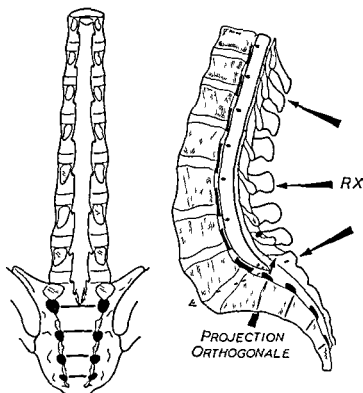


Fig 1 Schéma de face et de profil du cul de sac dural lombo sacré. On retiendra de face l'aspect festonné du cul de sac chaque émergence radiculaire déterminant une véritable enjambement de la dure mère. Sur le cliché de profil on conçoit la discordance qui peut exister entre le système de référence anatomique, référence orthogonale par rapport au rachis et la référence radiologique.

(examens myélographiques par myélographie gazeuse: lipiodol ou methiodal) qui permettent d'avoir une idée très précise sur la topographie du cul de sac dural et des racines.

Les examens radiologiques les plus précis sont constitués par des myélographies aux hydro-solubles. En effet leur résorption rapide permet d'injecter des quantités assez importantes pour obtenir un moule satisfaisant de l'ensemble du cul de sac. La faible opacité de ces produits donne une image satisfaisante des racines et de leur émergence.

Nous avons sélectionné 150 myélographies normales et pour chacune d'elles, nous avons étudié le niveau de terminaison, la forme du cul de sac, le niveau d'émergence des racines et leurs types morphologiques. Les données anatomiques nous ont été fournies soit par des dissections, soit par des moulages aux résines plastiques avec corrosion des pièces, soit enfin par injection du



Fig. 4. Radiographie d'un moulage de cul de sac. Méthode de corrosion. Les sillons plus clairs représentent ici l'empreinte des racines que l'on peut suivre jusqu'à leur sortie du fourreau du al.

et sa hauteur. À ce propos, il faut signaler quelques divergences entre les données anatomiques et radiologiques (Fig. 17).

Les constatations anatomiques se réfèrent à des projections orthogonales, c'est à dire perpendiculaires à l'axe du canal rachidien, le sujet étant en position indifférente. Par contre la projection radiographique est une projection conique divergente ne tenant aucun compte de l'axe rachidien, si bien qu'un cul de sac dural se terminant orthogonalement au niveau du disque S1—S2 se projette radiographiquement de face par la forte obliquité du sacrum au niveau du disque sus-jacent L5—S1.

Dimension du fourreau dural. La hauteur moyenne du cul de sac mesurée sur des moulages plastiques nous a paru être comprise entre 13 et 18 centimètres (Fig. 5).

De même l'immersion de ces moules nous a permis d'en déterminer le volume moyen (non compris le volume des racines détruites par la corrosion). Ce volume est compris entre 15 et 23 cm³.

Morphologie du fourreau dural. Jusqu'à la hauteur de L3—L4 le cul de sac présente une forme triangulaire correspondant aux parois du canal ostéo-fibreux qui l'entoure (Figs 6, 7, 8).

Au dessous de L4 le cul de sac varie de calibre de façon importante. Certains



Fig. 3 Aspects du cul de sac dural sur une dissection anatomique. L'émergence des racines n'a jamais lieu à la face postérieure du disque. Lorsque les racines croisent la partie postérieure du disque intervertébral, elles sont déjà assez éloignées du fourreau dural.

de 1 centimètre, perpendiculairement à l'axe du rachis, ces coupes passant soit par les corps vertébraux, soit par les disques permettent d'étudier les rapports antérieurs et latéraux du fourreau dural, ainsi que la disposition dans un plan horizontal des racines de la queue de cheval (Figs 6, 7, 8).

Les données anatomo-radiologiques permettent de fixer sa situation sa forme, ses mesures et ses rapports.

Situation du fourreau dural. Le fourreau dural lombo-sacré s'étend de l'interligne D12—L1 jusqu'à la région comprise entre S1—S2. En haut le fourreau dural fait suite à l'enveloppe dure méridienne de la moelle et du cône terminal. En bas, le fourreau se termine soit au niveau de l'interligne S1—S2, soit au niveau de l'interligne S2—S3 (Figs 1, 2, 18). Plus exceptionnellement, le fourreau dural se termine au milieu de S2, ou à la hauteur du disque S3—S4. Il est fréquent de rencontrer une terminaison du cul de sac d'autant plus basse que le cône terminal est lui-même plus bas situé.

Par contre, il ne semble exister aucune relation entre la forme du cul de sac



Fig. 4. Radiographie d'un moulage de cul-de sac. Méthode de corrosion. Les sillons plus clairs représentent ici l'empreinte des racines que l'on peut suivre jusqu'à leur sortie du fourreau du al.

et sa hauteur. À ce propos, il faut signaler quelques divergences entre les données anatomiques et radiologiques (Fig. 17).

Les constatations anatomiques se réfèrent à des projections orthogonales, c'est à dire perpendiculaires à l'axe du canal rachidien, le sujet étant en position indifférente. Par contre la projection radiographique est une projection conique divergente ne tenant aucun compte de l'axe rachidien si bien qu'un cul de sac dural se terminant orthogonalement au niveau du disque S1—S2 se projette radiographiquement de face par la forte obliquité du sacrum au niveau du disque sus-jacent L5—S1.

Dimension du fourreau dural. La hauteur moyenne du cul de sac mesurée sur des moulages plastiques nous a paru être comprise entre 13 et 18 centimètres (Fig. 5).

De même, l'immersion de ces moules nous a permis d'en déterminer le volume moyen (non compris le volume des racines détruites par la corrosion). Ce volume est compris entre 15 et 23 cm³.

Morphologie du fourreau dural. Jusqu'à la hauteur de L3—L4 le cul de sac présente une forme triangulaire correspondant aux parois du canal ostéo-fibreux qui l'entoure (Figs 6, 7, 8).

Au-dessous de L4 le cul de sac varie de calibre de façon importante. Certains



Fig 5 Moulages de cul de sac duraux. Pièces plastiques obtenues par corrosion. On remarquera les différences de calibre de terminaison et d'émergence radiculaires

d'entre eux, très larges, gardent à ce niveau la même configuration qu'à l'étage sus-jacent remplissent le canal lombo-sacré et prennent contact avec toutes ses parois, alors que d'autres, plus étroits, deviennent cylindriques et s'éloignent très nettement de la paroi postérieure de L5 et de l'interligne lombo-sacré (Fig 8). On conçoit que dans ces cas, le fourreau étant étroit, effilé, l'examen myélographique puisse rester négatif, même s'il existe une volumineuse hernie L5—S1 (LINDBLOM 1950).

Outre ces variations de hauteur correspondant à la terminaison du cul de sac, il existe nombreuses variations de formes bien étudiées par ARNELL (1948). Elles ont été schématisées sur la Fig 17.

Le fourreau dural ainsi disposé présente un aspect festonné en regard des pédicules, en 'dents de scie'. Cet aspect est déterminé par l'émergence de racines rachidiennes qui soulèvent à ce niveau la dure mère, déterminant ainsi une véritable fossette intra-durale. Nous les étudierons avec les racines de la queue de cheval (Figs 1, 15, 16).

Les racines de la queue de cheval

A l'intérieur du fourreau dural se trouvent disposées près de 15 racines sensitivo-motrices correspondant aux territoires lombaires, sacrés et coccygiens (y compris le filum terminale).

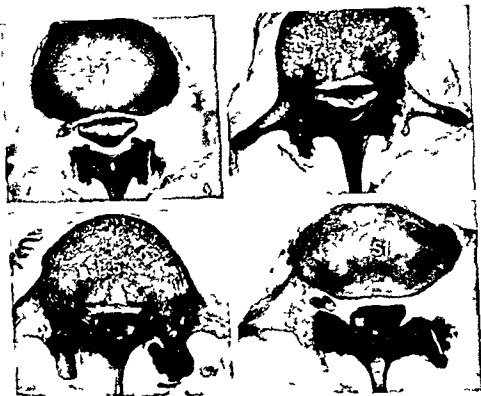


Fig 6 Coupes horizontales de rachis. Pêces congelées avec injection du cul-de sac dural au plomb. Ces coupes passent par L3—L4—L5—S1. Elles intéressent les corps vertébraux. En L4 et L5 l'émergence de racines correspondantes détermine de véritables évasements latéraux.

Les racines comme le montrent les coupes horizontales du rachis (Figs 6 7 8) sont disposées en arc de cercle ouvert en avant de telle sorte qu'aux extrémités de l'arc se trouvent les deux racines droite et gauche qui vont traverser le fourreau en s'éloignant vers le sommet postérieur de l'arc on trouve les racines les plus inférieures de part et d'autre du filum.

A chaque étage lombaire ou sacré deux racines sensitive et motrice de chaque côté abandonnent le fourreau dural et vont ainsi constituer le nerf rachidien. L'origine de ces racines et leur traversée duremérienne représentent des éléments anatomiques d'une certaine fixité. Il faut également signaler la mobilité de ces racines très relâchées en hyper extension et tendues rectilignes en hyper flexion (Fig 9). L'émergence durale de ces racines détermine on l'a vu une véritable fossette. Chaque racine motrice ou sensitive perfore la dure mère par un orifice distinct, les deux orifices étant séparés par un septum (Fig 15).

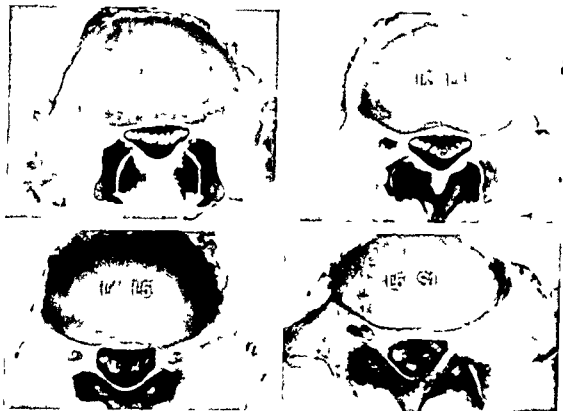


Fig. 7 Coupes horizontales du rachis. Pièces congelées avec injection du cul de sac dural au plomb. Ces coupes passent par les disques intervertébraux L2-L3, L3-L4, L4-L5 et L5-S1. Ici le cul de sac a une forme régulière triangulaire. Les racines à l'intérieur du fourreau sont disposées en arc de cercles. Au niveau des trous de conjugaison on aperçoit en L3-L4 et L4-L5 les racines émergentes.

D'autre part, l'évagination de la dure mère détermine au bord inférieur de celle-ci un véritable repli filiforme que l'on voit au cours de dissections et qui est nettement visible sur les myelogrammes.

À la partie inférieure et supérieure de ces racines, il existe deux fossettes l'une supérieure, l'autre inférieure. Ces deux fossettes sont déterminées par la racine elle-même qui vient isoler deux étages sous-arachnoïdiens à l'intérieur de l'évagination durale due à la traversée des racines.

Alors que les racines sous-jacentes sont disposées verticalement, les racines qui vont sortir du fourreau ont une courbure arciforme comme si elles étaient tendues sur la poulie que représentent à ce niveau les pédicules. Ce changement de direction (Figs 10, 11, 12, 13) est important à considérer, car il est souvent affecté par une hernie discale.

L'espace arachnoïdien sus-radicaire constitue une fossette, la fossette sus-radicaire, dont la forme est très variable. Elle se trouve comprise entre



Fig. 8 Coupes horizontales du rachis. Pièces congelées et injectées au minimum. Les 2 coupes de droite présentent un cul-de-sac très étroit. Les 2 coupes de gauche intéressent un cul-de-sac très large. On voit l'importante différence qui existe à l'étage L5—S1 entre les deux variétés de cul-de-sac. On conçoit qu'une hernie importante ne donne aucun signe myélographique dans le premier cas.

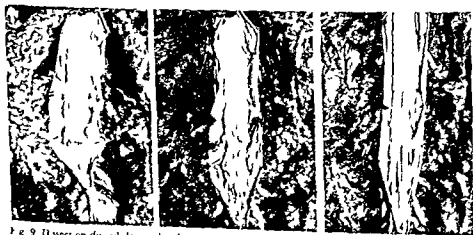


Fig. 9 Dissection du cul-de-sac du lumbosacral. Les racines sont photographiées de bas en haut, on peut constater l'induration et enfin en flexion. La flexion du rachis tend à bannir les racines comme les cordes d'un arc.



Fig 10 Émergence radiculaire avec fossettes sus et sous radiculaires longues. Cet aspect peut se voir au niveau de S1



Fig 11 Émergence radiculaire avec fossettes radiculaires à peine ébauchées



Fig 12 Émergence radiculaire avec aspect kystique d'un recessus



Fig 13 Émergence radiculaire d'aspect habituel avec fossette sous radiculaire triangulaire en console

les racines prêtes à sortir, et la paroi durale sus-jacente à sa sortie. Certaines sont triangulaires, d'autres quadrangulaires. De nombreuses variations peuvent se voir schématisées sur la Fig. 14.

La fossette sous radiculaire, par contre, présente une morphologie plus constante. Elle est pratiquement toujours de forme triangulaire, sa base étant rectiforme, à concavité inférieure. Sa constitution nous explique sa forme triangulaire, elle est limitée, en effet, par trois portions. En haut, la racine

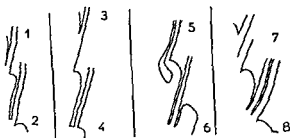


Fig 14 Schema des principaux types d'émergence radriculaire

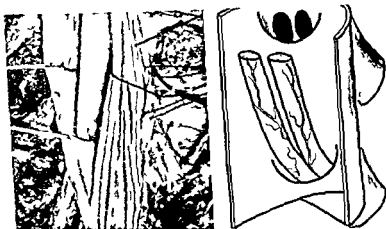


Fig 15 Dissection du cul-de sac dural. Vue interne d'une fossette radculaire. On distingue les 2 racines et le schéma représente leurs orifices de sortie distincts

qui traverse la dure mere en bas la faux de l'orifice de traversée en dedans, la racine sous jacente

Cet aspect existe de façon constante a tous les niveaux mais interesse surtout les racines de L2 a S1 ou S2 suivant le niveau plus ou moins bas de terminaison du sac dural. Cette fossette sousradiculaire plus large que la precedente est tres souvent comprimee et disparait si il existe une hernie discale meme de petit volume. La compression ou la disparition de cette fossette donne l'impression d'un elargissement apparent de la racine au moment de sa traversée. Ce signe decrit comme signe du tromblon était attribue a un oedeme radiculaire à ce niveau. Cet oedeme localise est d'autant moins probable qu'il est limite et qu'il est d'ailleurs exceptionnellement retrouve lors d'interventions neurochirurgicales. En fait cet elargissement apparent de la racine est du simplement à la compression directe de la hernie qui vient à ce niveau



Fig. 16. Coupe vertico frontale du cul de sac niveau des émergences radiculaires.

comprimer la dure mère, effaçant la fossette sous radiculaire. L'absence de cette fossette permet d'affirmer avec quasi certitude, l'existence d'une protrusion discale.

Les deux fossettes sont d'une longueur variable. En particulier, en regard de S1, elles peuvent être assez longues, et cela, d'autant plus que le cul de sac dural est plus étroit (Fig. 10). Il est assez rare, par contre, qu'elles soient peu marquées, le cul de sac ayant alors une forme cylindrique (Fig. 11).

Le niveau de la fossette sous radiculaire donne avec précision le niveau d'émergence dure-mère des racines. Au-delà de cette limite, il existe souvent une gaine arachnoïdienne, mais, elle ne s'injecte pratiquement jamais par l'emploi de produits iodés. Par contre, l'injection de pièces anatomiques au minimum nous a permis souvent d'opacifier la gaine arachnoïdienne sur une longueur un peu plus grande que sur les myelographies aux produits iodés hydro-solubles.

Les fossettes sus- et sous radiculaires communiquent largement avec les espaces sous arachnoïdiens du sac dural, et il serait faux de prétendre que chaque racine possède une gaine arachnoïdienne qui lui soit propre tout le long de son trajet intra-dural, et, que le liquide céphalo-rachidien qui l'occupe, ne puisse communiquer aisément autour des racines voisines.

On conçoit ainsi que, quelle que soit la méthode d'examen myelographique que l'on emploie, l'opacification du cul de sac et des fossettes radiculaires soit toujours satisfaisante.



Fig 17 Principaux types de terminaison de cul de sac dural

Il nous semble aussi pour cette raison assez demesure de pratiquer deux examens myelographiques droit et gauche alors qu'au cours d'un meme examen il suffit de retourner le malade pour obtenir une opacification tres satisfaisante des recessus radiculaires des deux cotes

Les donnees de dissection et l'analyse de myelographies montrent qu'il existe un niveau moyen d'emergence assez constant pour chaque racine (Fig 18) Les racines naissent d'autant plus bas que la terminaison du cul de sac est plus basse

On peut admettre lorsque le cul de sac s'arrete au niveau du disque S1—S2

1 Que la racine L2 quitte le cul de sac a mi hauteur de la deuxième lombaire

2 Que la 3eme racine lombaire quitte le cul de sac au 1/3 superieur environ de la troisieme piece lombaire

3 Que L4 quitte le cul de sac au 1/4 superieur de la quatrieme piece lombaire

4 Quant a L5 elle quitte le cul de sac au 1/5 superieur de la cinquieme vertebre lombaire alors que S1 le quitte soit au niveau soit quelques millimetres au dessus de l'interligne lombo sacre

Quand le cul de sac se termine plus bas a la hauteur du disque S2—S3 l'emergence des racines se fait plus bas que pour le cas precedent ainsi L3 naît au milieu du corps de L3 L4 vers le 1/3 superieur de L4 et L5 au niveau du 1/4 superieur de L5 tandis que S1 naît a la hauteur du disque L5—S1 soit a quelques millimetres au dessous

Enfin certaines anomalies de naissance se voient soit sur des dissections de pieces anatomiques soit sur des myelographies (CANNON HUNTER & PICAZA 1962)

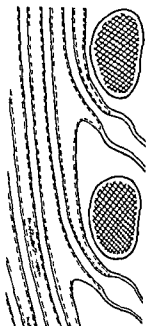


Fig. 16 Coupe vertico frontale du cul de sac niveau des émergences radiculaires

comprimer la dure mère, effaçant la fossette sous radiculaire. L'absence de cette fossette permet d'affirmer avec quasi certitude, l'existence d'une protrusion discale.

Les deux fossettes sont d'une longueur variable. En particulier en regard de S1, elles peuvent être assez longues, et cela, d'autant plus que le cul de sac dural est plus étroit (Fig. 10). Il est assez rare, par contre, qu'elles soient peu marquées, le cul de sac ayant alors une forme cylindrique (Fig. 11).

Le niveau de la fossette sous radiculaire donne avec précision le niveau d'émergence dural des racines. Au delà de cette limite, il existe souvent une gaine arachnoïdienne, mais, elle ne s'injecte pratiquement jamais par l'emploi de produits iodés. Par contre, l'injection de pièces anatomiques au minimum nous a permis souvent d'opacifier la gaine arachnoïdienne sur une longueur un peu plus grande que sur les myélographies aux produits iodés hydrosolubles.

Les fossettes sus et sous radiculaires communiquent largement avec les espaces sous arachnoïdiens du sac dural, et il serait faux de prétendre que chaque racine possède une gaine arachnoïdienne qui lui soit propre tout le long de trajet intra dural, et, que le liquide céphalo rachidien qui l'occupe, ne puisse communiquer aisément autour des racines voisines.

On conçoit ainsi que, quelle que soit la méthode d'examen myélographique que l'on emploie, l'opacification du cul de sac et des fossettes radiculaires soit toujours satisfaisante.



Fig 17 Principaux types de terminaison de cul de sac dural

Il nous semble aussi pour cette raison assez demesure de pratiquer deux examens myelographiques droit et gauche alors qu'au cours d'un meme examen il suffit de retourner le malade pour obtenir une opacification tres satisfaisante des recessus radiculaires des deux cotes

Les donnees de dissection et l'analyse de myelographies montrent qu'il existe un niveau moyen d'emergence assez constant pour chaque racine (Fig 18). Les racines naissent d'autant plus bas que la terminaison du cul de sac est plus basse

On peut admettre lorsque le cul de sac s'arrete au niveau du disque S1—S2

1 Que la racine L2 quitte le cul de sac a mi hauteur de la deuxieme lombaire

2 Que la 3eme racine lombaire quitte le cul de sac au 1/3 superieur environ de la troisieme piece lombaire

3 Que L4 quitte le cul de sac au 1/4 superieur de la quatrieme piece lombaire

4 Quant a L5 elle quitte le cul de sac au 1/5 superieur de la cinquieme vertebre lombaire alors que S1 le quitte soit au niveau soit quelques millimetres au dessus de l'interligne lombo sacre

Quand le cul de sac se termine plus bas a la hauteur du disque S2—S3 l'emergence des racines se fait plus bas que pour le cas precedent ainsi L3 nait au milieu du corps de L3 L4 vers le 1/3 superieur de L4 et L5 au niveau du 1/4 superieur de L5 tandis que S1 nait a la hauteur du disque L5—S1 soit à quelques millimetres au dessous

Enfin certaines anomalies de naissance se voient soit sur des dissections de pieces anatomiques soit sur des myelographies (CANNON HUNTER & PICAZA 1962)

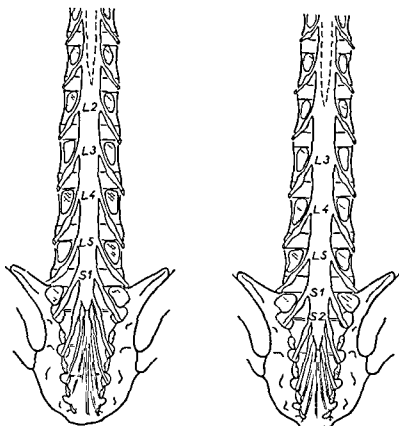


Fig. 18. Schéma des émergences radiculaires correspondant aux types les plus fréquemment rencontrés. Type S1 avec terminaison du cul de sac en S1—S2 ou terminaison en S2—S3 (87 des cas).

Discussion

Anatomie. La projection du cul de sac et des émergences radiculaires varie quelquefois avec celle que l'on observe sur les myélographies ou lors d'interventions chirurgicales. Dans le premier cas, il s'agit de références de projections différentes. Dans le second, la position opératoire du malade modifie quelque peu les rapports anatomiques, l'hyperflexion attirant de quelques millimètres vers la tête les racines sous-jacentes à L4.

La forme du cul de sac examinée en coupes est triangulaire sauf au niveau de la terminaison, variable sur le plan morphologique comme en hauteur (S1—S2).

Le cul de sac s'éloigne d'autant plus de la face postérieure des corps vertébraux que l'étage considéré est plus bas. Les racines sont disposées à l'intérieur du cul de sac, en arc de cercle.

Au niveau de leur émergence, les racines déterminent la formation de deux

recessus sus et sous radiculaires seul ce dernier est constant dans sa forme. Le niveau d'émergence radiculaire par rapport aux corps vertébraux est également assez constant.

Radiologie. On ne peut admettre qu'il existe de gaines sous arachnoïdiennes propre à chaque racine dans leur trajet intra dural. Les racines sont toutes à l'intérieur du fourreau dural et entourées de liquide céphalo rachidien.

L'existence des gaines radiculaires est une fausse impression optique créée par la myélographie le produit de contraste iode venant se déposer entre chaque racine.

Les myélographies montrent que le fourreau dural présente une certaine fixité jusqu'en L3—L4. De nombreuses variations sont observées à partir de L5 ce qui concorde nettement avec les données anatomiques.

Les fossettes sus et sous radiculaires sont déterminées par les émergences radiculaires.

La fossette sous radiculaire est souvent comprimée au cours de hernies discales ce qui explique le signe de tromblon beaucoup plus constamment que l'œdème radiculaire. Ce signe est certainement un signe de compression directe par la hernie.

La formation anatomique du cul de sac et des racines explique qu'une excellente myélographie puisse être obtenue quelle que soit la méthode employée la meilleure étant certainement la plus rapide et celle qui donne les images dont la définition est la meilleure.

Les clichés les plus importants sont ceux obtenus en oblique. Il peut être intéressant pour dégager ces divers recessus radiculaires de pratiquer quatre à cinq clichés sous des obliques différentes pour obtenir ainsi un véritable balayage de cette région.

RÉSUMÉ

Les auteurs ont étudié par diverses méthodes anatomiques et radio-anatomiques la situation par rapport aux vertèbres du cul-de sac dural lombo-sacré et de l'émergence des racines hors du fourreau dural. Ils expliquent pour quelles raisons les résultats de cette étude peuvent être en désaccord avec les constatations myélographiques ou per opératoires. Ils ont aussi étudié la forme du cul-de sac dural et la disposition des racines. Il n'y a pas une gaine arachnoïdienne intra-durale distincte pour chaque racine mais seulement une fossette sus et une fossette sous-radriculaire. Le signe radiculographique du tromblon semble dû le plus souvent à la compression de la fossette sous-radriculaire par la hernie discale plutôt qu'à l'œdème radiculaire.

SUMMARY

Using various anatomical and radiological methods the authors studied the dural sheaths and the emergence of the lumbosacral roots. They explain why the results of this study may disagree with the myelographic or operative findings. The shape of the dural sheath and the disposition of the roots was also studied. Each root does not have a distinct intradural arachnoidal sheath but on leaving the sheath produces an evagination of the dura forming two fossae, one above and one below the root. The sudden pain from the nerve roots would usually seem to be due to compression of the fossa below the root by the herniated disc, rather than to inflammation of the root.

ZUSAMMENFASSUNG

Mit Hilfe verschiedener anatomischen und röntgenologischen Methoden wurden die Durascheiden und die Austrittsstellen der Lumbosakralen Nervenwurzeln studiert. Diese Studien machen es klar, warum der Tatbestand nicht immer mit den myelographischen und operativen Befunden übereinzustimmen scheint. Die Form der Duralscheide und die Anordnung der Nervenwurzeln wurde erneut studiert. Jede einzelne Nervenwurzel hat nicht notwendigerweise ihre eigene intradurale Arachnoidscheide, aber sie hat an ihrer Austrittsstelle eine Ausstülpung der Dura, die zwei Gruben aufzeigt, eine oberhalb und eine unterhalb der Wurzel. Der plötzliche Schmerz, der von den Nervenwurzeln ausgeht, scheint durch Kompression der unteren Grube durch Diskusprolaps hervorgerufen zu werden und nicht durch Entzündung an der Wurzel.

BIBLIOGRAPHIE

- AMUNDSEN P, HELSINGEN P and KRISTIANSEN K. Evaluation of lumbar radiculography (myelography) with water soluble contrast media. *Acta radiol.* 3 Diagnosis (1963) 659.
- ARNELI S. Myelography with water soluble contrast. *Acta radiol.* (1948) Suppl. 70.
- BETOUTIERIS P, TILMILE J P et JANICOT J Y. La radiculographie lombo sacrée au méthiodal (Notes de technique d'après 300 examens). *J. Radiol. Electrol.* 8—9 (1960) 447.
- BONTE G, DEGOULA P, WAGHEMACHER J, CLICHE J P et HUART F. La radiculographie lombo sacrée en cours de lombalgie dans sciaticque. *J. Radiol. Electrol.* 6—7 (1961) 416.
- BULL J and McKISSOCK W. An atlas of positive contrast myelography. Grune and Stratton, London, 1962.
- CANNON B N, HUNTER S I and PICAZA J A. Nerve root anomaly in lumbar disc surgery. *J. Neurosurg.* 3 (1962) 208.
- CHAILAULT. Rapports des apophyses épineuses avec la moelle, les racines médullaires et les méninges. Thèse de Méd. Paris 1893.
- ECCOFFIER J. La radiculographie lombaire dans la sciaticque. Masson, Paris 1960.
- KEY A and RETZIUS G. Studien in der Anatomie des Nervensystems und des Bindegewebes. P. A. Norstedt & Soner, Stockholm 1875.
- KNUTSSON F. The myelogram following operation for herniated disc. *Acta radiol.* 32 (1949) 60.
- Lumbar myelography with water soluble contrast in cases of disc herniation. *Acta orthop. scand.* 20 (1951) 294.

- LATARJET M et MAGNIN P Relations des racines rachidiennes lombaires avec le sac dural et le système articulaire vertébral Etude anatomique J Med Lyon 8 (1941) 346
- LAUX G La moelle épinière et ses enveloppes en rapport avec les parois osseuses du canal vertébral Ann anat path 7 (1930) 629
- LAYANI F PERTUSET B et METZGER J La radiculographie lombaire après injection intrarachidienne de substance de contraste hydro soluble et résorbable Rev Rhum 3 (1957) 1
- LINDBLOM K. Technic and results in myelography and disc puncture Acta radiol 4—5 (1950) 370
- LOUIS R Contribution à l'étude des rapports des racines et de la moelle de l'adulte avec les lames et les disques vertébraux Thèse Méd Marseille 1961
- RIGGIERO G Traité de technique chirurgicale Masson Paris 1961
- SALAMON G LOUIS R FAURE J et COMALBERT A Les bases radio anatomiques de l'interprétation des myélographies aux hydro-solubles J Radiol Electrol 46 (1965) 547
- WORINGER E et LANGS A La myélographie ou Kontrast U (Moyen de diagnostic de la sciatique discale) J Radiol Electrol 31 (1950) 450
- BAL IGARTNER J & BRALN J P Le diagnostic de la hernie discale lombo-sacrée par la myélographie au mono-iodo-méthane sulfonate de sodium (A propos de 500 cas) Presse Med 16 (1955) 1583

FROM THE NEURORADIOLOGIC SECTION (CHIEF DR. M. M. SCHECHTER) OF THE
RADIOLOGY DEPARTMENT (DIRECTOR DR. M. ELKIN) OF THE ALBERT EINSTEIN
COLLEGE OF MEDICINE, NEW YORK, U.S.A.

THE SPINAL ARTERIES

by

MANNIE M. SCHECHTER and LAWRENCE H. ZINGESSER

Neuroradiology is a relatively young subspecialty of radiology. The growth of this subspecialty as well as the growth of the broader domain of radiology is due in part to the great technical achievements being made in our time. Another part of our body of knowledge, however, comes out of reassessment of material that has been with us for a relatively long period of time. Thus neglected aspects of radiologic anatomy take on a new meaning when our attention is drawn to the anatomy in question, and finally pathologic anatomy is recognized radiographically where it was passed over previously.

It is the purpose of this report to draw the attention of radiologists to the anterior and posterior spinal arteries. In a series of several hundred vertebral angiographies, the anterior spinal artery has been identified by us in the lateral view in 50 % of cases, and in a much smaller proportion of cases we could identify the posterior spinal plexus. In a recent series of vertebral angiographies performed via the brachial route reported by THOMAS et coll., the anterior spinal artery could be identified in 2 % of cases and KRAYENBUHL & YASARGIL (1957) identified these vessels positively in only three cases from their large series.

Because of the constant location of the anterior spinal artery in the anterior

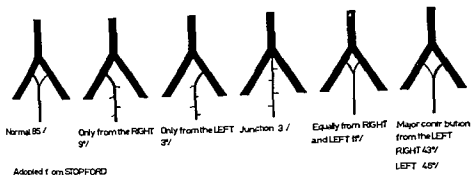


Fig 1 Variations in the origin of the anterior spinal artery

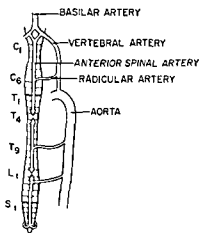
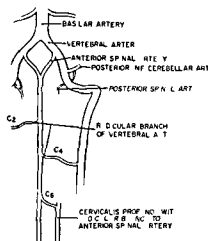
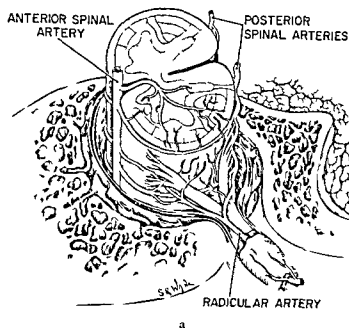
median raphe of the spinal cord demonstration of this artery angiographically allows an evaluation of the spinal cord position in relation to the vertebral canal. The plexus of vessels derived from the anastomoses between the posterior spinal arteries delineates the posterior aspect of the cord. Displacement of the spinal cord and these vessels may result from the patient's position (JIROUT 1959) but with the patient in the supine and the head and neck in the neutral position the anterior spinal artery lies within certain fixed limits. Displacement of this artery may be caused by a pathologic process involving structures within the spinal canal.

Another aspect of neuroradiologic significance relates to the possibility of the anterior spinal artery serving as a feeding vessel for an arteriovenous malformation or a vascular tumor within the spinal canal. Angiomas outlined by vertebral angiography have been reported by ZIEDES DES PLANTES (1953) LINDGREN (1956) HOOK & LIDVALL (1958) and MORRIS (1960).

Also the anterior spinal artery may serve as a pathway for collateral circulation where there is occlusive disease involving the proximal portions of the vertebral arteries. This has been recognized in the dog (DE LA TORRE et coll 1959) and we have seen this occur in an adult female.

GILLILAN (1958) reviewing the anatomy of the spinal arteries credits ADAMKIEWICZ (1881) for the first extensive investigation of the blood vessels of the spinal cord. This was followed by KADYI (1889), STOPFORD (1916) (see Fig 1) TUREN (1938) SUH & ALEXANDER (1939) and HERREN & ALEXANDER (1939). GILLILAN studied the spinal cords and brains of 100 human fetuses ranging in age from six months fetal life to full term. Corrosion studies of injected vessels were performed and observations made were confirmed in adult human material. She observed no difference in appearance, relative size or relationship between the arteries of fetuses and adults.

Fig 2 a) A schematic representation of the extrinsic vascular supply of the human spinal cord b) Segmental contribution to the anterior median spinal artery. Radicular branches from the vertebral arteries at the cervical 2 and cervical 4 levels and a branch from the cervical profunda at the cervical 6 level c) The posterior spinal plexus d) The shaded area of the cord at T 4 and at L 1 represent the watershed area



b

c

d

Our studies involved radiography of the vessels of the cord injected with barium gelatin solutions. We examined both the intact cord within the spinal canal and the cord after it had been removed. We also used corrosion techniques on cords which had the vessels injected with a plastic resin.

The anterior spinal artery extends the length of the spinal cord lying in close proximity to the anterior median fissure (Fig 2). The artery begins with the union of two vessels each coming off the distal vertebral arteries

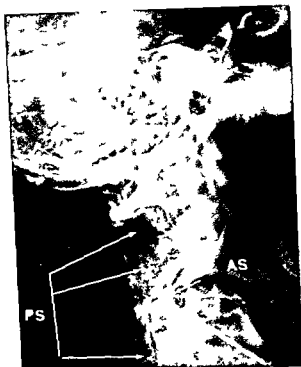


Fig 3 Lateral projection of a vertebral angiogram. The spinal cord outlined by the anterior spinal artery (AS) and by the posterior spinal plexus (PS)

The vessels vary in size and not infrequently after joining the two vessels extend separately for a length of the cord lying next to one another. Absence of one vessel has been seen in our corrosion specimens. Only rarely are both absent (SPILLER 1908).

Segmental arteries contribute to the anterior median spinal artery and these branches are not infrequently seen during vertebral angiography. The upper 3 to 5 cervical segments of the spinal cord are supplied by segmental branches of the cervical portion of the vertebral artery (GILLILAN 1958). The lower cervical region is supplied by various branches of the subclavian artery usually the ascending cervical or the profunda cervicalis (Fig 2 c).

The spinal cord down to the fourth thoracic (vertebral) segment is usually supplied by the anterior spinal artery, the segmental branches from the vertebral artery, the branches of the ascending cervical artery and by a branch of the profunda cervicalis which enters the canal through the intervertebral foramen between the 7th cervical and 1st thoracic vertebrae. Below this level



Fig. 4. A lateral vertebral angiogram (a) demonstrating the anterior spinal artery which identifies the anterior margin of the spinal cord and corresponds with the cord outlined in a subsequent cephalogram (b) on the same patient.

the cord is supplied by branches from the aorta (Fig. 2c). The territory between these two supply areas (referred to as a 'watershed area') is relatively less vascularized and suffers most with impaired circulation (Lazorthes 1958).

The anterior spinal artery is variable in width throughout its extent. It is usually well defined in the cervical region and gradually tapers from its origin towards the thoracic region, where it becomes hardly recognizable. The vessel may undulate from side to side, looping towards the medullary arteries as they anastomose with it, or the anterior medullary arteries may bifurcate sending one limb up and one limb down.

The segmental arteries, from which the medullary arteries arise, also supply the bone and dura. At the intervertebral foramen the vessel divides into an anterior radicular root and a posterior radicular root. These supply the corresponding nerve roots and disappear in these structures. Occasionally the posterior radicular artery extends into the spinal cord and supplies the posterior pial plexus (Fig. 3). Only at certain levels is there a second anterior or posterior branch of the radicular artery which joins the anterior or posterior spinal artery.

The intrinsic supply of the cord is by way of the anterior spinal artery the posterior spinal arteries and the fine network connecting them. Short arterial stems arise from the anterior spinal artery and penetrate the median fissure to supply the central portion of the cord. The more peripheral part is supplied by the vessels passing around the cord (Fig. 2).

The posterior spinal arteries are in fact one posterior plexiform channel, running longitudinally and lying on the dorsolateral aspect of the spinal cord (Figs 2c and 3). The upper ends of these vessels originate as branches from the intracranial portions of the vertebral arteries. They are distinct single vessels only at their origin and later become a network of anastomotic channels supplied by the posterior arteries arising from the radicular arteries. The posterior spinal channels are joined at intervals by the posterior medullary arteries (about six to eight in number).

Many of the vessels making up the extrinsic supply to the cervical and upper thoracic cord may be identified during vertebral angiography (Fig. 3).

Material and results

One hundred of our most recent vertebral angiographies performed by direct puncture were selected for this study. In 50 % of these, the anterior spinal artery could be recognized in the lateral projection. Rarely could it be recognized in the AP projection although a subtraction technique might help here. In 4 % the posterior spinal plexus could be identified (Fig. 3). In a small proportion of cases we were able to identify the segmental branches supplying the anterior spinal artery. Two measurements were made: 1) the width of the spinal canal at C2 and 2) the distance between the anterior spinal artery and the dorsal aspect of the body of the axis.

The result may be summarized as follows. A total of 100 vertebral angiographies (direct puncture) were studied. The anterior spinal artery was identified in 51 cases and was not identified in 49 cases. The posterior spinal plexus was identified in 4 cases (all had anterior spinals). The range of canal diameters at C2 was 1.6 to 2.4 cm and the range of the distance of the anterior spinal artery from the dorsal aspect of the body of C2 was 0.1 to 0.9 cm. The average distance of the anterior spinal artery from the dorsal aspect of the body of C2 was 0.3 cm. These measurements reflect the position of the anterior aspect of the spinal cord within the spinal canal in patients in the supine position with the head and neck in the neutral position. A deviation from the average measurement must be great in order to be pathologic for there is a wide range of normality.

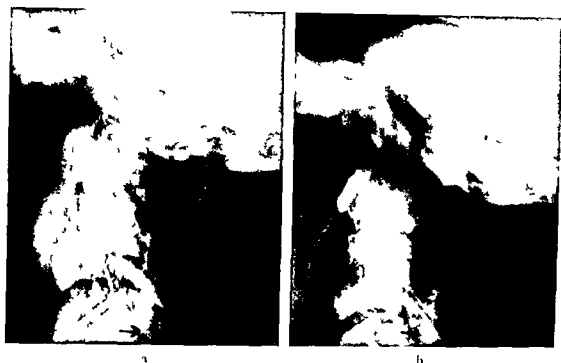


Fig. 4. A lateral vertebral angiogram (a) demonstrating the anterior spinal artery which identifies the anterior margin of the spinal cord and corresponds with the cord outlined in a subsequent encephalogram (b) on the same patient.

the cord is supplied by branches from the aorta (Fig. 2c). The territory between these two supply areas (referred to as a watershed area) is relatively less vascularized and suffers most with impaired circulation (Lazorthes 1958).

The anterior spinal artery is variable in width throughout its extent. It is usually well defined in the cervical region and gradually tapers from its origin towards the thoracic region, where it becomes hardly recognizable. The vessel may undulate from side to side looping towards the medullary arteries as they anastomose with it, or the anterior medullary arteries may bifurcate sending one limb up and one limb down.

The segmental arteries, from which the medullary arteries arise also supply the bone and dura. At the intervertebral foramen the vessel divides into an anterior radicular root and a posterior radicular root. These supply the corresponding nerve roots and disappear in these structures. Occasionally the posterior radicular artery extends into the spinal cord and supplies the posterior pial plexus (Fig. 3). Only at certain levels is there a second anterior or posterior branch of the radicular artery which joins the anterior or posterior spinal artery.

The intrinsic supply of the cord is by way of the anterior spinal artery the posterior spinal arteries and the fine network connecting them. Short arterial stems arise from the anterior spinal artery and penetrate the median fissure to supply the central portion of the cord. The more peripheral part is supplied by the vessels passing around the cord (Fig 2)

The posterior spinal arteries are in fact one posterior plexiform channel, running longitudinally and lying on the dorsolateral aspect of the spinal cord (Figs 2c and 3). The upper ends of these vessels originate as branches from the intracranial portions of the vertebral arteries. They are distinct single vessels only at their origin and later become a network of anastomotic channels supplied by the posterior arteries arising from the radicular arteries. The posterior spinal channels are joined at intervals by the posterior medullary arteries (about six to eight in number)

Many of the vessels making up the extrinsic supply to the cervical and upper thoracic cord may be identified during vertebral angiography (Fig 3)

Material and results

One hundred of our most recent vertebral angiographies performed by direct puncture were selected for this study. In 50 % of these the anterior spinal artery could be recognized in the lateral projection. Rarely could it be recognized in the AP projection although a subtraction technique might help here. In 4 % the posterior spinal plexus could be identified (Fig 3). In a small proportion of cases we were able to identify the segmental branches supplying the anterior spinal artery. Two measurements were made: 1) the width of the spinal canal at C2 and 2) the distance between the anterior spinal artery and the dorsal aspect of the body of the axis.

The result may be summarized as follows. A total of 100 vertebral angiographies (direct puncture) were studied. The anterior spinal artery was identified in 51 cases and was not identified in 49 cases. The posterior spinal plexus was identified in 4 cases (all had anterior spinals). The range of canal diameters at C2 was 1.6 to 2.4 cm and the range of the distance of the anterior spinal artery from the dorsal aspect of the body of C2 was 0.1 to 0.9 cm. The average distance of the anterior spinal artery from the dorsal aspect of the body of C2 was 0.3 cm. These measurements reflect the position of the anterior aspect of the spinal cord within the spinal canal in patients in the supine position with the head and neck in the neutral position. A deviation from the average measurement must be great in order to be pathologic, for there is a wide range of normality.

Acknowledgement

This work was supported in part by a special traineeship (B-1-937) from the National Institute of Neurologic Diseases and Blindness Public Health Service

SUMMARY

The anterior spinal artery can be identified in 50 % of vertebral angiographies performed by direct puncture. It can serve as a pathway for collateral circulation when the vertebral arteries proximally are involved by occlusive disease and it may feed a vascular pathologic process, this can be recognized angiographically. Measurement of the distance of the anterior spinal artery from the back of C2 may be used in evaluation of displacement of the spinal cord, but caution must be exercised for the range of normal variation is great. The posterior spinal plexus may be identified demonstrating the precise position of the posterior aspect of the cord and thus the size of the upper cervical spinal cord. The segmental branches although frequent findings at post mortem are only occasionally outlined *in vivo* during vertebral angiography.

ZUSAMMENFASSUNG

Die Art spinalis ant. kann mittels Angiographie der Art vertebralis in 50 % der Fälle identifiziert werden. Sie kann als Weg für die Kollateralkirkulation dienen wenn die Vertebralarterien proximal verschlossen sind und sie kann auch einen pathologischen Prozess mit Blut versorgen. Dies kann angiographisch nachgewiesen werden. Die Messung des Abstandes der Art spinalis ant. zum dorsalen Teil von C2 kann für die Untersuchung von Verlagerungen des Rückenmarks diagnostisch ausgewertet werden wobei jedoch wegen der normalerweise vorkommenden grossen Variation der Masse Vorsicht in der Beurteilung geboten ist. Durch den Nachweis des Plexus spinalis posterior kann die genaue Lage der hinteren Begrenzung des Rückenmarks und somit die Ausdehnung des oberen Cervikalmarks dargestellt werden. Obwohl die segmentalen Äste post mortem häufig gefunden werden kommen sie bei der vertebralen Angiographie *in vivo* nur gelegentlich zur Darstellung.

RÉSUMÉ

On peut identifier l'artère spinale antérieure dans 50 % des angiographies vertébrales faites par ponction directe. Elle peut servir à la circulation collatérale quand les artères vertébrales sont obstruées dans leur partie proximale et elle peut irriguer un processus pathologique vasculaire ceci est visible sur l'angiographie. La mesure de la distance de l'artère spinale antérieure à la face postérieure de C2 peut servir à apprécier le déplacement de la moelle, mais cette appréciation doit être prudente car les variations normales sont grandes. Le plexus spinal postérieur peut être identifié situant avec précision la face postérieure de la moelle et permettant ainsi de mesurer le diamètre de la moelle cervicale supérieure. Les branches segmentaires bien que souvent visibles post mortem ne sont que rarement visibles sur les angiographies vertébrales *in vivo*.

REFERENCES

- ADAMJEWICZ A Die Blutgefäße des menschlichen Rückenmarkes I Die Gefäße der Rückenmarksubstanz Sitzungsbd d k Akad d Wissensch in Wien math naturv Cl 84 (1881) 469
- ANDREYEV A Functional changes in the brain of the dog after reduction of the cerebral blood supply I Cerebral circulation and the development of anastomoses after ligation of the arteries Arch Neurol Psychiat 34 (1935) 481
- DE LA TORRE E NETSKY M and MESGHIAN I Intracranial and extracranial circulations in the dog anatomic and angiographic studies Amer J Anat 103 (1959) 343
- GILLILAN L The arterial blood supply of the human spinal cord J comp Neurol 110 (1958) 75
- HENSON R and CROFT P Spontaneous spinal subarachnoid hemorrhage Quart J Med 23 (1956) 53
- HERREN R and ALEXANDER L Sulcal and intrinsic blood vessels of human spinal cord Arch Neurol Psychiat 41 (1939) 6/8
- HOOB O and LIDVALL H Arteriovenous aneurysms of the spinal cord a report of 2 cases investigated by vertebral angiography J Neurosurg 15 (1958) 84
- JIROLT J The mobility of the cervical spinal cord under normal conditions Brit J Radiol 32 (1959) 744
- KADYI H Über die Blutgefäße des menschlichen Rückenmarkes Nach einer im XX Bande der Denkschriften d math naturw Cl d Akad d Wissensch in Krakau erschienenen Monographie aus dem Polnischen Übersetzt vom Verfasser Gubrynowicz and Schmidt Lemberg 1889
- LAZORTHES G POLLIES J BASTIDE G ROLLIEAT J et CHANCHOLLE A La vascularization artelle de la moelle Neuro-chirurgie 4 (1958) 3
- LINDGREN E Another method of vertebral angiography Acta radiol 46 (1956) 257
- MORRIS L Angioma of the cervical spinal cord Radiology 75 (1960) 785
- SPILLER W The symptom complex of a lesion of the uppermost portion of the anterior spinal and adjoining portion of the vertebral arteries J nerv ment Dis 35 (1908) 775
- STOPFORD J 1) The arteries of the pons and the medulla oblongata I art I J Anat 50 (1916) 131
- 2) The arteries of the pons and medulla oblongata I art II J Anat 50 (1916) 225
- SUHT and ALEXANDER L Vascular supply of the human spinal cord Arch Neurol Psychiat 41 (1939) 659
- THOMAS J HARDY W LIDNER D and GURDJIAN E Retrograde brachial angiography in cerebrovascular disease Arch Neurol 7 (1962) 339
- TUREN L Circulation of the spinal cord and the effect of vascular occlusion Ass Res nerv Dis Proc 23 (1938) 304
- ZIEDESS DES PLANTES B In discussion of angiographic papers of The Third Symposium Neuroradiologicum Acta radiol 40 (1953) 194
- ZULCH K Mangeldurchblutung aus der Grenz Zone zweier Gefäßgebiete als Ursache bisher ungeklärter Rückenmarksschädigungen Dtsch Z Nervenheilk 172 (1954) 81

RADIOLOGIC ASPECTS OF SPINAL BRUCELLOSIS

by

J. SOLÉ LLENAS, J. ROTÉS QUEROL and M. DALMAU CIRIA

Bone and nervous manifestations, particularly those affecting the spinal column, are frequently observed in brucellosis. There are two types of lesions: 1) osteoarticular lesions (spondylitis and sacroilitis), and 2) those affecting the intradural nervous structures (meningomyelitis and meningoradiculitis, with or without constrictive arachnoiditis).

The roentgen diagnosis is made by conventional radiography as well as by myelography.

Material. The total material consists of 192 cases during the period 1927—1963, in 156 of which a variable degree of involvement of the spinal column was observed; from the radiologic point of view this group includes 92 cases of spondylitis, 31 cases of sacroilitis and 9 cases of intradural changes, manifested radiologically by arachnoiditis.

The diagnosis of brucellosis was based on epidemiologic studies and agglutination tests and confirmed in some cases by blood and cerebrospinal fluid cultures.

Spondylitis

Spondylitis, the most common sign of osteoarticular brucellosis, occurred in 92 cases (58.9%). There was a marked predominance of males over females



Fig 1 Epiphysitis of the anterior margin of L4



Fig 2 Flattening of D7 with decrease in the height of the anterior border



Fig 3 Cervical lesions of the so-called soft type with extensive destruction of bone and disks and spinal deformity

with a higher incidence over the age of 50. Spondylitis is the rule in patients with bruceiosis over the age of 55.

The lumbar region was most frequently affected (74 cases). Several vertebrae usually non adjacent were involved a polytopic distribution in contrast to the monotopic distribution typical of Pott's disease. Two or three vertebral bodies L4, L3 and L2 in that order of frequency are generally affected. Lesions in the dorsal region are confined to D11 and D12. The cervical region is seldom the site of changes. The lesions seem to have a tendency to be superimposed upon traumatic and osteoarthritic lesions and congenital malformations.

Changes may be absent in the so called abortive form of the disease. They usually appear however as a focal lesion of the vertebral body. The trabecular structure appears blurred and irregular with osteoporotic zones alternating with increased bone density. In a later phase the lesion is more evident in the anterosuperior part of the vertebral body described as epiphysitis by PEDRO PONS (1929). The osteitic focus appears as a small loss of substance mostly localized to the same region (Fig 1). Marked destructive lesions and even detachment of the epiphyses may finally occur.

Although some changes in the shape of the vertebral body may be seen this is not the rule. However in some cases a flattening with a decrease in height

RADIOLOGIC ASPECTS OF SPINAL BRUCELLOSIS

by

J. SOLL LLENAS, J. ROTÉS QUEROL and M. DALMAU CIRIA

Bone and nervous manifestations, particularly those affecting the spinal column, are frequently observed in brucellosis. There are two types of lesions: 1) osteoarticular lesions (spondylitis and sacroilitis) and 2) those affecting the intradural nervous structures (meningomyelitis and meningoradiculitis with or without constrictive arachnoiditis).

The roentgen diagnosis is made by conventional radiography as well as by myelography.

Material. The total material consists of 192 cases during the period 1927—1963, in 156 of which a variable degree of involvement of the spinal column was observed; from the radiologic point of view this group includes 92 cases of spondylitis, 31 cases of sacroilitis and 9 cases of intradural changes manifested radiologically by arachnoiditis.

The diagnosis of brucellosis was based on epidemiologic studies and agglutination tests and confirmed in some cases by blood and cerebrospinal fluid cultures.

Spondylitis

Spondylitis, the most common sign of osteoarticular brucellosis, occurred in 92 cases (58.9%). There was a marked predominance of males over females



Fig. 5. Brucellar granuloma. Typical round mononuclear cells rich in eosinophilic protoplasm and with large nuclei.

Histology revealed that brucellar spondylitis consists of interstitial edema and infiltration of small and large monuclear cells through the cancellous bone, in some parts giving rise to granulomas. The most characteristic sign is the presence of mononuclear round cells with considerable eosinophilic protoplasm and large nuclei (Lowbeer's cells) (Fig. 5). In some areas the granulation tissue produces partial or total reabsorption of the bone trabeculae (zone of roentgen osteoporosis).

Nodules with a focus of necrosis may appear in the granulation tissue. These nodules may become calcified and even break down in 3 or 4 months. At the same time a reparative process starts as a proliferation of the connective tissue around the lesion with the formation of new trabeculae within the bone in the periosteal region and in the space between the disk and the ligaments. The formation of new bone would appear to be due to mechanical influences and to be completely independent of the inflammatory process.

Complication of spondylitis. A frequent complication is the appearance of an abscess. This seldom produces any clinical manifestation and is generally discovered during the radiologic examination. It was present in 12 of the



Fig. 4. Brucellar spondylitis of L2 and L3 with osteophytic reaction and narrowing of the intervertebral space.

of the anterior aspect of a dorsal vertebral body may be observed, the body may collapse as in tuberculous spondylitis (Fig. 2). A narrowing of the disk space was evident in 90 % of the cases and in some was the only sign of brucellar spondylitis. The disk lesions were generally associated with other bone lesions (Figs 1 and 4).

It is not unusual to observe geodic formations in the cancellous bone of the vertebral bodies near the intervertebral disk. These may be confused with Schmorl's nodes but are larger and more irregular. Lesions of the interapophyseal joints, with blurring of the articular facets, associated with subchondral osteoporosis, were present in one case.

Osteophytes often appear in advanced cases close to the osteolytic focus (Fig. 4). They appear generally in cases with marked narrowing of the disk space and displacement of the vertebrae. These lesions probably represent a nonspecific bone reaction to the direct brucellar destruction (ROTLS QUEROL).

Pathology. A pathologic study was performed by PEDRO BOTLT, CISCAR & J. ROTLS QUEROL in 4 cases. They stated that the destructive lesions are produced by granulation tissue that starts from the bone marrow, destroys the surrounding bone trabeculae and invades the disk through the geodic formations of the cancellous bone. The destruction of the intervertebral disk gives rise to the formation of osteophytes, these may be considered as signs of a reconstructive phenomenon.

trum in a cavity. The widening of the joint space may be regular or irregular and the margins of the joint may be undulating. The articular facets may be poorly defined, irregular, and even completely fragmented. Changes in density of the periarticular bone are also frequent.

Involvement of the intradural structures

Neurotropism is one of the characteristics of brucellosis. Involvement of the intradural nervous structures and their sheaths may take place by propagation of adjacent spondylitis or by independent hematogenous invasion through the meninges, the latter being the more frequent.

The meningeal participation is a constant phenomenon, manifested in most cases by adhesive arachnoiditis associated with a myelo- or radicular syndrome depending on the level. The lesions are produced by a hyperplastic proliferation of the meninges or by the formation of a true cyst. Out of 30 cases with myeloradicular manifestations only 9 had arachnoidal lesions on myelography.

A longer version of this paper was read at the Symposium.

SUMMARY

The characteristic radiologic signs of brucellar spondylitis and sacroilitis and some less common evidence of arachnoiditis are described with reference to 156 of a total material of 192 cases of brucellosis.

ZUSAMMENFASSUNG

Die charakteristischen Röntgenveränderungen der Wirbelsäule und der Sakroiliakal Gelenke sowie ungewöhnlichere Zeichen einer Arachnoiditis werden bei der Brucellose (Maltafieber) anhand von 156 Fällen von einer Gesamtzahl von 192 Fällen beschrieben.

RÉSUMÉ

Description des signes radiologiques caractéristiques des localisations rachidiennes et sacroiliques de la brucellose et de signes plus rares d'arachnoidite d'après 156 cas sur un total de 192 cas de brucellose.

REFERENCES

- ARCHER, V. W. Undulant fever with report of a case simulating Pott's disease. *South med J* 28 (1935) 1.
 ARDITI, J. Consideraciones generales y lesiones vertebrales cervicales brucelósicas. *Rev med de Córdoba* 33 (1945) 644.
 BARCELÓ, I., BATALLA, E., ROTES-QUEROL, J., VILASECA, J. M. Manifestaciones osteoarticulares de la brucelosis. IV Congreso Internacional de Higiene y Medicina Mediterránea (1953) 103.



Fig. 6 Brucellar sacroiliitis. Irregular widening of the joint space with blurring of its outline on the left side

present cases. An abscess in the lumbar region appears as a prominence of the psoas shadow and is usually bilateral. A dorsal abscess is generally unilateral and appears mainly in the lower part of the region between the insertions of the diaphragm and the spine. A cervical abscess usually lies in front of the spine and between it and the trachea.

Another complication of spondylitis is its propagation towards the vertebral canal, affecting the intradural nervous structures (spinal cord and nerve roots). This problem will be examined later.

Sacroiliitis

Sacroiliitis occurred in 31 cases of the material and tended to resolve spontaneously, without sequelae in 2 or 3 months.

Males were affected twice as often as females. The incidence was higher among younger patients, possibly due to the complete loss of mobility of the sacroiliac joint after the age of 50. The lesions are generally unilateral.

Sacroiliitis is characterized by its early appearance, 10 or 15 days after the onset of clinical signs, in contrast to tuberculous lesions. The initial lesion consists of an irregular diastasis of the articular space with blurring of the edges (Fig. 6). The diastasis may reach a width of 0.5 to 1 cm and even 2 cm and a fragment of cancellous bone which has been called an 'island' by ROTES QUEROL, may appear between the articular facets and suggest a seques-

trum in a cavity. The widening of the joint space may be regular or irregular and the margins of the joint may be undulating. The articular facets may be poorly defined, irregular, and even completely fragmented. Changes in density of the periarticular bone are also frequent.

Involvement of the intradural structures

Neurotropism is one of the characteristics of brucellosis. Involvement of the intradural nervous structures and their sheaths may take place by propagation of adjacent spondylitis or by independent hematogenous invasion through the meninges, the latter being the more frequent.

The meningeal participation is a constant phenomenon, manifested in most cases by adhesive arachnoiditis associated with a myelo- or radicular syndrome depending on the level. The lesions are produced by a hyperplastic proliferation of the meninges or by the formation of a true cyst. Out of 30 cases with myeloradicular manifestations only 9 had arachnoidal lesions on myelography.

A longer version of this paper was read at the Symposium

SUMMARY

The characteristic radiologic signs of brucellar spondylitis and sacroilitis and some less common evidence of arachnoiditis are described with reference to 156 of a total material of 192 cases of brucellosis.

ZUSAMMENFASSUNG

Die charakteristischen Röntgenveränderungen der Wirbelsäule und der Sakro-iliakal Gelenke sowie ungewöhnlichere Zeichen einer Arachnoiditis werden bei der Brucellose (Maltafieber) anhand von 156 Fällen von einer Gesamtzahl von 192 Fällen beschrieben.

RÉSUMÉ

Description des signes radiologiques caractéristiques des localisations rachidiennes et sacro-iliques de la brucellose et de signes plus rares d'arachnoidite d'après 156 cas sur un total de 192 cas de brucellose.

REFERENCES

- ARCHER V. W. Undulant fever with report of a case simulating Pott's disease. *South med J* 28 (1935) 1.
 ARDITI J. Consideraciones generales y lesiones vertebrales cervicales brucelósicas. *Rev. med de Córdoba* 33 (1945) 644.
 BARCELÓ P., BATALLA E., ROTES-QUEROL J., VILASECA J. M. Manifestaciones osteoarticulares de la brucelosis. IV Congreso Internacional de Higiene y Medicina Mediterránea (1953) 103.



Fig. 6. Brucellar sacroiliitis. Irregular widening of the joint space with blurring of its outline on the left side.

present cases. An abscess in the lumbar region appears as a prominence of the psoas shadow and is usually bilateral. A dorsal abscess is generally unilateral and appears mainly in the lower part of the region between the insertions of the diaphragm and the spine. A cervical abscess usually lies in front of the spine and between it and the trachea.

Another complication of spondylitis is its propagation towards the vertebral canal, affecting the intradural nervous structures (spinal cord and nerve roots). This problem will be examined later.

Sacroiliitis

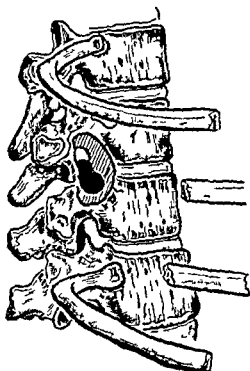
Sacroiliitis occurred in 31 cases of the material and tended to resolve spontaneously, without sequelae in 2 or 3 months.

Males were affected twice as often as females. The incidence was higher among younger patients, possibly due to the complete loss of mobility of the sacroiliac joint after the age of 50. The lesions are generally unilateral.

Sacroiliitis is characterized by its early appearance, 10 or 15 days after the onset of clinical signs, in contrast to tuberculous lesions. The initial lesion consists of an irregular diastasis of the articular space with blurring of the edges (Fig. 6). The diastasis may reach a width of 0.5 to 1 cm and even 2 cm and a fragment of cancellous bone, which has been called an island by ROTES QUEROL, may appear between the articular facets and suggest a seques-

- ROTES-QUEROL J Manifestaciones osteoarticulares de la Brucelosis Ed Jims Barcelona 1959
- SAEZ VAZQUEZ R y LEY A Contribución al estudio de las complicaciones nerviosas de la fiebre de Malta Rev Clin Esp 5 (1947) 419
- SANDSTROM O Multiple spondylitis in undulant fever Acta radiol 18 (1937) 253
- SCHREIBER F and HADDAD B Lumbar and sacral cysts causing pain J Neurosurg 8 (1951) 504
- SCHURR P H Sacral extradural cyst an uncommon cause of low back pain J Bone Jt Surg 37 B (1955) 601
- SERIO J Sulle Spondilite melitococcica Arch ital Pat Clin Med 6 (1927) 247
- SOLÉ LLENAS J Les kystes des racines sacrées et leur valeur pathologique Acta radiol (1963) 187
- SPINA W W Pathogenesis of human brucellosis Ann intern Med 29 (1948) 238
- STRULLY K J Meningeal diverticulae of sacral nerve roots (perineurial cysts) J Amer med Ass 161 (1956) 1147
- TERRANOVA R e NICOLA G C Arachnoiditi Spinali Ed Minerva Medica Torino 1959

- VILASECA J M Espondilitis melitococcica Clinica y Radiologia Med Clin 3 (1944) 184
- BASERGA A La sciatiche brucellari Gazz Osp Clin 60 (1939) 99
- BENDEK J Sciatic neuritis in undulant fever Gyógyszerész 71 (1931) 696
- BISHOP W A Vertebral lesions in undulant fever J Bone Jt Surg 21 (1939) 665
- BOULET P SERRE H PASSOUANT P et BERTRAND I Syndrome méningovertébrale melitococcique Bull Soc Med Paris 64 (1948) 883
- CALVET J Complications osseuses et vertébrales de la melitococcie Progr med 19 (1956) 1904
- CANTALOUBE P La fièvre de Malte en France Id Maloine Paris 1911
- CARNELLI R Spondilite cervicale melitococcique Not Diag et Ter 11 (1934) 3
- CATELLI J Spondilite da Brucellosi Rass int Clin 15 (1934) 649
- CISCAR F PEDRO BOTET J y CORNUDELLA R Estudio histopatológico de un caso de espondilitis melitococcica Congr de Med Mediterranea Barcelona 1953
- CLERICI C Sulla spondilite da febbre ondulante G Clin med 1 (1932) 2
- DALRYMPLE CHAUNLYS W Undulant fever Lancet 1 (1950) 429
- DI RIENZO S La Spondilitis brucellosica Rev argent Reum 10 (1945) 30
- Brucellar Spondilitis Fortschr Röntgenstr 73 (1950) 333
- LISTEIN B S The Spine Lea Febiger Philadelphia 1962
- LARRERUS P Neurobrucellosis Ed Marin Barcelona 1943
- LOZ A Valor de la reacción de fijación de complemento en la brucelosis humana IX Cong Int de Hig y Med Mediterraneas pág 173 Barcelona 1953
- GARCIA GAURE M Espondilitis melitococcica Dia méd 3 (1946) 257
- GAUTHIER J Spondilite melitococcique Lyon méd 155 (1935) 257
- HARDY A V JORDAN C S and BORTS J H Undulant fever Further epidemiologic and clinical observations J Amer med Ass 107 (1936) 559
- HERSON R N Undulant fever showing vertebral lesions Brit med J 1 (1942) 762
- HYNDMAN O R and GERBER W F Spinal extradural cysts congenital and acquired Report of cases J Neurosurg 4 (1946) 474
- JANON M Spondilite melitococcique avec paraplegie par compression Soc des Sc Med Montpellier 1945
- KULOWSKI J and WINKLE I H Undulant fever spondilitis J Amer med Ass 99 (1932) 1656
- MALDOVADO ALLENDE I Espondilitis brucellosica y hernia de disco intervertebral I Cong Interamericano sobre Brucellosis Mexico 1946 pag 590
- MASSERA L Le complicazioni vertebrali della brucellosi La Clin Ort 1 (1949) 4
- PEDRO BOTET J Aspectos anatomorradiológicos de la espondilitis brucelósica Rev esp Reum 4 (1951) 166
- PEDRO PONS A La espondilitis melitococcica Ann Med Barcelona (1929) 227
- y SORIANO M La espondilitis melitococcica Diagnóstico clínico y radiográfico An de la Clinica Médica Barcelona 1 (1932—33) 131
- PHALEN G S PRICKMAN L E and KRUSEN F H Brucellosis Spondilitis J Amer med Ass 118 (1942), 859
- RAVAULT P BERTHIER L et VIGNON G Deux cas de spondilite melitococcique Rev Rhum (1944) 332
- RIMBAU L et SERRE H Le mal de Pott cervical melitococcique Bull Acad Méd 614 (1943) 617
- ROGER H Les paraplegies brucellosesques Encéphale 3 (1954) 246



T ₆	_____	2
7	_____	2
8	_____	1
9	_____	2
10	_____	3
11		
T ₁₂		

Fig 1 Diagram of lateral approach operation for protruded thoracic disc (kind permission of A. HULME F.R.C.S.)

Fig 2 Levels affected in the 10 cases reported

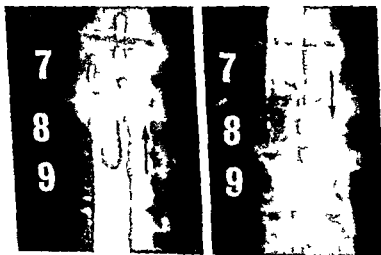


Fig 3 Case 1 Myelography. Elongated oval defect from T7-T8

MYELOGRAPHY IN DORSAL DISC PROTRUSION

by

J L G THOMSON

Thoracic disc protrusion is an uncommon lesion with little more than one hundred cases recorded in the literature, but as it is amenable to surgery it is important that it should be recognised.

It does seem, however, that for a benign compressive lesion of the cord the results of surgical treatment, as recorded, are often disappointing. Thus in *Logue's* (1952) series of eleven cases, six were better following operation and five were worse. In 1960 *Toni & Strang* reported improvement in four out of a series of fourteen cases. It may be of some relevance that the operation generally employed is the standard laminectomy procedure, for this does of necessity entail some handling of the spinal cord.

In 1960 *Hulme* described a lateral approach operation (Fig. 1) involving excision of the heads of two ribs, and widening of the appropriate intervertebral foramen (shaded area) to allow undercutting of the offending disc (shown black) and removal from in front. By this method the dura remains unopened and the spinal cord very little disturbed so that neurological trauma is at a minimum. In the Neurosurgical Unit at Bristol, England, there have been thirteen cases of thoracic disc protrusion in the last nine years, of which ten cases have been confirmed surgically. As the other three cases were treated medically, and are therefore unconfirmed, they will not be referred to again.



Fig 5 Case 2 myelography Almost complete obstruction to the upward flow of myodil

paper the conventional film and the tomographic findings are grouped together

Myelography is performed with the patient prone using 5 ml of myodil, the flow being screened and routine films taken. Should there be incomplete obstruction to the flow of myodil in the dorsal region great care is taken to exclude any other lesion higher up. It is also a basic principle that the myelographic defect should correspond with the clinical syndrome.

According to the myelographic findings there was complete obstruction in three cases, almost complete obstruction in one, a central filling defect in five, and a lateral J shaped defect in one. When the obstruction was complete or almost complete the shape of the myodil indicated extrathecal compression with deflection away from the back of the vertebral bodies in the lateral view, mostly adjacent to the disc space. The oval filling defect varied from 2 cm to 4 cm in length, the smaller defect corresponding quite clearly with the disc space. The rate of myodil flow was unaffected by the small lesion, hence the necessity for careful screening and routine films. Again in the lateral view there was some deflection away from the vertebral bodies at the disc space, and in one case a double profile was evident where some of the myodil deflected by the disc contrasted with myodil flowing around its side. With the



Fig 1 Case 1 Tomography Large osteophytes revealed

Of the ten cases operated, eight were approached laterally as outlined above, seven of these recovering well and the other one showing continued improvement. The other two cases had the standard laminectomy operation one is recovering well and the other remaining unimproved.

The objects of this paper therefore are firstly to draw attention to this particular operation, and secondly to review the radiological appearances of dorsal disc protrusion.

In our group there were six females with an average age of forty seven years, and four males with an average age of thirty eight years. The levels are indicated in Fig 2, all protrusions being single ones, as is usually the case.

Minor trauma may initiate symptoms, and five of our ten cases recalled antecedent incidents such as twisting movement, stretching or lifting heavy weights. Root pain may predominate if the protrusion is mainly lateral, but otherwise the symptoms resemble any other cord compressive lesion and the more central the protrusion the more motor and sensory loss there will be.

The cerebrospinal fluid findings are not typical and the diagnosis rests on the radiological findings.

Our routine in cases with spinal cord compression is to follow conventional films, where necessary, by myelography and then to proceed to lateral tomography should dorsal disc protrusion be suspected. For the purposes of this



Fig 7 Case 3 Left view Myelography Upward flow of myodil blocked below the disc space Right view Tomography Calcified disc material in the spinal canal and calcification in the disc space

Case 3 A 47 year old man had a sudden onset of pain in the back on lifting and within three weeks had become paraparetic. The myodil was completely blocked some distance below the disc space (Fig 7 left views). Lateral tomography showed calcification in the disc space and protruded disc material in the canal (Fig 7 right view).



Fig 8 Case 4 Left view Myelography Small half disc protrusion with myodil flowing up and down Right view Tomography Flecks of calcium in the spinal canal Calcification in the disc space



Fig 6 Case 2 Tomography Calcification in the disc space with small posterior osteophytes

patient supine the defect was usually less clear cut, confirming that the lesion was anteriorly placed in the spinal canal.

With myelographic findings such as these, suggestive of protruded thoracic disc, further information was obtained by lateral tomography of the spine. This examination revealed calcification in the disc space and posterior osteophytes in four cases, calcification in the disc space as well as posterior calcification in four cases, and a normal disc space in two cases. This information was considered diagnostic in eight cases. In the two cases where no abnormality could be demonstrated the diagnosis could be made at myelography, where the backward deflection of the myodil at a disc space was considered characteristic. In one case there was an incidental finding of calcification in an adjacent disc space and in four cases there was incidental Scheuermann's disease.

Examples

Case 1 A 32 year old female stretched in bed one morning and was seized by a sudden girdle pain. She became completely paraplegic within the next three hours. Myelography the same day (Fig 3) showed an elongated oval defect centrally from T7 to T9. Lateral tomography (Fig 4) showed calcification in the disc space and large osteophytes protruding into the spinal canal.

Case 2 A 59 year old female with gradual onset of numbness of the legs over six weeks. Myelography (Fig 5) showed an almost complete obstruction to myodil. The lateral tomogram (Fig 6) showed calcification in the disc space with small osteophytes posteriorly.

CAUDA EQUINA DAMAGE AFTER THORIUM DIOXIDE MYELOGRAPHY

by

HOWARD J. TUCKER, WILLIAM A. SIBLEY and LOWELL W. LAPHAM

Thorotrast, a colloidal solution of thorium dioxide, a radioactive material with a long half life (about 14 billion years) was widely used for myelography from about 1938 until 1945 (15, 16, 17, 18). Its use was curtailed because of concern about potential tissue damage and neoplasia (1, 2, 9, 10, 11, 12, 13, 14) and because more satisfactory contrast media became available.

Within the past six years we have examined three patients with severe cauda equina damage beginning five to eighteen years after Thorotrast myelography. A fourth patient with an identical clinical picture is presumed to have had Thorotrast myelography, but actual confirmation is lacking. All patients had paralysis of urinary and rectal sphincters, diminished or absent tendon reflexes in the lower extremities, and saddle analgesia. In some cases there was significant weakness and loss of proprioceptive sensibility in the legs. We know of no other reports of this complication except for a recent description of three similar cases by MALTBY (13). The occurrence of this late complication is probably due to the radioactivity of residual contrast media and is of special interest because of the long interval between myelography and the first symptom of neural damage.

Case 4 A 50 year old man twisted his back and developed numbness of his feet. At myelography a shelf could be demonstrated with the myodil flowing up and down (Fig. 8 left views). The lateral tomogram showed calcification in the disc space and flecks of calcium in the spinal canal (Fig. 8 right view). There is incidental Scheuermann's disease.

Case 5 A man of 29 with a one month's story of spinal cord compression showed a complete block to the flow of myodil following cisternal myelography. Tomography failed to show any abnormal calcification or osteophyte formation but a large disc protrusion was confirmed at operation.

Acknowledgement

Presentation of the paper at the Congress was assisted by the award of a Wellcome Research Travel Grant for which my sincere thanks are gratefully recorded.

SUMMARY

The findings at myelography in cases of dorsal disc protrusion are summarised in 10 cases that came to surgery. Lateral tomography of the spine gave considerable assistance in the confirmation of the diagnosis. Attention is drawn to the lateral approach operation for the removal of a protruded dorsal disc.

ZUSAMMENFASSUNG

Die myelographischen Befunde von 10 Fällen von dorsaler Diskusprotrusion, die zur Operation kamen, wurden zusammengefasst. Die laterale Tomographie des Rückens war für die Stellung der Diagnose von grosser Bedeutung. Zur Entfernung eines protrudierten dorsalen Diskus wird auf den lateralen Operationsweg aufmerksam gemacht.

RÉSUMÉ

Description des signes myélographiques de la protrusion discale dorsale d'après 10 cas opérés. La tomographie de profil du rachis a beaucoup facilité la confirmation du diagnostic. L'auteur attire l'attention sur l'abord chirurgical latéral pour l'exérèse d'une protrusion discale dorsale.

REFERENCES

- HULME A. The surgical approach to thoracic intervertebral disc protrusions. *J. Neurol. Neurosurg. Psychiat.* 23 (1960) 133.
 LOGUE V. Thoracic intervertebral disc prolapse with spinal cord compression. *J. Neurol. Neurosurg. Psychiat.* 15 (1952) 227.
 FOVI D. and STRANG R. R. Thoracic intervertebral disc protrusions. *Acta chir. scand.* (1960) Suppl. 267.

CAUDA EQUINA DAMAGE AFTER THORIUM DIOXIDE MYELOGRAPHY

by

HOWARD J. TUCKER WILLIAM A. SIBLEY and LOWELL W. LAPIER

Thorotrast a colloidal solution of thorium dioxide a radioactive material with a long half life (about 14 billion years) was widely used for myelography from about 1938 until 1945 (15 16 17 18). Its use was curtailed because of concern about potential tissue damage and neoplasia (1 2 9 10 11 12 13 14) and because more satisfactory contrast media became available.

Within the past six years we have examined three patients with severe cauda equina damage beginning five to eighteen years after Thorotrast myelography. A fourth patient with an identical clinical picture is presumed to have had Thorotrast myelography but actual confirmation is lacking. All patients had paralysis of urinary and rectal sphincters diminished or absent tendon reflexes in the lower extremities and saddle analgesia. In some cases there was significant weakness and loss of proprioceptive sensibility in the legs. We know of no other reports of this complication except for a recent description of three similar cases by MALTBY (13). The occurrence of this late complication is probably due to the radioactivity of residual contrast media and is of special interest because of the long interval between myelography and the first symptom of neural damage.

Case material

Case 1 A 42 year old woman was seen in 1959 because of increasing constipation for 7 years and progressive incontinence of urine for 3 months. In 1942 at age 26 Thorotrast myelography had been performed at another hospital and had revealed a definite large herniated intervertebral disc on the left side between L 5 and S 1. After a laminectomy she was entirely free of her previous complaint of left sciatica and remained asymptomatic until 1958.

Examination in 1959 showed a normal gait except for a limp favoring the left leg. She could not walk well on her heels and direct muscle testing confirmed mild weakness of the dorsiflexors of the feet bilaterally. Muscle strength in the lower extremities was otherwise intact. Straight leg raising was restricted to 45° on the right because of pain in the right buttock. The right knee jerk was depressed compared to the left. Ankle reflexes were absent bilaterally. Plantar responses were flexor. There was extensive anesthesia in a saddle distribution bilaterally, and anesthesia posteriorly in the right thigh and calf. Vibratory sensation was diminished in the right foot but position sense was preserved. Occasional fasciculations were noted in the right buttock. Rectal sphincter tone was definitely decreased.

Cystoscopy showed an atonic bladder with a capacity of 500 ml and a 350 ml volume of residual urine. Roentgenograms of the spine showed residual Thorotrast largely concentrated in the sacral spinal canal but present in lesser amounts as high as L 1 (Fig. 1). Lumbar puncture revealed clear fluid with normal pressures and dynamics but cerebrospinal fluid protein was 115 mg %. Myelography with Pantopaque in 1959 showed a free flow of contrast medium from the sacral cul de sac to the mid thoracic region.

In 1961 examination because of progressive difficulty in walking during the preceding 5 years showed more extensive weakness involving the dorsiflexors of the feet and gastrocnemius, gluteus maximus and hamstring muscle groups bilaterally. The right knee jerk was now absent but the left knee jerk was still present. Ankle jerks remained absent with flexor plantar responses. Sensory deficit was similar to that recorded in 1959 but the rectal sphincter was now patulous. There was complete urinary incontinence.

Case 2 This 57 year old man was first examined 1961 because of progressive urinary and fecal incontinence for 18 months. He had been treated at another hospital in 1941 for recurrent right sciatica and low back pain of many years duration. Thorotrast myelography in 1941 was said to be normal but a herniated intervertebral disc had been removed at L 4-5. He was then asymptomatic until the onset of the present complaints.

Examination in 1961 showed mild weakness of dorsiflexion of the left foot but good muscle strength was present in all other muscle groups including gluteal and hamstring muscles. Deep tendon reflexes were normally active except for an absent left ankle reflex. Sensory examination revealed marked loss of pain and touch sensation in a saddle distribution over the buttocks bilaterally corresponding to the second sacral to fifth sacral dermatomes. The rectal sphincter was patulous.

Roentgenograms of the lumbosacral spine showed evidence of an old laminectomy and fusion and the dural cul de sac was outlined by a rim of contrast medium (Fig. 1). Lumbar puncture revealed clear fluid with open manometrics and a cerebrospinal fluid protein value of 49 mg per 100 ml. Myelography with Pantopaque was normal.

Because of fecal incontinence a colostomy was performed in 1962 and he found it necessary to wear a urinal. No further leg weakness developed and there has been no change in his neurological deficit during the past 3 years.

Case 3 A 65 year old housewife was examined by us in 1959 with a complaint of constipa-



Fig 1 Conventional roentgenograms of lumbosacral spines of Cases 1 2 3 and 4 taken 17 20 18 and 0 years respectively after Thorotrast myelography

tion and occasional urinary and fecal incontinence of 9 years' duration and progressive leg weakness for 5 years.

In 1942 at age 49 she had had low back discomfort with a normal neurological examination. Thorotrast myelography elsewhere in 1943 revealed nothing of interest and at the time of discharge she was asymptomatic. In 1948 she developed urinary retention and a bladder neck resection was done. Examination in 1954 revealed a mild paraparesis and both patellar and ankle reflexes were absent. Plantar responses were flexor. The anal sphincter was patulous and there was a definite saddle analgesia. Spinal fluid examination showed an initial pressure of 103 mm of cerebrospinal fluid, normal dynamics, and a total protein value of 26 mg per 100 ml. The colloidal gold reaction was normal. By 1957 14 years after Thorotrast myelography the patient was no longer able to walk and used a wheelchair.

In 1958 she was admitted to University Hospitals for evaluation with moderate weakness of both lower extremities, more severe on the left and with greater involvement distally. No fasciculations were seen. Deep tendon reflexes were normal in the upper extremities but absent at the knees and ankles. There was hypalgesia and absent vibratory sensation below the knees. Position sense was markedly decreased in both feet, more severely so on the left. Saddle hypalgesia was present and the anus was patulous. Roentgenograms of the thoracic spine were normal but throughout the lumbar spinal canal there was residual Thorotrast (Fig 1). Myelography with Pantopaque showed free flow of the medium from the sacral cul-de-sac to the foramen magnum. The cerebrospinal fluid protein was 88 mg per 100 ml and there were no white cells in the fluid. Her weakness progressed and she died suddenly in 1961.

Case 4. A 56-year-old retired laborer was admitted in 1961 because of rectal incontinence for 2 months. In 1953 presumably for symptoms of prostatism he underwent transurethral resection and suprapubic prostatectomy. Since that time there had been total urinary incontinence and impotence. Since 1949 he had suffered from progressive weakness of the legs

Case material

Case 1 A 42 year old woman was seen in 1959 because of increasing constipation for 7 years, and progressive incontinence of urine for 5 months. In 1942, at age 26 Thorotrast myelography had been performed at another hospital and had revealed a definite large herniated intervertebral disc on the left side between L 5 and S 1. After a laminectomy she was entirely free of her previous complaint of left sciatica and remained asymptomatic until 1958.

Examination in 1959 showed a normal gait except for a limp favoring the left leg. She could not walk well on her heels and direct muscle testing confirmed mild weakness of the dorsiflexors of the feet bilaterally. Muscle strength in the lower extremities was otherwise intact. Straight leg raising was restricted to 45° on the right because of pain in the right buttock. The right knee jerk was depressed compared to the left. Ankle reflexes were absent bilaterally. Plantar responses were flexor. There was extensive anesthesia in a saddle distribution bilaterally and anesthesia posteriorly in the right thigh and calf. Vibratory sensation was diminished in the right foot but position sense was preserved. Occasional fasciculations were noted in the right buttock. Rectal sphincter tone was definitely decreased.

Cystoscopy showed an atonic bladder with a capacity of 500 ml and a 350 ml volume of residual urine. Roentgenograms of the spine showed residual Thorotrast largely concentrated in the sacral spinal canal but present in lesser amounts as high as L 1 (Fig. 1). Lumbar puncture revealed clear fluid with normal pressures and dynamics but cerebrospinal fluid protein was 115 mg %. Myelography with Pantopaque in 1959 showed a free flow of contrast medium from the sacral cul de sac to the mid thoracic region.

In 1964 examination because of progressive difficulty in walking during the preceding 5 years showed more extensive weakness involving the dorsiflexors of the feet and gastrocnemius, gluteus maximus and hamstring muscle groups bilaterally. The right knee jerk was now absent but the left knee jerk was still present. Ankle jerks remained absent with flexor plantar responses. Sensory deficit was similar to that recorded in 1959 but the rectal sphincter was now patulous. There was complete urinary incontinence.

Case 2 This 57 year old man was first examined in 1961 because of progressive urinary and fecal incontinence for 18 months. He had been treated at another hospital in 1941 for recurrent right sciatica and low back pain of many years' duration. Thorotrast myelography in 1941 was said to be normal but a herniated intervertebral disc had been removed at L 4-5. He was then asymptomatic until the onset of the present complaints.

Examination in 1961 showed mild weakness of dorsiflexion of the left foot but good muscle strength was present in all other muscle groups including gluteal and hamstring muscles. Deep tendon reflexes were normally active except for an absent left ankle reflex. Sensory examination revealed marked loss of pain and touch sensation in a saddle distribution over the buttocks bilaterally corresponding to the second sacral to fifth sacral dermatomes. The rectal sphincter was patulous.

Roentgenograms of the lumbosacral spine showed evidence of an old laminectomy and fusion and the dural cul de sac was outlined by a rim of contrast medium (Fig. 1). Lumbar puncture revealed clear fluid with open manometrics and a cerebrospinal fluid protein value of 49 mg per 100 ml. Myelography with Pantopaque was normal.

Because of fecal incontinence a colostomy was performed in 1962 and he found it necessary to wear a urinal. No further leg weakness developed and there has been no change in his neurological deficit during the past 3 years.

Case 3 A 65 year old housewife was examined by us in 1959 with a complaint of constipa-

each of our patients. This was considered especially important because of the progressive course in all patients and because three of the patients had elevated cerebrospinal fluid protein values. Pantopaque myelography was interpreted as normal in all four cases in spite of biopsy proven arachnoiditis in one of the patients and presumed adhesive arachnoiditis in the other three. It is evident, therefore, that the outline of the subarachnoid space as demonstrated by myelography with Pantopaque may not show the classical radiological picture of arachnoiditis though significant arachnoiditis is present.

It is probable that the cases reviewed here reflect only a small per cent of those developing neurological damage following Thorotrast myelography. Because of the time interval between injection of Thorotrast and the onset of symptoms the syndrome of thorium induced cauda equina damage may go unrecognized unless a careful history is elicited. The presence of the typical roentgenograms produced by Thorotrast retained in the lumbosacral canal should alert the examiner to this diagnosis.

SUMMARY

Four patients developed signs of progressive damage to the cauda equina many years after thorium dioxide myelography. The number of years elapsing between myelography and first symptoms of neural damage was inversely proportional to the amount of retained Thorotrast in the lumbosacral spinal canal. The clinical localization and extent of neurologic damage correlated with the position and estimated volume of residual contrast media. In all patients myelography with Pantopaque was normal after cauda equina damage had developed.

ZUSAMMENFASSUNG

Vier Patienten entwickelten viele Jahre nach einer Thoriumdioxid Myelographie Anzeichen einer progressiven Schädigung der Cauda equina. Das zeitliche Intervall zwischen Myelographie und den ersten Nervenstörungen ist umgekehrt proportional zur Menge des im lumbosacralen Spinalkanal reterierten Thorotrasts. Die klinische Lokalisierung und das Ausmass des Nervenschadens korrespondierte mit der Lage und einer bestimmten Menge reterierten Kontrastmittels. Bei allen Patienten, bei denen sich ein Cauda equina Schaden entwickelt hatte, war die Myelographie mit Pantopaque normal.

RÉSUMÉ

Quatre malades ont présenté des signes de lésion progressive de la queue de cheval de nombreuses années après une myélographie au dioxyde de thorium. Le nombre d'années écoulées entre la myélographie et les premiers symptômes de trouble neurologique est inversement proportionnel à la quantité de Thorotrast restant dans le canal rachidien lombo-sacré. La localisation clinique et l'étendue des signes neurologiques concorde avec la position et le volume du moyen de contraste résiduel. Chez tous ces malades, la myélographie au Pantopaque faite après le début des lésions de la queue de cheval a été normale.

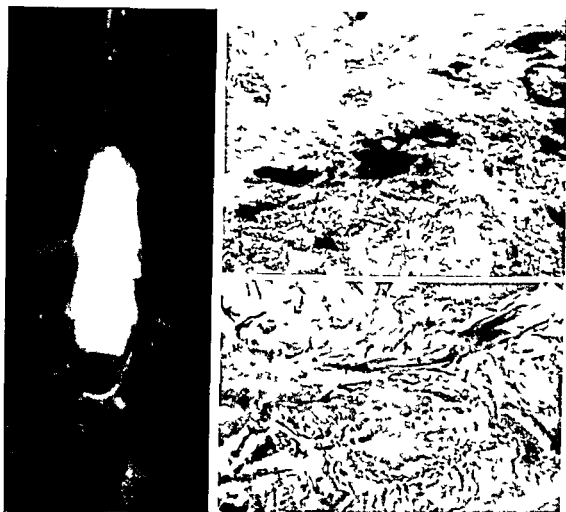


Fig. 2 Case 4. *Left view*. Myelogram. No significant distortion of the column of contrast medium in spite of biopsy proven arachnoiditis. *Right view*. Surgical biopsy of the arachnoid in the lumbosacral area. Deposits of brown granular material within dense connective tissue presumably Thorotrast. Hematoxylin eosin $\times 200$ (top) $\times 720$ (bottom).

which was more severe in the left leg 1 or the 18 months prior to his first examination by us in 1961 he had been confined to a wheelchair. Myelography had been performed in the early 1940s for obscure reasons and in 1947 roentgenograms of the lumbar spine at another hospital revealed contrast material outlining the entire lower spinal canal (Fig. 1).

On neurological examination paresis of the entire left lower extremity was noted. Except for marked weakness of the dorsiflexors of the toes and hamstring muscles there was good strength in all muscle groups of the right lower limb. Clonus strength was fair on both sides. Straight leg raising was limited bilaterally at 45° by pain in the buttocks. Knee and ankle jerks were absent. Anal and bulbocavernosus reflexes were absent and the anal sphincter was patulous. There was moderate atrophy of both lower extremities. No fasciculations were seen. Hypalgesia was present in the L3 dermatome and analgesia was found from L4 through

S-5 on the left and from S 2 through S 5 on the right. Position sense was lost in the left foot and vibratory sense was absent below the knees bilaterally.

Lumbar puncture revealed open manometrics and a cerebrospinal fluid protein of 96 mg per 100 ml. Myelography with Pantopaque in January 1961 showed nothing abnormal (Fig 2). No untoward reactions occurred after myelography. During the next 8 months there was progression of his symptoms and repeat examinations showed hypalgesia as high as L-1 on the left side. In August 1961 a laminectomy was performed. The ligamentum flavum was markedly adherent to the dura at the T 12 vertebral level; the dura was a dull yellow color and was markedly thickened. The arachnoid was greatly thickened and adherent to the nerve roots and the conus medullaris.

Microscopic examination of the ligamentum flavum showed excessive connective tissue with calcification; the arachnoid was fibrotic and hyalinized. Within the fragments of fibrosis several areas of brownish globular material were seen which were regarded as residual Thorotrast (Fig 2). (We have been unable to locate old hospital records to confirm that the contrast material at the initial myelography was thorium dioxide. We have presumed this to be Thorotrast because the residual contrast material on the roentgenograms had the same appearances as in the cases known to have had myelographies with Thorotrast. Further, the brown deposits in the biopsy specimen resemble the Thorotrast demonstrated by others in soft tissue (12) and is unlike the microscopic picture of either Lipiodol or Pantopaque. Lastly, the myelography was done during the few years in which Thorotrast myelography enjoyed a brief period of popularity in this area.)

The patient showed no improvement and was discharged to the care of his family. He died suddenly in January 1963.

Discussion

The four patients presented here and the three patients described by MALTBY (13) are similar with respect to certain historical features and neurological findings. All patients were examined by Thorotrast myelography in the early 1940's for clarification of acute low back pain or sciatica. Regardless of the nature of the original illness, the pain which prompted Thorotrast myelography subsided in all patients, either spontaneously or after operation. Then, after a lengthy symptom-free interval (range 5 to 15 years), each patient developed a neurological disturbance.

The clinical features of this post thorium dioxide myelography syndrome in these 7 patients are outlined below.

Symptoms and signs	Number of patients
Unilateral numbness	7
Weakness of legs	7
Absent ankle reflex	7
Sensory loss including the three patients reported by MALTBY	7
Rectal int. sphincter	6
Absent patella reflex	6
Pain in legs	4
Spasticity	4
Babinski sign	0
	0

Thus it can be seen that the most common symptoms and signs are urinary and fecal incontinence, absent ankle reflexes and weakness of the legs. In five of the seven cases urinary incontinence was the initial symptom. The extent of motor and sensory loss is variable from case to case and appeared to correlate with the amount and location of residual Thorotrast in our four patients. The latency between Thorotrast myelography and the beginning of the post myelography cauda equina syndrome was shorter in the patient having the largest amount of retained contrast media. In Case 3, only five years elapsed between myelography and the onset of urinary incontinence. This patient had a greater amount of retained Thorotrast than did the other three patients (Fig. 1, No. 3). All of our patients had saddle anesthesia, again reflecting major damage in the lower sacral segments due to a greater concentration of retained thorium in the sacral cul de sac. Although this distribution of sensory loss is not mentioned by MALTBY it seems probable that it was present in his patients since they, too, had urinary and fecal incontinence and other evidence of cauda equina damage. We believe that the neurological deficit in all of these cases is due to damage to the cauda equina secondarily to radiation effect.

Both clinical and experimental evidence has shown that the central nervous system is more radiosensitive than the peripheral nerve fibers (6, 7, 8). However, it is likely that the spinal cord is spared in our cases following Thorotrast myelography because of the distance of the retained contrast medium from the spinal cord in some of the cases and because of the low penetrating properties of alpha ray activity. It is known that 'chemically pure thorium dioxide may display increasing radioactivity for several years as disintegration products accumulate (1, 4), and that the alpha ray emitting properties of thorium are the most important emanation causing direct damage to tissue. However, the penetrating properties of alpha particles are estimated at only one millimeter (4). Therefore, the most severe disruption of function should occur in areas of highest concentration of residual Thorotrast, probably in the nerve roots as they emerge from the spinal canal. MALTBY (13) referred to this post thorium dioxide syndrome as a myelopathy. Since the spinal cord is probably not involved, or at least is not the major site of damage, the term myelopathy seems misleading.

Direct confirmation of the presumption that major damage occurs in the nerve roots of the cauda equina must await careful postmortem studies. However, that an intense reactive fibrosis occurs in the meninges in the area of retained thorium seems quite definite in view of the biopsy findings in Case 1.

Because Thorotrast is capable of inducing neoplasia, it seemed important to rule out the presence of an extramedullary tumor in the spinal canal in

each of our patients. This was considered especially important because of the progressive course in all patients and because three of the patients had elevated cerebrospinal fluid protein values. Pantopaque myelography was interpreted as normal in all four cases in spite of biopsy proven arachnoiditis in one of the patients and presumed adhesive arachnoiditis in the other three. It is evident therefore that the outline of the subarachnoid space as demonstrated by myelography with Pantopaque may not show the classical radiological picture of arachnoiditis though significant arachnoiditis is present.

It is probable that the cases reviewed here reflect only a small per cent of those developing neurological damage following Thorotrast myelography. Because of the time interval between injection of Thorotrast and the onset of symptoms the syndrome of thorium induced cauda equina damage may go unrecognized unless a careful history is elicited. The presence of the typical roentgenograms produced by Thorotrast retained in the lumbosacral canal should alert the examiner to this diagnosis.

SUMMARY

Four patients developed signs of progressive damage to the cauda equina many years after thorium dioxide myelography. The number of years elapsing between myelography and first symptoms of neural damage was inversely proportional to the amount of retained Thorotrast in the lumbosacral spinal canal. The clinical localization and extent of neurologic damage correlated with the position and estimated volume of residual contrast media. In all patients myelography with Pantopaque was normal after cauda equina damage had developed.

ZUSAMMENFASSUNG

Vier Patienten entwickelten viele Jahre nach einer Thoriumdioxid Myelographie Anzeichen einer progressiven Schädigung der Cauda equina. Das zeitliche Intervall zwischen Myelographie und den ersten Nervenstörungen ist umgekehrt proportional zur Menge des im lumbosacralen Spinalkanale retinierten Thorotrasts. Die klinische Lokalisierung und das Ausmass des Nervenschadens korrespondierte mit der Lage und einer bestimmten Menge retinierten Kontrastmittels. Bei allen Patienten bei denen sich einen Cauda equina Schaden entwickelt hatte war die Myelographie mit Pantopaque normal.

RÉSUMÉ

Quatre malades ont présenté des signes de lésion progressive de la queue de cheval de nombreuses années après une myélographie au dioxyde de thorium. Le nombre d'années écoulé entre la myélographie et les premiers symptômes de trouble neurologique est inversement proportionnel à la quantité de Thorotrast restant dans le canal rachidien lombo-sacré. La localisation clinique et l'étendue des signes neurologiques concorde avec la position et le volume du moyen de contraste résiduel. Chez tous ces malades la myélographie au Pantopaque faite après le début des lésions de la queue de cheval a été normale.

REFERENCES

- 1 AUB J. C., EVANS R. D., HEMPELMANN L. H. and MARTLAND H. S. The late effects of internally deposited radioactive materials in man. *Medicine* 31 (1952) 221.
- 2 BERRETTI A. and McRAE D. L. A follow up study after Thorotrast carotid arteriography. Abstract in *Radiology* 72 (1959) 613. *Canad. Med. Ass. J.* 78 (1959) 916.
- 3 BRADY L. W., CHANDLER D. E., GOKSON R. O. and CLIBERSON J. Perivascular extravasation of Thorotrast. Report of a case with 11 year follow up. *Radiology* 74 (1960) 392.
- 4 Council on Pharmacy and Chemistry. Thorotrast. *J. Amer. med. Ass.* 99 (1932) 2183.
- 5 COUGH J. H. Vocal cord paralysis occurring 17 years after extravasation of Thorotrast in the neck. *Brit. J. Radiol.* 36 (1963) 451.
- 6 GREENFIELD M. M. and STARK I. Post irradiation neuropathy. *Amer. J. Roentgenol.* 60 (1948) 617.
- 7 HICKS S. P. Effects of ionizing radiation on the adult and embryonic nervous systems. *Assoc. for Res. in Nerv. & Mental Dis.* 32 (1953) 439.
- 8 JANZEN A. H. and WARREN S. Effect of roentgen rays on peripheral nerve of rat. *Radiology* 38 (1942) 333.
- 9 KYLE R. H., OLER A., LASSER L. C. and ROSOMOFF H. L. Meningitis induced by thorium dioxide. *New Eng. J. Med.* 268 (1963) 80.
- 10 LLVOWITZ B. S., HUGHES R. F. and ALFORD F. C. Treatment of thorium dioxide granulomas of neck. *New Eng. J. Med.* 268 (1963) 340.
- 11 LOONEY W. B. Investigation of late clinical findings following Thorotrast (thorium dioxide) administration. *Amer. J. Roentgenol.* 83 (1960) 163.
- 12 —, ARNOLD J. S., Livi H. and CRR W. S. Autoradiographic and histopathological studies of thorium dioxide patients: deposition of thorium and its daughter radioelements in soft tissues and skeleton following thorium dioxide administration. *Arch. Path.* 60 (1955) 173.
- 13 MALTA C. I. Progressive thorium dioxide myelopathy. *New Eng. J. Med.* 270 (1964) 490.
- 14 MORA J. M. Granulomatous tumor following intramammary injection of colloidal thorium dioxide. *J. Amer. med. Ass.* 115 (1940) 363.
- 15 NICHOLS B. H. and NOSIK W. A. Myelography with use of thorium dioxide solution (Thorotrast) as contrast medium. *Radiology* 35 (1940) 459.
- 16 NOSIK W. A. Clinical application of Thorotrast myelography and subsequent forced drainage: report of case. *Cleveland Clin. Quart.* 3 (1938) 262.
- 17 —. Intraspinal Thorotrast. *Amer. J. Roentgenol.* 49 (1943) 214.
- 18 — and MORTENSEN O. A. Myelography with Thorotrast and subsequent removal by forced drainage: experimental study: preliminary report. *Amer. J. Roentgenol.* 39 (1938) 727.
- 19 PREZYNA A. P., AYRES W. W. and MULRY W. C. Late effects of Thorotrast in tissues. *Radiology* 60 (1953) 573.
- 20 WARREN S. Effects of radiation on normal tissues. *Arch. Path.* 35 (1943) 121.

Reflexions apres le VIIeme Symposium

Les procedés physiques sortent le neuroradiologiste de son monde anatomique directement accessible et l'introduisent dans un monde de signes indirects neurophysiologiques ou physiques. Pour la premiere fois dans l'histoire de nos Symposia de nombreuses communications se trouvent consacrees a des techniques non radiographiques. Mais le deroulement du Symposium a montre que la tomographie a ultra sons B nous ramene à l'anatomie. Je pense que notre President a bien fait de nous inviter vers des nouvelles frontieres pour nous familiariser avec des techniques physiques. « Jusqu'a present » dit Jean ROSTAND « on n'a jamais fait rien de mieux dans la nature que le cerveau » permettez nous d'ajouter — et rien de plus difficile a explorer¹.

Ces techniques biophysiques sont ambulatoires et complementaires, elles interrogent le cerveau vivant et souffrant en termes differents en plus des rayons de Roentgen les rayons gamma ou infra rouges les vibrations infra ou ultra sonores les oscillations electromagnetiques sont mis en oeuvre dans l'espoir de completer le manque d'information d'une methode par la reponse positive d'une autre egalement pour parer a l'erreur d'un procede par la rectification d'un autre.

Dans l'ouvrage de TAVERAS et WOOD Diagnostic Neuroradiology nos collegues distinguent la neuroroentgenologie de la neuroradiologie cette derniere comprend en plus des rayons de Roentgen un éventail de techniques se deployant du rayonnement gamma a l'infra rouge des oscillations infra ou ultra sonores aux oscillations electromagnetiques.

Precisons qu'il ne parait nullement obligatoire que le neuroradiologue pratique avec ses mains toutes ces techniques il devient par contre indispensable pour lui de connaitre les examens complementaires leur signification ainsi que leur articulation avec l'image neuroradiologique.

Dans le cadre d'une equipe de neurologie de neurochirurgie ou de neuroradiologie les techniques complementaires du systeme nerveux central doivent echoir aux specialistes competents la nature biophysique des techniques complementaires souligne l'utilite considerable d'un physicien a l'interieur de l'equipe l'autonomie la dependance ou l'indépendance de laboratoires ainsi specialises se developperont a la mesure des responsabilites exercees.

Ne cherchons pas de formules prefabriquees car pour ce dernier aspect le facteur humain prendra toujours le dessus.

